本発明の薬物複合体の多糖誘導体部分を構成するカルボキシC_{1-4}アルキルデキストランポリアルコールのポリアルコール化度は特に限定されないが、カルボキシC_{1-4}アルキルデキストランポリアルコールを構成するデキストランポリアルコールが、実質的に完全にポリアルコール化可能な条件下においてデキストランを処理して得られたデキストランポリアルコールであることが好ましい。例えば、デキストランに大過剰の過ヨウ素酸ナトリウムと水素化ホウ素ナトリウムとを順次作用させてデキストランを実質的に完全にポリアルコール化したデキストランポリアルコールを本発明の薬物複合体の原料化合物として好適に用いることができる。もっとも、デキストランのポリアルコール化の方法は上記のものに限定されることはなく、当業者に利用可能なものであればいかなる方法を採用してもよい。

デキストランの種類は特に限定されず、α-D-1,6- 結合を任意の割合で含んでいてもよい。例えば、α-D-1,6- 結合の割合が 85%以上、90% 以上、又は95% 以上のデキストランなどを用いることができる。デキストランの分子量は特に限定されないが、例えば 10,000 程度から 2,000,000程度のもの、好ましくは 50,000 程度から 800,000程度のものを用いることができる。カルボキシC_{1-4}アルキル基を構成するC_{1-4}アルキルとしては、直鎖又は分枝鎖のC_{1-4}アルキル、具体的にはメチル基、エチル基、n-プロピル基、イソプロピル基、n-ブチル基、sec-ブチル基などを用いることができるが、好ましくはメチル基を用いることができる。カルボキシC_{1-4}アルキル化は、例えば、デキストランポリアルコールの水酸基に対してクロル酢酸、ブロム酢酸、α－クロルプロピオン酸、α－メチル－α－クロルプロピオン酸、β－クロルプロピオン酸、α－メチル－β－クロルプロピオン酸、α－クロル酪酸、β－クロル酪酸、γ－クロル酪酸などのハロゲン化C_{1-4}アルキルカルボン酸、好ましくはクロル酢酸を反応させて水酸基を部分的又は完全にカルボキシC_{1-4}アルキル化することにより行うことができる。

例えば、デキストランポリアルコールを反応に関与しない不活性溶媒（例えば、水、N,N-ジメチルホルムアミド、ジメチルスルホキシド等）に溶解し、塩基（例えば、水酸化ナトリウムや水酸化カリウム等）の存在下にハロゲン化C_{1-4}アルキルカルボン酸またはその塩を添加し、氷冷下ないし100 ℃程度の温度範囲で数分ないし数日間反応させればよい。カルボキシC_{1-4}アルキル基の導入の程度は、例えば、カ

ルボキシC_{1-4}アルキル化の反応温度や試薬として用いるハロゲン化C_{1-4}アルキルカルボン酸及び塩基の量を適宜選択することにより容易に調節可能であり、そのような手段は当業者に周知である。デキストランポリアルコールの水酸基に対するカルボキシC_{1-4}アルキル化の程度は特に限定されないが、例えば、構成糖残基あたり0.01～2.0 の範囲、好ましくは 0.1～1.0 、より好ましくは 0.3～0.5 の範囲である。カルボキシC_{1-4}アルキルデキストランポリアルコールの分子量は、ゲルろ過法で測定した場合に 5,000から 500,000程度、好ましくは50,000～450,000 程度、より好ましくは200,000 ～400,000 程度である。

上記のカルボキシC_{1-4}アルキルデキストランポリアルコールは、薬物送達のキャリアーとして有用である。医薬化合物とカルボキシC_{1-4}アルキルデキストランポリアルコールとを結合させた薬物複合体は、例えば、腫瘍選択性などの優れた選択性を有しており、また高い血中濃度を長時間維持できるという特徴がある。医薬化合物とカルボキシC_{1-4}アルキルデキストランポリアルコールとの結合としては、例えば、エステル結合などで両者を直接結合させる方法、上記に説明したスペーサーなどの適宜のスペーサーを介して両者を結合させる方法などを採用することができる。

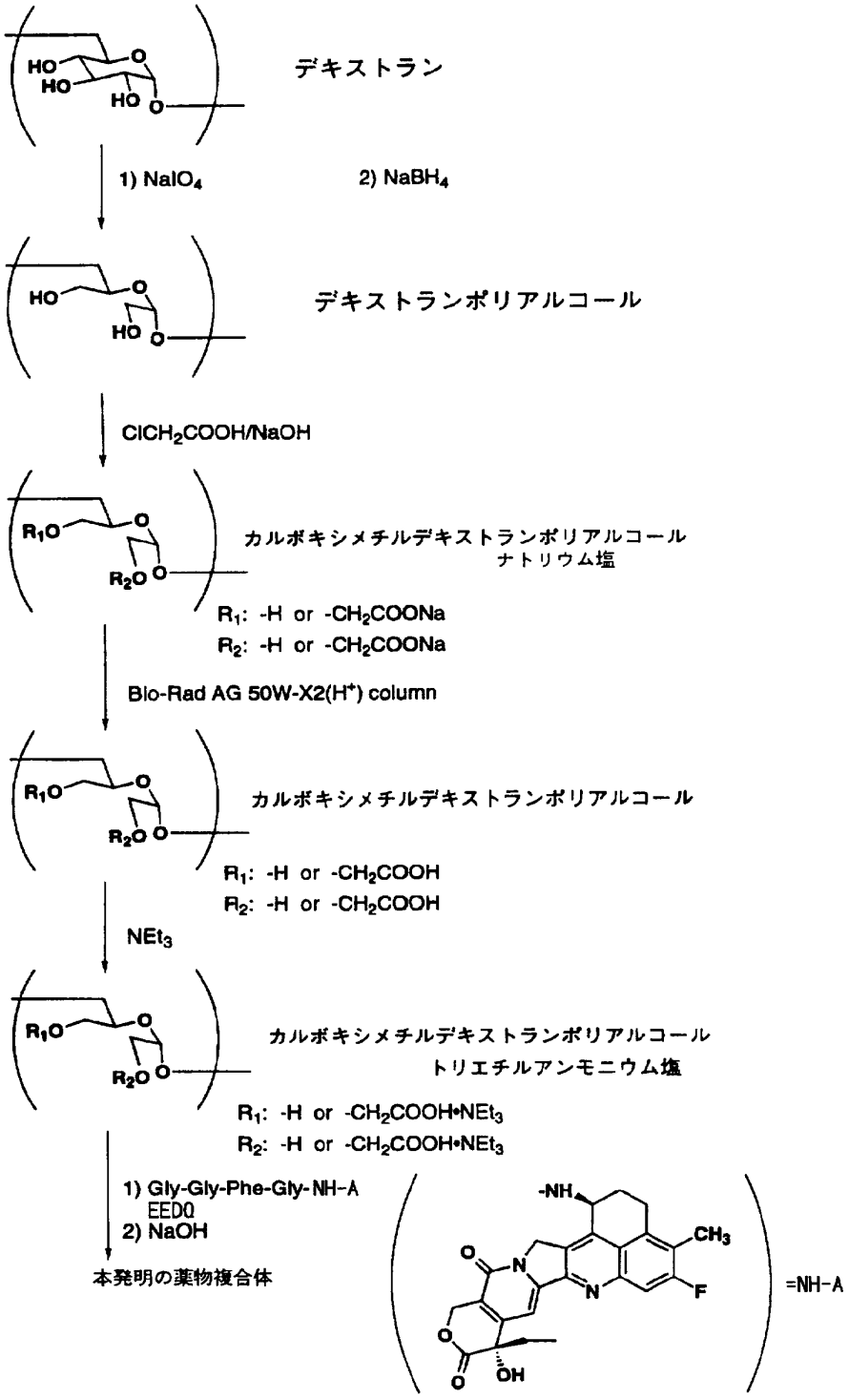
スペーサーを介して結合する薬物複合体に関しては、上記のようにして得られるカルボキシメチルデキストランポリアルコールのカルボキシル基に対して、医薬化合物の残基と結合させたスペーサーを結合することにより本発明の薬物複合体を製造することができる。スペーサーとカルボキシメチルデキストランポリアルコールのカルボキシル基との結合は、一般的には、スペーサーのＮ末端アミノ基とカルボキシメチルデキストランポリアルコールのカルボキシル基とを酸アミド結合により結合させることにより形成できる。もっとも、スペーサーとカルボキシメチルデキストランポリアルコールのカルボキシル基との結合は上記のものに限定されることはなく、他の化学結合や１又は２以上のスペーサーを利用した結合であってもよい。例えば、スペーサーのＣ末端カルボキシル基とカルボキシメチルデキストランポリアルコールのカルボキシル基とにより酸無水物を形成させてもよく、また、エチレンジアミン等のジアミン化合物をスペーサーとして用いてそれぞれのカルボキシル基をジアミンの各アミノ基に酸アミド結合させても

よい。

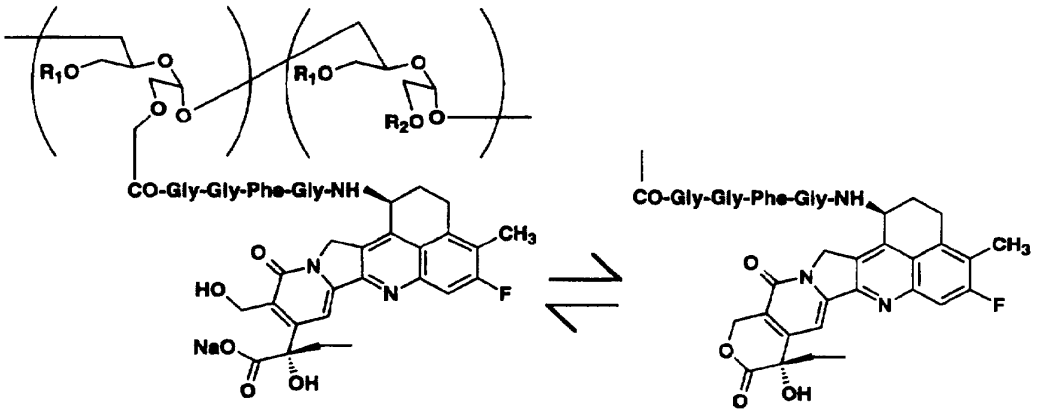
スペーサーのN末端アミノ基とカルボキシメチルデキストランポリアルコールのカルボキシル基とを酸アミド結合により結合させる場合には、ペプチド鎖の合成に用いる通常の脱水縮合剤、例えば、 N,N'-ジシクロヘキシルカルボジイミド(DCC) のような N,N'-ジシクロアルキルカルボジイミド類、1-エチル-3-(3-ジメチルアミノプロピル) カルボジイミド(EDAPC) 等のカルボジイミド誘導体、1-ヒドロキシベンゾトリアゾール(HOBT)のようなベンゾトリアゾール誘導体のほか、1-エトキシカルボニル-2- エトキシ-1,2- ジヒドロキシキノリン(EEDQ)などを用いることができる。また、活性エステル法や酸ハライド法などにより反応を行ってもよい。

カルボキシメチルデキストランポリアルコールに導入する医薬化合物残基の量は特に限定されないが、医薬化合物残基の物理化学的性質、並びに本発明の薬物複合体の体内動態、薬効、及び毒性などの観点から適宜選択すべきである。一般的には、0.1 ～30重量%、好ましくは 1～15重量%、さらに好ましくは 3～10重量%、特に好ましくは 5～6 重量%程度の範囲を選択することができる。カルボキシメチルデキストランポリアルコールに導入された医薬化合物残基の割合は、例えば、吸光度分析などにより容易に決定することが可能である。

本発明の薬物複合体の製造方法の一例として、特開平6-87746 号公報の請求項2に記載された抗腫瘍剤である医薬化合物の残基を導入する場合について、製造方法を以下のスキームに示すが、本発明の薬物複合体及びその製造方法はこのスキームに示されたものに限定されることはない。下記スキームにおいて、医薬化合物残基の導入量は、例えば 1～15重量%、好ましくは 2～10重量%程度である。また、下記スキーム中には、ポリアルコール類の構成単位のうち1個又は2個のカルボキシメチル基が導入された構成単位のみを例示的に記載したが、本発明の薬物複合体の多糖誘導体部分は上記構成単位の繰り返しによって構成されるものではないことを理解すべきである。


デキストラン
1) NaIO4
2) NaBH4
デキストランポリアルコール
ClCH2COOH/NaOH
カルボキシメチルデキストランポリアルコール
ナトリウム塩
R1: -H or -CH2COONa
R2: -H or -CH2COONa
Bio-Rad AG 50W-X2(H+) column
カルボキシメチルデキストランポリアルコール
R1: -H or -CH2COOH
R2: -H or -CH2COOH
NEt3
カルボキシメチルデキストランポリアルコール
トリエチルアンモニウム塩
R1: -H or -CH2COOH•NEt3
R2: -H or -CH2COOH•NEt3
1) Gly-Gly-Phe-Gly-NH-A
EEDQ
2) NaOH
本発明の薬物複合体
=NH-A

本発明の薬物複合体



上記の医薬化合物は、酸性水性媒体中（例えばpH 3程度）ではラクトン環を形成した化合物（閉環体）に平衡が偏り、一方、塩基性水性媒体中（例えばpH 10 程度）ではラクトン環が開環した化合物（開環体）に平衡が偏ることが知られているが、このような閉環体及び開環体に対応する残基を導入した薬物複合体は同等の抗腫瘍効果を有しており、いずれも本発明の範囲に包含されることはいうまでもない。なお、反応系中にラクトン環の開環した反応種が存在すると、ラクトン環に由来するカルボキシル基とスペーサー由来のアミノ基との間で縮合反応が進行して著しく反応収率が低下するだけでなく、目的とする均一な薬物複合体が得られない場合がある。このような副反応は反応種として選択的に閉環体を用いることによって回避することができる。

すなわち、カルボキシメチルデキストランポリアルコールのナトリウム塩をトリエチルアンモニウム塩に変換した後、非水系（水を含まない有機溶媒中）でカルボキシメチルデキストランポリアルコールのカルボキシル基に対して、上記の医薬化合物の残基を結合させたスペーサーのN末端アミノ基を縮合させることにより、副反応を抑制することができ、効率的に目的物を製造することが可能になる。有機溶媒に溶解可能なカルボキシメチルデキストランポリアルコールの塩としては、例えば、トリエチルアンモニウム塩やトリメチルアンモニウム塩などのトリアルキルアンモニウム塩のほか、N-メチルピロリジン、N-メチルモルホリン、ジメチルアミノピリジン（DMAP）などの有機塩基の塩を用いることが可能である。

有機溶媒としては、N,N-ジメチルホルムアミド、ジメチルスルホキシドなどを用いることができる。

本発明の薬物複合体は、医薬化合物の残基の種類（例えば、抗腫瘍剤または抗炎症剤などの医薬化合物の残基）に応じて、所望の医薬活性を腫瘍部位や炎症部位などの局所において特異的に発現させることができ、かつ、医薬化合物自体の有する毒性を低減できるという特徴を有する。いかなる特定の理論に拘泥するわけではないが、本発明の薬物複合体の多糖誘導体部分（例えばカルボキシメチルデキストランポリアルコール）は極めて優れた血中滞留性及び腫瘍・炎症部位への集積性を有するので薬物送達のキャリアーとして有用であり、本発明の薬物複合体は腫瘍選択性及び炎症部位選択性を有している。また、腫瘍部位や炎症部位ではプロテアーゼ（ペプチダーゼ）が発現されていると考えられるので、本発明の薬物複合体のスペーサーは容易に加水分解され、遊離した医薬化合物が薬効を発揮する。

本発明の薬物複合体を含む医薬は、通常、凍結乾燥品などの形態でバイアル等に充填することができ、用時溶解型の注射用または点滴用製剤等の非経口投与用製剤として臨床に提供されるが、本発明の医薬の製剤形態は上記態様に限定されることはない。上記製剤の製造には、例えば、溶解補助剤、pH調節剤、安定化剤など当業界で利用可能な製剤用添加物を用いることができる。本発明の医薬の投与量は特に限定されないが、通常は、医薬化合物残基を構成する医薬化合物の投与量、本発明の薬物複合体中に導入された医薬化合物の残基の量、患者の状態や疾患の種類などを勘案して決定すべきである。例えば、特開平6-87746 号公報の請求項２に記載された抗腫瘍剤の残基が約 6重量% 程度の割合で導入された本発明の薬物複合体を非経口投与する場合には、一般に一日あたり体表面積 1 m^2 につき約1～500 mg程度、好ましくは約10～100 mg の範囲で一回投与し、 3～4 週毎に繰り返すことが好ましい。

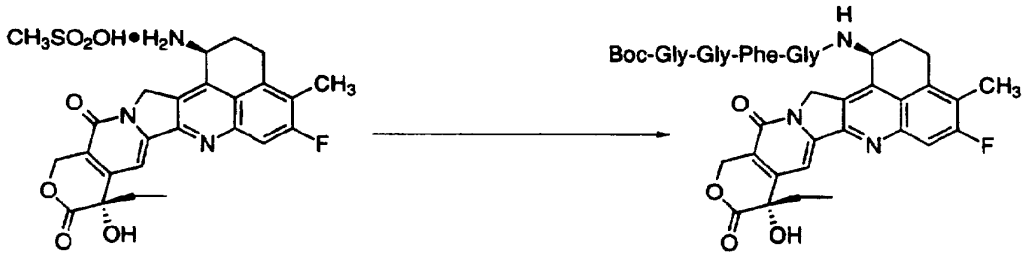
実施例

以下、本発明を実施例によりさらに具体的に説明するが、本発明の範囲は下記の実施例に限定されることはない。実施例中、「A-NH- 」は、特開平6-87746 号公

報の請求項２に記載された医薬化合物（実施例中で「DX-8951 」という場合がある）などのようにラクトン環を有する医薬化合物において、ラクトン環が閉環した医薬化合物を A-NH_2で表した場合の医薬化合物残基を表し、その一例は、上記のスキーム中にA-NH- で示した基（ラクトン環を形成したもの）である。また、A'-NH-は、A-NH- で表される医薬化合物残基中のラクトン環が閉環型若しくは開環型のいずれか又はそれらの混合形態であることを示し、-DXRはドキソルビシン由来の残基を示し、-D51-7059は例55に示されるタキソール誘導体由来の残基を示す。

また、実施例中、特に言及しない場合には、カルボキシメチルデキストランポリアルコールのカルボキシメチル化度（構成糖残基あたりのカルボキシメチル基の置換度）は、カルボキシメチルデキストランポリアルコールのナトリウム塩を遊離酸型に変換した後、 0.1N 水酸化ナトリウム水溶液に溶解して 0.1N 塩酸で滴定することにより求めた。カルボキシメチルデキストランポリアルコールのナトリウム塩の水溶液を Bio-Rad AG50W-x 2(H^+ 型）カラムに付して通過液を凍結乾燥して試料として用いた。この試料を所定過剰量の 0.1N 水酸化ナトリウム水溶液に溶解し、フェノールフタレンを指示薬として 0.1N 塩酸で滴定した。試料の採取量を s(mg)、 0.1N 水酸化ナトリウム水溶液の所定過剰量を a(ml)、 0.1N 塩酸の滴定量を b(ml)とし、カルボキシメチル化度を 13.4(a-b)/[s-5.8(a-b)] の式により求めた。また、薬物の導入量（重量%）は、薬物の特性吸収を利用した吸光度分析（362 nm付近）から求めた。さらに、ゲル濾過法は次の条件に従って行った（カラム：TSK gel G4000 PW_{XL}、溶離液： 0.1M NaCl、流速：0.8 ml/min、カラム温度：40℃）。

例１：3'-N-(Boc-Gly-Gly-Phe-Gly)-NH-A (A-NH_2 =DX-8951)



Boc-Gly-Gly-Phe-Gly (600 mg)および N- ヒドロキシスクシンイミド (160 mg) を N,N- ジメチルホルムアミド (20 ml)に溶解し、4℃に冷却した後、N,N'- ジシクロヘキシルカルボジイミド (280 mg) を添加した。この溶液に特開平6-87746号公報の請求項2に記載された医薬化合物のメタンスルホン酸塩 (600 mg: 上記公報の実施例50に記載された化合物) とトリエチルアミン (0.16 ml)を溶解したN,N-ジメチルホルムアミド (30 ml)溶液を加えて、遮光下に室温で16時間撹拌しながら反応させた。この反応液を減圧乾固し、残渣をシリカゲルカラムクロマトグラフィー (溶出液：0.5%酢酸を含むジクロロメタン：メタノール = 10:1 溶液) で精製して標記化合物 (1.0 g)を得た。

^{1}H-NMR (DMSO-d_6) δ: 8.40 (d, 1H, J=8.3 Hz), 8.10-8.17 (m, 2H), 7.91-8.01 (m, 1H), 7.78 (d, 1H, J=10.75 Hz), 7.32 (s, 1H), 6.94-6.96 (m, 1H), 6.50 (s, 1H), 5.57 (t, 1H, J= 4.5Hz), 5.43 (s, 2H), 5.23 (s, 2H), 3.77 (dd, 2H, J= 5.85Hz, J = 8.80Hz), 3.70 (d, 2H, J= 4.40Hz), 3.65 (d, 2H, J= 5.35Hz), 3.56 (d, 2H, J= 5.85), 3.15-3.25 (m, 2H), 2.40 (s, 3H), 2.05-2.25 (m, 1H), 1.86 (m, 2H), 1.35 (s, 9H), 0.88 (t, 3H, J= 7.35).

Mass (FAB): m/e 854 (M+1)

例2：3'-N-(Boc-Gly-Gly-Gly-Phe)-NH-A (A-NH_2 =DX-8951)の合成

Boc-Gly-Gly-Gly-Phe (600 mg)およびN-ヒドロキシスクシンイミド (160 mg) をN,N-ジメチルホルムアミド (20 ml)に溶解し、4℃に冷却した後、N,N'- ジシクロヘキシルカルボジイミド (280 mg) を添加した。この溶液に DX-8951 のメタンスルホン酸塩 (600 mg) とトリエチルアミン (0.16 ml)を溶解したN,N-ジメチルホルムアミド (30 ml)溶液を加えて、遮光下に室温で16時間撹拌しながら反応させた。この反応液を減圧乾固し、残渣をシリカゲルカラムクロマトグラフィー (溶出液：0.5%酢酸を含むジクロロメタン：メタノール = 10:1 溶液) で精製して標記化合物 (700 mg) を得た。

^{1}H-NMR (DMSO-d_6) δ: 8.57 (d, 1H, J= 7.8Hz), 8.19 (d, 1H), 8.05-8.07 (m, 2H), 7.79 (d, 1H, J= 11.2Hz), 7.32 (s, 1H), 7.10 (d, 2H, J= 7.8Hz), 6.93-7.03 (m, 4H), 6.51 (s, 1H), 5.52-5.55 (m, 1H), 5.44 (s, 2H), 5.18 (d, 1H, J= 18.5Hz), 4.84

(d, 1H, J= 18.5Hz), 4.57-4.59 (m, 1H), 3.57-3.71 (m, 6H), 3.15-3.25 (m, 2H), 3.00-3.02 (m, 1H), 2.80-2.90 (m, 1H), 2.40 (s, 3H), 2.05-2.25 (m, 1H), 1.86 (m, 2H), 1.35 (s, 9H), 0.88 (t, 3H, J= 7.35Hz).

Mass (FAB) ; m/e 854 (M+1)

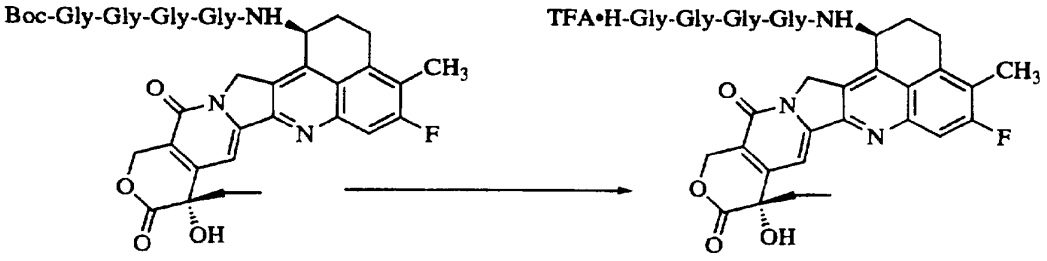
例３ : 3'-N-(Boc-Gly-Gly-Gly-Gly)-NH-A (A-NH_2 =DX-8951)の合成

Boc-Gly-Gly-Gly-Gly (120 mg)およびN-ヒドロキシスクシンイミド (39 mg)をN, N-ジメチルホルムアミド (20 ml)に溶解し、４℃に冷却した後、N, N'- ジシクロヘキシルカルボジイミド (70 mg)を添加した。この溶液に DX-8951 のメタンスルホン酸塩 (150 mg) とトリエチルアミン (0.039 ml) を溶解したN, N-ジメチルホルムアミド (10 ml)溶液を加えて、遮光下に室温で16時間撹拌しながら反応させた。この反応液を減圧乾固し、残渣をシリカゲルカラムクロマトグラフィー (溶出液 : ジクロロメタン : メタノール = 10:1 溶液) で精製して標記化合物 (100 mg) を得た。

^{1}H-NMR (DMSO-d_6) δ : 8.40 (d, 1H, J= 8.3 Hz), 8.10-8.17 (m, 2H), 7.91-8.01 (m, 1H), 7.78 (d, 1H, J= 10.75 Hz), 7.32 (s, 1H), 6.94-6.96 (m, 1H), 6.50 (s, 1H), 5.57 (t, 1H, J= 4.5Hz), 5.43 (s, 2H), 5.23 (s, 2H), 3.77 (dd, 2H, J= 5.85Hz, J = 8.80Hz), 3.70 (d, 2H, J= 4.40Hz), 3.65 (d, 2H, J= 5.35Hz), 3.56 (d, 2H, J= 5.85Hz), 3.15-3.25 (m, 2H), 2.40 (s, 3H), 2.05-2.25 (m, 1H), 1.86 (m, 2H), 1.35 (s, 9H), 0.88 (t, 3H, J= 7.35Hz).

Mass (FAB); m/e 764 (M+1)

例４ : 3'-N-(Gly-Gly-Gly-Gly)-NH-A (A-NH_2 =DX-8951)トリフルオロ酢酸塩の合成



3'-N-(Boc-Gly-Gly-Gly-Gly)-NH-A (A-NH_2 =DX-8951) (79 mg)をトリフルオロ酢

酸（3 ml）に溶かし、1時間放置した。溶媒を留去し、メタノール（30 ml)で共沸を2回、エタノール（30 ml)で共沸を2回行った後、残渣をエーテルで洗浄して、標記化合物（80 mg)を得た。

^{1}H-NMR (DMSO-d_6) δ: 8.59-8.61 (m, 1H), 8.50 (d, 1H, J= 8.3Hz), 8.21-8.27 (m, 2H), 7.91-8.01 (br, 3H), 7.81 (d, 1H, J= 11.2Hz), 7.32 (s, 1H), 6.50-6.52 (br, 1H), 5.57-5.59 (m, 1H), 5.43 (s, 2H), 5.23 (s, 2H), 3.80-3.82 (m, 3H), 3.70-3.75 (m, 3H), 3.15-3.25 (m, 2H), 2.41 (s, 3H), 2.05-2.25 (m, 1H), 1.86-1.88 (m, 2H), 0.88 (t, 3H, J= 7.35Hz).

例5：カルボキシメチルデキストランポリアルコールのトリエチルアンモニウム塩の合成

デキストランT2000(10 g, ファルマシア社製, 平均分子量 2,000,000）を 0.1 M酢酸緩衝液（pH 5.5, 1,000 ml）に溶解し、過ヨウ素酸ナトリウム（33.0 g）の水溶液（1000 ml)を加えた。遮光しながら4℃で10日間撹拌した後、エチレングリコール（7.0 ml）を加え、一晩撹拌した。反応液を氷冷下で 8 M水酸化ナトリウム水溶液を用いてpHを7.5 に調整した。水素化ホウ素ナトリウム（14 g）を加えて溶解した後、室温で一晩撹拌した。反応液を氷冷し、酢酸で pH5.5に調整して4℃で1時間撹拌した後、氷冷下で 8 M水酸化ナトリウム水溶液を用いてpHを7.5 に調整した。得られた水溶液をバイオマックス-30 膜（ミリポア社製）を用いて限外濾過法による低分子画分の除去を行なった。高分子画分を凍結乾燥して、デキストランポリアルコールを得た。このデキストランポリアルコールをpH 3.0で1時間処理した後、バイオマックス-50 膜で低分子画分を除去し、次いで高分子画分をバイオマックス-100膜で除去し、凍結乾燥して精製デキストランポリアルコール（2.0 g)を得た。この物質の分子量（ゲル濾過法、デキストラン標準）は、220 K であった。

この精製デキストランポリアルコール（1.8 g)を、水酸化ナトリウム（10.5 g）を水（45 ml)に溶かして得られる水溶液に加え、室温で溶解させた。この溶液に氷冷下でモノクロル酢酸（15 g）を加えて溶解させた後、室温で20時間反応させた。この反応液を酢酸でpHを8 に調整した後、バイオマックス-10 膜を用いて限外濾過法による低分子画分の除去を行なった。高分子画分を凍結乾燥して、カルボキシ

メチルデキストランポリアルコールのナトリウム塩（1.8 g)を得た。この物質の分子量（ゲル濾過、デキストラン標準）は330 K であり、カルボキシメチル化度は0.8 であった。

上記のカルボキシメチルデキストランポリアルコールのナトリウム塩（300 mg）を水に溶解し、Bio-Rad AG50W-X2（200-400 メッシュ、H^+ 型）カラム（1.5 × 8.6 cm)にのせ、水で溶出した。この溶出液にトリエチルアミン（0.5 ml）を加えた後、凍結乾燥してカルボキシメチルデキストランポリアルコールのトリエチルアンモニウム塩（380 mg）を得た。カルボキシメチルデキストランポリアルコールのナトリウム塩（各 300 mg)を上記と同様にカラム処理して、カルボキシメチルデキストランポリアルコールのトリエチルアンモニウム塩（380 mg, 400 mg）を得た。

例６：カルボキシメチルデキストランポリアルコールのナトリウム塩の合成

上記例５で得たカルボキシメチルデキストランポリアルコールのナトリウム塩（0.15 g）を、水酸化ナトリウム（1.05 g）を水（4.5 ml）に溶かして得られる水溶液に加え、室温で溶解させた。この溶液に氷冷下でモノクロル酢酸（1.5 g）を加えて溶解させた後、室温で18時間反応させた。この反応液を酢酸でpHを8 に調整し、90 ml のメタノール中に滴下した後、3 M 塩化ナトリウム水溶液（0.15 ml）を加えて、析出した沈澱を遠心分離（3500 rpm, ８分）により集めた。この沈澱をメタノールで洗浄した後、水（5 ml）に溶解し、3 M 塩化ナトリウム水溶液（0.15 ml)を加えた。この水溶液をミリポアフィルター（0.45μm)で濾過し、濾液を35 mlのエタノール中に滴下して、析出した沈澱を遠心分離（3500 rpm, ８分）により集めた。この沈澱をエタノールで洗浄した後、水に溶解し、透析膜（スペクトラポア１、カットオフ分子量 6,000-8,000）を用いて、純水に対して透析した。透析内液をミリポアフィルター（0.22μm)で濾過した後に凍結乾燥してカルボキシメチルデキストランポリアルコールのナトリウム塩（0.18 g）を得た。この物質の糖残基あたりのカルボキシメチル化度（アルカリ滴定法）は1.2 であった。

例７：カルボキシメチルデキストランポリアルコールのナトリウム塩の合成

例５で得た精製デキストランポリアルコール（0.2 g)を、水酸化ナトリウム（0.84 g）を水（6 ml）に溶かして得られる水溶液に加え、室温で溶解させた。この溶

液に氷冷下でモノクロル酢酸（1.2 g)を加えて溶解させた後、室温で18時間反応させた。この反応液を酢酸でpHを8 に調整し、120 mlのメタノール中に滴下した後、3 M 塩化ナトリウム水溶液（0.2 ml）を加えて、析出した沈澱を遠心分離（3500 rpm, 8分）により集めた。この沈澱をメタノールで洗浄した後、水（5 ml）に溶解し、3 M 塩化ナトリウム水溶液（0.2 ml）を加えた。この水溶液をミリポアフィルター（0.45μm)で濾過し、濾液を 35 mlのエタノール中に滴下して、析出した沈澱を遠心分離（3500 rpm, 8分）により集めた。この沈澱をエタノールで洗浄した後、水に溶解し、透析膜（スペクトラポア１、カットオフ分子量 6,000-8,000）を用いて、純水に対して透析した。透析内液をミリポアフィルター（0.22μm)で濾過した後、凍結乾燥してカルボキシメチルデキストランポリアルコールのナトリウム塩（0.20 g）を得た。この物質の糖残基あたりのカルボキシメチル化度（アルカリ滴定法）は0.4 であった。

例８：カルボキシメチルデキストランポリアルコール-Gly-Gly-Gly-Phe-NH-A'(A-NH_2 =DX-8951)の合成

例５で得たカルボキシメチルデキストランポリアルコールのトリエチルアンモニウム塩（380 mg, カルボキシメチル化度 0.8）をN,N-ジメチルホルムアミド（30 ml)に溶解した。この溶液に、3'-N-(Gly-Gly-Gly-Phe)-NH-A (A-NH_2 =DX-8951)のトリフルオロ酢酸塩（49 mg)のN,N-ジメチルホルムアミド（5 ml）溶液、トリエチルアミン（0.017 ml）、1-エトキシカルボニル -2-エトキシ -1,2-ジヒドロキシキノリン（380 mg）を順次加え、室温で一晩撹拌しながら反応させた。この反応液を1 M 水酸化ナトリウム水溶液で pH 10に調整した後、 25 mlのエタノール中に 5 ml ずつ滴下した。この混合物に3 M 塩化ナトリウム水溶液（1 ml）、ジエチルエーテル（5 ml）を加えて、析出した沈澱を遠心分離（3500 rpm, 8分）により集めた。

この沈澱を水に溶解し、透析膜（スペクトルポア１、カットオフ分子量 6,000-8,000）を用いて純水に対して透析し、透析内液をミリポアフィルター（0.22μm)で濾過した後、凍結乾燥した。得られた粗生成物を水（30 ml)に溶解し、0.1 M 水酸化ナトリウム水溶液でpH 9に調整し、37℃で１時間処理した。この処理液を上記と同様に透析した後、透析内液をミリポアフィルター（0.22μm)で濾過し、凍結

乾燥して標記化合物を 289 mg 得た。本化合物を 0.1 M塩化ナトリウム水溶液に溶解後、GPC （カラム：東ソー株式会社製 TSK Gel PW-4000XL、溶媒：0.1 M NaCl、流速：0.8 ml/min）で分析した結果、及び本化合物の紫外線吸収スペクトル（0.1 M トリス緩衝液, pH 9.0, 0.25 mg/ml）をそれぞれ図１及び図２に示す。本化合物の医薬化合物残基の含量を0.1 M トリス緩衝液（pH 9.0）中での 362 nm における吸光度に基づいて定量したところ 5.3%（W/W）であった。

例９：カルボキシメチルデキストランポリアルコール-Gly-Gly-Phe-Gly-NH-A'(A-NH_2 =DX-8951)合成

3'-N-(Boc-Gly-Gly-Phe-Gly)-NH-A (A-NH_2 =DX-8951)（50 mg)から例４と同様の方法により脱 Boc化して得られる 3'-N-(Gly-Gly-Phe-Gly)-NH-Aのトリフルオロ酢酸塩を、例８と同様の方法に従って、例５で得たカルボキシメチルデキストランポリアルコールのトリエチルアンモニウム塩（380 mg）に導入して標記化合物（300 mg）を合成した。本化合物を 0.1 M塩化ナトリウム水溶液に溶解後、GPC （カラム：東ソー株式会社製 TSK Gel PW-4000XL、溶媒：0.1 M NaCl、流速：0.8 ml/min）で分析した結果、及び本化合物の紫外線吸収スペクトル（0.1 M トリス緩衝液, pH 9.0, 0.19 mg/ml）をそれぞれ図３及び図４に示す。本化合物の医薬化合物残基の含量を0.1 M トリス緩衝液（pH 9.0）中での 362 nm における吸光度に基づいて定量したところ 5.3%（W/W）であった。

例10：カルボキシメチルデキストランポリアルコール-Gly-Gly-Gly-Gly-NH-A'(A-NH_2 =DX-8951)の合成

3'-N-(Boc-Gly-Gly-Gly-Gly)-NH-A (A-NH_2 =DX-8951)（41 mg)から例４と同様の方法により脱 Boc化して得られる 3'-N-(Gly-Gly-Gly-Gly)-NH-Aのトリフルオロ酢酸塩を、例８と同様の方法に従って、例５で得たカルボキシメチルデキストランポリアルコールのトリエチルアンモニウム塩（380 mg）に導入して標記化合物（190 mg）を合成した。本化合物の紫外線吸収スペクトル（0.1 M トリス緩衝液, pH 9.0, 0.34 mg/ml）を図５に示す。本化合物の医薬化合物残基の含量を0.1 M トリス緩衝液（pH 9.0）中での 362 nm における吸光度に基づいて定量したところ 5.3%（W/W）であった。

例11：本発明の薬物複合体の抗腫瘍作用

マウス線維肉腫 Meth A 細胞 1×10^6 個を BALB/c 系の雄マウス（7 週齢）の右鼠蹊部皮下に移植して Meth A 担癌マウスを作成した（1群7匹）。7 日目に注射用蒸留水に溶解した例9の薬物複合体を Meth A 担癌マウスの尾静脈内に4日毎に4回投与した。移植後21日目に腫瘍を摘出して重量を測定し、腫瘍増殖抑制率を次式：腫瘍増殖抑制率(%) =[1-(検体投与群の平均腫瘍重量／コントロール群の平均腫瘍重量)]×100 により算出した。その結果、例9で得られた本発明の薬物複合体は、毒性（体重減少）を発現することなく、上記医薬化合物自体（スペーサー及び多糖誘導体なし）に比較して抗腫瘍効果が大幅に増強されていた。多糖誘導体自体（例5）及びスペーサーのみを導入した医薬化合物残基（例1の化合物から例4の方法に従って脱BOC 化して得られたる H_2N-Gly-Gly-Phe-Gly-NH-A（A-NH_2 =DX-8951） のトリフルオロ酢酸塩）は無効であった。

表2

被検化合物	投与量(mg/kg)	抑制率(%)
医薬化合物自体	7.5 × 4	76
	1.875 × 4	46
	0.9375× 4	36
例9の化合物	1.4[1)] × 4	94
	0.7[1)] × 4	59
	0.35[1)]× 4	41

1)医薬化合物換算量

例12：本発明の薬物複合体の抗腫瘍作用

例11と同様の方法によりMeth A担癌マウスを作成し（1群6匹）、7 日目に例8及び例9の薬物複合体を単回投与した場合の抗腫瘍作用を比較した。その結果、抗腫瘍作用の程度は（多糖誘導体)-Gly-Gly-Phe-Gly-NH-A' ＞（多糖誘導体)-Gly-Gly-Gly-Phe-NH-A' ＞医薬化合物自体であった。スペーサーを介することなく医

薬化合物残基を例５のカルボキシメチルデキストランポリアルコールのカルボキシル基に直接結合した化合物（医薬化合物残基の導入量： 6.2重量% ）は無効であった。

表３

被検化合物	投与量(mg/kg)	抑制率(%)
医薬化合物自体	60	77
	20	59
例８の化合物	10[1)]	85
	5[1)]	76
例９の化合物	5[1)]	98
	2.5[1)]	87

[1)]医薬化合物換算量

例13：カルボキシメチルデキストランポリアルコールのトリエチルアンモニウム塩の合成

デキストランT500（10 g，ファルマシア社製，分子量 500K ）を0.1 M 酢酸緩衝液（pH5.5，1000 ml）に溶解し、過ヨウ素酸ナトリウム（33 g）の水溶液（1000 ml)を加えた。遮光しながら４℃で10日間撹拌した後、エチレングリコール（7.0 ml）を加え、一晩撹拌した。反応液を8 M 水酸化ナトリウム水溶液を用いてpHを 7.5に調整した。水素化ホウ素ナトリウム（14 g）を加えて溶解した後、一晩撹拌した。反応液を氷冷し、酢酸でpH 5.5に調整して４℃で１時間撹拌した後、8 M 水酸化ナトリウム水溶液でpH 7.5に調整して溶液１を得た。別に、デキストランT500（10 g，ファルマシア社製，分子量500K）について、上記の一連の操作を行い、溶液２を得た。さらに、デキストランT250（各10 g，ファルマシア社製，分子量250K ）について、上記の一連の操作を行い、溶液３と溶液４を得た。これらの溶液１～４を合して、バイオマックス-50 膜を用いて限外濾過法により、低分子画分

の除去を行った。高分子画分を凍結乾燥して、デキストランポリアルコール（25 g）を得た。この物質の分子量（ゲル濾過、プルラン標準）は、163Kであった。

このデキストランポリアルコール（11 g）を、水酸化ナトリウム（46.2 g）を水（330 ml）に溶かして得られる水溶液に加え、室温で溶解させた。この溶液に氷冷下でモノクロル酢酸（66 g）を加えて溶解させた後、室温で一晩反応させた。この反応液を酢酸でpHを９に調整した後、バイオマックス-30 膜を用いた限外濾過法により脱塩した。膜を通過しない残留溶液を凍結乾燥してカルボキシメチルデキストランポリアルコールのナトリウム塩（13 g）を得た。この物質の分子量（ゲル濾過、プルラン標準）は 228K であり、カルボキシメチル化度は 0.4であった。

このカルボキシメチルデキストランポリアルコールのナトリウム塩（600 mg）を水に溶解し、Bio-Rad AG 50W-X2 （200-400 メッシュ、H^+ 型）カラム（直径44mm、長さ210mm)にのせ、水で溶出した。この溶出液にトリエチルアミン（0.93 ml)を加えた後、凍結乾燥して標記化合物（690 mg）を得た。

例14：3'-N-(Gly-Gly-Phe-Gly)-NH-A (A-NH_2 =DX-8951)トリフルオロ酢酸塩の合成

例１で得た3'-N-(Boc-Gly-Gly-Phe-Gly)-NH-A (A-NH_2 =DX-8951)（79 mg)をトリフルオロ酢酸（3 ml）に溶かし、１時間放置した。溶媒を留去し、メタノール(30 ml)で共沸を２回、エタノール（30 ml)で共沸を２回行った後、残渣をエーテルで洗浄して、標記化合物（80 mg)を得た。

^{1}H-NMR (DMSO-d_6) δ: 8.53 (d, 1H, J= 8.3Hz), 8.40-8.48 (m, 2H), 8.28 (d, 1H, J= 8.3Hz), 7.95-8.07 (br, 3H), 7.81 (d, 1H, J= 10.2Hz), 7.30-7.37 (m, 2H), 7.15-7.30 (m, 5H), 6.50-6.55 (br, 1H), 5.50-5.57 (m, 1H), 5.41 (d, 2H, J= 7.82Hz), 5.25 (s, 2H), 4.55-4.62 (m, 1H), 3.55-3.92 (m, 6H), 3.15-3.25 (br, 2H), 2.98-3.03 (m, 1H), 2.73-2.82 (m, 1H), 2.40 (s, 3H), 2.05-2.25 (m, 1H), 1.84-1.92 (m, 2H), 0.88 (t, 3H, J= 7.35Hz).

例15：カルボキシメチルデキストランポリアルコール-Gly-Gly-Phe-Gly-NH-A'(A-NH_2 =DX-8951)の合成

例13で得たカルボキシメチルデキストランポリアルコールのナトリウム塩（400 mg）をトリエチルアンモニウム塩（470 mg）に変換し、N,N-ジメチルホルムアミド(30 ml）に溶解させた。この溶液に、例14で得た3'-N-(Gly-Gly-Phe-Gly)-NH-

A (A-NH_2 =DX-8951) のトリフルオロ酢酸塩 (62 mg)のN,N-ジメチルホルムアミド (5 ml) 溶液、トリエチルアミン(0.02 ml) 、1-エトキシカルボニル-2- エトキシ-1,2- ジヒドロキシキノリン (470 mg) を順次加え、遮光して室温で一晩撹拌しながら反応させた。この反応液の5 mlずつを各10 ml のエタノール中に滴下した。これに3 M 塩化ナトリウム水溶液 (2.5 ml) 、ジエチルエーテル (20 ml)を加えて、析出した沈澱を遠心分離により集めた。この沈澱を0.5 M 塩化ナトリウム水溶液に溶解し、氷冷下0.1 M 水酸化ナトリウム水溶液でpH 9に調整した後、透析膜 (スペクトルポア1、カットオフ分子量 6000-8000) を用いて、純水に対して透析した。透析内液をミリポアフィルター (0.22μm)で濾過した後、凍結乾燥して標記化合物 (600 mg) を得た。本化合物を0.1 M 塩化ナトリウム水溶液に溶解後、 GPC (カラム：東ソー TSK Gel PW-4000XL、溶媒： 0.1 M NaCl 、流速： 0.8 ml/min)で分析した結果、及び本化合物の紫外線吸収スペクトル (0.1 M トリス緩衝液、pH 9.0、0.1 mg/ml) をそれぞれ図6及び図7に示す。本化合物の医薬化合物残基の含量を0.1 M トリス緩衝液 (pH 9.0) 中での 362 nm における吸光度に基づいて定量したところ 5.8% (W/W) であった。

例16：3'-N-(Gly-Gly-Gly-Phe)-NH-A (A-NH_2 =DX-8951)トリフルオロ酢酸塩の合成

例2で得た3'-N-(Boc-Gly-Gly-Gly-Phe)-NH-A (A-NH_2 =DX-8951) (79 mg)をトリフルオロ酢酸 (3 ml) に溶かし、1時間放置した。溶媒を留去し、メタノール(30 ml) で共沸を2回、エタノール(30 ml) で共沸を2回行った後、残渣をエーテルで洗浄して、標記化合物(80 mg) を得た。

^{1}H-NMR (DMSO-d_6) δ： 8.62-8.66 (m,2H), 8.23 (d,1H,J= 8.3Hz), 8.18-8.20 (m,1H), 7.98-8.10 (br,2H), 7.79 (d,1H,J= 10.7Hz), 7.32 (s,1H), 7.09 (d,2H,J= 7.3Hz), 6.93-7.03 (m,4H), 6.50-6.60 (br,1H), 5.52-5.55 (m,1H), 5.44(s,2H), 5.18 (d,1H,J= 18.5Hz), 4.80 (d,1H,J= 18.5Hz), 4.57-4.59 (m,1H), 3.57-3.71 (m,6H), 3.15-3.25 (m,2H), 3.00-3.02 (m,1H), 2.80-2.90 (m,1H), 2.50 (s,3H), 2.05-2.25 (m,1H), 1.86-2.00 (m,2H), 0.88 (t,3H,J= 7.35Hz).

例17：カルボキシメチルデキストランポリアルコール-Gly-Gly-Gly-Phe-NH-A'(A-NH_2 =DX-8951)の合成

例13で得たカルボキシメチルデキストランポリアルコールのナトリウム塩 (1.

0 g)をトリエチルアンモニウム塩(1.2 g) に変換し、N,N-ジメチルホルムアミド(90 ml) に溶解させた。この溶液に、例16で得た3'-N-(Gly-Gly-Gly-Phe)-NH-A (A-NH_2 =DX-8951) のトリフルオロ酢酸塩 (158 mg) のN,N-ジメチルホルムアミド(15 ml) 溶液、トリエチルアミン(0.05 ml) 、1-エトキシカルボニル-2- エトキシ-1,2- ジヒドロキシキノリン(1.2 g) を順次加え、遮光して室温で一晩撹拌しながら反応させた。この反応液の5 mlずつを各10 ml のエタノール中に滴下した。これに3 M 塩化ナトリウム水溶液 (2.5 ml) 、ジエチルエーテル(20 ml) を加えて、析出した沈澱を遠心分離により集めた。この沈澱を0.5 M 塩化ナトリウム水溶液に溶解し、氷冷下0.1 M 水酸化ナトリウム水溶液で pH 9 に調整した後、透析膜 (スペクトルポア１、カットオフ分子量 6000-8000) を用いて、純水に対して透析した。透析内液をミリポアフィルター (0.22μm)で濾過した後、凍結乾燥して標記化合物 (1.4 g) を得た。本化合物の医薬化合物残基の含量を0.1 M トリス緩衝液 (pH 9.0) 中での 362 nm における吸光度に基づいて定量したところ 5.2% (W/W) であった。

例18：Boc-Gly-Phe-Leu-OHの合成

H-Gly-Phe-Leu-OH (3.0 g)を 50%ジオキサン水溶液(48 ml) に加えて氷冷した。この溶液に1 N 水酸化ナトリウム水溶液(9.45 ml) と $(Boc)_2O$ (2.27 g) を含むジオキサン(24 ml) 溶液を加え、１晩撹拌した。反応液に1 N 塩酸(9.45 ml) を加え、溶媒を溜去した。得られた残渣をシリカゲルカラムクロマトグラフィー (溶出液：ジクロロメタン：メタノール＝５：１溶液) で精製して標記化合物(2.5 g) を得た。

例19：Boc-Gly-Phe-Leu-Gly-OBzlの合成

例18で得たBoc-Gly-Phe-Leu-OH (2.4 g)およびN-ヒドロキシスクシンイミド (656 mg) をN,N-ジメチルホルムアミド(50 ml) に溶解し、４℃に冷却した後、N,N'-ジシクロヘキシルカルボジイミド (1.17 g) を添加し、２時間撹拌した。この溶液に H-Gly-OBzl のトシル酸塩(1.9 g) とトリエチルアミン(0.79 ml) を溶解したN,N-ジメチルホルムアミド(40 ml) 溶液を加えて、室温で16時間撹拌しながら反応させた。この反応液を減圧乾固し、残渣をシリカゲルカラムクロマトグラフィー (溶出液：ジクロロメタン：メタノール＝50：１溶液) で精製して標記化合物(2.0 g) を得た。

^{1}H-NMR(DNSO-d_6) δ : 8.20-8.30 (m,1H), 8.12 (d,1H,J= 8.3Hz), 7.83 (d,1H, J= 8.3Hz), 7.32-7.37 (m,5H), 6.89-6.95 (m,1H), 5.12 (s,1H), 4.52-4.59 (br, 1H), 4.34 (dd,1H,J= 7.3Hz, J= 15.1Hz), 3.93 (dd,1H,J= 5.5Hz, J= 17.2Hz), 3 .84 (dd,1H,J= 5.5Hz, J= 17.2Hz), 3.54 (dd,1H,J= 5.9Hz, J= 16.7Hz), 3. 42 (dd,J= 5.9Hz, J= 16.7Hz), 3.00 (dd,1H,J= 4.4Hz, 13.7Hz), 2.78 (dd,1H, J= 8.8Hz, J= 13.2Hz), 1.50-1.65 (m,1H), 1.45 (t,2H,J= 7.3Hz), 1.36 (s,9H), 0.86 (d,3H,J= 6.4Hz), 0.82 (d,3H,J= 6.4Hz).

例20：Boc-Gly-Phe-Leu-Gly-OHの合成

例19で得たBoc-Gly-Phe-Leu-OBzl(1.7 g) を酢酸エチル(30 ml) とメタノール (30 ml) の混合溶液に溶解させた後、5 % Pd-C (1.5 g)を加え、接触還元を行った。反応液を濾過し、濾液を減圧乾固して、標記化合物 (1.15 g) を得た。

例21：3'-N-(Boc-Gly-Phe-Leu-Gly)-NH-A (A-NH_2 =DX-8951)の合成

例20で得たBoc-Gly-Phe-Leu-Gly-OH (200 mg) およびN-ヒドロキシスクシンイミド(58 mg) をN,N-ジメチルホルムアミド (5 ml) に溶解し、4℃に冷却した後、N,N'- ジシクロヘキシルカルボジイミド (104 mg) を加えて溶解させた。この溶液に DX-8951 のメタンスルホン酸塩 (224 mg) とトリエチルアミン (0.059 ml) を溶解したN,N-ジメチルホルムアミド (5 ml) 溶液を加えて、遮光下に室温で16時間撹拌しながら反応させた。この反応液を減圧乾固し、残渣をシリカゲルカラムクロマトグラフィー (溶出液：0.5 % 酢酸を含むジクロロメタン：メタノール＝10：1 溶液) で精製して標記化合物 (200 mg) を得た。

^{1}H-NMR (DMSO-d_6) δ : 8.35 (d,1H,J=7.8Hz), 8.08-8.18 (m,2H), 7.75-7.85 (m, 2H), 7.32 (s,1H), 7.10 (d,2H,J=6.8Hz), 7.08-7.13 (m, 3H), 6.85-6.95 (br, 1H), 6.40-6.65 (br,1H), 5.52-5.55 (m,1H), 5.46 (d,1H,J=18.5Hz), 5.37(d,1H, J=18.5Hz), 5.24 (s,2H), 4.44-4.52 (m,1H), 4.15-4.25 (m,1H), 3.68-3.72 (m, 2H), 3.40-3.52 (m,2H), 3.15-3.25 (br,2H), 2.85-2.95 (m,1H), 2.65-2.75 (m, 1H), 2.40 (s,3H), 2.05-2.25 (m,1H), 1.80-1.91 (m,2H), 1.50-1.65 (m,1H), 1.45 (t,2H,J=7.3Hz), 1.35 (s,9H), 0.88 (t,3H,J=7.4), 0.86 (d,3H,J=6.4Hz), 0.82 (d,3H,J=6.4Hz).

例22：3'-N-(Gly-Phe-Leu-Gly)-NH-A (A-NH_2 =DX-8951)トリフルオロ酢酸塩の合成

例21で得た3'-N-(Boc-Gly-Phe-Leu-Gly)-NH-A (A-NH_2 =DX-8951) (97 mg)をトリフルオロ酢酸 (3 ml) に溶かし、1時間放置した。溶媒を留去し、メタノール(30 ml) で共沸を2回、エタノール(30 ml) で共沸を2回行った後、残渣をエーテルで洗浄して、標記化合物(95 mg) を得た。

^{1}H-NMR (DMSO-d_6) δ : 8.57 (d, 1H, J=8.3Hz), 8.47 (d, 1H, J=8.3Hz), 8.32 (d, 1H, J=7.8Hz), 8.17 (t, 1H, J=5.5Hz), 7.81-7.91 (br, 3H), 7.79 (d, 1H, J=10.7Hz), 7.32 (s, 1H), 7.21-7.23 (m, 5H), 7.12-7.17 (m, 1H), 6.45-6.55 (br, 1H), 5.57 (q, 1H, J=4.4Hz), 5.43 (d, 1H, J=16.1Hz), 5.34 (d, 1H, J=16.1Hz), 5.23 (s, 2H), 4.67 (dt, 1H, J=4.0Hz, J=9.0Hz), 4.31 (dd, 1H, J=8.5Hz, J=15.0Hz), 4.0-4.4 (br, 1H), 3.74-3.76 (m, 2H), 3.56 (dd, 1H, J=6.0Hz, J=16.0Hz), 3.41 (dd, 1H, J=6.0Hz, J=16.0Hz), 3.17-3.19 (br, 2H), 3.02 (dd, 1H, J=4.0Hz, J=14.0Hz), 2.70 (dd, 1H, J=10.0Hz, J=14.0Hz), 2.40 (s, 3H), 2.05-2.15 (m, 1H), 1.85 (dt, 2H, J=7.0Hz, J=14.0Hz), 1.50-1.55 (m, 1H), 1.45 (t, 2H, J=6.0Hz), 1.35 (s, 9H), 0.88 (t, 3H, J=7.4), 0.85 (d, 3H, J=6.4Hz), 0.80 (d, 3H, J=6.4Hz).

例23：カルボキシメチルデキストランポリアルコール-Gly-Phe-Leu-Gly-NH-A'(A-NH_2 =DX-8951)の合成

例13で得たカルボキシメチルデキストランポリアルコールのトリエチルアンモニウム塩 (690 mg) をN,N-ジメチルホルムアミド(50 ml) に溶解させた。この溶液に、例22で得た3'-N-(Gly-Phe-Leu-Gly)-NH-A (A-NH_2 =DX-8951) のトリフルオロ酢酸塩 (95 mg)のN,N-ジメチルホルムアミド(10 ml) 溶液、トリエチルアミン(0.03 ml) 、1-エトキシカルボニル-2- エトキシ-1,2- ジヒドロキシキノリン (690 mg) を順次加え、室温で一晩撹拌しながら反応させた。この反応液の5 mlずつを各10 ml のエタノール中に滴下した。これに3 M 塩化ナトリウム水溶液 (2.5 ml) 、ジエチルエーテル(20 ml) を加えて、析出した沈澱を遠心分離により集めた。この沈澱を0.5 M 食塩水に溶解し、氷冷下0.1 M 水酸化ナトリウム水溶液で pH 9 に調整した後、透析膜 (スペクトルポア1、カットオフ分子量 6000-8000) を用いて、純水に対して透析した。透析内液をミリポアフィルター (0.22μm)で濾過した後、濾液を凍結乾燥して標記化合物 (600 mg) を得た。本化合物の医薬化合物残基の含量を0.1 M トリス緩衝液 (pH 9.0) 中での 362 nm における吸光度に基づい

て定量したところ、 4.8% (W/W) であった。

例24：カルボキシメチルデキストランポリアルコールのトリエチルアンモニウム塩の合成

デキストランT500 (50 g, ファルマシア社製, 分子量 500K) を0.1 M 酢酸緩衝液 (pH5.5, 5000 ml) に溶解し、過ヨウ素酸ナトリウム(165.0 g) の水溶液(5000 ml) を加えた。遮光しながら4 ℃で10日間撹拌した後、エチレングリコール(35.0 ml) を加え、一晩撹拌した。反応液を8 M 水酸化ナトリウム水溶液を用いて pH 7.5 に調整した。水素化ホウ素ナトリウム (70 g) を加えて溶解した後、一晩撹拌した。反応液を氷冷し、酢酸で pH 5.5 に調整して4 ℃で1時間撹拌した後、8 M 水酸化ナトリウム水溶液を用いて pH 7.5 に調整した。得られた水溶液をバイオマックス-50 膜を用いて限外濾過法による低分子画分の除去を行なった。高分子画分を凍結乾燥して、デキストランポリアルコール (27.1 g) を得た。この物質の分子量 (ゲル濾過、プルラン標準) は、140Kであった。

このデキストランポリアルコール(5 g) を、水酸化ナトリウム (21 g) を水 (150 ml) に溶かして得られる水溶液に加え、室温で溶解させた。この溶液に氷冷下でモノクロル酢酸 (30 g) を加えて溶解させた後、室温で一晩反応させた。この反応液を酢酸でpHを8に調整した後、バイオマックス-50 膜を用いた限外濾過法により脱塩した。膜を通過しない残留溶液を凍結乾燥してカルボキシメチルデキストランポリアルコールのナトリウム塩(5.6 g) を得た。この物質の分子量 (ゲル濾過、プルラン標準) は 263K であり、カルボキシメチル化度は0.4 であった。

このカルボキシメチルデキストランポリアルコールのナトリウム塩(2.0 g) を水に溶解し、Bio -Rad AG 50W-X2 (200-400 メッシュ、 H^+ 型) カラム (直径 44 mm、長さ 210 mm)にのせ、水で溶出した。この溶出液にトリエチルアミン (4 ml) を加えた後、凍結乾燥して標記化合物(2.2 g) を得た。

例25：カルボキシメチルデキストランポリアルコールのトリメチルアンモニウム塩の合成

例24で得たカルボキシメチルデキストランポリアルコールのナトリウム塩(1.0 g) を水に溶解し、Bio-Rad AG 50W-X2 (200-400 メッシュ、$Me_3N\ H^+$ 型) カラムにのせ、水で溶出した。この溶出液を凍結乾燥して標記化合物 (950 mg) を得た。

例26：3'-N-(Gly-Gly-Phe-Gly)-NH-A (A-NH_2 =DX-8951)塩酸塩の合成

例14と同様の方法で3'-N-(Boc-Gly-Gly-Phe-Gly)-NH-A (A-NH_2 =DX-8951) (400 mg) から得た3'-N-(Gly-Gly-Phe-Gly)-NH-A トリフルオロ酢酸塩を水-MeOH (1:4) に溶解して、Bio-Rad AG 1-X8 (200-400 メッシュ、Cl^- 型) カラム (1.5 cm × 8.6 cm) にのせ、上記溶媒で溶出した。この溶出液を濃縮した後、凍結乾燥して標記化合物 (310 mg) を得た。

^{1}H-NMR (DMSO-d_6) δ : 8.53 (d, 1H, J=8.5Hz), 8.46-8.48 (m, 1H), 8.37-8.39 (m , 1H), 7.95 (d, 1H, J=8.0Hz), 7.80 (s, 3H), 7.78 (d, 1H, J=11.1Hz), 7.34 (s, 1H), 7.14-7.24 (m, 5H), 6.50(s, 1H), 5.56-5.60 (m, 1H), 5.35-5.40 (m, 2H), 5.24 (s, 2H), 4.51-4.56 (m, 1H), 3.86 (dd, J=4.8, 13.5Hz, 1H), 3.68-3.79 (m, 3H), 3.54 (s, 2H), 3.15-3.22 (m, 2H), 3.01 (dd, J=5.6, 13.5Hz, 1H), 2.78 (dd, J=9.6, 3.5Hz, 1H), 2.41 (s, 3H), 2.12-2.23 (m, 2H), 1.81-1.89 (m, 2H), 0.88 (t, 3H, J=7.2Hz).

Mass (FAB); m/e 753 (M+1)

例27：カルボキシメチルデキストランポリアルコール-Gly-Gly-Phe-Gly-NH-A'(A-NH_2 =DX-8951)の合成

例25で得たカルボキシメチルデキストランポリアルコールのトリメチルアンモニウム塩(0.1 g) をN,N-ジメチルホルムアミド (6 ml) に溶解させた。この溶液に、例26で得た 3'-N-(Gly-Gly-Phe-Gly)NH-A (A-NH_2 =DX-8951) の塩酸塩 (24 mg) のN,N-ジメチルホルムアミド(10 ml) 溶液、トリエチルアミン(5μl)、1-エトキシカルボニル-2- エトキシ-1,2- ジヒドロキシキノリン(0.1 g) を順次加え、室温で一晩撹拌しながら反応させた。この反応液の5 mlずつを各10 ml のエタノール中に滴下した。これに3 M 塩化ナトリウム水溶液 (2.5 ml) 、ジエチルエーテル(20 ml) を加えて、析出した沈澱を遠心分離 (3500 rpm, 8分) により集めた。この沈澱を0.5 M 食塩水に溶解し、氷冷下0.1 M 水酸化ナトリウム水溶液で pH 9 とした。得られた水溶液をバイオマックス-30 膜を用いた限外濾過法により脱塩した。膜を通過しない残留溶液をミリポアフィルター(0.22 μm)で濾過した後、凍結乾燥して標記化合物(90 mg) を得た。本化合物の医薬化合物残基の含量を0.1 M トリス緩衝液 (pH 9.0) 中での 362 nm における吸光度に基づいて定量したところ 11% (W/

W)であった。

例28：カルボキシメチルデキストランポリアルコール-Gly-Gly-Phe-Gly-NH-A'(A-NH_2 =DX-8951)の合成

例25で得たカルボキシメチルデキストランポリアルコールのトリメチルアンモニウム塩(0.1 g)をN,N-ジメチルホルムアミド（6 ml）に溶解させた。この溶液に、例26で得た3'-N-(Gly-Gly-Phe-Gly)-NH-A（A-NH_2 =DX-8951） の塩酸塩（36 mg）のN,N-ジメチルホルムアミド(10 ml）溶液、トリエチルアミン(8μl)、1-エトキシカルボニル-2- エトキシ-1,2- ジヒドロキシキノリン(0.1 g）を順次加え、室温で一晩撹拌しながら反応させた。この反応液の5 mlずつを各10 ml のエタノール中に滴下した。これに3M塩化ナトリウム水溶液（2.5 ml）、ジエチルエーテル(20 ml）を加えて、析出した沈澱を遠心分離（3500 rpm, 8分）により集めた。この沈澱を0.5 M 食塩水に溶解し、氷冷下0.1 M 水酸化ナトリウム水溶液で pH 12とした。得られた水溶液をバイオマックス-30 膜を用いた限外濾過法により脱塩した。膜を通過しない残留溶液をミリポアフィルター(0.22 μm)で濾過した後、凍結乾燥して標記化合物(80 mg）を得た。本化合物を0.1 M 塩化ナトリウム水溶液に溶解後、GPC（カラム：東ソー TSK Gel PW-4000XL、溶媒： 0.1M NaCl、流速：0.8 ml/min）で分析した結果、及び本化合物の紫外線吸収スペクトル（0.1 M トリス緩衝液、pH 9.0、 36 μg/ml）をそれぞれ図８及び図９に示す。本化合物の医薬化合物基の含量を0.1 M トリス緩衝液（pH 9.0）中での 362 nm における吸光度に基づいて定量したところ15%（W/W）であった。

例29：カルボキシメチルデキストランポリアルコール-Gly-Gly-Gly-Phe-NH-A'(A-NH_2 =DX-8951)の合成

デキストランT250(20 g, EXTRASYNTHESE製, 平均分子量 250K)を0.1 M 酢酸緩衝液（pH5.5, 2000 ml）に溶解し、過ヨウ素酸ナトリウム（66.0 g）の水溶液(2000 ml）を加えた。遮光しながら４℃で10日間撹拌した後、エチレングリコール(14.0 ml）を加え、一晩撹拌した。反応液を氷冷下で8 M 水酸化ナトリウム水溶液を用いてpHを7.5 に調整した。水素化ホウ素ナトリウム（28 g）を加えて溶解した後、室温で一晩撹拌した。反応液を氷冷し、酢酸で pH 5.5 に調整して４℃で１時間撹拌した後、氷冷下で8 M 水酸化ナトリウム水溶液を用いてpHを7.5 に調整した。得

られた水溶液をバイオマックス-30 膜を用いた限外濾過法により低分子画分を除去して、膜を通過しない残留溶液1を得た。別に、デキストランT250(50 g, EXTRASYNTHESE製, 平均分子量 250K)を0.1 M 酢酸緩衝液 (pH5.5, 5000 ml) に溶解し、過ヨウ素酸ナトリウム(165 g) の水溶液(5000 ml) を加えた。遮光しながら4℃で10日間撹拌した後、エチレングリコール(35.0 ml) を加え、一晩撹拌した。反応液を氷冷下で8 M 水酸化ナトリウム水溶液を用いてpHを7.5 に調整した。水素化ホウ素ナトリウム (70 g) を加えて溶解した後、室温で一晩撹拌した。反応液を氷冷し、酢酸で pH 5.5 に調整して4℃で1時間撹拌した後、氷冷下で8 M 水酸化ナトリウム水溶液を用いてpHを7.5 に調整した。得られた水溶液をバイオマックス-30 膜を用いた限外濾過法により低分子画分を除去して、膜を通過しない残留溶液2を得た。残留溶液1と残留溶液2を合して、限外濾過法によりバイオマックス-50 膜を通過する画分をバイオマックス-30 膜を用いて低分子画分を除去し、凍結乾燥してデキストランポリアルコール (25.7 g) を得た。この物質の分子量 (ゲル濾過、プルラン標準) は、47K であった。

このデキストランポリアルコール(5 g) を、水酸化ナトリウム (35 g) を水 (150 ml) に溶かして得られる水溶液に加え、室温で溶解させた。この溶液に氷冷下でモノクロル酢酸 (50 g) を加えて溶解させた後、室温で18時間反応させた。この反応液を酢酸でpHを8に調整した後、バイオマックス-50 膜を用いた限外濾過法により脱塩した。膜を通過しない残留溶液を凍結乾燥して、カルボキシメチルデキストランポリアルコールのナトリウム塩(7.2 g) を得た。この物質の分子量 (ゲル濾過、プルラン標準) は 127K であり、カルボキシメチル化度は0.8 であった。このカルボキシメチルデキストランポリアルコールのナトリウム塩(2.2 g) を水に溶解し、Bio-Rad AG 50W-X2 (200-400 メッシュ、 H^+ 型) カラム (直径 44 mm、長さ 210 mm)にのせ、水で溶出した。この溶出液にトリエチルアミン (4 ml) を加えた後、凍結乾燥してカルボキシメチルデキストランポリアルコールのトリエチルアンモニウム塩 (2.69 g) を得た。

このカルボキシメチルデキストランポリアルコールのトリエチルアンモニウム塩 (2.67 g) をN,N-ジメチルホルムアミド (200 ml) に溶解した。この溶液に、例2と同様に合成した3'-N-(Boc-Gly-Gly-Gly-Phe)-NH-A (A-NH_2 =DX-8951) (350

mg）から例16と同様の方法で脱Boc 化して得られる3'-N-(Gly-Gly-Gly-Phe)-NH-A のトリフルオロ酢酸塩とトリエチルアミン（0.116 ml）をN,N-ジメチルホルムアミド（10 ml)に溶かして得られる溶液、1-エトキシカルボニル-2- エトキシ-1,2- ジヒドロキシキノリン（2.67 g）をN,N-ジメチルホルムアミド(10 ml）に溶かして得られる溶液を順次加え、室温で一晩撹拌しながら反応させた。この反応液に3 M 塩化ナトリウム水溶液（100 ml）を加え、8 mlずつを各30 ml のエタノール中に滴下した。それぞれに3 M 塩化ナトリウム水溶液（1 ml）、ジエチルエーテル(5 ml）を加えて、析出した沈澱を遠心分離（3500 rpm, 8分）により集めた。この沈澱をアセトンで洗浄した後、水に溶解し、3 M 塩化ナトリウム水溶液(10 ml) を加えた後、0.1 M 水酸化ナトリウム水溶液で pH 9 に調整し、37℃で1時間処理した。この処理液をバイオマックス-10 膜を用いた限外濾過法により脱塩した。膜を通過しない残留溶液をミリポアフィルター(0.22 μm)で濾過した後、凍結乾燥して標記化合物（2.30 g）を得た。本化合物を0.1 M 塩化ナトリウム水溶液に溶解後、GPC （カラム：東ソー TSK Gel PW-4000XL、溶媒： 0.1M NaCl、流速：0.8 ml/min）で分析した結果、及び本化合物の紫外線吸収スペクトル（0.1 M トリス緩衝液, pH 9.0, 0.20 mg/ml）をそれぞれ図10及び図11に示す。本化合物の医薬化合物残基の含量を0.1 M トリス緩衝液（pH 9.0）中での 362 nm における吸光度に基づいて定量したところ、 5.8%（W/W）であった。

例30：<u>カルボキシメチルデキストランポリアルコールのトリエチルアンモニウム塩の合成</u>

デキストランT10 （20 g, ファルマシア社製、平均分子量10K ）の0.1 M 酢酸緩衝液（pH 5.5）溶液（2000 ml)に、過ヨウ素酸ナトリウム（66.0 g）の水溶液(2000 ml）を加えた。遮光しながら4℃で10日間撹拌した後、エチレングリコール(14.0 ml）を加え、一晩撹拌した。反応液を氷冷下で8 M 水酸化ナトリウム水溶液を用いて pH 7.5 に調整した。水素化ホウ素ナトリウム（28 g）を加えて溶解した後、室温で一晩撹拌した。反応液を氷冷し、酢酸で pH 5.5 に調整して4℃で1時間撹拌した後、氷冷下で8 M 水酸化ナトリウム水溶液を用いて pH 7.5 に調整した。得られた水溶液をバイオマックス-5膜（ミリポア社製）を用いた限外濾過法により低分子画分を除去して、膜を通過しない残留溶液をバイオマックス-30 膜を通過させ

た。得られた通過液を凍結乾燥して、デキストランポリアルコール(8.0 g) を得た。この物質の分子量（ゲル濾過、プルラン標準）は、13K であった。

このデキストランポリアルコール(3.7 g) を、水酸化ナトリウム (25.9 g) を水 (111 ml) に溶かして得られる水溶液に加え、室温で溶解させた。この溶液に氷冷下でモノクロル酢酸 (37 g) を加えて溶解させた後、室温で20時間反応させた。この反応液を酢酸で pH 8 に調整した後、バイオマックス-5膜を用いた限外濾過法により脱塩した。膜を通過しない残留溶液を凍結乾燥して、カルボキシメチルデキストランポリアルコールのナトリウム塩(6.2 g) を得た。この物質の分子量（ゲル濾過、プルラン標準）は、37K であり、カルボキシメチル化度は0.9 であった。

このカルボキシメチルデキストランポリアルコールのナトリウム塩(6.0 g) を水に溶解し、Bio-Rad AG 50W-X2 (200-400 メッシュ、H^+ 型) カラムにのせ、水で溶出した。この溶出液にトリエチルアミン (9.3 ml) を加えた後、凍結乾燥して標記化合物(7.2 g) を得た。

例31：カルボキシメチルデキストランポリアルコールのトリエチルアンモニウム塩の合成

例30で得たデキストランポリアルコール(3.9 g) を、水酸化ナトリウム (16.3 g) を水 (117 ml) に溶かして得られる水溶液に加え、室温で溶解させた。この溶液に氷冷下でモノクロル酢酸 (23.4 g) を加えて溶解させた後、室温で18時間反応させた。この反応液を酢酸で pH 8 に調整した後、バイオマックス-5膜を用いた限外濾過法により脱塩した。膜を通過しない残留溶液を凍結乾燥して、カルボキシメチルデキストランポリアルコールのナトリウム塩(5.0 g) を得た。この物質の分子量（ゲル濾過、プルラン標準）は、28K であり、カルボキシメチル化度は0.5 であった。このカルボキシメチルデキストランポリアルコールのナトリウム塩(4.8 g) を例30と同様にトリエチルアンモニウム塩に変換して、標記化合物(5.6 g) を得た。

例32：カルボキシメチルデキストランポリアルコールのトリエチルアンモニウム塩の合成

デキストラン4 (20 g 、フナコシ社製、平均分子量 4K-6K) の0.1 M 酢酸緩衝液 (pH 5.5) 溶液(2000 ml) に、過ヨウ素酸ナトリウム (66.0 g) の水溶液(2000

ml）を加えた。遮光しながら４℃で10日間撹拌した後、エチレングリコール(14.0 ml）を加え、一晩撹拌した。反応液を氷冷下で8 M 水酸化ナトリウム水溶液を用いてpHを7.5 に調整した。水素化ホウ素ナトリウム（28 g）を加えて溶解した後、室温で一晩撹拌した。反応液を氷冷し、酢酸で pH 5.5 に調整して４℃で１時間撹拌した後、氷冷下で8 M 水酸化ナトリウム水溶液を用いて pH 7.5 に調整した。得られた水溶液をバイオマックス-3膜（ミリポア社製）を用いた限外濾過法により低分子画分を除去した。得られた通過液を凍結乾燥してデキストランポリアルコール(6.0 g）を得た。この物質の分子量（ゲル濾過、プルラン標準）は、9Kであった。このデキストランポリアルコール(2.7 g）を、水酸化ナトリウム（18.9 g）を水(81 ml）に溶かして得られる水溶液に加え、室温で溶解させた。この溶液に氷冷下でモノクロル酢酸（27 g）を加えて溶解させた後、室温で20時間反応させた。この反応液を酢酸で pH 8 に調整した後、バイオマックス-5膜を用いた限外濾過法により脱塩した。膜を通過しない残留溶液を凍結乾燥して、カルボキシメチルデキストランポリアルコールのナトリウム塩(4.2 g）を得た。この物質の分子量（ゲル濾過、プルラン標準）は、20K であり、カルボキシメチル化度は0.9 であった。

このカルボキシメチルデキストランポリアルコールのナトリウム塩(4.0 g）を例30と同様にトリエチルアンモニウム塩に変換して、標記化合物(4.8 g）を得た。

例33：カルボキシメチルデキストランポリアルコールのトリエチルアンモニウム塩の合成

例32で得たデキストランポリアルコール(2.7 g）を、水酸化ナトリウム（11.3 g）を水(81 ml）に溶かして得られる水溶液に加え、室温で溶解させた。この溶液に氷冷下でモノクロル酢酸（16.2 g）を加えて溶解させた後、室温で18時間反応させた。この反応液を酢酸で pH 8 に調整した後、バイオマックス-5膜を用いた限外濾過法により脱塩した。膜を通過しない残留溶液を凍結乾燥して、カルボキシメチルデキストランポリアルコールのナトリウム塩(2.7 g）を得た。この物質の分子量（ゲル濾過、プルラン標準）は、16K であり、カルボキシメチル化度は0.5であった。このカルボキシメチルデキストランポリアルコールのナトリウム塩(2.7 g）を例30と同様にトリエチルアンモニウム塩に変換して、標記化合物(3.1 g）を得た。

例34：カルボキシメチルデキストランポリアルコール-Gly-Gly-Phe-Gly-NH-A'(A-NH_2 =DX-8951)の合成

例30で得たカルボキシメチルデキストランポリアルコールのトリエチルアンモニウム塩(1.5 g) N,N-ジメチルホルムアミド(90 ml) 溶解させた。この溶液に、トリエチルアミン(0.07 ml) と3'-N-(Gly-Gly-Phe-Gly)-NH-A (A-NH_2 =DX-8951)のトリフルオロ酢酸塩 (210 mg) のN,N-ジメチルホルムアミド(40 ml) 溶液、1-エトキシカルボニル-2- エトキシ-1,2- ジヒドロキシキノリン(1.5 g) を順次加え、室温で一晩撹拌しながら反応させた。この反応液の5 mlずつを各10 ml のエタノール中に滴下した。それぞれに3 M 塩化ナトリウム水溶液 (2.5 ml) 、ジエチルエーテル(20 ml) を加えて、析出した沈澱を遠心分離 (3500 rpm, 8分) により集めた。この沈澱を0.5 M 食塩水に溶解し、氷冷下0.1 M 水酸化ナトリウム水溶液で pH 9 とした。得られた水溶液をバイオマックス-3膜を用いた限外濾過法により脱塩した。膜を通過しない残留溶液をミリポアフィルター(0.22 μm)で濾過した後、凍結乾燥して標記化合物(1.3 g) を得た。本化合物を0.1 M 塩化ナトリウム水溶液に溶解後、GPC (カラム：東ソー TSK Gel PW-4000XL、溶媒： 0.1M NaCl、流速： 0.8 ml/min) で分析した結果、及び本化合物の紫外線吸収スペクトル (0.1 M トリス緩衝液、pH 9.0、 65 μg/ml) をそれぞれ図12及び図13に示す。本化合物の医薬化合物残基の含量を0.1 M トリス緩衝液 (pH 9.0) 中での 362 nm における吸光度に基づいて定量したところ 6.4% (W/W) であった。

例35：カルボキシメチルデキストランポリアルコール-Gly-Gly-Phe-Gly-NH-A'(A-NH_2 =DX-8951)の合成

例31で得たカルボキシメチルデキストランポリアルコールのトリエチルアンモニウム塩(1.2 g) をN,N-ジメチルホルムアミド(90 ml) 溶解させた。この溶液に、トリエチルアミン (0.056 ml) と3'-N-(Gly-Gly-Phe-Gly)-NH-A (A-NH_2 =DX-8951) のトリフルオロ酢酸塩 (168 mg) のN,N-ジメチルホルムアミド(30 ml) 溶液、1-エトキシカルボニル-2- エトキシ-1,2- ジヒドロキシキノリン(1.2 g) を順次加え、室温で一晩撹拌しながら反応させた。この反応液の5 mlずつを各10 ml のエタノール中に滴下した。それぞれに3 M 塩化ナトリウム水溶液 (2.5 ml) 、ジエチルエーテル(20 ml) を加えて、析出した沈澱を遠心分離 (3500 rpm, 8分) により集

めた。この沈澱を0.5 M 食塩水に溶解し、氷冷下0.1 M 水酸化ナトリウム水溶液で pH 9 とした。得られた水溶液をバイオマックス-3膜を用いた限外濾過法により脱塩した。膜を通過しない残留溶液をミリポアフィルター(0.22 μm)で濾過した後、凍結乾燥して標記化合物(1.0 g) を得た。本化合物の医薬化合物残基の含量を0.1 M トリス緩衝液 (pH 9.0) 中での 362 nm における吸光度に基づいて定量したところ、 4.8% (W/W) であった。

例36：カルボキシメチルデキストランポリアルコール-Gly-Gly-Phe-Gly-NH-A'(A-NH_2 =DX-8951)の合成

例32で得たカルボキシメチルデキストランポリアルコールのトリエチルアンモニウム塩(1.2 g) をN,N-ジメチルホルムアミド(90 ml) 溶解させた。この溶液に、トリエチルアミン (0.056 ml) と3'-N-(Gly-Gly-Phe-Gly)-NH-A (A-NH_2 =DX-8951) のトリフルオロ酢酸塩 (168 mg) のN,N-ジメチルホルムアミド(30 ml) 溶液、1-エトキシカルボニル-2- エトキシ-1,2- ジヒドロキシキノリン(1.2 g) を順次加え、室温で一晩撹拌しながら反応させた。この反応液の5 mlずつを各10 ml のエタノール中に滴下した。それぞれに3 M 塩化ナトリウム水溶液 (2.5 ml) 、ジエチルエーテル(20 ml) を加えて、析出した沈澱を遠心分離 (3500 rpm, 8分) により集めた。この沈澱を0.5 M 食塩水に溶解し、氷冷下0.1 M 水酸化ナトリウム水溶液で pH 9 とした。得られた水溶液をバイオマックス-3膜を用いた限外濾過法により脱塩した。膜を通過しない残留溶液をミリポアフィルター(0.22 μm)で濾過した後、凍結乾燥して標記化合物(1.0 g) を得た。本化合物の医薬化合物残基の含量を0.1 M トリス緩衝液 (pH 9.0) 中での 362 nm における吸光度に基づいて定量したところ、 5.9% (W/W) であった。

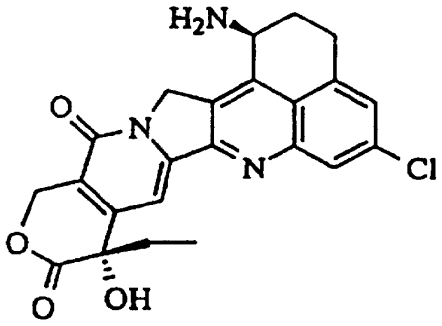
例37：カルボキシメチルデキストランポリアルコール-Gly-Gly-Phe-Gly-NH-A'(A-NH_2 =DX-8951)の合成

例33で得たカルボキシメチルデキストランポリアルコールのトリエチルアンモニウム塩(1.5 g) をN,N-ジメチルホルムアミド(90 ml) 溶解させた。この溶液に、トリエチルアミン(0.07 ml) と3'-N-(Gly-Gly-Phe-Gly)-NH-A (A-NH_2 =DX-8951) のトリフルオロ酢酸塩 (210 mg) のN,N-ジメチルホルムアミド(40 ml) 溶液、1-エトキシカルボニル-2- エトキシ-1,2- ジヒドロキシキノリン(1.5 g) を順次加え、

室温で一晩撹拌しながら反応させた。この反応液の5 mlずつを各10 ml のエタノール中に滴下した。それぞれに3 M 塩化ナトリウム水溶液（2.5 ml）、ジエチルエーテル(20 ml）を加えて、析出した沈澱を遠心分離（3500 rpm, 8分）により集めた。この沈澱を0.5 M 食塩水に溶解し、氷冷下0.1 M 水酸化ナトリウム水溶液で pH 9 とした。得られた水溶液をバイオマックス-3膜を用いた限外濾過法により脱塩した。膜を通過しない残留溶液をミリポアフィルター(0.22 μm)で濾過した後、凍結乾燥して標記化合物(1.3 g）を得た。本化合物の医薬化合物残基の含量を0.1 M トリス緩衝液（pH 9.0）中での 362 nm における吸光度に基づいて定量したところ、4.6%（W/W）であった。

例38：Boc-Gly-Gly-Phe-Gly-NH-A（A-NH_2 =DW-8286）の合成

Boc-Gly-Gly-Phe-Gly（42 mg）およびN-ヒドロキシスクシンイミド(12 mg）をN,N-ジメチルホルムアミド（2 ml）に溶解し、4℃に冷却した後、N,N'- ジシクロヘキシルカルボジイミド(22 mg）を添加した。この溶液に下記式：



で表される化合物［(1s,9s)-1-アミノ-5- クロロ-9- エチル-2,3- ジヒドロ-9-ハイドロキシ-1H,12H-ベンゾ[de]ピラノ[3',4':6,7] インドリジノ[1,2-b] キノリン-10,13(9H,15H)- ジオン：DW-8286]の塩酸塩(50 mg）とトリエチルアミン(0.01 ml）を溶解したN,N-ジメチルホルムアミド（6 ml）溶液を加えて、遮光して、室温で16時間撹拌しながら反応させた。この反応液を減圧乾固し、残渣をシリカゲルカラムクロマトグラフィー（溶出液：0.5% 酢酸を含むジクロロメタン：メタノール＝10：1 溶液）で精製して標記化合物(27 mg）を得た。

^{1}H-NMR($CDCl_3$) δ：8.10-8.20 (br,1H), 7.95-8.05 (br,1H), 7.70-7.80 (br,2H), 7.50-7.60 (br,1H), 7.40-7.50 (br,1H), 7.10-7.25 (m,5H), 7.05-7.15 (br,1H),

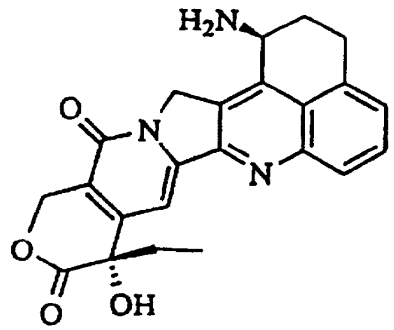
5.85-5.95 (br, 1H), 5.50-5.60 (br, 1H), 5.40-5.50 (m, 1H), 5.25-5.35 (m, 1H), 5.05-5.15 (m, 1H), 4.90-5.00 (m, 1H), 4.70-4.80 (br, 1H), 4.10-4.25 (br, 2H), 3.60-3.90 (m, 4H), 3.10-3.40 (m, 3H), 2.95-3.05 (br, 1H), 2.15-2.30 (br, 1H), 1.75-1.90 (br, 2H), 1.39 (s, 9H), 0.80-1.00 (m, 3H).

例39：カルボキシメチルデキストランポリアルコール-Gly-Gly-Phe-Gly-NH-A'(A-NH_2 =DW-8286)の合成

例24で得たカルボキシメチルデキストランポリアルコールのトリエチルアンモニウム塩（175 mg）をN,N-ジメチルホルムアミド(20 ml）に溶解させた。この溶液に、例38で得られた3'-N-(Boc-Gly-Gly-Phe-Gly)-NH-A (A-NH_2 =DW-8286) (27 mg)から例4と同様の方法で脱Boc 化して得られる 3'-N-(Gly-Gly-Phe-Gly)-NH-Aのトリフルオロ酢酸塩(29 mg) とトリエチルアミン(9 μl)のN,N-ジメチルホルムアミド（5 ml）溶液、1-エトキシカルボニル-2- エトキシ-1,2- ジヒドロキシキノリン（175 mg）を順次加え、室温で一晩撹拌しながら反応させた。この反応液の5 mlずつを各10 ml のエタノール中に滴下した。これに3 M 塩化ナトリウム水溶液（2.5 ml）、ジエチルエーテル(20 ml）を加えて、析出した沈澱を遠心分離（3500 rpm, 8分）により集めた。この沈澱を0.5 M 食塩水に溶解し、氷冷下0.1 M 水酸化ナトリウム水溶液で pH 9 とした。得られた水溶液をバイオマックス-30 膜を用いた限外濾過法により脱塩した。膜を通過しない残留溶液をミリポアフィルター(0.22 μm)で濾過した後、凍結乾燥して標記化合物（135 mg）を得た。本化合物を0.1 M 塩化ナトリウム水溶液に溶解後、GPC （カラム：東ソー TSK Gel PW-4000XL、溶媒：0.1M NaCl、流速： 0.8 ml/min ）で分析した結果、及び本化合物の紫外線吸収スペクトル（0.1 M トリス緩衝液、Ph 9.0、 99 μg/ml）をそれぞれ図14及び図15に示す。本化合物の医薬化合物残基の含量は、0.1 M トリス緩衝液（pH 9.0）中での 362 nm における吸光度に基づいて定量したところ、 6.1% (W/W) であった。

例40：3'-N-(Boc-Gly-Gly-Phe-Gly)-NH-A (A-NH_2 =DW-8089)の合成

Boc-Gly-Gly-Phe-Gly (163 mg)およびN-ヒドロキシスクシンイミド(45 mg) をN,N-ジメチルホルムアミド(10 ml）に溶解し、4 ℃に冷却した後、N, N'-ジシクロヘキシルカルボジイミド(79 mg) を添加した。この溶液に下記の式：



で表される化合物 [(1s,9s)-1-アミノ-9- エチル-2,3- ジヒドロ-9- ハイドロキシ-1H,12H-ベンゾ[de]ピラノ[3',4':6,7] インドリジノ[1,2-b] キノリン-10,13(9H,15H)- ジオン: DW-8089]のトシル酸塩 (170 mg) とトリエチルアミン (0.054 ml) を溶解したN,N-ジメチルホルムアミド(30 ml) 溶液を加えて、遮光下に室温で一晩撹拌しながら反応させた。この反応液を減圧乾固し、残渣をシリカゲルカラムクロマトグラフィー (溶出液：0.5%酢酸を含むジクロロメタン：メタノール＝94：6溶液) で精製して標記化合物 (100 mg) を得た。

^{1}H-NMR (DMSO-d_6) δ: 8.51 (d,1H,J=8.5Hz), 8.41 (t,1H,J=5.6Hz), 8.29 (s,1H), 8.17 (d,1H,J=8.0Hz), 8.03 (d,1H,J=8.0Hz), 7.90 (dd,1H,J=4.8,5.6Hz), 7.79 (t,1H,J=5.6Hz), 7.53 (d,1H,J=7.2Hz), 7.36 (s,1H), 7.13-7.25 (m,5H), 6.94-6.95 (m,1H), 5.60-5.63 (m,1H), 5.36-5.47 (m,2H), 5.21-5.30 (m,2H), 4.42-4.47 (m,1H), 3.63-3.96 (m,3H), 3.51-3.59 (m,3H), 3.31-3.40 (m,1H), 3.09-3.21 (m,1H), 3.02 (dd,1H,J=4.8,13.5Hz), 2.76-2.81 (m,1H), 2.13-2.17 (m,2H), 1.85-1.90 (m,2H), 1.37 (s,9H), 0.89 (t,3H,J=8.0Hz).

Mass (FAB); m/e 822 (M+1)

例41：カルボキシメチルデキストランポリアルコール-Gly-Gly-Phe-Gly-NH-A'(A-NH_2 =DW-8089)の合成

例24で得たカルボキシメチルデキストランポリアルコールのトリエチルアンモニウム塩(1.6 g) をN,N-ジメチルホルムアミド(60 ml) に溶解させた。この溶液に、例40で得られた3'-N-(Boc-Gly-Gly-Phe-Gly)-NH-A (A-NH_2 =DW-8089) (200 mg) から例４と同様の方法で脱Boc 化して得られる 3'-N-(Gly-Gly-Phe-Gly)-NH-Aのトリフルオロ酢酸塩とトリエチルアミン(0.07 ml) をN,N-ジメチルホルムアミド(20

ml）に溶かして得られる溶液、1-エトキシカルボニル-2- エトキシ-1, 2-ジヒドロキシキノリン(1.6 g）を順次加え、室温で一晩撹拌しながら反応させた。この反応液の5 mlずつを各10 ml のエタノール中に滴下した。それぞれに3 M 塩化ナトリウム水溶液（2.5 ml）、ジエチルエーテル(25 ml）を加えて、析出した沈澱を遠心分離（2500 rpm, 8分）により集めた。この沈澱をエタノールで洗浄した後、水に溶解し、3 M 塩化ナトリウム水溶液(20 ml）を加え、0.1 M 水酸化ナトリウム水溶液で pH 9 に調整した。この溶液をバイオマックス-10 膜を用いた限外濾過法により脱塩した。膜を通過しない残留溶液をミリポアフィルター(0.22 μm)で濾過した後、凍結乾燥して標記化合物（1.20 g）を得た。本化合物を0.1 M 塩化ナトリウム水溶液に溶解後、GPC （カラム：東ソー TSK Gel PW-4000XL、溶媒： 0.1M NaCl、流速：0.8 ml/min）で分析した結果、及び本化合物の紫外線吸収スペクトル（0.1 M トリス緩衝液, pH 9.0, 0.26 mg/ml）をそれぞれ図16及び図17に示す。本化合物の医薬化合物残基の含量を0.1 M トリス緩衝液（pH 9.0）中での 362 nm における吸光度に基づいて定量したところ、 5.0% (W/W) であった。

例42：Trt-Gly-Gly-Phe-Gly-OHの合成

Trt-Gly-Gly-Phe-Gly-OBzl (670 mg）、10% Pd-C (100mg)およびギ酸アンモニウム（200 mg）をDMF (5 ml)中に加え、3時間撹拌した。反応液を濾過し、濾液を減圧乾固した後、残渣をシリカゲルカラムクロマトグラフィー（溶出液：ジクロロメタン：メタノール＝８：１溶液）で精製して標記化合物（300 mg）を得た。

^{1}H-NMR(CD_3OD) δ： 7.16-7.45 (m, 20H), 4.66 (dd, 1H, J=9.8, 5.4Hz), 3.93 (d, 1H, J=16.6Hz), 3.80 (d, 1H, J=17.6Hz), 3.78 (d, 1H, J=16.6Hz), 3.68 (d, 1H, J=17.1Hz), 3.23 (dd, 1H, J=14.2, 5.4Hz), 2.90 (d, 1H, J=13.7Hz), 2.90 (s, 1H).

例43：3'-N-(Gly-Gly-Phe-Gly)-DXR塩酸塩の合成

Trt-Gly-Gly-Phe-Gly-OH (100 mg) およびN-ヒドロキシスクシンイミド(22 mg)をDMF (4 ml)に溶かし、氷冷下N, N'- ジシクロヘキシルカルボジイミド(40 mg)を加え４℃で２時間撹拌した。この溶液にN-メチルモルホリン（0.019 ml）とドキソルビシン(DXR) 塩酸塩(92 mg) を溶解したDMF (20 ml) 溶液を加えて、４℃で16時間攪拌した。この反応液を減圧乾固し、残渣をシリカゲルカラムクロマトグラフィー（溶出液：ジクロロメタン：メタノール＝２０：１溶液）で精製した。得

られた化合物を 75%酢酸 1 ml に溶解し、1時間撹拌した。水 (20 ml)を加えて析出した固体を濾過して除き、濾液を凍結乾燥して、得られた粉末を水 (5 ml) に溶かした。この溶液をAG-1X8 (Cl^- 型) カラムに通し、水で溶出した後、ジクロロメタンで洗い、水層を凍結乾燥して、標記化合物(40 mg) を得た。

^{1}H-NMR(CD_3OD) δ : 7.95 (d, 1H, J=7.3Hz), 7.82 (t, 1H, J=7.8Hz), 7.54 (d, 1H, J=8.3Hz), 7.16-7.26 (m, 5H), 5.43 (d, 1H, J=3.4Hz), 5.14 (br, 1H), 4.72 (s, 2H), 4.42 (dd, 1H, J=8.3, 6.8Hz), 4.30 (q, 1H, J=6.8Hz), 4.14-4.18 (m, 1H), 4.03 (d, 1H, J=16.6Hz), 4.02 (s, 3H), 3.86 (d, 1H, J=18.5Hz), 3.83 (d, 1H, J=17.1Hz), 3.75 (d, 1H, J=16.1Hz), 3.73 (d, 1H, J=16.1Hz), 3.62 (br, 1H), 3.58 (d, 1H, J=16.6Hz), 3.10-3.15 (m, 2H), 3.00 (d, 1H, J=18.6Hz), 2.94 (dd, 1H, J=14.2, 8.8Hz), 2.38 (d, 1H, J=14.2Hz), 2.18 (dd, 1H, J=14.2, 4.4Hz), 1.94-2.00 (m, 1H), 1.71 (dd, 1H, J=12.7, 4.4Hz), 1.28 (d, 3H, J=6.3Hz).

例44：カルボキシメチルデキストランポリアルコール-Gly-Gly-Phe-Gly-DXRの合成

例24で得たカルボキシメチルデキストランポリアルコールのナトリウム塩(1.5 g) を例25と同様の方法でトリメチルアンモニウム塩(1.2 g) に変換した後、この 400 mg をN,N-ジメチルホルムアミド(24 ml) に溶解させた。この溶液に、3'-N-(Gly-Gly-Phe-Gly)-DXRの塩酸塩(76 mg) のN,N-ジメチルホルムアミド(24 ml) 溶液、トリエチルアミン(24 μl)、1-エトキシカルボニル-2- エトキシ-1,2- ジヒドロキシキノリン (400 mg) を順次加え、室温で一晩撹拌しながら反応させた。この反応液の5 mlずつを各10 ml のエタノール中に滴下した。これに3 M 塩化ナトリウム水溶液 (2.5 ml) 、ジエチルエーテル(20 ml) を加えて、析出した沈澱を遠心分離 (3500 rpm, 8分) により集めた。この沈澱を0.5 M 食塩水に溶解し、バイオマックス-30 膜を用いた限外濾過法により脱塩した。膜を通過しない残留溶液をミリポアフィルター(0.22 μm)で濾過した後、凍結乾燥して標記化合物(40 mg) を得た。本化合物を0.1 M 塩化ナトリウム水溶液に溶解後、GPC (カラム：東ソー TSK Gel PW-4000XL、溶媒： 0.1M NaCl、流速： 0.8 ml/min) で分析した結果、及び本化合物の紫外線吸収スペクトル (0.01 Mトリス緩衝液、pH 7.4、 36 μg ml) をそれぞれ図18及び図19に示す。本化合物の医薬化合物残基の含量は、PBS (pH 7.4)中での 480 nm における吸光度に基づいて定量したところ、 6.0% (W/W)

であった。

例45：カルボキシメチルデキストランポリアルコールのトリエチルアンモニウム塩の合成

デキストランT150（20 g、ファルマシア社製、平均分子量 150K ）を0.1 M 酢酸緩衝液（pH 5.5、2000 ml)に溶解し、過ヨウ素酸ナトリウム（66.0 g）の水溶液(2000 ml）を加えた。遮光しながら４℃で10日間撹拌した後、エチレングリコール(14.0 ml）を加え、一晩撹拌した。反応液を氷冷下で8 M 水酸化ナトリウム水溶液を用いてpHを7.5 に調整した。水素化ホウ素ナトリウム（28 g）を加えて溶解した後、室温で一晩撹拌した。反応液を氷冷して、酢酸で pH 5.5 に調整し、４℃で１時間撹拌した。氷冷下で8 M 水酸化ナトリウム水溶液を用いてpHを7.5 に調整した。得られた水溶液をバイオマックス-5膜（ミリポア社製）を用いた限外濾過法により、500 mlまで濃縮して溶液１を得た。別に、デキストランT110（20 g）について上記の一連の操作を行い、溶液２を得た。溶液１と溶液２を混合し、混合溶液のpHを3.0 とし、40℃で４時間インキュベートした後、pHを７に調整して低分子化されたデキストランポリアルコールを含む溶液を得た。バイオマックス-30 膜を通過させ、次いでバイオマックス-5膜を用いて脱塩した後、凍結乾燥してデキストランポリアルコール(4.6 g）を得た。この物質の分子量（ゲル濾過、プルラン標準）は、17K であった。

このデキストランポリアルコール(2.5 g）を、水酸化ナトリウム（17.5 g）を水(75 ml）に溶かして得られる水溶液に加え、室温で溶解させた。この溶液に氷冷下でモノクロル酢酸（25 g）を加えて溶解させた後、室温で20時間反応させた。この反応液を酢酸でpHを９に調整した後、バイオマックス-5膜を用いた限外濾過法により脱塩した。膜を通過しない残留溶液を凍結乾燥して、カルボキシメチルデキストランポリアルコールのナトリウム塩(4.0 g）を得た。この物質の分子量（ゲル濾過、プルラン標準）は 45Kであり、CM化度は0.9 であった。

このカルボキシメチルデキストランポリアルコールのナトリウム塩(3.7 g）を水に溶解し、Bio-Rad AG 50W-X2 (200-400 メッシュ、 H^+ 型）カラムにのせ、水で溶出した。この溶出液にトリエチルアミン（5.8 ml）を加えた後、凍結乾燥して標記化合物(4.4 g）を得た。

例46：カルボキシメチルデキストランポリアルコール-Gly-Gly-Gly-Phe-NH-A'(A-NH_2 =DX-8951)の合成

例45で得られたカルボキシメチルデキストランポリアルコールのトリエチルアンモニウム塩(4.4 g)をN,N-ジメチルホルムアミド（300 ml）に溶解させた。この溶液に、トリエチルアミン(0.19 ml）と3'-N-(Gly-Gly-Gly-Phe)-NH-A (A-NH_2 =DX-8951)のトリフルオロ酢酸塩（580 mg）を含むN,N-ジメチルホルムアミド(45 ml)溶液、1-エトキシカルボニル-2- エトキシ-1,2- ジヒドロキシキノリン(4.4 g)を順次加え、遮光して室温で一晩撹拌しながら反応させた。この反応液を1 M 水酸化ナトリウム水溶液で pH 10に調整した後、5 mlずつを各25 ml のエタノール中に滴下した。これに3 M 塩化ナトリウム水溶液（1 ml）、ジエチルエーテル（5 ml）を加えて、析出した沈澱を遠心分離（3500 rpm, 8分）により集めた。この沈澱を水に溶解し、透析膜（スペクトルポア１、カットオフ分子量 6000-8000）を用いて、純水に対して透析し、透析内液をミリポアフィルター(0.22 μm)で濾過した後、凍結乾燥して標記化合物(3.4 g）を得た。本化合物の医薬化合物残基の含量を0.1 トリス緩衝液（pH 9.0）中での 362 nm における吸光度に基づいて定量したところ、 4.6%（W/W）であった。

例47：α－メチルカルボキシメチルデキストランポリアルコール-Gly-Gly-Gly-Phe-NH-A'(A-NH_2 =DX-8951)の合成

例45で得られたデキストランポリアルコール(2 g）を、水酸化ナトリウム（14 g）を水(60 ml）に溶かして得られる水溶液に加え、室温で溶解させた。この溶液に氷冷下でα－ブロモプロピオン酸(19 ml）を加えて溶解させた後、室温で18時間反応させた。この反応液を酢酸で pH 8 に調整した後、バイオマックス-50膜を用いた限外濾過法により脱塩した。膜を通過しない残留溶液を凍結乾燥して、α－メチルカルボキシメチルデキストランポリアルコールのナトリウム塩（2.95 g）を得た。この物質の分子量（ゲル濾過、プルラン標準）は、 45Kであった。糖残基あたりのα－メチルカルボキシメチル化度は、カルボキシメチルデキストランポリアルコールの場合に準じて以下の様に求めた。α－メチルカルボキシメチルデキストランポリアルコールのナトリウム塩の水溶液を Bio-Rad AG 50W-X 2 (H^+ 型）カラムに付し、通過液を凍結乾燥して試料として用いた。この試料を所

定過剰量の0.1 N 水酸化ナトリウム水溶液に溶解し、フェノールフタレインを指示薬として0.1 N 塩酸で滴定した。試料の採取量を s mg 、0.1 N 水酸化ナトリウム水溶液の所定過剰量を a (ml) 、0.1 N 塩酸の滴定量を b (ml) とし、α－メチルカルボキシメチル化度を 13.4(a-b)/[s-7.2(a-b)] の式により求めた。その結果α－メチルカルボキシメチル化度は0.8 であった。

このα－メチルカルボキシメチルデキストランポリアルコールのナトリウム塩(2.2 g) を水に溶解し、Bio-Rad AG 50W-X2 (200-400 メッシュ、H^+ 型) カラム (直径 44 mm、長さ 210 mm)にのせ、水で溶出した。この溶出液にトリエチルアミン (4 ml) を加えた後、凍結乾燥してα－メチルカルボキシメチルデキストランポリアルコールのトリエチルアンモニウム塩 (2.69 g) を得た。

このα－メチルカルボキシメチルデキストランポリアルコールのトリエチルアンモニウム塩 (2.68 g) をN,N-ジメチルホルムアミド(60 ml) に溶解した。この溶液に、例２と同様に合成した3'-N-(Boc-Gly-Gly-Gly-Phe)-NH-A (A-NH_2 =DX-8951) (350 mg) から例16と同様の方法で脱Boc 化して得られる3'-N-(Gly-Gly-Gly-Phe)-NH-A のトリフルオロ酢酸塩とトリエチルアミン (0.116 ml) をN,N-ジメチルホルムアミド (10 ml) に溶かして得られる溶液、1-エトキシカルボニル-2- エトキシ-1,2- ジヒドロキシキノリン (2.68 g) をN,N-ジメチルホルムアミド(10 ml) に溶かして得られる溶液を順次加え、室温で一晩撹拌しながら反応させた。この反応液に3 M 塩化ナトリウム水溶液(40 ml) を加え、6 mlずつを各30 ml のエタノール中に滴下した。それぞれに3 M 塩化ナトリウム水溶液 (1 ml) 、ジエチルエーテル (5 ml) を加えて、析出した沈澱を遠心分離 (3500 rpm, ８分) により集めた。この沈澱をアセトンで洗浄した後、水に溶解し、3 M 塩化ナトリウム水溶液(10 ml) を加え、0.1 M 水酸化ナトリウム水溶液で pH 9 に調整し、37℃で１時間処理した。この処理液をバイオマックス-10 膜を用いた限外濾過法により脱塩した。膜を通過しない残留溶液をミリポアフィルター(0.22 μm)で濾過した後、凍結乾燥して標記化合物 (2.15 g) を得た。本化合物を0.1 M 塩化ナトリウム水溶液に溶解後、GPC (カラム：東ソー TSK Gel PW-4000XL、溶媒： 0.1M NaCl、流速： 0.8 ml min) で分析した結果、及び本化合物の紫外線吸収スペクトル (0.1 M トリス緩衝液, pH 9.0, 0.21 mg/ ml)をそれぞれ図20および図21に示す。本化合物の医薬化合

物残基の含量を0.1 M トリス緩衝液（pH 9.0）中での 362 nm における吸光度に基づいて定量したところ、 5.9%（W/W）であった。

例48：3'-N-(Gly-Phe-Gly)-NH-A（A-NH_2 =DX-8951）トリフルオロ酢酸塩の合成

Phe-Gly-OBzlのp-トルエンスルホン酸塩（3.06 g）、Boc-Gly-OH（1.10 g）、N-ヒドロキシスクシンイミド（941 mg）、N-メチルモルフォリン（0.725 ml）、N,N-ジメチルホルムアミド(40 ml）の混合物を4℃に冷却した後、N,N'- ジシクロヘキシルカルボジイミド（1.56 g）を加えた。室温で一晩撹拌しながら反応させた後、反応液を減圧乾固した。残渣をシリカゲルカラムクロマトグラフィー（溶出液：ジクロロメタン：メタノール＝98：2溶液）で精製してBoc-Gly-Phe-Gly-OBzl（1.93 g）を得た。

^{1}H-NMR（DMSO-d_6）δ：8.52（dd, 1H, J=5.6, 6.4Hz), 7.97（d, 1H, J=8.8Hz), 7.30-7.39（m, 5H), 7.15-7.26（m, 5H), 6.83（t, 1H, J=5.6Hz), 5.14（s, 1H), 4.52-4.57（m, 1H), 3.87-3.96（m, 2H), 3.57（dd, 1H, J=5.6, 16.7Hz), 3.43（dd, 1H, J=5.6, 16.7Hz), 3.01（dd, 1H, J=4.8, 14.3Hz), 2.77（dd, 1H, J=5.6, 14.3Hz), 1.37（s, 9H).

得られたBoc-Gly-Phe-Gly-OBzl（1.78 g）を酢酸エチル(60 ml）に溶解し、5%-Pd-C（1.8 g）存在下、24時間接触還元した。触媒を濾去し、濾液を減圧濃縮し、Boc-Gly-Phe-Gly-OH（1.41 g）を得た。

^{1}H-NMR（DMSO-d_6）δ：8.35（t, 1H, J=5.6Hz), 7.94（d, 1H, J=8.8Hz), 7.15-7.26（m, 5H), 6.85（dd, 1H, J=5.6, 6.4Hz), 4.52-4.58（m, 1H), 3.76（d, 2H, J=5.6Hz), 3.56（dd, 1H, J=6.4, 16.7Hz), 3.43（dd, 1H, J=5.6, 16.7Hz), 3.03（dd, 1H, J=5.0, 13.5Hz), 2.79（dd, 1H, J=9.5, 13.5Hz), 1.37（s, 9H).

上で得られたBoc-Gly-Phe-Gly-OH（500 mg）およびN-ヒドロキシスクシンイミド（161 mg）をN,N-ジメチルホルムアミド(10 ml）に溶解した。この溶液に DX-8951のメタンスルホン酸塩（530 mg）とトリエチルアミン（0.146 ml）を溶解したN,N-ジメチルホルムアミド(50 ml）溶液を加えて、4℃に冷却した後、N,N'- ジシクロヘキシルカルボジイミド（268 mg）を加えて、遮光下に室温で一晩撹拌しながら反応させた。この反応液を減圧乾固し、残渣をシリカゲルカラムクロマトグラフィー（溶出液：ジクロロメタン：メタノール＝96：4溶液）で精製して3'-N-(Boc

-Gly-Phe-Gly)-NH-A (A-NH_2 =DX-8951) (100 mg) を得た。

^{1}H-NMR (DMSO-d_6) δ: 8.39 (d, 1H, J=8.0Hz), 8.34 (t, 1H, J=5.6Hz), 7.98 (d, 1H, J=7.2Hz), 7.78 (d, 1H, J=10.3Hz), 7.33 (s, 1H), 7.13-7.24 (m, 5H), 6.80 (dd, 1H, J=5.6, 6.4Hz), 5.55-5.61 (m, 1H), 5.44 (d, 1H, J=16.0Hz), 5.41 (d, 1H, J=16.0Hz), 5.25 (s, 2H), 4.43-4.46 (m, 1H), 3.69-3.79 (m, 2H), 3.50 (dd, 1H, J=5.6, 16.7Hz), 3.41 (dd, 1H, J=5.6, 16.7Hz), 3.16-3.19 (m, 2H), 2.98 (dd, 1H, J=4.8, 14.3Hz), 2.79 (dd, 1H, J=9.5, 14.3Hz), 2.41 (s, 3H), 2.19-2.25 (m, 1H), 2.10-2.15 (m, 1H), 1.82-1.90 (m, 2H), 1.35 (s, 9H), 0.88 (t, 3H, J=8.0Hz).

Mass (FAB); m/e 797 (M+1)

得られた3'-N-(Boc-Gly-Phe-Gly)-NH-A (A-NH_2 =DX-8951) (100 mg) をトリフルオロ酢酸 (3 ml) に溶かし、1時間放置した。溶媒を留去し、メタノール(30 ml) で共沸を2回、エタノール(30 ml) で共沸を2回行った後、残渣をエーテルで洗浄して、標記化合物(80 mg) を得た。

^{1}H-NMR (DMSO-d_6) δ: 8.52-8.62 (m, 1H), 7.94 (s, 3H), 7.79 (t, 1H, J=11.1Hz), 7.34 (s, 1H), 7.15-7.27 (m, 5H), 6.52 (s, 1H), 5.57-5.61 (m, 1H), 5.36-5.46 (m, 2H), 5.24 (s, 2H), 4.66-4.70 (m, 1H), 3.69-3.81 (m, 2H), 3.61-3.68(m, 1H), 3.40-3.47 (m, 1H), 3.15-3.23 (m, 1H), 3.01 (dd, 1H, J=4.0, 13.5Hz), 2.77 (dd, 1H, J=9.5, 13.5Hz), 2.12-2.23 (m, 2H), 1.81-1.91 (m, 2H), 0.89 (t, 3H, J=7.2Hz).

Mass (FAB); m/e 697 (M+1)

例49：3'-N-(Phe-Gly)-NH-A (A-NH_2 =DX-8951)トリフルオロ酢酸塩の合成

Boc-Phe-Gly(771 mg) およびN-ヒドロキシスクシンイミド (300 mg) をN,N-ジメチルホルムアミド(10 ml) に溶解した。この溶液に DX-8951 のメタンスルホン酸塩(1058 mg) とトリエチルアミン (0.293 ml) を溶解したN,N-ジメチルホルムアミド(50 ml) 溶液を加えて、4℃に冷却した後、N,N'- ジシクロヘキシルカルボジイミド (494 mg) を加えて、遮光下に室温で一晩撹拌しながら反応させた。この反応液を減圧乾固し、残渣をシリカゲルカラムクロマトグラフィー (溶出液：ジクロロメタン：メタノール＝98：2溶液) で精製して3'-N-(Boc-Phe-Gly)-NH-A (A-NH_2 =DX-8951)(1.20 g)を得た。

^{1}H-NMR (DMSO-d_6) δ: 8.29 (d, 1H, J=8.0Hz), 8.21 (t, 1H, J=4.8Hz), 7.76 (d, 1H, J=10.3Hz), 7.32 (s, 1H), 7.13-7.25 (m, 5H), 6.92 (d, 1H, J=7.2Hz), 6.49 (s, 1H), 5.56-5.61 (m, 1H), 5.44 (d, 1H, J=15.9Hz), 5.38 (d, 1H, J=15.9Hz), 5.25 (s, 2H), 4.08-4.12 (m, 1H), 3.78 (d, 1H, J=4.8Hz), 3.16-3.25 (m, 2H), 2.99 (dd, 1H, J=4.0, 13.5Hz), 2.72 (dd, 1H, J=10.3, 13.5Hz), 2.40 (s, 3H), 2.09-2.35 (m, 2H), 1.80-1.91 (m, 2H), 1.16 (s, 9H), 0.88 (t, 3H, J=8.0Hz).

Mass (FAB); m/e 741 (M+1)

上で得られた3'-N-(Boc-Phe-Gly)-NH-A (170 mg)をトリフルオロ酢酸 (4 ml) に溶かし、1時間放置した。溶媒を留去し、メタノール(10 ml) で共沸を2回、エタノール(10 ml) で共沸を2回行った後、残渣をエーテルで洗浄して、標記化合物 (100 mg) を得た。

^{1}H-NMR (DMSO-d_6) δ: 8.88 (t, 1H, J=4.8Hz), 8.68 (d, 1H, J=8.7Hz), 8.05-8.15 (m, 3H), 7.79 (d, 1H, J=11.1Hz), 7.26-7.36 (m, 5H), 6.52 (d, 1H, J=7.2Hz), 5.57-5.62 (m, 1H), 5.43 (d, 1H, J=15.9Hz), 5.38 (d, 1H, J=15.9Hz), 5.19-5.28 (m, 1H), 4.10-4.18 (m, 1H), 3.93 (dd, 1H, J=4.8, 16.7Hz), 3.82 (dd, 1H, J=4.8, 16.7Hz), 3.17-3.24 (m, 2H), 3.14 (dd, 1H, J=4.8, 13.5Hz), 2.95 (dd, 1H, J=8.0, 13.5Hz), 2.42 (s, 3H), 2.14-2.25 (m, 2H), 1.83-1.91 (m, 2H), 0.89 (t, 3H, J=8.0Hz).

Mass (FAB); m/e 640 (M+1)

例50：3'-N-Gly-NH-A (A-NH_2 =DX-8951)トリフルオロ酢酸塩の合成

DX-5981 のメタンスルホン酸塩 (530 mg) とトリエチルアミン(0.28 ml) をN, N-ジメチルホルムアミド(10 ml) に溶解し、4℃に冷却した後、Boc-Gly のN-ヒドロキシスクシンイミドエステル (327 mg) を加えた。遮光下に室温で一晩撹拌しながら反応させた。この反応液を減圧乾固し、残渣をシリカゲルカラムクロマトグラフィー (溶出液：ジクロロメタン：メタノール＝98：2溶液) で精製して3'-N-(Boc-Gly)-NH-A (A-NH_2 =DX-8951) (500 mg) を得た。

^{1}H-NMR (DMSO-d_6) δ: 8.38 (d, 1H, J=8.3Hz), 7.77 (d, 1H, J=10.7Hz), 7.31 (s, 1H), 6.89-6.91 (m, 1H), 6.49 (s, 1H), 5.55-5.59 (m, 1H), 5.45 (d, 1H, J=16.1Hz), 5.38 (d, 1H, J=16.1Hz), 5.27 (d, 1H, J=19.0Hz), 5.18 (d, 1H, J=19.0Hz), 3.50-3.62 (m, 2H), 3.15-3.19 (m, 2H), 2.41 (s, 3H), 2.18-2.24 (m, 1H), 2.08-2.12

(m, 1H), 1.81-1.91 (m, 2H), 1.31 (s, 9H), 0.87 (t, 3H, J=8.0Hz).

Mass (FAB); m/e 593 (M+1)

上で得られた3'-N-(Boc-Gly)-NH-A (100 mg)をトリフルオロ酢酸 (2 ml) に溶かし、1時間放置した。溶媒を留去し、メタノール(10 ml) で共沸を2回、エタノール(10 ml) で共沸を2回行った後、残渣をエーテルで洗浄して、標記化合物(70 mg) を得た。

^{1}H-NMR (DMSO-d_6) δ: 8.88 (d, 1H, J=8.8Hz), 8.08 (s, 3H), 7.81 (d, 1H, J=11.2Hz), 7.34 (s, 1H), 6.52 (s, 1H), 5.63-5.67 (m, 1H), 5.45 (d, 1H, J=16.7Hz), 5.40 (d, 1H, J=16.7Hz), 5.36 (d, 1H, J=19.1Hz), 5.25 (d, 1H, J=19.1Hz), 3.56 (s, 2H), 3.11-3.19 (m, 2H), 2.43 (s, 3H), 2.23-2.28 (m, 1H), 2.11-2.19 (m, 1H), 1.81-1.91 (m, 2H), 0.88 (t, 3H, J=8.0Hz).

Mass (FAB); m/e 493 (M+1)

例51：<u>カルボキシメチルデキストランポリアルコールのトリメチルアンモニウム塩の合成</u>

デキストランT500 (50 g, ファルマシア社製, 分子量 500K) を0.1 M 酢酸緩衝液 (pH5.5, 5000 ml) に溶解し、過ヨウ素酸ナトリウム(165.0 g) の水溶液(5000 ml) を加えた。遮光しながら4℃で10日間撹拌した後、エチレングリコール(35.0 ml) を加え、一晩撹拌した。反応液を8 M 水酸化ナトリウム水溶液を用いて pH 7 に調整した。水素化ホウ素ナトリウム (70 g) を加えて溶解した後、一晩撹拌した。反応液を氷冷し、酢酸で pH 5.5 に調整して4℃で1時間撹拌した後、8 M 水酸化ナトリウム水溶液を用いて pH 7.5 に調整した。得られた水溶液をバイオマックス-50 膜を用いて限外濾過法による脱塩を行なった。膜を通過しない残留溶液を凍結乾燥して、デキストランポリアルコール (20.2 g) を得た。この物質の分子量 (ゲル濾過、プルラン標準) は、159Kであった。

このデキストランポリアルコール(7.5 g) を、水酸化ナトリウム (31.5 g) を水 (225 ml) に溶かして得られる水溶液に加え、室温で溶解させた。この溶液に氷冷下でモノクロル酢酸 (45 g) を加えて溶解させた後、室温で一晩反応させた。この反応液を酢酸でpHを8に調整した後、バイオマックス-50 膜を用いた限外濾過法により脱塩した。膜を通過しない残留溶液を凍結乾燥してカルボキシメチルデキ

ストランポリアルコールのナトリウム塩(8.5 g) を得た。この物質の分子量（ゲル濾過、プルラン標準）は 274K であり、カルボキシメチル化度は0.4 であった。このカルボキシメチルデキストランポリアルコールのナトリウム塩(2.0 g) を水に溶解し、Bio-Rad AG 50W-X2 (200-400 メッシュ、H^+ 型）カラム（直径 44 mm、長さ 210 mm)にのせ、水で溶出した。この溶出液にトリエチルアミン（4 ml）を加えた後、凍結乾燥して標記化合物(2.2 g) を得た。

例52：カルボキシメチルデキストランポリアルコール-Gly-Phe-Gly-NH-A'(A-NH_2 =DX-8951)の合成

例51で得たカルボキシメチルデキストランポリアルコールのトリエチルアンモニウム塩（200 mg）をN,N-ジメチルホルムアミド（7 ml）に溶解させた。この溶液に、例48で得た3'-N-(Gly-Phe-Gly)-NH-A (A-NH_2 =DX-8951) のトリフルオロ酢酸塩(41 mg) のN,N-ジメチルホルムアミド（5 ml）溶液、トリエチルアミン（0.014 ml）、1-エトキシカルボニル-2- エトキシ-1,2- ジヒドロキシキノリン（100 mg）を順次加え、室温で一晩撹拌しながら反応させた。この反応液の5 mlずつを各10 ml のエタノール中に滴下した。これに3 M 塩化ナトリウム水溶液（2.0 ml）、ジエチルエーテル(25 ml) を加えて、析出した沈澱を遠心分離（3500 rpm, 8分）により集めた。この沈澱を0.5 M 食塩水に溶解し、氷冷下0.1 M 水酸化ナトリウム水溶液で pH 9 とした。得られた水溶液をバイオマックス-50 膜を用いた限外濾過法により脱塩した。膜を通過しない残留溶液をミリポアフィルター(0.22 μm)で濾過した後、凍結乾燥して標記化合物（190 mg）を得た。本化合物の医薬化合物残基の含量を0.1 M トリス緩衝液（pH 9.0）中での 362 nm における吸光度に基づいて定量したところ 4.5% (W/W) であった。

例53：カルボキシメチルデキストランポリアルコール-Phe-Gly-NH-A'(A-NH_2 =DX-8951)の合成

例24で得たカルボキシメチルデキストランポリアルコールのナトリウム塩(2.5 g) を水に溶解し、Bio-Rad AG 50W-X2 (200-400 メッシュ、Et_3N H^+ 型）カラムにのせ、水で溶出した。この溶出液を凍結乾燥してカルボキシメチルデキストランポリアルコールのトリエチルアンモニウム塩(2.5 g) を得た。

このカルボキシメチルデキストランポリアルコールのトリエチルアンモニウム

塩（200 mg）をN,N-ジメチルホルムアミド(12 ml）に溶解させた。この溶液に、例49で得た3'-N-(Phe-Gly)-NH-A（A-NH_2 =DX-8951） のトリフルオロ酢酸塩(42 mg) とトリエチルアミン（0.016 ml）のN,N-ジメチルホルムアミド（5 ml）溶液、1-エトキシカルボニル-2- エトキシ-1,2- ジヒドロキシキノリン（200 mg）を順次加え、遮光して室温で一晩撹拌しながら反応させた。この反応液に水（300 ml）を加え、限外濾過膜10K （フィルトロン社製）を用いて限外濾過した。膜を通過しない残留溶液を0.1 N 水酸化ナトリウム水溶液で pH 10とし、濾過膜（0.16μm 、フィルトロン社製）を通過させた。通過した溶液をバイオマックス-50 膜を用いた限外濾過法により脱塩し、次いでミリポアフィルター(0.22 μm)で濾過した後、凍結乾燥して標記化合物（180 mg）を得た。本化合物の医薬化合物残基の含量を0.1 M トリス緩衝液（pH 9.0）中での 362 nm における吸光度に基づいて定量したところ 6.1%（W/W）であった。

例54：カルボキシメチルデキストランポリアルコール-Gly-NH-A'(A-NH_2 =DX-8951)の合成

例51で得たカルボキシメチルデキストランポリアルコールのトリエチルアンモニウム塩（370 mg）をN,N-ジメチルホルムアミド(10 ml）に溶解させた。この溶液に、例50で得た3'-N-Gly-NH-A（A-NH_2 =DX-8951） のトリフルオロ酢酸塩(57 mg) のN,N-ジメチルホルムアミド（3 ml）溶液、トリエチルアミン（0.027 ml）、1-エトキシカルボニル-2- エトキシ-1,2- ジヒドロキシキノリン（185 mg）を順次加え、室温で一晩撹拌しながら反応させた。この反応液の5 mlずつを各10 ml のエタノール中に滴下した。これに3 M 塩化ナトリウム水溶液（2.0 ml）、ジエチルエーテル(25 ml）を加えて、析出した沈澱を遠心分離（3500 rpm, 8分）により集めた。この沈澱を0.5 M 食塩水に溶解し、氷冷下0.1 M 水酸化ナトリウム水溶液で pH 9 とした。得られた水溶液をバイオマックス-50 膜を用いた限外濾過法により脱塩した。膜を通過しない残留溶液をミリポアフィルター(0.22 μm)で濾過した後、凍結乾燥して標記化合物（290 mg）を得た。本化合物の医薬化合物残基の含量を0.1 M トリス緩衝液（pH 9.0）中での 362 nm における吸光度に基づいて定量したところ 0.5%（W/W）であった。

例55：カルボキシメチルデキストランポリアルコール-Gly-Gly-Phe-Gly-D51-7059

の合成

Boc-Gly-Gly-Phe-Gly-OH (200 mg) をトリフルオロ酢酸 (4 ml) に溶かし、1.5 時間撹拌した。溶媒を留去し、メタノール(10 ml) で共沸を2回、エタノール(10 ml) で共沸を2回行った後、残渣をエーテルで洗浄して、Gly-Gly-Phe-Gly-OHのトリフルオロ酢酸塩 (225 mg) を得た。

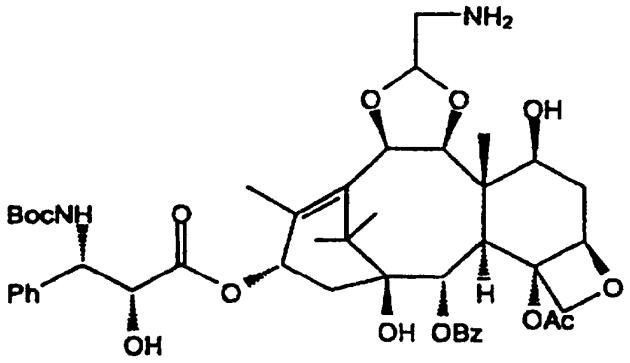
^{1}H-NMR (DMSO-d_6) δ: 8.48 (dd, 1H, J=5.6, 5.6Hz), 8.59 (dd, 1H, J=5.6, 6.4Hz), 8.29 (d, 1H, J=4.8Hz), 7.23-7.26 (m, 4H), 7.16-7.20 (m, 1H), 4.58 (ddd, 1H, J=4.8, 4.8, 10.4Hz), 3.89 (dd, 1H, J=5.6, 16.7Hz), 3.76-3.79 (m, 2H), 3.67 (dd, 1H, J=5.6, 16.7Hz), 3.56 (s, 2H).

上で得られたGly-Gly-Phe-Gly-OHのトリフルオロ酢酸塩 (200 mg) を、水(10 ml) に溶解し、トリエチルアミンを加えて pH 9.0 に調整した後、9-フレオレニルメチルN-ヒドロキシスクシンイミジルカルボネート (200 mg) のアセトニトリル (5 ml) 溶液を加え、次いでトリエチルアミンを用いて pH 8.0-8.5 に維持しながら室温で4時間撹拌した。反応液に1.5 N 塩酸 (50 ml)を加え、析出した沈澱を濾取し、水で洗浄した後、シリカゲルカラムクロマトグラフィー (溶出液：ジクロロメタン：メタノール＝4：1溶液) で精製してFmoc-Gly-Gly-Phe-Gly-OH (151 mg)を得た。

^{1}H-NMR (DMSO-d_6) δ: 8.28-8.32 (m, 1H), 8.08-8.12 (m, 1H), 7.85-7.89 (m, 2H), 7.68-7.72 (m, 2H), 7.57-7.65 (m, 1H), 7.38-7.43 (m, 2H), 7.29-7.34 (m, 2H), 7.20-7.25 (m, 4H), 7.14-7.17 (m, 1H), 4.45-4.52 (m, 1H), 4.26-4.30 (m, 2H), 4.19-4.24 (m, 1H), 3.77 (dd, 1H, J=5.6, 16.7Hz), 3.58-3.69 (m, 4H), 3.42-3.52 (m, 1H), 3.06 (dd, 1H, J=4.0, 13.5Hz), 2.78 (dd, 1H, J=4.0, 13.5Hz).

上で得られたFmoc-Gly-Gly-Phe-Gly-OH (24 mg) 、下記の式：

OnCusp
Ex. 1002



で表されるタキソール誘導体（D51-7059: 9,10-O-(2-アミノエチリデン)-13-O-[3-(tert-ブトキシカルボニルアミノ)-2-ヒドロキシ-3- フェニル]-プロパノイル-10-デアセチル-9- ジヒドロバカチン III）（20 mg）およびN-ヒドロキシスクシンイミド（7 mg）をN,N-ジメチルホルムアミド（1 ml）に溶解した。この溶液を4℃に冷却した後、N, N'-ジシクロヘキシルカルボジイミド（9 mg）を添加し、室温で一晩撹拌しながら反応させた。この反応液を減圧乾固し、残渣をシリカゲルカラムクロマトグラフィー（溶出液：ジクロロメタン：メタノール＝96：4溶液）で精製してFmoc-Gly-Gly-Phe-Gly-D51-7059（21 mg）を得た。

^{1}H-NMR ($CDCl_3$) δ: 8.06 (d, 2H, J=8.1Hz), 7.75 (d, 2H, J=8.1Hz), 7.18-7.61 (m, 23H), 7.62 (dd, 1H, J=7.2, 8.0Hz), 6.07 (dd, 1H, J=7.9, 8.8Hz), 5.98 (d, 1H, J=4.8Hz), 5.63 (d, 1H, J=8.8Hz), 5.00-5.40 (m, 4H), 4.92 (s, 1H), 4.60-4.69 (m, 2H), 4.41 (d, 2H, J=6.4Hz), 4.35 (d, 1H, J=8.0Hz), 4.29 (d, 1H, J=8.0Hz), 4.21 (t, 1H, J=7.5Hz), 3.96-4.07 (m, 3H), 3.73-3.86 (m, 4H), 3.37-3.41 (m, 1H), 3.19-3.23 (m, 1H), 3.00 (dd, 1H, J=8.0, 13.5Hz), 2.85-2.89 (m, 3H), 2.29 (s, 3H), 2.05-2.40 (m, 4H), 1.57 (s, 3H), 1.56 (s, 3H), 1.53 (s, 3H), 1.40 (s, 9H), 1.22 (s, 3H).

Mass (FAB); m/e 1413 (M+Na)

上記で得られたFmoc-Gly-Gly-Phe-Gly-D51-7059（21 mg）をジクロロメタン（1.8 ml）に溶解させ、ピペラジン（0.2 ml）を加えた後、室温で1時間反応させた。この反応液をシリカゲルカラムクロマトグラフィー（溶出液：ジクロロメタン：メタノール＝94：6溶液）で精製してGly-Gly-Phe-Gly-D51-7059（16 mg)を得た。

^{1}H-NMR ($CDCl_3$) δ: 8.10 (d, 2H, J=8.1Hz), 7.89-7.94 (m, 1H), 7.62 (dd, 1H, J=7.2, 8.0Hz), 7.45-7.50 (m, 2H), 7.17-7.42 (m, 12H), 7.10-7.16 (m, 1H), 6.97 (dd, 1H, J=5.6, 6.4Hz), 6.08 (dd, 1H, J=8.0, 8.7Hz), 6.02 (d, 1H, J=4.8Hz), 5.62 (d, 1H, J=11.1Hz), 5.23-5.30 (m, 1H), 5.23 (d, 1H, J=7.2Hz), 5.10 (s, 1H), 4.98-5.00 (m, 1H), 4.60-4.63 (m, 1H), 4.38 (d, 1H, J=8.8Hz), 4.33 (d, 1H, J=8.8Hz), 4.13 (s, 1H), 4.04 (dd, 1H, J=5.6, 16.7Hz), 3.93 (dd, 1H, J=5.6, 16.7Hz), 3.82 (d, 1H, J=7.2Hz), 3.73-3.82 (m, 2H), 3.43-3.49 (m, 1H), 3.30-3.38 (m, 2H), 3.24 (dd, 1H, J=6.4, 14.3Hz), 3.04 (dd, 1H, J=8.0, 14.3Hz), 2.89-3.07 (m, 3H), 2.30 (s, 3H), 2.01-2.50 (m, 4H), 1.70 (s, 3H), 1.62 (s, 3H), 1.61 (s, 3H), 1.40 (s, 9H), 1.26 (s, 3H).

Mass (FAB); m/e 1169 (M+1)

以上の方法で合成したGly-Gly-Phe-Gly-D51-7059(33 mg) をN,N-ジメチルホルムアミド (0.5 ml) に溶解させた。この溶液に、例24で得たカルボキシメチルデキストランポリアルコールのトリエチルアンモニウム塩 (180 mg) のN,N-ジメチルホルムアミド (7 ml) 溶液、1-エトキシカルボニル-2- エトキシ-1,2- ジヒドロキシキノリン (180 mg) を順次加え、室温で一晩撹拌しながら反応させた。この反応液の4 mlずつを各10 ml のエタノール中に滴下した。それぞれに3 M 塩化ナトリウム水溶液 (2.0 ml) 、ジエチルエーテル(25 ml) を加えて、析出した沈澱を遠心分離 (2500 rpm, 8分) により集めた。この沈澱をエタノールで洗浄した後、水に溶解し、Bio-Rad AG 50W-X2 (200-400 メッシュ、Na^+ 型) カラム (直径 15 mm、長さ 85 mm) にのせ、水で溶出し、溶出液1を得た。別に、Gly-Gly-Phe-Gly-D51-7059 (10 mg) をN,N-ジメチルホルムアミド (0.5 ml) に溶解させた後、例24で得たカルボキシメチルデキストランポリアルコールのトリエチルアンモニウム塩(60 mg) のN,N-ジメチルホルムアミド (5 ml) 溶液、1-エトキシカルボニル-2- エトキシ-1,2- ジヒドロキシキノリン(60 mg) のN,N-ジメチルホルムアミド(0.25 ml) 溶液を順次加え、室温で一晩撹拌しながら反応させた。この反応液を10 ml のエタノール中に滴下した後、3 M 塩化ナトリウム水溶液 (2.0 ml) 、ジエチルエーテル(25 ml) を加え、析出した沈澱を遠心分離 (2500 rpm, 8分) により集めた。この沈澱をエタノールで洗浄した後、水に溶解し、Bio-Rad AG 50W-X2 (200-400 メッシ

ュ、Na^+ 型）カラム（直径 15 mm、長さ 85 mm）にのせ、水で溶出し、溶出液２を得た。溶出液１と溶出液２を合した後、バイオマックス-50 膜を用いた限外濾過法により脱塩した。膜を通過しない残留溶液をミリポアフィルター(0.22 μm)で濾過した後、凍結乾燥して標記化合物（208 mg）を得た。本化合物を0.1 M 塩化ナトリウム水溶液に溶解後、GPC （カラム：東ソー TSK Gel PW-4000XL、溶媒： 0.1M NaCl、流速： 0.8 ml/min ）で分析した結果、及び本化合物の紫外線吸収スペクトル（メタノール：水＝10：１溶液、1.69 mg/ml）をそれぞれ図22および図23に示す。本化合物の医薬化合物残基の含量をメタノール：水＝10：１溶液中での 240 nm における吸光度に基づいて定量したところ、 5.3% (W/W) であった。

例56：本発明の薬物複合体の抗腫瘍作用

例11と同様の方法により Meth A 担癌マウスを作成し（１群６匹）、例15の薬物複合体について、例12と同様の方法で単回投与した場合の抗腫瘍作用を調べた。その結果、例15の薬物複合体は例12の医薬化合物自体に比べて、顕著な抗腫瘍効果の増強と有効用量域の拡大を示した。

被検化合物	投与量(mg/kg)[1)]	抑制率(%)
例15の化合物	10	100
	5	99
	2.5	95
	1.25	83

1)医薬化合物換算量

例57：本発明の薬物複合体の抗腫瘍作用

ヒト胃癌 SC-6 の腫瘍塊をヌードマウス（BALB/c-nu/nu, 雄）の右鼠径部皮下に移植して SC-6 担癌ヌードマウスを作成した（１群５匹）。移植後24日目に注射用蒸留水に溶解した例15の薬物複合体を静脈内に単回投与し、抗腫瘍作用を医薬化合物自体と比較した。その結果、例15の薬物複合体は医薬化合物自体に比べて、毒性死を示すことなく、高い抗腫瘍効果を発揮した。

被検化合物	投与量(mg/kg)	抑制率(%)	死亡マウス数／使用マウス数
医薬化合物自体	60	98	2/5
	15	61	0/5
例15の化合物	8[1)]	100	0/5
	2[1)]	71	0/5

1)医薬化合物換算量

例58：本発明の薬物複合体の抗腫瘍作用

例57と同様の方法によりヒト肺癌 QG-90担癌ヌードマウスを作成した（１群５匹）。移植後16日目に注射用蒸留水に溶解した例15の薬物複合体を静脈内に単回投与し、抗腫瘍作用を医薬化合物自体と比較した。その結果、例15の薬物複合体は医薬化合物自体に比べて、顕著な抗腫瘍効果の増強と有効用量域の拡大を示した。

被検化合物	投与量(mg/kg)	抑制率(%)	死亡マウス数／使用マウス数
医薬化合物自体	50	60	0/5
	12.5	51	0/5
例15の化合物	7[1)]	98	0/5
	1.75[1)]	97	0/5

1)医薬化合物換算量

例59：本発明の薬物複合体の抗腫瘍作用

例11と同様の方法により Meth A 担癌マウスを作成し（１群６匹）、例12と同様の方法で例41の薬物複合体を単回投与した場合の抗腫瘍作用を医薬化合物自体と比較した。その結果、例41の薬物複合体は医薬化合物自体に比べて、顕著な抗腫瘍効果の増強と有効用量域の拡大を示した。

被検化合物	投与量(mg/kg)	抑制率(%)
医薬化合物自体	100	64
	50	56
	25	34
例41の化合物	25[1)]	99
	12.5[1)]	95
	6.25[1)]	81
	3.125[1)]	61

[1)]医薬化合物換算量

例60：本発明の薬物複合体の抗腫瘍作用

例11と同様の方法により Meth A 担癌マウスを作成し（１群６匹）、例12と同様の方法で例29、例46および例47の各薬物複合体をそれぞれ単回投与した場合の抗腫瘍作用を調べた。

その結果、何れの薬物複合体も高い抗腫瘍効果と広い有効用量域を示した。

被検化合物	投与量(mg/kg)[1)]	抑制率(%)
例29の化合物	30	99
	20	99
	10	89
	5	79
例46の化合物	100	94
	80	92
	40	82
	20	75
例47の化合物	100	96

80	94
40	97
20	75

1)医薬化合物換算量

例61：本発明の薬物複合体の抗腫瘍作用

例11と同様の方法により Meth A 担癌マウスを作成し（１群６匹）、例44の薬物複合体について、例12と同様の方法で単回投与して抗腫瘍作用を医薬化合物自体（ドキソルビシン）と比較した。その結果、例44の薬物複合体は医薬化合物自体に比べて、顕著な抗腫瘍効果の増強と有効用量域の拡大を示した。

被検化合物	投与量(mg/kg)	抑制率(%)	死亡マウス数／使用マウス数
医薬化合物自体	20		6/6
	10	64	0/6
	5	39	0/6
例44の化合物	40[1)]	96	0/6
	20[1)]	96	0/6
	10[1)]	87	0/6
	5[1)]	76	0/6

1)医薬化合物換算量

例62：本発明の薬物複合体の体内動態

例11と同様の方法により Meth A 担癌マウスを作成し、例15の薬物複合体について、例12と同様の方法で単回投与（10 mg/kg：医薬化合物換算量）して、薬物複合体の各組織内における濃度推移を調べた。その結果、例15の薬物複合体は著しく高い血中滞留性、腫瘍組織への高い移行性および肝臓と小腸に対する高い腫瘍選択性を示した。結果を図24に示す。

産業上の利用可能性

例えば抗腫瘍剤である医薬化合物の残基を導入した本発明の薬物複合体は、腫瘍部位選択性に優れており、高い抗腫瘍作用を発揮できるとともに、毒性の発現も軽減されているという特徴を有している。

OnCusp
Ex. 1002

請 求 の 範 囲

1．1個のアミノ酸からなるスペーサー又はペプチド結合した 2～8 個のアミノ酸からなるスペーサーを介してカルボキシC_{1-4}アルキルデキストランポリアルコールと医薬化合物の残基とが結合していることを特徴とする薬物複合体。

2．カルボキシC_{1-4}アルキルデキストランポリアルコールを構成するデキストランポリアルコールが、実質的に完全にポリアルコール化可能な条件下でデキストランを処理して得られたデキストランポリアルコールであることを特徴とする、請求の範囲第1項に記載の薬物複合体。

3．カルボキシC_{1-4}アルキルデキストランポリアルコールがカルボキシメチルデキストランポリアルコールである請求の範囲第1項または第2項に記載の薬物複合体。

4．医薬化合物が抗腫瘍剤又は抗炎症剤である請求の範囲第1項ないし第3項のいずれか1項に記載の薬物複合体。

5．医薬化合物が濃度依存型の抗腫瘍作用を発現する抗腫瘍剤である請求の範囲第4項に記載の薬物複合体。

6．医薬化合物が時間に依存した抗腫瘍作用を発現する抗腫瘍剤である請求の範囲第4項に記載の薬物複合体。

7．抗腫瘍剤がドキソルビシン又は（1S,9S)-1- アミノ-9- エチル-5- フルオロ-2,3- ジヒドロ-9- ハイドロキシ-4- メチル-1H,12H-ベンゾ[de]ピラノ[3',4':6,7] インドリジノ[1,2-b] キノリン-10,13(9H,15H)- ジオンである請求の範囲第4項に記載の薬物複合体。

8．スペーサーが -X-Z-で表されるジペプチド（-X-Z- は疎水性アミノ酸(X) と親水性アミノ酸(Z) とがそれぞれN末端側及びC末端側となってペプチド結合して形成されるジペプチドのN末端のアミノ基及びC末端のカルボキシル基から、それぞれ1個の水素原子及び1個の水酸基を除いた残基を示す）であるか、又は該ジペプチドを部分ペプチド配列として含むスペーサーである請求の範囲第5項ないし7項のいずれか1項に記載の薬物複合体。

9．疎水性アミノ酸がフェニルアラニンであり、親水性アミノ酸がグリシンであ

る請求の範囲第８項に記載の薬物複合体。

１０．スペーサーが（N 末端)-Gly-Gly-Phe-Gly-である請求の範囲第９項に記載の薬物複合体。

１１．抗腫瘍剤の残基の導入量が 1～15重量% の範囲である請求の範囲第５項ないし第１０項のいずれか１項に記載の薬物複合体。

１２．抗腫瘍剤の残基の導入量が 3～10重量% の範囲である請求の範囲第５項ないし第１０項のいずれか１項に記載の薬物複合体。

１３．抗腫瘍剤の残基の導入量が 5～6 重量% の範囲である請求の範囲第５項ないし第１０項のいずれか１項に記載の薬物複合体。

１４．H_2N-Gly-Gly-Phe-Gly-COOHで示されるペプチドのN末端がカルボキシメチルデキストランポリアルコールのカルボキシル基に酸アミド結合しており、該ペプチドのC末端が（1S,9S)-1- アミノ-9- エチル-5- フルオロ-2,3- ジヒドロ-9- ハイドロキシ-4- メチル-1H,12H-ベンゾ[de]ピラノ[3',4':6,7] インドリジノ[1,2-b] キノリン-10,13(9H,15H)- ジオンの1-アミノ基と酸アミド結合した請求の範囲第１項に記載の薬物複合体。

１５．（1S,9S)-1- アミノ-9- エチル-5- フルオロ-2,3- ジヒドロ-9- ハイドロキシ-4- メチル-1H,12H-ベンゾ[de]ピラノ[3',4':6,7] インドリジノ[1,2-b] キノリン-10,13(9H,15H)- ジオン残基の導入量が 2～10重量% の範囲である請求の範囲第14項に記載の薬物複合体。

１６．カルボキシC_{1-4}アルキルデキストランポリアルコールが分子量 5,000ないし 500,000の範囲のカルボキシメチルデキストランポリアルコールであり、カルボキシメチル化度が 0.01 ～2.0 の範囲である請求の範囲第14項又は第15項に記載の薬物複合体。

１７．カルボキシC_{1-4}アルキルデキストランポリアルコールが分子量50,000～450,000 の範囲のカルボキシメチルデキストランポリアルコールであり、カルボキシメチル化度が 0.1～1.0 の範囲である請求の範囲第14項又は第15項に記載の薬物複合体。

１８．カルボキシC_{1-4}アルキルデキストランポリアルコールが分子量 200,000～400,000 の範囲のカルボキシメチルデキストランポリアルコールであり、カルボキシメ

チル化度が 0.3～0.5 の範囲である請求の範囲第14項又は第15項に記載の薬物複合体。

１９．(1S,9S)-1- アミノ-9- エチル-5- フルオロ-2,3- ジヒドロ-9- ハイドロキシ-4- メチル-1H,12H-ベンゾ[de]ピラノ[3',4':6,7] インドリジノ[1,2-b] キノリン-10,13(9H,15H)- ジオン残基の導入量が 5～6 重量% の範囲であり、カルボキシC_{1-4}アルキルデキストランポリアルコールの分子量が約 228,000であり、カルボキシメチル化度が約 0.4である請求の範囲第14項に記載の薬物複合体。

２０．医薬化合物を結合するための薬物送達のキャリアーであって、カルボキシC_{1-4}アルキルデキストランポリアルコールからなる薬物送達のキャリアー。

２１．カルボキシC_{1-4}アルキルデキストランポリアルコールの分子量が 5,000～500,000 の範囲であり、カルボキシC_{1-4}アルキル化度が0.01～2.0 の範囲である請求の範囲第20項に記載の薬物送達のキャリアー。

２２．カルボキシC_{1-4}アルキルデキストランポリアルコールの分子量が50,000～450,000 の範囲であり、カルボキシC_{1-4}アルキル化度が 0.1～1.0 の範囲である請求の範囲第20項に記載の薬物送達のキャリアー。

２３．カルボキシC_{1-4}アルキルデキストランポリアルコールの分子量が 200,000～400,000 の範囲であり、カルボキシC_{1-4}アルキル化度が 0.3～0.5 の範囲である請求の範囲第20項に記載の薬物送達のキャリアー。

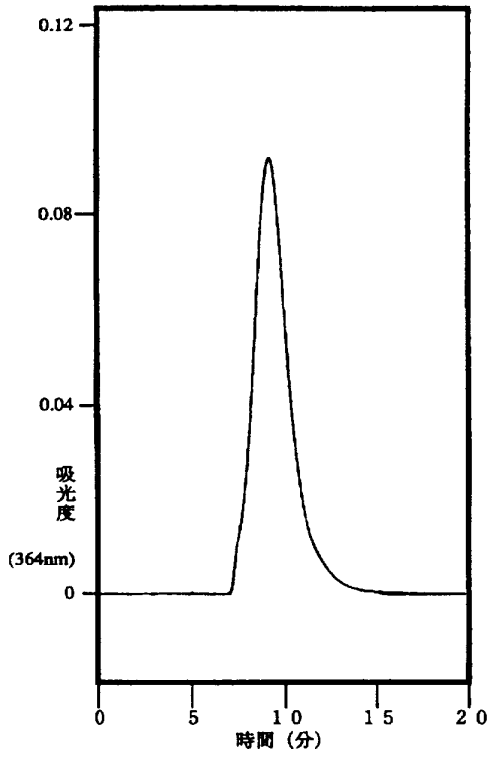
２４．カルボキシC_{1-4}アルキルデキストランポリアルコールがカルボキシメチルデキストランポリアルコールである請求の範囲第20項ないし第23項のいずれか１項に記載の薬物送達のキャリアー。

２５．医薬化合物の残基と結合したカルボキシC_{1-4}アルキルデキストランポリアルコールを含む薬物複合体の製造のためのカルボキシC_{1-4}アルキルデキストランポリアルコールの使用。

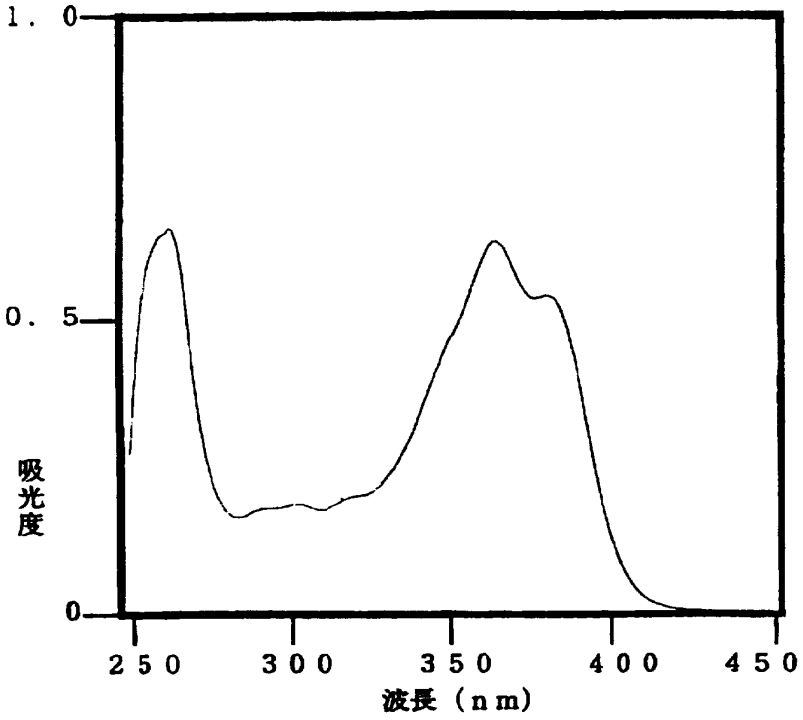
２６．医薬化合物の残基とカルボキシC_{1-4}アルキルデキストランポリアルコールとがスペーサーを介して、又はスペーサーを介さずに結合した薬物複合体の製造のためのカルボキシC_{1-4}アルキルデキストランポリアルコールの使用。

OnCusp
Ex. 1002

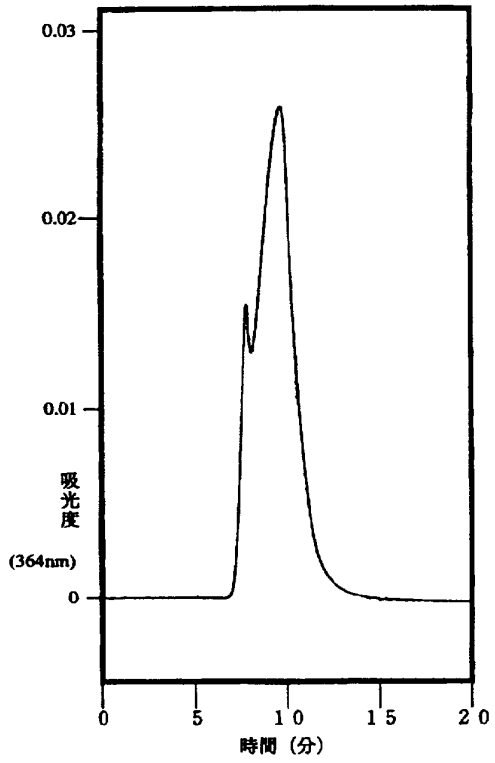
第１図



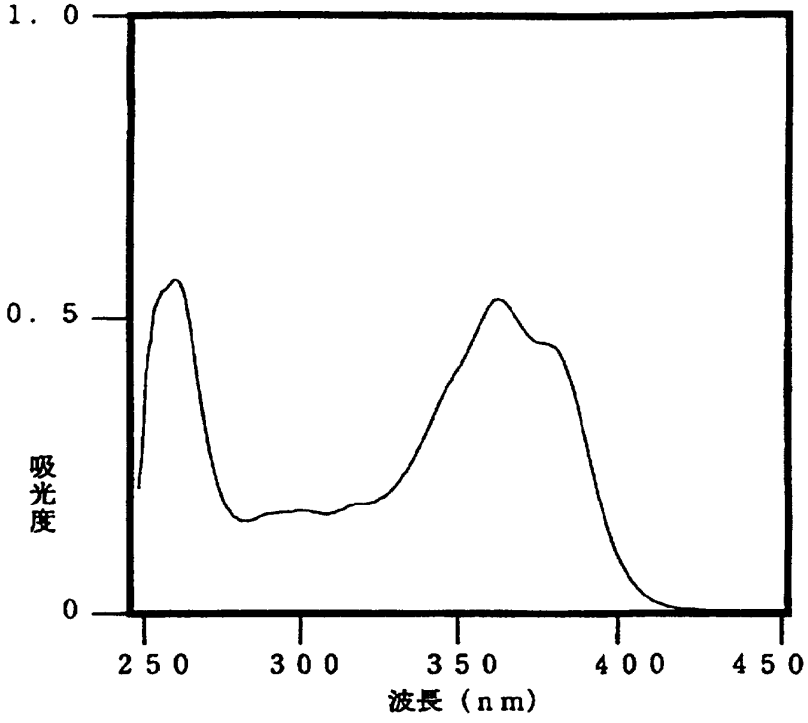
第２図



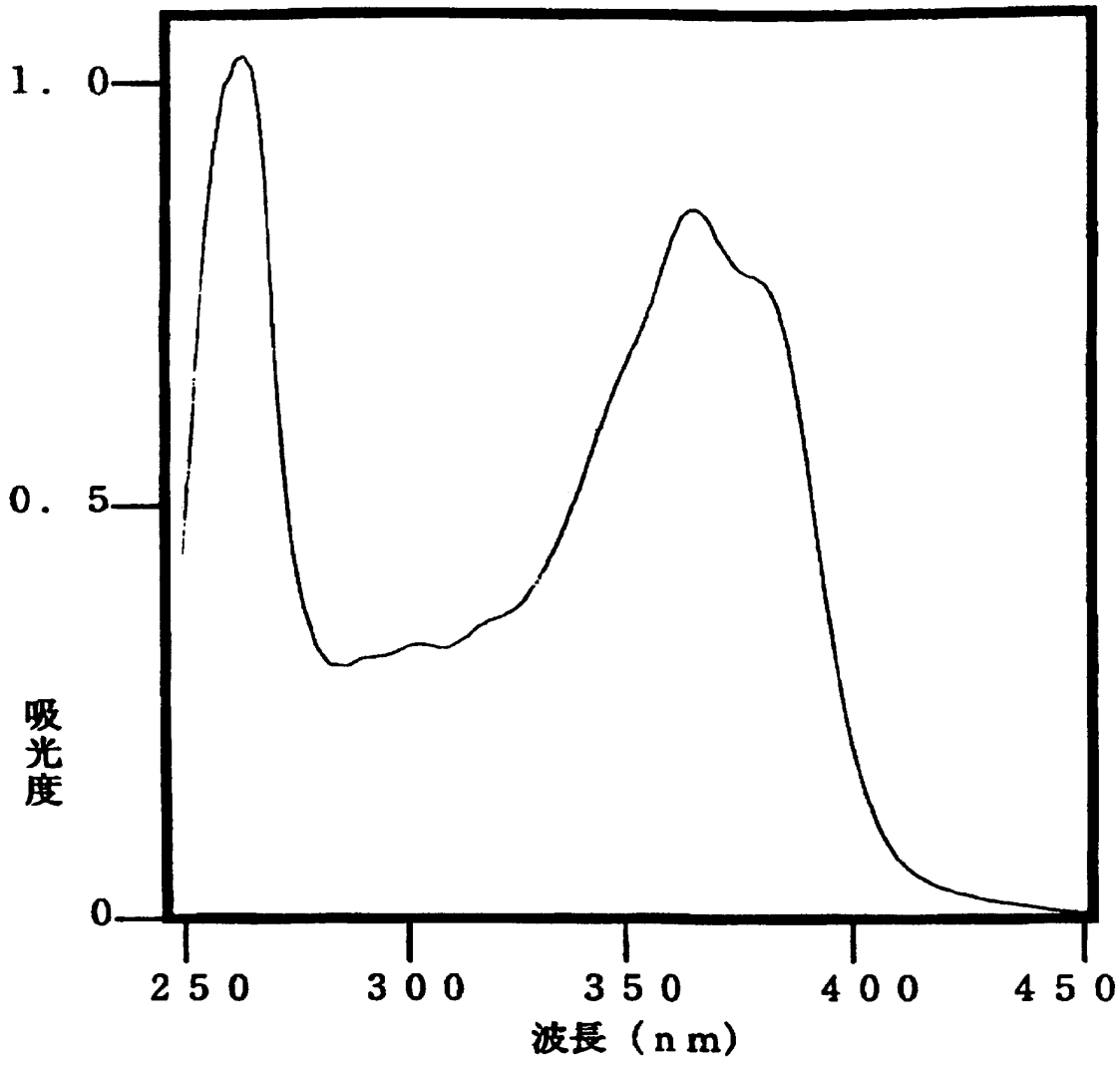
第３図


0.03
0.02
0.01
吸光度
(364nm)
0
0
5
10
15
20
時間（分）

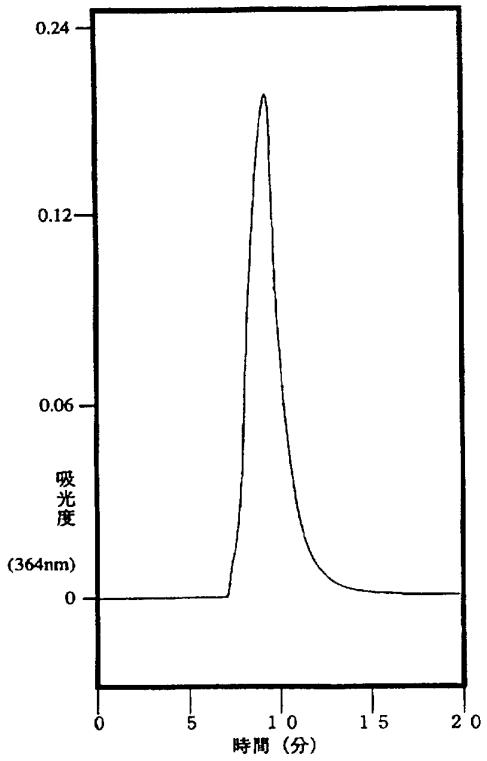
第４図


1．0
0．5
0
吸光度
250
300
350
400
450
波長（nm）

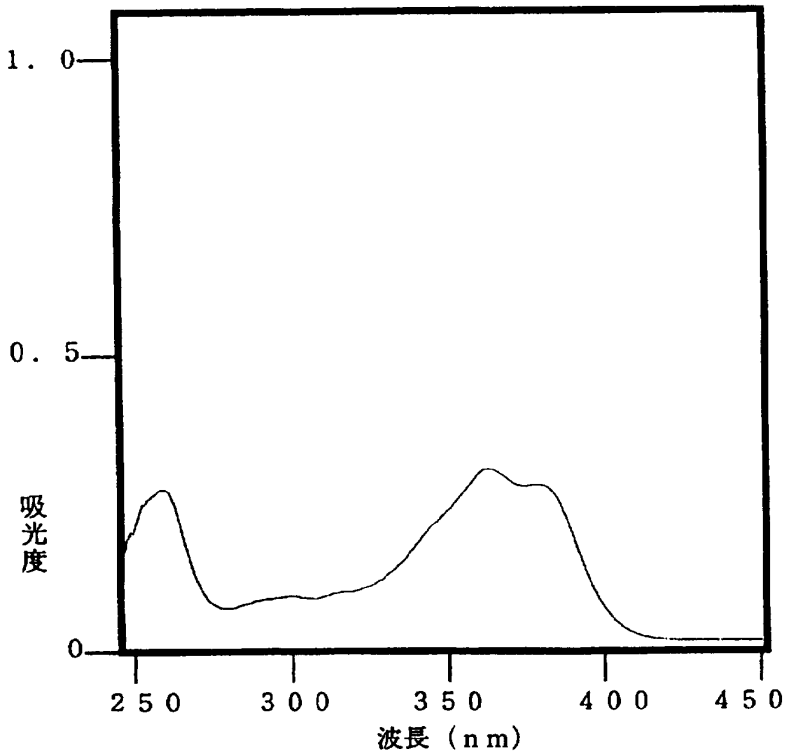
第５図



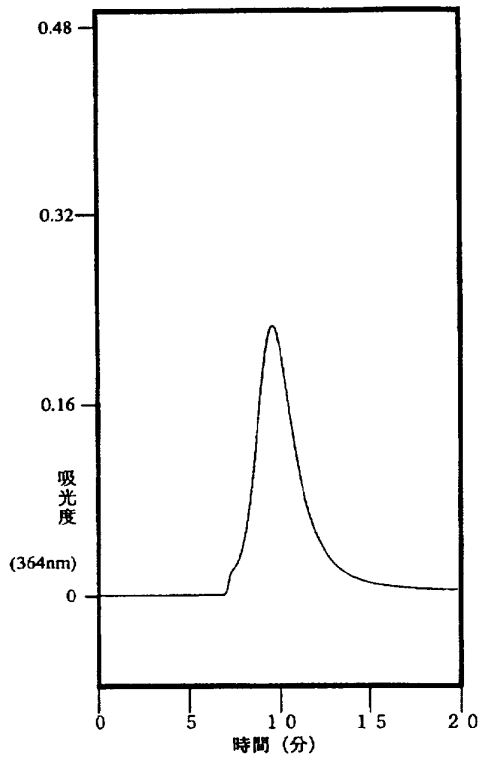
第６図


0.24
0.12
0.06
吸光度
(364nm)
0
0
5
10
15
20
時間（分）

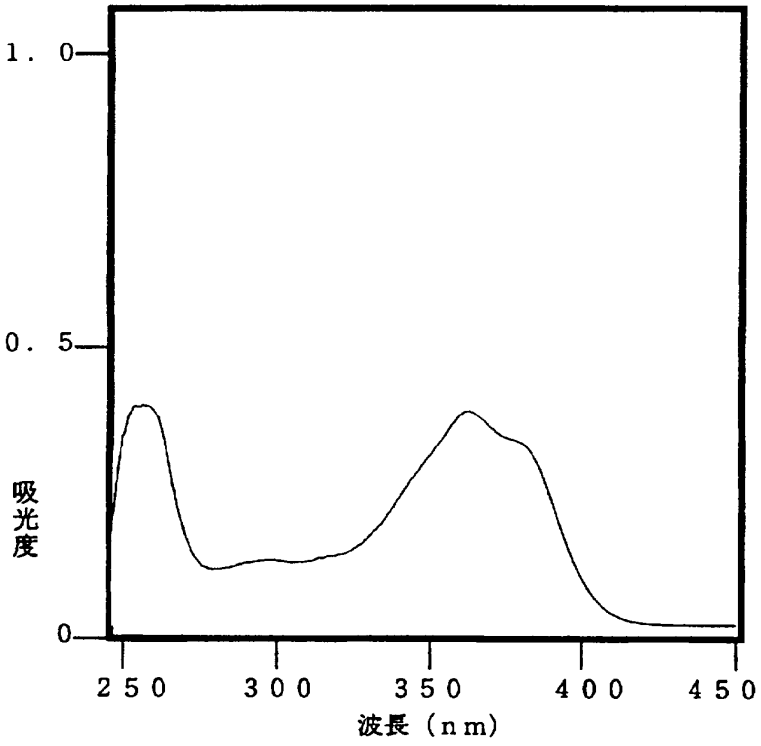
第７図


1．0
0．5
0
吸光度
250
300
350
400
450
波長（nm）

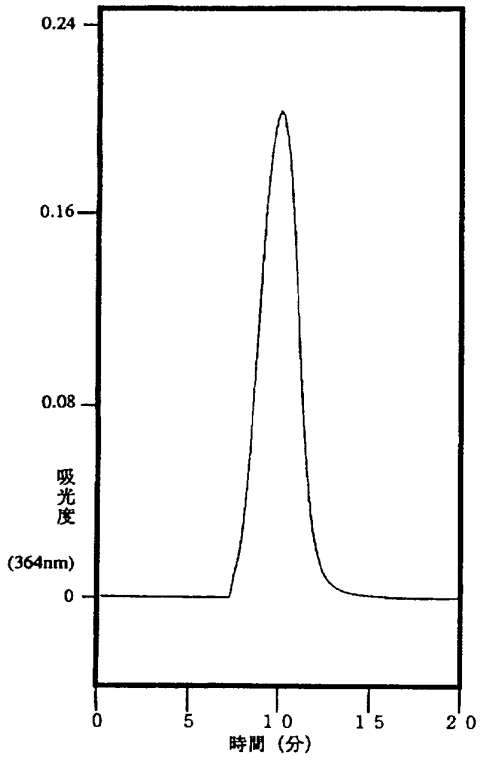
第８図


0.48
0.32
0.16
吸光度
(364nm)
0
0
5
10
15
20
時間（分）

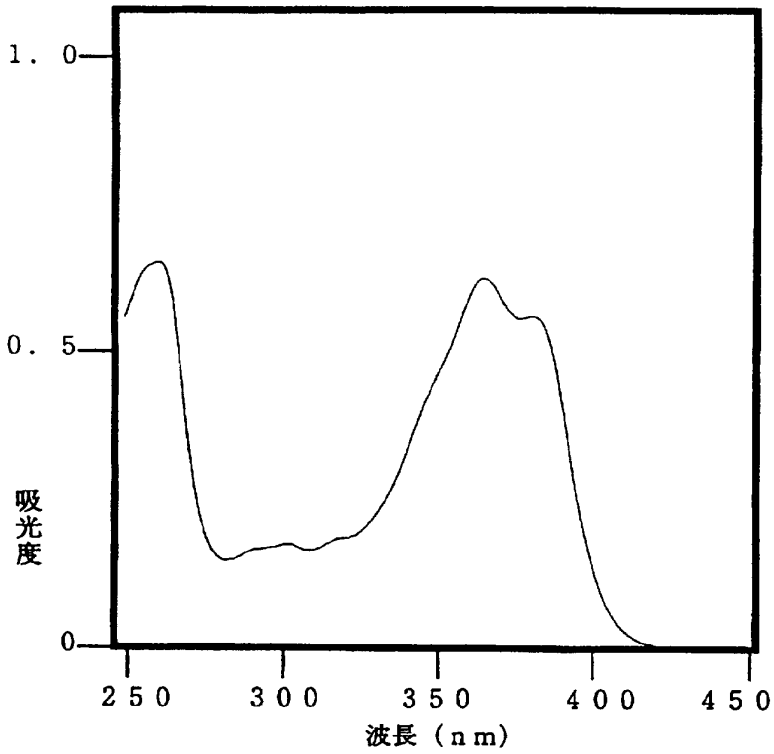
第９図


1．0
0．5
0
吸光度
250
300
350
400
450
波長（nm）

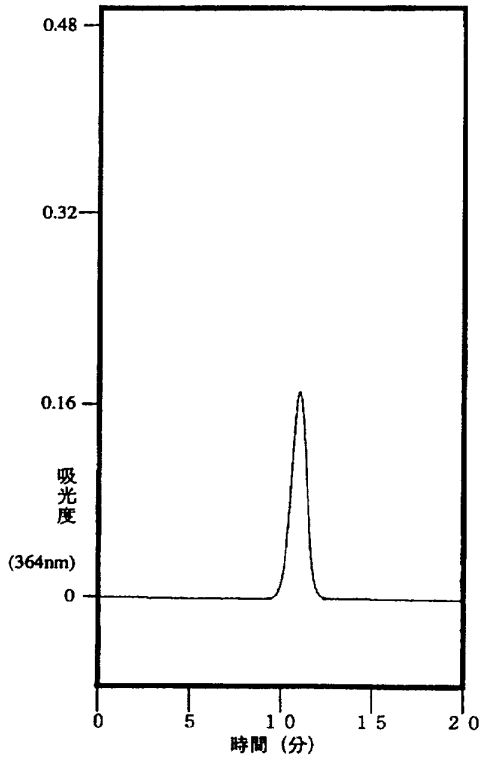
第10図


0.24
0.16
0.08
吸光度
(364nm)
0
0
5
10
15
20
時間（分）

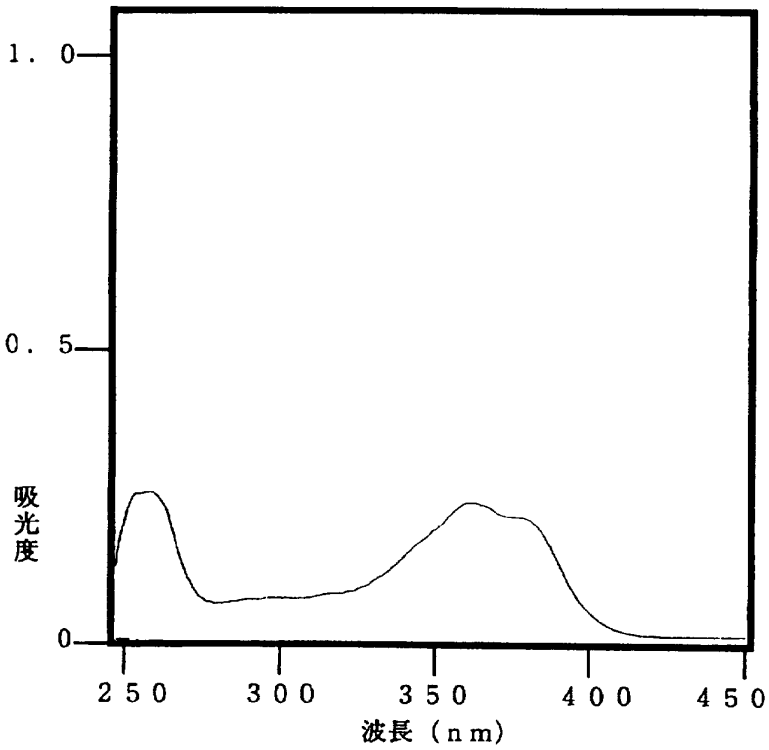
第11図


1．0
0．5
0
吸光度
250
300
350
400
450
波長（nm）

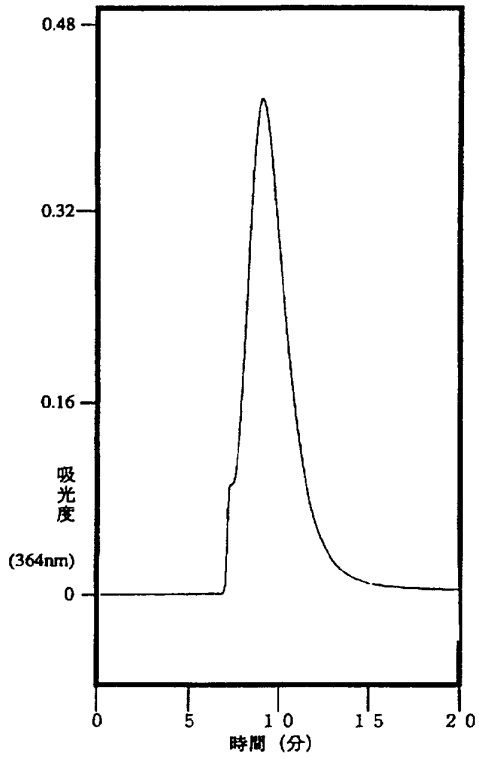
第12図


0.48
0.32
0.16
吸光度
(364nm)
0
0
5
10
15
20
時間（分）

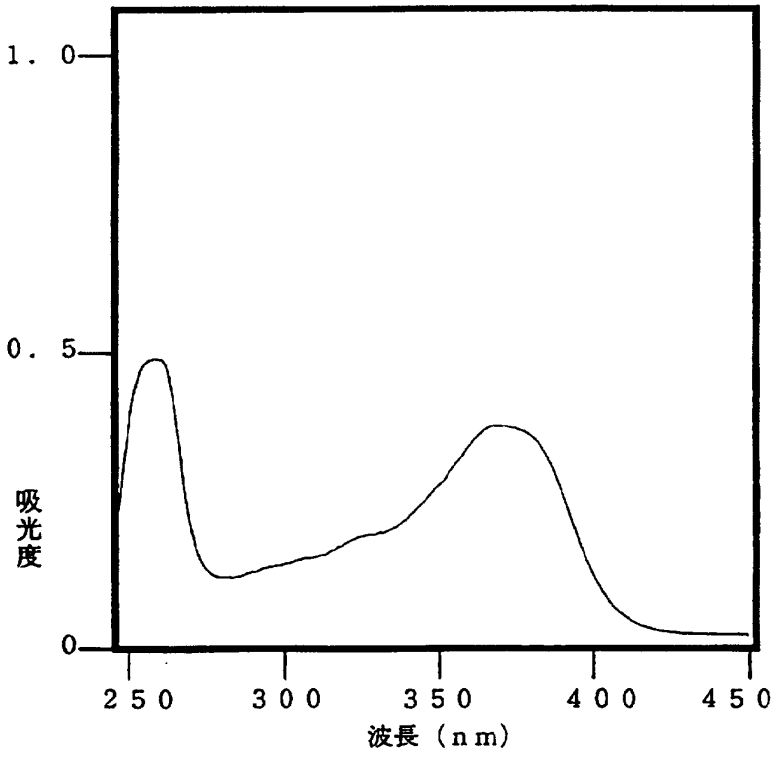
第13図


1．0
0．5
吸光度
0
250
300
350
400
450
波長（nm）

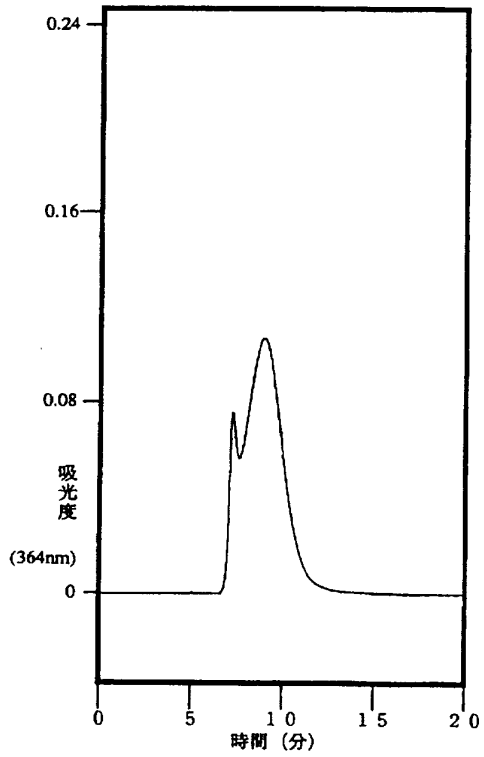
第14図


0.48
0.32
0.16
吸光度
(364nm)
0
0
5
10
15
20
時間（分）

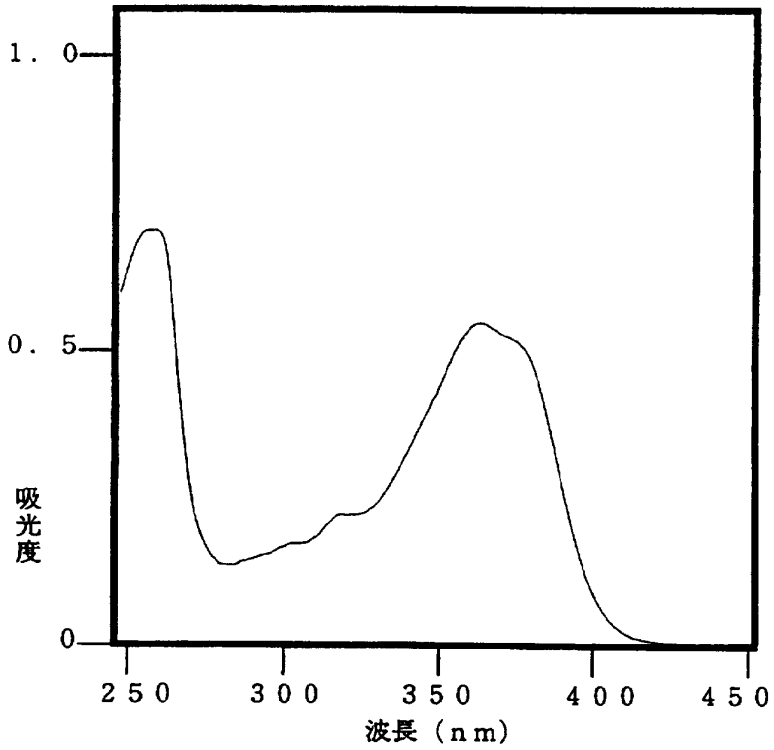
第15図


1.0
0.5
吸光度
0
250
300
350
400
450
波長（nm）

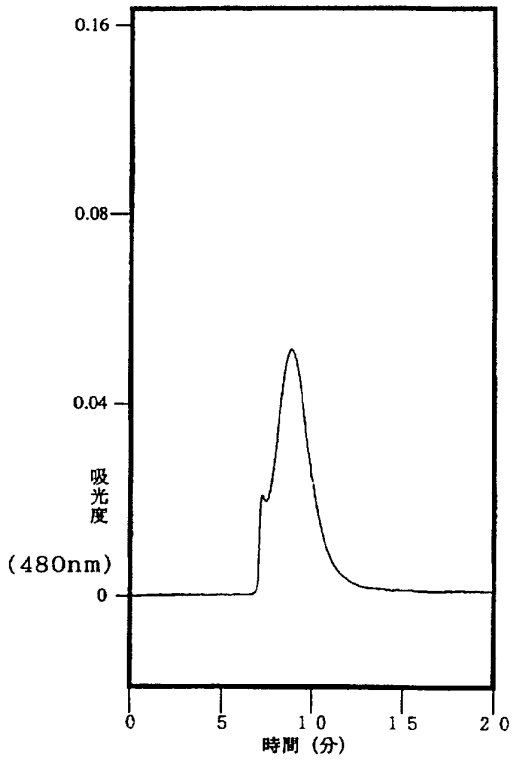
第16図


0.24
0.16
0.08
吸光度
(364nm)
0
0
5
10
15
20
時間（分）

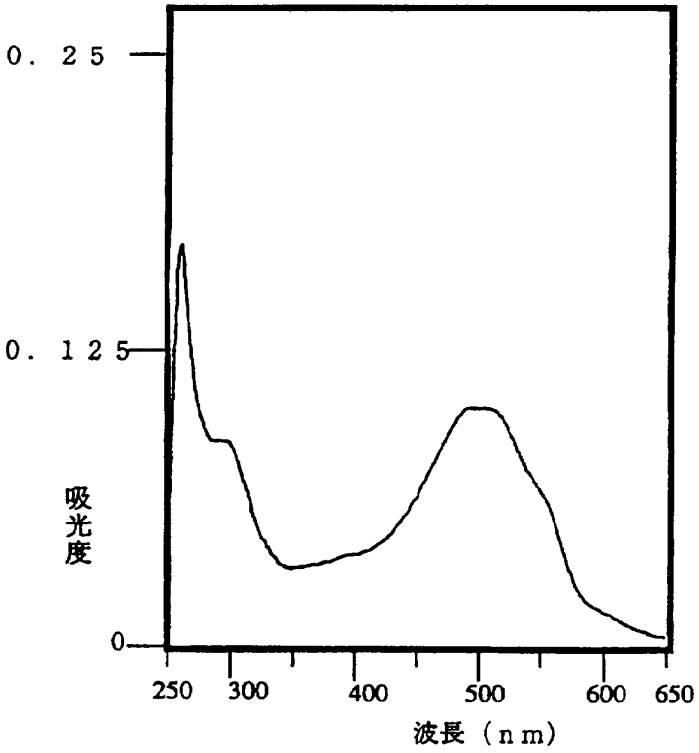
第17図


1．0
0．5
0
吸光度
250
300
350
400
450
波長（nm）

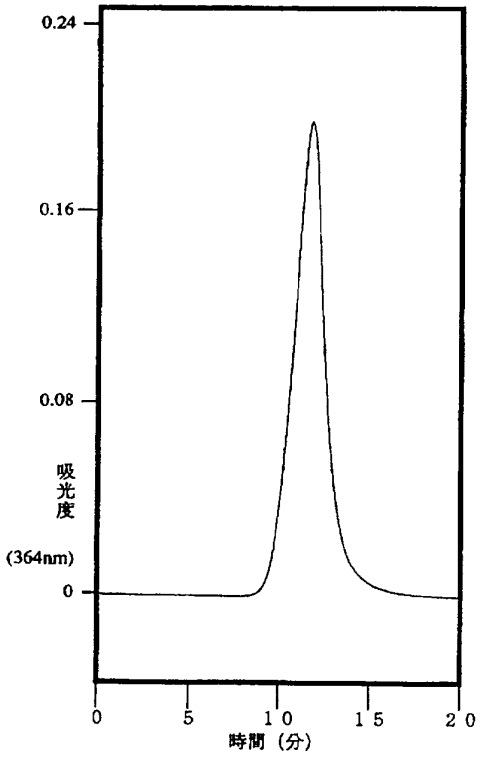
第18図


0.16
0.08
0.04
吸光度
(480nm)
0
0
5
10
15
20
時間（分）

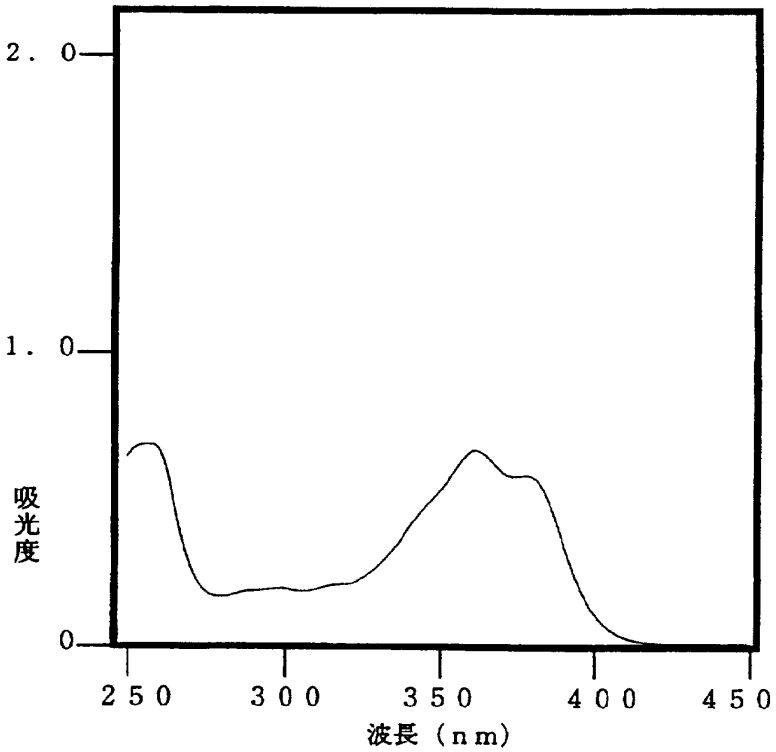
第19図


0．25
0．125
吸光度
0
250
300
400
500
600
650
波長（nm）

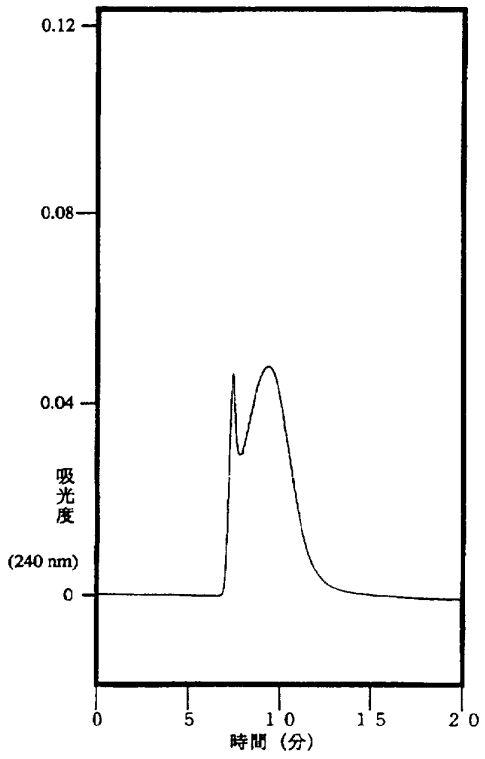
第20図


0.24
0.16
0.08
吸光度
(364nm)
0
0
5
10
15
20
時間（分）

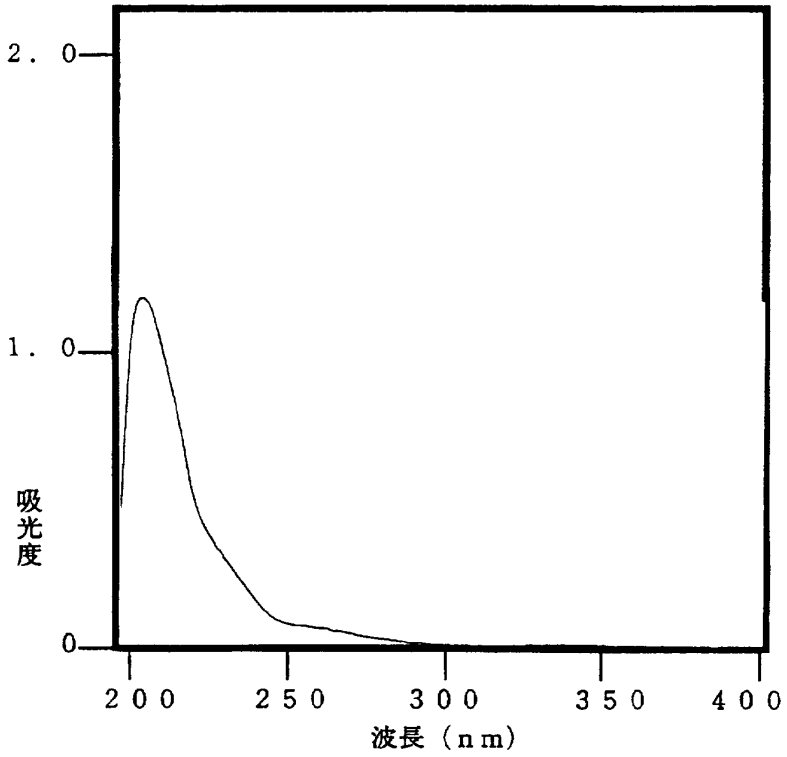
第21図


2．0
1．0
0
吸光度
250
300
350
400
450
波長（nm）

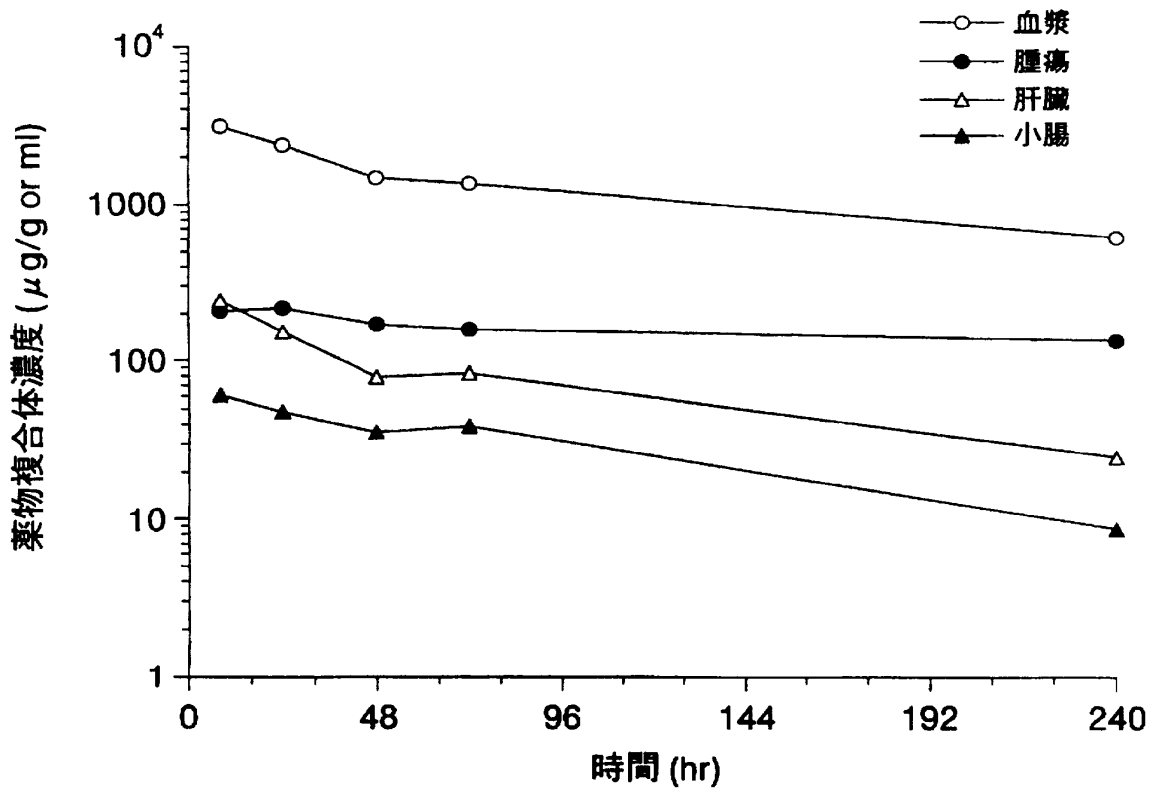
第22図


0.12
0.08
0.04
吸光度
(240 nm)
0
0
5
10
15
20
時間（分）

第23図


2．0
1．0
吸光度
0
200
250
300
350
400
波長（nm）

第24図


血漿
腫瘍
肝臓
小腸
薬物複合体濃度 (μg/g or ml)
10^4
1000
100
10
1
0
48
96
144
192
240
時間 (hr)

INTERNATIONAL SEARCH REPORT

International application No.
PCT/JP97/01914

A. CLASSIFICATION OF SUBJECT MATTER

Int. Cl^6 A61K47/48

According to International Patent Classification (IPC) or to both national classification and IPC

B. FIELDS SEARCHED

Minimum documentation searched (classification system followed by classification symbols)

Int. Cl^6 A61K47/48

Documentation searched other than minimum documentation to the extent that such documents are included in the fields searched

Electronic data base consulted during the international search (name of data base and, where practicable, search terms used)

C. DOCUMENTS CONSIDERED TO BE RELEVANT

Category*	Citation of document, with indication, where appropriate, of the relevant passages	Relevant to claim No.
A	JP, 5-39306, A (Drug Delivery System Institute, Ltd.), February 19, 1993 (19. 02. 93)(Family: none)	1 - 26
A	JP, 59-220197, A (Snow Brand Milk Products Co., Ltd.), December 11, 1984 (11. 12. 84)(Family: none)	1 - 26

☐ Further documents are listed in the continuation of Box C. ☐ See patent family annex.

* Special categories of cited documents:
"A" document defining the general state of the art which is not considered to be of particular relevance
"E" earlier document but published on or after the international filing date
"L" document which may throw doubts on priority claim(s) or which is cited to establish the publication date of another citation or other special reason (as specified)
"O" document referring to an oral disclosure, use, exhibition or other means
"P" document published prior to the international filing date but later than the priority date claimed
"T" later document published after the international filing date or priority date and not in conflict with the application but cited to understand the principle or theory underlying the invention
"X" document of particular relevance; the claimed invention cannot be considered novel or cannot be considered to involve an inventive step when the document is taken alone
"Y" document of particular relevance; the claimed invention cannot be considered to involve an inventive step when the document is combined with one or more other such documents, such combination being obvious to a person skilled in the art
"&" document member of the same patent family

Date of the actual completion of the international search	Date of mailing of the international search report
August 11, 1997 (11. 08. 97)	August 19, 1997 (19. 08. 97)
Name and mailing address of the ISA/ Japanese Patent Office Facsimile No.	Authorized officer Telephone No.

Form PCT/ISA/210 (second sheet) (July 1992)

国際調査報告

国際出願番号　ＰＣＴ／ＪＰ９７／０１９１４

Ａ．　発明の属する分野の分類（国際特許分類（ＩＰＣ））

Ｉｎｔ．Ｃｌ[6]　Ａ６１Ｋ４７／４８

Ｂ．　調査を行った分野

調査を行った最小限資料（国際特許分類（ＩＰＣ））

Ｉｎｔ．Ｃｌ[6]　Ａ６１Ｋ４７／４８

最小限資料以外の資料で調査を行った分野に含まれるもの

国際調査で使用した電子データベース（データベースの名称、調査に使用した用語）

Ｃ．　関連すると認められる文献

引用文献のカテゴリー＊	引用文献名　及び一部の箇所が関連するときは、その関連する箇所の表示	関連する請求の範囲の番号
Ａ	ＪＰ，５－３９３０６，Ａ（株式会社デイ・デイ・エス研究所），19.2月.1993 (19.02.93)，（ファミリーなし）	１－２６
Ａ	ＪＰ，５９－２２０１９７，Ａ（雪印乳業株式会社），11.12月.1984(11.12.84)，（ファミリーなし）	１－２６

☐ Ｃ欄の続きにも文献が列挙されている。

☐ パテントファミリーに関する別紙を参照。

＊　引用文献のカテゴリー
「Ａ」特に関連のある文献ではなく、一般的技術水準を示すもの
「Ｅ」先行文献ではあるが、国際出願日以後に公表されたもの
「Ｌ」優先権主張に疑義を提起する文献又は他の文献の発行日若しくは他の特別な理由を確立するために引用する文献（理由を付す）
「Ｏ」口頭による開示、使用、展示等に言及する文献
「Ｐ」国際出願日前で、かつ優先権の主張の基礎となる出願の日の後に公表された文献
「Ｔ」国際出願日又は優先日後に公表された文献であって出願と矛盾するものではなく、発明の原理又は理論の理解のために引用するもの
「Ｘ」特に関連のある文献であって、当該文献のみで発明の新規性又は進歩性がないと考えられるもの
「Ｙ」特に関連のある文献であって、当該文献と他の１以上の文献との、当業者にとって自明である組合せによって進歩性がないと考えられるもの
「＆」同一パテントファミリー文献

国際調査を完了した日	国際調査報告の発送日
１１．０８．９７	19.08.97
国際調査機関の名称及びあて先 日本国特許庁（ＩＳＡ／ＪＰ） 郵便番号１００ 東京都千代田区霞が関三丁目４番３号	特許庁審査官（権限のある職員）　４Ｃ　７４３３ 弓ム 真　　謙二　　印 電話番号　０３－３５８１－１１０１　内線　３４５２

様式ＰＣＴ／ＩＳＡ／２１０（第２ページ）（１９９２年７月）

OnCusp
Ex. 1002



mAbs

ISSN: 1942-0862 (Print) 1942-0870 (Online) Journal homepage: https://www.tandfonline.com/loi/kmab20

Impact of linker and conjugation chemistry on antigen binding, Fc receptor binding and thermal stability of model antibody-drug conjugates

Mauro Acchione, Hyewon Kwon, Claudia M. Jochheim & William M. Atkins

To cite this article: Mauro Acchione, Hyewon Kwon, Claudia M. Jochheim & William M. Atkins (2012) Impact of linker and conjugation chemistry on antigen binding, Fc receptor binding and thermal stability of model antibody-drug conjugates, mAbs, 4:3, 362-372, DOI: 10.4161/mabs.19449

To link to this article: https://doi.org/10.4161/mabs.19449

Published online: 26 Apr 2012.

Submit your article to this journal

Article views: 1160

Citing articles: 56 View citing articles

Full Terms & Conditions of access and use can be found at
https://www.tandfonline.com/action/journalInformation?journalCode=kmab20

mAbs 4:3, 362-372; May/June 2012; © 2012 Landes Bioscience

Impact of linker and conjugation chemistry on antigen binding, Fc receptor binding and thermal stability of model antibody-drug conjugates

Mauro Acchione,[1] Hyewon Kwon,[1] Claudia M. Jochheim[2] and William M. Atkins[1,*]

[1]Department of Medicinal Chemistry; University of Washington; Seattle, WA USA; [2]CMC Consulting; Seattle, WA USA

Keywords: conjugate, thermostability, Fc, linker, SPR, DSC, amine, thiol, carbohydrate, CD32b

Abbreviations: SPR, surface plasmon resonance; DSC, differential scanning calorimetry; FcγIIb, Fcgamma receptor IIb; T_m, melting temperature; ADC, antibody-drug conjugate; MSP, membrane scaffold protein; RU, response units; SD, standard deviation

Antibody-drug conjugates (ADCs) with biotin as a model cargo tethered to IgG1 mAbs via different linkers and conjugation methods were prepared and tested for thermostability and ability to bind target antigen and Fc receptor. Most conjugates demonstrated decreased thermostability relative to unconjugated antibody, based on DSC, with carbohydrate and amine coupled ADCs showing the least effect compared with thiol coupled conjugates. A strong correlation between biotin-load and loss of stability is observed with thiol conjugation to one IgG scaffold, but the stability of a second IgG scaffold is relatively insensitive to biotin load. The same correlation for amine coupling was less significant. Binding of antibody to antigen and Fc receptor was investigated using surface plasmon resonance. None of the conjugates exhibited altered antigen affinity. Fc receptor FcγIIb (CD32b) interactions were investigated using captured antibody conjugate. Protein G and Protein A, known inhibitors of Fc receptor (FcR) binding to IgG, were also used to extend the analysis of the impact of conjugation on Fc receptor binding. $H10_4$PEG4 was the only conjugate to show significant negative impact to FcR binding, which is likely due to higher biotin-load compared with the other ADCs. The ADC $aHIS_4$LC and $aHIS_1$PEG8 demonstrated some loss in affinity for FcR, but to much lower extent. The general insensitivity of target binding and effector function of the IgG1 platform to conjugation highlight their utility. The observed changes in thermostability require consideration for the choice of conjugation chemistry, depending on the system being pursued and particular application of the conjugate.

The US Food and Drug Administration's approval of brentuximab vedotin (Adcetris™) in August 2011 demonstrates the therapeutic potential of antibody-drug conjugates (ADCs) to treat many cancers. The therapeutic effects of ADCs can result from a complex combination of mechanisms, including anti-proliferative or cell-killing potential through delivery of cytotoxic agents, apoptotic signaling, antibody-dependent cell-mediated cytotoxicity (ADCC) and complement dependent cytotoxicity (CDC). The inherent specificity of ADCs, coupled with their long serum half-life and low immunogenicity have generated substantial interest and investment toward improving these drug delivery platforms.

The choice of linker that connects the drug to the antibody scaffold is a critical factor in determining the effectiveness of ADC therapy. There has been notable progress recently in linker technology and the range of chemical reagents available for coupling the antibody to the drug of interest.[1] Several factors contribute to optimal linker function, including stability in vivo, immunogenicity and efficiency of drug release from ADC. The linker should be sufficiently stable to allow the antibody to carry the toxic payload to the cell of interest and subsequently into the cell, where it must then release the active cytotoxic drug. This last step may be of critical importance, and it depends on the method of cellular uptake and internalization of the ADC, which in turn may change with linker properties.[2,3] Furthermore, a linker should be chosen that induces no or minimal immunogenicity or off-target binding.

The site of conjugation must also be considered. Ideally, the site for conjugation must not interfere with any therapeutic function, nor significantly disrupt regions that may confer fold stability. The most common approach in preparing ADCs is to use heterobifunctional linkers. These consist of a spacer with chemically distinct reactive groups on either end that can couple to various functional groups on the respective antibody or drug molecule. This provides considerable control and flexibility in how one attaches the linker. There are several targets on the antibody available for conjugation. Three common strategies include thiol coupling to reduced cysteines, amine coupling to lysine

*Correspondence to: William M. Atkins; Email: winky@uw.edu
Submitted: 02/05/12; Accepted: 03/12/12
http://dx.doi.org/10.4161/mabs.4.3.19449

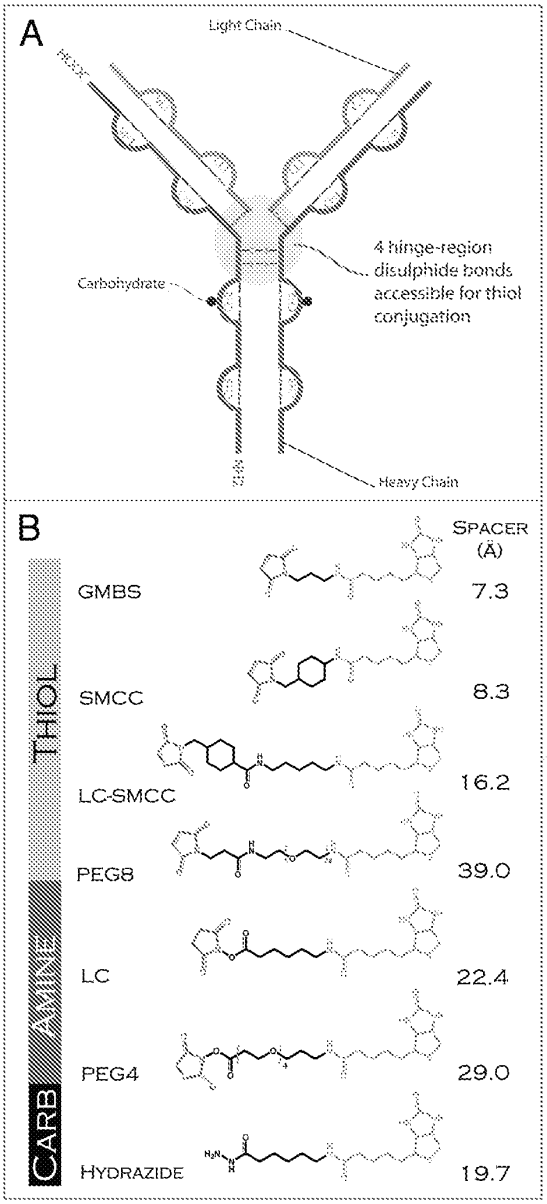


Figure 1. (A) Schematic representation of an IgG1 antibody showing sites of conjugation (thiol, amine and carbohydrate) used in generating the antibody-biotin conjugates. (B) Structure and length of linkers used in conjugating biotin (biocytin) to antibody. N-hydroxysuccinimide (blue), spacer arm (black), maleimide (violet), biotin (biocytin) (green).

residues and coupling to oxidized sugar residues on glycosylated mAbs. In principle, each method offers advantages and disadvantages with regard to product heterogeneity, stability and potential impact on effector function. Because in some cases modification of antibody residues spatially distant from the CDR domains can affect antigen binding, it is reasonable to expect that conjugation to the different functional groups may have different functional affects.[4]

Since different IgG1s can in principle have different sensitivities to conjugation with drugs, it is important to determine whether the trends observed in effects of conjugation for one IgG1 can be generalized to others. In addition to variable linkers and coupling strategies, we compared two distinct IgG1 scaffolds, to determine if different Fab domains would differentially be affected by the different linkers. The IgG1s used here include anti-6xHis (aHIS), which is directed against his-tags and therefore can be used with varying antigens that vary in size or other property, and HyHEL-10 (H10) anti-hen lysozyme, which provides a well-characterized scaffold with well-understood interactions with its antigen. In effect, we constructed a matrix of linker, IgG1 scaffold and conjugation chemistry to explore their effects on in vitro properties of ADCs.

Although the available literature suggests indirectly that the optimal choice of linker and conjugation site may vary with mAb idiotype, drug payload, conjugation site and antigen, no direct comparison of the effects of linker characteristics on functional properties for multiple mAbs and variable antigen has been reported in the public domain. General 'rules' about the advantages or disadvantages of specific linkers or conjugation methods are not well documented. Here we systematically evaluate the impact of linker and coupling chemistry on the properties of two model IgG1 antibodies (**Fig. 1A**). The results demonstrate some general trends concerning optimal linker strategies.

Results

Overall strategy. To explore the effects of IgG1 structure, conjugation chemistry and linker on ADC properties, we exploited two model IgG1 scaffolds, with multiple linkers of variable length and hydrophobicity. The linkers were used to attach the model 'drug' biotin to amines, reduced thiols, or oxidized carbohydrates on each IgG. In all cases, the form of biotin used for conjugation was biocytin, which allows for facile amine coupling of the biotin. Amine and carbohydrate linkers were purchased with this biocytin attached. For clarity, we refer to the group as biotin rather than biocytin in the remainder of this report. The structures of the linkers and biotin are shown in **Figure 1B**. For ADC identification, the subscripts 'N', 'T' and 'C' refer to coupling to amines, thiols or carbohydrates respectively. Biotin was chosen as a model drug for several reasons. Biotin, while hydrophobic, has a relatively low propensity to form aggregates or to bind non-specifically to protein surfaces. It also provides a rapid method to verify conjugation via SPR, quantify the level of biotin load on the ADC (**Table 1**) and verify that the recognition of biotin by streptavidin is not compromised in the conjugates. All IgG-linker-biotin conjugates synthesized showed positive capture by the Biacore streptavidin-linked CAP sensor chip surface (data not shown). IgG1 idiotype monoclonal antibodies (mAbs), such as the mouse H10 and aHIS, are the most abundant and commonly used mAb platform for ADCs, and the IgG1 idiotype contains a total of 16 disulfide bonds including four interchain (2 heavy-heavy, two heavy-light) and 12 intrachain disulfide bonds (**Fig. 1A**). The four interchain disulfide bonds are accessible to

OnCusp
Ex. 1002

Table 1. Impact of linker and conjugation chemistry on ADC thermal stability as measured by DSC

ADC[a]	Transition Temperature T_m (°C)			
	Component 1	Component 2	Component 3	Component 4
H10	77.5	74.2		
H10/w TCEP	76.4	74.8		
$H10_NPEG4_L$	76.4	73.3		
$H10_NPEG4_H$	75.1	71.8		
$H10_TSMCC$	77.6	72.5	70.0	
$H10_TLC$-SMCC	78.2	72.4	69.0	
$H10_TGMBS$	77.4	72.9	66.8	
$H10_TPEG8$	77.5	72.9	67.3	
$H10_C$	76.8	74.8		
aHIS	78.9	71.2	67.5	61.7
aHIS/w TCEP	79.0	65.8	63.2	60.1
$aHIS_NPEG4$	78.3	70.7	67.1	61.3
$aHIS_NLC$	78.1	70.6	67.0	61.1
$aHIS_TSMCC$	78.0		60.8	58.3
$aHIS_TLC$-SMCC	78.1		60.7	58.0
$aHIS_TGMBS$	78.2		60.7	58.0
$aHIS_TPEG8$	77.7		60.5	57.9

[a]N, amine; T, thiol; C, Carbohydrate; L, low linker ratio; H, high linker ratio

reduction without unfolding the antibody. This gives a total of eight potential conjugation sites, assuming reduction of all four bonds. In practice, a mixture of thiol conjugates with different load (0, 2, 4, 6 and 8) is presumed. For amine coupling there are many surface accessible lysine residues distributed over a characteristic IgG1 structure. No attempt was made here to separate mixtures of antibodies loaded with different levels of biotin, and the average number of biotins per ADC were used as a measure of biotin load (**Table 2**).

Thermal stability. DSC was used to characterize each antibody and its corresponding ADCs to determine effects of linker and coupling strategy on thermal stability. Each DSC thermogram was fit to multiple components. A shift to lower T_m for a component is indicative of a loss in stability. Replicates for SD analysis are not available for each ADC. When evaluating significance of changes to T_m for a particular ADC from the naked antibody we used the conservative value of greater than 1°C as a minimum. In fact in the samples where a significant change in T_m is noted, the values reported are much greater than those characteristic for replicate samples with this instrument.[5] The naked H10 antibody unfolds in two distinct but overlapping irreversible transitions (**Fig. 2A**), whereas the naked aHIS antibody unfolds with four distinct but overlapping irreversible transitions (**Fig. 2C**). IgG1 mAbs often exhibit two or more transitions in DSC thermograms due to the vastly different stabilities[6] of the immunoglobin structural domains. The heterogeneity in drug-load with all ADC preparations is expected to cause some broadening of transitions seen in DSC thermograms. However, all DSC thermograms fit well to between two and four components using a non-two state model. In the absence of knowledge regarding the degree of heterogeneity in biotin load, a relative comparison of linkers and conjugation chemistries was pursued.

Table 2. Impact of linker and conjugation chemistry on ADC binding to antigen

ADC[a]	K_D (pM)		BTN:Ab[b]	
H10	397	±32.5		
$H10_NPEG4_L$	546	±80.4	6.4	±0.3
$H10_NPEG4_H$	825	±172.0	14.2	±0.4
$H10_TSMCC$	451	±52.4	4.9	±0.2
$H10_TLC$-SMCC	297	±38.6	4.9	±0.8
$H10_TGMBS$	376	±63.3	6.6	±0.3
$H10_TPEG8$	356	±1.1	6.5	±0.4
$H10_C$	371	±34.4	0.7	±0.1
aHIS	20.8	±1.8		
$aHIS_NPEG4$	24.1	±0.1	3.6	±1.1
$aHIS_NLC$	21.8	±0.3	3.7	±0.9
$aHIS_TSMCC$	22.6	±0.6	5.7	±1.4
$aHIS_TLC$-SMCC	22.5	±0.4	6.0	±2.3
$aHIS_TGMBS$	22.8	±2.4	4.9	±0.6
$aHIS_TPEG8$	23.3	±2.8	7.7	±0.04

[a]N, amine; T, thiol; C, Carbohydrate; L, low linker ratio; H, high linker ratio; [b]BTN, biotin; Ab, antibody

With H10 generated ADCs, the amine and carbohydrate conjugation chemistries did not alter the pattern of two component

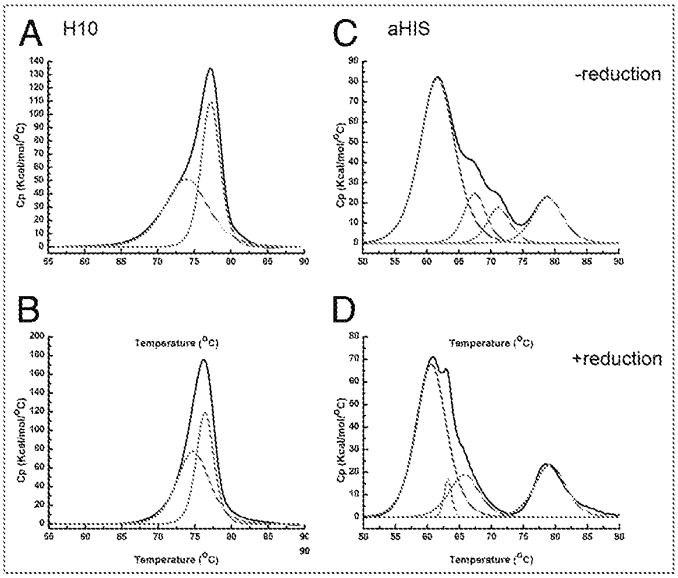


Figure 2. DSC thermograms and deconvoluted component transitions for the two unconjugated IgG1 antibodies in the presence and absence of TCEP. Left parts: (A) H10 without reducing agent (B) H10 with reducing agent; Right parts (C) aHIS without reducing agent (D) aHIS with reducing agent. Raw thermogram is shown in black. Individual transitions from non-two state fit are color coded as component 1 (red), component 2 (green), component 3 (magenta) and component 4 (blue).

transitions seen with the naked antibody (**Figs. 3A, C and D and Table 1**). Amine conjugation to accessible surface lysine residues presents an additional strategy for conjugation of drugs, with the potential to modify stability of the antibody fold. There was a clear difference in stability observed with the amine coupled ADCs with a drop in T_m for both components 1 and 2. The greater the biotin load (**Table 2**) the greater the change in T_m. For the corresponding thiol conjugates (**Fig. 3B and Table 1**), a new component is observed with a much lower thermostability than the other two components. While component 1 does not change significantly in T_m for the thiol generated ADCs, the presence of this new lower temp transition results in ADC that are significantly less stable than the naked antibody, with $H10_tGMBS$ beginning to partially unfold at a T_m 7.4°C below that of any component in the naked antibody. This ADC was also the one with the highest biotin load.

For the aHIS ADCs, the pattern of component transitions observed with DSC again differs depending on conjugation chemistry (**Fig. 3E–G and Table 1**). However, unlike H10 the number of visible components decreases from 4 with the naked antibody and amine-coupled ADCs to 3 for the thiol ADCs. It is unclear whether the lack of a component 2 for thiol-coupled ADCs reflects its superposition with another component in the thermogram that makes it indistinguishable. For amine aHIS ADCs, components 1–4 remain largely unaffected, even with higher biotin load (**Table 2**). For the thiol aHIS ADCs component 3 shows a large decline in T_m relative to the naked antibody of between 7.0-6.7°C which is comparable to the difference observed between components 2 and 3 for the thiol H10 ADCs. Component 4 showed a modest decline in T_m compared with the naked antibody, decreasing as much as 3.8°C for $aHIS_TPEG8$. So, in comparison to aHIS, the impact of thiol conjugation to thermostability was greater for H10 ADCs with comparable biotin load. The results for the shifts in low temperature DSC components with different model ADCs are summarized in **Figure 4**. In general, the results clearly demonstrate that different thiol-conjugates IgGs yield ADCs with significantly different sensitivity to drug load, even with the same linkers.

For this work, we were interested in changes in thermostability that may be important for the manufacture and use of these 'model' therapeutics. Therefore, we focused on notable changes in the relative components with the lowest temperature transition. For thiol conjugates, H10 showed a strong correlation ($R^2 = 0.87$) between higher biotin load and loss of stability. For aHIS, no correlation was observed for the corresponding thiol conjugates when comparing the lowest temperature transitions. However, among different DSC components there are similarities. This suggests that conjugation to free thiols located in the hinge region can differentially affect IgG1 scaffolds in ways that could have implications for their manufacture. With amine conjugates there were only two linkers used for each antibody. For amine H10 conjugates the correlation between biotin load and change in T_m for the low temperature component is less than that of thiol H10 conjugates. With amine aHIS conjugates the two T_m values are too close to confidently assess the correlation between biotin load and change in T_m. However, both values are below that observed with any of the thiol conjugates when those data sets are extrapolated to comparable biotin loads. What is clear from this data are that amine coupling has had less impact on thermostability compared with thiol conjugation for both antibodies. Also, for thiol conjugation the impact on thermostability with biotin load is very different among the two antibodies tested.

To determine the affect of reduction without chemical elaboration of the hinge region disulfides alone, both antibodies were unfolded in the presence of TCEP as the reducing agent. At the concentrations tested here (10 mM), TCEP had negligible impact on the DSC baseline. As stated previously, the H10 antibody has two characteristic component transitions (**Fig. 2A**) and the number of components, as well as the transition temperatures, did not change in the presence of this reducing agent (**Fig. 2B**). For the aHIS antibody, reduction of the hinge inter-chain disulfides with TCEP showed a slight negative affect on thermogram components 2, 3 and 4 with decreased thermostability (**Fig. 2D**). These data demonstrate that the effect of thiol reduction on stability can be IgG dependent, but the reduction of IgG by itself does not cause a significant decrease in thermal stability in either antibody used here.

In addition to thiol and amine conjugation strategies, we examined the effect of linking via carbohydrate. IgGs include N-linked oligosaccharides on two conserved asparagine residues (Asn297) in the CH_2 domain of the Fc region and approximately

15–20% also have N-linked oligosaccharides in the variable region.[7] Oxidation of these N-linked sugars offers a convenient means of conjugation of a drug or small molecule at a defined location, with potentially less of a destabilizing effect than hinge-region thiol conjugation. Among the conjugation strategies we tested, the carbohydrate linked ADCs had the smallest changes in T_m for DSC profile compared with the unconjugated antibody (**Fig. 3D**). This may be in part due to the much lower level of conjugation (**Table 2**). However, even taking this into account, the affect of conjugation on T_m was much less than that for the thiol or amine conjugated antibodies.

Antigen binding. Because tight binding to its target is inherent in the strategy when using these drug delivery platforms, any effects on antigen binding due to conjugation are important. Such effects are possible, in principle, due to long range structural effects transmitted from conjugation sites to the antigen binding sites, or in the case of amine-conjugation potentially affecting hotspot lysine residues at the interface. Given the moderate role for disulfides in antibody stability (**Fig. 2**), we also studied whether conjugation to hinge-region disulfides affects antigen binding.[8] Each individual antibody and its respective ADCs were tested for binding to antigen. Representative sensorgrams are shown in **Figure 5**; comparisons of K_D were made by assessment of differences (>2-fold difference from unconjugated antibody) with conjugation chemistry or linker. None of ADCs for either antibody were different than the unconjugated antibody (**Table 2**). For the mAbs tested in this study, there was no clear disadvantage to antigen binding for any of the linkers or chemistries investigated here. The amine-conjugated $H10_NPEG4_H$ ADC was the one notable exception, and most likely reflects modification of a lysine residue at or near the paratope when the biotin load is sufficiently high.

Effector function and Fc binding. Effector functions mediated by binding of the Fc region of IgG1 antibodies to Fc receptors (FcR) can play an important role in the overall effectiveness of ADC therapies.[9-11] Modifciation of residues directly involved or near the Fc recdeptor binding site, such as regions of glycosylation on antibodies, may have an important role in FcR binding and in the structural integrity.[12,13] The potential therapeutic benefits of FcR activation or binding to other 'FcR-like' proteins make these interactions a target for optimization. All three conjugation strategies and linkers explored in this study could have direct or indirect effects on the structure and accessibility of the Fc region of the antibody. To test this, we captured the ADC to a SPR sensor surface on which native antigen was immobilized and then investigated binding of FcR to the captured ADC (**Figs. 6–8**). Effectively we began with a surface of ADC that was already bound to its corresponding antigen. This approach had several advantages over coupling of the antibody directly to the CM5 dextran surface of the chip or the Fc receptor. Because one of the approaches undertaken in conjugation involved amine coupling, the amine-sites available for coupling the ADCs to a CM5 sensor chip were much lower. Capturing the antibody on the SPR chip via its antigen also minimizes the possibility of interactions between the chip surface and the Fc region that could be confused with effects of N-linked biotin on the Fc region. The SPR data of FcR binding to ADC captured on the chip surface all fit very well to a one-site binding model. There was no statistically significant improvement of the fits to the data for a two-site binding model with non-equivalent binding sites, as observed by others.[14] As noted above, one important distinction to other work using SPR in this area is that in our experiments the antibody/ADC was captured to the chip surface via the antigen rather than using direct amine coupling.

Some conjugation strategies were found to have a significant affect on binding to certain FcR-binding partners. For $H10_NPEG4_H$ the affinity was reduced 17-fold for Protein G (**Table 3**). This may be due to coupling to lysine residues proximal to, or

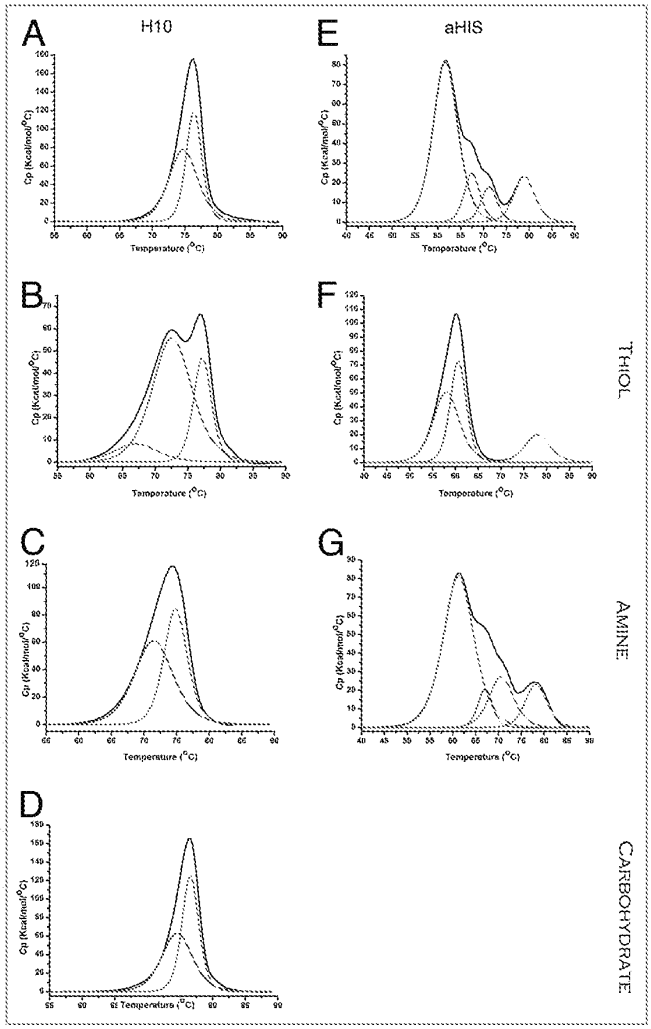


Figure 3. DSC thermograms comparing ADCs prepared with different conjugation chemistries. Raw thermograms are shown in black. Individual transitions are color coded as: component 1 (red), component 2 (green), component 3 (magenta) and component 4 (blue). (A) H10, (B) $H10_SSMCC$ (C) $H10_NPEG4_H$ (D) $H10_C$ (E) aHIS (F) $aHIS_{LC}$-SMCC (G) $aHIS_NPEG4$.

OnCusp
Ex. 1002

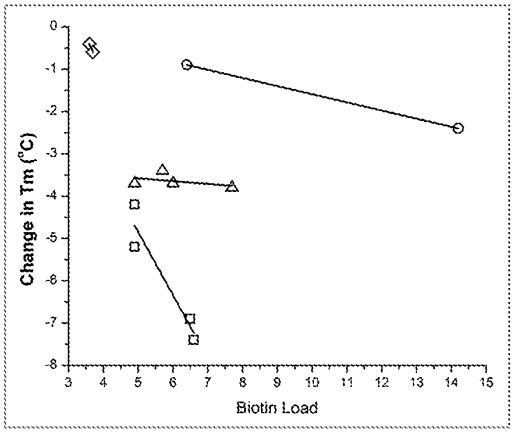


Figure 4. Correlation between biotin load and change in T_m for low-temperature components from DSC for ADC, grouped according to conjugation chemistry and/or antibody. (circle) amine-conjugated H10, (diamond) amine-conjugated aHIS, (triangle) thiol-conjugated aHIS and (square) thiol-conjugated H10.

in direct contact with, Protein G binding residues. There was also a decrease in binding to Protein G observed with amine coupled $aHIS_NLC$. The $aHIS_TPEG_8$ ADC was the only one to show some negative affect on binding with all FcR model proteins (CD32b, Protein A and Protein G). For this conjugate, the higher ratio of biotin load may be one reason for this (**Table 2**). CD32b is an inhibitor for Fcγ receptors that are often involved in effector functions such as ADCC and C1q mediated complement activation. A reduction in expression of CD32b has been associated with enhanced antitumor activity for antibodies.[15] These results suggest that amine coupling at high load-ratios can have a significant affect on binding to the Fc domain, and a similar evaluation would prove useful for any therapeutic ADC targeting effector function and using this conjugation chemistry. Other reports suggest a strong correlation with pegylation of antibodies and a reduction in FcR binding.[16,17] We observed a large reduction, but only with one ADC binding to one particular FcR.

Discussion

The lack of any significant change to antigen binding, or in most cases FcR binding, with any of the linkers or conjugation methods used, support the important role for antibodies as robust drug platforms for therapeutics. One attractive aspect to amine conjugation is the potential for increased drug load compared with using the fixed eight thiols presented by the IgG1 hinge disulfides. Because increased drug load on the ADC might be expected to improve therapeutic efficacy, the relatively mild perturbations to both Fc receptor binding and antigen binding observed in this work suggest that this advantage might be exploitable. However, in the case of thiol ADC, an increase in drug load does not necessarily correlate with improved therapeutic outcome.[18] With amine coupling, these results suggest that an analysis of FcR binding may prove useful when comparing leads that may present differences in serum half-life.

Table 3. Impact of linker and conjugation chemistry on ADC binding to Fc receptor

ADC[a]	K_D (nM)					
	CD32b		Protein G		Protein A	
H10	168.7	±13.1	134.3	±7.5	434.3	±3.2
$H10_NPEG4_L$	150.3	±10.8	324.3	±17.1	510.0	±5.2
$H10_NPEG4_H$	87.9	±12.1	2314.0	±175.0	334.0	±5.2
$H10_TSMCC$	134.0	±10.5	124.3	±18.9	495.3	±10.4
$H10_TLC$-SMCC	267.7	±14.0	99.2	±9.6	442.3	±56.7
$H10_TGMBS$	136.3	±20.4	110.0	±3.5	445.3	±59.5
$H10_TPEG8$	227.3	±10.6	132.3	±18.6	454.3	±55.4
$H10_C$	124.7	±6.4	90.5	±18.2	454.7	±34.5
aHIS	203.0	±9.5	119.6	±28.1	309.6	±28.6
$aHIS_NPEG4$	163.4	±20.5	137.0	±25.1	361.6	±73.4
$aHIS_NLC$	163.2	±16.3	197.9	±9.3	368.8	±50.2
$aHIS_TSMCC$	138.8	±27.9	157.3	±36.3	165.9	±39.4
$aHIS_TLC$-SMCC	139.2	±25.6	163.3	±8.4	164.8	±36.7
$aHIS_TGMBS$	206.5	±15.0	149.6	±5.5	232.0	±36.3
$aHIS_TPEG8$	448.7	±68.3	253.4	±9.1	523.0	±88.1

[a]N, amine; T, thiol; C, Carb

Increasing circulating half-life has often been associated with improved therapeutic efficacy for ADCs. Correlation between protein stability and in vivo half-life has been known for some time.[19,20] The more obvious correlation would be expected for changes in neonatal Fc receptor (FcRn) binding, which is a major factor in determining the rate of catabolism of IgGs not displaying target-mediated disposition, although there is some evidence that other factors may play a more significant role in serum half-life than affinity for FcRn.[21] We chose the bacterial receptors Protein G and Protein A as surrogates for natural FcR since they are both known to overlap with FcR binding sites and compete for their binding.[22,23] Our results suggest that binding to FcRn would not be expected to change with any of the conjugation chemistries or linkers investigated here. Therefore, the circulating half-life is not expected to change as a direct result of these modifications. However, catabolic mechanisms mediated by the cytosol are a possibility with any of these ADCs. Since terminal amine residues are a determining factor in that pathway, there is potential for influence on half-life in the case of amine coupling to the N-terminus of the antibody.

Biotin is small and somewhat water soluble whereas many chemotherapeutics are larger and more hydrophobic. Our results with biotinylating IgG1 antibodies demonstrate little or no impact on antigen/Fc receptor binding. With the exception of $H10_NPEG4_H$, these results are in contrast to several other reports which suggest that coupling of PEG molecules to an antibody can have a significant detrimental impact on antigen binding.[24] The results with the $H10_NPEG4_H$ ADC more likely reflect a difference in biotin load and location of conjugation on the antibody rather than the identity of the linker itself. The physiochemical characteristics and ultimate cellular disposition

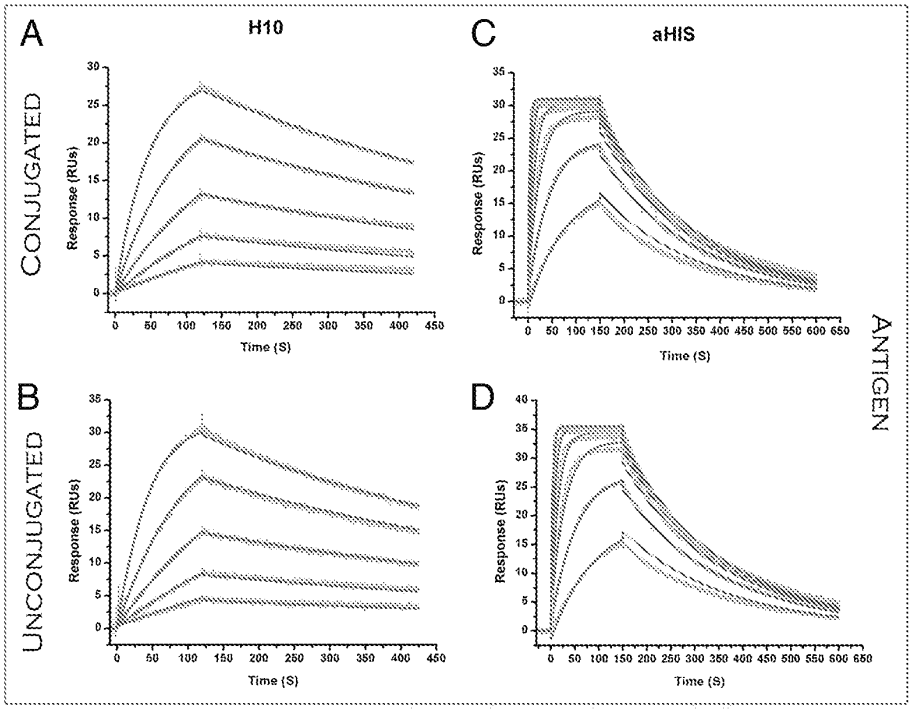


Figure 5. SPR sensorgrams comparing binding of ADC (analyte) to antigen (ligand). (A) H10 binding to JQL (B). $H10_2PEG8$ binding to JQL. (C) aHIS binding to 6xHis peptide (D). $aHIS_6PEG4$ binding to 6xHis peptide. Raw sensorgrams are shown in gray with results from fitting that data to a 1:1 binding model depicted in red.

of the drug should also be considered when interpreting these results. Consideration of unintended consequences to secondary roles mediated through Fc receptor mediated binding would seem to warrant a similar analysis for ADCs currently being developed. There remains the possibility that a different small molecule, peptide, protein or nucleic acid bound to a different antibody via these methods might have a significant impact on antigen/Fc receptor binding. However, we tested two distinct IgG1 antibodies with completely different targets, and our results suggest a more general relationship in the case of smaller molecules. Clearly, many of the current chemotherapeutic drugs employed or explored for therapy differ significantly in size, charge and hydrophobicity from biotin. With much larger drug payloads like bacterial exotoxins we would expect that steric hindrance could play a significant role in modulating antigen/Fc receptor binding. While not a drug, there is clear evidence that with much larger PEG moieties used in the linker, the negative impact on antigen binding can be dramatic;[17,25-27] In cases where the drug payload is highly hydrophobic and 'sticky', the chemical identity and length of the linker may influence the ability of those drug molecules to self-associate and promote aggregation.

While this report focuses on the relative thermal stability of conjugates, there has been much interest in investigating the stability of linkers in vivo. The work here demonstrates that linker identity has little or no impact on the inherent stability of the ADC construct, especially when compared with the relative impact of conjugation chemistry. Although outside the scope of this study, it would be interesting to compare conjugation chemistries known to impact thermal stability of an ADC with similar linkers and drugs to see if there is any correlation with the stability of a given linker to processing in vivo.

For all ADCs synthesized here, conjugation had some impact on thermostability of the molecule that could influence decisions for the manufacturing and storage for any particular ADC and may guide initial decisions on coupling strategies for therapeutic use based on possible correlations between thermal stability for the protein fold and serum half-life. Of the three functional groups investigated, thiol conjugation resulted in the greatest decreases in observed T_m as monitored by DSC. Furthermore, the degree of change in T_m is correlated with the number of biotin molecules linked to the antibody via thiols. The degree to which the T_m was independent of the length of the linker used or its hydrophobicity when the molecule being attached to the antibody is small and slightly hydrophobic. It remains to be seen if this relationship holds for much larger or more hydrophobic drugs such as exotoxins or auristatins. DSC showed clear differences in the number of components observed in thermograms for the two IgG1 antibodies and those differences also extended to how those component transitions were differentially impacted by conjugation chemistry. Perhaps most importantly, the results demonstrate the potential utility of DSC as a method to study comparability between ADC preparations.

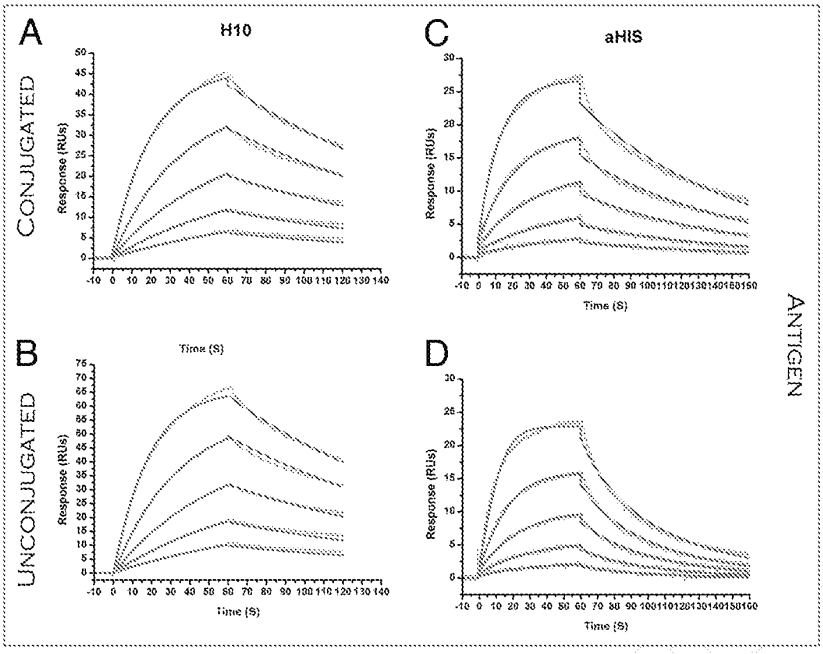


Figure 6. SPR sensorgrams comparing binding of ADC (ligand) to Protein G (analyte). (A) H10 (B). $H10_4PEG8$ (C) aHIS (D). $aHIS_4PEG4$. Raw sensorgrams are shown in gray with results from fitting that data to a 1:1 binding model depicted in red.

Materials and Methods

Materials. Buffer salts and biocytin for ADC synthesis and purification were purchased from Sigma. Heterobifuctional linkers, both with and without biotin attached, T-gel and Zeba columns were obtained from Thermo Scientific. Concentrated hybridoma supernatant containing mouse HyHEL-10 IgG1 (H10) whole antibody was provided by Dr. Sandi Smith-Gill, (National Cancer Institute, Frederick, MD). Japanese quail lysozyme was purified from egg white. Purified mouse monoclonal anti-6xHis IgG1 (aHIS) whole antibody was purchased from Invitrogen and dialyzed into PBS, pH 7.2. Hexa histidine peptides were obtained from AnaSpec. An engineered variant of apolipoprotein A1 (MSP1D1) was purified using the hepta-histidine tag via Ni-affinity chromatography as previously described in reference 28. Reagents and consumables for DSC and SPR analysis were obtained from GE Health Sciences.

Purification of H10 antibody. Concentrated fractions of H10 antibody from hybridoma cultures were clarified by centrifugation at 50,000x g for 20 min at 4°C. The supernatant was then applied to a T-gel column and purified according to the manufacturer's instructions. Antibody fractions were concentrated via Millipore Amicon-Ultra 0.5 spin-ultrafiltration columns and then passed through a GE Superose 10/300 GL gel filtration column pre-equilibrated with HBS buffer (10 mM HEPES, 150 mM NaCl, 3 mM EDTA, pH 7.4). Purified antibody was stored in HBS at 4°C until further use.

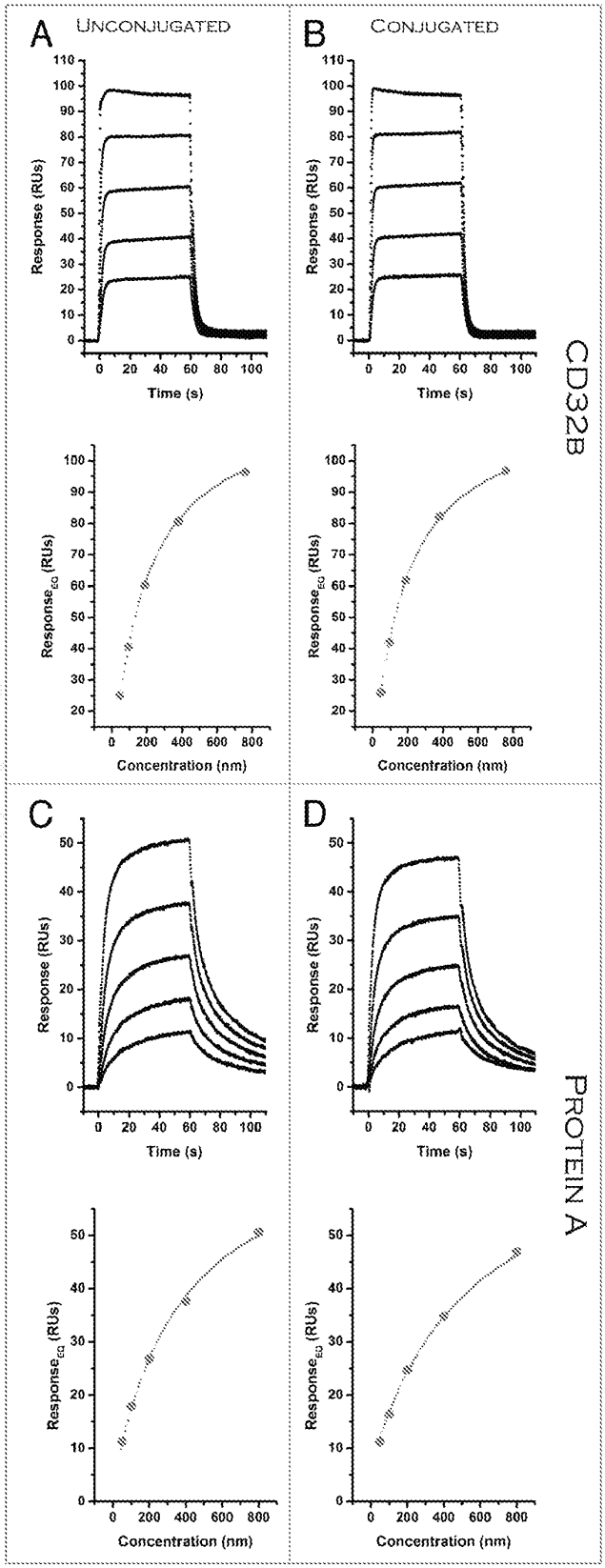
Preparation of thiol conjugated ADCs. Stock solutions containing 5 μM H10 and aHIS were reduced with 10 mM TCEP in nitrogen purged phosphate buffer (10 mM sodium phosphate, 150 mM NaCl, 5 mM EDTA, pH 7.2) for 2 h at 37°C. A fresh solution of 30 mM SMCC (**Fig. 1B**) in DMSO was prepared and mixed with biocytin at a ratio of 1:20 in Phosphate Buffer for 2 h at 37°C. Initial attempts to reduce disulfide bonds in these antibodies to form thiol-linked conjugate using low ratios of TCEP:Ab[29] proved unsuccessful. When using ratios below 5:1 no significant level of conjugate was observed. Considerably higher ratios of reducing agent:mAb were required (2,000:1) at elevated temperatures, which is more consistent with those reported for other IgG1s.[30] The reduced antibody was then buffer exchanged into HBS (PBS for aHIS) buffer using three Zeba desalting columns equilibrated with HBS buffer. Removal of TCEP reducing agent during this step prevented inhibition of the maleimide reaction.[31] The reduced antibody was then mixed with 1/10 volume equivalent of the SMCC-biocytin reaction mixture and allowed to equilibrate at room temperature for 2.5 h in the dark. An excess of L-cysteine was then added to cap unreacted thiol groups and the mixture was allowed to incubate for 30 min at room temperature.

Preparation of amine conjugated ADCs. NHS-PEG4-Biotin (**Fig. 1B**) was re-suspended in PBS and mixed with HyHEL-10 IgG in a final molar ratio of 20:1 and 40:1 and both reactions were incubated at room temperature for 2 h. For aHIS IgG, NHS-LC-Biotin (**Fig. 1B**) prepared in DMSO and NHS-PEG4-Biotin (**Fig. 1B**) were re-suspended in PBS and mixed with aHIS IgG in final molar ratio of 25:1 and incubated at room temperature for 30 min. In both cases, excess linker was removed with Zeba desalting columns.

Preparation of carbohydrate conjugated ADCs. Stock solutions of 50 μM H10 were oxidized in freshly prepared sodium periodate in PBS at room temperature in the dark for 2 h.[32] Excess oxidizing agent was removed with Zeba desalting columns and the oxidized antibodies were immediately reacted with the hydrizide-biocytin linker (**Fig. 1B**) at a ratio of 1:20 for 2 h at room temperature.

Purification, determination of biotin-load and storage of ADCs. All ADC mixtures were further purified and buffer exchanged using a Superose 10/300 GL size exclusion column pre-equilibrated with HBS-E (10 mM HEPES, 150 mM NaCl, 3 mM EDTA) for H10 ADCs and PBS (10 mM sodium phosphate, 150 mM NaCl, pH 7.2) for aHIS ADCs at a flow rate of 0.55 mL/min, with UV detection at 280 nm. Protein fractions corresponding to the ADC peak (based on retention times of unconjugated antibody) were pooled and stored at 4°C

Figure 7. SPR equilibrium data comparing ADC (ligand) binding to CD32b and Protein A (analyte). (A) H10 (B). $H10_hPEG4_L$ (C) H10 (D) $H10_hPEG4_L$. Raw sensorgrams are shown in black with corresponding results from fitting that data to a 1:1 binding model depicted in a binding isotherm below.



until further use. Typical reaction yields after purification were between 30–55%. Degree of biotin conjugation on ADC was determined using the fluorescence biotin quantification kit from Thermo Scientific.

Stability analysis of conjugates using DSC. Differential scanning calorimetry was used to determine the affect of ligand and conjugation chemistry on the stability of all antibodies and ADCs. Samples were prepared immediately prior to analysis and any aggregates formed during storage were removed by size-exclusion chromatography in HBS-E buffer (10 mM HEPES, 150 mM NaCl, 3 mM EDTA, pH 7.4) or PBS for aHIS ADCs. Concentrations of antibody and conjugate used were 4–6 μM. All samples were analyzed using a Microcal VP-Capillary DSC equipped with autosampler and temperature controlled sample storage accessories. Unfolding was monitored between 10°C and 90°C (20°C and 90°C for aHIS ADCs) with a ramp rate of 1°C/min and a filtering period of 16 sec with no gain. H10 antibody was analyzed by DSC using ramp rates of 0.5°C/min and 1.5°C/min and there was no siginificant change in T_m or component profiles in the thermograms. Thermograms were normalized for concentration and then baseline corrected prior to fitting to a non-two-state unfolding model to determine transition melting temperature T_m for each component.

Determination of binding affinity for HEL antigen using SPR. SPR was used to compare effects of conjugation on ADC binding to its antigen. All experiments were conducted on a Biacore T100 with CM5 sensor chips. The antibodies were amine coupled to the sensor surface using 10 mM sodium acetate, pH 5.0 at a level that resulted in a maximum analyte response no higher than 40 response units (RUs). This, together with a flow rate of 100 μL/min, negated any significant mass transport effects for this very tight association. Several different concentrations of analyte diluted in HBS-EP running buffer (10 mM HEPES, 150 mM NaCl, 3 mM EDTA, 0.005% v/v P20) were injected for 120 sec followed by monitoring dissociation for 10 min. Raw sensorgrams were double reference subtracted using a reference flow cell with no ADC immobilized and by injections of running buffer. Corrected sensorgrams were fit globally to a 1:1 interaction model using the Biacore evaluation software. The quality of the nonlinear fit to this model was evaluated using coefficient of variance (CV) values and residuals. Unless otherwise stated in the figure captions, all values reported for apparent affinity K_D are an average of three independent measurements made from separate dilutions of analyte stock. All experimental cycles were conducted at 25°C. Chip surfaces were regenerated after each cycle using 10 mM Glycine, pH 1.5.

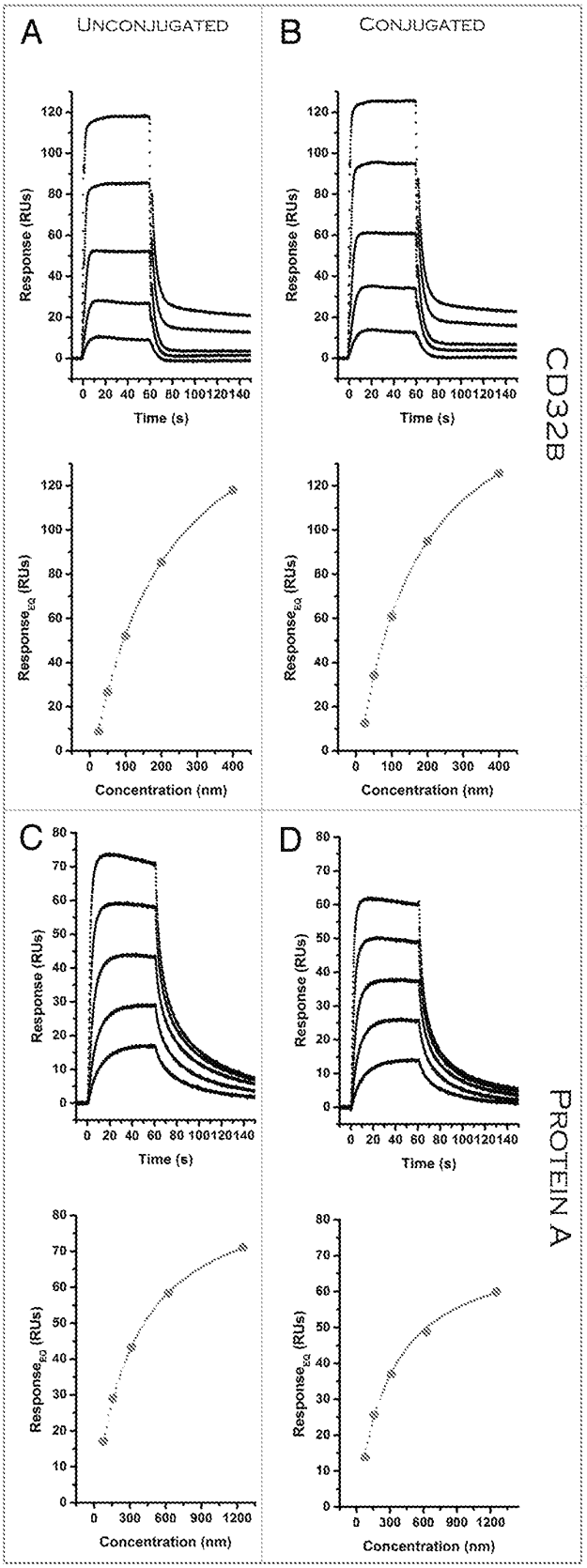


Figure 8. SPR equilibrium data comparing ADC (ligand) binding to CD32b and Protein A (analyte). (A) aHIS (B). aHIS$_6$ LC (C) aHIS (D) aHIS$_6$ PEG4. Raw sensorgrams are shown in black with corresponding results from fitting that data to a 1:1 binding model depicted in a binding isotherm below.

Determination of binding affinity for 6xHis peptide antigen using SPR. ADCs were diluted into 10 mM sodium acetate buffer, pH 5.0 at a concentration of 10 μg/mL and immobilized on CM5 sensor surface chips using amine-coupling chemistry to give a maximum analyte response of approximately 40 response units (RUs). All binding analysis of antibodies with 6xHis peptides antigen were performed at 25°C in PBS (pH 7.2) as running buffer. Several concentrations of 6xHis peptides diluted in running buffer were injected for 150 sec at a flow rate of 50 μL/min followed by monitoring dissociation for 450 sec. Raw sensorgrams were double referenced by both subtracting a flow cell with no antibodies immobilized and subtracting a run of buffer only injection. The surface was regenerated with 10 mM glycine, pH 2.0 at a flow rate of 20 μL/min.

Determination of binding affinity for Fc receptor using SPR. Assessing the effect of conjugation on effector role function was done by first immobilizing the antigenic HEL ligand (a His-tagged apolipoprotein A1 variant for aHIS) onto a CM5 sensor surface onto which a high level of conjugate was captured. This configuration allows us to assess whether antigen bound ADC can still effectively bind Fc receptor. Between 3,500–4,000 RUs of capture ligand (antigen) was immobilized on each flow cell including the reference flow cell. To this was then captured approximately 500–1,000 RUs of ADC diluted in SPR running buffer HBS-EP (PBS for aHIS). The level of captured ADC was chosen to give sufficient signal to provide good signal to noise for fitting while at the same time minimizing (for Protein G) the potential for mass transport limitations. Several concentrations of Fc receptor analyte were freshly prepared and injected over the antigen-captured ADC surface.

For Protein G, the protocol used was for kinetic measurements with a flow rate of 10 μL/min, an association time of 60 sec and a dissociation time of 60 sec (120 sec for aHIS). To assess potential mass-transport limitations tests with higher flow rates of 20 μL/min and 40 μL/min were conducted. No significantly change in on-rate was observed. Chip surfaces were regenerated after each cycle using 10 mM Glycine, pH 2.5. Analyte binding level was consistent among replicates, decreasing less than 5% after repeated regeneration cycles, and calculated rate used in determination of K_D were highly reproducible from cycle to cycle. Raw sensorgrams were double referenced using a flow cell with no ligand immobilized and by injections of running buffer. Corrected sensorgrams were fit globally to a 1:1 interaction model using the Biacore evaluation software. Quality of the nonlinear fitting to this model was evaluated using CV values and the residuals. Values reported for apparent affinity K_D are an average of three independent measurements made from separate dilutions of analyte stock.

Determination of binding affinity for CD32b and protein A by equilibrium binding. For both CD32b binding and Protein A binding, the on rates and off rates were too fast

to be measured with confidence using the T100. Therefore the apparent affinity was determined by measuring equilibrium binding levels at several different analyte concentrations in HBS-EP buffer. After correcting raw sensorgrams for the reference flow cell and buffer injections, equilibrium responses were plotted against analyte concentration using Biacore evaluation software and fit to a 1:1 association model using nonlinear Scatchard analysis. Each concentration was measured in triplicate and both methods were conducted using a sensor surface temperature of 25°C.

Disclosure of Potential Conflicts of Interest Statement

No potential conflicts of interest were disclosed.

Acknowledgements

We wish to thank Sandi Smith-Gill from the National Cancer Institute for the kind gift of the mouse H10 IgG1 antibody. We would also like the thank John Sumida from the Bioanalytical Pharmacy Core, the Center for Intracellular Delivery Biologics and the Washington State Life Sciences Discovery Fund.

References

1. Ojima I, Geng X, Wu X, Qu C, Borella CP, Xie H, et al. Tumor-specific novel taxoid-monoclonal antibody conjugates. J Med Chem 2002; 45:5620-3; PMID:12477344; http://dx.doi.org/10.1021/jm025540g.
2. Smith LM, Nesterova A, Alley SC, Torgov MY, Carter PJ. Potent cytotoxicity of an auristatin-containing antibody-drug conjugate targeting melanoma cells expressing melanotransferrin/p97. Mol Cancer Ther 2006; 5:1474-82; PMID:16818506; http://dx.doi.org/10.1158/1535-7163.MCT-06-0026.
3. Razani B, Woodman SE, Lisanti MP. Caveolae: from cell biology to animal physiology. Pharmacol Rev 2002; 54:431-67; PMID:12223531; http://dx.doi.org/10.1124/pr.54.3.431.
4. Torres M, Casadevall A. The immunoglobulin constant region contributes to affinity and specificity. Trends Immunol 2008; 29:91-7; PMID:18191616; http://dx.doi.org/10.1016/j.it.2007.11.004.
5. Wen J, Arthur K, Chemmalil L, Muzammil S, Gabrielson J, Jiang Y. Applications of differential scanning calorimetry for thermal stability analysis of proteins: qualification of DSC. J Pharm Sci 2012; 101:955-64; PMID:22147423; http://dx.doi.org/10.1002/jps.22820.
6. Vermeer AW, Norde W. The thermal stability of immunoglobulin: unfolding and aggregation of a multi-domain protein. Biophys J 2000; 78:394-404; PMID:10620303; http://dx.doi.org/10.1016/S0006-3495(00)76602-1.
7. Holland M, Yagi H, Takahashi N, Kato K, Savage CO, Goodall DM, et al. Differential glycosylation of polyclonal IgG, IgG-Fc and IgG-Fab isolated from the sera of patients with ANCA-associated systemic vasculitis. Biochim Biophys Acta 2006; 1760:669-77.
8. Harris RJ. Heterogeneity of recombinant antibodies: linking structure to function. Dev Biol (Basel) 2005; 122:117-27; PMID:16375256.
9. Sibéril S, Dutertre CA, Fridman WH, Teillaud JL. FcgammaR: The key to optimize therapeutic antibodies? Crit Rev Oncol Hematol 2007; 62:26-33; PMID:17240158; http://dx.doi.org/10.1016/j.critrevonc.2006.12.003.
10. Natsume A, Niwa R, Satoh M. Improving effector functions of antibodies for cancer treatment: Enhancing ADCC and CDC. Drug Des Devel Ther 2009; 3:7-16; PMID:19920917.
11. Moore GL, Chen H, Karki S, Lazar GA. Engineered Fc variant antibodies with enhanced ability to recruit complement and mediate effector functions. MAbs 2010; 2:181-9; PMID:20150767; http://dx.doi.org/10.4161/mabs.2.2.11158.
12. Radaev S, Sun PD. Recognition of IgG by Fcgamma receptor. The role of Fc glycosylation and the binding of peptide inhibitors. J Biol Chem 2001; 276:16478-83; PMID:11297533; http://dx.doi.org/10.1074/jbc.M100351200.
13. Krapp S, Mimura Y, Jefferis R, Huber R, Sondermann P. Structural analysis of human IgG-Fc glycoforms reveals a correlation between glycosylation and structural integrity. J Mol Biol 2003; 325:979-89; PMID:12527303; http://dx.doi.org/10.1016/S0022-2836(02)01250-0.
14. Vaccaro C, Zhou J, Ober RJ, Ward ES. Engineering the Fc region of immunoglobulin G to modulate in vivo antibody levels. Nat Biotechnol 2005; 23:1283-8; PMID:16186811; http://dx.doi.org/10.1038/nbt1143.
15. Clynes RA, Towers TL, Presta LG, Ravetch JV. Inhibitory Fc receptors modulate in vivo cytotoxicity against tumor targets. Nat Med 2000; 6:443-6; PMID:10742152; http://dx.doi.org/10.1038/74704.
16. Cunningham-Rundles C, Zhuo Z, Griffith B, Keenan J. Biological activities of polyethylene-glycol immunoglobulin conjugates. Resistance to enzymatic degradation. J Immunol Methods 1992; 152:177-90; PMID:1500728; http://dx.doi.org/10.1016/0022-1759(92)90139-K.
17. Anderson WL, Tomasi TB. Polymer modification of antibody to eliminate immune complex and Fc binding. J Immunol Methods 1988; 109:37-42; PMID:3128614; http://dx.doi.org/10.1016/0022-1759(88)90439-5.
18. Hamblett KJ, Senter PD, Chace DF, Sun MM, Lenox J, Cerveny CG, et al. Effects of drug loading on the antitumor activity of a monoclonal antibody drug conjugate. Clin Cancer Res 2004; 10:7063-70; PMID:15501986; http://dx.doi.org/10.1158/1078-0432.CCR-04-0789.
19. McLendon G, Radany E. Is protein turnover thermodynamically controlled? J Biol Chem 1978; 253:6335-7; PMID:687388.
20. Fontana A, Zambonin M, Polverino de Laurero P, De Filippis V, Clementi A, Scaramella E. Probing the conformational state of apomyoglobin by limited proteolysis. J Mol Biol 1997; 266:223-30; PMID:9047359; http://dx.doi.org/10.1006/jmbi.1996.0787.
21. Gurbaxani B, Dela Cruz LL, Chintalacharuvu K, Morrison SL. Analysis of a family of antibodies with different half-lives in mice fails to find a correlation between affinity for FcRn and serum half-life. Mol Immunol 2006; 43:1462-73; PMID:16139891; http://dx.doi.org/10.1016/j.molimm.2005.07.032.
22. Sulica A, Medesan C, Laky M, Onica D, Sjöquist J, Ghetie V. Effect of protein A of Staphylococcus aureus on the binding of monomeric and polymeric IgG to Fc receptor-bearing cells. Immunology 1979; 38:173-9; PMID:511216.
23. Stone GC, Sjöbring U, Björck L, Sjöquist J, Barber CV, Nardella FA. The Fc binding site for streptococcal protein G is in the Cgamma2--Cgamma3 interface region of IgG and is related to the sites that bind staphylococcal protein A and human rheumatoid factors. J Immunol 1989; 143:565-70; PMID:2738404.
24. Chapman AP. PEGylated antibodies and antibody fragments for improved therapy: a review. Adv Drug Deliv Rev 2002; 54:531-45; PMID:12052713; http://dx.doi.org/10.1016/S0169-409X(02)00026-1.
25. Kitamura K, Takahashi T, Yamaguchi T, Noguchi A, Noguchi A, Takashina K, et al. Chemical engineering of the monoclonal antibody A7 by polyethylene glycol for targeting cancer chemotherapy. Cancer Res 1991; 51:4310-5; PMID:1868453.
26. Suzuki T, Kanbara N, Tomono T, Hayashi N, Shinohara I. Physicochemical and biological properties of poly(ethylene glycol)-coupled immunoglobulin G. Biochim Biophys Acta 1984; 788:248-55; PMID:6743669; http://dx.doi.org/10.1016/0167-4838(84)90268-1.
27. Takashina K, Kitamura K, Yamaguchi T, Noguchi A, Noguchi A, Tsurumi H, et al. Comparative pharmacokinetic properties of murine monoclonal antibody A7 modified with neocarzinostatin, dextran and polyethylene glycol. Jpn J Cancer Res 1991; 82:1145-50; PMID:1720116; http://dx.doi.org/10.1111/j.1349-7006.1991.tb01769.x.
28. Ritchie TK, Grinkova YV, Bayburt TH, Denisov IG, Zolnerciks JK, Atkins WM, et al. Chapter 11--- Reconstitution of membrane proteins in phospholipid bilayer nanodiscs. Methods Enzymol 2009; 464:211-31; PMID:19903557; http://dx.doi.org/10.1016/S0076-6879(09)64011-8.
29. Sun MM, Beam KS, Cerveny CG, Hamblett KJ, Blackmore RS, Torgov MY, et al. Reduction-alkylation strategies for the modification of specific monoclonal antibody disulfides. Bioconjug Chem 2005; 16:1282-90; PMID:16173809; http://dx.doi.org/10.1021/bc050201y.
30. Liu H, Chumsae C, Gaza-Bulseco G, Hurkmans K, Radziejewski CH. Ranking the susceptibility of disulfide bonds in human IgG1 antibodies by reduction, differential alkylation, and LC-MS analysis. Anal Chem 2010; 82:5219-26; PMID:20491447; http://dx.doi.org/10.1021/ac100575n.
31. Getz EB, Xiao M, Chakrabarty T, Cooke R, Selvin PR. A comparison between the sulfhydryl reductants tris(2-carboxyethyl)phosphine and dithiothreitol for use in protein biochemistry. Anal Biochem 1999; 273:73-80; PMID:10452801; http://dx.doi.org/10.1006/abio.1999.4203.
32. Hermanson GT. Bioconjugate techniques. Amsterdam; Boston: Elsevier Academic Press 2008.

Cancer Immunol Immunother (2006) 55: 717–727
DOI 10.1007/s00262-005-0058-x

ORIGINAL ARTICLE

Camellia W. Adams · David E. Allison · Kelly Flagella
Leonard Presta · Janet Clarke · Noel Dybdal
Kathleen McKeever · Mark X. Sliwkowski

Humanization of a recombinant monoclonal antibody to produce a therapeutic HER dimerization inhibitor, pertuzumab

Received: 28 April 2005 / Accepted: 24 June 2005 / Published online: 3 September 2005
© Springer-Verlag 2005

Abstract Dimerization is essential for activity of human epidermal growth factor receptors (HER1/EGFR, HER2/ErbB2, HER3/ErbB3, and ErbB4) and mediates intracellular signaling events leading to cancer cell proliferation, survival, and resistance to therapy. HER2 is the preferred dimerization partner. Activation of HER signaling pathways may be blocked by inhibition of dimer formation using a monoclonal antibody (MAb) directed against the dimerization domain of HER2. The murine MAb 2C4 that specifically binds the HER2 dimerization domain was cloned as a chimeric antibody, humanized using a computer-generated model to guide framework substitutions, and variants were tested as Fabs. Pharmacokinetics and toxicology were evaluated in rodents and cynomolgus monkeys. Cloning the variable domains of MAb 2C4 into a vector containing human kappa and CH1 domains allowed construction of a mouse-human chimeric Fab. DNA sequencing of the chimeric clone permitted identification of CDR residues. The full-length IgG1 of variant F-10 was equivalent in binding to chimeric IgG1 and was designated pertuzumab (rhuMAb 2C4; Omnitarg). Pertuzumab pharmacokinetics was best described by a two-compartment model with a distribution phase of < 1 day, terminal half-life of ~10 days, and volume of distribution of ~40 mL/kg that approximates serum volume. With the exception of diarrhea, pertuzumab was generally well tolerated in cynomolgus monkeys. Pertuzumab, a recombinant humanized IgG1 MAb, is the first of a new class of agents known as HER dimerization inhibitors. Inhibition of HER dimerization may be an effective anticancer strategy in tumors with either normal or elevated expression of HER2.

Keywords Pertuzumab · 2C4 · rhuMAb 2C4 · HER2 · HER dimerization inhibitor (HDI) · Monoclonal antibody humanization

C. W. Adams (✉) · D. E. Allison · K. Flagella · L. Presta
J. Clarke · N. Dybdal · K. McKeever · M. X. Sliwkowski
Genentech Inc., One DNA Way,
South San Francisco, CA 94080, USA
E-mail: adams.camellia@gene.com
Tel.: +1-650-2252071
Fax: +1-650-2254343

Present address: L. Presta
DNAX Research Institute, Palo Alto, CA, USA

Present address: J. Clarke
Biogen Idec Inc., Cambridge, MA, USA

Introduction

Dimerization is essential for the activity of the transmembrane human epidermal growth factor receptors (HER1/EGFR, HER2/ErbB2, HER3/ErbB3, and ErbB4) (reviewed in Ref. [54]). Interactions between HER receptors and specific stromal ligands, the formation of different homodimers or heterodimers, and receptor cross talk, both within the HER family and with other growth factor receptors, govern the activation of specific intracellular signaling pathways, such as mitogen-activated protein kinase (MAPK) and phosphatidylinositol 3-kinase (PI3 K)/Akt [21, 39, 47]. Multiple HER ligands with different binding affinities for specific receptors have been identified, and include transforming growth factor alpha (ligand for EGFR), epidermal growth factor (EGFR), epiregulin (EGFR and HER4), beta-cellulin (EGFR), heparin-binding-EGF (EGFR and HER4), amphiregulin (EGFR), heregulin/neuregulin 1 (HER3 and HER4), and neuregulins 2,3,4 (HER4) (reviewed in Ref. [54]). Dysregulation of the complex HER signaling network is known to be associated with malignant transformation and cancer progression (reviewed in Ref. [23]). Studies have demonstrated that HER receptor dimerization mediates intracellular signaling events that lead to cancer cell proliferation, survival, and resistance to anticancer therapy in tumor cells associated with HER dysregulation [1, 2, 4, 7, 49].

The mechanisms of HER dimerization have now been elucidated through a series of elegant crystallography studies [5, 8, 17]. EGFR, HER3, and HER4 are inactive until ligand binding stabilizes the dimer-competent

formation. In the inactive form, the dimerization domain (domain II) is tethered to domain IV preventing the formation of dimers with other HER receptors. Substantial domain rearrangement is triggered when ligand binds to the receptor at extracellular domains I and III. This rearrangement exposes the dimerization domain for interactions with the dimerization domain of other HER receptors that are in the active conformation. In contrast, HER2, which lacks any known ligand, is constitutively in the active conformation and structurally resembles activated ligand-bound EGFR. As a result, the dimerization domain is permanently exposed and ready to form dimers with ligand-activated HER receptors. This explains why HER2 is the preferred binding partner for other HER receptors [21]. It has also been shown that HER2-containing heterodimers are the most prevalent and the most active of all dimer combinations [21]. For example, treatment with the HER3 ligand heregulin was able to induce transformation of cells expressing HER2-HER3, but not cells that express HER3 alone [49]. Other experiments have shown that the HER2-EGFR heterodimer may be associated with greater and more prolonged proliferative signals than EGFR homodimers [21, 25, 37]. Interestingly, HER2-HER3 and HER2-EGFR heterodimers were also more effective inducers of vascular endothelial growth factor than other HER heterodimer combinations [55].

Using a stably transfected NIH 3T3 cell line expressing the HER2 gene, several IgG1κ monoclonal antibodies (MAbs) targeting HER2 were developed and shown to bind different epitopes on the extracellular domain of the receptor [14]. One of these, the MAb 2C4, was subsequently shown to bind to the putative dimerization domain (domain II) [16]. Agents specifically targeting domain II could inhibit HER dimerization, thus preventing activation of HER signaling pathways that mediate cancer cell proliferation and survival [5]. Moreover, it is logical to target the dimerization domain of HER2 because it is the most common receptor in HER dimer combinations [21]. Since the clinical utility of murine MAbs is limited by a human antimouse antibody (HAMA) response [42], 2C4 was humanized. This paper describes the humanization of 2C4 and the evaluation of pharmacokinetics and safety in preclinical models. The principal objective of this study was to create a humanized MAb that specifically binds to the extracellular dimerization domain on the HER2 receptor, therefore inhibiting HER dimerization and the resultant activation of intracellular signaling pathways associated with cancer cell proliferation and survival.

Materials and methods

Construction of chimeric and humanized 2C4 Fabs

The murine MAb 2C4 that specifically binds the extracellular domain of HER2 (ErbB2) has been described previously [14]. To construct a mouse-human chimeric Fab, total RNA was isolated from 2C4 hybridoma cells using a Stratagene RNA extraction kit and manufacturer's protocols (Stratagene, La Jolla, CA, USA). The variable domains were amplified by reverse transcriptase polymerase chain reaction (RT-PCR), gel purified, and inserted into a pUC119-based plasmid containing a human kappa constant domain and human CH1 domain as previously described [6, 40]. Plasmids were transformed into *Escherichia coli* strain XL1-Blue (Stratagene, La Jolla, CA, USA) for preparation of double-stranded DNA.

For the chimera and each subsequent variant both light (L) and heavy (H) chains were completely sequenced using an automated ABI Stretch 3700 sequencer and Big Dye reagents [Applera Corp., Applied Biosystems (ABI)]. Sequences of the murine variable light (VL) and variable heavy (VH) domains (Fig. 1) [26] were used to construct a computer graphics model to determine which framework residues should be incorporated into the humanized antibody. Construction of models was performed as previously described by Carter and co-workers [6, 13].

The vector template for humanized Fab contained a consensus human kappa subgroup I L chain, a consensus human subgroup III heavy chain (VH-CH1), an alkaline phosphatase promoter, and an f1 phage origin for production of single-stranded DNA [6, 40]. To construct the first humanized variant, the complementarity-determining region (CDR)-swap Fab-1, site-directed mutagenesis [29] was performed on a deoxyuridine-containing single-stranded DNA template prepared from *E. coli* strain CJ236 (BioRad, Hercules, CA, USA). Thus all six CDRs were changed to the 2C4 sequence. Plasmids for other Fab variants were constructed using Fab-1 as the template.

Chimeric 2C4 Fab and humanized Fab variants were transformed into *E. coli* strain 16C9, a derivative of MM294, for protein expression and cultured using AP5 modified medium for protein induction. Fabs were purified using protein G-Sepharose CL-4B (Pharmacia Biotech, Amersham Biosciences Corp., Piscataway, NJ, USA) [40], buffer exchanged into 10 mM sodium succinate, 140 mM NaCl, pH 6.0, and concentrated to a volume of 0.5 mL using a Centricon-10 (Ambicon, Millipore, Billerica, MA, USA). A 500 mL culture yielded 0.1–0.3 mg protein. Protein concentrations were determined by quantitative amino acid analysis.

Construction of chimeric and humanized 2C4 IgG1

Full-length chimeric IgG1 (chIgG1) or humanized 2C4 IgG1 (rhuMAb 2C4; pertuzumab) were generated by subcloning the murine or humanized (Fab-10, Table 1) variable domains of the L and H chains from the respective Fabs into separate pRK vectors [19]. The L and H chain plasmids were co-transfected into an ade-

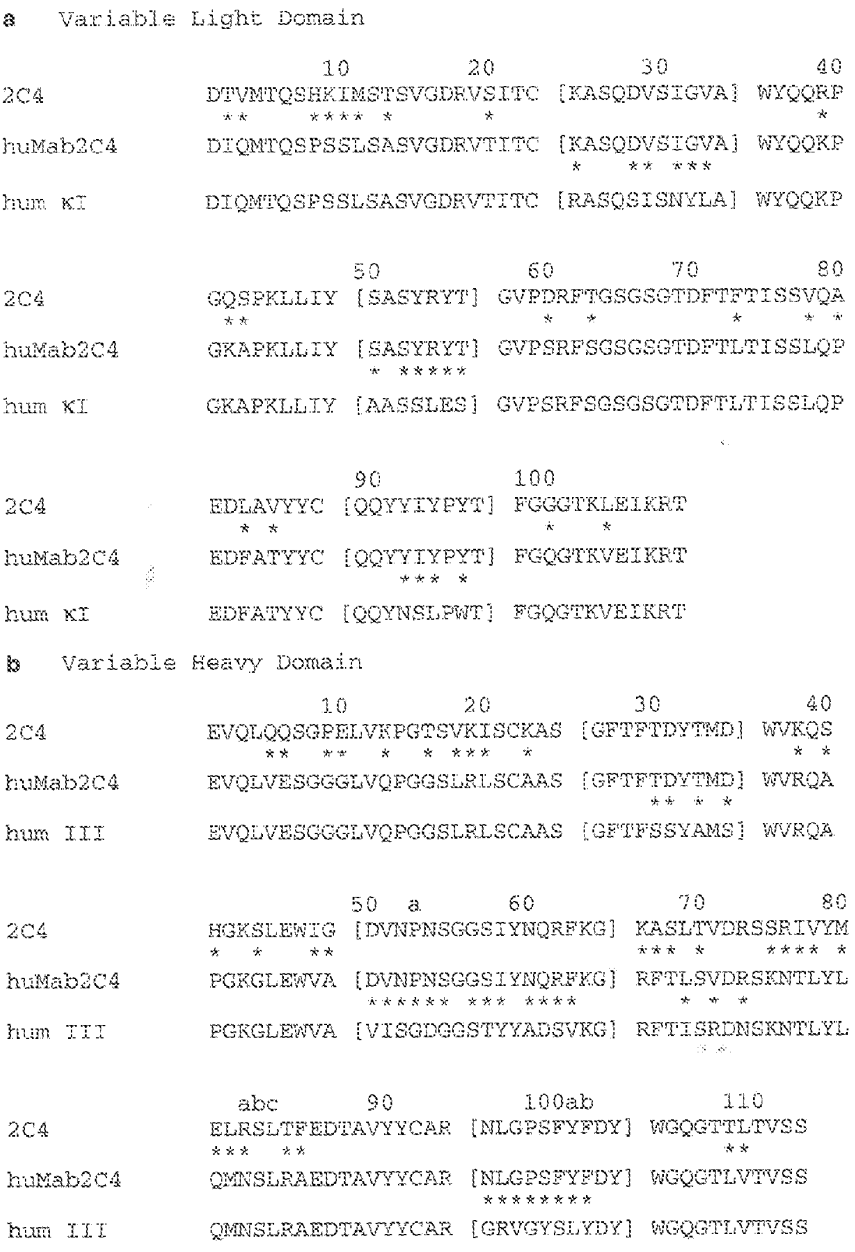


Fig. 1 Amino acid sequences of murine 2C4, humanized 2C4 (Fab-10) (pertuzumab), and human consensus sequences of L chain subgroup kappa I (humκI) and H chain subgroup III (hum III). CDR loops are enclosed in *brackets*, and differences between sequences are denoted by an *asterisk* (*). Residue numbering is according to Kabat et al. [26]. a VL domain. b VH domain

novirus-transformed human embryonic kidney cell line 293 [20] using a high-efficiency procedure [19]. Media were changed to serum-free and harvested after 4 days. Antibodies were purified from the supernatants using protein A-Sepharose CL-4B with the buffer exchanged and concentrated, using the same buffer as for the Fab. Chinese hamster ovary (CHO) cells were transfected with di-cistronic vectors to achieve stable expression of pertuzumab (rhuMAb 2C4).

HER2-extracellular domain (HER2-ECD) binding assay

To measure the binding activity of Fab and immunoglobulin Gs (IgGs), NUNC maxisorp plates were coated with 1 μg/mL of HER2-ECD (Genentech Inc., South San Francisco, CA, USA) in 50 mM carbonate buffer, pH 9.6, overnight at 4°C, and then blocked with enzyme-linked immunosorbent assay (ELISA) diluent

Table 1 Binding of humanized anti-HER2 Fab variants to HER2-ECD

Variant	Template	Changes[a]	Purpose	EC_{50} Fab-X/EC_{50} chimeric Fab[b]		
				Mean	SD[c]	*n*
Chimera	Chimeric Fab			1.0		
Fab-1	Human FR		Straight CDR Swap	No binding		3
Fab-2	Fab-1	Arg H71 **Val**	CDR-H2 conformation	35.0	3.5	3
Fab-3	Fab-1	Asp H73 **Arg**	Framework loop in VH	> 10,000		6
Fab-4	Fab-1	Arg H71 **Val** Asp H73 **Arg**	CDR-H2 conformation Framework loop in VH	4.0	0.3	4
Fab-5	Fab-4	Ala H49 **Gly**	CDR-H2 conformation	1.6	0.6	3
Fab-6	Fab-4	Phe H67 **Ala**	CDR-H2 conformation	1.7	0.9	2
Fab-7	Fab-4	Ala H49 **Gly** Phe H67 **Ala**	CDR-H2 conformation CDR-H2 conformation	1.4	0.6	2
Fab-8	Fab-4	Leu H78 **Val**	CDR-H2 conformation	2.9	0.6	2
Fab-9	Fab-4	Asn H76 **Arg**	Framework loop in VH	1.8	0.7	2
Fab-10	Fab-4	Ile H69 **Leu**	CDR-H2 conformation	1.0	0.3	4

H heavy chain, *Arg H71 Val* indicates change in the arginine at position 71 on the heavy chain to valine, *Ala* alanine, *Arg* arginine, *Asp* aspartic acid, *Asn* asparagine, *Gly* glycine, *Ile* isoleucine, *Leu* leucine, *Phe* phenylalanine, *Val* valine

[a]Murine residues are in *bold* type; *residue numbers* are according to Kabat et al. [26]

[b]The murine/human chimeric Fab was used as the standard. Equivalent binding to that of the chimera is indicated by an EC_{50} (50% effective concentration) Fab-X/EC_{50} chimeric Fab ratio of 1, while an increase in the ratio to greater than unity indicates relative binding affinity is proportionately less than the chimera. EC_{50} values were determined from titration curves. The EC_{50} for chimeric Fab was 0.13 mg/mL

[c]SD is standard deviation for $n > 2$ measurements; when $n = 2$ numbers are average difference from the mean

(0.5% BSA, 0.05% Polysorbate 20, PBS) at room temperature for 1 h. Serial dilutions of samples in ELISA diluent were incubated on the plates for 2 h. After washing, bound Fab or IgG molecules were detected with biotinylated murine anti-human kappa antibody (ICN 634771) followed by streptavidin-conjugated horseradish peroxidase (Sigma, St. Louis, MO, USA) using 3,3′,5,5′-tetramethyl benzidine (Kirkegaard and Perry Laboratories, Gaithersburg, MD, USA) as substrate. Absorbance was read at 450 nm. Chimera binding served as the standard. Titration curves were fit with a four-parameter nonlinear regression curve-fitting program (KaleidaGraph; Synergy Software, Reading, PA, USA). Concentrations of Fab variants corresponding to the midpoint absorbance of the titration curve of the standard were calculated and then divided by the concentration of the standard at that point.

Pharmacokinetics and toxicology in animals

All animal studies were conducted in accordance with institutional guidelines. Pertuzumab (26.7 mg/mL rhuMAb 2C4, Genentech Inc., South San Francisco, CA, USA) and vehicle (10 mM L-histidine at pH 6.0, 240 mM sucrose, 0.02% polysorbate 20) were stored at 2–8°C. All blood samples were collected without anticoagulant and allowed to clot at room temperature, and were stored frozen prior to thawing for analysis of pertuzumab serum concentrations. Mouse, rat, and cynomolgus monkey serum samples for pertuzumab concentrations were assayed using a receptor-binding ELISA. The assay uses immobilized antigen HER2-ECD (Genentech Inc., South San Francisco, CA, USA) to capture pertuzumab (rhuMAb 2C4) from serum samples [43]. Bound pertuzumab was detected with mouse anti-human Fc-horseradish peroxidase with tetramethyl benzidine used as the substrate for color development to quantify serum pertuzumab against a known standard curve. The assay has a minimum quantifiable concentration of 0.25–0.40 μg/mL of pertuzumab in mouse, rat, and cynomolgus monkey serum.

Single-dose pharmacokinetics in mice and rats

Male CD-1 mice (Charles River, Raleigh, NC, USA) weighing 0.022–0.028 kg were randomized into three groups (36 per group) that received 3, 30, or 90 mg/kg of pertuzumab by intravenous (IV) bolus. Male Sprague Dawley rats (Charles River) weighing 0.25–0.30 kg were randomized into three groups (six per group) that received 3, 30, or 90 mg/kg per animal of pertuzumab by IV bolus. For both species, blood was collected for pharmacokinetic analyses predose and at various times from 5 min to 36 days postdose.

Single-dose pharmacokinetics in monkeys

Six male and six female cynomolgus monkeys (SNBL, Everett, WA, USA), aged approximately 2–3 years and weighing 1.94–2.24 kg, were randomized into three groups (two animals per sex group) that received 15, 50, or 150 mg/kg per animal of pertuzumab by IV bolus. Blood was collected for pharmacokinetic analyses of pertuzumab at predose, and from 30 min to 28 days postdose.

Multi-dose toxicology study in monkeys

Cynomolgus monkeys were deemed the most appropriate animal model for assessing safety because of the 99% amino acid sequence homology between cynomolgus monkey and human HER2-ECD, similar binding affinity of pertuzumab to human and cynomolgus monkey HER2 (data not shown), and a lack of antibody binding to the mouse homolog (*c-neu*). A toxicology study was conducted in 20 males and 20 females' cynomolgus monkeys that were healthy and free from obvious abnormalities, aged 2.5–3.0 years, and weighing 2.1–3.3 kg. Animals were randomized into four groups, vehicle or 15, 50, or 150 mg/kg per animal of pertuzumab. All doses were administered as a IV bolus, once weekly for 7 weeks. Two males and two female monkeys in the control and 150 mg/kg groups were retained after the dosing period for evaluation during a 4-week recovery period. Blood was collected for toxicokinetic analyses predose, and frequently from 45 min to 7 days following the first and seventh doses. For the second to sixth doses, blood samples were collected at peak and trough at alternating intervals. Additional blood samples were collected from the recovery animals from days 57 to 80.

Animals were monitored twice daily for general health and three times on dosing days. Detailed observations were performed once weekly and on the day of scheduled euthanasia (day 49 or 80). Body weight, temperature, blood pressure, heart rate, electrocardiogram (ECG), ophthalmic parameters, clinical pathology (including standard clinical chemistry analyses, serum creatinine kinase isoenzyme, troponin T, hematology parameters, and urinalysis), and anatomic pathology parameters (including organ weights, gross pathology, and histopathology) were assessed.

Statistical analysis of toxicology data

Toxicology data from treatment groups were compared statistically with the data from the same gender control group. With the exception of clinical pathology data, only data collected on or after the first day of treatment were analyzed statistically, using one-way analysis of variance (ANOVA) or covariance (ANCOVA) [51, 52]. Dunnett's *t*-test [11] was used for control versus treated group comparisons if ANOVA or ANCOVA were significant ($p \leq 0.05$). Group comparisons were evaluated at the 5% two-tailed probability level.

Results

Humanization of 2C4 monoclonal antibody

A mouse-human chimeric Fab was constructed by cloning the variable domains of 2C4 murine MAb into a vector that contains human kappa and CH1 domains and permits expression of Fab fragments in *E. coli*. DNA sequencing of the chimeric clone allowed identification of the CDR residues (Fig. 1). For the purpose of this work, definitions of the CDRs based on sequence hypervariability as described by Kabat et al. [26] were used, except in the case of CDR-H1. For this CDR, the residues in the structure-based definition [9] were combined with the residues identified by sequence variability [26] and include residues H26–H35.

The consensus sequence for the human L chain subgroup kappa I and human H chain subgroup III comprised the framework for humanization (Fig. 1) [26]. This framework has been successfully used in humanization of other murine antibodies [6, 12, 40, 41, 50]. Since Fabs can be conveniently expressed and purified from *E. coli*, all humanized variants were initially constructed and screened for binding as Fabs. The initial variant, Fab-1, was a straight CDR swap in which the six murine CDRs were grafted onto the human framework. This Fab showed no detectable binding to HER2-ECD (Table 1).

As shown in Table 1, in Fab-2, H71 was changed from the human to the murine amino acid (Arg H71 Val) since this residue had previously been shown to affect the conformations of CDR-H1 and CDR-H2 [46, 53]. This change increased the binding from undetectable to 35-fold less than observed with the chimera. Residue H73 occurs in a framework loop adjacent to CDR-H1 and CDR-H2 and was previously shown to affect binding of other antibodies [40, 50]. In Fab-3, the residue at H73 was changed from the human to the murine amino acid (Asp H73 Arg). A slight increase in binding of Fab-3 was seen compared with Fab-1. However, when both the H71 and H73 changes were combined in Fab-4, binding was increased to within a fourfold difference from the chimera.

Several buried residues were evaluated based on their importance in previous humanizations. H49, shown to play a role in CDR-H2 conformation [40], was changed from the human to the murine amino acid (Ala H49 Gly). Phe H67, a large residue that might influence packing and conformation of CDR-H2 [50], was changed from the human to the murine amino acid (Phe H67 Ala). Each of these changes resulted in a very slight increase in binding compared with the template, Fab-4. The combination of H49 and H67 changes (Fab-7) was not improved over either mutation alone. Based on the model used, H78, which is buried and plays a role in supporting the conformation of CDR-H1 [40], was also investigated. However, binding decreased when Leu found in the human sequence at this position was changed to the murine amino acid (Leu H78 Val). None of these three changes were kept in the final humanized Fab.

A second residue in the Framework-3 loop, Asn H76, was previously observed to influence binding [12] and was therefore changed to the murine amino acid at this position (Asn H76 Arg) resulting in variant Fab-9. This

Table 2 Binding of 2C4 Fabs to HER2-ECD using surface plasmon resonance[a]

Variant	Fab bound, Rmax (RU)	k_{off} (10^{-4} s^{-1})	k_{on} (10^6 M^{-1} s^{-1})	K_d (nM)
Chimera	30	8.7 ± 1.5	9.5 ± 0.2	9.2 ± 1.6
Fab-10	25	9.5 ± 0.5	11.2 ± 0.1	8.5 ± 0.4

[a]Binding of Fab fragments to immobilized HER2-ECD was measured with a CM5-biosensor chip on a BIAcore-2000 system essentially as described [18]. Twofold serial dilutions of Fab from 125 nM to 1000 nM were injected at 25°C at a flow rate of 0.02 mL/min, and the net binding (in response units, RU) of Fab to a flowcell with HER2-ECD was measured versus a control flowcell with an unrelated IgG immobilized. Association (k_{on}) and dissociation (k_{off}) rate constants were calculated using global fitting with the BIA evaluation software, and the equilibrium dissociation constant, K_d was calculated as k_{off}/k_{on}

change slightly increased binding affinity, but as the residue may be solvent-exposed and could contribute to immunogenicity, the human amino acid at this position (Asn) was retained. Further mutations were made to explore the importance of the L chain and other buried residues of the H chain. None of these changes improved binding (data not shown). Finally, the buried amino acid residue at position H69 in the human sequence was replaced by the murine amino acid at this position (Ile H69 Leu). This resulted in variant Fab-10 with binding equal to that of the chimeric Fab. Binding kinetics of Fab-10 and the chimeric Fab were compared using surface plasmon resonance. The studies confirmed that Fab-10 has binding equal to that of the starting chimeric antibody (Table 2) [18].

Full-length MAbs of variant Fab-10 and the chimera were constructed by fusing the respective VL and VH domains to the constant domains of human kappa L chain and human IgG1 H chain. The full-length IgG1 of variant

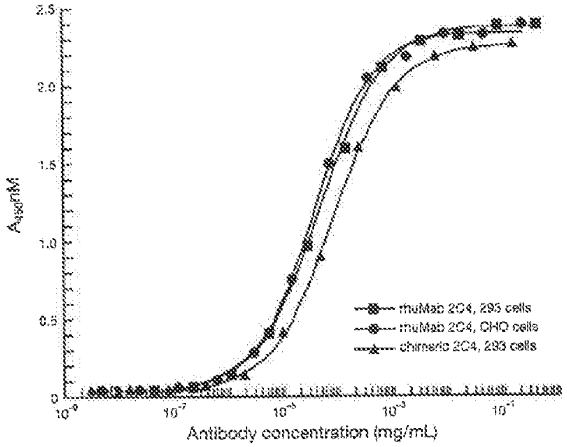


Fig. 2 Humanized 2C4 IgG1 (pertuzumab) expressed from either 293 cells (*filled square*) or CHO cells (*filled circle*) binds HER2-ECD equally well compared with the 2C4 chimeric full-length IgG1 antibody (*filled triangle*)

F-10 was equivalent in binding to the chimeric IgG1 (Fig. 2) and was designated pertuzumab (rhuMAb 2C4).

Pharmacokinetics

Table 3 summarizes pharmacokinetic parameters for pertuzumab. Pertuzumab serum concentration-time data from single-dose studies in mice and rats, and single-dose and multiple-dose studies in cynomolgus monkeys exhibited biphasic disposition and were fit into a two-compartment pharmacokinetic model. The distribution phase of pertuzumab was < 1 day, the terminal elimination half-life was approximately 10 days, and the volume of distribution was 27–58 mL/kg. The volume of distribution of the central compartment approximated the serum volume in all models and did not change with increasing dose in multiple-dose studies in cynomolgus monkeys. However, clearance increased by approximately 30% when the dose was increased from 50 mg/kg to 150 mg/kg in these multiple-dose studies. Figure 3 shows predicted clearance in humans by allometric interspecies scaling [24].

Safety evaluation of pertuzumab in cynomolgus monkeys

Pertuzumab (15, 50, and 150 mg/kg IV weekly for 7 weeks) was generally well tolerated and there were no treatment-related effects on physical examination, blood pressure, heart rate, ECG, cardiac markers (creatinine kinase isoenzymes and troponin T), ophthalmic parameters, clinical pathology tests, and anatomic pathology parameters. Treatment with pertuzumab was associated with an increased incidence and occurrence of liquid and non-formed feces (Table 4). Although diarrhea was observed in all groups, including control, it was most notable in animals given 150 mg pertuzumab per kg. Diarrhea did not adversely affect body weight (except in one animal), and did not result in dehydration or changes in clinical or anatomic pathology parameters. Moreover, diarrhea was reversible, although not completely normalized, and improved by day 80 of the 4-week recovery period.

Discussion

Based on the hypothesis that inhibiting HER dimerization may block intracellular signaling pathways associated with cancer cell proliferation and survival, this work was undertaken to produce a novel anticancer therapeutic by humanizing a murine MAb that targets the dimerization domain on the HER2 receptor. The murine MAb 2C4 was successfully humanized using consensus framework sequences for L and H chains, VLκI and VHIII, to produce pertuzumab (recombinant humanized MAb 2C4), which represents the first of a

Table 3 Pharmacokinetic parameters for pertuzumab[a]

Study type	Species/strain	No./sex	Route	Doses (mg/kg)	CL (mL/day/kg)	V_c (mL/kg)	V_{ss} (mL/kg)	αHL (day)	βHL (day)
SD PK	Mouse/CD-1	144/M	IV	3, 30, 90	5.6–9.2	45–58	102–148	0.1–0.3	11.4–15.7
SD PK	Rat/SD	18/M	IV	3, 30, 90	7.2–10.1	27–44	91–121	0.2–0.4	8.9–9.2
SD PK	Monkey/Cyno	8/M, 8/F	IV	15, 50, 150	5.0–5.2	31–37	68–73	0.3–0.9	9.9–10.4
MD Tox	Monkey/Cyno	14/M, 14/F	IV	15, 50, 150	5.1–7.4	36–41	64–80	0.5–0.6	8.1–10.6

CL clearance, V_c volume of distribution of the central compartment, V_{ss} volume of distribution at steady state, *αHL* initial half-life, *βHL* terminal half-life, *SD* Single-dose, *MD* Multi-dose, *PK* Pharmacokinetic, *Tox* Toxicology, *IV* Intravenous

[a]Pharmacokinetics were characterized using a two-compartment model for the serum concentration-time data of individual animals (WinNonlin Professional Version 3.1, Pharsight Corp., Mountain View, CA, USA) using the Gauss–Newton algorithm and a reiterative weighting scheme ($1/\hat{Y}$). Serum pertuzumab concentrations found in the less-than-reportable range of the assay (LTR; < 0.25 μg/mL) were not used for pharmacokinetic analysis, or in the group summary calculations. Data are ranges of group means

new class of agents designated HER dimerization inhibitors. Results from both the toxicology and pharmacokinetic studies reported in this paper supported the initiation of human clinical studies using doses of 0.5–15 mg/kg of pertuzumab administered every 3 weeks.

Consensus frameworks have been used successfully in several previous humanizations [6, 13, 40, 41, 50]; the current work further illustrates the utility of this approach. Transferring CDRs from the murine antibody to the human framework resulted in complete loss of binding to HER2-ECD. Remarkably, altering only three non-CDR residues in the H chain was sufficient to restore binding to that of the parent MAb. From the model, it was anticipated that two of these residues, H69 and H71, are buried and on the same side of a beta strand with their side chains directed toward CDR-H2. Thus, it was thought that they would play an important role in maintaining the conformation of this CDR. In the crystal structure of the humanized 2C4 Fab now available (Fig. 4) [48], it can be seen that this hypothesis is correct. When Leu is substituted for Ile at position H69, the packing is improved due to a better fit into a pocket between CDRH2 and framework 3. At position H71, the large human residue, Arg, would probably impinge on the Pro at position 52a on CDR H2, thereby changing the conformation of this loop. The substitution of Val, a much smaller and uncharged residue, allows CDRH2 to maintain the optimal conformation. In a sense, the pertuzumab sequence is a hybrid with respect to positions H69 and H71, since it has the closest homologue (Ile) of the favored Leu found at position H69 in subgroup III, and the favored Val from subgroup II at position 71. In the model, it appears that H73 is solvent exposed, thus it was postulated that this residue might interact directly with antigen. In the crystal structure of the pertuzumab–receptor complex [16], H73, changed to Arg in pertuzumab, can be seen to directly interact with the receptor, thus explaining the preference for Arg over Asp at this position. Position H73 is quite variable, and may play a direct role in antigen binding of other antibodies. None of the residues in the L chain were changed to derive the humanized antibody.

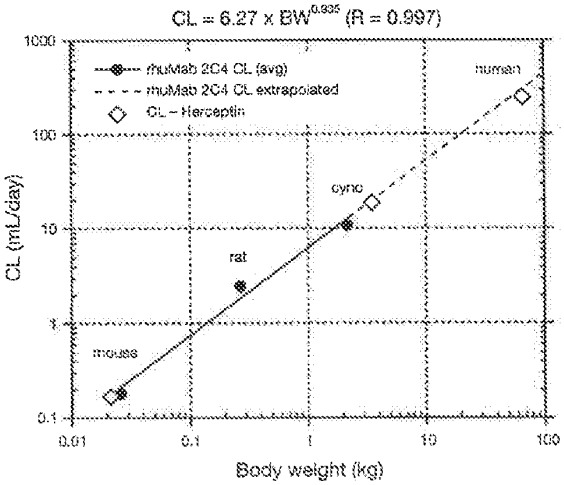


Fig. 3 Interspecies scaling used to predict human clearance. The predicted CL of pertuzumab in humans by allometric scaling is approximately 330 mL/day, which is equivalent to 4.76 mL/day/kg for a 70 kg individual

Evidence from previously published in vitro and in vivo studies supports the putative mechanism of action of pertuzumab as an inhibitor of HER dimerization [2, 16]. A recent study determined the X-ray crystal structure of the soluble HER2-ECD in a complex with the antigen-binding fragment of pertuzumab [16]. The study showed that pertuzumab binds near the center of the second cysteine-rich dimerization domain (extracellular domain II), a region of the HER receptor family that is highly conserved and previously shown to be necessary for EGFR homodimerization. Experiments in which the binding site was altered by mutation indicated a steric mechanism for the ability of pertuzumab to inhibit HER2 receptor dimerization and signaling [16]. Of note, pertuzumab binds to a different extracellular domain of the HER2 receptor compared with trastuzumab, which binds at domain IV [8, 14].

In vitro studies showed that pertuzumab is far more effective than trastuzumab in disrupting the formation of HER3-heregulin-HER2 complexes in MCF-7 (low/normal HER2 expression) and SK-BR3 (high HER2 expression) breast cancer cell lines [2]. Inhibition of HER dimer formation by pertuzumab was also shown

Table 4 Incidence and frequency of diarrhea in male (*M*) and female (*F*) cynomolgus monkeys treated for 7 weeks with 15, 50, and 150 mg/kg pertuzumab IV for 7 weeks

Pertuzumab (mg/kg)	Non-formed feces						Liquid feces					
	Acclimation		Treatment		Recovery		Acclimation		Treatment		Recovery	
	M	F	M	F	M	F	M	F	M	F	M	F
Number of animals affected/number of animals per group												
0	1/5	3/6	2/6	2/6	1/2	0/2	0/5	0/6	1/6	0/6	0/2	0/2
15	0/4	3/4	3/4	4/4	–	–	0/4	0/4	1/4	2/4	–	–
50	3/4	2/4	2/4	3/4	–	–	0/4	0/4	2/4	2/4	–	–
150	4/6	4/6	6/6	5/6	2/2	1/2	1/6	2/6	3/6	5/6	1/2	0/2
Number of days observed (± SD)												
0	0.2 (0.4)	0.8 (1.2)	0.7 (1.2)	0.7 (1.2)	1.5 (2.1)	0.0 (0.0)	0.0 (0.0)	0.0 (0.0)	0.2 (0.4)	0.0 (0.0)	0.0 (0.0)	0.0 (0.0)
15	0.0 (0.0)	3.0 (2.9)	1.5 (1.3)	17.0 (15.5)	–	–	0.0 (0.0)	0.0 (0.0)	0.3 (0.5)	2.0 (2.8)	–	–
50	1.0 (0.8)	1.3 (1.5)	12.0 (14.0)	8.0 (12.1)	–	–	0.0 (0.0)	0.0 (0.0)	5.3 (6.4)	1.5 (2.4)	–	–
150	2.3 (2.6)	6.0 (6.9)	12.2 (9.4)	4.2 (3.5)	6.5 (4.9)	0.5 (0.7)	1.7 (4.1)	1.0 (1.5)	6.7 (8.9)	11.2 (17.3)	0.5 (0.7)	0.0 (0.0)

SD standard deviation

to block the heregulin-dependent phosphorylation signal of HER2 and to inhibit downstream MAPK and Akt signaling pathways in MCF-7 cells [2]. Activity was seen for intact pertuzumab and the Fab fragment [2]. In addition, pertuzumab was found to inhibit ligand-dependent receptor activation and signaling in several other cell lines, including ovarian cancer [45], androgen-independent prostate cancer [35], colon cancer [34], breast cancer [30], and lung epithelial cells [32].

In vivo experiments support the hypothesis that inhibition of HER dimerization and downstream signaling will have antiproliferative effects against a range of different tumor types. Both pertuzumab and trastuzumab inhibited breast cancer xenografts with high HER2 expression (BT474), and importantly, pertuzumab also inhibited xenografts with low levels of HER2 expression (MCF-7), achieving 59% growth inhibition compared with controls or trastuzumab ($p < 0.001$) [2]. In the androgen-independent prostate cancer xenograft, CWRSA6, which is not responsive to trastuzumab, pertuzumab produced 82% growth inhibition compared with controls [2]. A dose-response relationship was also observed in CWRR22R androgen-independent xenografts [2]. In xenograft models of non-small cell lung cancer (NSCLC) treated with pertuzumab, tumor growth inhibition of >80% was obtained in NCI-H522 (NSCLC HER2 1+) and in Calu-3 (NSCLC HER2 3+) [33]. This degree of tumor growth inhibition was seen at trough serum concentrations of 5–25 μg/mL of pertuzumab [33].

Pertuzumab entered clinical development based on evidence of biological activity in xenograft tumor models, using a dose regimen that was supported by the preclinical and toxicology models reported in this paper. The disposition of pertuzumab in humans was expected to be similar to that of other humanized MAbs that share the same IgG1 framework, trastuzumab and bevacizumab [15, 31], because preclinical pharmacokinetics were comparable between these molecules and allometric interspecies scaling predicted similar clearance.

In a Phase Ia clinical study, patients with incurable, locally advanced, recurrent or metastatic solid tumors that had progressed during or after standard therapy were administered pertuzumab intravenously every 3 weeks at doses escalating from 0.5 mg/kg to 15 mg/kg [3]. Pharmacokinetic results of pertuzumab doses from 2 mg/kg to 15 mg/kg showed that the systemic clearance (CL) did not change with dose (grand mean = 3.42 ± 1.20 mL/day/kg), the volume of distribution (Vd) approximated the serum volume (grand mean = 40.6 ± 6.6 mL/day/kg) and the terminal elimination half-life was approximately 2–3 weeks (grand mean = 18.9 ± 8.0 days). There was good agreement between pertuzumab pharmacokinetics observed in this study and expected from preclinical studies.

In comparison, a population pharmacokinetic model in patients with metastatic breast cancer estimated the clearance of trastuzumab to be 225 mL/day (3.24 mL/day/kg for a 69 kg patient) [22]. Moreover, dosing

OnCusp
Ex. 1002

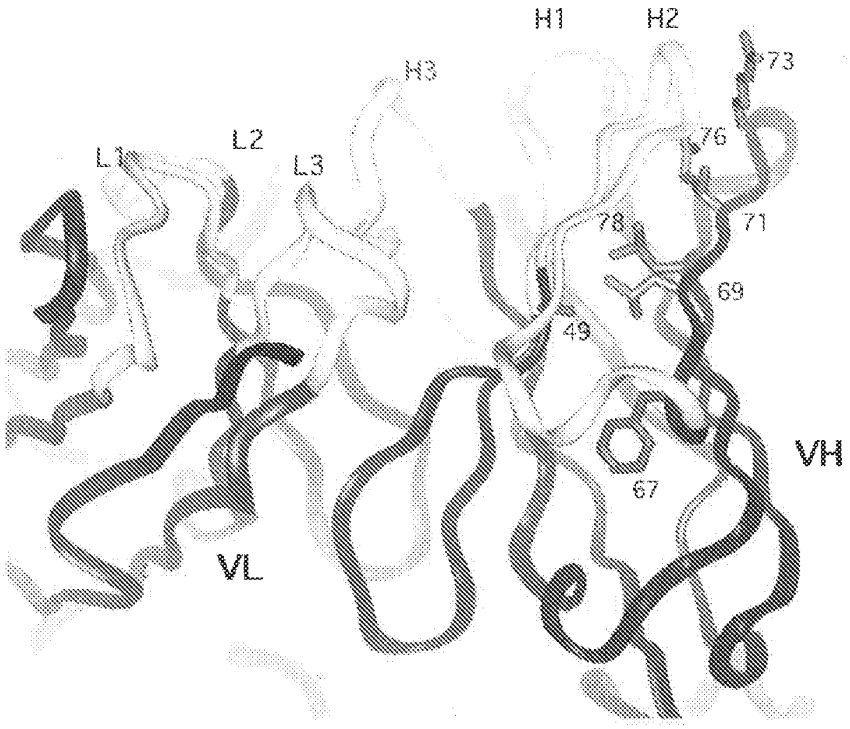


Fig. 4 X-ray structure of humanized 2C4 Fab (pertuzumab) [48] (PDB accession number 1L71). The CDR loops of the light (L1-3) and heavy chains (H1-3) are indicated. Side chains of VH residues that were investigated or changed during humanization are shown (refer to Table 1 for details for specific changes and their effect on binding relative to the chimera)

trastuzumab every 3 weeks has been shown to be feasible and effective [31]. As pertuzumab and trastuzumab appear to have comparable pharmacokinetic profiles, an every 3-week dosing schedule was recommended for clinical testing of pertuzumab.

Since pertuzumab was associated with minimal toxicity and a large safety factor in the 7-week toxicology study in cynomolgus monkeys, a starting dose of 0.5 mg/kg every 3 weeks was recommended for clinical testing. An upper dose of 15.0 mg/kg every 3 weeks was recommended by estimating the dose required to exceed serum trough concentrations of pertuzumab associated with efficacy in xenograft models (5–25 μg/mL) [33]. Pharmacokinetic simulations predicted that doses between 5.0 mg/kg and 15.0 mg/kg administered every 3 weeks would achieve targeted serum trough concentrations of 20 μg/mL in most subjects. The dose range 0.5–15.0 mg/kg represents a safety factor of 300-fold to tenfold com

pared with the highest dose of pertuzumab (150 mg/kg) used in the multi-dose toxicology studies in cynomolgus monkeys. In the 7-week toxicology study, diarrhea was the only significant toxicity and was observed in all dose groups treated with pertuzumab for 7 weeks. Diarrhea improved during the recovery period and in most cases was responsive to supportive care. Similarly, diarrhea was also observed in a chronic dosing study in which cynomolgus monkeys were treated with pertuzumab (15, 50, and 150 mg/kg IV) for 26 weeks (data not shown). Unlike in the 7-week study, diarrhea-related dehydration was observed in the 26-week study. Agents targeting the EGF receptor tyrosine kinase have also been associated with diarrhea [28, 38], although they have a different mechanism of action from pertuzumab. Pertuzumab does not bind to EGFR, but it does inhibit formation of EGFR/HER2 heterodimers [2]. EGFR may be a negative regulator of chloride secretion; therefore, inhibition of receptor activity could lead to increased fluid secretion into the intestinal lumen [27].

There was no evidence of cardiotoxicity in cynomolgus monkeys. In the clinical setting, decreased left ventricular function has been observed in patients treated the anti-HER2 MAb trastuzumab, particularly when used in combination with anthracycline therapy [44]. Evidence from preclinical studies indicates that the HER2-signaling pathway in cardiac myocytes may play an important role in the cardiotoxicity of anti-HER2 therapy [10, 36], therefore, monitoring of potential cardiac effects is mandatory in ongoing clinical studies of pertuzumab.

In the Phase Ia study, pertuzumab was generally well tolerated and no evidence of decreased left ventricular function was observed, except in one patient who had an intercurrent myocardial infarction [3]. Of note, the study also provided evidence of antitumor activity. Tumor regression was achieved in 3 of 20 patients evaluable for response (ovarian cancer, islet cell carcinoma of the pancreas, and prostate cancer). Two patients had confirmed partial responses. Stable disease lasting for more than 2.5 months was observed in 6 of 21 patients. Antibodies to pertuzumab were not detected.

In conclusion, the recombinant humanized MAb pertuzumab is the first HER dimerization inhibitor to enter clinical development. Inhibiting HER receptor dimerization by targeting the dimerization domain of HER2 prevents the activation of HER signaling pathways that mediate cancer cell proliferation and survival. Preclinical and preliminary clinical evidence suggests that inhibition of HER dimerization may be an effective anticancer strategy in tumors expressing HER2 either at normal or elevated levels.

Acknowledgments The authors gratefully acknowledge the important contributions of Tim Breece and Charlie Schmaizer (for protein purification), Henry Lowman (for BIAcore assays), Mubashira A. Malik (for assistance with PK assays) and the Oligosynthesis and DNA Sequencing Groups at Genentech Inc.

References

1. Agus DB, Akita RW, Fox WD, Lofgren JA, Higgins B, Maiese K, Scher HI, Sliwkowski MX (2000) A potential role for activated HER-2 in prostate cancer. Semin Oncol 27:76–83
2. Agus DB, Akita RW, Fox WD, Lewis GD, Higgins B, Pisacane PI, Lofgren JA, Tindell C, Evans DP, Maiese K, Scher HI, Sliwkowski MX (2002) Targeting ligand-activated ErbB2 signaling inhibits breast and tumor growth. Cancer Cell 2:127–137
3. Agus DB, Gordon MS, Taylor C, Natale RB, Karlan B, Mendelson DS, Press MF, Allison DE, Sliwkowski MX, Lieberman G, Kelsey SM, Fyfe G (2005) Phase I clinical study of pertuzumab, a novel HER dimerization inhibitor, in patients with advanced cancer. J Clin Oncol 23:2534–2543
4. Alimandi M, Romano A, Curia MC, Muraro R, Fedi P, Aaronson SA, Di Fiore PP, Kraus MH (1995) Cooperative signaling of ErbB3 and ErbB2 in neoplastic transformation and human mammary carcinomas. Oncogene 10:1813–1821
5. Burgess AW, Cho HS, Eigenbrot C, Ferguson KM, Garrett TP, Leahy DJ, Lemmon MA, Sliwkowski MX, Ward CW, Yokoyama S (2003) An open-and-shut case? Recent insights into the activation of EGF/ErbB receptors. Mol Cell 12:541–552
6. Carter P, Presta L, Gorman CM, Ridgway JB, Henner D, Wong WL, Rowland AM, Kotts C, Carver ME, Shepard HM (1992) Humanization of an anti-p185HER2 antibody for human cancer therapy. Proc Natl Acad Sci USA 89:4285–4289
7. Chen X, Yeung TK, Wang Z (2000) Enhanced drug resistance in cells coexpressing ErbB2 with EGF receptor or ErbB3. Biochem Biophys Res Commun 277:757–763
8. Cho HS, Mason K, Ramyar KX, Stanley AM, Gabelli SB, Denney DW Jr, Leahy DJ (2003) Structure of the extracellular region of HER2 alone and in complex with the Herceptin Fab. Nature 421:756–760
9. Chothia C, Lesk AM, Tramontano A, Levitt M, Smith-Gill SJ, Air G, Sheriff S, Padlan EA, Davies D, Tulip WR, Colman PM, Spinelli S, Alzari PM, Poljak RJ (1989) Conformations of immunoglobulin hypervariable regions. Nature 342:877–883
10. Crone SA, Zhao YY, Fan L, Gu Y, Minamisawa S, Liu Y, Peterson KL, Chen J, Kahn R, Condorelli G, Ross J Jr, Chien KR, Lee KF (2002) ErbB2 is essential in the prevention of dilated cardiomyopathy. Nat Med 8:459–465
11. Dunnett CW (1964) New tables for multiple comparisons with a control. Biometrics 20:482–491
12. Eigenbrot C, Gonzalez T, Mayeda J, Carter P, Werther W, Hotaling T, Fox J, Kessler J (1994) X-ray structures of fragments from binding and nonbinding versions of a humanized anti-CD18 antibody: structural indications of the key role of VH residues 59 to 65. Proteins 18:49–62
13. Eigenbrot C, Randal M, Presta L, Carter P, Kossiakoff AA (1993) X-ray structures of the antigen-binding domains from three variants of humanized anti-p185HER2 antibody 4D5 and comparison with molecular modeling. J Mol Biol 229:969–995
14. Fendly BM, Winget M, Hudziak RM, Lipari MT, Napier MA, Ullrich A (1990) Characterization of murine monoclonal antibodies reactive to either the human epidermal growth factor receptor or HER2/neu gene product. Cancer Res 50:1550–1558
15. Fernando NH, Hurwitz HI (2003) Inhibition of vascular endothelial growth factor in the treatment of colorectal cancer. Semin Oncol 30(Suppl 6):39–50
16. Franklin MC, Carey KD, Vajdos FF, Leahy DJ, de Vos AM, Sliwkowski MX (2004) Insights into ErbB signaling. Cancer Cell 5:317–328
17. Garrett TP, McKern NM, Lou M, Elleman TC, Adams TE, Lovrecz GO, Kofler M, Jorissen RN, Nice EC, Burgess AW, Ward CW (2003) The crystal structure of a truncated ErbB2 ectodomain reveals an active conformation, poised to interact with other ErbB receptors. Mol Cell 11:495–505
18. Gerstner RB, Carter P, Lowman HB (2002) Sequence plasticity in the antigen-binding site of a therapeutic anti-HER2 antibody. J Mol Biol 321:851–862
19. Gorman CM, Gies DR, McCray G (1990) Transient production of proteins using an adenovirus transformed cell line. DNA Prot Eng Tech 2:3–10
20. Graham FL, Smiley J, Russell WC, Nairn R (1977) Characteristics of a human cell line transformed by DNA from human adenovirus type 5. J Gen Virol 36:59–74
21. Graus-Porta D, Beerli RR, Daly JM, Hynes NE (1997) ErbB-2, the preferred heterodimerization partner of all ErbB receptors, is a mediator of lateral signaling. EMBO J 16:1647–1655
22. Harris KA, Washington CB, Lieberman G, Lu JF, Mass R, Bruno R (2002) A population pharmacokinetic (PK) model for trastuzumab (Herceptin) and implications for clinical dosing. Proc Am Soc Clin Oncol 21 (abstr 488)
23. Holbro T, Civenni G, Hynes NE (2003) The ErbB receptors and their role in cancer progression. Exp Cell Res 284:99–110
24. Ings RMJ (1990) Interspecies scaling and comparisons in drug development and toxicokinetics. Xenobiotica 20:1125–1135
25. Jones JT, Akita RW, Sliwkowski MX (1999) Binding specificities and affinities of egf domains for ErbB receptors. FEBS Lett 447:227–231
26. Kabat EA, Wu TT, Perry H, Gottesmann KS, Foeller C (1991) Sequences of proteins of immunological interest, 5th edn. Public Health Service, National Institutes of Health Bethesda, MD
27. Keely SJ, Uribe JM, Barrett KE (1998) Carbachol stimulates transactivation of epidermal growth factor receptor and mitogen-activated protein kinase in T84 cells. Implications for carbachol-stimulated chloride secretion. J Biol Chem 273:27111–27117
28. Kris MG, Natale RB, Herbst RS, Lynch TJ Jr, Prager D, Belani CP, Schiller JH, Kelly K, Spiridonidis H, Sandler A, Albain KS, Cella D, Wolf MK, Averbuch SD, Ochs JJ, Kay AC (2003) Efficacy of gefitinib, an inhibitor of the epidermal growth factor receptor tyrosine kinase, in symptomatic patients with non-small cell lung cancer: a randomized trial. JAMA 290:2149–2158
29. Kunkel TA (1985) Rapid and efficient site-specific mutagenesis without phenotypic selection. Proc Natl Acad Sci USA 82:488–492
30. Lee H, Akita RW, Sliwkowski MX, Maihle NJ (2001) A naturally occurring secreted human ErbB3 receptor isoform inhibits heregulin-stimulated activation of ErbB2, ErbB3, and ErbB4. Cancer Res 61:4467–4473
31. Leyland-Jones B, Gelmon K, Ayoub JP, Arnold A, Verma S, Dias R, Ghahramani P (2003) Pharmacokinetics, safety, and efficacy of trastuzumab administered every three weeks in combination with paclitaxel. J Clin Oncol 21:3965–3971
32. Liu J, Kern JA (2002) Neuregulin-1 activates the JAK-STAT pathway and regulates lung epithelial cell proliferation. Am J Resp Cell Mol Biol 27:306–313

33. Malik MA, Totpal K, Balter I, Sliwkowski MX, Pelletier N, Reich M, Crocker L, Friess T, Bauer S, Fiebig HH, Allison DE (2003) Dose-response studies of recombinant humanized monoclonal antibody 2C4 in tumor xenograft models. Proc Am Assoc Cancer Res 44:150 (abstr 773)
34. Mann M, Sheng H, Shao J, Williams CS, Pisacane PI, Sliwkowski MX, DuBois RN (2001) Targeting cyclooxygenase 2 and HER-2/neu pathways inhibits colorectal carcinoma growth. Gastroenterology 120:1713–1719
35. Mendoza N, Phillips GL, Silva J, Schwall R, Wickramasinghe D (2002) Inhibition of ligand-mediated HER2 activation in androgen-independent prostate cancer. Cancer Res 62:5485–5488
36. Negro A, Brar BK, Lee KF (2004) Essential roles of Her2/erbB2 in cardiac development and function. Recent Prog Horm Res 59:1–12
37. Olayioye MA, Graus-Porta D, Beerli RR, Rohrer J, Gay B, Hynes NE (1998) ErbB-1 and ErbB-2 acquire distinct signaling properties dependent upon their dimerization partner. Mol Cell Biol 18:5042–5051
38. Perez-Soler R, Chachoua A, Hammond LA, Rowinsky EK, Huberman M, Karp D, Rigas J, Clark GM, Santabarbara P, Bonomi P (2004) Determinants of tumor response and survival with erlotinib in patients with non-small-cell lung cancer. J Clin Oncol 22:3238–3247
39. Pinkas-Kramarski R, Soussan L, Waterman H, Levkowitz G, Alroy I, Klapper L, Lavi S, Seger R, Ratzkin BJ, Sela M, Yarden Y (1996) Diversification of Neu differentiation factor and epidermal growth factor signaling by combinatorial receptor interactions. EMBO J 15:2452–2467
40. Presta LG, Chen H, O'Connor SJ, Chisholm V, Meng YG, Krummen L, Winkler M, Ferrara N (1997) Humanization of an anti-vascular endothelial growth factor monoclonal antibody for the therapy of solid tumors and other disorders. Cancer Res 57:4593–4599
41. Presta LG, Lahr SJ, Shields RL, Porter JP, Gorman CM, Fendly BM, Jardieu PM (1993) Humanization of an antibody directed against IgE. J Immunol 151:2623–2632
42. Schroff RW, Foon KAA, Beatty SSM, Odham RK, Morgan AC Jr (1985) Human anti-murine immunoglobulin response in patients receiving monoclonal antibody therapy. Cancer Res 45:879–885
43. Sias PE, Kotts CE, Vetterlein D, Shepard M, Wong WL (1990) ELISA for quantitation of the extracellular domain of p185HER2 in biological fluids. J Immunol Methods 132:73–80
44. Suter TM, Cook-Bruns N, Barton C (2004) Cardiotoxicity associated with trastuzumab (Herceptin) therapy in the treatment of metastatic breast cancer. Breast 13:173–183
45. Totpal K, Balter I, Akita R, Bargsiochi F, Phillips GL, Shwkowski MX (2003) Targeting ErbB2/HER2's role as a coreceptor with rhuMAb2C4 inhibits Erb/HER ligand-dependent signaling and proliferation of ovarian tumor cell lines. Proc Am Assoc Cancer Res 44:151 (abstr 776)
46. Tramontano A, Chothia C, Lesk AM (1990) Framework residue 71 is a major determinant of the position and conformation of the second hypervariable region in the VH domains of immunoglobulins. J Mol Biol 215:175–182
47. Tzahar E, Waterman H, Chen X, Levkowitz G, Karunagaran D, Lavi S, Ratzkin BJ, Yarden Y (1996) A hierarchical network of interreceptor interactions determines signal transduction by Neu differentiation factor/neuregulin and epidermal growth factor. Mol Cell Biol 16:5276–5287
48. Vajdos FF, Adams CW, Breece TN, Presta LG, de Vos AM, Sidhu SS (2002) Comprehensive functional maps of the antigen-binding site of an anti-ErbB2 antibody obtained with shotgun scanning mutagenesis. J Mol Biol 320:415–428
49. Wallasch C, Weiss FU, Niederfellner G, Jallal B, Issing W, Ullrich A (1995) Heregulin-dependent regulation of HER2/neu oncogenic signaling by heterodimerization with HER3. EMBO J 14:4267–4275
50. Werther WA, Gonzalez TN, O'Connor SJ, McCabe S, Chan B, Hotaling T, Champe M, Fox JA, Jardieu PM, Berman PW, Presta LG (1996) Humanization of an anti-lymphocyte function-associated antigen (LFA)-1 monoclonal antibody and reengineering of the humanized antibody for binding to rhesus LFA-1. J Immunol 157:4986–4995
51. Winer BJ (1971) Analysis of covariance. In: Statistical principles in experimental design, 2nd edn. McGraw-Hill, New York, pp 752–812
52. Winer BJ (1971) Design and analysis of single-factor experiments. In: Statistical principles in experimental design. 2nd edn. McGraw-Hill, New York, pp 149–260
53. Xiang J, Sha Y, Jia Z, Prasad L, Delbaere LT (1995) Framework residues 71 and 93 of the chimeric B72.3 antibody are major determinants of the conformation of the heavy-chain hypervariable. J Mol Biol 253:385–390
54. Yarden Y, Sliwkowski MX (2001) Untangling the ErbB signalling network. Nat Rev Mol Cell Biol 2:127–137
55. Yen L, Benlimame N, Nie ZR, Xiao D, Wang T, Al Moustafa AE, Esumi H, Milanini J, Hynes NE, Pages G, Alaoui-Jamali MA (2002) Differential regulation of tumor angiogenesis by distinct ErbB homo- and heterodimers. Mol Biol Cell 13:4029–4044

Oncogene (1995) 10, 1813–1821

Cooperative signaling of ErbB3 and ErbB2 in neoplastic transformation and human mammary carcinomas

Maurizio Alimandi[1], Alfredo Romano[2], Maria Cristina Curia[1], Raffaella Muraro[3], Paolo Fedi[4], Stuart A Aaronson[4], Pier Paolo Di Fiore[1] and Matthias H Kraus[1]

[1]*Laboratory of Cellular and Molecular Biology, National Cancer Institute, National Institutes of Health, Bethesda, Maryland 20892, USA;* [2]*Laboratory of Experimental Carcinogenesis, National Cancer Institute, National Institutes of Health, Bethesda, Maryland 20892, USA;* [3]*Istituto di Patologia Umana e Medicina Sociale, Universitá 'G D'Annunzio', 66013 Chieti, Italy;* [4]*Derald H Ruttenberg Cancer Center, Mount Sinai Medical Center, New York, NY 10029-6574, USA*

In the present study we demonstrate that *erbB*-3 and *erbB*-2 cooperate in neoplastic transformation. Under conditions in which neither gene alone induced transformation, they readily transformed NIH3T3 cells if co-expressed. Furthermore, at high expression levels of ErbB2 which cause transformation, ErbB3 enhanced focus formation by one order of magnitude. Synergy required an intact ErbB2 extracellular domain and tyrosine kinase activity. Cooperation between ErbB3 and ErbB2 involved heterodimerization and increased tyrosine phosphorylation of ErbB3. Signaling by the heterodimer resulted in increased PI 3-kinase recruitment as well as quantitative and qualitative differences in substrate phosphorylation. Evidence for signaling by an active ErbB3-ErbB2 heterodimer in four mammary tumor cell lines indicated relevance of this mechanism for human neoplasia. Our detection of the NDF/heregulin transcript in NIH3T3 cells implicates an autocrine loop involving this ligand in signaling by the ErbB3-ErbB2 heterodimer in the model system, whereas heregulin-independent mechanisms likely exist for co-operative signaling by ErbB3 and ErbB2 chronically activated in some human mammary carcinomas.

Keywords: *erbB* receptor family; oncogenes; tyrosine phosphorylation; heterodimerization; PI3-kinase

Introduction

The *erbB* family of receptor tyrosine kinases (RTKs) includes the epidermal growth factor receptor (EGFR), *erbB*-2/HER-2/*neu*, *erbB*-3/HER-3 (Ullrich and Schlessinger, 1990 and references therein), and *erbB*-4/HER-4 (Plowman *et al.*, 1993). Members of this family have frequently been implicated in human neoplasia due to their overexpression in the presence or absence of gene amplification (Yokota *et al.*, 1986; Slamon *et al.*, 1987, 1989; Kraus *et al.*, 1987; van de Vijver *et al.*, 1987; Berger *et al.*, 1988). In the case of *erbB*-2, gene amplification in mammary and ovarian carcinomas has been associated with decreased disease-free survival (Slamon *et al.*, 1987, 1989). Understanding of the physiologic functions of these receptors has been greatly aided by studies in cell model systems in which they have been exogenously expressed individually or in combination. Such investigations have established, for instance, that ligand activation was indispensable for EGFR biological activity (Di Fiore *et al.*, 1987a; Velu *et al.*, 1987; Riedel *et al.*, 1988), while normal ErbB2 exhibited constitutive activity in the apparent absence of a specific ligand (Di Fiore *et al.*, 1987b; Hudziak *et al.*, 1987). Furthermore, structural receptor alterations were able to upregulate intrinsic catalytic properties of either EGFR or ErbB2 proteins (Di Fiore *et al.*, 1987b; Bargmann and Weinberg, 1988; Segatto *et al.*, 1988; Haley *et al.*, 1989). Finally, EGF-dependent phosphorylation of ErbB2 by the EGFR and biological cooperation of both molecules implicated transphosphorylation and heterodimerization in signal transduction by this class of receptors (King *et al.*, 1988; Stern and Kamps, 1988; Kokai *et al.*, 1989).

Employing a chimeric EGFR/ErbB3 receptor, we and others have demonstrated that a third member of this receptor family, ErbB3, is capable of transducing mitogenic signals in NIH3T3 fibroblasts (Kraus *et al.*, 1993; Fedi *et al.*, 1994; Prigent and Gullick, 1994). The mechanisms responsible for ErbB3-induced mitogenesis, however, are not clear. Concerns about the intrinsic enzymatic ability of ErbB3 arose from possibly inactivating amino acid substitutions in the predicted ErbB3 catalytic domain with respect to other RTKs (Kraus *et al.*, 1989; Plowman *et al.*, 1990). Our initial results showed that ErbB3 is capable of autophosphorylation *in vitro* (Kraus *et al.*, 1993). However, the ErbB3 enzymatic activity might be significantly lower than that of the EGFR, as was shown in subsequent studies (Guy *et al.*, 1994).

Recent evidence provides a framework for delineating the role of ErbB3 in mitogenesis. It was reported that the EGFR is capable of transphosphorylating ErbB3, an event associated with recruitment of phosphatidylinositol 3-kinase (PI 3-kinase) (Soltoff *et al.*, 1994). In addition, we found that a ligand-stimulated EGFR/ErbB3 receptor can efficiently couple to PI 3-kinase, but not to phospholipase Cγ (PLCγ) or GTPase-activating protein (GAP), revealing striking differences as compared to the EGFR and ErbB2 proteins (Fedi *et al.*, 1994). Moreover, members of the NDF/heregulin family of EGF-like molecules (Holmes *et al.*, 1992; Wen *et al.*, 1992; Falls *et al.*, 1993; Marchionni *et al.*, 1993) bind to ErbB3 (Carraway *et al.*, 1994). However, co-expression of ErbB2 and ErbB3 in COS cells indicated that a putative heterodimer between these molecules bound heregulin 10- to 100-fold more efficiently than ErbB3 alone (Sliwkowski *et al.*, 1994; Carraway and Cantley, 1994). It is therefore conceivable that NDF/heregulin and/or other putative

Correspondence: MH Kraus
Received 19 January 1995; accepted 9 February 1995

ligands normally associate with ErbB3-containing heterodimers. In this setting, ErbB3 would contribute its unique ability when compared with EGFR and ErbB2, to recruit PI 3-kinase, and possibly other second messengers. The mitogenic ability of ErbB3 might therefore depend in part on an intrinsic, albeit reduced, kinase activity and in part on its ability to heterodimerize with other *erbB* family members which are often co-expressed in various cell types.

ErbB3 has been found to be expressed at varying levels in human mammary carcinomas (Kraus *et al*., 1989; Lemoine *et al*., 1992). Furthermore, chronic ErbB3 tyrosine phosphorylation in a significant fraction of such tumor cell lines indicated constitutive activation of the ErbB3 signaling function in these tumors (Kraus *et al*., 1993). We reasoned that ErbB3 might cooperate with other *erbB* family members by simultaneous recruitment of complementary signal transduction pathways. In the present study we tested this hypothesis. We demonstrate that co-expression of ErbB3 and ErbB2 in NIH3T3 cells results in significantly increased transforming activity when compared to ErbB3 or ErbB2 expressed individually. Analysis of cytoplasmic signaling pathways indicated that cooperative transformation was associated with qualitative and quantitative differences in substrate phosphorylation, including a striking increase in PI 3-kinase recruitment. Simultaneous activation of ErbB3 and ErbB2 signaling functions at both receptor and substrate levels was observed in certain human breast tumor cell lines, underscoring the relevance of biological cooperation between ErbB2 and ErbB3 for human neoplasia. Finally, lack of heregulin expression in mammary tumor cell lines harboring concomitantly activated ErbB2 and ErbB3, raises the possibility that heregulin-independent mechanisms exist for cooperation of ErbB2 and ErbB3 in human neoplasia.

Results

Evidence for concomitant activation of ErbB3 and ErbB2 in human mammary tumor cell lines

We have previously demonstrated constitutive ErbB3 tyrosine phosphorylation in some human mammary tumor cell lines, including MDA-MB453, BT474, SK-BR-3 and MDA-MB175 (Kraus *et al*., 1993 and Table 1). As the same cell lines have also been shown to overexpress ErbB2, but not the EGFR (Kraus *et al*., 1987), we sought to determine the state of ErbB2 tyrosine phosphorylation in the same cell lines. As shown in Figure 1, the ErbB2 protein was detected at varying levels in 10 mammary tumor cell lines, with highest expression in MDA-MB453, BT474, MDA-MB361 and SK-BR-3 (Figure 1). When anti-ErbB2 immunoprecipitates were subjected to immunoblot analysis with anti-P-Tyr, ErbB2 tyrosine phosphorylation was readily detected in MDA-MB453, BT474, MDA-MB175 and SK-BR-3 (Figure 1). These findings coincided with the presence of constitutive ErbB3 phosphorylation in the same cell lines (Table 1). ErbB2 tyrosine phosphorylation was not solely a function of its level of expression as evident from a comparison of MDA-MB175 and MDA-MB361 cells (Figure 1). These findings indicated concomitant chronic tyrosine phosphorylation of ErbB3 and ErbB2 in human mammary tumor cell lines, raising the possibility that ErbB3 and ErbB2 might be active synergistically.

Table 1 Concomitant activation of ErbB3 and ErbB2 signaling in human mammary carcinomas

Mammary carcinoma cell lines	*ErbB3*		*ErbB2*	
	Protein	*P-Tyr*	*Protein*	*P-Tyr*
MDA-MB453	+ +	+ +	+ +	+
BT474	+ +	+ +	+ + +	+ +
MDA-MB175	(+)	+ +	+	+
SK-BR-3	+	+	+ + +	+ +
MDA-MB134	+ +	–	(+)	–
MCF-7	+	–	(+)	–
MDA-MB361	+ +	–	+ +	–
MDA-MB415	+	–	(+)	–
ZR-75-1	+	–	+	–
MDA-MB468	+ +	–	(+)	–

Relative ErbB3 or ErbB2 protein and phosphotyrosine levels were determined by immunoblot analysis with protein-specific peptide antisera and anti-P-Tyr antibodies, following immunoprecipitation from 1 mg protein lysates with receptor-specific monoclonal antibodies. Relative signal intensities were evaluated semiquantitatively: + + +/+ + /+ positive, (+) weakly positive, – not detectable. ErbB3 phosphotyrosine and protein levels have been previously reported (Kraus *et al*., 1993)

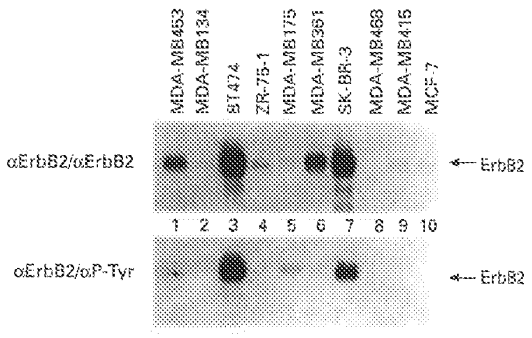


Figure 1 ErbB2 tyrosine phosphorylation in human mammary tumor cell lines. One mg lysate of the indicated mammary tumor cell lines prepared in SDS-containing buffer were immunoprecipitated with the ErbB2-specific monoclonal antibody E2-1. Immunoprecipitates were divided for immunoblot analysis with ErbB2 peptide antiserum M6 (Di Fiore *et al*., 1990) or monoclonal anti-P-Tyr antibodies (PY20, PY69; ICN)

Cooperative transformation of NIH3T3 cells by ErbB2 and ErbB3

To investigate the possibility of cooperation between ErbB3 and ErbB2 in transformation, we cotransfected expression vectors for these proteins into NIH3T3 cells. In this model system, transformation by the normal ErbB2 protein has previously been shown to depend on its expression level (Di Fiore *et al*., 1987b), whereas ErbB3 does not induce detectable focus formation (Kraus *et al*., 1993). As shown in Figure 2, cotransfection with ErbB3 resulted in greatly enhanced ErbB2 transformation as compared to ErbB2 alone (Figure 2). LTR-ErbB3 cotransfection increased LTR-ErbB2 transforming ability by at least 10-fold, while it had no effect on EGFR-induced transformation, either in the presence or absence of EGF stimulation (Table 2). Strikingly, ErbB3 co-expression was able to unmask ErbB2 transforming ability at low levels of ErbB2 expression under SV40 transcriptional control. Co-

versely, ErbB3 did not synergize with an ATP-binding site mutant of ErbB2, LTR-ErbB2$_{R753}$ (Segatto *et al.*, 1990) or with an amino-terminally truncated ErbB2, LTR-ΔNErbB2 (Di Fiore *et al.*, 1987b), (Table 2) indicating a requirement for both intact ErbB2 tyrosine kinase activity and the presence of its extracellular domain.

Cooperative transformation by ErbB3 and ErbB2 is associated with increased ErbB3 phosphorylation and receptor heterodimerization

To investigate the effects of cotransfection on receptor activity, cotransfectants were marker selected and grown up to mass cultures. Following immunoprecipitation with ErbB3 or ErbB2-specific antibodies, immunoprecipitates were subjected to immunoblotting with anti-receptor or anti-P-Tyr. In an attempt to avoid receptor coprecipitation, lysates were prepared in the presence of ionic detergents. As shown in Figure 3A, ErbB3 was expressed at comparable levels in LTR-ErbB3 transfectants and cotransfectants with either LTR-ErbB2 or LTR-ErbB2$_{R753}$ (lane 7, 9 and 10), while endogenous mouse ErbB3 and ErbB2 proteins were not detectable (lanes 1 and 6). Expression levels of the normal ErbB2 protein were similar in cotransfectants with a control vector or with LTR-ErbB3 (lanes 3 and 4). By comparison, the ErbB2 kinase-negative mutant protein was expressed at about threefold lower levels in cotransfectants with LTR-ErbB3 (lane 5).

Analysis of ErbB2 immunoprecipitates with anti-P-Tyr antibodies demonstrated similar levels of ErbB2-specific tyrosine phosphorylation in cotransfectants with LTR-neo or LTR-ErbB3 (lanes 3 and 4), while no ErbB2 tyrosine phosphorylation was detectable in ErbB2$_{R753}$ mutant co-expressed with the ErbB3 protein (lane 5). These findings indicated that ErbB3 did not noticeably affect ErbB2 tyrosine phosphorylation. In

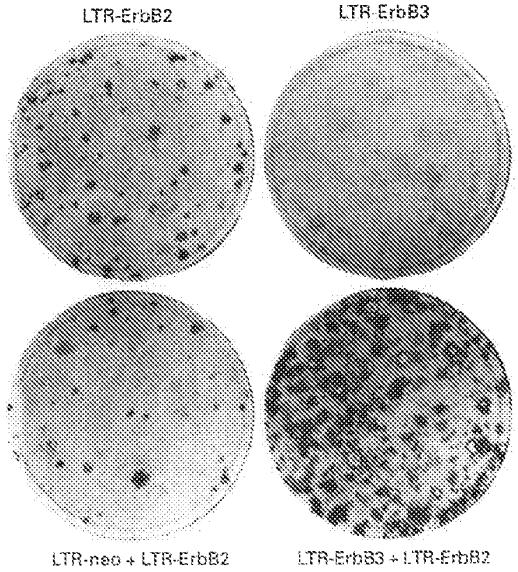


Figure 2 Biological phenotype of NIH3T3 transfectants. LTR-neo (1 μg), LTR-ErbB3 (1 μg) and LTR-ErbB2 (0.01 μg) expression vectors were transfected by calcium phosphate precipitation. Plates were stained with GIEMSA 14 days following transfection

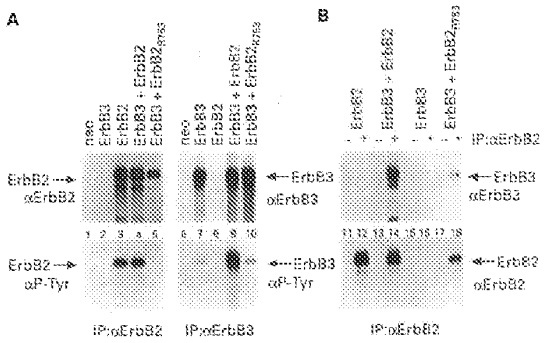


Figure 3 ErbB3 transphosphorylation and heterodimerization with ErbB2. Selected mass cultures of LTR-neo (neo) and LTR-ErbB3 (ErbB3) transfectants, or cotransfectants LTR-ErbB2/LTR-neo (ErbB2), LTR-ErbB3/LTR-ErbB2 (ErbB3+ErbB2) and LTR-ErbB3/LTR-ErbB2$_{R753}$ (ErbB3+ErbB2$_{R753}$) were serum-starved for 48 h and lysed in the presence of phosphatase inhibitors. (**A**) One mg lysate was immunoprecipitated (IP) in the presence of ionic detergents with αErbB2 peptide antiserum M6 or αErbB3 monoclonal antibody E3-1 (Kraus *et al.*, 1993). Immunoprecipitates were divided for immunoblot analysis with αErbB2 (M6) and αErbB3 (Kraus *et al.*, 1993) peptide antisera or monoclonal αP-Tyr antibody. Direct immunoblot analysis confirmed relative ErbB3 and ErbB2 expression levels in these transfectants (data not shown). Furthermore, comparison with previously characterized transfectants (Di Fiore *et al.*, 1987b; Kraus *et al.*, 1993) indicated ErbB3 and ErbB2 receptor numbers of $\sim 1 \times 10^5$ and $\sim 2 \times 10^5$, respectively, whereas ErbB2$_{R753}$ was expressed at $\sim 7 \times 10^4$ molecules per cell. (**B**) Four mg fresh lysates prepared in the absence of ionic detergents were immunoprecipitated with αErbB2 monoclonal antibody E2-1 (+) or a non-immune control MOPC21 (−). Four fifth and 1/5 of immunoprecipitates were subjected to immunoblot analysis with αErbB3 and αErbB2 peptide antisera, respectively

Table 2 Biological cooperation of ErbB3 and ErbB2 in NIH3T3 cells

	LTR-neo (0.1)		*LTR-ErbB3 (0.1)*	
	FFU/plate	*CFU/plate*	*FFU/plate*	*CFU/plate*
SV40-ErbB2 (1)	<1	NT	22 (2)	NT
LTR-ErbB2 (0.01)	16 (4)	76 (13)	104 (10)	26 (6)
LTR-ErbB2$_{R753}$ (0.01)	<1	63 (12)	<1	12 (4)
LTR-ΔNErbB2 (0.01)	30 (4)	8 (2)	32 (6)	2 (1)
LTR-EGFR (0.1)	<1	79 (29)	1 (0.3)	35 (10)
LTR-EGFR (0.1) + EGF	13 (3)	NT	12 (4)	NT

NIH3T3 cells were transfected by the calcium phosphate precipitation method using 40 μg of calf thymus high molecular weight DNA as a carrier. FFU (standard error): Focus-forming units. CFU (standard error): Number of colonies exhibiting simultaneous resistance to G418 as well as kHAT, indicate stable transfection of both constructs. LTR-neo and LTR-ErbB3 vectors confer G418 resistance, where as LTR-driven ErbB2 and EGFR constructs carry the Ecogpt marker. Amounts (μg) of expression vector DNA transfected are listed in parentheses. Data were obtained from at least two independent transfection assays performed in duplicate

striking contrast, the level of ErbB3 tyrosine phosphorylation was elevated five- to 10-fold when co-expressed specifically with the normal ErbB2 protein (lane 7 and 9). There was no effect of co-expression with the ErbB2 ATP-binding site mutant (lanes 7 and 10) nor the activated ErbB2 protein (ΔNErbB2) that lacked most of its extracellular domain (data not shown). Thus, cooperative transformation of ErbB3 and ErbB2 was associated with a significant increase in ErbB3 tyrosine phosphorylation, suggesting transphosphorylation of ErbB3 by the ErbB2 protein.

We next sought to determine whether heterodimers between ErbB3 and ErbB2 could be demonstrated in the cotransfectants by testing the ability of ErbB2 to co-immunoprecipitate the ErbB3 protein. To minimize dissociation of receptor complexes, immunoprecipitation experiments were conducted on fresh lysates prepared in the absence of ionic detergents. Lysates were subjected to immunoprecipitation with an ErbB2-specific monoclonal antibody and then immunoblotted with peptide antibodies specific for ErbB3 or ErbB2 proteins, respectively. As shown in Figure 3B, the ErbB3 protein was readily recovered from ErbB2 immunoprecipitates of LTR-ErbB3/LTR-ErbB2 cotransfectants (lane 14). The specificity of this co-immunoprecipitation was confirmed by the absence of the ErbB3 protein in immunoprecipitates of the same lysates using non-immune IgG, or in ErbB2 immunoprecipitates of LTR-ErbB3 transfectants (Figure 3B, lanes 13 and 16). These results demonstrated that ErbB3 and ErbB2 aggregate *in vivo* to form heterodimeric receptor complexes. Of note, heterodimer formation occurred independently of ErbB3 or ErbB2 tyrosine phosphorylation, since quantitatively proportional ErbB3 protein was co-immunoprecipitated with anti-ErbB2 from cells co-expressing ErbB3 and the ErbB2 ATP-binding site mutant protein (Figure 3B, lane 18).

ErbB3-mediated recruitment of PI 3-kinase activity is enhanced by co-expression of ErbB2

In efforts to investigate whether the biological cooperation observed between ErbB3 and ErbB2 was associated with alterations in their intracellular signaling capacities, we initially investigated PI 3-kinase activity in the cotransfectants. As shown in Figure 4, significantly elevated levels of PI 3-kinase activity were observed in anti-P-Tyr or anti-ErbB3 immunoprecipitates of LTR-ErbB3/LTR-ErbB2 cotransfectants when compared to LTR-neo or LTR-ErbB3 as well as LTR-neo/LTR-ErbB2 or LTR-ErbB3/LTR-ErbB2$_{R753}$ cotransfectants (Figure 4A). Standardization of the PIP signal relative to p85 expression levels in the same lysates indicated a 2–5-fold increase of PI 3-kinase activity. Thus, the increase in PI 3-kinase recruitment paralleled the increased level of ErbB3 tyrosine phosphorylation observed in LTR-ErbB3/LTR-ErbB2 cotransfectants.

We next compared association of the p85 subunit of PI 3-kinase with the fraction of phosphotyrosine-containing proteins in these transfectants. Immunoblot analysis with anti-p85 demonstrated that the highest levels of p85 were detected in anti-P-Tyr immunoprecipitates of ErbB3/ErbB2 cotransfectants (Figure 4B, lane 4). Relative to p85 expression levels in the same lysates, a 2.8-fold or 5.5-fold increase was estimated in these cotransfectants when compared to transfectants

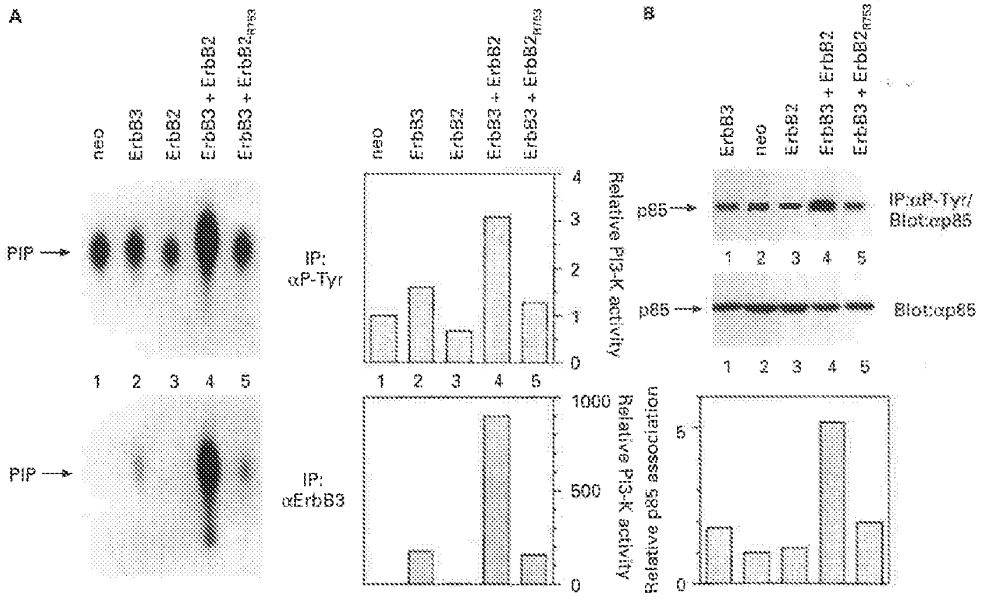


Figure 4 Enhanced signaling through PI 3-kinase by ErbB3-ErbB2 heterodimers. Two mg fresh lysates were immunoprecipitated with αP-Tyr or αErbB3 monoclonal antibodies and divided for PI 3-kinase assay (A) or immunoblot analysis with an αp85 antibody (UBI), (B). 100 μg of the same lysates were subjected to direct immunoblotting with αp85 (B). PIP (phosphatidylinositol 3-phosphate) and p85 signal intensities were determined by phosphor-imager analysis. Relative PI 3-kinase activity = PIP signal intensity/p85 protein. Relative p85 association = p85 signal intensity from αP-Tyr immunoprecipitates/p85 protein

containing only ErbB3 or ErbB2, respectively. Thus, heterodimerization of ErbB3 and ErbB2 was associated with a significant increase of PI 3-kinase signaling in NIH3T3 cells.

Cooperative transformation by ErbB3 and ErbB2 involves differences in substrate phosphorylation by receptor heterodimers

To explore whether other differences in substrate recruitment or phosphorylation by an ErbB2-ErbB3 heterodimer could be demonstrated, we sought to compare patterns of phosphotyrosine-containing proteins in transfectants expressing similar levels of ErbB3, ErbB2 or both proteins by two-dimensional gel analysis. As shown in Figure 5, phosphotyrosine-containing proteins were less abundant in LTR-ErbB3 as compared with ErbB2 transfectants. Comparison of cotransfectants expressing ErbB3 as well as ErbB2 with an ErbB2 control revealed a number of common spots. Some of these P-Tyr-containing proteins showed increased intensity in the cotransfectants and were detectable at lower intensity in the LTR-ErbB3 transfectant (Figure 5). These findings suggested a quantitative increase of substrate phosphorylation in LTR-ErbB3/LTR-ErbB2 cotransfectants. Of note, three major spots were uniquely detected in LTR-ErbB3/LTR-ErbB2 cotransfectants (Figure 5, right panel, arrowheads). Two of these proteins migrated in the molecular weight range of 120–130 kDa, whereas the third exhibited an estimated molecular mass of 65 kDa. None of these spots was visualized using antisera specific for carboxyl-terminal epitopes of ErbB2 or ErbB3 (data not shown), suggesting that they are not receptor degradation products but rather reflect tyrosine kinase substrates specifically phosphorylated by heterodimeric ErbB2-ErbB3 receptors. Two spots observed in the ErbB2 transfectant were not evident in the ErbB2/ErbB3 cotransfectant. It is not known whether the 65 kDa protein in the latter represents a differentially phosphorylated isoform of one of these two unique spots in the ErbB2 transfectants. In any case, these findings provide evidence for qualitative as well as quantitative differences in substrate phosphorylation in NIH3T3 cells cooperatively transformed by ErbB2 and ErbB3.

Evidence for ErbB3-mediated signaling in human breast tumor cell lines

Based upon the known differences in efficiency of ErbB3 and ErbB2 with respect to PI 3-kinase recruitment, we investigated the pattern of PI 3-kinase activation in six human breast tumor cell lines including four lines that exhibited active ErbB3 and ErbB2. PI 3-kinase activity was determined following serum-starvation and was normalized for p85 expression levels in these cell lines. Analysis of anti-P-Tyr and anti-ErbB3 immunoprecipitates revealed an increase in associated PI 3-kinase activity in MDA-MB361, MDA-MB453, MDA-MB175, BT474 and SK-BR-3 as compared to MDA-MB134 cells which showed little if any associated PI 3-kinase activity. Moreover, analysis of anti-ErbB3 immunoprecipitates revealed relatively higher levels of associated PI 3-kinase activity in cell lines exhibiting chronic ErbB3 and ErbB2 tyrosine phosphorylation (Figure 6A). All of these findings suggested increased coupling of ErbB3 with PI 3-kinase in the ErbB3 activated tumor cell lines.

We next analysed these same tumor cell lines for evidence of ErbB3-ErbB2 heterodimers. As shown in Figure 6B, ErbB3 co-immunoprecipitation with ErbB2 was most pronounced in the four cell lines with constitutively activated ErbB3 including MDA-MB453, BT474, SK-BR-3 and MDA-MB-175, whereas little co-immunoprecipitation was observed in MDA-MB361 cells. The extent of ErbB3 co-immunoprecipitation with ErbB2 in these cell lines corresponded to relative levels of chronic ErbB3 tyrosine phosphorylation as well as ErbB3-associated PI 3-kinase activity. Thus, the results with human breast tumor lines are consistent with heterodimer formation and PI 3-kinase recruitment observed in NIH3T3 cells cooperatively transformed by ErbB2 and ErbB3.

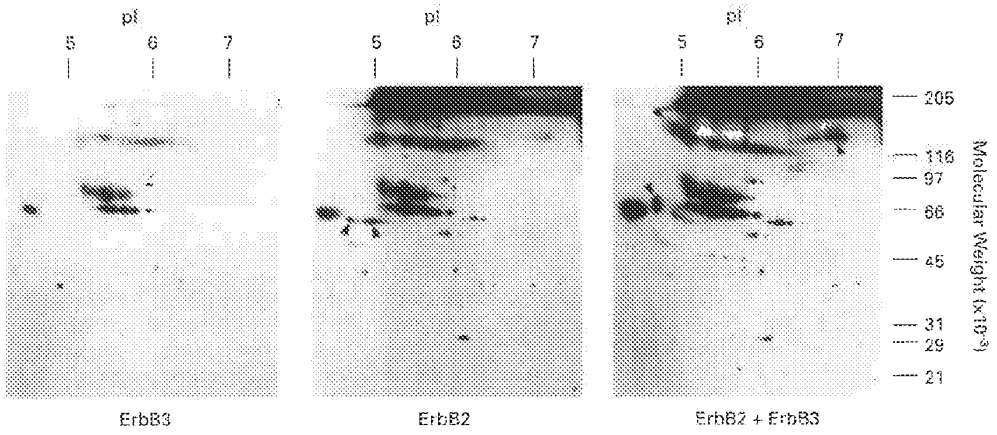


Figure 5 Two-dimensional analysis of phosphotyrosine-containing proteins in NIH3T3 transfectants. Serum-starved NIH3T3 transfectants were lysed in 1% Triton buffer containing phosphatase inhibitors. Six mg of total proteins were immunoprecipitated with excess of αP-Tyr antibody (UBI) and processed for 2-D analysis as described (Romano *et al*., 1994). Following electrotransfer phosphotyrosine-containing proteins were visualized with αP-Tyr antibody (UBI)

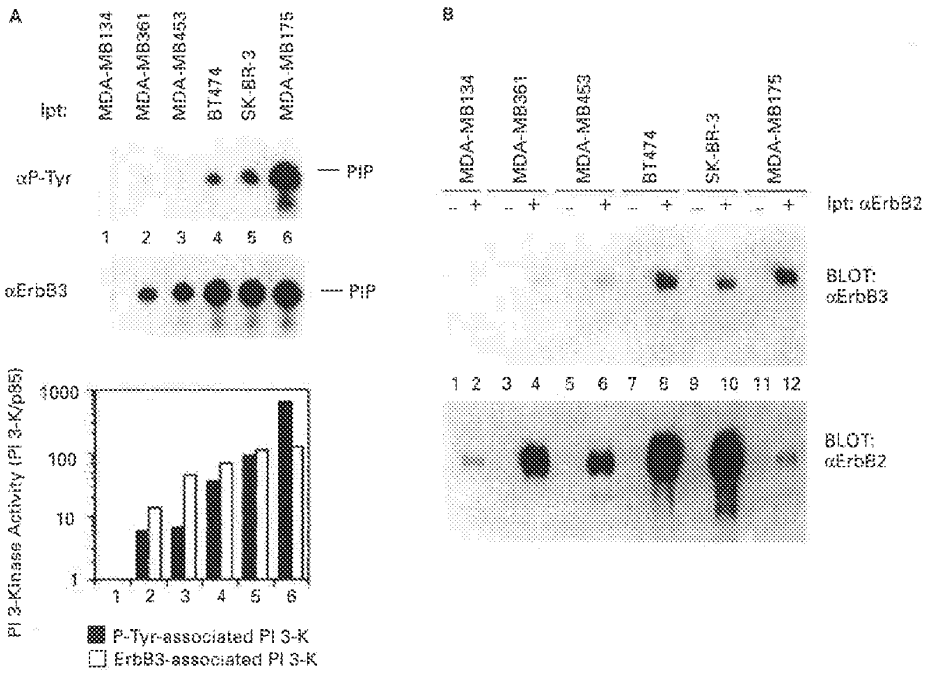


Figure 6 Signaling by an ErbB3-ErbB2 heterodimer in human mammary tumor cell lines. (**A**) PI 3-kinase activity associated with αP-Tyr or αErbB3 immunoprecipitates was determined as described in legend to Figure 4. (**B**) ErbB3-ErbB2 heterodimer formation was analysed in the indicated mammary tumor cell lines as described in Figure 3B

Ligand-dependent activation of ErbB3-ErbB2 heterodimers

Co-expression of ErbB2 and ErbB3 has been reported to reconstitute a high-affinity receptor for NDF/heregulin (Carraway and Cantley, 1994; Sliwkowski *et al*., 1994). Thus, NDF/heregulin might be involved in ErbB3-ErbB2 heterodimer formation in NIH3T3 cells as well as breast tumor cell lines co-expressing these molecules. We tested these cell lines for NDF/heregulin transcripts by reverse transcriptase-polymerase chain reaction (RT-PCR). Oligonucleotide primers were designed in invariant regions of the gene to allow PCR amplification of the rodent homologue (NDF) as well as 4 human isoforms of heregulin, HRG-α, HRG-β1, HRG-β2 and HRG-β3. As shown in Figure 7A, the predicted 567 bp NDF/heregulin fragment was amplified from RNA of NIH3T3 and a human leiomyosarcoma derived cell line, SK-LMS-1, which served as a positive control. Under these same conditions, the NDF/heregulin transcript was not detectable in MDA-MB134, MDA-MB361, SK-BR-3, MDA-MB175, BT474 or MDA-MB453. A *β*-actin control demonstrated integrity of the mRNA in each cell line (Figure 7A). The expression of NDF/heregulin transcript in NIH3T3 cells is consistent with the concept that this ligand is responsible for autocrine triggering of ErbB3-ErbB2 heterodimers in these cells.

To investigate the possibility of other ligands responsible for ErbB2-ErbB3 heterodimerization in mammary tumor cell lines, we tested conditioned medium for the ability to induce ErbB3 tyrosine phosphorylation in MDA-MB134 cells. This cell line expresses relatively high ErbB3 and low ErbB2 protein levels neither of which exhibits detectable tyrosine phosphorylation (Figure 1 and Kraus *et al*., 1993). When serum-starved MDA-MB134 were exposed to conditioned medium prepared from breast tumor cell lines with active ErbB2 and ErbB3, conditioned medium of MDA-MB175 induced ErbB3 tyrosine phosphorylation, whereas SK-BR-3, BT474 and MDA-MB453 lacked similar activity. Thus, endogenous ligand production might be responsible for activated signaling by an ErbB3-ErbB2 heterodimer in MDA-MB175 cells. Whether this activity represents an alternatively spliced form of NDF/heregulin whose transcript was not detectable by RT-PCR or a different molecule, is not yet known.

Discussion

ErbB2 has been implicated in human malignancies due to gene amplification/overexpression and its ability to induce transformation in model systems *in vitro* and *in vivo*. In NIH3T3 cells, normal ErbB2 transforming activity was only evident at high levels of expression (Di Fiore *et al*., 1987b; Hudziak *et al*., 1987). In human malignancy, similarly high ErbB2 protein levels are observed in 20–30% of breast or ovarian carcinomas and are invariably associated with gene amplification (Yokota *et al*., 1986; Kraus *et al*., 1987; Slamon *et al*., 1987; van de Vijver *et al*., 1987; Berger *et al*., 1988). However, a similar fraction of breast tumors and tumor-derived cell lines does not display gene amplification, but overexpresses ErbB2 at moderate levels, insufficient to produce the malignant phenotype in the NIH3T3 model system (Di Fiore *et al*., 1987b;

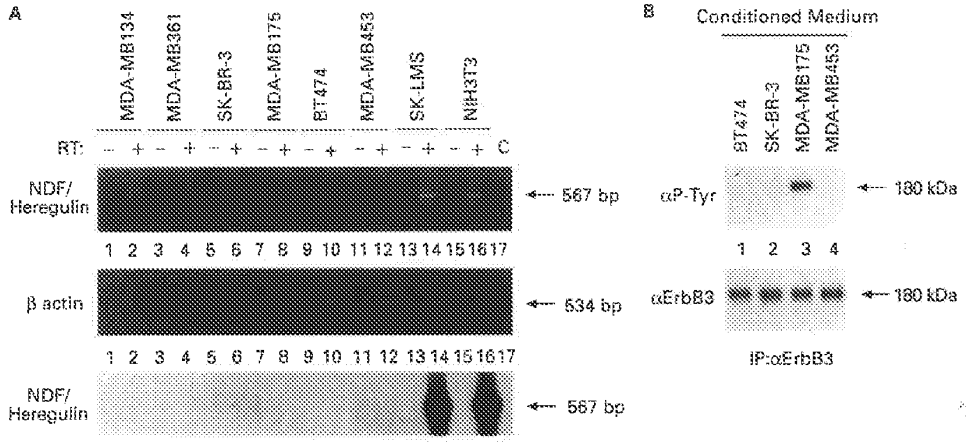


Figure 7 Ligand involvement in ErbB2-ErbB3 heterodimer activation. (A) Five μg total RNA from the indicated cell lines were analysed for the presence of NDF/heregulin transcript by RT-PCR. To ascertain RNA-specific amplification, reactions were performed in the presence or absence of reverse transcriptase (RT). In addition, a negative control for PCR amplification was conducted in the absence of template (C). Top: Ethidium bromide stain of NDF/heregulin products. Center: Ethidium bromide stain of β actin products. Bottom: Southern blot analysis of gel shown in top panel employing an internal NDF/heregulin-oligonucleotide as a probe. The predicted 567 bp fragment was independently confirmed as NDF/heregulin by restriction analysis with PstI and BclI. (B) Serum-starved MDA-MB134 cells were triggered with conditioned medium harvested from the indicated cell lines. Two mg lysate was immunoprecipitated with αErbB3 monoclonal antibody E3-1 and subjected to immunoblot analysis with αP-Tyr antibody (ICN) or αErbB3 peptide antiserum

Kraus *et al.*, 1987; Berger *et al.*, 1988; Slamon *et al.*, 1989). Our present studies show that ErbB3 cooperates with ErbB2 in the neoplastic transformation of NIH3T3 cells. ErbB3 activates ErbB2 transforming potential at intermediate expression levels and substantially enhances neoplastic transformation, when ErbB2 is expressed at high protein levels. These observations in a model system were paralleled by evidence of concurrent activation of ErbB2 and ErbB3 signaling function in a number of human breast tumor cell lines. These results imply that biological cooperation between these two *erbB* family members can occur in human malignancy.

We demonstrated that biological cooperation between ErbB2 and ErbB3 was associated with heterodimer formation and increased steady state ErbB3 tyrosine phosphorylation. The formation of a heterodimer *in vivo* may facilitate transphosphorylation of ErbB3 by ErbB2 or such heterodimers may possess higher intrinsic catalytic activity than the monomer. We further showed that an ErbB2 mutant lacking most of its extracellular domain, ΔNErbB2, was unable to cooperate for transformation with ErbB3. Based upon the current understanding of receptor dimerization (Schlessinger, 1988), such a mutant would not display heterodimerization properties with ErbB3. This possibility was consistent with our finding that ErbB3 does not display increased tyrosine phosphorylation in ΔNErbB2/ErbB3 cotransfectants (data not shown). Heterodimer formation between the EGFR and ErbB2 has previously been reported to be associated with a cooperative transforming activity of these molecules (Kokai *et al.*, 1989). However, constitutive EGFR-ErbB2 heterodimers were not reported in human tumor cells due to a lack of co-expression of these two receptors at sufficient protein levels (Goldman *et al.*, 1990). Conversely, ErbB3 and ErbB2 are found simultaneously expressed in several human mammary tumor cell lines at intermediate or high protein levels. Moreover, an active ErbB3-ErbB2 heterodimer in MDA-MB175 suggests that simultaneously increased signaling can occur even at lower expression of both receptors.

The question arises as to the underlying mechanisms of ErbB2 and ErbB3 heterodimer formation. Our observations suggest involvement of multiple molecular mechanisms. Previous studies have indicated that receptor homodimerization and heterodimerization occur in response to ligand or, as in the case of ErbB2, may result from structural alterations mimicking ligand activation (Weiner *et al.*, 1989; Honegger *et al.*, 1990; Spivak-Kroizman *et al.*, 1992). Based upon constitutive ErbB3 tyrosine phosphorylation in NIH3T3 cells, we have previously suggested that these cells may produce an ErbB3 ligand (Kraus *et al.*, 1993). Consistent with this finding, we detected endogenous NDF/heregulin expression in NIH3T3 cells by RT-PCR. In addition, conditioned medium from NIH3T3 cells was able to trigger ErbB3 tyrosine phosphorylation in MDA-MB134 cells (data not shown). Thus, autocrine NDF/heregulin production is likely responsible for ErbB3-ErbB2 heterodimerization in this model system.

In all four mammary tumor cell lines displaying constitutive activation of ErbB2 and ErbB3, we failed to detect NDF/heregulin expression by RT-PCR. This observation does not rule out alternatively spliced NDF/heregulin transcripts escaping detection by RT-PCR. Such a NDF/heregulin variant might be present in MDA-MB175, since we observed soluble ErbB3-triggering activity as well as higher molecular weight transcripts hybridizing with a human heregulin probe in Northern blot analysis (data not shown). In SK-BR-3, MDA-MB453 and BT474, however, lack of NDF/heregulin detection by RT-PCR was paralleled by lack of transcript detection in Northern blot analysis (data

not shown and Holmes *et al*., 1992) and absence of ErbB3 triggering activity from conditioned medium. These findings raise the possibility that ErbB2-ErbB3 heterodimerization in these cell lines involves a still unknown, cell-associated ligand activity or ligand-independent mechanisms including mutations or high receptor density.

We demonstrated enhanced signaling through the PI 3-kinase pathway in NIH3T3 cells as well as human tumor cell lines exhibiting co-expression of chronically activated ErbB2 and ErbB3. These findings can be explained by the enhanced tyrosine phosphorylation of ErbB3 co-expressed with ErbB2 which by itself does not efficiently couple with PI 3-kinase. Substantial evidence implicates PI 3-kinase in mitogenic signaling (Cantley *et al*., 1991; Valius and Kazlauskas, 1993; Rodriguez-Viciana *et al*., 1994). Thus, increased recruitment of PI 3-kinase might participate in enhanced signaling by an ErbB3-ErbB2 heterodimer. However, it appears unlikely that PI 3-kinase alone is responsible for this effect. SV40-ErbB2 transfected NIH3T3 cells, for instance, did not exhibit a transformed morphology even upon exposure to high concentrations of insulin, a potent activator of PI 3-kinase (Cantley *et al*., 1991 and PP Di Fiore, unpublished observations), whereas they were readily transformed by co-expression of ErbB3. Indeed, we identified by 2-dimensional gel analysis three phosphotyrosine proteins that are uniquely phosphorylated in the cotransfectant, but not by ErbB3 or ErbB2 alone. Thus, biological cooperation does not only involve additive recruitment of ErbB3 and ErbB2 signaling pathways, but is determined by qualitative differences in substrate recruitment by a receptor heterodimer. Characterization of these substrate proteins should provide insight in the mechanism of action by an ErbB2-ErbB3 heterodimer.

In human breast cancer, ErbB2 overexpression associated with gene amplification has been shown to possess prognostic value for decreased survival in lymph-node positive disease, while a diagnostic role in stage I tumors was not unequivocally established (Slamon *et al*., 1987, 1989; Tandon *et al*., 1989; Paterson *et al*., 1991). In addition, ErbB2 overexpression at intermediate levels affecting a significant subset of human mammary carcinomas, could not be associated with disease progression. Based on our results, it appears worthwhile to evaluate breast tumors for ErbB2 overexpression in light of simultaneous ErbB3 expression as well as ligands activating the signaling function of a heterodimer. Evidence for biological synergism of ErbB3 and ErbB2 in a model system and human breast tumor cell lines raises the possibility that determination of a simultaneously activated ErbB3 and ErbB2 signaling function may improve the predictability of disease-free survival in human breast cancer.

Materials and methods

Tumor cell lines

Human tumor cell lines were obtained from the American Type Culture Collection (ATCC) and were maintained in Dulbecco's Modified Eagle Medium (DMEM) containing 10% fetal calf serum.

Preparation of conditioned medium and triggering of MDA-MB134

Confluent monolayers of cell lines seeded on fibronectin-coated plates were washed twice with PBS (phosphate-buffered saline) and exposed to 0.1 ml per cm^2 serum-free medium (DMEM containing 5 $\mu g\ ml^{-1}$ transferrin and 10^{-8} M selenium) for 48 h. Conditioned media were harvested and clarified at 10 000 *g*. MDA-MB134 mammary tumor cells were plated on fibronectin-coated plates and grown to confluence. Following serum starvation for 18h, monolayers were triggered with 0.1 ml per cm^2 of conditioned medium for 10 min at 37°C. Mock treatment with serum-free medium or conditioned medium of MDA-MB134 cells served as negative controls.

Generation of αErbB2 monoclonal antibody E2-1

A monoclonal antibody against the extracellular domain of ErbB2 was raised by immunization of Balb/c mice with live LTR-ErbB2 NIH3T3 transfectants as previously described (Kraus *et al*., 1993). Hybridoma supernatants were screened by enzyme-linked immunosorbent assay (ELISA). Following double cloning by limiting dilution, supernatants were analysed by immunofluorescence and immunoprecipitation. One monoclonal antibody, MAb E2-1, was further characterized as IgG1 isotype. It specifically recognized the ErbB2 protein, and did not show cross-reactivity with EGFR, ErbB3 or ErbB4 proteins overexpressed in NIH3T3 cells.

Protein analysis

Immunoprecipitation and immunoblot analyses were conducted essentially as previously described (Kraus *et al*., 1987, 1993). Immunoprecipitations using monoclonal antibodies were performed using Gammabind G agarose precoated with goat anti-mouse immunoglobulin G secondary antibody. For receptor co-immunoprecipitation, cells were serum-starved for 16 h and lysed in a buffer containing 20 mM Tris-HCl 7.5, 100 mM NaCl, 5 mM EGTA, 1% Nonidet P-40 (NP-40), protease and phosphatase inhibitors. Receptor-specific immunoprecipitations were performed in StaphA buffer (10 mM sodium phosphate pH 7.4, 100 mM NaCl, 5 mM EGTA, 1% Triton, 0.1% SDS, 0.5% deoxycholate), whereas immunoprecipitations with anti-P-Tyr (UBI) were conducted in 1% Triton buffer (Fedi *et al*., 1994). PI 3-kinase assays (Fedi *et al*., 1994) and 2-D analyses (Romano *et al*., 1994) were performed as previously reported.

Reverse transcriptase-polymerase chain reaction (RT-PCR)

RT-PCR was conducted by standard methodology using a commercial preamplification system (Gibco-BRL). First strand-synthesis was primed from 5 μg total RNA using random hexamers (Pharmacia) and 200 units Superscript reverse transcriptase. Following inactivation of the enzyme at 95°C for 5 min, samples were treated for 20 min with 2.5 units of RNase H (Gibco-BRL). Forty cycles of PCR amplification (1 min at 95°C, 2 min at 55°C, 2 min at 72°C) were carried out in 100 μl using Taq polymerase (Boehringer Mannheim) and 1 μM of the following primers:

NDF/heregulin:

5′-GAGCGCAAAGAAGGCAGAGG-3′ and 5′-CACACAGAAAGTTTTCTCCTT-3′ (Holmes *et al*., 1992; Wen *et al*., 1992).

β actin:

5′-TTCTACAATGAGCTGCGTGTG-3′ and 5′-CAGGAAGGAAGGCTGGAAGA-3′ (Gunning *et al*., 1983; Nudel *et al*., 1983).

Southern blot hybridization

Following gel electrophoresis the NDF/heregulin RT-PCR products were transferred to nitrocellulose and hybridized with an internal NDF/heregulin-specific oligonucleotide matching NDF, HRGα and HRGβ1-3 (Wen *et al*., 1992; Holmes *et al*., 1992; 5′-CTTTGCACATATACTCTCCAG-3′), as previously described (Kraus and Aaronson, 1991) except using 8 × Denhardt's for hybridization. Stringencies during hybridization and washing were reduced by 28°C and 21°C, respectively (Kraus and Aaronson, 1991).

Acknowledgements

We thank Steven R Tronick for support and helpful discussions, Silvio Gutkind for advice on the PI 3-kinase assay and Yaurice Starks for technical assistance.

R.M. was supported by grants from CNR (project ACRO 94.01172.PF39) and AIRC

References

Bargmann CI and Weinberg RA. (1988). *EMBO J.*, **7**, 2043–2052.
Berger MS, *et al*. (1988). *Cancer Res.*, **48**, 1238–1243.
Cantley LC, *et al*. (1991). *Cell*, **64**, 281–302.
Carraway III KL and Cantley LC. (1994). *Cell*, **78**, 5–8.
Carraway III KL, *et al*. (1994). *J. Biol. Chem.*, **269**, 14303–14306.
Di Fiore PP, *et al*. (1987a). *Cell*, **51**, 1063–1070.
Di Fiore PP, *et al*. (1987b). *Science*, **237**, 178–182.
Di Fiore PP, *et al*. (1990). *Science*, **248**, 79–83.
Falls DL, *et al*. (1993). *Cell*, **72**, 801–815.
Fedi P, Pierce JH, Di Fiore PP and Kraus MH. (1994). *Mol. Cell. Biol.*, **14**, 492–500.
Goldman R, Ben Levy R, Peles E and Yarden Y. (1990). *Biochemistry*, **29**, 11024–11028.
Gunning P, *et al*. (1983). *Mol. Cell. Biol.*, **3**, 787–795.
Guy PM, *et al*. (1994). *Proc. Natl. Acad. Sci. USA*, **91**, 8132–8136.
Haley JD, Hsuan JJ and Waterfield MD. (1989). *Oncogene*, **4**, 273–283.
Holmes WE, *et al*. (1992). *Science*, **256**, 1205–1210.
Honegger AM, Schmidt A, Ullrich A and Schlessinger J. (1990). *Mol. Cell. Biol.*, **10**, 4035–4044.
Hudziak RM, Schlessinger J and Ullrich A. (1987). *Proc. Natl. Acad. Sci. USA*, **84**, 7159–7163.
King CR, *et al*. (1988). *EMBO J.*, **7**, 1647–1651.
Kokai Y, *et al*. (1989). *Cell*, **58**, 287–292.
Kraus MH and Aaronson SA. (1991). *Methods Enzymol.*, **200**, 546–556.
Kraus MH, *et al*. (1993). *Proc. Natl. Acad. Sci. USA*, **90**, 2900–2904.
Kraus MH, *et al*. (1989). *Proc. Natl. Acad. Sci. USA*, **86**, 9193–9197.
Kraus MH, Popescu NC, Amsbaugh SC and King CR. (1987). *EMBO J.*, **6**, 605–610.
Lemoine NR, *et al*. (1992). *Br. J. Cancer*, **66**, 1116–1121.
Marchionni MA, *et al*. (1993). *Nature*, **362**, 312–318.
Nudel U, *et al*. (1983). *Nucleic Acids Res.*, **11**, 1759–1771.
Paterson MC, *et al*. (1991). *Cancer Res.*, **51**, 556–567.
Plowman GD, *et al*. (1993). *Proc. Natl. Acad. Sci. USA*, **90**, 1746–1750.
Plowman GD, *et al* (1990). *Proc. Natl. Acad. Sci. USA*, **87**, 4905–4909.
Prigent SA and Gullick WJ. (1994). *EMBO J.*, **13**, 2831–2841.
Riedel H, Massoglia S, Schlessinger J and Ullrich A. (1988). *Proc. Natl. Acad. Sci. USA*, **85**, 1477–1481.
Rodriguez-Viciana P, *et al*. (1994). *Nature*, **370**, 527–532.
Romano A, *et al*. (1994). *Oncogene*, **9**, 2923–2933.
Schlessinger J. (1988). *Trends Biochem. Sci.*, **13**, 443–447.
Segatto O, *et al*. (1988). *Mol. Cell. Biol.*, **8**, 5570–5574.
Segatto O, *et al*. (1990). *New Biol.*, **2**, 187–195.
Slamon DJ, *et al*. (1987). *Science*, **235**, 177–182.
Slamon DJ, *et al*. (1989). *Science*, **244**, 707–712.
Sliwkowski MX, *et al*. (1994). *J. Biol. Chem.*, **269**, 14661–14665.
Soltoff SP, *et al*. (1994). *Mol. Cell. Biol.*, **14**, 3550–3558.
Spivak-Kroizman T, *et al*. (1992). *J. Biol. Chem.*, **267**, 8056–8063.
Stern DF and Kamps MP. (1988). *EMBO J.*, **7**, 995–1001.
Tandon AK, *et al*. (1989). *J. Clin. Oncol.*, **7**, 1120–1128.
Ullrich A and Schlessinger J. (1990). *Cell*, **61**, 203–212.
Valius M and Kazlauskas A. (1993). *Cell*, **73**, 321–334.
Van de Vijver M, *et al*. (1987). *Mol. Cell. Biol.*, **7**, 2019–2023.
Velu TJ, *et al*. (1987). *Science*, **238**, 1408–1410.
Wada T, Qian X and Greene MI. (1990). *Cell*, **61**, 1339–1347.
Weiner DB, *et al*. (1989). *Nature*, **339**, 230–231.
Wen D, *et al*. (1992). *Cell*, **69**, 559–572.
Yokota J, *et al*. (1986). *Lancet*, **1**, 765–767.

Available online at www.sciencedirect.com
ScienceDirect
Current Opinion in Chemical Biology

Antibody–drug conjugates: targeted drug delivery for cancer

Stephen C Alley, Nicole M Okeley and Peter D Senter

The antibody–drug conjugate field has made significant progress recently owing to careful optimization of several parameters, including mAb specificity, drug potency, linker technology, and the stoichiometry and placement of conjugated drugs. The underlying reason for this has been obtained in pre-clinical biodistribution and pharmacokinetics studies showing that targeted delivery leads to high intratumoral free drug concentrations, while non-target tissues are largely spared from chemotherapeutic exposure. Recent developments in the field have led to an increase in the number of ADCs being tested clinically, with 3 in late stage clinical trials: brentuximab vedotin (also referred to as SGN-35) for Hodgkin lymphoma; Trastuzumab-DM1 for breast cancer; and inotuzumab ozogamicin for non-Hodgkin lymphoma. This review highlights the recent pre-clinical and clinical advances that have been made.

Address
Seattle Genetics, Inc., 21823 30th Drive SE, Bothell, WA 98021, United States

Corresponding author: Alley, Stephen C (SAlley@seagen.com)

Current Opinion in Chemical Biology 2010, 14:529–537

This review comes from a themed issue on
Next Generation Therapeutics
Edited by Michael Gelb and Adrian Whitty

Available online 17th July 2010

1367-5931/$ – see front matter
© 2010 Elsevier Ltd. All rights reserved.

DOI 10.1016/j.cbpa.2010.06.170

More than 20 monoclonal antibodies (mAbs) have been approved for use in many indications, including cancer [1]. There are multiple mechanisms by which mAbs can exert therapeutic efficacy, but often their activity is not sufficient to produce a lasting benefit. Hence, several strategies have been employed to enhance their activity. Antibody–drug conjugates (ADCs) represent one approach, where the ability to harness mAb specificity and target the delivery of a cytotoxic agent to the tumor may significantly enhance both mAb and drug activities. Conjugation also has an effect on the biodistribution of the drug, sparing normal tissue exposure to the cytotoxic agent and allowing the use of potent agents that would prove too toxic for systemic use. Optimization of a variety of ADC parameters has recently met with considerable success [2–5,6•], and 3 ADCs are now in late-stage clinical trials with about 10 others in earlier stage trials.

Development of optimized ADCs

Optimization parameters

Extensive optimization of several ADC parameters has taken place over multiple decades, and clinical development of ADCs has required attention to these details. Table 1 lists these optimization parameters and different solutions for producing pharmacologically active ADCs. There are 3 key components of an ADC: the mAb, the drug, and the linker. Ideally, the mAb will specifically bind to an antigen with substantial expression on tumor cells but limited expression on normal tissues. Specificity allows the utilization of drugs that otherwise would be too toxic for clinical application. Thus, most of the recent work in this field has centered on the use of highly potent cytotoxic agents. This requires the development of linker technologies that provide conditional stability, so that drug release occurs after tumor binding, rather than in circulation. Finally, the method of ADC conjugation, which determines the drug loading stoichiometry and homogeneity, has been shown to play roles not only in pharmacokinetics, but also in activity, potency, and tolerability.

Antigen binding and drug release

Many different antigens have been evaluated for ADCs [2,4,5,6•]. The vast majority undergo rapid internalization once the ADC binds through a process known as receptor mediated endocytosis, in which antigens localized to clathrin-coated pits or lipid rafts are internalized along with bound antibody [5]. For some antigens, unconjugated mAb and ADC have been observed to internalize with the same rate [7], while for other antigens ADC has been observed to internalize much more efficiently than unconjugated mAb [8], suggesting that internalization processes are variable across antigens and depend on multiple parameters. Once internalized, the ADC is delivered to lysosomes (although there are some exceptions [9]) where effective drug release takes advantage of the catabolic environment found within these organelles. Following release from the lysosome, the drug either binds to its pharmacological target or leaves the cell via active or passive processes [2]. ADCs have demonstrated intracellular accumulation of released drug in antigen positive cells [10,11] but no intracellular accumulation in antigen negative cells [11], highlighting the antigen specificity of drug delivery by ADCs. There have also been some reports that poorly internalized antigens can successfully be targeted with ADCs potentially utilizing drug release strategies that occur in the tumor microenvironment rather than inside cells [12,13]. The requirements for antigen internalization to yield active ADCs is an area of active investigation, and the results may be

Table 1

Key ADC parameters

Parameter	Description	Leading examples	References
Antigen	Substantial expression on tumor, limited expression on normal tissues	Her2, CD30, CD33	[2,4,5,6*]
Linker	High stability to avoid systemic release	Dipeptides, direct linkage, some hydrazones and disulfides	[17–19]
Drug	High potency since delivery is limited by antigen copy number	Auristatins, maytansines, calicheamicin	[3,14,15]
Drug loading level	Maintain mAb PK by limiting drug loading	3–4 drugs per mAb often optimal	[24]
Conjugation site	Homogeneous drug loading by site-specific conjugation to avoid subpopulations with altered PK	Chemical methods, cysteine point mutants	[21–23]

dependent not only on the linker technology used for drug attachment, but also on the fate of the drug once it is released from the mAb carrier.

Drugs and linkers

Early ADCs relied on drugs that were already approved for use as small molecules, such as vinblastine and doxorubicin, and suffered from lack of potency and low clinical activities [4,5]. Substantially more potent drugs that were too toxic to use in an untargeted manner have been more promising as ADCs. These include auristatins (Figure 1), maytansines (Figure 2), and calicheamicins (Figure 3). Auristatins and maytasines both exert their cytotoxic effects by binding to tubulin, causing G2/M cell cycle arrest, and subsequently leading to apoptosis. Monomethylauristatin E, conjugated through a protease-cleavable dipeptide linker (vcMMAE, **1**) [14], and monomethylauristatin F, conjugated directly to mAbs through maleimidocaproic acid (mcMMAF, **3**) [8], are synthetic analogs of dolastatin 10, a natural product originally isolated from the Indian ocean sea hare *Dolabella auricularia*. DM1, conjugated through a disulfide (**5**) or directly through the heterobifunctional succinimidyl 4-[N-maleimidomethyl]cyclohexane-1-carboxylate (SMCC) linker (**8**), and DM4, conjugated through a disulfide (**10**), are semi-synthetic analogs of maytansine, a natural product originally isolated from the Ethiopian shrub *Maytenus ovatus* [3]. Calicheamicin, a DNA strand cleaving agent conjugated through an acid-sensitive hydrazone (**13**), is a semi-synthetic analog of a *Micromonospora echinospora* ssp. calichensis fermentation product [15].

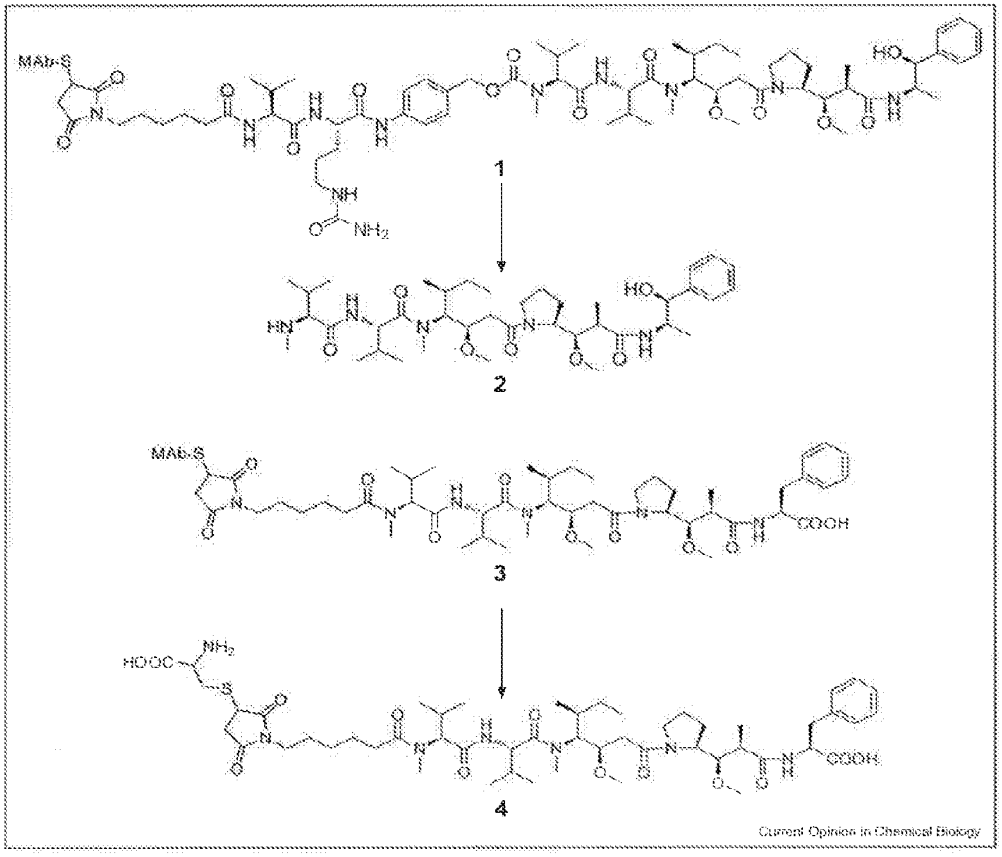
There are a variety of catabolic processes that occur to release drug from an ADC. The vcMMAE protease-cleavable drug-linker (**1**) was designed to release MMAE (**2**) in target cells [7], and indeed MMAE was reported as the only intracellular released drug in cancer cell lines (Figure 1) [11]. The directly conjugated mcMMAF drug-linker (**3**) was observed to release cys-mcMMAF (**4**) after ADC catabolism, consistent with proteolytic degradation of the mAb to release the drug (Figure 1) [16]. For maytansines, directly linked SMCC ADCs and disulfide-linked ADCs both yield ε-amino lysine-linked drugs (**6**, **9**, **11**). The disulfide-linked drugs can also be reduced to the free thiol and subsequently S-methylated or cysteinylated (**7**, **12**) (Figure 2). These various small molecules have different potencies and cellular permeabilities, presumably because of differences in charged groups on the various catabolites [10]. Not all drug classes may be tolerant of modification with an amino acid, and could be inactive in this form.

Stability of the drug-linker in circulation is important because the long circulating half-life of the ADC provides exposure for several days post injection. Directly linked ADCs and protease-cleavable linkers are generally more stable in circulation than disulfides and hydrazones [17–19], although the stability of the latter two linkers can be tuned by altering the neighboring chemical structure. For example, substituents on the aromatic group adjacent to the hydrazone in calicheamicin conjugates were observed to significantly affect the rate of calicheamicin release and ADC potency [15]. DM4 has a gem-dimethyl group next to the disulfide, which increases disulfide bond stability compared to DM1 that has a single adjacent methyl group [20].

Conjugation methods

The method of making ADCs, including the drug loading stoichiometry and resulting conjugation heterogeneity, should maintain the pharmacokinetic properties of the mAb. There are three common methods for conjugating mAbs: alkylation of reduced interchain disulfides, acylation of lysines, and alkylation of genetically engineered cysteines. There are 8 interchain cysteines and up to 100 lysines available for conjugation on IgG1 mAbs, and conjugation to these sites results in heterogeneous mixtures. Cysteine conjugates provide a greater degree of uniformity than lysine-based conjugates [21], while recombinant methods in which cysteines are specifically introduced into the mAb backbone are more uniform still [22,23]. In some instances, it has been observed that the location of the conjugated drug is not as important as the

Figure 1



Structures of auristatin antibody-drug conjugates and catabolic products. ADCs made from vcMMAE (1) are converted to MMAE (2), while ADCs made from mcMMAF (3) are converted to cys-mcMMAF (4).

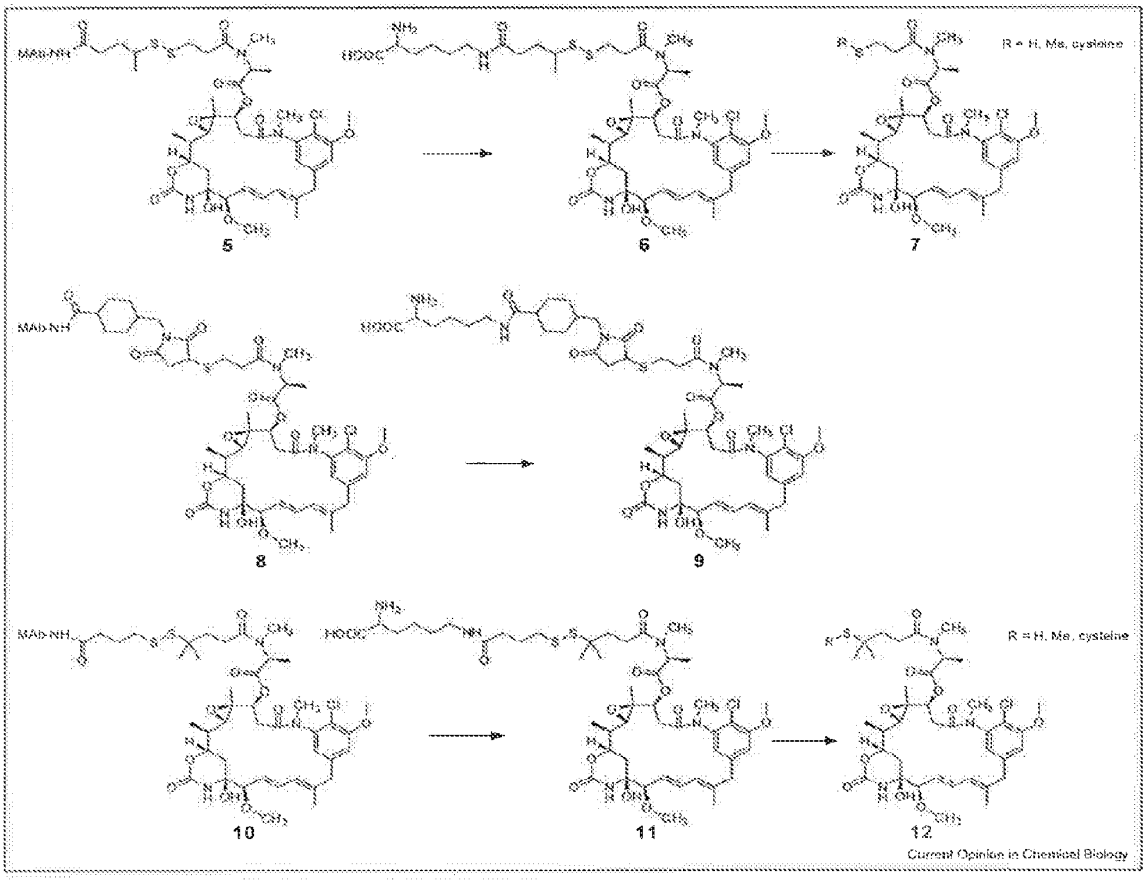
stoichiometry of drug attachment [21,23]. ADCs with two to four drugs per antibody are generally superior to more heavily loaded conjugates that clear very rapidly from the circulation [24]. Using chemical methods for conjugate formation, it has proven difficult to prepare ADCs with only 2 drugs/mAb because a large fraction of the mAb will not be conjugated to any drug. Recombinant methods have been described for this purpose [22,23], and in one case the resulting engineered conjugate had an improved therapeutic window relative to a chemically produced ADC [22]. However the drug loading stoichiometry of the two conjugates were markedly different. The precise roles that conjugation site and stoichiometry play in ADC efficacy and tolerability warrant further investigation.

Pharmacology of ADCs

Ideally, an ADC acts as an inactive prodrug in circulation and only upon internalization into target cells or localization to the tumor is an active drug released. However, only a small amount of the ADC will ever reach the target cells [3,25••], highlighting the importance of using a highly potent drug. The remainder will be catabolized in normal tissues, which may cause exposure to the released drug. An optimal drug for ADCs will therefore be one that does not have a long residence time once released in normal tissues, while maintaining a high concentration in the tumor for an extended time.

To evaluate ADC biodistribution, an anti-CD70 mcMMAF ADC with two unique radiolabels was

Figure 2

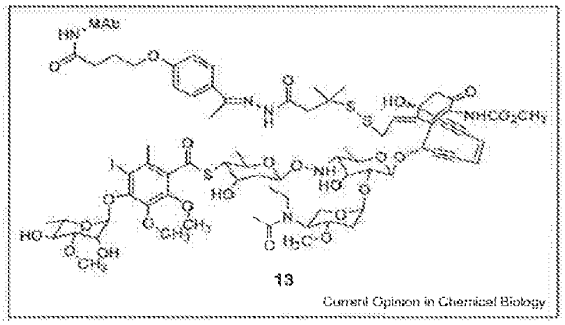


Structures of maytansine antibody–drug conjugates and catabolic products, DM1 (6) and DM4 (10) disulfide ADCs are converted to lysine-linked disulfides (6, 11), which are subsequently reduced to the free thiol and then S-methylated or cystineylated (7, 12). DM1 linked through SMCC (8) is converted to the lysine-linked drug (9).

prepared to track the mAb (^{3}H) and drug (^{14}C) simultaneously in mice bearing tumor xenografts. Two radiolabels were used because once the ADC is catabolized and drug released, tracking just the mAb would not be able to determine the biodistribution of the released drug. Antibody-bound drug and released drug were distinguished by precipitating the mAb-bound drug with organic solvent and scintillation counting the supernatant containing the released drug. Both radiolabels quickly accumulated in the tumor, but the mAb peak was 1 d post dose while the drug peak was 2 d post dose. The proportion of released drug relative to conjugated drug increased over time in the tumor. In most normal tissues, both the mAb and drug decreased over time in conjunction with the serum levels, except in organs involved in hepatobiliary clearance where there was a peak 4 h post dose followed by a rapid decrease (Figure 4a). This difference in tumor versus normal biodistribution and release kinetics yielded a tumor exposure to released drug tens to hundreds of times higher than that of normal tissues [26•].

The size of the ADC delivery vehicle also plays a role in how effectively drug will be delivered to tumors. Diabodies are single-chain variable domain fragments (scFvs) with a linker between the light and heavy chains that promotes dimerization. The biodistributions of vcMMAF-conjugated anti-CD30 mAb and diabody were

Figure 3

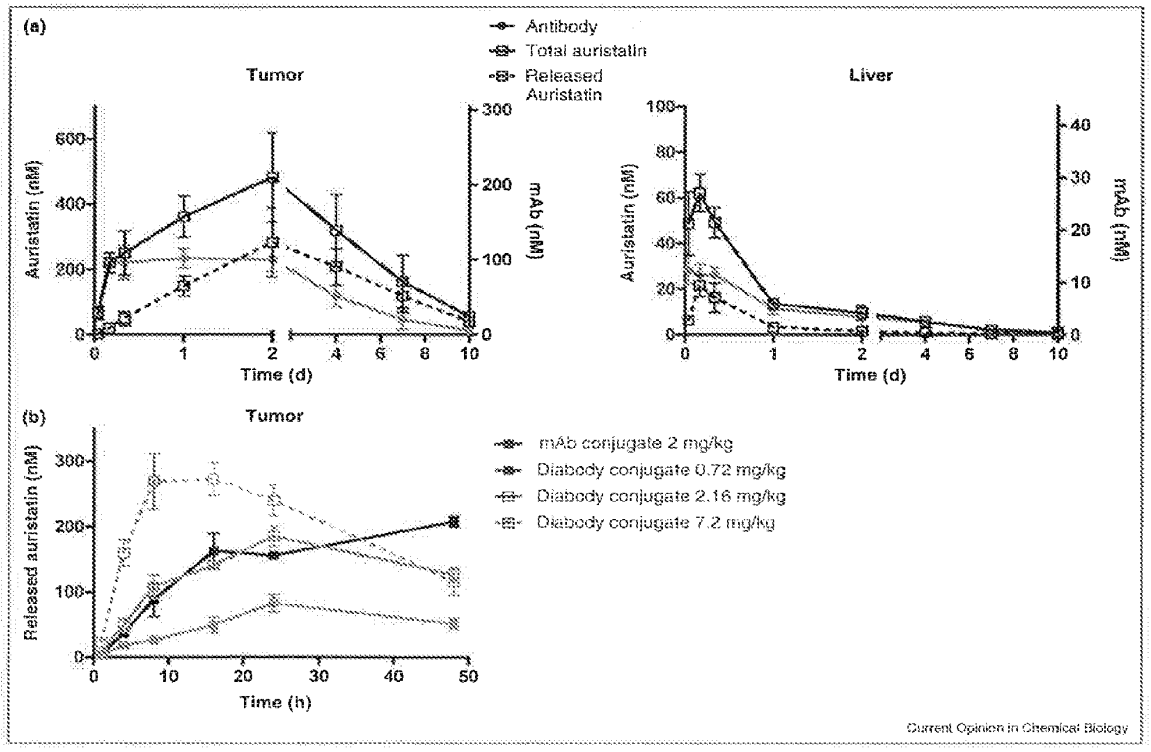


Structure of calicheamicin antibody–drug conjugate.

compared using a single radiolabel on the drug. Since the diabody clears much faster than the mAb, the kinetics of tumor accumulation were distinct: released drug from the diabody conjugate reached peak concentrations within 1 d post dose while the released drug concentration from the mAb conjugate was still increasing at 2 d post dose (Figure 4b). Despite the rapid clearance of the diabody, the tumor exposure to the drug for diabody and mAb could be matched with a larger diabody dose, but at the expense of the diabody exposing the normal tissues to much higher concentrations of conjugated and released drug. Thus, the tumor to normal tissue released drug exposure ratios were found to be superior using a mAb for drug delivery, compared to the lower molecular weight diabody [27].

These findings are consistent with a subsequently published study involving mathematical modeling and

Figure 4



Biodistribution studies of ADCs in tumor bearing mice. (a) Anti-CD70 mcMMAF ADC simultaneously labeled on the mAb (^{3}H) and drug (^{14}C) was administered to 786-O tumor-bearing mice (2 mg/kg). At indicated time points, tumor and normal tissues including liver were harvested and the concentrations of mAb, total auristatin (conjugated plus released), and released auristatin were determined by liquid scintillation counting. (b) Anti-CD30 vcMMAF mAb and diabody conjugates labeled on the drug (^{3}H) were administered to Karpas 299 tumor-bearing mice at 2 mg/kg for the mAb and 0.72, 2.16, and 7.2 mg/kg for the diabody (delivering 1, 3, and 10 fold as much drug as the mAb). At indicated time points, tumors were harvested and the concentration of released auristatin determined by liquid scintillation counting. Adapted from [17,27].

experimental observations of the relationship between molecular weight of the delivery agent and the extent of tumor targeting. Calculations in agreement with previous experimental results predicted that the minimum tumor uptake occurred with ~25 kDa vehicles such as scFvs, while maximum tumor uptake should take place with ~150 kDa mAbs and small drugs with very low molecular weights. The long circulating half-life of mAbs more than compensated for a decrease in tumor penetration relative to smaller vehicles [25••]. mAb conjugates may therefore be the optimal vehicle for drug delivery owing to their maximal tumor uptake, as long as normal tissues are minimally exposed to released drug by careful target, drug, and linker selection.

Maytansine ADCs have also been evaluated for their ability to localize to tumors using ^{3}H labeled drug. Mice with tumor xenografts were dosed with anti-CanAg ADCs and the total amount of ^{3}H drug (mAb bound and released) in tumor evaluated. A directly linked SMCC-DM1 ADC achieved ~2-fold higher tumor concentrations than disulfide-linked DM1 and DM4 ADCs. Samples were also analyzed for the identity of drug released by ADC catabolism, with the same species observed *in vivo* and *in vitro*. The tumor concentration of ε-amino lysine-linked DM1 was also ~2 fold higher than the sum of the S-methyl and cysteinyl DM1 and DM4 [28].

ADCs in clinical development

Approved ADCs

Table 2 lists ADCs currently in the clinic, and recently released clinical data are presented below. Also listed is the ADC Gemtuzumab ozogamicin, an anti-CD33 mAb conjugated to calicheamicin. This ADC was approved in 2000 but has been withdrawn and is no longer commercially available to new patients (http://www.fda.gov/NewsEvents/Newsroom/PressAnnouncements/ucm216448.htm). Gemtuzumab ozogamicin was approved for the treatment of relapsed acute myeloid leukemia in patients older than 60 years based on a response rate of about 30% [29]. The approved dose is 9 mg/m^{2}, or about 0.22 mg/kg for a 65 kg adult, a very low dose that reflects the high potency of calicheamicin.

Late clinical stage ADCs

ADCs in late stage clinical trials include brentuximab vedotin (SGN-35), an anti-CD30 mAb conjugated to vcMMAE, currently in a pivotal trial for relapsed or refractory Hodgkin lymphoma (HL) following an autologous stem cell transplant, using a dose of 1.8 mg/kg every 3 weeks. The rationale for a pivotal trial was based on data from a Phase I dose escalation trial that included both HL and systemic anaplastic large cell lymphoma (sALCL) patients, whereas those treated with ≥1.2 mg/kg of SGN-35 showed an objective response rate of 54% (15/28), with 9 complete responses. Nearly all (93%) of the patients experienced tumor regression during the course of therapy [30••]. In a second Phase I trial with weekly dosing, patients receiving 0.4–1.4 mg/kg had an objective response rate of 56% (22/39). Among the 5 sALCL patients, 4 had complete responses [31].

Trastuzumab-DM1, also in late-stage clinical trials, uses the approved anti-Her2 mAb Trastuzumab (Herceptin) directly conjugated to DM1 via SMCC for the treatment of metastatic breast cancer. In a Phase II trial in third line metastatic breast cancer with 3.6 mg/kg Trastuzumab-DM1 dosed every 3 weeks, a 33% objective response rate in 110 patients was observed [32••], demonstrating single agent activity in a population heavily pretreated with agents including Trastuzumab. A Phase III trial investigating Trastuzumab-DM1 versus capecitabine

Table 2

ADCs in the clinic

Agent	Target	Drug class	Indication	Clinical status
Brentuximab vedotin (SGN-35) [30••,31]	CD30	Auristatin	Hodgkin lymphoma	Phase II (pivotal)
CDX-011 (CR011-vcMMAE) [34,35]	GPNMB	Auristatin	Melanoma, breast cancer	Phase II
SGN-75 [53]	CD70	Auristatin	NHL, RCC	Phase I
PSMA ADC [54]	PSMA	Auristatin	Prostate cancer	Phase I
MEDI-547 [40]	EphA2	Auristatin	Solid tumors	Phase I
MN immunoconjugate [41]	MN	Auristatin	Cancer	Phase I
Trastuzumab-DM1 [32••]	Her2	Maytansine	Breast cancer	Phase III
IMGN901 [36,37]	CD56	Maytansine	Multiple myeloma, solid tumors	Phase I
IMGN388 [55]	α_v integrin	Maytansine	Solid tumors	Phase I
SAR3914 [38]	CD19	Maytansine	NHL	Phase I
BT-062 [39,56]	CD138	Maytansine	Multiple myeloma	Phase I
BIIB015 [42]	Cripto	Maytansine	Solid tumors	Phase I
Gemtuzumab ozogamicin [29]	CD33	Calicheamicin	AML	Approved, withdrawn from market
Inotuzumab ozogamicin [33]	CD22	Calicheamicin	NHL	Phase III
MEDX-1209 [43]	CD70	Duocarmycin	NHL, RCC	Phase I

Data gathered from the listed references, clinicaltrials.gov, and sponsor web sites.

and lapatinib in second line metastatic breast cancer and a Phase II trial investigating Trastuzumab-DM1 versus Trastuzumab and docetaxel in front line therapy are currently ongoing.

Inotuzumab ozogamicin, which uses the same calicheamicin drug-linker as Gemtuzumab ozogamicin, is an anti-CD22 ADC for non-Hodgkin lymphoma (NHL) currently in a Phase III trial in combination with Rituximab. In a Phase I/II dose escalation trial, the maximum tolerated dose (MTD) was found to be 1.8 mg/m^2 when dosed every 4 weeks and an expansion cohort was enrolled at this dose. In this expansion cohort, the objective response rate was 88% (14/16) for follicular lymphoma and 71% (10/14) for diffuse large B-cell lymphoma (10/14) [33].

Early clinical stage ADCs

ADCs in earlier stage clinical trials include CDX-011 (CR011-vcMMAE), being evaluated in both melanoma and breast cancer, an anti-glycoprotein NMB mAb conjugated to vcMMAE. In Phase I/II studies for both indications, 1.88 mg/kg dosed every 3 weeks was found to be the MTD. In 37 melanoma patients at all dose levels there were 2 partial responses [34], while in 32 breast cancer patients treated at 1.88 mg/kg there were 4 partial responses [35].

Several maytansine ADCs currently in the clinic have had Phase I dose escalation and MTD expansion cohort data reported, including the anti-CD56 IMGN901, a disulfide-linked DM1 ADC for multiple myeloma and solid tumors, the anti-CD19 SAR3419, a disulfide-linked DM4 ADC for NHL, and the anti-CD138 BT-062, a disulfide-linked DM4 ADC for multiple myeloma. Treatment with IMGN901 showed 1 partial response in the first 26 multiple myeloma patients [36] and 5 objective responses in 113 patients with a variety of solid tumors [37]. Objective responses from SAR3419 treatment were obtained in 5 of 27 patients [38], while 2 of 25 patients treated with BT-062 had objective responses [39].

A number of other ADCs have just recently entered clinical trials. SGN-75, an anti-CD70 mAb directly conjugated to the drug-linker mcMMAF [36]. This ADC is being tested in both NHL and renal cell carcinoma (RCC), where CD70 expression has been demonstrated. Additional auristatin ADCs in the clinic target PSMA [37], EphA2 [40], and MN (carbonic anhydrase IX) [41], while additional maytansine ADCs in the clinic target α_v integrin [40] and cripto [42]. A final ADC recently entering the clinic uses a DNA minor groove binding duocarmycin conjugated to an anti-CD70 mAb [43].

Pre-clinical ADCs

The drug-linkers being used in ADCs in the clinic have also been evaluated pre-clinically for a variety of targets, including CD19 [43,44], CD20 [44–46], CD79b [44,47], CD133 [44], BCMA [45], CEACAM6 [46], TMEFF2 [47], PSCA [48], MUC16 [22,49], p97 [9], EphB2 [50], and 5T4 [51]. Many more ADCs such as these can be expected to enter clinical trials soon [52•].

Conclusions

Optimization of the parameters influencing ADC activity has led to the development of new agents with promising activities. Recent clinical results have sparked significant additional interest and the number of ADC candidates in clinical development is growing rapidly. Use of highly potent drugs, stable linkers, optimized drug stoichiometry, and appropriate antigen target selection have been crucial in advancing the technology to where it is today. A detailed understanding of ADC pharmacokinetics, catabolism, and biodistribution will facilitate the development of new agents for clinical evaluation.

References and recommended reading

Papers of particular interest, published within the annual period of review, have been highlighted as:

- • of special interest
- •• of outstanding interest

1. Fleichert JM: **Monoclonal antibodies as innovative therapeutics.** *Curr Pharm Biotechnol* 2008, **9**:423-430.

2. Carter PJ, Senter PD: **Antibody–drug conjugates for cancer therapy.** *Cancer J* 2008, **14**:154-169.

3. Chari RV: **Targeted cancer therapy: conferring specificity to cytotoxic drugs.** *Acc Chem Res* 2008, **41**:98-107.

4. Senter PD: **Potent antibody drug conjugates for cancer therapy.** *Curr Opin Chem Biol* 2009, **13**:235-244.

5. Alley SC, Benjamin D, Law C-L: In *Antibody–Drug Conjugate Therapy*. Edited by An Z. Hoboken, NJ: John Wiley & Sons, Inc.; 2009.

6. • Teicher BA: **Antibody–drug conjugate targets.** *Curr Cancer Drug Targets* 2009, **9**:982-1004.
A thorough review of ADC targets being evaluated clinically and pre-clinically.

7. Sutherland MS, Sanderson RJ, Gordon KA, Andreyka J, Cerveny CG, Yu C, Lewis TS, Meyer DL, Zabinski RF, Doronina SO *et al.*: **Lysosomal trafficking and cysteine protease metabolism confer target-specific cytotoxicity by peptide-linked anti-CD30-auristatin conjugates.** *J Biol Chem* 2006, **281**:10540-10547.

8. Law CL, Cerveny CG, Gordon KA, Klussman K, Mixan BJ, Chace DF, Meyer DL, Doronina SO, Siegall CB, Francisco JA *et al.*: **Efficient elimination of B-lineage lymphomas by anti-CD20-auristatin conjugates.** *Clin Cancer Res* 2004, **10**:7842-7851.

9. Smith LM, Nesterova A, Alley SC, Torgov MY, Carter PJ: **Potent cytotoxicity of an auristatin-containing antibody–drug conjugate targeting melanoma cells expressing melanotransferrin/p97.** *Mol Cancer Ther* 2006, **5**:1474-1482.

10. Erickson HK, Park PU, Widdison WC, Kovtun YV, Garrett LM, Hoffman K, Lutz RJ, Goldmacher VS, Blattler WA: **Antibody-maytansinoid conjugates are activated in targeted cancer cells by lysosomal degradation and linker-dependent intracellular processing.** *Cancer Res* 2006, **66**:4426-4433.

11. Okeley NM: **Intracellular activation of SGN-35, a potent anti-CD30 antibody–drug conjugate.** *Clin Cancer Res* 2010, **16**:888-897.

12. Dijoseph JF, Dougher MM, Armellino DC, Kalyandrug L, Kunz A, Boghaert ER, Hamann PR, Damle NK: **CD20-specific antibody-targeted chemotherapy of non-Hodgkin's B-cell lymphoma**

using calicheamicin-conjugated rituximab. *Cancer Immunol Immunother* 2007, **56**:1107-1117.

13. Polson AG, Calemine-Fenaux J, Chan P, Chang W, Christensen E, Clark S, de Sauvage FJ, Eaton D, Elkins K, Elliott JM *et al.*: **Antibody–drug conjugates for the treatment of non-Hodgkin's lymphoma: target and linker-drug selection.** *Cancer Res* 2009, **69**:2358-2364.

14. Doronina SO, Toki BE, Torgov MY, Mendelsohn BA, Cerveny CG, Chace DF, DeBlanc RL, Gearing RP, Bovee TD, Siegall CB *et al.*: **Development of potent monoclonal antibody auristatin conjugates for cancer therapy.** *Nat Biotechnol* 2003, **21**:778-784.

15. Hamann PR, Hinman LM, Hollander I, Beyer CF, Lindh D, Holcomb R, Hallett W, Tsou HR, Upeslacis J, Shochat D *et al.*: **Gemtuzumab ozogamicin, a potent and selective anti-CD33 antibody-calicheamicin conjugate for treatment of acute myeloid leukemia.** *Bioconjug Chem* 2002, **13**:47-58.

16. Doronina SO, Mendelsohn BA, Bovee TD, Cerveny CG, Alley SC, Meyer DL, Oflazoglu E, Toki BE, Sanderson RJ, Zabinski RF *et al.*: **Enhanced activity of monomethylauristatin F through monoclonal antibody delivery: effects of linker technology on efficacy and toxicity.** *Bioconjug Chem* 2006, **17**:114-124.

17. Alley SC, Benjamin DR, Jeffrey SC, Okeley NM, Meyer DL, Sanderson RJ, Senter PD: **Contribution of linker stability to the activities of anticancer immunoconjugates.** *Bioconjug Chem* 2008, **19**:759-765.

18. Sanderson RJ, Hering MA, James SF, Sun MM, Doronina SO, Siadak AW, Senter PD, Wahl AF: **In vivo drug-linker stability of an anti-CD30 dipeptide-linked auristatin immunoconjugate.** *Clin Cancer Res* 2005, **11**:843-852.

19. Lewis Phillips GD, Li G, Dugger DL, Crocker LM, Parsons KL, Mai E, Blattler WA, Lambert JM, Chari RV, Lutz RJ *et al.*: **Targeting HER2-positive breast cancer with trastuzumab-DM1, an antibody-cytotoxic drug conjugate.** *Cancer Res* 2008, **68**:9280-9290.

20. Widdison WC, Wilhelm SD, Cavanagh EE, Whiteman KR, Leece BA, Kovtun Y, Goldmacher VS, Xie H, Steeves RM, Lutz RJ *et al.*: **Semisynthetic maytansine analogues for the targeted treatment of cancer.** *J Med Chem* 2006, **49**:4392-4408.

21. Sun MM, Beam KS, Cerveny CG, Hamblett KJ, Blackmore RS, Torgov MY, Handley FG, Ihle NC, Senter PD, Alley SC: **Reduction-alkylation strategies for the modification of specific monoclonal antibody disulfides.** *Bioconjug Chem* 2005, **16**:1282-1290.

22. Junutula JR, Raab H, Clark S, Bhakta S, Leipold DD, Weir S, Chen Y, Simpson M, Tsai SP, Dennis MS *et al.*: **Site-specific conjugation of a cytotoxic drug to an antibody improves the therapeutic index.** *Nat Biotechnol* 2008, **26**:925-932.

23. McDonagh CF, Turcott E, Westendorf L, Webster JB, Alley SC, Kim K, Andreyka J, Stone I, Hamblett KJ, Francisco JA *et al.*: **Engineered antibody–drug conjugates with defined sites and stoichiometries of drug attachment.** *Protein Eng Des Sel* 2006, **19**:299-307.

24. Hamblett KJ, Senter PD, Chace DF, Sun MM, Lenox J, Cerveny CG, Kissler KM, Bernhardt SX, Kopcha AK, Zabinski RF *et al.*: **Effects of drug loading on the antitumor activity of a monoclonal antibody drug conjugate.** *Clin Cancer Res* 2004, **10**:7063-7070.

25. • Schmidt MM, Wittrup KD: **A modeling analysis of the effects of molecular size and binding affinity on tumor targeting.** *Mol Cancer Ther* 2009, **8**:2861-2871.
An excellent mathematical model of tumor uptake of targeting agents based on size and affinity.

26. • Alley SC, Zhang X, Okeley NM, Anderson M, Law CL, Senter PD, Benjamin DR: **The pharmacologic basis for antibody-auristatin conjugate activity.** *J Pharmacol Exp Ther* 2009, **330**:932-938.
Evaluation of biodistribution of ADCs in a mouse xenograft model using two radiolabels for mAb and drug simultaneously.

27. Kim KM, McDonagh CF, Westendorf L, Brown LL, Sussman D, Feist T, Lyon R, Alley SC, Okeley NM, Zhang X *et al.*: **Anti-CD30 diabody drug conjugates with potent antitumor activity.** *Mol Cancer Ther* 2008, **7**:2486-2497.

28. Erickson HK, Widdison WC, Mayo MF, Whiteman K, Audette C, Wilhelm SD, Singh R: **Tumor delivery and in vivo processing of disulfide-linked and thioether-linked antibody-maytansinoid conjugates.** *Bioconjug Chem* 2009.

29. Larson RA, Boogaerts M, Estey E, Karanes C, Stadtmauer EA, Sievers EL, Mineur P, Bennett JM, Berger MS, Eten CB *et al.*: **Antibody-targeted chemotherapy of older patients with acute myeloid leukemia in first relapse using Mylotarg (gemtuzumab ozogamicin).** *Leukemia* 2002, **16**:1627-1636.

30. •• Younes A, Forero-Torres A, Bartlett NL, Leonard JP, Lynch C, Kennedy DA, Sievers EL: **Multiple complete responses in a Phase 1 dose-escalation study of the antibody–drug conjugate SGN-35 in patients with relapsed or refractory CD30-positive lymphomas.** *Blood (ASH Annual Meeting Abstracts), vol 112*. 2008:1006.
Clinical data with a single agent ADC demonstrating objective responses in heavily pretreated Hodgkin lymphoma patients.

31. Fanale M, Bartlett NL, Forero-Torres A, Rosenblatt JD, Horning SJ, Franklin AR, Lynch C, Sievers EL, Kennedy DA: **The antibody–drug conjugate brentuximab vedotin (SGN-35) induced multiple objective responses in patients with relapsed or refractory CD30-positive lymphomas in a phase 1 weekly dosing study.** *Blood (ASH Annual Meeting Abstracts)*. 2009., abstract 2731.

32. •• Krop I, LoRusso P, Miller KD, Modi S, Yardley D, Rodriguez G, Zheng M, Amler L, Rugo H: **A phase II study of Trastuzumab-DM1 (T-DM1), a novel HER2 antibody–drug conjugate, in patients with HER2+ metastatic breast cancer (MBC) who were previously treated with an antihracycline, a taxane, capecitabine, lipatinib, and trastuzumab.** *32nd Annual San Antonio Breast Cancer Symposium; San Antonio, TX: 2009., abstract 710*.
Clinical data with a single agent ADC demonstrating objective responses in heavily pretreated metastatic breast cancer patients.

33. Fayad L, Patel H, Verhoef G, Smith MR, Johnson PWM, Czuczman MS, Coiffier B, Hess G, Gine E, Advani A *et al.*: **Safety and clinical activity of the anti-CD22 immunoconjugate inotuzumab ozogamicin (CMC-544) in combination with rituximab in follicular lymphoma or diffuse large B-cell lymphoma: preliminary report of a phase 1/2 study.** *Blood (ASH Annual Meeting Abstracts)*. 2008., abstract 266.

34. Hwu P, Sznol M, Pavlick A, Kluger H, Kim KB, Boasberg P, Sanders D, Simantov R, Crowley E, Hamid O: **A phase I/II study of CR011-vcMMAE, an antibody–drug conjugate (ADC) targeting glycoprotein NMB (GPNMB) in patients (pts) with advanced melanoma.** *J Clin Oncol* 2009, **27(15S)** abstract 9032.

35. Burris H, Saleh M, Bendell J, Hart L, Rose AAN, Dong Z, Siegel PM, Crane MF, Donovan D, Crowley E *et al.*: **A phase I/II study of CR011-vcMMAE (CDX-011), an antibody–drug conjugate, in patients with locally advances or metastatic breast cancer.** *32nd Annual San Antonio Breast Cancer Symposium; San Antonio, TX: 2009., abstract 6096*.

36. Chanan-Khan A, Wolf J, Gharibo M, Jagannath S, Munshi N, Anderson KC, DePaolo D, Lee K, Miller KC, Guild R *et al.*: **Phase 1 Study of IMGN901, used as monotherapy, in patients with heavily pre-treated CD56-positive multiple myeloma. A preliminary safety and efficacy analysis.** *Blood (ASH Annual Meeting Abstracts)*. 2009., abstract 2283.

37. Fosselia F, Woll PJ, Lorigan P, Tolcher A, O'Brien M, O'Keeffe J, Zidijan S, Oin A, O'Leary J, Villalona-Calero M: **Investigation of IMGN901 in CD56+ solid tumors: results from a phase I/II trial (study 001) and a phase I trial (study 002).** *13th World Conference on Lung Cancer*. 2009.

38. Younes A, Gordon L, Kim S, Romaguera J, Copeland AR, de Castro Faria S, Kwak L, Fayad L, Hagemeister F, Fanale M *et al.*: **Phase 1 multi-dose escalation study of the anti-CD19 maytansinoid immunoconjugate SAR3419 administered by IV infusion every 3 weeks to patients with relapsed/refractory B-cell NHL.** *Blood (ASH Annual Meeting Abstracts)*. 2009., abstract 585.

39. Chanan-Khan A, Jagannath S, Heffner T, Avigan D, Lee K, Lutz RJ, Haeder T, Ruehle M, Uherek C, Wartenberg-Demand A *et al.*: **Phase 1 Study of BT062 given as repeated single dose once every 3 weeks in patients with relapsed or relapsed/refractory multiple myeloma.** *Blood (ASH Annual Meeting Abstracts)*. 2009., abstract 1862.

40. Lee JW, Han HD, Shahzad MM, Kim SW, Mangala LS, Nick AM, Lu C, Langley RR, Schmandt R, Kim HS *et al.*: **EphA2 immunoconjugate as molecularly targeted chemotherapy for ovarian carcinoma**. *J Natl Cancer Inst* 2009, **101**: 1193-1205.

41. Al-Ahmadie HA, Alden D, Qin LX, Olgac S, Fine SW, Gopalan A, Russo P, Motzer RJ, Reuter VE, Tickoo SK: **Carbonic anhydrase IX expression in clear cell renal cell carcinoma: an immunohistochemical study comparing 2 antibodies**. *Am J Surg Pathol* 2008, **32**:377-382.

42. Gong YP, Yarrow PM, Carmalt HL, Kwun SY, Kennedy CW, Lin BP, Xing PX, Gillett DJ: **Overexpression of Cripto and its prognostic significance in breast cancer: a study with long-term survival**. *Eur J Surg Oncol* 2007, **33**:438-443.

43. Zhang Q, Derwin D, Sufi B, Chen L, Guerlavais V, Green L, Passmore D, Sung J, Rangan V, Dai H *et al.*: **The critical role of cleavable linkers for efficacy and low toxicity with minor groove binding alkylating agent (MGBA) based antibody–drug conjugates**. *American Association of Cancer Research 100th Annual Meeting*, 2009, : abstract 1722.

44. Smith LM, Nesterova A, Ryan MC, Duniho S, Jonas M, Anderson M, Zabinski RF, Sutherland MK, Gerber HP, Van Orden KL *et al.*: **CD133/prominin-1 is a potential therapeutic target for antibody–drug conjugates in hepatocellular and gastric cancers**. *Br J Cancer* 2008, **99**:100-109.

45. Ryan MC, Hering M, Peckham D, McDonagh CF, Brown L, Kim KM, Meyer DL, Zabinski RF, Grewal IS, Carter PJ: **Antibody targeting of B-cell maturation antigen on malignant plasma cells**. *Mol Cancer Ther* 2007, **6**:3009-3018.

46. Strickland LA, Ross J, Williams S, Ross S, Romero M, Spencer S, Erickson R, Sutcliffe J, Verbeke C, Polakis P *et al.*: **Preclinical evaluation of carcinoembryonic cell adhesion molecule (CEACAM) 6 as potential therapy target for pancreatic adenocarcinoma**. *J Pathol* 2009, **218**:380-390.

47. Afar DE, Bhaskar V, Ibsen E, Breinberg D, Henshall SM, Kench JG, Drobnjak M, Powers R, Wong M, Evangelista F *et al.*: **Preclinical validation of anti-TMEFF2-auristatin E-conjugated antibodies in the treatment of prostate cancer**. *Mol Cancer Ther* 2004, **3**:921-932.

48. Ross S, Spencer SD, Holcomb I, Tan C, Hongo J, Devaux B, Rangell L, Keller GA, Schow P, Steeves RM *et al.*: **Prostate stem cell antigen as therapy target: tissue expression and in vivo efficacy of an immunoconjugate**. *Cancer Res* 2002, **62**:2546-2553.

49. Chen Y, Clark S, Wong T, Dennis MS, Luis E, Zhong F, Bheddah S, Koeppen H, Gogineni A, Ross S *et al.*: **Armed antibodies targeting the mucin repeats of the ovarian cancer antigen. MUC16, are highly efficacious in animal tumor models**. *Cancer Res* 2007, **67**:4924-4932.

50. Mao W, Luis E, Ross S, Silva J, Tan C, Crowley C, Chui C, Franz G, Senter P, Koeppen H *et al.*: **EphB2 as a therapeutic antibody drug target for the treatment of colorectal cancer**. *Cancer Res* 2004, **64**:781-788.

51. Boghaert ER, Sridharan L, Khandke KM, Armellino D, Ryan MG, Myers K, Harrop R, Kunz A, Hamann PR, Marquette K *et al.*: **The oncofetal protein, 5T4, is a suitable target for antibody-guided anti-cancer chemotherapy with calicheamicin**. *Int J Oncol* 2008, **32**:221-234.

52. Ducry L, Stump B: **Antibody–drug conjugates: linking cytotoxic payloads to monoclonal antibodies**. *Bioconjug Chem* 2010, **21**:5-13.
* A review focused on the various linkers used in ADCs and their impact on stability and drug release.

53. Oflazoglu E, Stone IJ, Gordon K, Wood CG, Repasky EA, Grewal IS, Law CL, Gerber HP: **Potent anticarcinoma activity of the humanized anti-CD70 antibody h1F6 conjugated to the tubulin inhibitor auristatin via an uncleavable linker**. *Clin Cancer Res* 2008, **14**:6171-6180.

54. Ma D, Hopf CE, Malewicz AD, Donovan GP, Senter PD, Goeckeler WF, Maddon PJ, Olson WC: **Potent antitumor activity of an auristatin-conjugated, fully human monoclonal antibody to prostate-specific membrane antigen**. *Clin Cancer Res* 2006, **12**:2591-2596.

55. Chen Q, Millar HJ, McCabe FL, Manning CD, Steeves R, Lai K, Kellogg B, Lutz RJ, Trikha M, Nakada MT *et al.*: **Alphav integrin-targeted immunoconjugates regress established human tumors in xenograft models**. *Clin Cancer Res* 2007, **13**:3689-3695.

56. Ikeda H, Hideshima T, Fulciniti M, Lutz RJ, Yasui H, Okawa Y, Kiziltepe T, Vallet S, Pozzi S, Santo L *et al.*: **The monoclonal antibody nBT062 conjugated to cytotoxic Maytansinoids has selective cytotoxicity against CD138-positive multiple myeloma cells in vitro and in vivo**. *Clin Cancer Res* 2009, **15**:4028-4037.

整理番号:PD20-0012D　発送番号:284957　発送日:平成29年 7月 4日　1

特許査定

（分割）

特許出願の番号	特願２０１６－１１７０９６
起案日	平成２９年　６月２２日
特許庁審査官	三木　寛　４１５１　４Ｐ００
発明の名称	抗体－薬物コンジュゲート
請求項の数	３
特許出願人	第一三共株式会社
代理人	大野　聖二（外　４名）

この出願については、拒絶の理由を発見しないから、特許査定をします。

上記はファイルに記録されている事項と相違ないことを認証する。
認証日　平成29年 6月29日　経済産業事務官　山田　忠男

注意：この書面を受け取った日から３０日以内に特許料の納付が必要です。

整理番号:PD20-0012D　発送番号:284957　発送日:平成29年 7月 4日　3/E

参考情報

特許出願の番号　特願２０１６－１１７０９６

１．調査した分野（ＩＰＣ，ＤＢ名）

ＣＯ７Ｄ　４９１／２２
ＣＡｐｌｕｓ／ＲＥＧＩＳＴＲＹ（ＳＴＮ）

２．参考特許文献

特表２００９－５３８６２９	（ＪＰ，Ａ）
特表２００８－５２１８２８	（ＪＰ，Ａ）
特表２００５－５１１６２７	（ＪＰ，Ａ）
国際公開第２００２／０００７３４	（ＷＯ，Ａ１）
特開平１１－０９２４０５	（ＪＰ，Ａ）
特開平１０－０９５８０２	（ＪＰ，Ａ）
特許第５９５３３７８	（ＪＰ，Ｂ１）
特許第６０３０２６７	（ＪＰ，Ｂ１）
特開平０６－０８７７４６	（ＪＰ，Ａ）
国際公開第２０１１／０２１３９７	（ＷＯ，Ａ１）
特表２００７－５２７８７２	（ＪＰ，Ａ）
特表２０１０－５１３５２４	（ＪＰ，Ａ）

３．参考図書雑誌

Journal of Medicinal Chemistry, ２０１１年, Vol.54, p.4077-4091
↳添付ﾌｧｲﾙ

整理番号:PD20-0012D　発送番号:284957　発送日:平成29年 7月 4日　2

1．出願種別　分割
2．参考文献　有
3．特許法第３０条適用　無
4．発明の名称の変更　無

5．国際特許分類（ＩＰＣ）

Ｃ０７Ｄ４９１／２２	ＣＳＰ	＝
Ａ６１Ｋ　３１／４７４５	ＺＮＡ	,
Ａ６１Ｐ　３５／００		,
Ｃ０７Ｋ　１６／２８		,
Ａ６１Ｋ　３９／３９５		Ｌ

6．菌寄託

7．出願日の遡及を認めない旨の表示

正本

1515487

檔　　號：
保存年限：9

經濟部智慧財產局專利核准審定書

機關地址：臺北市大安區辛亥路2段185號3樓
聯 絡 人：蔡付樺
聯絡電話：(02)23765380
查詢領證事宜請撥 (02)81769009
電子郵件：lion20663@tipo.gov.tw
傳　　真：(02)23779875

受文者：日商第一三共股份有限公司（代理人：丁國隆　專利代理人）

發文日期：中華民國107年4月11日
發文字號：（107）智專二（五）01203字第10720305960號
速　　別：
密等及解密條件或保密期限：
附　　件：如文

10720305960

IPC：*A61K 47/50 (2017.01)*　*A61K 31/4745 (2006.01)*　*A61K 39/395 (2006.01)*
A61P 35/00 (2006.01)

一、申請案號數：104103127

二、發明名稱：抗ＨＥＲ２抗體－藥物結合物

三、申請人：

名稱：日商第一三共股份有限公司

地址：日本

四、代理人：

姓名：丁國隆　專利代理人

地址：臺北市大安區敦化南路2段77號8樓

五、申請日期：104年1月30日

六、優先權項目：

1 2014/01/31 日本 2014-017777

2 2014/08/22 日本 2014-168944

3 2014/11/10 日本 2014-227886

TAIPEI
13 APR 2018
RECEIVED

1070413014

七、審查人員姓名：蔡付樺 委員

八、主文：應予專利。

九、注意事項：

(一)本案應於本審定書送達後3個月內，繳納證書費及第1年年費，始予公告，並自公告之日起給予發明專利權；屆期未繳費者不予公告。（檢附申領專利證書暨延緩公告申請書；申請人如欲洽詢領證事宜，請撥(02)81769009）。

(二)專利權人為自然人、學校或中小企業者，得依專利法第95條及專利年費減免辦法規定，向本局申請減收專利年費。

(三)專利之實施依其他法令規定須取得許可者，應依規定向有關主管機關申請之。

(四)本案發明專利名稱包含醫療功效用語，專利權人日後實施該專利權，仍須符合相關法規之規定。

十、本案係依申請時所提摘要、說明書、申請專利範圍及圖式、107年1月17日修正之申請專利範圍第1-3頁進行審查。

十一、檢送本案檢索報告1份。

附件

第104103127號專利申請案檢索報告

1. 申 請 日：	104年1月30日
2. 優先權日：	2014年1月31日、2014年8月22日、2014年11月10日
3. 本案國際專利分類號(IPC)：	***A61K47/50*** (2017.01) , ***A61K31/4745*** (2006.01) ***A61K39/395*** (2006.01) , *A61P35/00* (2006.01)
4. 檢索國際專利分類號(IPC)範圍：	A61K/47/50, A61K/31/4745, A61K/39/395, A61P/35/00 A61K47/50 (2017.01), A61K31/4745 (2006.01), A61K39/395 (2006.01), A61P35/00 (2006.01)
5. 檢索使用資料庫名稱：(關鍵詞)	TIPO 國內外專利資料庫，EPO，USPTO，JPO，GOOGLE SCHOLAR，中國專利訊息資料庫

關聯性代碼	引用文獻資料與相關段落處	相關聯請求項
A	1. CN 102481364 A 2012/05/30 【全文】	1-10
A	2. CN 101023100 A 2007/08/22 【全文】	1-10

關聯性代碼說明：

X：單獨引用即足以否定發明新穎性或進步性之特別相關的文獻。

Y：結合一或多篇其他文獻後足以否定發明進步性之特別相關的文獻。

A：一般技術水準之參考文獻。

D：說明書已記載之文獻。

E：申請在前、公開／公告在後之專利文獻。

O：公開使用、販賣或展覽陳列之文件。

P：申請日與優先權日間公開之文獻。

L：其他理由引用之文獻。

完成日： 107年4月10日

簽收時間 107/04/13(2018/04/13) 09:02:53

Australian Government
IP Australia

Delivering a world leading IP system

www.ipaustralia.gov.au

ABN: 38 113 072 755

13 September 2019

Examination report No. 2 for standard patent application

Pizzeys Patent and Trade Mark Attorneys Pty Ltd
GPO Box 1374
BRISBANE QLD 4001
Australia

Your reference	49212DAI/KS
Application number	2014371934
Applicant name	Daiichi Sankyo Company, Limited, Sapporo Medical University
Earliest priority date	25 December 2013

Final date for acceptance: **21 June 2020**
Date of this report: 13 September 2019
Examination request date: 15 November 2018

Dear Pizzeys Patent and Trade Mark Attorneys Pty Ltd,

Your application has been examined under *section 45 of the Patents Act 1990*. I consider that this application does not meet the requirements of the Act because there are issues with the application that are explained in the report details.

You have until **21 June 2020** to overcome all my objection(s) otherwise this application will lapse.

You will also need to pay any annual continuation fees that apply. Your next continuation fee is due on **24 December 2019**.

Details of this patent application can be viewed on AusPat, our Australian patent search database.

Yours sincerely,

Shawn Lyons
Section: CHEM 3 – BIOTHERAPEUTICS
Phone: (612) 6283 2081

Your reference 49212DAI/KS
Application number 2014371934

Report details

Basis of the report

In examining this application I have considered:

- the verified translation of the PCT pamphlet as originally filed
- allowed and/or proposed amendment/s under S104 up to and including amendment item number 2, filed on 6 September 2019.

Summary of novelty, inventive step and patentable subject matter

	Satisfy requirements?	*Claim numbers*
Novelty/inventive step	**Yes**	1-39
	No	NONE
Patentable subject matter	**Yes**	1-39
	No	NONE

Detailed objections on issues that have been identified

Section 40 (support, disclosure, clarity, lack of unity)

2 Claims 26-31, 37-39 are not supported. More specifically, the claims are directed to an antitumor and or anticancer drug comprising the anti-TROP2 antibody conjugate, pharmaceutical compositions comprising the claimed anti-TROP2 antibody conjugate suitable for treating various cancers and the use of the claimed anti-TROP2 antibody for treating tumours and/or cancers broadly and various other claimed cancers.

It is not reasonable to expect that the conjugate can be used for treating cancers where TROP2 is not implicated. D9 is considered representative of the common general knowledge in the art and discloses that TROP2 overexpression on several types of carcinomas is associated with tumour invasiveness and poor prognosis. However, TROP2 is not overexpressed in all cancers e.g. TROP2 is not upregulated in head and neck cancer (see the first paragraph of the Discussion on page 706; the paragraph bridging pages 704 and 705). Furthermore, the applicant's specification demonstrates that not all cancer cells are positive for TROP2 including the lung cancer cell line Calu-6 and the human cutaneous melanoma cell line A375 (See Example 22 of the applicant's specification).

In the absence of a principle of general application that enables the whole scope of the claims, the claimed invention will only be supported if the body of the specification provides adequate guidance in the form of explicit instructions and/or sufficiently representative examples that enable the skilled person in the art to perform the invention over the full scope of the claims. In the present application, however, such instructions or examples have not been provided.

Thus, for the reasons provided above, I am not satisfied that the body of the specification

Your reference 49212DAI/KS
Application number 2014371934

provides the support required by s 40(3).

I apologise for not raising this objection in the previous report.

Documents cited or considered relevant

D1 : T. M. CARDILLO ET AL, "Humanized Anti-Trop-2 IgG-SN-38 Conjugate for Effective Treatment of Diverse Epithelial Cancers: Preclinical Studies in Human Cancer Xenograft Models and Monkeys", CLINICAL CANCER RESEARCH, (2011-03-03), vol. 17, no. 10, doi:10.1158/1078-0432.CCR-10-2939, ISSN 1078-0432, pages 3157 - 3169 [1]

Category: **A** Claims: 1-39

D2 : WO 2011068845 A1 (IMMUNOMEDICS, INC et al.) 09 June 2011 [1]

Category: **A** Claims: 1-39

D3 : US 20080131363 A1 (GOVINDAN SERENGULAM et al.) 05 June 2008 [1]

Category: **A** Claims: 1-39

D4 : MORITZ N WENTE ET AL, "DE-310, a macromolecular prodrug of the topoisomerase-I-inhibitor exatecan (DX-8951), in patients with operable solid tumors", INVESTIGATIONAL NEW DRUGS ; THE JOURNAL OF NEW ANTICANCER AGENTS, KLUWER ACADEMIC PUBLISHERS, BO, (2005-08-01), vol. 23, no. 4, doi:10.1007/S10637-005-1442-2, ISSN 1573-0646, pages 339 - 347 [1]

Category: **A** Claims: 1-39

D5 : YUSUKE OCHI ET AL, "A possible mechanism for the long-lasting antitumor effect of the macromolecular conjugate DE-310: mediation by cellular uptake and drug release of its active camptothecin analog DX-8951", CANCER CHEMOTHERAPY AND PHARMACOLOGY, SPRINGER, BERLIN, DE, (2005-04-01), vol. 55, no. 4, doi:10.1007/S00280-004-0911-1, ISSN 1432-0843, pages 323 - 332 [1]

Category: **A** Claims: 1-39

D6 : YOSHINOBU SHIOSE ET AL, "Systematic Research of Peptide Spacers Controlling Drug Release from Macromolecular Prodrug System, Carboxymethyldextran Polyalcohol-Peptide-Drug Conjugates", BIOCONJUGATE CHEMISTRY, (2009-01-21), vol. 20, no. 1, doi:10.1021/bc800238f, ISSN 1043-1802, pages 60 - 70 [1]

Category: **A** Claims: 1-39

D7 : US 20110293513 A1 (GOVINDAN SERENGULAM V et al.) 01 December 2011 [1]

Category: **A** Claims: 1-39

D8 : IKUO MITSUI ET AL., "A New Water-soluble Camptothecin Derivative, DX-8951f, Exhibits Potent Antitumor Activity against Human Tumors in vitro and in vivo", JPN. J. CANCER RES., (1995), vol. 86, pages 776 - 782 [1]

Category: **A** Claims: 1-39

D9 : STEPAN L.P. et al., "Expression of Trop2 Cell Surface Glycoprotein in Normal and Tumor Tissues: Potential Implications as a cancer Therapeutic Target", Journal of Histochemistry & Cytochemistry, Vol. 59, No. 7, pages 701-710 [2]

Category: **A** Claims: 26-31, 37-39

Your reference 49212DAI/KS
Application number 2014371934

[1] Cited in the search/examination report of EP 3088419

[2] Document found in an informal state of the art search for common general knowledge. See attached Search Information Statement for details.

Note that this report has cited non-patent literature document/s. Copies of non-patent literature document/s can be requested for a fee (see *Patent Regulations, schedule 7, fee item 233 and 234*) through online services.

Please provide the citation details and associated patent application number with your request. Note that because of copyright restrictions we can only provide copies of hard copy books, journals and newspapers (see the Australian Patent Office Manual of Practice and Procedure at part 2.13.14 Copying of Material and Copyright Implications). However copies of any remaining documents should be readily obtainable from known electronic database sources.

New Documents

Informal state of the art search was performed for common general knowledge.

I apologise for any inconvenience that raising new citation/s at this stage may have caused.

Special categories of cited documents:

Y: The claimed invention cannot be considered to involve an inventive step under *subsection 7(2)* of the Act in light of the common general knowledge when considered together with a combination of the document and one or more other such documents.
A: Document defining the general state of the art which is not considered to be of particular relevance.

Your reference 49212DAI/KS
Application number 2014371934

Search information statement

Search details

Application number: 2014371934
Earlier search results available: Yes
Search completion date: 13 September 2019

Search strategy

Informal state of the art search of the Internet using Google and the following keywords:

TROP2 antibody and cancer - **First 20 results viewed**

END OF REPORT

The Open Breast Cancer Journal, 2009, *1*, 25-30

Open Access

Trastuzumab-DM1: A Review of the Novel Immuno-Conjugate for HER2-Overexpressing Breast Cancer

Myra F. Barginear[*,1] and Daniel R. Budman[2]

[1]*The Mount Sinai School of Medicine, The Breast Cancer Medicine Program at the Tisch Cancer Institute, One Gustave L. Levy Place, Box 1079, New York, NY 10029, USA*

[2]*New York University School of Medicine, Don Monti Division of Oncology, Monter Cancer Center of North Shore University Hospital, USA*

Abstract: Trastuzumab is a monoclonal antibody targeted against the HER2 tyrosine kinase receptor. Although trastuzumab is a very active agent in HER2-expressing breast cancer, the majority of patients with metastatic HER2 overexpressing breast cancer who initially respond to trastuzumab develop resistance within one year of initiation of treatment, and in the adjuvant setting, progress despite trastuzumab-based therapy. The immuno-conjugate Trastuzumab-DM1 (T-DM1) was designed to combine the biological activity of trastuzumab with the targeted delivery of a highly potent antimicrotubule agent, DM1, a maytansine derivative, to HER2-expressing breast cancer cells. T-DM1 is the first immuno-conjugate with a non-reducible thioether linker in clinical trials. Here, we summarize evidence from pre-clinical studies, analyze clinical data, and discuss the potential clinical implications of T-DM1.

INTRODUCTION

Several methods to enhance and improve the selectivity of cytotoxic drugs, and thus significantly improve the therapeutic index, are currently being pursued. One particular method is targeting drug carriers such as antibodies; this is the objective of immuno-conjugates, in which cytotoxic drugs are attached *via* chemical linkers to antibodies that recognize cancer cell antigens and deliver the cytotoxic drug only to the cells of interest.

The therapeutic concept of drug targeting was founded on Paul Ehrlich's vision of "the magic bullet" [1]. As such, he predicted the emergence of targeted agents which have lessened effects on host tissue. However, serotherapy was limited by the lack of appropriate targets, the inability to make discrete antibodies with high specificity in large quantities, and the reproducibility of the characteristics of the poly-antisera. In the late 1970's, George Köhler and César Milstein fundamentally changed Immunology by developing the technology of hybridomas, the production of a desired specific antibody in large amounts [2]. These investigators showed that antibody-producing cells, of any given specificity, could be fused with a myeloma cell line and create an unlimited amount of monoclonal antibodies carrying that specificity [3]. This finding has led researchers, clinicians, and especially biotechnology companies to focus on new diagnostic and therapeutic agents.

Lessons from the development of immunoconjugates can be learned from the biodistribution of immunoconjugates and the relationship between toxicity and efficacy. This is observed by the success of Yttrium-90 (^{90}Y)-ibritumomab tiuxetan (Zevalin®, Biogen) and Iodine-131 (^{131}I)-tositumomab (Bexxar®, Glaxo SmithKline) [4, 5]. Both of these radio-immunoconjugate therapies target the CD20 antigen that is expressed within normal pre-B lymphocytes but not on stem cells or plasma cells. The anatomic distribution of CD20- cells on both normal and malignant lymphocytes within blood and bone marrow may influence the activity and toxicity of radio-immunoconjugates.

Trastuzumab is a monoclonal antibody targeted against the HER2 tyrosine kinase receptor. Although trastuzumab is a very active agent in HER2-expressing breast cancer, the majority of patients with metastatic HER2 overexpressing breast cancer who initially respond to trastuzumab develop resistance within one year of initiation of treatment, and in the adjuvant setting, progress despite trastuzumab-based therapy [6-9]. The immuno-conjugate Trastuzumab-DM1 (T-DM1) was designed to combine the biological activity of trastuzumab (Herceptin®, Genentech) with the targeted delivery of a highly potent antimicrotubule agent, DM1 (ImmunoGen), a maytansine derivative, to human epidermal growth factor receptor type 2 (HER2)-expressing breast cancer cells. The aim of immuno-conjugates such as T-DM1 is to target intracellular delivery of both drugs with high specificity to avoid normal tissues.

The anti-mitotic drug maytansine was chosen for use in the targeted delivery approach because of its high *in vitro* potency [10, 11]. It was originally isolated from members of the plant families *Rhamnaceae* and *Euphorbiaceae*, as well as some mosses [12]. The maytansinoids bind tubulin competitively with vinca alkaloids and are approximately 100 times more potent than vincristine [12-14]. To link maytansinoids to antibodies through disulfide bonds, a thiol-containing maytansinoid, DM1 (N-methyl-N-[3-mercapto-1-oxopropyl]-L-alanine ester of maytansinol), an analog of the clinically-studied drug maytansine) was synthesized. In the case of T-DM1, DM1 is linked to trastuzumab using the

*Address correspondence to this author at the Tisch Cancer Institute, The Mount Sinai School of Medicine, One Gustave L. Levy Place, Box 1079, New York, NY 10029, USA; Tel: (212) 241-3650; Fax: (212) 876-5276; E-mail: Myra.Barginear@mssm.edu

1876-8172/09 2009 Bentham Open

bifunctional reagent, SMCC (*N*-succinimidyl-4-(maleimidomethyl) cyclohexanecarboxylate.) SMCC is first added to lysine residues on the protein to produce a linker modified antibody. The thiol group in DM1 is then reacted with the maleimide group of the linker to form the non-reducible thioether bond (Fig. 1). Each antibody contains an average of 3.5 drugs, however the product contains a distribution from 0 to 8 drugs per antibody [15]. T-DM1 is the first immuno-conjugate with a nonreducible thioether linker in clinical trials.

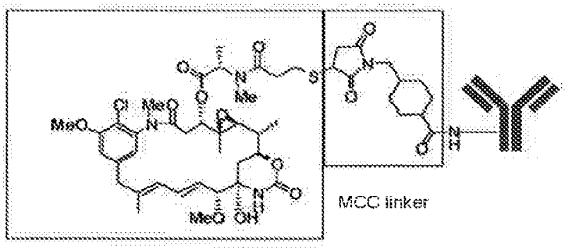


Fig. (1). Illustration of T-DM1. The average number of DM1 molecules per monoclonal antibody is 3.5 [45].

A review of the literature regarding T-DM1, its safety, efficacy, and toxicities was conducted by searches on Medline, Embase, Web of Science, and scientific meeting proceedings. Here, we summarize evidence from pre-clinical studies, analyze clinical data, and discuss the potential clinical implications of T-DM1.

HER2 POSITIVE BREAST CANCER

Overexpression of HER2, also referred to as HER2/neu or ErbB-2, was first described more than two decades ago [16, 17]. HER2 overexpression or gene amplification is observed in approximately 20 to 30% of invasive breast cancers. HER2 overexpression has been reported to be a poor prognostic factor and a predictive risk factor for decreased disease-free survival and overall survival in patients with breast cancer [18, 19]. Consequently, therapies which target HER2 are attractive in treating HER2-overexpressing breast cancer. One such therapy is trastuzumab, a humanized monoclonal immunoglobulin (IgG) that targets the extracellular domain of the HER2 receptor. Trastuzumab was approved in 1998 for the treatment of metastatic breast cancer and in 2006 for the adjuvant treatment of HER2 overexpressing breast cancer [20].

The exact mechanisms in which trastuzumab causes regression of HER2-overexpressing tumors are still being clarified, but several effects have been reported in the literature [21]. They include antibody-dependent cellular cytotoxicity, angiogenesis inhibition, and reduced downstream signaling through phosphatidylinositol 3-kinase and mitogen-activated protein kinase, ultimately resulting in cell-cycle arrest and apoptosis [21-25].

Trastuzumab Resistance

Although the selection of trastuzumab is based on the presence of HER2 overexpression, the simple presence of HER2 is not sufficient to ensure that trastuzumab will be effective in first-line treatment or guarantee that resistance will not develop.

The objective response rates for patients with HER2 overexpressing tumors to single agent trastuzumab range from 12% to 34%, for a median duration of 9 months [7, 8, 26, 27]. The median time to progression in patients who have not received prior chemotherapy and who have received prior chemotherapy for HER2 overexpressing metastatic breast cancer, is 4.9 months and 7.4, respectively [7, 8]. Thus, patients who respond to trastuzumab develop resistance within one year.

In the adjuvant setting, the administration of trastuzumab in combination with or following chemotherapy improves the disease-free and overall survival rates in patients with early stage breast cancer [6, 9]. However, approximately 15% of these women still develop metastatic disease despite trastuzumab-based adjuvant chemotherapy. Understanding the mechanisms that contribute to trastuzumab resistance and identifying novel agents is critical to improving the survival of patients whose tumors overexpress HER2.

Trastuzumab – DM1

A normal breast cell may have 20,000 HER2 receptors, whereas a breast cancer cell may express as many as 1.5 million copies per cell, which makes HER2 a potential target for immuno-conjugate therapy [28]. Preclinical and clinical studies indicate that trastuzumab combines extremely well with microtubule-directed agents [29, 30]. Thus, it was of particular interest to conjugate trastuzumab to the extremely potent drug maytansine.

The immuno-conjugates in development have been reported that use either antibody lysines or cysteines as the sites of drug attachment (31-34). Immuno-conjugates containing DM1 have previously been reported using several targeting antibodies [13-35]. In these studies, the linker attaching the drug to the protein lysines used a partially hindered, but still reducible disulfide. Trastuzumab linked to DM1 through a nonreducible thioether linker (SMCC) was compared to versions using disulfide linkers and appeared to offer improvements to both safety and efficacy [37]. Although the non-reducible linker is significantly more stable in circulation than the disulfide, it can still release active DM1 following internalization into tumor cells [36]. Work by Erickson, *et al.* [38] suggests that the immuno-conjugate is proteolytically degraded to release lysine-MCC-DM1, which is still a potent anti-mitotic agent.

TRASTUZUMAB-DM1 CLINICAL TRIALS

Pre-Clinical

Lewis-Phillips and colleagues reported the pharmacokinetics, efficacy, and toxicity of T-DM1[37]. The biological effects of disulfide linkers were investigated by constructing various T-DM1 conjugates; the stability of the linker not only compromises potency but can also exacerbate toxicity. Trastuzumab conjugated to DM1 through a nonreducible thioether linkage displayed better efficacy and lower toxicity than trastuzumab conjugated with reducible disulfide linkers. This was also confirmed by Kovtun and colleagues [38]. T-DM1 is internalized upon binding to HER2-overexpressing tumor cells and it is believed that

maytansine is released secondary to intracellular proteolytic degradation.

The antiproliferative effects of T-DM1 were evaluated in normal (MCF 10A breast epithelial cells) and tumor (breast carcinoma BT-474, SK-BR-3, MCF7, MDA-MB-468, MDAMB- 361, HCC1954, lung carcinoma Calu 3, and ovarian carcinoma line SK-OV-3) cell lines. HER2-overexpressing, trastuzumab-resistant tumor cells responded to T-DM1 whereas cell lines without overexpression were unaffected. Cell cycle analysis of conjugate-treated cells revealed cell cycle arrest in the G_2-M phase.

In vivo efficacy was determined in HER2-overexpressing breast cancer mouse models. Complete tumor regression for the duration of the study (126 days) was observed in mice receiving T-DM1. In contrast, unconjugated trastuzumab induced an initial decrease in tumor size, followed by regrowth upon cessation of treatment. In addition, T-DM1 was active in HER2-overexpressing, trastuzumab-refractory tumors [37].

Junttila and colleagues recently reported that trastuzumab conjugated to DM1 did not affect the mechanism of action of traztuzumab [39]. Cell lines overexpressing HER2 were used to assess *in vitro* efficacy and a trastuzumabinsensitive, HER2-transgenic mouse model was used to assess *in vivo* efficacy. The affinity of T-DM1 for HER2 was nearly identical to trastuzumab. Drug conjugation did not adversely affect trastuzumab's inhibition of HER2 shedding or down-regulation of AKT signaling. Notably, T-DM1 was active against mouse models that were insensitive to either trastuzumab or lapatinib (Tykerb®, GlaxoSmithKline). These results, along with the favorable efficacy and safety profile of trastuzumab linked to DM1 through a non-reducible linker, have advanced T-DM1 into clinical development.

Clinical

Two phase I studies have been conducted with T-DM1, administered weekly or every 3 weeks, in patients with advanced HER2 overexpressing breast cancer [40, 41]. Beeram *et al.* reported six dose levels of intravenous TDM1, scheduled every three weeks, in twenty-four HER2 positive breast cancer patients [40]. Patients had progressed on at least one trastuzmab-containing regimen with the median number of 92 weeks of prior trastuzumab therapy. Patients with significant cardiac disease, who had received prior doses of anthracyclines, and/or Grade 2 neuropathy, were excluded. The median age was 51 and all patients had an ECOG performance status of 0 or 1 (Table 1) [40].

The six dose levels of T-DM1 were administered: 0.3 mg/kg (n=3), 0.6 mg/kg (n=1), 1.2 mg/kg (n=1), 2.4 mg/kg (n=1), 3.6 mg/kg (n=15), and 4.8 mg/kg (n=3). Side effects included grade 1 and 2 transaminase elevations, thrombocytopenia, fatigue and nausea. Constipation, anemia, and neuropathy were also reported. Grade 3 and 4 thrombocytopenia was reported in three patients of whom two had Grade 4 events at 4.8 mg/kg, the dose limiting toxicity. One patient experienced Grade 3 neutropenia and another pulmonary hypertension. No cardiac events were reported.

The median progression-free survival at 3.6 mg/kg, the maximum tolerated dose, was 9.8 months. Additionally, thrombocytopenia, at the maximum tolerated does, was reported to be grade 1, rapidly reversible, and not cumulative. Partial responses were observed in 6/16 patients at 2.4 mg/kg (n=1) and 3.6 mg/kg (n=5). These patients had prior treatment with trastuzumab and other tublin-binding cytotoxic agents such as paclitaxel, docetaxel, and vinorelbine. An additional 9 patients were reported to have stable disease.

In the second phase I trial, Holden and colleagues reported weekly dosing of T-DM1 in fifteen patients with advanced HER2-positive breast cancer [41]. Patients had progressed on at least one trastuzmab-containing regimen with the median number of 122 weeks of prior trastuzumab therapy and an average of two prior chemotherapy regimens. The median age was 53 and all patients had an ECOG performance status of 0 or 1. T-DM1 was dosed at 1.2 mg/kg (n=3), 1.6 mg/kg (n=3), 2.0 mg/kg (n=3), 2.4 mg/kg (n=7), and 2.9 mg/kg (n=3) intravenously weekly.

Burris and colleagues initially reported phase II data of T-DM1 in HER2-positive metastatic breast cancer at the American Society of Clinical Oncology Breast Cancer Symposium and updated the results at the San Antonio Breast Cancer Symposium, December 2008 [42-44]. Enrollment completed with 112 patients. Patients were eligible if they had progression of disease on or within sixty days of receiving HER2 directed therapy and no active brain metastases, defined as symptomatic or requiring treatment within the last three months. Additional eligibility criteria included prior treatment with one or more chemotherapy regimens and no history of significant cardiac disease. The median age was 55 (33-79). The majority of patients had an ECOG performance status of 0 or 1, 68% had more than three metastatic sites, primarily liver and lung, and 8% had brain metastases. The median number of prior cytotoxic therapies was three (1-12) with 68% receiving an anthracycline. The median duration of prior traztuzumab was 77 weeks. Fifty-five percent of patients had received prior lapatinib therapy with a median duration of prior lapatinib therapy for 26 weeks.

Patients were treated with T-DM1 dosed at 3.6 mg/kg intravenously every three weeks and assessed every two cycles for toxicity and efficacy. Echocardiograms or MUGA scans were done after cycle 1 and cycle 2 and every other cycle thereafter. The average number of cycles administered was five; three patients were dose reduced to 3 mg/kg every three weeks. Pharamacokinetic parameters indicated the average terminal half-life was 89 hours and peak serum levels were less than 10 ng/ml. The preliminary pharmacokinetic analyses were similar to those reported for the maximum tolerated does in the phase I study by Beerman and colleagues [45].

The most common adverse advents were fatigue, nausea, and headache. Grade 3 and 4 adverse events included thrombocytopenia (n=8), hypokalemia (n=6), fatigue (n=4), infection (n=3), musculoskeletal chest pain (n=2), convulsions (n=2), thromboses (n=2), dyspnea (n=3), pleural effusion (n=3), and epistaxis (n=2). There were no Grade 3 or 4 cardiac dysfunction reported.

Fifty-six of the 112 patients have discontinued the study. Forty-four patients have discontinued the study secondary to

Table 1. Clinical Data Available, to Date, for T-DM1 in Patients with Metastatic HER2 Overexpressed Breast Cancer on Previous HER2 Directed Therapy

	Phase	N	Median # Prior Tx	Median T Dose (mg/kg/week)	Dose Levels	SD	PR	CR	Grade 3 or 4 AE	Conclusion
Beeram et al.	I	24	5†	91.6	3-4.8 mg/kg every 3 weeks	5/16	6/16	6/16	Thrombocytopenia Neutropenia	MTD: 3.6 mg/kg every 3 weeks
Thistlethwaite et al.	I	28	5‡	122	1.2-2 mg/kg weekly	NR	15/26	NR	Thrombocytopenia	MTD: 2.4 mg/kg every 3 weeks
Perez et al.	II	11	5§	76.6	3.6 mg/kg every 3 weeks	12/30	12/30	1/30	Thrombocytopenia Hypokalemia Fatigue Infection Musculoskeletal chest pain Convulsions Thromboses Dyspnea Pleural effusions Epistaxis	Antitumor activity in trastuzumab and lapatinib pre-treated pts Single agent activity in Her2-positive breast cancer Phase III in 2009

T: trastuzumab, N: number, SD: stable disease, PR: partial response, CR: complete response, AE: adverse event, NR: not reported, MTD: maximum tolerated dose.

progression of disease, six secondary to patient or physician's decision to discontinue the study, five secondary to adverse events unrelated to T-DM1, and one death on the study secondary to progression of disease.

The primary endpoint was overall response rate; the objective overall response rate was 39.3% (95% confidence interval (CI) =30-49), and the confirmed overall response rate, repeat imaging done on two occasions more than four weeks apart, was 27% (95% CI=19.4-36.1). Of the 62 patients exposed to prior lapatinib therapy, sixty were evaluable for efficacy. Objective responses were observed in 23/60 (38.30%, 95% CI=19.4-36.1).

In October 2008, Genentech indicated that they plan to initiate a Phase III, randomized, multicenter, international trial designed to compare the safety and efficacy of T-DM1 with that of capecitabine (Xeloda®, Roche) and lapatinib in patients with metastatic breast cancer that overexpress HER2. A total of 580 patients will be enrolled at approximately 260 sites worldwide. The company has also announced that they have initiated a Phase II trial comparing T-DM1, given as a single agent, to trastuzumab plus docetaxel as a first-line treatment in metastatic HER2-positive breast cancer. Currently, Genentech is enrolling a multicenter, open-label extension study. Patients who received T-DM1 in a Genentech-sponsored study and completed T-DM1 or who continue to receive T-DM1 at the time of the parent study closure are eligible for continued treatment. Patients can receive T-DM1 until disease progression or unacceptable toxicity for as long as the extension study remains open. More information on these trials can be found at www.clinicaltrials.gov.

DISCUSSION

The immono-conjugate T-DM1 has displayed significant *in vitro* and *in vivo* potency. Patients enrolled in the Phase I and II trials were heavily pretreated with cytotoxic therapy as well as HER2-targeted therapy. The median duration of prior traztuzumab or lapatinib therapy was over 1 year [43]. This finding establishes that HER2 remains a viable target, in HER2 overexpresing breast cancer, even after trastuzumab is ineffective.

There is clinical evidence that continued treatment with trastuzumab beyond progression improves activity of subsequent chemotherapy in patients with HER2–positive breast cancer [46]. Trastuzumab can induce an immunemediated, target-cell killing by antibody-dependent, cellmediated cytotoxicity [47, 48]. It is hypothesized that, under the selective pressure of continuous antibody exposure, breast cancer cells may be able to bypass the antiproliferative action of trastuzumab but leave a chemotherapy-sensitizing mechanism intact [46]. The reintroduction or continuation of trastuzumab *via* T-DM1 may be very effective in patients with metastatic breast cancer who are heavily pretreated.

The delivery of the active cytotoxic agent, maytansine, through the drug delivery system of trastuzumab is significant. The linker chemistry is of upmost importance with regards to efficacy and tolerability. The thio-ether linked T-DM1 increases serum stability relative to a disulfide linker version (37) and appears to undergo endosomal degradation (17), resulting in intracellular release of the cytotoxic agent (17), thereby improving efficacy and tolerability.

T-DM1 is also well tolerated. Grade 3 and 4 thrombocytopenia and elevated transaminases were reported to be reversible [45]. Notably, there were no Grade 3 or 4 cardiac dysfunction reported, and nearly 40% of patients enrolled in the Phase II trial had received a prior anthracycline. Cardiotoxicity remains a major concern withthe use of trastuzumab. The association between impairment of the left cardiac ventricle and trastuzumab was first observed in one of the early prospective trastuzumab trials; cardiotoxicity was seen in 27% of patients treated with trastuzumab and anthracyclines, concurrently, in 13% of patients treated with trastuzumab and paclitaxel, and in 5% of patients treated with trastuzumab alone [8].

In addition, T-DM1's antitumor results are extremely note-worthy in a heavily pretreated patient population. The overall response rates were observed in over 38% of patients. These developments provide us with optimism for the future, but further investigation of T-DM1 will need to focus on the mechanisms of resistance and toxicity, so that T-DM1 can be integrated into treatment schemes safely. The use of T-DM1 with other immuno-conjugates, which could possibly provide non-cross-resistant therapeutic effects without cumulative toxicities, should also be explored [49].

FUTURE DIRECTIONS

In the past few decades we have seen significant progress in the development of immuno-conjugates as anti-cancer agents. Improving the therapeutic index of these drugs is imperative and will probably result from targeting antigens and increasing linker stability, as demonstrated by T-DM1. The progress made in the targeted delivery approach with TDM1 as well as the clinical and pre-clinical results have been very promising. It is plausible that T-DM1 may be a treatment strategy for patients with HER2 overexpressed breast cancer that progress on first line HER2- directed therapy. The Phase III data results for T-DM1 are anxiously awaited.

REFERENCES

[1] Lekaj J, John C. [ilya ilich metchnikov and paul ehrlich: 1908 nobel prize winners for their research on immunity]. Epidemiol Mikrobiol Imunol 2008; 57: 119-24.

[2] Funaro A, Horenstein AL, Santoro P, *et al.* Monoclonal antibodies and therapy of human cancers. Biotechnol Adv 2000; 18: 385-401.

[3] Uhr JW. The 1984 Nobel Prize in medicine. Science 1984; 226: 1025-28.

[4] Kaminski MS, Tuck M, Estes J, *et al.* 131i-tositumomab therapy as initial treatment for follicular lymphoma. N Engl J Med 2005; 352: 441-49.

[5] Jacobs SA, Vidnovic N, Joyce J, *et al.* Full-dose 90y ibritumomab tiuxetan therapy is safe in patients with prior myeloablative chemotherapy. Clin Cancer Res 2005; 11: 7146s-50s.

[6] Piccart-Gebhart MJ, Procter M, Leyland-Jones B, *et al.* Trastuzumab after adjuvant chemotherapy in her2-positive breast cancer. N Engl J Med 2005; 353: 1659-72.

[7] Seidman AD, Fornier MN, Esteva FJ, *et al.* Weekly trastuzumab and paclitaxel therapy for metastatic breast cancer with analysis of efficacy by her2 immunophenotype and gene amplification. J Clin Oncol 2001; 19: 2587-95.

[8] Slamon DJ, Leyland-Jones B, Shak S, *et al.* Use of chemotherapy plus a monoclonal antibody against her2 for metastatic breast cancer that overexpresses her2. N Engl J Med 2001; 344: 783-92.

[9] Romond EH, Perez EA, Bryant J, *et al.* Trastuzumab plus adjuvant chemotherapy for operable her2-positive breast cancer. N Engl J Med 2005; 353: 1673-84.

[10] Higashide E, Asai M, Ootsu K, *et al.* Ansamitocin, a group of novel maytansinoid antibiotics with antitumour properties from nocardia. Nature 1977; 270: 721-22.

[11] Cassady JM, Chan KK, Floss HG, *et al.* Recent developments in the maytansinoid antitumor agents. Chem Pharm Bull (Tokyo) 2004; 52: 1-26.

[12] Yu TW, Bai L, Clade D, *et al.* The biosynthetic gene cluster of the maytansinoid antitumor agent ansamitocin from actinosynnema pretiosum. Proc Natl Acad Sci U S A 2002; 99: 7968-73.

[13] Tassone P, Goldmacher VS, Neri P, *et al.* Cytotoxic activity of the maytansinoid immunoconjugate b-b4-dm1 against cd138+ multiple myeloma cells. Blood 2004; 104: 3688-96.

[14] Wang L, Amphlett G, Blattler WA, *et al.* Structural characterization of the maytansinoid-monoclonal antibody immunoconjugate, hun901-dm1, by mass spectrometry. Protein Sci 2005; 14: 2436-2446.

[15] Blattler WA, Chari RVJ, Vite GD, Altmann KH, Eds. Anticancer Agents – Frontiers in Cancer Chemotherapy. American Chemical Society, Washington 2001; 317-38.

[16] Schechter AL, Stern DF, Vaidyanathan L, *et al.* An erb-b-related gene encoding a 185,000-mr tumour antigen. Nature 1984; 312: 513-16.

[17] Hudis CA. Trastuzumab--mechanism of action and use in clinical practice. N Engl J Med 2007; 357: 39-51.

[18] Pegram MD, Pauletti G, Slamon DJ. Her-2/neu as a predictive marker of response to breast cancer therapy. Breast Cancer Res Treat 1998; 52: 65-77.

[19] Slamon DJ, Clark GM, Wong SG, *et al.* Human breast cancer: Correlation of relapse and survival with amplification of the her-2/neu oncogene. Science 1987; 235: 177-82.

[20] Tokunaga E, Oki E, Nishida K, *et al.* Trastuzumab and breast cancer: Developments and current status. Int J Clin Oncol 2006; 11: 199-08.

[21] Nahta R, Esteva FJ. Her2 therapy: Molecular mechanisms of trastuzumab resistance. Breast Cancer Res 2006; 8: 215.

[22] Baselga J, Albanell J, Molina MA, *et al.* Mechanism of action of trastuzumab and scientific update. Semin Oncol 2001; 28: 4-11.

[23] Arnould L, Gelly M, Penault-Llorca F, *et al.* Trastuzumab-based treatment of her2-positive breast cancer: An antibody-dependent cellular cytotoxicity mechanism? Br J Cancer 2006; 94: 259-67.

[24] Izumi Y, Xu L, di Tomaso E, *et al.* Tumour biology: Herceptin acts as an anti-angiogenic cocktail. Nature 2002; 416: 279-80.

[25] Wen XF, Yang G, Mao W, *et al.* Her2 signaling modulates the equilibrium between pro- and antiangiogenic factors *via* distinct pathways: Implications for her2-targeted antibody therapy. Oncogene 2006; 25: 6986-96.

[26] Cobleigh MA, Vogel CL, Tripathy D, *et al.* Multinational study of the efficacy and safety of humanized anti-her2 monoclonal antibody in women who have her2-overexpressing metastatic breast cancer that has progressed after chemotherapy for metastatic disease. J Clin Oncol 1999; 17: 2639-48.

[27] Vogel CL, Cobleigh MA, Tripathy D, *et al.* Efficacy and safety of trastuzumab as a single agent in first-line treatment of her2-overexpressing metastatic breast cancer. J Clin Oncol 2002; 20: 719-26.

[28] Carter P, Smith L, Ryan M. Identification and validation of cell surface antigens for antibody targeting in oncology. Endocr Relat Cancer 2004; 11: 659-87.

[29] Baselga J, Norton L, Albanell J, *et al.* Recombinant humanized anti-her2 antibody (herceptin) enhances the antitumor activity of paclitaxel and doxorubicin against her2/neu overexpressing human breast cancer xenografts. Cancer Res 1998; 58: 2825-31.

[30] Pegram M, Hsu S, Lewis G, *et al.* Inhibitory effects of combinations of her-2/neu antibody and chemotherapeutic agents used for treatment of human breast cancers. Oncogene 1999; 18: 2241-51.

[31] Carter PJ, Senter PD. Antibody-drug conjugates for cancer therapy. Cancer J 2008; 14: 154-69.

[32] Lambert JM. Drug-conjugated monoclonal antibodies for the treatment of cancer. Curr Opin Pharmacol 2005; 5: 543-49.
[33] Damle NK. Antibody-drug conjugates ace the tolerability test. Nat Biotechnol 2008; 26: 884-5.
[34] Hamblett KJ, Senter PD, Chace DF, *et al.* Effects of drug loading on the antitumor activity of a monoclonal antibody drug conjugate. Clin Cancer Res 2004; 10: 7063-70.
[35] Smith SV. Technology evaluation, Hun901-dm1, immunogen. Curr Opin Mol Ther 2005; 7: 394-401.
[36] Kratz F, Abu Ajaj K, Warnecke A. Anticancer carrier-linked prodrugs in clinical trials. Expert Opin Investig Drugs 2007; 16: 1037-58.
[37] Lewis Phillips GD, Li G, Dugger DL, *et al.* Targeting her2-positive breast cancer with trastuzumab-dm1, an antibody-cytotoxic drug conjugate. Cancer Res 2008; 68: 9280-90.
[38] Erickson HK, Park PU, Widdison WL, *et al.* Antibody-Maytansinoid Conjugates Are Activated in Targeted Cancer Cells by Lysosomal Degradation and Linker-Dependent Intracellular Processing. Cancer Res 2006; 66: 4426-33.

Received: March 10, 2009 Revised: July 28, 2009 Accepted: September 2, 2009

© Barginear and Budman; Licensee *Bentham Open.*

This is an open access article licensed under the terms of the Creative Commons Attribution Non-Commercial License (http://creativecommons.org/licenses/by-nc/3.0/) which permits unrestricted, non-commercial use, distribution and reproduction in any medium, provided the work is properly cited.

Cancer Letters 306 (2011) 171–179

Contents lists available at ScienceDirect

Cancer Letters

journal homepage: www.elsevier.com/locate/canlet

Trastuzumab-DM1 is highly effective in preclinical models of HER2-positive gastric cancer ☆

Mark Barok [a], Minna Tanner [b], Katri Köninki [a], Jorma Isola [a,*]

[a] Institute of Medical Technology, University of Tampere, Tampere, Finland
[b] Tampere University Hospital, Department of Oncology, Finland

ARTICLE INFO

Article history:
Received 17 January 2011
Received in revised form 3 March 2011
Accepted 3 March 2011

Keywords:
Herceptin
T-DM1
Maytansine
Antibody–drug conjugate
Trastuzumab resistance

ABSTRACT

Background: A novel antibody–drug conjugate (trastuzumab-DM1, T-DM1) is currently in clinical trials for patients with trastuzumab resistant HER2-positive breast cancer. Since no clinical data is available from gastric cancer, we studied T-DM1 on HER2-positive human gastric cancer cells and xenograft tumors.

Methods: Effects of T-DM1 were studied in four HER2-positive gastric cancer cell lines (N-87, OE-19, SNU-216 and MKN-7) *in vitro*. Xenograft tumors from N-87 and OE-19 were studied to determine the effect of T-DM1 *in vivo*.

Results: T-DM1 was found more effective than trastuzumab in N-87 and OE-19, and moderately effective in MKN-7 cells. On SNU-216 cells both trastuzumab and T-DM1 showed limited efficacy. In xenograft tumor experiments, complete pathological response was observed in all OE-19 xenografted mice and in half of the N-87 xenografted mice. The results were equally good irrespective of the tumor burden at therapy initiation, or preceding trastuzumab treatment. T-DM1 treatment showed direct effects (apoptotic cell death and aberrant mitosis) as well as it mediated antibody-dependent cellular cytotoxcity (ADCC).

Conclusions: T-DM1 showed a promising anti-tumor effect in HER2-positive gastric cancer cell lines *in vitro* and *in vivo*, even in tumors which had developed resistance to trastuzumab. T-DM1 therapy may warrant clinical trials for HER2-positive gastric cancer patients.

© 2011 Elsevier Ireland Ltd. All rights reserved.

1. Introduction

Gastric cancer is one of the most frequent human malignancies and the second leading cause of cancer-related death in the world [1]. Because the early disease is often asymptomatic, many gastric cancer patients are diagnosed when their cancer is already beyond curative surgery [2,3]. Treatment options for these patients include radiotherapy and chemotherapy, but cancer progression is common and the 5-year survival rate is less than 30% [2,3]. Therefore, a high unmet medical need exists to develop new highly potent therapies.

One possible target is HER2 (ErbB2) oncoprotein, a member of the epidermal growth factor receptor (EGFR) family of receptor tyrosine kinases. Its overexpression occurs in ~20% of gastric cancers and is associated with poor clinical outcome [4,5]. Trastuzumab, a recombinant humanized monoclonal antibody against the extracellular domain of HER2, has shown significant antitumor effect in both *in vitro* and *in vivo* models of HER2-positive gastric cancer [4–8]. Very recently, a randomized phase III clinical trial (ToGA trial) showed that trastuzumab is highly effective in untreated

Abbreviations: ADCC, antibody-dependent cellular cytotoxicity; BAC, bacterial artificial chromosome; BSA, bovine serum albumin; GAHIG, goat anti-human immunoglobulin; FISH, fluorescence in situ hybridization; H&E, hematoxylin and eosin; i.p., intraperitoneally; i.v., intravenously; LDH, lactate dehydrogenase; SCID, severe combined immunodeficiency.

☆ Author contributions: B.M., M.T. and J.I. conceived and designed the experiments; B.M. and K.K. performed the experiments; B.M. and J.I. analyzed data; and B.M. and J.I. wrote the paper.

* Corresponding author. Tel.: +358 50 300 5609; fax: +358 3 3551 8923.
E-mail address: jorma.isola@uta.fi (J. Isola).

0304-3835/$ - see front matter © 2011 Elsevier Ireland Ltd. All rights reserved.
doi:10.1016/j.canlet.2011.03.002

advanced HER2-positive gastric cancer patients and significantly improved overall survival when given in combination with standard chemotherapy [9]. These data show that trastuzumab is a valuable drug for the treatment of the HER2-positive subset of gastric cancers. Unfortunately, a sizable fraction of HER2-positive patients in the ToGA trial did progress on treatment [9,10]. This denotes that developing trastuzumab resistance might be a problem also in gastric cancer, similar to the situation in breast cancer [11]. For this reason, several research strategies have focused on alternative HER2 directed treatments.

A new strategy of anti-HER2 targeted therapy has been achieved using the antibody–drug conjugate technology. The monoclonal antibody trastuzumab has been conjugated with cytotoxic molecule DM1 (derivative of maytansine 1). The resulting conjugate, named trastuzumab-DM1 (T-DM1) is designed to deliver the highly potent DM1 into the HER2 overexpressing cells via receptor-mediated endocytosis [12]. Active lysine-mcc-DM1 is released by lysosomal degradation [13]. Free intracellular DM1 is a potent inhibitor of microtubule assembly thereby causing cell death [14,15]. T-DM1 is effective both *in vitro* and *in vivo* models of trastuzumab-insensitive breast cancer [12], furthermore, it showed remarkable activity in phase I and II studies in which it was given to patients with trastuzumab-insensitive HER2-positive breast cancer [16–18].

Because trastuzumab is effective in HER2-positive gastric cancer, and T-DM1 shows promising efficacy in trastuzumab insensitive breast cancer, we wanted to test the efficacy and mechanisms of T-DM1 on gastric cancer cell models. In this paper we report that T-DM1 displayed strong anti-tumor effect in OE-19 and N-87 gastric cancer *in vitro* and in xenograft tumors *in vivo*. Furthermore, T-DM1 was highly effective even on large tumors which progressed on prior trastuzumab. This is the first study which shows the efficacy of T-DM1 on gastric cancer cells *in vivo*.

2. Materials and methods

2.1. Cells

OE-19 human gastric cancer cell line was obtained from the European Collection of Cell Culture (CAMR Centre for Applied Microbiology and Research, Wiltshire, United Kingdom). MKN-7 and N-87 human gastric cancer cell lines were obtained from American Type Culture Collection (ATCC, Manassas, VA). SNU-216 human gastric cancer cell line was obtained from the Korean Cell Line Bank (Seoul, Korea). Human breast cancer cell lines MCF-7 and SKBR-3 (ATCC) were used as a control. The cell lines were cultured according to recommended specifications.

2.2. Antibodies

Trastuzumab (Herceptin®) and rituximab (Mabthera®) were purchased from Roche Ltd. (Basel, Switzerland). Trastuzumab-DM1 (T-DM1) was provided by Genentech Inc. (South San Francisco, CA) through a Materials Transfer Agreement. FITC-conjugated goat anti-human immunoglobulin (GAHIG) was obtained from Jackson ImmunoResearch Europe Ltd. (Newmarket, Suffolk, UK). Rabbit monoclonal antibodies against human HER2 (clone SP3) and human Ki-67 (clone SP6) were obtained from NeoMarkers/Lab Vision (Fremont, CA). Mouse M30 CytoDeath antibody was obtained from Roche Ltd.

2.3. Flow cytometry

For flow cytometric measurements trypsinized cells were centrifuged and resuspended in 50 μl PBS (pH 7.4) supplemented with 1% BSA and labeled with a saturating concentration (40 μg/ml) of unlabeled trastuzumab or T-DM1 for 30 min (at 4 °C). After labeling, the cells were washed twice with PBS then labeled with FITC-GAHIG (30 min at 4 °C). The cells were then washed twice with PBS and fixed in 1% formaldehyde. The fluorescence intensity of FITC was determined using a Coulter1 EPICS XL-MCL flow cytometer (Beckman Coulter, Inc., Fullerton, CA) or Accuri C6 Flow Cytometer (Accuri Cytometers, Inc., Ann Arbor, MI).

2.4. Fluorescence in situ hybridization (FISH)

HER2 gene copy numbers were determined by using the dual-color fluorescence in situ hybridization (FISH). After trypsinization and washing with PBS, the cells were fixed with methanol–acetic acid (3:1) and air-dried on slides. A bacterial artificial chromosome (BAC) clone specific to HER2 DNA was labeled with dUTP-FITC (Fermentas, Burlington, Canada) and the chromosome 17 centromere probe (p17H8) was labeled with chromatide Alexa Fluor 594-5-dUTP (Invitrogen, Carlsbad, CA) using nick-translation and FISH was performed as described previously [19].

2.5. In vitro assay of drug sensitivity

The effects of trastuzumab and T-DM1 on the cell growth were examined by the AlamarBlue method (Invitrogen, Carlsbad, CA). The cells were trypsinized and plated in 96-well, flat-bottomed, tissue culture plates. The effects of trastuzumab and T-DM1 were tested at a concentration of 0.001, 0.01, 0.1, 1 and 10 μg/ml. MCF-7 breast cancer cell line with low trastuzumab binding capacity was used as a negative control. The number of viable cells was tested at 72 h after drug exposure by adding the AlamarBlue reagent. Fluorescence was measured with excitation at 544 nm and emission at 590 nm using a Wallac Victor2 plate reader (Perkin–Elmer, Turku, Finland). Fluorescence values of samples were normalized with values of the cell culture media without cells. The results presented as the proportion of viable cells were calculated by dividing the fluorescence values of drug treated samples by the fluorescence values of untreated control samples.

2.6. Measurement of antibody-dependent cellular cytotoxicity (ADCC)

ADCC was analysed by measuring the lactate dehydrogenase (LDH) released from the cancer cells as a result of ADCC activity of peripheral blood mononuclear cells (PBMC). PBMCs were separated from the heparinized blood of a single healthy donor by Ficoll density gradient centrifugation (Histopaque-1077, Sigma–Aldrich, St Louis, MO).

Cancer cells (target; 5000–10,000 per well) and PBMCs (effector) were co-incubated at 1:40 target:effector ratio in 100 μL DMEM containing 5% FCS in a 96-well U-bottomed plate in quadruplicate for 6 h at 37 °C with trastuzumab, T-DM1 or negative control antibody, rituximab. ADCC was measured in a 6-h LDH release assay (CytoTox Non-Radioactive Cytotoxicity Assay, Promega Corporation, Madison, WI). The absorbance at 490 nm was recorded by using a microplate reader (Model 680XR, Bio-Rad, Hercules, CA). The negative control sample (target spontaneous) was prepared identically, contained trastuzumab or T-DM1 or rituximab, but did not contain PBMCs; effector spontaneous sample contained no target cells. Tumor cells killed by freezing at −80 °C for 1 h then warming up to 37 °C served as positive control (target maximum). The percentage of cells killed was calculated according the following formula: (experimental − effector spontaneous − target spontaneous)/(target maximum − target spontaneous) × 100.

2.7. In vivo assay of drug sensitivity

5- to 8-week-old female SCID mice (Harlan Netherlands, Horst, Netherlands) were given a single subcutaneous injection of 5×10^6 N-87 or OE-19 cells suspended in 100 μl cell culture medium. Rituximab (5 μg/g) and trastuzumab (5 μg/g) were given intraperitoneally (i.p.) once per week. This dosing has been shown to saturate HER-2 receptor on breast cancer xenografts [26]. T-DM1 (5 or 15 μg/g) was administered intravenously (i.v.) once per week, as shown effective by Lewis Phillips et al. [12]. No signs of general toxicity were seen in T-DM1 treated animals. No animals died during the experiment or had to be sacrificed prematurely because of signs of systemic illness. Tumor growth was measured with a caliper and tumor volume was calculated using the formula $T_{vol} = \pi/6 \times$ larger diameter $\times$ (smaller diameter)^2 [20]. Animals were euthanized by CO_2 inhalation. The experiments were done with the approval by the National Animal Experiment Board.

2.8. Immunohistochemistry

Animals were euthanized by CO_2 inhalation. Samples of xenograft tumors were fixed in 4% buffered formaldehyde for 24 h, processed into paraffin, then sectioned at 5 μm. Sections were deparaffinized and stained with hematoxylin and eosin (H&E). For immunohistochemistry, tissue sections were deparaffinised followed by antigen-retrieval in Tris–EDTA buffer (0.01 M pH 9.0) at high temperature (water bath, 30 min at 98 °C). After blocking for non-specific binding, primary antibodies (see above) were applied at optimized concentrations and incubated (30 min at room temperature). Standard peroxidase-polymer kit (PowerVision + poly-HRP IHC Detection Systems, Leica Biosystems, UK) was used for visualization, with diaminobenzidine as

Table 1
HER-2 gene copy number and trastuzumab binding capacity of human gastric cancer cell lines.

Cell line	HER-2 gene copy number per cell[a]	Trastuzumab binding capacity (%, relative to SKBR-3)[b]
N-87	19	87
OE-19	23	76
MKN-7	13	26
SNU-216	17	26
MCF-7[c]	2	5
SKBR-3[d]	30	100

[a] Determined by FISH.
[b] Determined by flow cytometer.
[c] Breast cancer cells were used as negative control.
[d] Breast cancer cells were used as positive control.

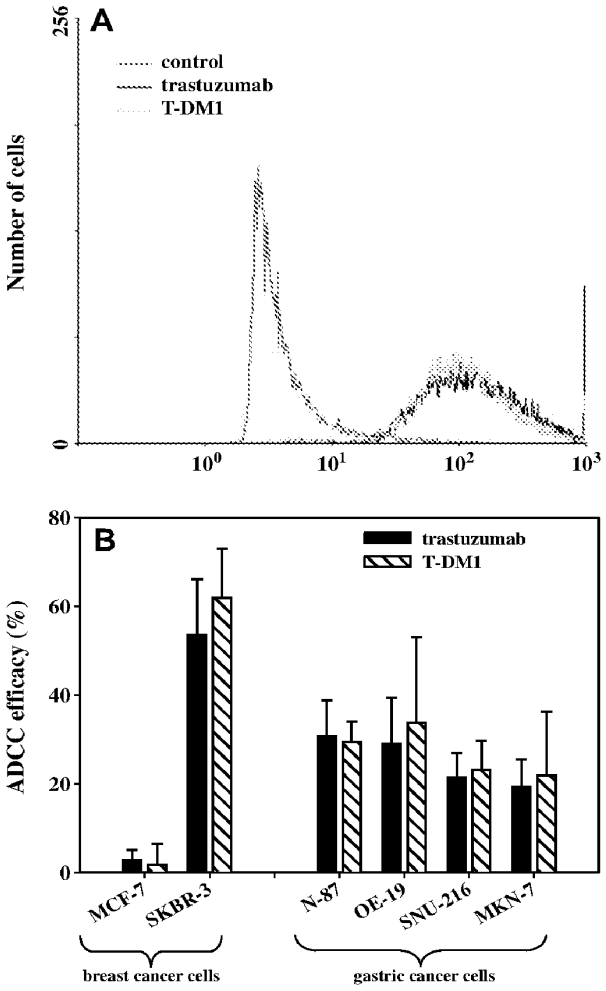


Fig. 1. (A) Binding of trastuzumab and T-DM1 to HER2-positive gastric cancer cells. Trypsinised OE-19 gastric cancer cells were incubated with control antibody (rituximab; *red*), trastuzumab (*black*) or T-DM1 (*green*), followed by goat anti-human FITC. Fluorescence intensities were determined by flow cytometry. Trastuzumab and T-DM1 bound to the OE19 cells in a similar manner. (B) Trastuzumab and T-DM1 mediate ADCC on HER2-positive gastric cancer cells *in vitro*. Target tumor cells (N-87, OE-19, SNU-216, MKN-7) were mixed with peripheral blood mononuclear effector cells (PBMCs) freshly isolated from peripheral blood at effector/target ratio 40:1. ADCC was analyzed by measuring the lactate dehydrogenase (LDH) released from the cancer cells as a result of ADCC activity of PBMCs in the presence of trastuzumab, T-DM1 or control antibody (rituximab). Trastuzumab (*black column*) and T-DM1 (*hatched column*) evoked similar tumor cell killing on the HER2-positive gastric cancer cell lines. Breast cancer cell lines SKBR-3 and MCF-7 were used as a positive and negative controls, respectively.

the chromogen (Vector Labs). Slide scanning was done using Aperio ScanScope XT at superresolution (40×). Cells with normal and aberrant mitotic shape were defined morphologically as describer earlier [21]. Cells with normal and aberrant mitotic shape were counted in hematoxylin and eosin stained histological sections. Apoptotic cells were counted as positive cells using CytoDeath antibody immunohistochemistry [22]. Cells with normal and aberrant mitotic shape and apoptotic cells were counted on a minimum of 10 randomly selected ×40 high-power fields containing representative sections of tumor. Data are presented as the average of positive cells ± SD/field.

2.9. Statistical analysis

Data are expressed as the mean ± SE. The statistical significance of the differences between means were determined using Student's *t* test for two samples after verifying that data passed the normality test and the groups compared have equal variance. Unpaired groups were compared with the Mann-Whitney *U* test. Differences were statistically significant at $P < 0.05$.

3. Results

3.1. HER2 oncogene amplification and protein expression levels of human gastric cancer cell lines

Using FISH analysis we confirmed that the HER2 oncogene is amplified in all gastric cancer cell lines studied. By flow cytometric analysis we showed that HER2 protein is highly overexpressed in N-87 and OE-19, comparable to that of breast cancer cell line SKBR-3. HER2 protein in MKN-7 and SNU-216 cells was also overexpressed, being about one third of that in N-87 and OE-19 (Table 1). Conjugation of trastuzumab with DM1 did not influence of binding to the OE19 gastric cancer cells (Fig. 1A).

3.2. Trastuzumab- and T-DM1-mediated ADCC against HER2-positive gastric cancer cells

Because antibody-dependent cellular cytotoxicity (ADCC) has a key role in the *in vivo* effect of trastuzumab [23,24], we compared trastuzumab and T-DM1 in an ADCC assay. Trastuzumab and T-DM1 evoked ADCC similarly on all four gastric cancer cell lines. Therefore, conjugation of trastuzumab with DM1 seemed not to alter the ability of trastuzumab to mediate ADCC (Fig. 1B).

3.3. In vitro sensitivity of HER2-positive gastric cancer cells to trastuzumab and T-DM1

Next we compared the effects of trastuzumab and T-DM1 on four HER2-positive gastric cancer cell lines *in vitro*. After 72 h incubation, a concentration of 1 μg/ml trastuzumab inhibited the growth of the cell lines described as trastuzumab sensitive previously (OE-19, 86 ± 5%; N-87, 82 ± 1%; SNU-216, 91 ± 1%), while the growth of trastuzumab resistant cells was not inhibited in MKN-7 (105 ± 6%). T-DM1 inhibited the growth of N-87 and OE-19 cells in a dose-dependent manner. The growth inhibition was significantly stronger compared to trastuzumab in the concentration range of 0.01–1 μg/ml ($P < 0.05$). Growth inhibition by T-DM1 on trastuzumab resistant MKN-7 cells was also significant at a relatively high concentration (1 μg/ml ($P < 0.05$)). In contrast, T-DM1 had no superior inhibitory effect on SNU-216 cells compared to trastuzumab. Concentration of 10 μg/ml of T-DM1 inhibited also the growth of the HER2-negative control cell line (MCF-7), suggesting a non-specific toxic effect (Fig. 2).

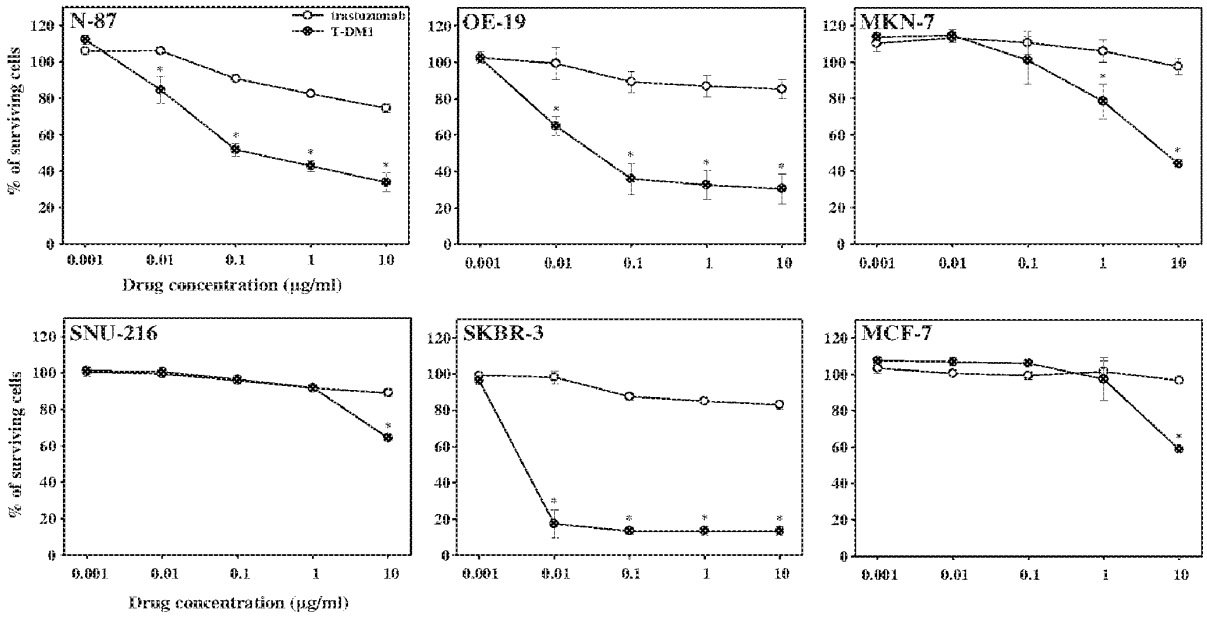


Fig. 2. Growth inhibitory effects of trastuzumab and T-DM1 on HER2-positive gastric cells *in vitro*. The effects of trastuzumab (*white circle*) and T-DM1 (*black circle*) was tested at a concentrations 0.001, 0.01, 0.1, 1 μg/ml and 10 μg/ml on OE-19, N-87, MKN-7 and SNU-216 gastric cancer cells *in vitro*. The results are presented as the proportion of viable cells (AlamarBlue assay). T-DM1 inhibited the growth of OE-19 and N87 gastric cancer cells in a dose-dependent manner. The effect of T-DM1 was stronger than that of trastuzumab in the concentration range of 0.01–1 μg/ml (*$P < 0.05$). Growth inhibition by T-DM1 on MKN-7 cells was also significant at a concentration of 1 μg/ml (*$P < 0.05$). No difference was detected between the inhibition by trastuzumab and T-DM1 on SNU-216 cells. HER2-positive SKBR-3 breast cancer cells and HER2-negative MCF-7 breast cancer cells were used as a positive and negative control, respectively. A high concentration of T-DM1 (10 ug/ml) inhibited also the growth of MCF-7 cells, indicating a non-specifically toxic effect.

3.4. Effect of T-DM1 on N-87 and OE-19 xenografts

Of the four cell lines, N-87 and OE-19 were capable of forming subcutaneous xenograft tumors in SCID mice. Tumors were formed in all mice inoculated with N-87 cell suspension in 7 days ($n = 18$, mean tumor volume 24 ± 3 mm^3). Thereafter, three weekly treatments with trastuzumab ($n = 6$) or T-DM1 ($n = 6$) were administered on days 14, 21 and 28. Rituximab ($n = 6$) was used as negative control agent. A rapid tumor shrinkage was seen by T-DM1 from day 19. From day 37 onwards, none of T-DM1 treated tumors were measurable. Histologically, a pathological complete response was seen in three mice (3/6), and residual tumor cells in the other three (3/6) at the end of the experiment (day 55). Overall, the

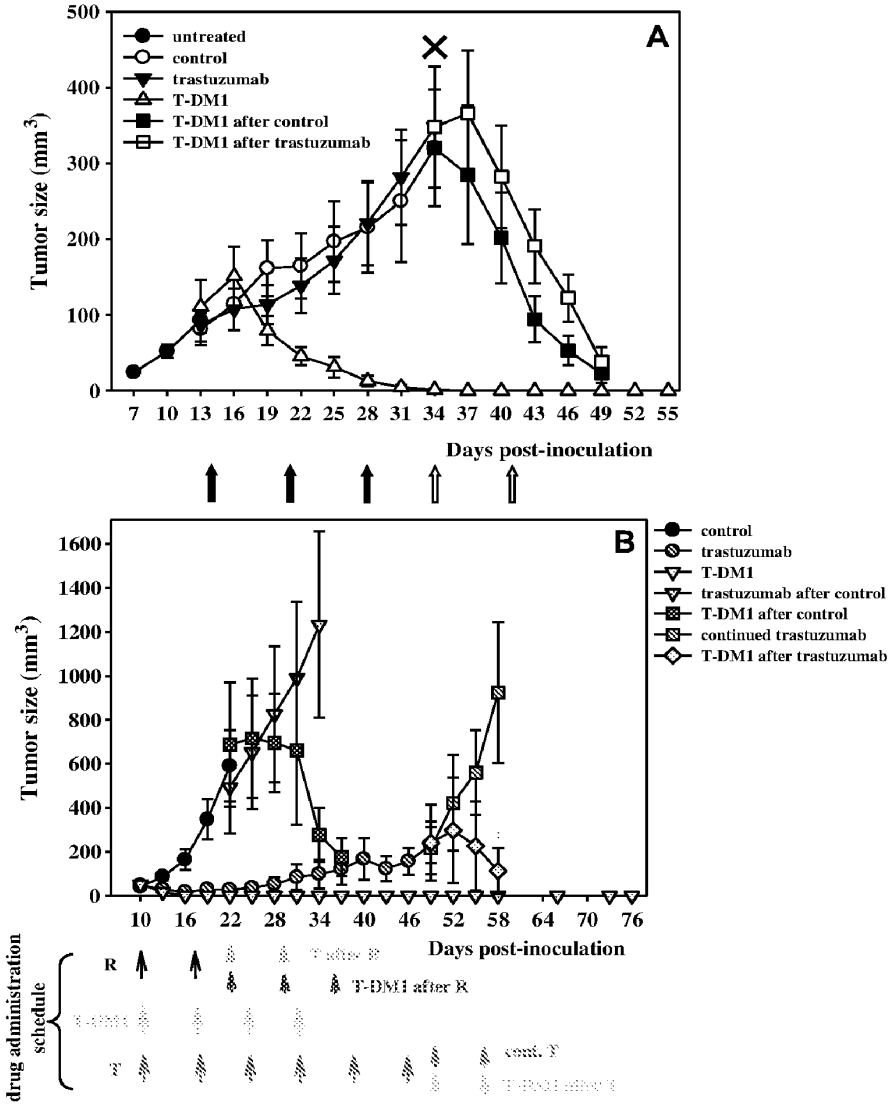


Fig. 3. (A) Effect of T-DM1 on the growth of N-87 xenografts. SCID mice with N-87 xenografts were treated on a weekly basis with control antibody (rituximab, 5 μg/g, i.p., *white circles*, $n = 6$), trastuzumab (5 μg/g, i.p., *black triangles*, $n = 6$) or T-DM1 (15 μg/g, i.v., *white triangles*, $n = 6$). Drug administration schedule is shown by *black arrows*. Trastuzumab had no effect on tumor growth (*black triangles*). Rapid tumor shrinkage was seen by T-DM1 from day 19 (*white triangles*). From day 37 onwards all T-DM1 treated tumors had shrunken to non-palpable. Histologically, residual cancer cells were found in three out of these mice (3/6), but a complete pathological response was suggested in the other three (3/6). Trastuzumab and control treatment of N-87 xenografts was discontinued on day 29 and switched to T-DM1 (15 μg/g, i.v.; *white arrows*) from the day 34 onwards (marked by ×). In this setting, rapid tumor shrinkage was seen by T-DM1 in both control- and trastuzumab-pretreated mice (*black squares* and *white squares*, respectively). (B). Effect of T-DM1 on the growth of OE-19 xenografts. SCID mice with OE-19 xenografts were treated on a weekly basis with control antibody (rituximab, 5 μg/g, i.p., *black circles*, $n = 6$), trastuzumab (5 μg/g, i.p., *red circles*, $n = 6$) and T-DM1 (5 μg/g, i.v., *green triangles*, $n = 7$). Drug administration schedule is shown by *arrows*. By day 19, all T-DM1 treated tumors (*green triangles*) shrank to non-palpable and remained non-palpable and histologically carcinoma-free at the end of the experiment (day 76). Trastuzumab treatment was discontinued and switched to T-DM1 in three mice (5 μg/g, i.v., *cyan squares*) from the day 49 (marked by *black* ×) and continued for another 2 weeks in the other three (5 μg/g, i.p., *pink squares*). In this setting, trastuzumab treated tumors grew further, while tumors were shrunk by T-DM1; significant tumor inhibition was seen by T-DM1 on day 58 (*cyan star*, $P < 0.05$). Control tumors reaching an average size of 590 ± 163 mm^3 (*black circles* were treated with trastuzumab (5 μg/g, i.p., *gray triangles*, $n = 3$) or T-DM1 (5 μg/g, i.p., *blue squares*, $n = 3$) from the day 22 onwards (marked by *red* ×). In this setting, tumors started to shrink by T-DM1, while trastuzumab treated tumors continued to grow.

effect of T-DM1 on tumor growth was much stronger than that of trastuzumab ($P < 0.05$) (Fig. 3A). The experiment was repeated to obtain tumor samples from T-DM1 treated animals. Despite lower drug dosing (5 μg/g vs. 15 μg/g), a similar shrinkage of the tumors was seen (data not shown). This experiment was terminated before complete shrinkage of the tumors.

Tumors were formed in all SCID mice inoculated with OE-19 cells in 10 days ($n = 19$, mean tumor volume 47 ± 6 mm^3). T-DM1 administration was started on day 10, and by day 19 all T-DM1 treated tumors shrank to non-palpable (7/7). Thereafter, the tumors remained non-palpable in all of these mice until the end of the experiment (day 76). No tumor cells were found even in histological examination, indicating a pathological complete response of all T-DM1 treated mice. In this setting, trastuzumab also inhibited the tumor growth in comparison to the negative control, but the effect of T-DM1 on tumor growth was much stronger when compared to trastuzumab ($P < 0.05$) (Fig. 3B). When OE-19 tumors reached 590 ± 163 mm^3 in size in the negative control group, treatment was switched to trastuzumab or T-DM1 from the day 22 onwards. In this setting, these large tumors shrank by T-DM1, while trastuzumab treated tumors continued to grow exponentially (Fig. 3B).

3.5. Effect of T-DM1 on N-87 and OE-19 xenografts pretreated with trastuzumab

Trastuzumab treatment of N-87 xenografts was discontinued when no inhibitory effect was seen compared to control (day 29). The treatment was switched to T-DM1 from the day 34 onwards. Rapid and complete tumor shrinkage was also seen in trastuzumab-pretreated mice (Fig. 3A). T-DM1 was tested also on OE-19 xenografts which received six trastuzumab treatments. For half of these mice trastuzumab was discontinued and switched to T-DM1 from the day 49 onwards. In this setting, tumors were shrunk by T-DM1, while trastuzumab treated tumors grew further (Fig. 3B).

3.6. T-DM1 decreases the number of mitoses and increases the number of cells with aberrant mitosis in gastric cancer xenografts

Histological sections of the N-87 and OE-19 xenograft tumors were prepared and stained with hematoxylin and eosin. Because T-DM1 treatment abolished the OE-19 xenograft tumors, histological examination was done on the large tumors initially treated with trastuzumab. When enumerating the number of mitoses with normal morphology, we found no differences between trastuzumab and T-DM1 treated OE-19 tumors (Figs. 4A and 5A). In contrast, we detected a significantly lower number of mitoses in T-DM1 treated N-87 tumors in comparison to trastuzumab treated ones ($P < 0.05$) (Fig. 4A). Conversely, T-DM1 significantly increased the number of cells with aberrant mitotic morphology in OE-19 tumors when compared to trastuzumab ($P < 0.05$) (Figs. 4B and 5B), while no differences in the number of cells with aberrant mitotic morphology were found in N-87 xenografts (Fig. 4B).

3.7. T-DM1 evokes apoptosis in gastric cancer xenografts

Apoptotic cells were detected using CytoDeath staining, which localizes a caspase-activated breakdown product of cytokeratin subtype 18. In this analysis we found significantly increased number of apoptotic cells in both N-87 and OE-19 tumors treated with T-DM1 in comparison to the trastuzumab treated ones ($P < 0.05$) (Figs. 4C, 5E and F).

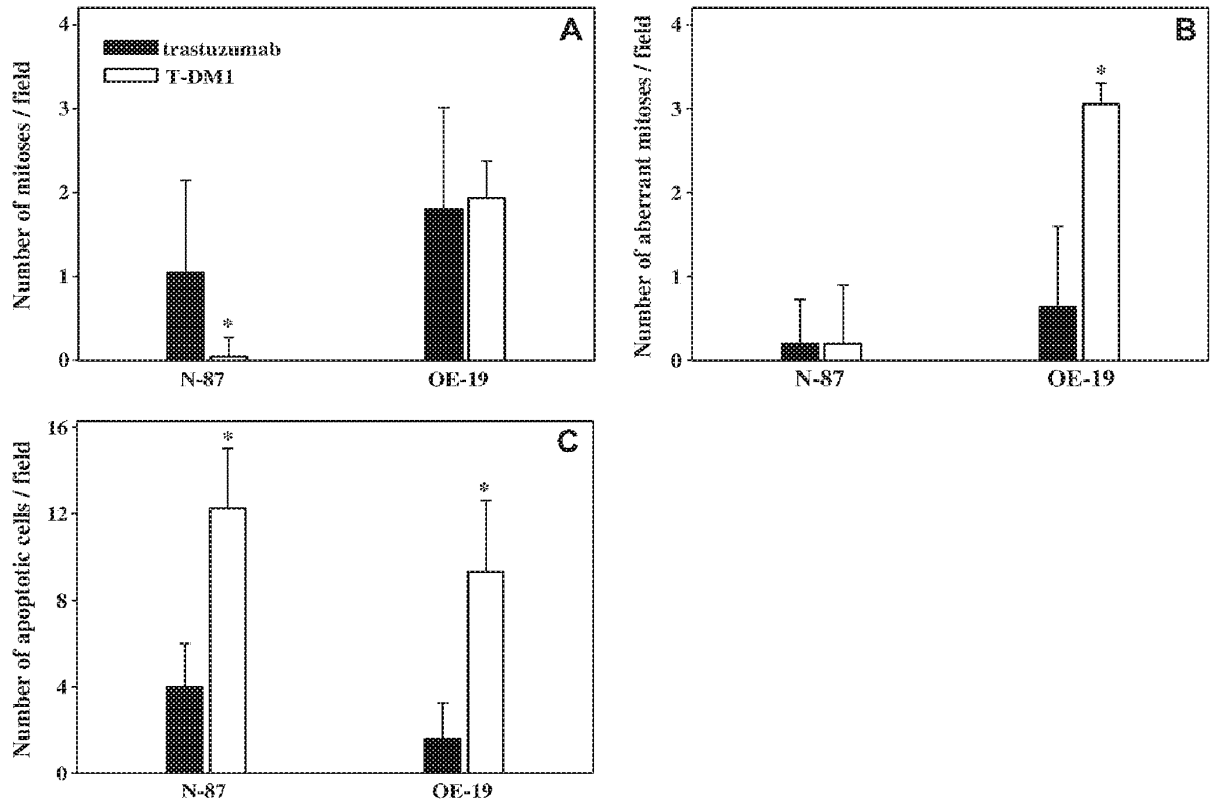


Fig. 4. T-DM1 induced aberrant mitosis and apoptosis in gastric cancer xenografts. For histology, samples from T-DM1 treated N-87 tumors were obtained from the experiment which was terminated before tumor shrinkage. Because complete pathological response of OE-19 xenografts was seen after T-DM1 treatment, samples were taken from animals whose trastuzumab treatment was switched to T-DM1. Samples from trastuzumab and T-DM1 treated tumors were compared (*black* and *hatched columns*, respectively). The number of morphologically normal mitoses was lower T-DM1 treated N-87 tumors (A, $^*P < 0.05$) but did not differ in OE-19 (A). The number of aberrant mitoses was significantly higher in T-DM1 treated OE-19 tumors (compared to trastuzumab treatment) (B, $^*P < 0.05$). No difference was seen in N-87 xenografts (B). The number of apoptotic cells (by CytoDeath staining) was higher in T-DM1 treated N-87 and OE-19 compared to the trastuzumab treated ones (C, $^*P < 0.05$).

3.8. Expression of HER2 protein on trastuzumab and T-DM1 treated xenografts

Immunohistochemical staining localizing extracellular epitopes of the HER2 protein were performed. No major qualitative changes in the cell membrane staining of HER2 expression were observed. Virtually all tumor cells showed strongly positive cell membrane staining reaction. It is noteworthy that trastuzumab treated N-87 and OE-18 tumors were positive for HER2 in spite of their intrinsic or acquired resistance to trastuzumab (Fig. 5C and D).

3.9. Histological evaluation of residual N-87 cancer cells

As we mentioned above, residual tumor cells were found at the inoculation site in three samples (3/6) (Fig. 6A). Immunohistochemical staining of the HER2 protein showed that all residual tumor cells were strongly positive for HER2 (Fig. 6B). The fraction of proliferating cells (by Ki-67 staining) positive cells was small among the residual tumor cells (Fig. 6C).

4. Discussion

Trastuzumab-DM1 (T-DM1) is a new antibody–drug conjugate which has been developed to improve the therapy of HER2-positive breast cancer. So far T-DM1 has not been extensively studied in preclinical models of gastric cancer. In this study, we showed the efficacy of T-DM1 on gastric cancer xenograft tumors.

We applied different treatment strategies when testing T-DM1 in tumor xenografts. A complete pathological response was observed in all of the OE-19 xenografts and in half of the N-87 xenografts when T-DM1 was given to mice carrying small subcutaneous tumors. Surprisingly, the effect was not dependent on tumor burden, since rapid tumor shrinkage was seen also for large established tumors. Most importantly, T-DM1 was highly effective even on large tumors which had become resistant to prior trastuzumab treatment. Both N-87 and OE-19 tumors which had become resistant to trastuzumab started to shrink already 1 week after switching the treatment to T-DM1, despite the fact that trastuzumab and T-DM1 should compete in binding to the same epitope of HER2. These results suggest that N-87 and OE-19 gastric cancer cells must have relatively rapid HER2 protein turnover, which produces enough trastuzumab-free HER2 for T-DM1 binding. In the clinical setting this suggests that lengthy wash-out periods

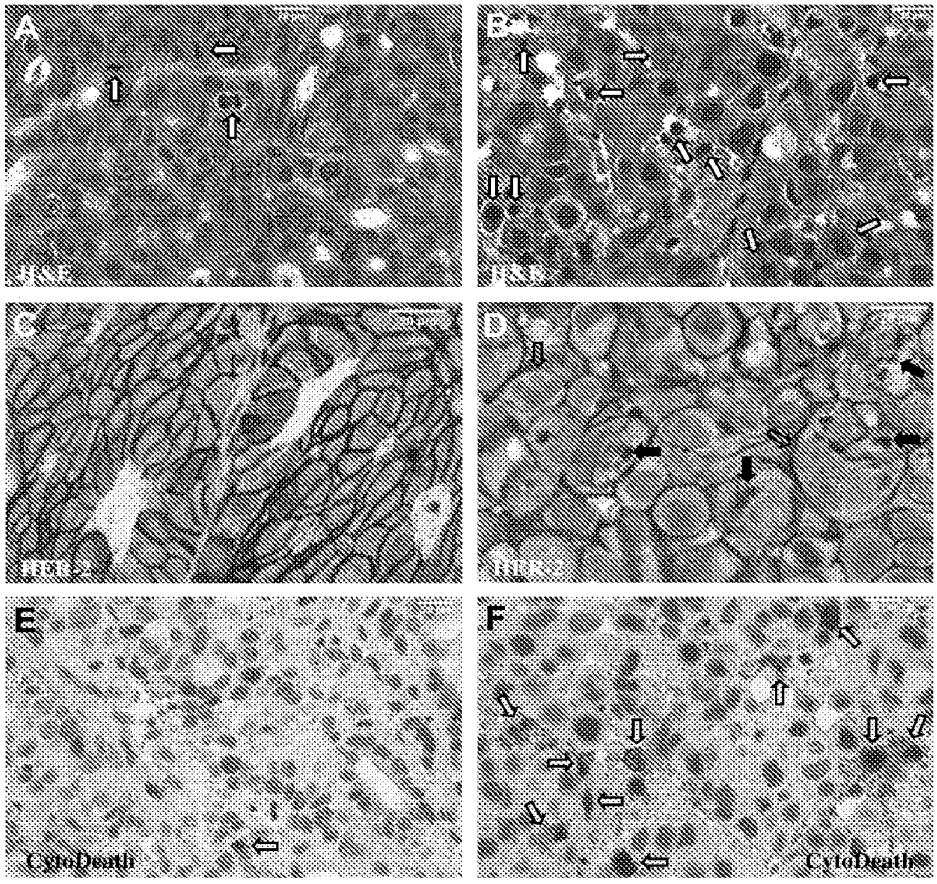


Fig. 5. Histological characterization of T-DM1 induced changes in gastric cancer xenografts. OE-19 xenografts were obtained from mice treated with trastuzumab (A, C, E) or T-DM1 after prior trastuzumab (B, D, F). Histological sections were stained with hematoxylin and eosin (H&E, A and B), immunohistochemically for HER2 protein (C and D) and apoptotic cells (CytoDeath staining) (E and F). Many aberrant mitoses were seen in T-DM1 treated tumors (*blue arrows*, B). Apoptotic cells were evident in the T-DM1 treated tumors with H&E (*white arrows*, A and B) and CytoDeath stainings (*green arrows*, E and F). Mitoses with normal morphology were found both in trastuzumab and T-DM1 treated OE-19 tumors (*yellow arrows*, A). Tumor cells retained their strong (3+) HER2 positivity after long-term trastuzumab (C) or T-DM1 treatment (D). Interestingly, HER2 staining positive intracytoplasmic granules (*black arrows*) were seen in T-DM1 treated tumors (D). Giant multinucleated cells (*red arrows*) were seen in T-DM1 treated samples (D).

when switching from trastuzumab to T-DM1 are not needed.

The main mechanism of T-DM1 is the release of free intracellular DM1 after degradation in the lysosomes. DM1 is a potent inhibitor of microtubule assembly thereby causing cell death [14,15]. In line with this observation, T-DM1 treatment was associated with apoptotic cell death and mitotic catastrophe in breast cancer cells [12] and (Barok et al. submitted for publication). Here we showed that the cellular response to T-DM1 was apoptosis and aberrant mitosis also in gastric tumors.

Very recently, studies in breast cancer have shown direct cytotoxicity is not the only mechanism for T-DM1 action. T-DM1 can evoke antibody-mediated cellular cytotoxicity (ADCC), similar to unconjugated trastuzumab (26). ADCC was evidenced with similar efficacy on HER2-positive gastric cancer cells. Because ADCC has a key role in the efficacy of trastuzumab *in vivo* [23,24], we believe that ADCC might be an important contributor also in the *in vivo* effect of T-DM1 in gastric cancer.

In our experiments the effect of T-DM1 was much stronger in N-87 and OE-19 cells than that of trastuzumab. Of the gastric cancer cells with lower level HER2 overexpression, T-DM1 had a clear inhibitory effect on trastuzumab resistant MKN-7 cells, while trastuzumab and T-DM1 were both relatively ineffective on SNU-216 cells. As all gastric cancer cell lines studied were FISH-positive, this may suggest that responders could be identified by their HER2 protein expression levels. However, this may refer only to direct cytotoxic response, since strength of ADCC was showed no correlation to the HER2 protein expression levels.

Interestingly, residual tumor cells could be identified in half of the mice whose N-87 tumors had macroscopically disappeared. Thus, these cells were able to survive the T-DM1 treatment despite their high HER2 overexpression. These cells showed low proliferation activity (Ki-67) suggesting that they might be in a dormant state. In an immunohistochemical assay these cells did not reveal stem cell-like properties [25], since they were immunohistochemically CD44 negative (data not shown). The presence of residual cancer cells indicates a possibility for a relapse after long latency period. Therefore, combination of T-DM1 with other cytotoxic drugs (such as taxanes) should be considered.

In summary, we found that T-DM1 is strongly effective on HER-2 positive gastric cancer cells both *in vitro* and *in vivo*. T-DM1 also inhibited the large tumors which had become trastuzumab resistant. To our knowledge, this is the first published demonstration of efficacy of T-DM1 in gastric cancer xenografts, and gives the theoretical background for testing this drug clinically in gastric carcinoma patients whose treatment with trastuzumab has failed.

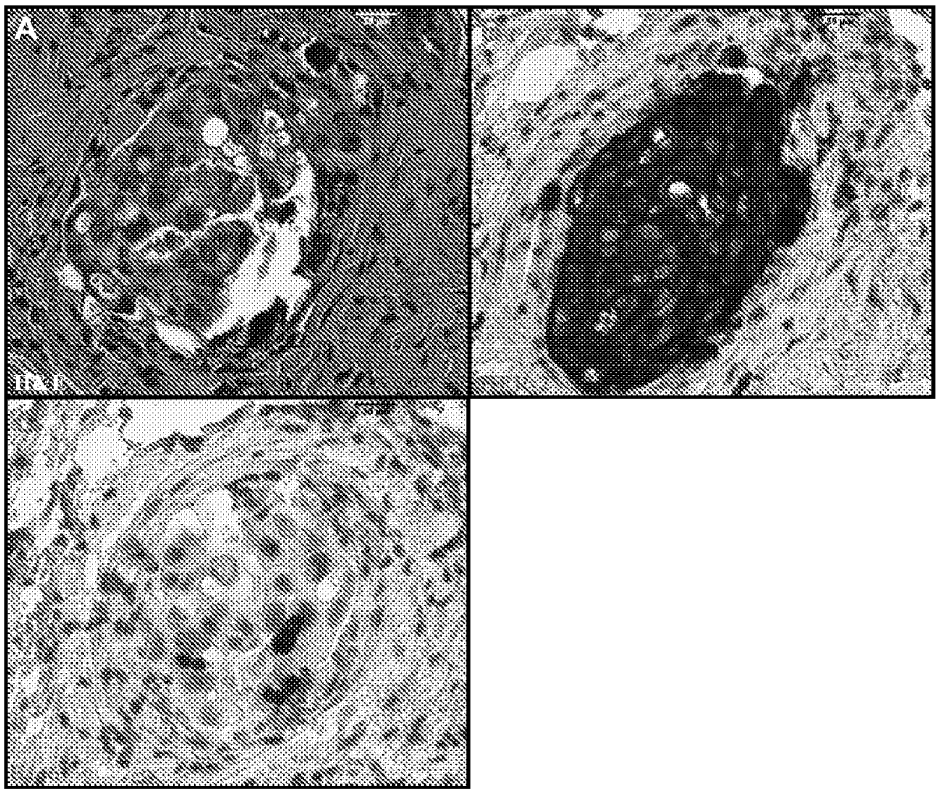


Fig. 6. Residual cancer cells in T-DM1 treated N-87 xenografts. Residual cancer cell aggregates were found from the skin samples in three of six N-87 xenografted mice after T-DM1 treatment (G). These cells were strongly HER2-positive (I), but displayed only few Ki-67 positive cells suggesting tumor dormancy (H).

Conflict of interest

The authors disclose no financial conflicts of interest that could influence the present work.

Role of the funding source

This study was financially supported by the Tampere University Hospital Research Foundation, Academy of Finland, Sigrid Juselius Foundation and Finnish Cancer Foundation. The sponsors had no influence on the study design, in the collection, analysis and interpretation of data; in the writing of the manuscript; and in the decision to submit the manuscript for publication.

Acknowledgements

The skillful technical assistance of Ms. Kristiina Ryömä, Mrs. Sari Toivola and Ms. Barbara Német is greatly appreciated. We thank Genentech Inc. for providing T-DM1.

References

[1] D.M. Parkin, F. Bray, J. Ferlay, P. Pisani, Global cancer statistics, 2002, CA Cancer J. Clin. 55 (2005) 74–108.
[2] R. Wesolowski, C. Lee, R. Kim, Is there a role for second-line chemotherapy in advanced gastric cancer?, Lancet Oncol 10 (2009) 903–912.
[3] F. Rivera, M.E. Vega-Villegas, M.F. Lopez-Brea, Chemotherapy of advanced gastric cancer, Cancer Treat. Rev. 33 (2007) 315–324.
[4] M. Tanner, M. Hollmen, T.T. Junttila, A.I. Kapanen, S. Tommola, Y. Soini, H. Helin, J. Salo, H. Joensuu, E. Sihvo, K. Elenius, J. Isola, Amplification of HER-2 in gastric carcinoma: association with topoisomerase IIalpha gene amplification, intestinal type, poor prognosis and sensitivity to trastuzumab, Ann. Oncol. 16 (2005) 273–278.
[5] C. Gravalos, A. Jimeno, HER2 in gastric cancer: a new prognostic factor and a novel therapeutic target, Ann. Oncol. 19 (2008) 1523–1529.
[6] K. Fujimoto-Ouchi, F. Sekiguchi, H. Yasuno, Y. Moriya, K. Mori, Y. Tanaka, Antitumor activity of trastuzumab in combination with chemotherapy in human gastric cancer xenograft models, Cancer Chemother. Pharmacol. 59 (2007) 795–805.
[7] S.Y. Kim, H.P. Kim, Y.J. Kim, Y. Oh do, S.A. Im, D. Lee, H.S. Jong, T.Y. Kim, Y.J. Bang, Trastuzumab inhibits the growth of human gastric cancer cell lines with HER2 amplification synergistically with cisplatin, Int. J. Oncol. 32 (2008) 89–95.
[8] Y. Matsui, M. Inomata, M. Tojigamori, K. Sonoda, N. Shiraishi, S. Kitano, Suppression of tumor growth in human gastric cancer with HER2 overexpression by an anti-HER2 antibody in a murine model, Int. J. Oncol. 27 (2005) 681–685.
[9] Y.J. Bang, E. Van Cutsem, A. Feyereislova, H.C. Chung, L. Shen, A. Sawaki, F. Lordick, A. Ohtsu, Y. Omuro, T. Satoh, G. Aprile, E. Kulikov, J. Hill, M. Lehle, J. Ruschoff, Y.K. Kang, Trastuzumab in combination with chemotherapy versus chemotherapy alone for treatment of HER2-positive advanced gastric or gastro-oesophageal junction cancer (ToGA): a phase 3, open-label, randomised controlled trial, Lancet.
[10] A.F. Okines, D. Cunningham, Trastuzumab in gastric cancer, Eur. J. Cancer 46, 1949–1959.
[11] R. Nahta, D. Yu, M.C. Hung, G.N. Hortobagyi, F.J. Esteva, Mechanisms of disease: understanding resistance to HER2-targeted therapy in human breast cancer, Nat. Clin. Pract. Oncol. 3 (2006) 269–280.
[12] G.D. Lewis Phillips, G. Li, D.L. Dugger, L.M. Crocker, K.L. Parsons, E. Mai, W.A. Blattler, J.M. Lambert, R.V. Chari, R.J. Lutz, W.L. Wong, F.S. Jacobson, H. Koeppen, R.H. Schwall, S.R. Kenkare-Mitra, S.D. Spencer, M.X. Sliwkowski, Targeting HER2-positive breast cancer with trastuzumab-DM1, an antibody–cytotoxic drug conjugate, Cancer Res. 68 (2008) 9280–9290.
[13] Y.V. Kovtun, V.S. Goldmacher, Cell killing by antibody–drug conjugates, Cancer Lett. 255 (2007) 232–240.
[14] R.V. Chari, Targeted cancer therapy: conferring specificity to cytotoxic drugs, Acc. Chem. Res. 41 (2008) 98–107.
[15] S. Remillard, L.I. Rebhun, G.A. Howie, S.M. Kupchan, Antimitotic activity of the potent tumor inhibitor maytansine, Science 189 (1975) 1002–1005.
[16] I.E. Krop, M. Beeram, S. Modi, S.F. Jones, S.N. Holden, W. Yu, S. Girish, J. Tibbitts, J.H. Yi, M.X. Sliwkowski, F. Jacobson, S.G. Lutzker, H.A. Burris, Phase I study of trastuzumab-DM1, a HER2 antibody–drug conjugate, given every 3 weeks to patients with HER2-positive metastatic breast cancer, J. Clin. Oncol.
[17] C. Vogel, H. Burris, S. Limentani, et al., A phase II study of trastuzumab-DM1 (T-DM1), a HER2 antibody–drug conjugate (ADC), in patients (pts) with HER2+ metastatic breast cancer (MBC): final results, Proc. Am. Soc. Clin. Oncol. 27 (Suppl. 15) (2009) 1017 (Abstr.).
[18] I. Krop, P. LoRusso, K. Miller, S. Modi, D. Yardley, G. Rodriguez, S. Agresta, M. Zheng, L. Amler, H. Rugo, A phase II study of trastuzumab-DM1 (T-DM1), a novel HER2 antibody–drug conjugate, in patients previously treated with lapatinib, trastuzumab, and chemotherapy, in: 32nd Annual San Antonio Breast Cancer Symposium, San Antonio, TX, USA, December 9–13, 2009, Abstr. 5090.
[19] M. Tanner, P. Jarvinen, J. Isola, Amplification of HER-2/neu and topoisomerase IIalpha in primary and metastatic breast cancer, Cancer Res. 61 (2001) 5345–5348.
[20] M. Tanner, A.I. Kapanen, T. Junttila, O. Raheem, S. Grenman, J. Elo, K. Elenius, J. Isola, Characterization of a novel cell line established from a patient with herceptin-resistant breast cancer, Mol. Cancer Ther. 3 (2004) 1585–1592.
[21] B.D. Chang, E.V. Broude, J. Fang, T.V. Kalinichenko, R. Abdryashitov, J.C. Poole, I.B. Roninson, p21Waf1/Cip1/Sdi1-induced growth arrest is associated with depletion of mitosis-control proteins and leads to abnormal mitosis and endoreduplication in recovering cells, Oncogene 19 (2000) 2165–2170.
[22] M.P. Leers, W. Kolgen, V. Bjorklund, T. Bergman, G. Tribbick, B. Persson, P. Bjorklund, F.C. Ramaekers, B. Bjorklund, M. Nap, H. Jornvall, B. Schutte, Immunocytochemical detection and mapping of a cytokeratin 18 neo-epitope exposed during early apoptosis, J. Pathol. 187 (1999) 567–572.
[23] R.A. Clynes, T.L. Towers, L.G. Presta, J.V. Ravetch, Inhibitory Fc receptors modulate in vivo cytoxicity against tumor targets, Nat. Med. 6 (2000) 443–446.
[24] M. Barok, J. Isola, Z. Palyi-Krekk, P. Nagy, I. Juhasz, G. Vereb, P. Kauraniemi, A. Kapanen, M. Tanner, J. Szollosi, Trastuzumab causes antibody-dependent cellular cytotoxicity-mediated growth inhibition of submacroscopic JIMT-1 breast cancer xenografts despite intrinsic drug resistance, Mol. Cancer Ther. 6 (2007) 2065–2072.
[25] S. Takaishi, T. Okumura, S. Tu, S.S. Wang, W. Shibata, R. Vigneshwaran, S.A. Gordon, Y. Shimada, T.C. Wang, Identification of gastric cancer stem cells using the cell surface marker CD44, Stem Cells 27 (2009) 1006–1020.
[26] Z. Pályi-Krekk, M. Barok, J. Isola, M. Tammi, J. Szöllosi, P. Nagy, Hyaluronan-induced masking of ErbB2 and CD44-enhanced trastuzumab internalisation in trastuzumab resistant breast cancer, Eur. J. Cancer 43 (2007) 2423–2433.

Phase II Study of Weekly Intravenous Recombinant Humanized Anti-p185^{HER2} Monoclonal Antibody in Patients With HER2/*neu*-Overexpressing Metastatic Breast Cancer

By José Baselga, Debasish Tripathy, John Mendelsohn, Sharon Baughman, Christopher C. Benz, Lucy Dantis, Nancy T. Sklarin, Andrew D. Seidman, Clifford A. Hudis, Jackie Moore, Paul P. Rosen, Thomas Twaddell, I. Craig Henderson, and Larry Norton

Purpose: **Breast cancer frequently overexpresses the product of the HER2 proto-oncogene, a 185-kd growth factor receptor (p185^{HER2}). The recombinant humanized monoclonal antibody (rhuMAb) HER2 has high affinity for p185^{HER2} and inhibits the growth of breast cancer cells that overexpress HER2. We evaluated the efficacy and toxicity of weekly intravenous administration of rhuMAb HER2 in patients with HER2-overexpressing metastatic breast cancer.**

Patients and Methods: **We treated 46 patients with metastatic breast carcinomas that overexpressed HER2. Patients received a loading dose of 250 mg of intravenous rhuMAb HER2, then 10 weekly doses of 100 mg each. Patients with no disease progression at the completion of this treatment period were offered a maintenance phase of 100 mg/wk.**

Results: **Study patients had extensive metastatic disease, and most had received extensive prior anticancer therapy. Adequate pharmacokinetic levels of rhuMAb HER2 were obtained in 90% of the patients. Toxicity was minimal and no antibodies against rhuMAb HER2 were detected in any patients. Objective responses were seen in five of 43 assessable patients, and included one complete remission and four partial remissions (overall response rate, 11.6%; 95% confidence interval, 4.36 to 25.9). Responses were observed in liver, mediastinum, lymph nodes, and chest wall lesions. Minor responses, seen in two patients, and stable disease, which occurred in 14 patients, lasted for a median of 5.1 months.**

Conclusion: **rhuMAb HER2 is well tolerated and clinically active in patients with HER2-overexpressing metastatic breast cancers that had received extensive prior therapy. This is evidence that targeting growth factor receptors can cause regression of human cancer and justifies further evaluation of this agent.**

J Clin Oncol 14:737-744. © 1996 by American Society of Clinical Oncology.

DURING THE LAST DECADE, proto-oncogenes that encode growth factors and growth factor receptors have been found to play important roles in the pathogenesis of several human malignancies, including breast cancer.[1] The HER2 gene (also known as *neu* and as *c-erbB*-2) encodes a 185-kd transmembrane glycoprotein receptor (p185^{HER2}) that has partial homology with the epidermal growth factor receptor, and that shares with that receptor intrinsic tyrosine kinase activity.[2-4] HER2 is overexpressed in 25% to 30% of human breast cancers[5,6] and predicts for a worse prognosis in patients with primary disease that involves axillary lymph nodes.[5,7,8] Several lines of evidence support a direct role for HER2 in the pathogenesis and clinical aggressiveness of HER2-overexpressing tumors: The introduction of HER2 into nonneoplastic cells causes their malignant transformation.[9,10] Transgenic mice that express HER2 develop mammary tumors.[11] HER2 overexpression is common in ductal carcinomas in situ and in their associated invasive cancers.[12,13] Antibodies directed at p185^{HER2} can inhibit the growth of tumors and of transformed cells that express high levels of this receptor.[14-18]

The latter observation suggests that p185^{HER2} may be a potential target for the treatment of breast cancer or preinvasive breast lesions because these cells commonly overexpress HER2. The murine monoclonal antibody (MAb) 4D5, directed against the extracellular domain of p185^{HER2} (ECD^{HER2}), is a potent inhibitor of growth, in vitro and in xenograft models, of human breast cancer cells that overexpress HER2.[19-21] However, murine antibodies are limited clinically because they are immunogenic. To facilitate further clinical investigations, therefore, MAb 4D5 was humanized. The resulting recombinant humanized anti-p185^{HER2} monoclonal antibody (rhuMAb HER2) was found to be safe and to have dose-dependent pharmacokinetics in two prior phase I clinical trials.

From the Department of Medicine, Services of Breast and Gynecological Cancer Medicine and Clinical Immunology, Department of Pathology, Memorial Sloan-Kettering Cancer Center, New York, NY; Division of Oncology, University of California, San Francisco; and Pharmacokinetics and Metabolism and Clinical Research, Genentech, Inc, South San Francisco, CA.

Submitted August 8, 1995; accepted October 10, 1995.

Supported in part by an American Society of Clinical Oncology Career Development Award (to J.B. and A.D.S.), a SPORE grant (p50-CA58207) from The National Cancer Institute, Bethesda, MD, and Genentech Inc, South San Francisco, CA.

Address reprint requests to José Baselga, MD, Breast and Gynecological Cancer Medicine Service, Memorial Sloan-Kettering Cancer Center, 1275 York Ave, New York, NY 10021-6007.

© 1996 by American Society of Clinical Oncology.

0732-183X/96/1403-0008$3.00/0

We now report the results of a phase II study of multiple-dose intravenous administration of rhuMAb HER2 in patients with metastatic breast cancer. The objectives of this trial were to determine the antitumor activity of rhuMAb HER2 in this patient population, as well as to define further the toxicity profile and pharmacokinetics of rhuMAb HER2.

PATIENTS AND METHODS

Preparation and Humanization of rhuMAb HER2 Antibody

MAb 4D5 was initially derived by immunizing mice with cells that expressed high levels of the HER2 gene product, $p185^{HER2}$.[19] MAb 4D5, directed at the extracellular domain of $p185^{HER2}$ (ECD^{HER2}), inhibits the in vitro growth of breast cancer cells that contain high levels of $p185^{HER2}$.[19,20] rhuMAb HER2 was engineered by inserting the complementarity determining regions of MAb 4D5 into the framework of a consensus human immunoglobulin G_1 (IgG_1).[22] The resulting rhuMAb HER2 has high affinity for $p185^{HER2}$ (Dilohation constant [K_d] = 0.1 nmol/L), markedly inhibits, in vitro and in human xenografts, the growth of breast cancer cells that contain high levels of $p185^{HER2}$, and induces antibody-dependent cellular cytotoxicity (ADCC).[22,23] rhuMAb HER2 is produced by a genetically engineered Chinese hamster ovary (CHO) cell line, grown in large scale, that secretes rhuMAb HER2 into the culture medium. Antibody is purified from the CHO culture media using standard chromatographic and filtration methods. Each lot of antibody used in this study was assayed to verify identity, purity, and potency, as well as to meet Food and Drug Administration requirements for sterility and safety.

Selection of Patients

Patients eligible for this study were adult women whose metastatic breast carcinomas overexpressed HER2 (see later). All patients had measurable disease, a Karnofsky's performance status of at least 60%, and preserved hematologic, liver, renal, and pulmonary function. Patients with lymphangitic pulmonary metastasis, history of brain metastasis, or bone metastases as the only site of measurable disease were excluded. Chemotherapy or additive hormonal therapy within 3 weeks before study entry (6 weeks for mitomycin or nitrosureas) was not permitted. Informed consent was obtained and documented in writing before study entry.

Tumor expression of HER2 was determined by immunohistochemical analysis, as previously described,[5,6] of a set of thin sections prepared from the patient's paraffin-archived tumor blocks. The primary detecting antibody used was murine MAb 4D5, which has the same complementarity determining regions as rhuMAb HER2. Tumors were considered to overexpress HER2 if at least 25% of tumor cells exhibited characteristic membrane staining for $p185^{HER2}$.

Antibody Administration

The pharmacokinetic goal was to achieve rhuMAb HER2 trough serum concentrations greater than 10 μg/mL, a level associated with optimal inhibition of cell growth in the preclinical model.[22] The optimal dose and schedule of rhuMAb HER2 was based on two prior phase I clinical trials, conducted at University of California, Los Angeles, and Memorial Sloan-Kettering Cancer Center, which had documented dose-dependent pharmacokinetics. In this current trial, rhuMAb HER2 was administered intravenously over a period of 90 minutes in the outpatient setting. Each patient received a loading dose of 250 mg of rhuMAb HER2 on day 0, and beginning on day 7,100 mg weekly for a total of 10 doses. At the completion of this treatment period, patients with stable disease or minor, partial, or complete responses were entered onto a maintenance phase of weekly rhuMAb HER2 administration until disease progression.

Evaluation of Toxicity

Toxicity was scored based on a modified National Cancer Institute common toxicity criteria. Complete blood cell counts, urinalysis, coagulation profile, and hepatic enzyme, renal, and electrolyte studies were performed weekly while on the study.

Pharmacokinetics, Determination of Extracellular Domain of $p185^{HER2}$ Levels, and Antibodies Directed Against rhuMAb HER2

Blood samples for pharmacokinetic analysis were collected just before each treatment with rhuMAb HER2 and within the first hour following the end of each rhuMAb HER2 infusion. Serum concentrations of rhuMAb HER2 were determined in a receptor binding assay that detects binding with ECD^{HER2}. The nominal limit of detection for rhuMAb HER2 in serum samples was 156 ng/mL. The presence of antibodies to rhuMAb HER2 was determined with a bridging-type filter enzyme-linked immunosorbent assay (ELISA). Circulating concentrations of ECD^{HER2} shed by patients' tumors were also determined using an ELISA.[24] The pair of antibodies used for the assay were 7C2 as coat and 2C4 as horseradish peroxidase–conjugated antibody; the lower limit of detection for this assay ranged from 2.8 to 8.3 ng/mL (Baly D, Wong WL, unpublished data, November 1994).

Serum levels of rhuMAb HER2 as a function of time were analyzed for each patient using a one-compartment model. Model parameters (volume and the elimination rate constant [K_e]) were estimated for each patient using a maximum-likelihood estimation procedure.[25] rhuMAb HER2 half-life ($t_{1/2}$) was calculated by dividing ln 2 by K_e.

Tumor Response

Tumor response was determined at the completion of the initial 11-week treatment period. All responses were confirmed by an independent extramural evaluation committee composed of an oncologist and a radiologist. Complete response was defined as the disappearance of all radiographically and/or visually apparent tumor, partial response as a ≥ 50% reduction in the sum of the products of the perpendicular diameters of all measurable lesions, minimal response as a ≥ 25% and less than 50% reduction in the diameters, stable disease as no change greater than 25% in the size of measurable lesions, and progressive disease as a ≥ 25% increase in any measurable lesion or the appearance of any new lesion. Although bone metastases were considered not measurable for response, patients had to have at least stability of bone lesions to be considered responders. Patients who had entered the maintenance phase of the study had tumor responses evaluated every 11 weeks, or earlier if clinically indicated. Time to tumor progression was calculated from the beginning of therapy to progression. Confidence limits for response rates were calculated using the exact method for a single proportion.[26]

Table 1. Patient Characteristics

Characteristic	Patients (N = 46) No.	%
Age, years		
Median	50	
Range	30-65	
Karnofsky performance status		
Median	90	
Range	60-100	
Level of HER2 expression*		
25%-50% cells	7	15.2
> 50% cells	39	84.8
Receptor status		
Estrogen receptor-positive (n = 40)	17	42.5
Progesterone receptor-positive (n = 39)	15	38.5
No. of metastatic sites		
1	16	34.5
2	14	30.4
≥ 3	16	34.5
Dominant site of metastasis		
Viscera	37	80.4
Skeleton	1	2.2
Soft tissues	8	17.4
Prior therapy		
Chemotherapy	45	97.8
Adjuvant chemotherapy	26	56.5
Neoadjuvant chemotherapy	4	8.7
Metastatic disease (no. of regimens)		
None	8	17.4
1	9	19.6
2	9	19.6
> 2	20	43.5
Median	2	
Range	0-7	
Hormonal therapy		
Adjuvant tamoxifen	7	15.2
Metastatic disease	21	45.6

*In percent of tumor cells with cytoplasmic membrane staining.

RESULTS

Patients characteristics are listed in Table 1. A total of 46 patients were enrolled onto the study. Their level of tumor overexpression of HER2 was relatively high, with more than 80% of the tumors having more than half of their cells exhibit positive membrane staining. Our patient population had extensive metastatic disease: 34.5% of patients had three or more metastatic sites. Dominant sites of metastases were visceral in 80% of cases (lung in 18, liver in 13, both liver and lung in five, and ovary in one). Only 17.4% of cases had dominant metastases in soft tissues (skin and lymph nodes) and only one patient had bone as the dominant site of disease. The total number of patients with bone disease was 18 (39%). All but one of the patients had received prior chemotherapy, with 82.6% having received at least one regimen for metastatic disease and 63% having received two or more regimens. Of this latter group, four patients had previously received high-dose chemotherapy with hematopoietic stem-cell support.

Data on rhuMAb HER2 pharmacokinetics are available from 45 patients (Table 2). More than 90% of the examined population (41 patients) had rhuMAb HER2 trough levels above the targeted 10-μg/mL level. The mean serum $t_{1/2}$ of rhuMAb HER2 was 8.3 ± 5.0 days. The rhuMAb HER2 serum $t_{1/2}$ was found to be dependent on the presence of circulating ECD^{HER2} released from the tumor into the serum (Table 2). Representative examples of pharmacokinetics profiles are shown in Fig 1. Figure 1A shows the serum levels of rhuMAb HER2 in a patient with undetectable level of circulating ECD^{HER2}; stable, therapeutic serum levels of the drug were maintained in this patient for more than 1 year. Figure 1B shows the serum levels of rhuMAb HER2 in a patient with high levels of circulating ECD^{HER2}; trough levels of rhuMAb HER2 were consistently below detectable levels throughout the treatment course and until disease progression. Antibodies against rhuMAb HER2 (human antihuman antibodies [HAHA]) were not detected in any patients.

Treatment with rhuMAb HER2 was remarkably well tolerated. Of a total of 768 administrations of rhuMAb HER2, only 11 events occurred that were considered to be related to the use of the antibody (Table 3). Fever and chills occurred on five occasions after the first administration of rhuMAb HER2. The fever lasted less than 8 hours in all cases and did not recur on subsequent administrations of the antibody. Three patients experienced chest pain in areas of tumor involvement shortly after the infusion of the first dose of rhuMAb HER2; in one case this required an overnight hospital admission for pain control. The pain did not recur on successive administrations of the antibody. None of the patients whose cancer regression met the formal criteria for complete or partial response had pain at a tumor site after administration of rhuMAb HER2.

The number of patients assessable for treatment response on evaluation day 77 was 43. Three patients were not assessable for response. One had a bacteremic infection of an intravenous catheter that required prolonged administration of antibiotics, which precluded treatment

Table 2. ECD^{HER2}-Dependent Pharmacokinetics of rhuMAb HER2

N	Patient Group	rhuMAb HER2 $t_{1/2}$ (days)
45	All patients	8.3 ± 5.0
40	Circulating ECD^{HER2} < 500 ng/mL	9.1 ± 4.7
5	Circulating ECD^{HER2} > 500 ng/mL	1.8 ± 1.0

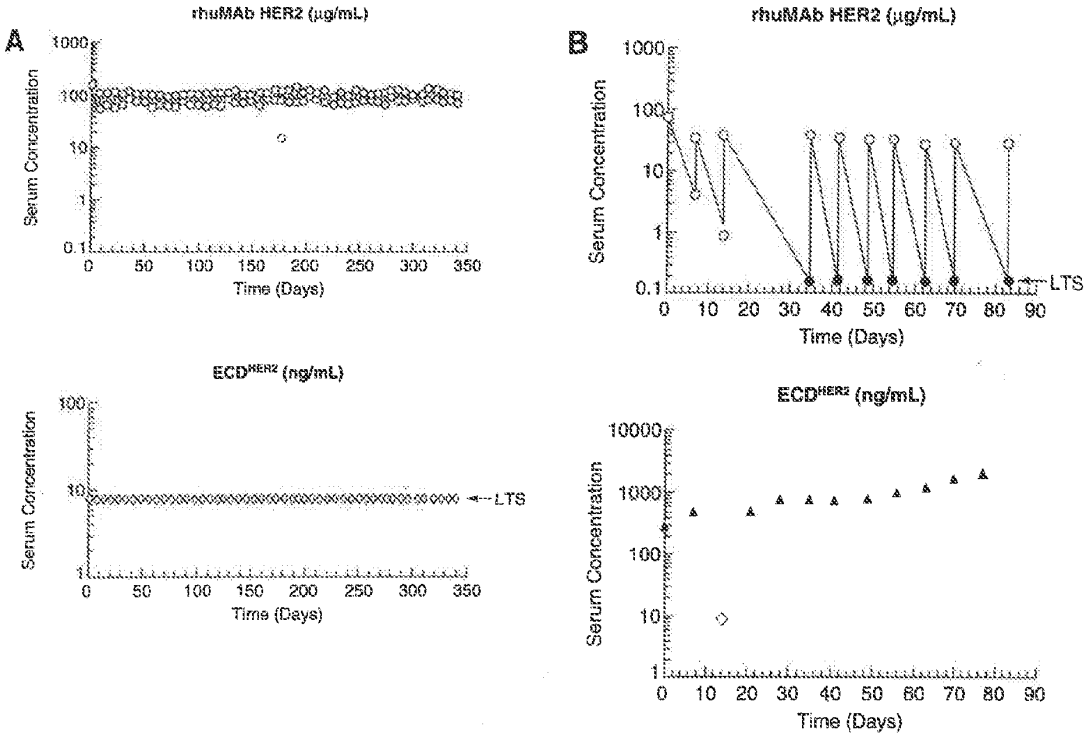


Fig 1. Effect of serum ECD^{HER2} on rhuMAb HER2 pharmacokinetics. Stable serum levels of rhuMAb HER2 in a patient with absence of ECD^{HER2} (A) v suboptimal rhuMAb HER2 serum levels in a patient with high ECD^{HER2} (B). Note that log scales on the Y-axis describing the serum ECD^{HER2} differ among charts. LTS, less than lowest assay standard. (○) observed rhuMAb HER2 serum concentration; (✱) LTS for rhuMAb HER2 serum concentration; (▲) ECD^{HER2} serum concentration; (◇) LTS for ECD^{HER2} serum concentration.

with rhuMAb HER2. A second declined to continue on the study for personal reasons. The third died of congestive heart failure associated with prior doxorubicin treatment. Among 43 assessable patients, 5 had tumor responses: one patient had a complete remission and four had partial remissions. Therefore, the overall response rate (complete plus partial responses) for assessable patients is 11.6% (95% confidence interval, 4.36 to 25.9). Details of responses are listed in Tables 4 and 5, and examples of the responses are shown in Fig 2.

Table 3. rhuMAb HER2-Related Toxicity

Toxicity	Moderate (grade 2)	Severe (grade 3)
Fever and chills	5	
Pain at tumor site	2	1
Diarrhea	2	
Nausea and emesis	1	

NOTE. In number of events of a total of 768 administrations.

Two patients had minor responses and 14 patients had stable disease at day 77. These patients entered a maintenance phase of weekly antibody administration until progression of disease. The median time to progression for the patients with either minor or stable disease was 5.1 months. An additional patient had a greater than 50% reduction in the size of the metastatic disease on her mediastinum and chest wall after 2 weeks of treatment. While the duration of response was greater than 4 weeks, by evaluation day 77 the lesion had begun to regrow from the size of maximal response to therapy. Per protocol guidelines, this patient was therefore considered not to have had a response to therapy, but rather progression of disease.

DISCUSSION

During the last decade, overexpression of the HER2 gene has been shown to play an important role in the pathogenesis and poor prognosis of breast cancer. As a

OnCusp
Ex. 1002

Table 4. Response Rate Obtained With rhuMAb HER2 in 43 Assessable Patients

Response	No. of Patients	%
Complete response	1	2.3
Partial response	4	9.3
Overall response	5	11.6
Minor response	2	4.6
Stable disease	14	32.6
Progression of disease	22	51.2

consequence, strategies directed at interference with HER2 expression or the function of its protein, $p185^{HER2}$, have been anticipated to have therapeutic value. Extensive preclinical studies have shown that certain MAbs directed against $p185^{HER2}$ can inhibit growth of HER2-overexpressing tumor cells.[15-19] This study provides the first clinical evidence of the antitumor activity of one of these agents, rhuMAb HER2.

Of 43 patients with $p185^{HER2}$-positive tumors assessable for response after treatment with rhuMAb HER2, five experienced a complete or partial remission, for an overall response rate of 11.6%. One additional patient had a greater than 50% shrinking of her cancer that lasted more than 1 month, but was not considered a responder by our protocol definition. The objective antitumor responses observed were of clinical importance, since two patients had regression of cancers in the liver and one patient achieved a pathologically-proven complete response of chest wall disease, which has persisted for 24 months. Our patients were selected to have many sites of metastatic involvement, one of the most dire prognostic characteristics regarding response to therapy. This selection was the consequence of the rule that patients with disease involving only bone were ineligible for accrual, because bone is the solitary site of initial metastatic involvement in up to 60% of cases.[27] It is reasonable to hypothesize that the percentage of patients who show objective tumor regression to rhuMAb HER2 will be higher when patients with less extensive breast cancer are treated, since laboratory studies have shown that the response to antireceptor antibodies is greater with lower tumor burden.[28] It would be also of interest to analyze the response rate to rhuMAb HER2 in a patient population with no prior chemotherapy for stage IV disease, since prior experience has shown that untreated patients usually respond better to new anticancer drugs.[29]

Another important point about the probability of response to rhuMAb HER2 concerns the observation that 37% of patients achieved minimal responses or stable disease. In the laboratory, rhuMAb HER2 or the parent antibody 4D5 has been noted to be cytostatic, which causes growth arrest, rather than cytocidal, which causes cell death. In clinical trials of many anticancer drugs, particularly chemotherapy, the achievement of stable disease is not considered a reliable measure of anticancer activity. However, with rhuMAb HER2, stable disease may be an authentic reflection of the biologic action of the drug, which differs markedly from conventional anticancer agents. The unusually long durations of minimal responses and stable disease seen in our trial may relate to this distinction. These data are specially interesting in light of the absence of significant toxicity observed here, for in a setting in which palliation is a main objective, quality of life while on treatment should be a main end point.

The dose and schedule of rhuMAb HER2 administration used in this protocol provided adequate serum concentrations in all patients, except in those with circulating levels of tumor-shed ECD^{HER2} at serum concentrations ≥

Table 5. Characteristics of Patients Who Achieved a Response to Treatment

Patient No.	HER2*	Site of Metastatic Disease	Prior Systemic Therapy	Best Response	Duration of Response (months)
1	3+	Chest wall	Doxorubicin	Complete response†	> 24
2	3+	Liver	Doxorubicin, mitoxantrone, paclitaxel	Partial response	6.7
3	2+	Mediastinum	CMFVP, doxorubicin, tamoxifen, paclitaxel	Partial response	7.7
4	3+	Liver + retroperitoneal lymph nodes + bone	CMF, docetaxel	Partial response	1
5	2+	Chest wall	Paclitaxel	Partial response	3.4

Abbreviations: CMFVP, cyclophosphamide, methotrexate, fluorouracil, vincristine, and prednisone; CMF, cyclophosphamide, methotrexate, and fluorouracil.

*By immunohistochemistry: 2+, 25% to 50% of tumor cells with cytoplasmic membrane staining; 3+, > 50% of tumor cells with cytoplasmic membrane staining.

†Patient's complete response was pathologically proven with several biopsies at tumor site. Patient bone scan, head, thoracic, abdominal, and pelvic computed tomographic scans are negative.

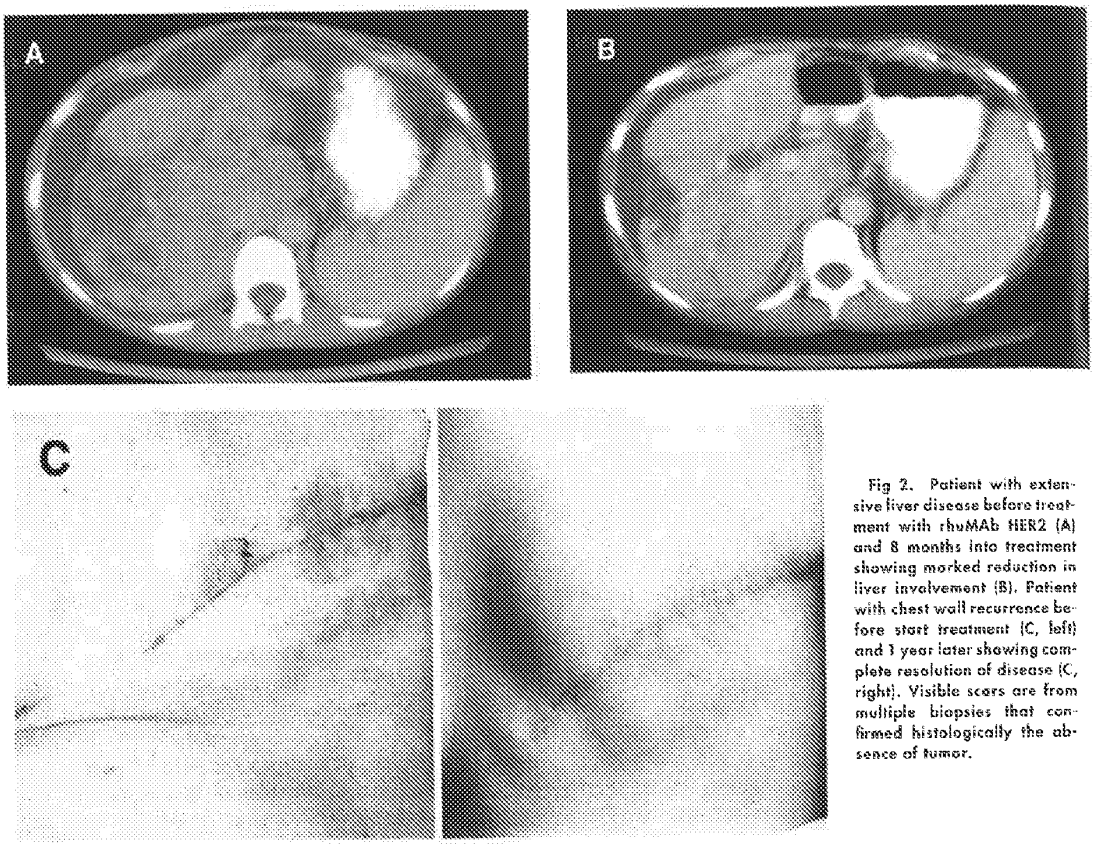


Fig 2. Patient with extensive liver disease before treatment with rhuMAb HER2 (A) and 8 months into treatment showing marked reduction in liver involvement (B). Patient with chest wall recurrence before start treatment (C, left) and 1 year later showing complete resolution of disease (C, right). Visible scars are from multiple biopsies that confirmed histologically the absence of tumor.

500 ng/mL. ECD^{HER2} is known to be released by some breast cancer cells that overexpress HER2,[30-32] and elevated ECD^{HER2} serum levels have been previously reported in patients with breast cancer.[31,33,34] The most likely explanation for the short serum $t_{1/2}$ values and subtherapeutic trough levels of rhuMAb HER2 in this group of patients is that in the presence of ECD^{HER2} in the serum, antigen-antibody complexes form and are rapidly cleared from the circulation. Of interest, no anticancer responses were observed in the group of patients with serum concentrations of $ECD^{HER2} \geq 500$ ng/mL. Hence, the interpretation of results of future trials of agents that bind to or exert their function through $p185^{HER2}$ should take ECD^{HER2} release from the tumors into account; at present, patients with high levels of ECD^{HER2} should continue to participate in these studies.

There are several possible mechanisms, not mutually exclusive, that could explain the clinical results observed. An important fact is that rhuMAb HER2 induces a marked downregulation of $p185^{HER2}$.[19] Antibody-induced downregulation of $p185^{HER2}$ has been shown to induce reversion of the transformed phenotype in HER2-transformed cells.[14] By a similar mechanism, the continuous exposure to rhuMAb HER2 at adequate concentrations achieved in our trial could be reversing the malignant phenotype of the clinical cancers by downregulating their level of $p185^{HER2}$. Another possibility is that the known partial agonistic effects of rhuMAb HER2[35] could result in the activation of a signal transduction pathway that leads to inhibition of tumor-cell proliferation. Both of these potential antitumor mechanisms would require, in addition to receptor expression, intact receptor function. Little is known about the functional status of $p185^{HER2}$ in breast tumor specimens, but it is conceivable that not all overexpressing tumors have functional receptors. In support of this view is the observation that HER2-overexpressing tumor-cell lines that are not growth-inhibited by anti-$p185^{HER2}$ antibodies have been described and well charac-

terized[36]; it is noteworthy that some of these antibody-resistant tumor cells also overexpressed truncated forms of ECD^{HER2}. Furthermore, in vitro studies suggest that those breast cancer cell lines that have the highest basal level of p185^{HER2} phosphorylation are the most growth-inhibited by anti-p185^{HER2} antibodies.[20] If this were the case in the clinic, the recently produced antiserum that specifically recognizes only overexpressed tyrosine-phosphorylated p185^{HER2} might prove useful in predicting the subset of p185^{HER2}-positive tumors most likely to respond to rhuMAb HER2.[8]

Another possible mechanism of action concerns the observation that rhuMAb HER2 is a potent inducer of ADCC.[32] However, while this immune-mediated mechanism might play a role in the observed clinical responses, ADCC is obviously not involved in the pronounced growth-inhibitory effects of the antibody in vitro.

The observed activity of rhuMAb HER2 against advanced breast cancers that overexpress HER2 provides the first clinical evidence that anti–growth factor receptor-directed strategies may be useful in the treatment of human breast cancer. Therefore, continued research with this agent and other HER2-targeted treatment strategies appears warranted. The response to rhuMAb HER2 in a less heavily pretreated population and in those with less extensive metastatic disease would be of interest since both parameters have historically correlated with a higher response to drugs,[29] and this same principle may apply to antibody-based therapy.[37] In preclinical studies, both in vitro and in xenografts, rhuMAb HER2 markedly potentiated the antitumor effects of several chemotherapeutic agents, including cisplatin, doxorubicin, and paclitaxel,[25,38] without increasing their toxicity. Laboratory studies of the mechanism of this effect and clinical trials of such combination therapy are currently in progress.

ACKNOWLEDGMENT

We are indebted to Drs Mary Ellen Moynahan, George Raptis, Violante E. Currie, David W. Fennelly, John P. Crown (Department of Medicine), and Patrick Borgen (Department of Surgery), Memorial Sloan-Kettering Cancer Center, for accrual and care of patients; Katherine Trainer for data management (Memorial Sloan-Kettering Cancer Center); Judy Tomsic and Anita Harrison for data management and Dr David Kirn, Diane Craig, Diane Kennedy, and Becki Moore for care of patients (University of California, San Francisco); and Gracie Lieberman, Maureen Ash, and Annabel Vaghai (Genentech Inc) for data and statistical analysis; and Andrew Nuijens, Cheryl Schofield, Wai Lee Wong, and Deborah Baly (Genentech Inc) for their tremendous efforts in developing and interpreting data from the assays for rhuMAb HER2 serum concentrations, extracellular domain of p185^{HER2} (ECD^{HER2}), and the presence of antibodies to rhuMAb HER2. We also acknowledge Mark Sliwkowski (Genentech Inc) for careful review of the manuscript and useful suggestions.

REFERENCES

1. Aaronson SA: Growth factors and cancer. Science 254:1146-1153, 1991

2. Coussens L, Yang-Feng TL, Liao Y-C, et al: Tyrosine kinase receptor with extensive homology to EGF receptor shares chromosomal location with *neu* oncogene. Science 230:1132-1139, 1985

3. Akiyama T, Sudo C, Ogawara H, et al: The product of the human c-erbB-2 gene: A 185-kilodalton glycoprotein with tyrosine kinase activity. Science 232:1644-1646, 1986

4. Stern DF, Heffernan PA, Weinberg RA: p185, a product of the *neu* proto-oncogene, is a receptorlike protein associated with tyrosine kinase activity. Mol Cell Biol 6:1729-1740, 1986

5. Slamon DJ, Godolphin W, Jones LA, et al: Studies of the HER-2/*neu* proto-oncogene in human breast and ovarian cancer. Science 244:707-712, 1989

6. Slamon DJ, Clark GM, Wong SG, et al: Human breast cancer: Correlation of relapse and survival with amplification of the HER2/*neu* oncogene. Science 235:177-182, 1987

7. Ravdin PV, Chamness GC: The c-erbB-2 proto-oncogene as a prognostic and predictive marker in breast cancer: A paradigm for the development of other macromolecular markers—A review. Gene 159:19-27, 1995

8. Hynes NE, Stern DF: The biology of *erbB-2/neu*/HER-2 and its role in cancer. Biochim Biophys Acta 1198:165-184, 1994

9. Hudziak RM, Schlessinger J, Ullrich A: Increased expression of the putative growth factor receptor p185^{HER2} causes transformation and tumorigenesis of NIH 3T3 cells. Proc Natl Acad Sci USA 84:7159-7163, 1987

10. Di Fiore PP, Pierce JH, Kraus MH, et al: *erbB-2* is a potent oncogene when overexpressed in NIH-3T3 cells. Science 237:178-182, 1987

11. Guy CT, Webster MA, Schaller M, et al: Expression of the neu protooncogene in the mammary epithelium of transgenic mice induces metastatic disease. Proc Natl Acad Sci USA 89:10578-10582, 1992

12. Gusterson BA, Machin LG, Gullick WJ, et al: Immunohistochemical distribution of c-erbB-2 in infiltrating and in situ breast cancer. Int J Cancer 42:842-845, 1988

13. van de Vijver MJ, Peterse JL, Mooi WJ, et al: *NEU*-protein overexpression in breast cancer—Association with comedo-type ductal carcinoma in situ and limited prognostic value in stage II breast cancer. N Engl J Med 319:1239-1245, 1988

14. Drebin JA, Link VC, Stern DF, et al: Down-modulation of an oncogene protein product and reversion of the transformed phenotype by monoclonal antibodies. Cell 41:695-706, 1985

15. McKenzie SJ, Marks PJ, Lam T, et al: Generation and characterization of monoclonal antibodies specific for the human *neu* oncogene product, p185. Oncogene 4:543-548, 1989

16. Stancovski I, Hurwitz E, Leitner D, et al: Mechanistic aspects of the opposing effects of monoclonal antibodies to the *erbB-2* receptor on tumor growth. Proc Natl Acad Sci USA 88:8691-8695, 1991

17. Hancock MC, Langton BC, Chan T, et al: A monoclonal antibody against the c-erbB-2 protein enhances the cytotoxicity of cis-diamminedichloroplatinum against human breast and ovarian tumor cell lines. Cancer Res 51:4575-4580, 1991

18. Harwerth IM, Wels W, Schlegel J, et al: Monoclonal antibodies directed to the erbB-2 receptor inhibit in vivo tumour cell growth. Br J Cancer 68:1140-1145, 1993

19. Hudziak RM, Lewis GD, Winget M, et al: p185^{HER2} monoclonal antibody has antiproliferative effects in vitro and sensitizes human breast tumor cells to tumor necrosis factor. Mol Cell Biol 9:1165-1172, 1989

20. Lewis GD, Figari I, Fendly B, et al: Differential responses of human tumor cell lines to anti-p185^{HER2} monoclonal antibodies. Cancer Immunol Immunother 37:255-263, 1993

21. Shepard HM, Lewis GD, Sarup JC, et al: Monoclonal antibody therapy of human cancer: Taking the HER2 protooncogene to the clinic (review). J Clin Immunol 11:117-127, 1991

22. Carter P, Presta L, Gorman CM, et al: Humanization of an anti-p185HER2 antibody for human cancer therapy. Proc Natl Acad Sci USA 89:4285-4289, 1992

23. Baselga J, Norton L, Coplan K, et al: Anti-HER2 humanized monoclonal antibody alone and in combination with chemotherapy against human breast carcinoma xenografts. Proc Am Soc Clin Oncol 13:63, 1994 (abstr 53)

24. Sias PE, Kotts CE, Vetterlein D, et al: ELISA for quantitation of the extracellular domain of p185^{HER2} in biological fluids. J Immunol Methods 132:73-80, 1990

25. D'Argenio DZ, Schumitzky A: ADAPT II User's Guide (ed 2). Los Angeles, CA, Biomedical Simulations Resource, University of Southern California, 1990

26. Fleiss JL: Statistical Methods for Rates and Proportions (ed 2). New York, NY, Wiley, 1981, pp 13-17

27. Hayes DF, Kaplan WD: Evaluation of patients following primary therapy, in Harris JR, Hellman S, Kinne DW (eds): Breast Diseases (ed 2). Philadelphia, PA, Lippincott, 1991, pp 505-525

28. Fan Z, Baselga J, Masui H, et al: Antitumor effect of anti-epidermal growth factor receptor monoclonal antibodies plus cis-diamminedichloroplatinum on well established A431 cell xenografts. Cancer Res 53:4637-4642, 1993

29. Norton L: Salvage chemotherapy of breast cancer. Semin Oncol 21:19-24, 1994

30. Zabrecky JR, Lam T, McKenzie SJ, et al: The extracellular domain of p185/*neu* is released from the surface of human breast carcinoma cells, SK-BR-3. J Biol Chem 266:1716-1720, 1991

31. Pupa SM, Menard S, Morelli D, et al: The extracellular domain of the c-erbB-2 oncoprotein is released from tumor cells by proteolytic cleavage. Oncogene 8:2917-2923, 1993

32. Lin YJ, Clinton GM: A soluble protein related to the HER-2 proto-oncogene product is released from human breast carcinoma cells. Oncogene 6:639-643, 1991

33. Hayes DF, Cirincione C, Carney W, et al: Elevated circulating HER2/*neu* related protein (NRP) is associated with poor survival in patients with metastatic breast cancer. Proc Am Soc Clin Oncol 12:58, 1993 (abstr 35)

34. Kandil H, Seymour L, Bezwoda WR: Soluble c-erbB-2 fragment in serum correlates with disease stage and predicts for shortened survival in patients with early-stage and advanced breast cancer. Br J Cancer 70:739-742, 1994

35. Scott GK, Dodson JM, Montgomery PA, et al: p185HER2 signal transduction in breast cancer cells. J Biol Chem 266:14300-14305, 1991

36. Scott GK, Robles R, Park JW, et al: A truncated intracellular HER2/neu receptor produced by alternative RNA processing affects growth of human carcinoma cells. Mol Cell Biol 13:2247-2257, 1993

37. Riethmuller G, Schneider-Gadicke E, Schlimok G, et al: Randomised trial of monoclonal antibody for adjuvant therapy of resected Dukes' C colorectal carcinoma. Lancet 343:1177-1183, 1994

38. Pietras RJ, Fendly BM, Chazin VR, et al: Antibody to HER-2/*neu* receptor blocks DNA repair after cisplatin in human breast and ovarian cancer cells. Oncogene 9:1829-1838, 1994

OnCusp
Ex. 1002

Int. J. Cancer: 62, 472–479 (1995)
© 1995 Wiley-Liss, Inc.

Publication of the International Union Against Cancer
Publication de l'Union Internationale Contre le Cancer

THE EPITHELIAL/CARCINOMA ANTIGEN EGP-1, RECOGNIZED BY MONOCLONAL ANTIBODY RS7-3G11, IS PHOSPHORYLATED ON SERINE 303

Amartya BASU[1], David M. GOLDENBERG[2] and Rhona STEIN[2,3]

[1]*Department of Biochemistry and Molecular Biology, Graduate School of Biomedical Science, University of Medicine and Dentistry of New Jersey, Newark, NJ 07103;* [2]*Garden State Cancer Center at the Center for Molecular Medicine and Immunology, Newark, NJ 07103, USA.*

RS7-3G11 is a murine monoclonal antibody (MAb) raised against human non-small-cell lung carcinoma, and is under clinical evaluation. The epithelial/carcinoma antigen EGP-1, defined by RS7-3G11, was isolated and purified to homogeneity from a cervical carcinoma cell line, ME180. EGP-1 is a glycoprotein with an average molecular mass of 47.8 kDa. Metabolic labeling of the antigen with ^{32}P-orthophosphate and subsequent immunoprecipitation with RS7-3G11 showed that it is a phosphoprotein. Phosphoamino acid analysis of the *in vivo* phosphorylated EGP-1 revealed that the phosphorylation is on serine. *In vitro* analysis with purified antigen demonstrated that protein kinase C, and not protein kinase A, is involved in phosphorylating the antigen *in vitro*. *In vitro* analysis indicated a stoichiometry of phosphorylation of 0.54 mole of phosphate per mole of EGP-1. Phosphoamino acid analysis and phosphopeptide mapping of the antigen phosphorylated *in vitro* by protein kinase C showed that phosphorylation occurred on a serine residue, specifically on serine 303, located in the cytoplasmic domain of EGP-1. Treatment of ME180 cells with phorbol ester increased the phosphorylation of EGP-1. The biological function of EGP-1 remains to be elucidated. In this report we elucidate an involvement of protein kinase C in phosphorylating EGP-1, which may signify a role for this antigen in signal transduction across the cell membrane.
© *1995 Wiley-Liss, Inc.*

An epithelial/carcinoma glycoprotein of 46–48 kDa molecular mass is defined by the murine pancarcinoma RS7-3G11 MAb (Stein *et al.,* 1993). Following the proposal of the Third International IASLC Workshop on Lung Tumor and Differentiation Antigens, we are adopting the nomenclature *epithelial glycoprotein-1* (EGP-1) to designate this antigen (De Leij *et al.,* 1994).

The RS7-3G11 MAb, which was raised against human non-small-cell lung carcinoma, reacts with various human tumors of epithelial origin, including breast, bladder, lung, ovary, prostate, pancreas, and stomach. Although most normal human tissues are unreactive to RS7-3G11, the antigen is found to be expressed in several normal glandular and epithelial cells, including glands in the bronchus, breast, prostate, and skin, and ducts and acini of the pancreas (Stein *et al.,* 1990). Nevertheless, radiolabeled RS7-3G11 has been found to target several carcinoma types in patients (data not shown).

The antigen has been affinity purified using the RS7-3G11 MAb and partially sequenced (Stein *et al.,* 1994). Sequence data indicated a likely identity to the deduced sequence of the GA733-1 gene, which has been cloned previously (Linnenbach *et al.,* 1989). GA733-1, along with GA733-2, forms a family of genes coding for proteins that are highly immunogenic in the mouse and that have been exploited effectively in applications involving tumor targeting and site-directed immunotherapy (Szala *et al.,* 1990; Ross *et al.,* 1986). The GA733-1 gene is an intronless transposon formed by retroposition of the GA733-2 gene via an mRNA intermediate (Linnenbach *et al.,* 1993). At the amino acid level EGP-1 and EGP-2 (the gene products of GA733-1 and GA733-2, respectively) are 49% identical. Evidence by Litvinov *et al.* (1994) suggests that EGP-2 is an epithelial-specific intercellular adhesion molecule.

The sequence investigation of GA733-1 cDNA indicates that EGP-1 is a type I transmembrane glycoprotein with homology to nidogen, a matrix protein involved in cell adhesion, human and bovine thyroglobulin type I repeat unit, α-subunit of the interleukin-2 growth factor receptor of human and mouse, and HLA-DR-associated invariant chain (Linnenbach *et al.,* 1993). The molecular mass of the protein moiety of EGP-1 is approximately 35 kDa (corresponding to the predicted mass of the GA733-1 gene product, 35.7 kDa), with heterogeneous N-linked glycosylation on its extracellular domain ranging from 11 to 13 kDa. The protein moiety has been shown to be antigenic to RS7-3G11 and the antigenicity is based on a conformational epitope (Stein *et al.,* 1993). The extracellular domain is rich in cysteine residues, which might bear some functional significance.

Analysis of the predicted amino acid sequence of EGP-1 suggested possible phosphorylation sites within the cytoplasmic domain of this antigen. However, it is interesting to note that neither EGP-2 nor the homologous antigen nidogen contain any phosphorylation sites in their cytoplasmic domains. The present studies were initiated to determine the phosphorylation status of EGP-1. This report demonstrates that EGP-1 is indeed a phosphoglycoprotein and a substrate for protein kinase C (PKC), the Ca^{2+}-dependent protein kinase. The phosphorylation occurs on serine 303 in the cytoplasmic domain of EGP-1. This information implies a role for EGP-1 in signal transduction.

MATERIAL AND METHODS

Cell culture

The human cervical carcinoma cell line ME-180, a carcinoma of epithelial origin, was grown in RPMI 1640 medium supplemented with 5% fetal bovine serum, 10% defined equine serum, penicillin (100 U/ml), streptomycin (100 μg/ml), and L-glutamine (2 mM) at 37°C in a 5% CO_2 environment. Cells were passaged after detachment with trypsin, 0.2% EDTA.

Preparation of crude extract from ME-180 cells

ME180 cells were grown to confluency. After removing the medium by thorough washing with cold PBS, cells were lysed in lysis buffer [0.1 M NaCl, 50 mM Tris-HCl at pH 7.4, 1 mM

[3]To whom correspondence and reprint requests should be addressed. Fax: 201 982 7047.

Abbreviations used: BSA, bovine serum albumin; ELISA, enzyme-linked immunosorbent assay; EGP-1, Epithelial glycoprotein-1; MAb, monoclonal antibody; PBS, phosphate buffered saline; PKA, protein kinase A; PKC, protein kinase C; PAGE, polyacrylamide gel electrophoresis; PVDF, polyvinylidene fluoride; PS, phosphatidylserine.

Received: March 13, 1995.

5101 of 14295

OnCusp
Ex. 1002

EDTA, 1.0% Nonidet P-40, phenylmethylsulfonyl fluoride (200 nM), aprotinin (0.6 μg/ml), and leupeptin (1.0 μg/ml)] at 0–4°C for 1 hr. To ensure lysis and antigen solubilization, the extract was sonicated approximately 10 times for 10 sec each. The cell debris and nuclei were removed by centrifugation at 12,000g (Sorval SS-34 rotor, Du Pont, Wilmington, DE) for 20–30 min at 4°C. The supernatant was stored at −80°C before use.

Purification of EGP-1 from ME180 cells

EGP-1 was purified from the ME180 cell extract using concanavalin A-Sepharose (Pharmacia, Piscataway, NJ) column chromatography and RS7-3G11-Affi-Gel Hz column chromatography as described previously (Stein *et al.*, 1993). To achieve maximum purity, the antibody column-purified sample was passed through a Sephacryl S-300 (superfine) column (Pharmacia). The fractions (1.0 ml each) were assayed by a capture-probe ELISA. The ELISA-positive fractions were pooled, and concentrated using Centricon-10 (Amicon, Beverly, MA). The Sephacryl S-300 column-resolved EGP-1 sample was analyzed by 10% SDS-PAGE followed by silver staining (Blum *et al.*, 1987).

Metabolic labeling of EGP-1 with ^{32}P-orthophosphate

ME180 cells were grown to approximately 80% confluency in T25 flasks. The cells were washed first with cold PBS and then with cold phosphate-free RPMI-1640 medium (Specialty Media, Lavallette, NJ) without any supplement. The cells were allowed to grow in phosphate-free RPMI-1640 medium without any supplement for 1–2 hr and then in phosphate-free RPMI-1640 medium supplemented with L-glutamine, antibiotics, 5% fetal bovine serum, and 250 μCi/ml of ^{32}P-orthophosphate (Du Pont NEN) for 6 hr at 37°C.

Immunoprecipitation of EGP-1

The lysate from ME180 cells was prepared as described above. The lysate was first cleared with 50 μl of a 50% suspension of protein A-agarose beads (BioRad, Melville, NY) for 60 min. The beads were removed by a brief centrifugation and the concentration of $MnCl_2$ in the supernatant was adjusted to 10 mM. The cleared lysate was then incubated with concanavalin A-Sepharose beads (100 μl, 50% packed resin from Pharmacia) for 2 hr. After a brief centrifugation, the supernatant was discarded and the concanavalin A-Sepharose beads with bound antigen was washed with 1.5 ml of lysis buffer. The antigen was eluted from the beads with 1.0 ml of lysis buffer containing 1 M methyl α, D-mannopyranoside rotating end-to-end for 30 min. The concanavalin A-Sepharose beads were removed by centrifugation and the eluant was incubated with MAb-protein A-agarose beads for 3 hr. The MAb-protein A-agarose beads were prepared by incubating 1 μg of antibodies with 50 μl of protein A-agarose beads in 500 μl of PBS for 3 hr, followed by washing with lysis buffer. The beads were collected and washed with 0.5 M NaCl-containing lysis buffer (1.5 ml), then with lysis buffer supplemented with 2% BSA, 0.5% sodium deoxycholate, and 0.1% SDS (4.5 ml), and finally with unsupplemented lysis buffer (3.0 ml). All the above steps were performed at 4°C and in the presence of 1 mM sodium orthovanadate.

The washed immunoprecipitate was solubilized in Laemmli (1970) sample buffer by boiling for 5 min. The agarose beads were separated by centrifugation and the supernatant was subjected to 10% SDS-PAGE without reduction. The gel was either dried and autoradiographed or transferred to polyvinylidene fluoride (PVDF) membrane for Western blotting, as described previously (Stein *et al.*, 1993).

In vitro *phosphorylation of EGP-1 by protein kinases*

Phosphorylation of EGP-1 was performed *in vitro* using 200 ng of purified antigen (more than 95% purity as determined by silver staining; data not shown) and 20 ng of PKC (a mixture of α, β, and γ subunits purified from the rat brain; Upstate Biotechnology, Lake Placid, NY). The reaction mixture contained Tris-HCl at pH 7.5 (20 mM), $MgCl_2$ (5 mM), Triton X-100 (0.03%), $CaCl_2$ (0.3 mM or without), phosphatidylserine (0.31 mg/ml or without; Sigma, St. Louis, MO), diolein (0.4 μM or without; ICN, Costa Mesa, CA), free arachidonic acid (0.4 mM or without; ICN), and 0.25 μM [γ-^{32}P]-ATP (2.5 μCi; Amersham, Arlington Heights, IL) in a final volume of 20 μl (Sekiguchi *et al.*, 1988). Under calcium-depleted conditions, EGTA (5 mM) was added to the reaction mixtures. Histone type III-SS (0.4 μg, Sigma) from calf thymus was used as a positive control. The reaction mixtures were incubated at 30°C for 1 hr and were stopped by boiling the samples for 5 min after adding 2× SDS-PAGE sample buffer with or without 2-mercaptoethanol. Approximately 10–12.5 ng of EGP-1 and 25 ng of histone type III-SS from the reaction mixtures were analyzed by 10% SDS-PAGE. Gels were dried and autoradiographed.

The competition experiment with ATP was performed by adding unlabeled ATP at final concentrations of 0.5 μM, 5.0 μM, 12.5 μM, and 25.0 μM in reaction mixtures containing Ca^{2+} (1 mM) and phosphatidylserine (0.31 mg/ml).

To determine the stoichiometry of phosphorylation of EGP-1, 4.7 μg (100 pmole) of purified EGP-1 was allowed to react *in vitro* in the presence of Ca^{2+} (1 mM), phosphatidylserine (0.31 mg/ml), 2 mM cold ATP, and 8.34 nM [γ-^{32}P]ATP with 100 ng of PKC for 1 hr at 30°C. The sample was resolved in 10% SDS-PAGE under non-reducing conditions. Following staining of the gel with Coomassie blue, the antigen band was excised and radioactivity was measured in a β-scintillation counter (Packard TriCarb, Meriden, CT; Liquid Scintillation Spectrometer 3255).

Protein kinase A (PKA) was assayed in the presence of Mg^{2+} as the divalent cation. The reaction mixtures included $MgCl_2$ (5 mM), Tris at pH 7.4 (20 mM), EGTA (1 mM), 0.25 μM [γ-^{32}P]ATP (2.5 μCi), 0.2 μg EGP-1, or 0.4 μg of histone type III-SS as substrate and 20 ng of PKA in a final volume of 20 μl (Park and Campaisi, 1990). The reaction mixtures were incubated at 30°C for 1 hr. Reactions were stopped by boiling for 10 min after adding 2× sample buffer and the proteins were resolved using 10% SDS-PAGE. The gel was dried and autoradiographed.

In vitro *dephosphorylation of EGP-1 by calf intestinal alkaline phosphatase*

Purified EGP-1 (50 ng) was phosphorylated *in vitro* by PKC as described above. Following inactivation of PKC by boiling for 10 min, 5 units of calf intestinal alkaline phosphatase and reaction buffer (New England Biolabs, Beverly, MA) were added. The reaction mixture was incubated at 37°C for 1 hr, and the reaction was stopped by adding 2× sample buffer and boiling for 5 min. It was then analyzed by 10% SDS-PAGE without reduction. The gel was dried and autoradiographed. Histone type III-SS was used as a positive control.

Phosphoamino acid analysis

The two-dimensional phosphoamino acid analysis of the ^{32}P-labeled EGP-1 was performed as described by Cooper *et al.* (1983). The phosphorylated EGP-1 was resolved in 10% SDS-PAGE. The gel was dried and autoradiographed. The ^{32}P-EGP-1 band was excised and eluted overnight at 37°C with 50 mM ammonium bicarbonate containing 0.1% SDS and 0.05% 2-mercaptoethanol with continuous shaking. The eluted sample was precipitated with 20% ice-cold TCA in the presence of 10 μg RNase A and then washed. An aliquot was subjected to partial acid hydrolysis (6 N HCl) for 1 hr at 110°C. The remainder of the sample was saved for tryptic digestion. Alternatively, the ^{32}P-EGP-1 was transferred onto a PVDF membrane and then subjected to partial acid hydrolysis. Phosphoamino acids were analyzed on a cellulose plate (100 μm; Polygram Cel 300, Macherey-Nagel, Doren, Germany) by

thin layer electrophoresis at pH 1.9 (formic acid/acetic acid/H_2O, 5:15.6:179.4) in the first dimension and at pH 3.5 (acetic acid/pyridine/H_2O, 10:1:189) in the second dimension. The ^{32}P-labeled phosphoamino acids were detected first by autoradiography and then the unlabeled phosphoserine, phosphotyrosine, and phosphothreonine, used as internal standards, were stained with 0.25% ninhydrin in acetone.

Tryptic digestion and peptide mapping

Complete tryptic digestion of the *in vitro* ^{32}P-labeled EGP-1 was performed following the method described by Boyle and Hunter (1991) with slight modifications. Briefly, the tryptic digestion was performed for 48 hr at 37°C with the addition of 2 more aliquots of trypsin, 5 μg each, at 12 hr intervals. The total tryptic digest was then lyophilized, resuspended in 1.0 ml of water, and lyophilized again. It was then resuspended in 100 μl 50 mM ammonium bicarbonate at pH 7.8 and passed through a Sephadex G-25 (fine grade; BioRad, Melville, NY) equilibrated with the same buffer. The column was calibrated with stachyose (M, 666.6) and maltose (M, 342.6) before the run. The fractions (0.6 ml) were counted by liquid scintillation. The peak fractions were pooled, lyophilized, resuspended in 2.5 ml of water, and lyophilized again. Finally, the sample was resuspended in 10 μl of water and an aliquot (1.5 μl) was subjected to phosphopeptide analysis in 2 dimensions on a 20 × 20 cm thin layer cellulose plate (100 μm). The digest was analyzed by electrophoresis in the first dimension using pH 8.9 buffer (1.0% ammonium bicarbonate adjusted to pH 8.9 with 30% ammonium hydroxide) and then chromatography was employed in the second dimension using n-butanol/pyridine/acetic acid/H_2O (7.5:5:1.5:6).

To confirm the identity of the phosphopeptide as phosphorylated S-G-K, synthetic phosphotripeptide (*i.e.*, phospho-S-G-K-COOH, synthesized for us by Quality Controlled Biochemicals, Hopkinton, MA) was run as an internal standard along with the sample during phosphopeptides separation. The plate was first autoradiographed and then stained with 0.25% ninhydrin.

RESULTS

EGP-1 is phosphorylated in vivo

In order to establish whether EGP-1 is phosphorylated *in vivo*, ME180 cells were metabolically labeled with ^{32}P-orthophosphate. This cell line was selected due to a high level of expression of EGP-1 (Stein *et al.*, 1994). Since it had been observed that the expression of EGP-1 increases with increasing cell density (data not shown), labeling experiments were performed using cells at greater than 90% confluency. As shown in Figure 1*a*, MAb RS7-3G11 immunoprecipitates a phosphorylated product with a molecular mass of 46–48 kDa (Fig. 1*a*, lane 1). The migration of the phosphorylated protein in SDS-PAGE corresponded to the migration of purified EGP-1 and immunoprecipitated EGP-1 metabolically labeled with [^{35}S]cysteine (data not shown). Immunoprecipitation of the ^{32}P-labeled cell lysate with the non-specific MAb Ag8 did not yield any phosphorylated product corresponding to the molecular mass of EGP-1 (Fig. 1*a*, lane 2). These results indicate that EGP-1 is a phosphoglycoprotein.

Identification of the phosphorylated residue

Since the cytoplasmic domain of EGP-1 contains serine and tyrosine residues, and the consensus site of tyrosine phosphorylation is not well defined (Hanks and Quinn, 1991), we investigated the possibility of phosphorylation of both serine and tyrosine residues. A tyrosine residue is located at position 306 in the context of -S-G-K-Y-K-K- (residues 303–308) in the cytoplasmic domain of EGP-1. To determine whether the EGP-1 is phosphorylated on tyrosine, antiphosphotyrosine MAb 4G10 was used to immunoprecipitate EGP-1 in the presence of 1 mM sodium orthovanadate. Immunoprecipitation studies with 4G10 and RS7-3G11 indicated that the antiphosphotyrosine MAb 4G10 does not recognize EGP-1, implying that EGP-1 is not phosphorylated on tyrosine (data not shown).

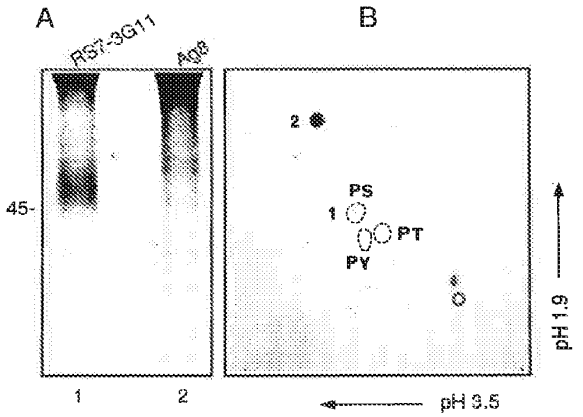


FIGURE 1 – Immunoprecipitation of phosphorylated EGP-1 metabolically labeled with ^{32}P-orthophosphate. *(a)* SDS-PAGE. ME180 cells were incubated with ^{32}P-orthophosphate (250 μCi/ml) for 6 hr in phosphate-free RPMI-1640 medium. The EGP-1 was immunoprecipitated with RS7-3G11 and Ag8 MAbs and resolved by 10% SDS-PAGE without reduction. The gel was dried and autoradiographed. All the steps of immunoprecipitation were performed at 4°C and in the presence of 1 mM sodium orthovanadate. Lane 1: proteins immunoprecipitated with RS7-3G11; lane 2: proteins immunoprecipitated with Ag8. Molecular weight marker ($\times 10^3$) is indicated in the margin. *(b)* Phosphoamino acid analysis of the ^{32}P-EGP-1. Following resolution by 10% SDS-PAGE (unreduced), proteins were blotted onto PVDF membrane and autoradiographed. The band corresponding to ^{32}P-EGP-1 was excised from the blot and hydrolyzed in 6 N HCl for 1 hr. Phosphoamino acids were analyzed as described in the methodology section. Spot 1 corresponds to phosphoserine and spot 2 to ^{32}P-orthophosphate. The origin is shown by 'O' and the directions of electrophoresis are indicated by arrows. Locations of the unlabeled phosphoamino acids are shown by broken circles. The PS, PT, and PY stand for phosphoserine, phosphothreonine, and phosphotyrosine, respectively.

Identification of the phosphorylated residue in EGP-1 was performed by phosphoamino acid analysis of the ^{32}P-EGP-1, phosphorylated *in vivo*. The metabolically labeled ^{32}P-EGP-1 was immunoprecipitated with RS7-3G11 from ME180 cell extract, resolved in 10% SDS-PAGE, transferred onto PVDF membrane, and autoradiographed. The band corresponding to ^{32}P-EGP-1 was excised from the PVDF membrane and then subjected to partial acid hydrolysis followed by electrophoresis (cathode to anode) in 2 dimensions on a thin layer cellulose plate. Unlabeled phosphoserine, phosphothreonine, and phosphotyrosine were included as internal standards. The locations of the standards after 2-dimensional electrophoresis are shown by broken circles in Figure 1*b*. Co-migration of the labeled spot (spot 1) with unlabeled phosphoserine (marked by PS in Fig. 1*b*) indicated that EGP-1, *in vivo*, was phosphorylated on serine and not on tyrosine or threonine residues.

In vitro *phosphorylation of EGP-1 by protein kinases*

There are 2 serine residues in the cytoplasmic domain of EGP-1 that potentially can be phosphorylated, serine 303 and serine 322. The contexts of these serine residues were compared with the consensus motifs of PKA and PKC. PKC, the calcium-dependent protein kinase, recognizes the motifs

OnCusp
Ex. 1002

R/K_{1-3}-X_{0-2}-S/T-X_{0-2}-R/K_{1-3} > S/T-X_{0-2}-R/K_{1-3} > R/K_{1-3}-X_{0-2}-S/T for phosphorylation. PKA, the cyclic AMP-dependent protein kinase, recognizes the motifs R-R/K-X-S/T > R-X-X-S/T = R-X-S/T, where X is any amino acid (Kennelly and Krebs, 1991). The contexts of both of the cytoplasmic domain serine residues in EGP-1 (serine 303, R-R-K-S-G-K, and serine 322, R-K-E-P-S-L) are compatible to PKC consensus sequences and close to PKA consensus sequences. Due to the inherent flexibility of the consensus sequences it was necessary to consider the possibility that EGP-1 could be a substrate for either kinase.

Both kinases were examined for their ability to phosphorylate purified EGP-1 *in vitro*. In this study only phosphatidylserine was used as an activator in the reaction mixture of PKC in the presence of Ca^{2+}. The PKA reaction was performed in the presence of 5 mM Mg^{2+}. The results of these experiments are shown in Figure 2. The sample was used, both untreated and after boiling, to examine both native and denatured forms. No bands of phosphorylated EGP-1 were observed when either untreated (*i.e.*, native) or boiled (*i.e.*, denatured) EGP-1 was incubated with PKA (Fig. 2*a*, lanes 3 and 4, respectively). Histone type III-SS (both unboiled and boiled), used as a positive control, was phosphorylated by PKA (Fig. 2*a*, lanes 1 and 2, respectively). On the other hand, when incubated with PKC, purified EGP-1 became phosphorylated *in vitro* and was observed as a 47 kDa band (Fig. 2*b*, lane 2). Reduction of purified EGP-1 had been shown to yield a doublet around 45 kDa. A similar doublet pattern was also observed with the phosphorylated form of EGP-1 (Fig. 2*b*, lane 3), as indicated by minor arrows on the right margin of Figure 2*b*. Phosphorylation of histone type III-SS, used as a control, is also shown (Fig. 2*b*, lane 1, unreduced and lane 4, reduced). The band of autophosphorylated PKC (approximately 80 kDa) is marked by the major arrows on the left and right margins in Figure 2*b*. These results demonstrate that PKC and not PKA is involved in phosphorylating EGP-1 *in vitro*. The effect of Mn^{2+} instead of Mg^{2+} as the divalent cation on phosphorylation of EGP-1 by PKA has not been examined.

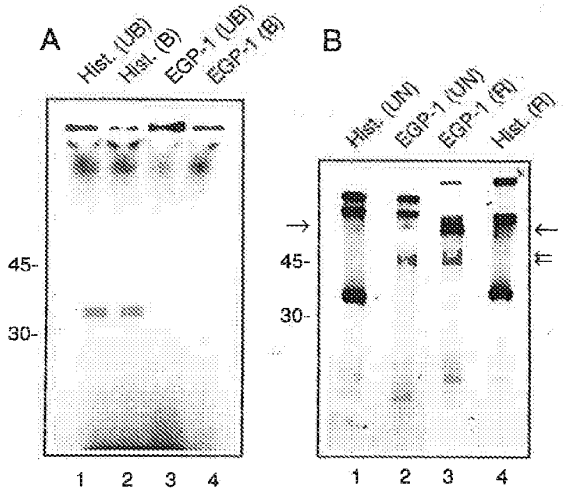


FIGURE 2.—Phosphorylation of EGP-1 by protein kinases. *(a)* Purified EGP-1 (200 ng, both boiled and unboiled) was incubated *in vitro* with PKA (catalytic subunit, 20 ng) in the presence of [γ-^{32}P]ATP (0.84 μCi) and 5 mM Mg^{2+}. Histone type III-SS (400 ng) was used as positive control. The reaction mixtures were resolved in 10% SDS-PAGE, and the gel was dried and autoradiographed. Lanes 1 and 2: unboiled (UB) and boiled (B) histone type III-SS (HIST.); lanes 3 and 4: unboiled and boiled EGP-1. *(b)* Purified EGP-1 (200 ng) incubated with protein kinase C (20 ng) in the presence of [γ-^{32}P]ATP (2.5 μCi), Ca^{2+} (1 mM), and phosphatidylserine. Histone type III-SS (400 ng) was used as positive control. Lanes 1 and 4: unreduced (UN) and reduced (R) histone type III-SS; lanes 2 and 3: unreduced and reduced phosphorylated EGP-1 (47 kDa), respectively. The autophosphorylated PKC is indicated by the major arrows. The bands of reduced EGP-1 (lane 3) are shown by minor arrows. Phosphorylated histone is seen at approximately 35 kDa.

Confirmation of the enzymatic labeling of EGP-1 by PKC

To confirm the involvement of PKC in the phosphorylation of EGP-1, control studies were performed under various reaction conditions. PKC requires calcium and phosphatidylserine for its activity (Takai *et al.*, 1979*a*). Among different phospholipids, phosphatidylserine has been shown to be the most effective phospholipid for activation of PKC (Takai *et al.*, 1979*b*). Diolein, a synthetic unsaturated diacylglycerol, and free arachidonic acid have been shown to augment the activity of PKC when used at low concentrations (Sekiguchi *et al.*, 1988; Takai *et al.*, 1979*c*). It has also been reported by Sekiguchi *et al.* (1988) that at a concentration of 0.4 mM or higher, free arachidonic acid inhibits the activities of the α-, β-, and γ-subtypes of PKC to varying extents (Sekiguchi *et al.*, 1988). The effects of calcium, phosphatidylserine, diolein, and free arachidonic acid on EGP-1 phosphorylation were evaluated to confirm the participation of PKC in this reaction *in vitro*. The results of these experiments are shown in Figure 3. The phosphorylation of EGP-1 (47 kDa band) was increased when diolein was added to the reaction mixtures containing either Ca^{2+} alone (Fig. 3*a*, lanes 1 and 3) or only phosphatidylserine (Fig. 3*b*, lanes 1 and 3) or both (Fig. 3*c*, lanes 1 and 3) indicating increased activity of PKC under these conditions. Free arachidonic acid at a concentration of 0.4 mM, on the other hand, inhibited EGP-1 phosphorylation under all of the conditions examined (lane 2 in Fig. 3*a–c*). Phosphorylation of EGP-1 was greater in the presence of phosphatidylserine alone (Fig. 3*b*, lane 1) than in the presence of Ca^{2+} alone (Fig. 3*a*, lane 1). The phosphorylation of EGP-1 by PKC was even greater when both Ca^{2+} and phosphatidylserine were present (Fig. 3*c*, lane 1). In the absence of both Ca^{2+} and phosphatidylserine, phosphorylation of EGP-1 by PKC was not observed (data not shown). Although dependency of PKC *in vitro* on Ca^{2+}, phosphatidylserine, and diacylglycerol varies with phosphate acceptor (Nishizuka, 1989), these results are typical of those characteristics reported for PKC. The consistency of these results with the known properties of PKC, along with the fact that no phosphorylation occurred on EGP-1 in the absence of PKC (data not shown), demonstrated the involvement of PKC in phosphorylating EGP-1 *in vitro*.

In another approach to show that the phosphorylation of purified EGP-1 is an enzyme-mediated process, the competition between [γ-^{32}P]ATP and excess of unlabeled ATP in the reaction mixture of PKC was evaluated. The study utilized approximately 50-, 500-, 1,250-, and 2,500-fold excess of unlabeled ATP. There was a gradual decrease of the signal intensities of ^{32}P-EGP-1 in the autoradiogram from uncompeted to the increasingly competed samples (data not shown), suggesting that other variables remaining constant, phosphorylation of EGP-1 *in vitro* is ATP dependent.

Calf intestinal alkaline phosphatase was used to show that phosphorylated EGP-1 is a substrate for phosphatase. The *in vitro* labeled ^{32}P-EGP-1 was allowed to react with 5 U of calf intestinal alkaline phosphatase. Phosphorylated EGP-1 and phosphatase-treated phosphorylated EGP-1 were resolved in 10% SDS-PAGE and autoradiographed. Histone type III-SS was used as positive control. The results are shown in Figure 4. The disappearance of the band corresponding to ^{32}P-EGP-1 (Fig. 4, lane 1) after alkaline phosphatase treatment (Fig. 4, lane 3) demonstrated that ^{32}P-EGP-1 could be dephosphory-

OnCusp
Ex. 1002

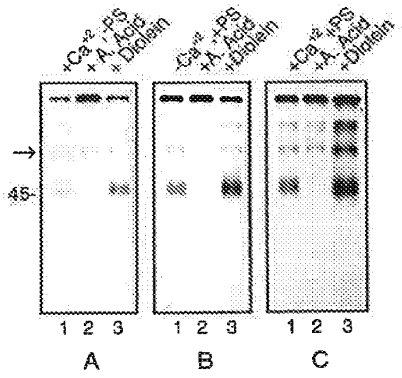


FIGURE 3 – Effects of Ca^{2+}, phosphatidylserine (PS), diolein, and free arachidonic acid on *in vitro* phosphorylation of EGP-1 by PKC. EGP-1 (200 ng) was phosphorylated (2.5 μCi of [^{32}P]ATP) *in vitro* by PKC under various conditions. Aliquots of the reaction mixtures (approximately 12.5 ng of EGP-1) were resolved in 10% SDS-PAGE, and the gel was dried and then autoradiographed. *(a)* Reactions performed in the presence of Ca^{2+} (0.5 mM) and without phosphatidylserine. Lane 1: Ca^{2+} only; lane 2: with 0.4 mM free arachidonic acid (A. acid); lane 3: with 4.0 μM diolein. *(b)* Reactions performed in the presence of phosphatidylserine (0.31 mg/ml) and without Ca^{2+}. Lane 1: PS only; lane 2: with 0.4 mM free arachidonic acid; lane 3: with 0.4 μM diolein. *(c)* Reactions performed in the presence of both Ca^{2+} (0.5 mM) and phosphatidylserine (0.31 mg/ml). Lane 1: both Ca^{2+} and PS; lane 2: with free arachidonic acid (0.4 mM); lane 3: with diolein (0.4 μM). EGTA (5 mM) was added to those reaction mixtures without Ca^{2+}. The 47 kDa bands represent the phosphorylated EGP-1. Arrow indicates the autophosphorylated PKC. Molecular weight markers ($\times 10^3$) are indicated in the margin.

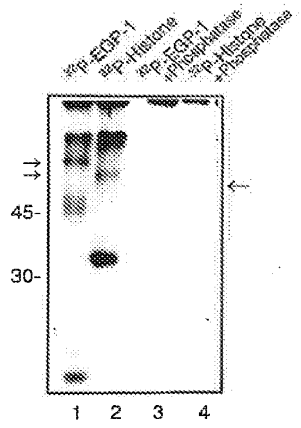


FIGURE 4 – Dephosphorylation of phosphorylated EGP-1 with calf intestinal alkaline phosphatase. Purified EGP-1 was phosphorylated *in vitro* by PKC with [γ-^{32}P]ATP (0.84 μCi). The phosphorylated EGP-1 (50 ng) was treated with 5 units of alkaline phosphatase. ^{32}P-EGP-1 and phosphatase treated ^{32}P-EGP-1 were subjected to 10% SDS-PAGE, and the gel was then dried and autoradiographed. Histone type III-SS was used as a positive control. Lane 1: phosphorylated EGP-1 (12.5 ng); lane 2: phosphorylated histone (25 ng); lane 3: phosphatase-treated phosphorylated EGP-1 (25 ng); lane 4: phosphatase-treated phosphorylated histone (50 ng). Autophosphorylated PKC is indicated by minor arrows. Molecular weight markers ($\times 10^3$) are indicated in the margin. The bands (marked by the major arrow) in the dephosphorylation lanes (lanes 3 and 4) are probably enzyme backgrounds.

lated by calf intestinal alkaline phosphatase. Phosphorylated and dephosphorylated histone type III-SS are shown in Figure 4, lanes 2 and 4, respectively.

The stoichiometry of phosphorylation of EGP-1 by PKC *in vitro* was determined in the presence of Ca^{2+} (1 mM) and phosphatidylserine (0.31 mg/ml). No activator of PKC, *e.g.*, diolein, was added to the reaction mixture. The incorporation of phosphate was 0.54 mole of phosphate per mole of the EGP-1, which is in the biologically relevant range.

Serine residue(s) is phosphorylated by PKC in vitro

In order to determine whether serine or threonine or both these residues of EGP-1 were phosphorylated by PKC *in vitro*, phosphoamino acid analysis of the *in vitro*-phosphorylated ^{32}P-EGP-1 was performed. The result of 2-dimensional analysis of the phosphoamino acids is shown in Figure 5. Co-migration of the labeled spot (spot 1) with the unlabeled phosphoserine internal standard (shown by broken circle and marked by PS) indicated that serine was the only amino acid phosphorylated *in vitro* by PKC. The phosphorylation of serine in EGP-1 *in vitro* by PKC and the *in vivo* phosphorylation of EGP-1 on serine suggest that PKC is most likely engaged in phosphorylating EGP-1 *in vivo*.

Phosphorylation of EGP-1 on serine 303 by PKC in vitro

The phosphorylation of EGP-1 by PKC could either be on serine 303 or serine 322 or both in the contexts of -R-K-S-G-K-Y-K- (residue 301–307) and -R-K-E-P-S-L (residue 318–323). To determine which serine residue(s) is phosphorylated, phosphopeptide mapping of the ^{32}P-EGP-1 was performed. Based on the established sequence of EGP-1 (Linnenbach *et al.*, 1989), complete digestion of EGP-1 with trypsin should yield either a tripeptide consisting of the sequence -S (PO_3)-G-K-, or a tetrapeptide consisting of the sequence -E-P-S(PO_3)-L, or both. The tryptic digest was passed through a Sephadex G-25 column and only one radiolabeled peak was obtained. Due to the acidic nature of the expected phosphopeptides, first-dimension electrophoresis of the tryptic digest was performed using pH 8.9 buffer. Being more hydrophobic than the phosphotripeptide, the phosphotetrapeptide should migrate at a different location when chromatographed in the second dimension using organic solvent. Figure 6 shows the result of phosphopeptide mapping of the ^{32}P-EGP-1. Two spots appeared in the autoradiogram. Spot 1 represents the majority of the phosphorylated product. Unlabeled phosphotripeptide, S(PO_3)-G-K, used as an internal standard and stained with ninhydrin, migrated at the same spot (indicated by broken circle) where the majority of the radioactivity was retained (spot 1), thus confirming the sequence of the labeled peptide. The minor spot in the autoradiogram (indicated by a minor arrow and representing less than 5% of the radioactivity in spot 1) may represent either inefficiently phosphorylated tetrapeptide or incompletely digested phosphopeptide generated from the (^{32}P-serine$_{303}$)-EGP-1. These possibilities were not investigated further. The results of this study suggest that the sequence R-R-K-S-G-K (residue 300–305) is the major site of phosphorylation on EGP-1 and that serine 303, present in the cytoplasmic domain, is the target amino acid for PKC. Whether serine 303 is the only site or the major site of phosphorylation on EGP-1 for PKC remains to be confirmed.

Phosphorylation of EGP-1 in vivo *by PKC*

Phorbol esters are known to activate PKC directly *in vivo*, circumventing normal activation processes (Castagna *et al.*, 1982). To determine whether EGP-1 is phosphorylated by PKC *in vivo*, ME180 cells were treated with phorbol 12-myristate 13-acetate (PMA, 150 ng/ml) for 15 min after metabolically labeling the cells with ^{32}P-orthophosphate (150

OnCusp
Ex. 1002

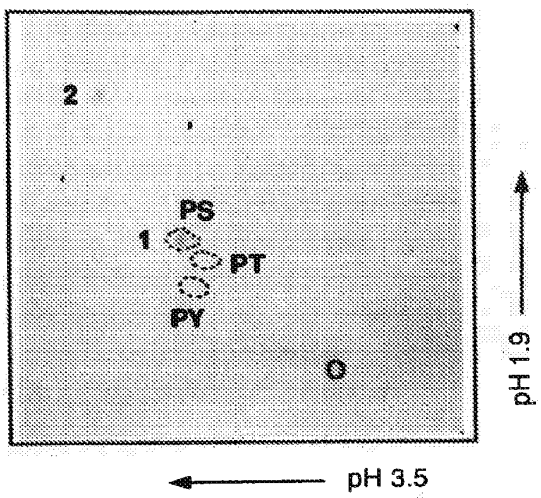


FIGURE 5 – Phosphoamino acid analysis of EGP-1 phosphorylated *in vitro* by PKC. Purified EGP-1 (200 ng) was phosphorylated *in vitro* using [γ-^{32}P]ATP (0.84 μCi). The ^{32}P-EGP-1 was digested with 6 N HCl for 1 hr and the phosphoamino acids were analyzed as described in the methodology sections. Spot 1 corresponds to phosphoserine; spot 2 corresponds to ^{32}P-orthophosphate. The origin is marked by 'O'. The directions of electrophoresis are indicated by arrows. Broken circles represent the locations of unlabeled phosphoamino acids. PS, PT, and PY stand for phosphoserine, phosphothreonine, and phosphotyrosine, respectively.

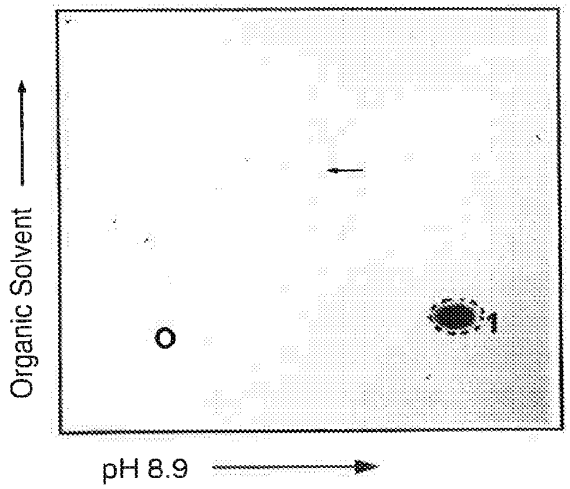


FIGURE 6 – Peptide analysis of ^{32}P-EGP-1 phosphorylated *in vitro* by PKC. *In vitro* phosphorylated EGP-1 was digested with trypsin for 48 hr. The trypsin-digested sample was then passed through a Sephadex G-25 column and the fractions were collected. An aliquot of the fraction corresponding to the peak activity was subjected to 2-dimensional peptide-mapping analysis on a thin layer cellulose plate along with an internal standard [S(PO_3)-G-K], as described in the methodology section. The plate was autoradiographed. Spot 1 represents the location of the phosphotripeptide. The origin is indicated by 'O' and the minor spot by an arrow. The unlabeled phosphotripeptide was detected by ninhydrin staining. The directions of electrophoresis with pH 8.9 buffer and thin layer chromatography with organic solvents are shown by arrows.

μCi/ml) for 6 hr. Cells were lysed and equal quantities of cell extracts (either treated or control) were subjected to immunoprecipitation with either RS7-3G11 or Ag8 in the presence of sodium orthovanadate (1 mM). Half of each immunoprecipitated sample was analyzed in 10% SDS-PAGE and autoradiographed. The results are shown in Figure 7. When treated with PMA, phosphorylation of EGP-1 was increased approximately 2-fold above the basal level (compare lanes 2 and 3 in Fig. 7). No phosphorylated EGP-1 was observed in the immunoprecipitate of non-specific antibody, Ag8 (Fig. 7, lane 1). These results support the involvement of PKC in phosphorylating the EGP-1 *in vivo*. Further investigation is under way to reveal the identity of the low m.w. phosphorylated product (approx. 21 kDa), which was co-immunoprecipitated with EGP-1 (Fig. 7, lanes 2 and 3). The signal intensity of the 21 kDa band immunoprecipitated with RS7-3G11 increased approximately 3-fold when ME180 cells were stimulated with PMA, compared with the unstimulated cells. This may be due to either increased association of the phosphorylated 21 kDa protein with EGP-1 or to increased phosphorylation of the 21 kDa protein under these conditions.

Discussion

PKC activation, induced by diacyl glycerol, is a major pathway by which information from external signals is transferred into the cell interior. Several lines of evidence suggest that PKC is a target of tumor promotors, which presumably have both positive and negative actions depending on the function of the target substrate protein. PKC has been proposed to be involved in a number of short- and long-term cellular responses in different tissues and cells. These include secretion of mucins, various hormones, enzymes, and neurotransmitters, transport of glucose and hexose, inhibition of gap junctions, muscle contraction, steroidogenesis, and lipogenesis, and activation of B and T cells (Nishizuka, 1986). The number of proposed substrate proteins of PKC is increasing as more cellular processes are studied in detail (Nishizuka, 1986). We report here that the epithelial/carcinoma-associated antigen EGP-1 is phosphorylated *in vivo* and that it is a substrate for PKC. Specifically, serine 303, present in the cytoplasmic domain of EGP-1, is phosphorylated. *In vivo* studies showed that when ME180 cells were treated with PMA, phosphorylation of EGP-1 was increased by approximately 2-fold above the level in the untreated cells, suggesting the involvement of PKC in phosphorylating the antigen *in vivo*.

Some basic proteins or polypeptides undergo non-enzymatic phosphorylation when incubated with α-^{32}P- or γ-^{32}P-labeled ATP at high pH (Abdel-Ghany *et al.*, 1988). Since the cytoplasmic domain of EGP-1 is basic in nature (containing 9 out of 25 basic amino acid residues), it was necessary to demonstrate that the phosphorylation we observed was indeed enzymatic. In fact, the chance of nonenzymatic phosphorylation on serine residue(s) in the cytoplasmic domain of EGP-1 could not be ruled out even if the pH used for the phosphorylation assays *in vitro* were physiological. This point was confirmed by several lines of evidence: 1) *in vitro* studies with purified EGP-1 showed no autophosphorylation when incubated at 30°C and pH 7.5 in the presence of [γ-^{32}P]ATP (data not shown); 2) competition of the [γ-^{32}P]ATP with increasing concentrations of unlabeled ATP showed that there is a distinct dependence on ATP for the phosphorylation of EGP-1 in the presence of PKC; 3) alkaline phosphatase recognizes the phosphorylated antigen as a substrate, which probably would not be expected for a non-enzymatically phosphorylated product; 4) there was modulation of phosphorylation of EGP-1 by

OnCusp
Ex. 1002

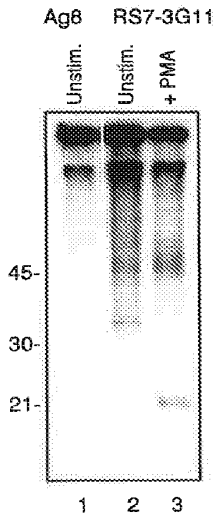


FIGURE 7 – Effect of PMA on the phosphorylation state of EGP-1. ME180 cells were metabolically labeled with ^{32}P-orthophosphate for 6 hr, and then stimulated with PMA (150 ng/ml) for 15 min. ^{32}P-EGP-1 was immunoprecipitated with either RS7-3G11 or Ag8. Following resolution in 10% SDS-PAGE, the gel was autoradiographed. Lane 1: immunoprecipitate of Ag8; lanes 2 and 3: immunoprecipitates of RS7-3G11, untreated and treated with PMA, respectively.

Ca^{2+}, phosphatidylserine, diolein, and free arachidonic acid in the presence of PKC; and 5) the stoichiometry of phosphorylation for EGP-1 (0.54 mol of phosphate per mole of EGP-1), determined *in vitro*, was in the physiologically expected range.

The PKC utilized in these studies (United Biochemical, Lake Success, NY) was a mixture of α-, β-, and γ-subtypes from rat brain. Different conditions lead to preferential activation or inactivation of a particular subtype of PKC (Sekiguchi *et al.*, 1988; Kaibuchi *et al.*, 1981). All the subtypes of PKC are activated by diolein to variable extents in the presence of Ca^{2+} and phosphatidylserine. Phosphatidylserine alone, at a high concentration of Ca^{2+}, can cause a substantial activation of all subtypes. Type I, the γ-subtype, is less sensitive to diolein and is activated about 50% by a low concentration (50 μM) of free arachidonic acid. At a high concentration (400 μM), however, arachidonic acid inhibits the γ-subtype. Type II, the β-subtype, is well activated by diolein and also, to a reasonable degree, by a high concentration of free arachidonic acid. This subtype also shows about 60% of its activity without any added Ca^{2+}. Type III, the α-subtype, responds well to diolein and exhibits almost full activity with free arachidonic acid in the presence of high concentrations of Ca^{2+} without requiring phosphatidylserine or diolein. The various subspecies of PKC are expressed differentially in diverse tissues (for review see Sekiguchi *et al.*, 1988). Type I (γ-subspecies) is expressed only in the brain and spinal cord. Among the type II kinds (β-subspecies), βII is more prevalent than βI in many tissues including heart, liver, lung, kidney, spleen, and testis. Only type III (α-subspecies) is expressed universally. Which subtype of PKC is engaged in EGP-1 phosphorylation remains to be established. The γ-subspecies of PKC is the only subtype that becomes almost completely inactivated at a high concentration of free arachidonic acid and since EGP-1 could not be phosphorylated by PKC (*i.e.*, the mixture of α-, β-, and γ-subspecies) under different conditions in the presence of 0.4 mM arachidonic acid, it appeared logical to believe that the γ-subspecies of PKC was involved in phosphorylating EGP-1 *in vitro*. However, considering the expression of EGP-1 in different tissues we can speculate that probably PKC type III (α-subspecies) is responsible for the phosphorylation of EGP-1 *in vivo*. Whether EGP-1 is constitutively phosphorylated by PKC in vivo or this phosphorylation is a response to a definite stimulus also remains to be evaluated.

The dependence of phosphorylation of EGP-1 on phosphatidylserine and Ca^{2+} suggests that EGP-1 is a component of a Ca^{2+}-dependent signal transduction pathway, probably the inositol triphosphate/diacylglycerol-dependent pathway driven by a ligand involving PKC. However, the specific role of EGP-1 in cellular processes in relation to the activity of PKC remains to be elucidated. In different cell lines, rapid internalization of tumor necrosis factor receptor or transferrin receptor can be induced by phorbol esters irrespective of ligand occupancy (Aggarwal and Eessalu, 1987; Klausner *et al.*, 1984). Hyperphosphorylation of transferrin receptors by PKC stimulated by phorbol ester has been shown to be the cause of internalization of these receptors in HL60 cells (May *et al.*, 1984). The rates of internalization induced by ligand or phorbol ester are comparable (Klausner *et al.*, 1984). It had been shown by Stein *et al.* (1993) that the rate of internalization of EGP-1-RS7-3G11 complex is fairly rapid in an adenocarcinoma cell line, Calu-3. Whether internalization is facilitated by phosphorylation of EGP-1 on serine 303 *in vivo* remains to be determined. If this is found to be the case, then the existence of an as yet unidentified ligand interacting with EGP-1 is likely.

It has been suggested that EGP-2, the other member of this gene family, is involved in cell-cell adhesion and epithelial-specific cell sorting in a calcium-independent manner (Litvinov *et al.*, 1994). The expression of EGP-1 is more restricted than EGP-2, being negative, for example, in colon cancer and normal colon epithelium (Stein *et al.*, 1993, 1990). The tissue distribution, along with the evidence presented in this report, suggests that EGP-1 may have a more specific function involving signal transduction.

ACKNOWLEDGEMENTS

This work was supported in part by Outstanding Investigator Grant CA39841 from the National Cancer Institute, NIH (DMG).

REFERENCES

ABDEL-GHANY, M., RADEN, D. and KATCHALSKI-KATZIR, E., Phosphorylation of synthetic random polypeptides by protein kinase P and other protein-serine (threonine) kinases and stimulation or inhibition of kinase activities by microbial toxins. *Proc. nat. Acad. Sci. (Wash.)*, **85**, 1408–1411 (1988).

AGGARWAL, B.B. and EESSALU, T.E., Effect of phorbol esters on down-regulation and redistribution of cell surface receptors for tumor necrosis factor-α. *J. biol. Chem.*, **262**, 16450–16455 (1987).

BLUM, H., BEIER, H. and GROSS, H.J., Improved silver staining of plant proteins, RNA and DNA in polyacrylamide gels. *Electrophoresis*, **8**, 93–99 (1987).

BOYLE, B. and HUNTER, T., *Laboratory manual of Hunter thin layer electrophoresis system*. C.B.S., Del Mar, CA (1991).

CASTAGNA, M., TAKAI, Y., KAIBUCHI, K., SANO, K., KIKKAWA, U. and NISHIZUKA, Y., Direct activation of calcium-activated, phospholipid-dependent protein kinase by tumor-promoting phorbol esters. *J. biol. Chem.*, **257**, 7847–7851 (1982).

COOPER, J.A., SEFTON, B.M. and HUNTER, T., Detection and quantifi-

cation of phosphotyrosine in proteins. *Methods Enzymol.* **99,** 387–402 (1983).

De Leij, L., Helrich, W., Stein, R. and Mattes, M.J., SCLC-cluster-3 antibodies detect the pancarcinoma/epithelial glycoprotein EGP-2. *Int. J. Cancer,* Suppl **8,** 60–63 (1994).

Hanks, S.K., and Quinn, A.M. Protein kinase catalytic domain sequence database: identification of conserved features of primary structure and classification of family members. *Methods Enzymol.,* **200,** 38–81 (1991).

Kaibuchi, K., Takai, Y. and Nishizuka, Y., Cooperative roles of various membrane phospholipids in the activation of calcium-activated, phospholipid-dependent protein kinase. *J. biol. Chem.,* **256,** 7146–7149 (1981).

Kennelly, P.J. and Krebs, E.G., Consensus sequences as substrate specificity determinants for protein kinases and protein phosphatases. *J. biol. Chem.,* **266,** 15555–15558 (1991).

Klausner, D., Harford, J. and Renswoude, J.V., Rapid internalization of the transferrin receptor in K562 cells is triggered by ligand binding or treatment with a phorbol ester. *Proc. nat. Acad. Sci. (Wash.),* **81,** 3005–3009 (1984).

Laemmli, U.K., Cleavage of structural proteins during the assembly of the head of bacteriophage. *Nature (Lond.),* **227,** 680–685 (1970).

Linnenbach, A.J., Seng, B.A., Wu, S., Robbins, S., Scollon, M., Pyrc, J.J., Druck, T. and Huebner, K., Retroposition in a family of carcinoma-associated antigen genes. *Mol. cell. Biol.,* **13,** 1507–1515 (1993).

Linnenbach, A.J., Wojcierowski, J., Wu, S., Pyrc, J.J., Ross, A.H., Dietzschold, B., Speicher, D. and Koprowski, H., Sequence investigation of the major gastrointestinal tumor-associated antigen gene family, GA733. *Proc. nat. Acad. Sci. (Wash.),* **86,** 27–31 (1989).

Litvinov, S.V., Velders, M.P., Bakker, H.A.M., Fleuren, G.J. and Warnaar, S.O., Ep-CAM: a human epithelial antigen is a homophilic cell-cell adhesion molecule. *J. Cell Biol.,* **125,** 437–446 (1994).

May, W.S., Jacobs, S. and Cuatrecasas, P., Association of phorbol ester-induced hyperphosphorylation and reversible regulation of transferrin membrane receptors in HL60 cells. *Proc. nat. Acad. Sci. (Wash.),* **81,** 2016–2020 (1984).

Nishizuka, Y., Studies and perspectives of protein kinase C. *Science,* **233,** 305–312 (1986).

Nishizuka, Y., Studies and prospectives of the protein kinase C family for cellular regulation. *Cancer,* **63,** 1892–1903 (1989).

Park, H.-Y. and Campaisi, J., Posttransiational control of cyclic AMP-dependent protein kinase by phorbol ester in normal but not in chemically transformed 3T3 cells. *Cancer Res.,* **50,** 7145–7152 (1990).

Ross, A.H., Lubeck, M., Steplewski, Z. and Koprowski, H., Identification and characterization of the CO17-1A carcinoma-associated antigen. *Hybridoma* **5,** Suppl. **1,** s21–s28 (1986).

Sekiguchi, K., Tsukuda, M., Ase, K., Kikkawa, U. and Nishizuka, Y., Mode of activation and kinetic properties of three distinct forms of protein kinase C from rat brain. *J. Biochem.,* **103,** 759–765 (1988).

Stein, R., Basu, A., Chen, S., Shih, L.B. and Goldenberg, D.M., Specificity and properties of MAb RS7-3G11 and the antigen defined by this pancarcinoma monoclonal antibody. *Int. J. Cancer,* **55,** 938–946 (1993).

Stein, R., Basu, A., Goldenberg, D.M., Lloyd, K.O. and Mattes, M.J., Characterization of cluster 13: the epithelial/carcinoma antigen recognized by MAb RS7. *Int. J. Cancer,* Suppl. **8,** 98–102 (1994).

Stein, R., Chen, S., Sharkey, R.M. and Goldenberg, D.M., Murine monoclonal antibodies raised against human non-small cell carcinoma of the lung: specificity and tumor targeting. *Cancer Res.,* **50,** 1330–1336 (1990).

Szala, S., Froenlich, M., Scollon, M., Kasai, Y., Steplewski, Z., Koprowski, H. and Linnenbach, A.J., Molecular cloning of cDNA for the carcinoma associated antigen GA733-2. *Proc. nat. Acad. Sci. (Wash.),* **87,** 3542–3546 (1990).

Takai, Y., Kishimoto, A., Iwasa, Y., Kawahara, Y., Mori, T. and Nishizuka, Y., Calcium-dependent activation of a multifunctional protein kinase by membrane phospholipids. *J. biol. Chem.,* **254,** 3692–3695 (1979*a*).

Takai, Y., Kishimoto, A., Iwasa, Y., Kawahara, Y., Mori, T., Nishizuka, Y., Tamura, A. and Fujii, T., A role of membranes in the activation of a new multifunctional protein kinase system. *J. Biochem.,* **86,** 575–578 (1979*b*).

Takai, Y., Kishimoto, A., Kikkawa, U., Mori, T. and Nishizuka, Y., Unsaturated diacylglycerol as a possible messenger for the activation of calcium-activated, phospholipid-dependent protein kinase system. *Biochem. biophys. Res. Comm.,* **91,** 1218–1224 (1979*c*).

May 9, 2016

DISCOVERY MEDICINE

Article Published in the Author Account of

Alain Beck

The Next Generation of Antibody–drug Conjugates Comes of Age

Published on October 16, 2010

Author: Alain Beck

Specialty: Drug Discovery, Immunology, Chemistry
Institution: Centre d'Immunologie Pierre Fabre (CIPF)
Address: St Julien-en-Genevois, 74164, France

Author: Jean-Francois Haeuw

Specialty: Drug Discovery, Immunology, Chemistry
Institution: Centre d'Immunologie Pierre Fabre (CIPF)
Address: St Julien-en-Genevois, 74164, France

Author: Thierry Wurch

Specialty: Drug Discovery, Immunology, Chemistry
Institution: Centre d'Immunologie Pierre Fabre (CIPF)
Address: St Julien-en-Genevois, 74164, France

Author: Liliane Goetsch

Specialty: Drug Discovery, Immunology, Chemistry
Institution: Centre d'Immunologie Pierre Fabre (CIPF)
Address: St Julien-en-Genevois, 74164, France

Author: Christian Bailly

Specialty: Drug Discovery, Immunology, Chemistry
Institution: Centre d'Immunologie Pierre Fabre (CIPF)
Address: St Julien-en-Genevois, 74164, France

Author: Nathalie Corvaia

Specialty: Drug Discovery, Immunology, Chemistry
Institution: Centre d'Immunologie Pierre Fabre (CIPF)
Address: St Julien-en-Genevois, 74164, France

Abstract: Monoclonal antibodies (mAbs) and derivatives are currently the fastest growing class of therapeutic molecules. More than 30 G-type immunoglobulins (IgG) and related agents have been approved over the past 25 years mainly for cancers and inflammatory diseases. In oncology, mAbs are often combined with cytotoxic drugs to enhance their therapeutic efficacy. Alternatively, small anti-neoplastic molecules can be chemically conjugated to mAbs, used both as carriers (increased half-life) and as targeting agents (selectivity). Potential benefits of antibody–drug conjugates (ADCs), strategies, and development challenges are discussed in this review. Several examples of ADCs are presented with emphasis on three major molecules currently in late clinical development as well as next generation thio-mAbs conjugates with improved therapeutic index.

Access PDF as a Subscriber
Purchase/Download This F
Related Articles
Email This Article
Share This Article

Introduction/Background: Conjugating Cytotoxic Drugs to Antibodies

Antibody drug-conjugates (also called immuno-conjugates) are constituted by a recombinant antibody covalently bound by a synthetic linker to a given cytotoxic chemical (Chari, 2008). The main objective is to combine the pharmacological potency of "small" cytotoxic drugs (300 to 1,000 Da) and the high specificity of monoclonal antibodies (150 kDa, Figure 1) for tumor-associated antigen targets. Anti-neoplastic drugs like doxorubicin, daunomycin, vinca-alkaloids, and taxoids, to name a few, have demonstrated their ability to kill cancer cells (Bailly, 2009), but generally with limited selectivity and high toxic

effects on normal cells yielding marginal therapeutic indices. On the other hand, approved naked antibody drugs such as rituximab, trastuzumab, cetuximab, bevacizumab, panitumumab, alemtuzumab, and ofatumumab have demonstrated their therapeutic utility in malignancies, but often in combination with small cytotoxic drugs to achieve significant clinical efficacy. Since the use of mAbs as a single agent is sub-optimal, many strategies are investigated including enhancement of intrinsic Fc-linked effector functions by glycoengineering (Beck et al., 2010a), the use of bispecific antibodies, polyclonal antibodies, and conjugates (Beck et al., 2010b; Beck et al., 2010c). Covalent conjugation of mAbs and drugs with synthetic chemical linkers is not a recent concept. In the 1960s the use of ADCs in animal models was described in the literature, and in the 1980s, clinical trials with murine IgG-based ADCs were conducted.

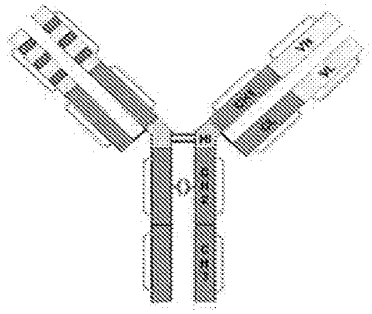


Figure 1. Structure of humanized IgG1. All current approved therapeutic antibodies are IgGs or their derivatives. Human G immunoglobulins are tetrameric glycoproteins (150 kDa) composed of two heavy chains (HC, 50 kDa) and two light chains (LC, 25 kDa). They are divided in four subclasses or isotypes defined by different heavy chains (γ1, γ2, γ3, and γ4). They share greater than 90% sequence homology in their constant domains but differ significantly in the hinge region. Disulfide bridges (sixteen for IgG1 and IgG4; eighteen for IgG2) and non-covalent interactions maintain their 3-dimensional structure. The heavy and light chains are linked by one disulfide bond and the heavy chains by two (for IgG1 and IgG4) or three (for IgG2) disulfide bonds, all located in the small hinge domain, which also contains a papain cleavage site yielding two Fab and one Fc fragments (50 kDa each). The other twelve or fourteen cysteine bridges are intramolecular and delimit six different globular domains: one variable (VL) and one constant (CL) for the light chain; one variable (VH) and three constant (CH1, CH2, and CH3) for the heavy chain. Each variable domain contains also 3 Complementary Determining Regions (CDRs), a short sequence up to 13 amino acids. The CDRs are the most variable parts of IgGs and contribute to their diversity by making contacts with a specific antigen, allowing IgGs to recognize a vast repertoire of antigens with a high affinity (Beck et al., 2009).

Unfortunately so far, the clinical successof immuno-conjugates is very limited compared to naked IgGs (Haeuw et al., 2009). Only onedrug, namely gemtuzumab ozogamicin (Mylotarg; anti-CD33 mAb conjugated to calicheamycin, Pfizer/Wyeth) has been approved by the Food and Drug Administration (FDA) in 2000 for the treatment of patients with acute myeloid leukemia (AML). This ADC was never approved in Europe and recently was voluntarily withdrawn from the U.S. market by the sponsor company. The required post-approval study combining chemotherapy and Mylotarg did not demonstrate improved survival and furthermore the fatal toxicity rate was higher in patients treated with gemtuzumab plus chemotherapy compared to patients treated with chemotherapy alone. Gemtuzumab ozogamicin is a heterogeneous mixture of 50% conjugates (0 to 8 calicheamycin moieties per IgG molecules with an average of 2 or 3, randomly linked to solvent exposed lysyl residues of the antibody) and 50% unconjugated antibody (Bross et al., 2001; Labrijn et al., 2009). Nonetheless, this first compound may be considered as a Trojan horse for the ADC field. All the extensive recorded data and the lessons learned from this first-in-class ADC helped to pave the way for the next generation immuno-conjugates. At least fifteen promising new immuno-conjugates are currently investigated in clinical trials (Table 1). They include molecules with optimized linkers that are hydrolysable in the cytoplasm, resistant or susceptible to proteases, or resistant to multi-drug resistance efflux pumps that are associated with highly cytotoxic drugs. Selection of targets, drugs, and linkers are discussed in the next sections.

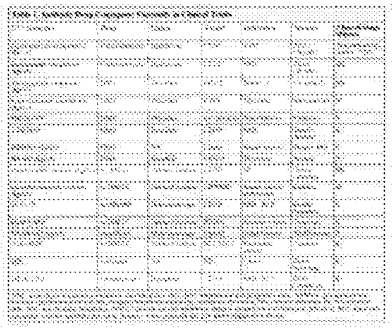
Tumor-associated Antigens Selection

Antigens must have high tumor cell selectivity to limit toxicity and off-target effects (less evident). A plethora of tumor-associated antigens have been investigated in pre-clinical models and in clinical trials including antigens over-expressed in B-cells (e.g., CD20, CD22, CD40, CD79), T-cells (CD25, CD30), carcinoma cells (HER2, EGFR, EpCAM, EphB2, PSMA, Cripto), endothelial (endoglin), or stroma cells (fibroblast activated protein), to name a few (Teicher, 2009). As an illustration, those retained for the most advanced ADC investigation as well as new potential targets are briefly discussed below. A major and critical property for ADC targets is their ability to be internalized: this can be an intrinsic feature of the antigen by itself, or it can be induced by the binding of the antibody to its antigen. Indeed, ADC internalization is crucial to reduce toxicity associated with an extracellular delivery of the drug payload.

HER2

HER2 is a particularly interesting target, validated by 12 years of therapeutic use of trastuzumab in HER2 positive breast cancer patients. Nevertheless, acquired resistance to this mAb (Nahta et al., 2006), as well as primary resistance (Kruser and Wheeler, 2010), are clearly established drawbacks. Interestingly, among the multiple mechanisms of action of trastuzumab — blocking HER2 dimerization, blocking of HER2 extracellular domain cleavage, antibody-dependent cell-mediated cytotoxicity (ADCC), and HER2 internalization and degradation, the last one is of prime interest to ensure specific drug internalization in cancer cells. This surface antigen was chosen as target for the current most clinically advanced ADC (see below) in HER2-positive patients refractory to trastuzumab (Hughes, 2010).

Hematological malignancies



Cancers of blood cells including leukemia, lymphoma, and multiple myeloma are frequently chosen indications to study new ADC-based experimental treatments (Lutz and Whiteman, 2009; Polson et al., 2009; Ryan et al., 2010; Gerber, 2010; Polson et al., 2010). Malignant blood cells are more accessible to antibodies than solid tumors (e.g., AML, NHL) (Table 1) (Schmidt and Wittrup, 2009).

Targeting tumor vasculature

Reducing the blood supply of tumors is another efficient option to fight cancer. Bevacizumab, an anti-VEGF mAb, is now an established key therapeutic approach that targets endothelial cells within the tumor in combination with other chemotherapeutics. Again, the antitumor activity of bevacizumab as a single agent drug is limited and the development of vasculature targeting ADCs looks promising. Other endothelial cell-linked antigens like integrins or endoglin have been chosen as targets for immuno-conjugates (Gerber et al., 2009). The aim is to induce anti-tumor effects via the selective destruction of blood vessels within established tumors, leading to tumor cell death due to ischemia.

Selection of Highly Cytotoxic Drugs

In contrast to the vast variety of putative antigen targets, only three main families of cytotoxic drugs used as payloads in ADCs are currently actively investigated in clinical trials: calicheamycin (Pfizer), maytansinoids (DM1 and DM4; ImmunoGen + Genentech/ Roche, Sanofi-Aventis, Ravenn Idec, Centocor/Johnson & Johnson, Millennium/Takeda), and auristatins (MMAE and MMAF; Seattle Genetics + Genentech/Roche, MedImmune/AstraZeneca, Bayer-Schering, Celldex, Progenics, Genmab) (Table 1). The first one is a DNA minor groove binder whereas the other two are tubulin depolymerization agents. One of their common features is their high free drug potency (10^{-9} to 10^{-11} M) in comparison, for example, to doxorubicin (10^{-7} M) used in the first generation ADCs. Another key element for success is the clear knowledge of a "permissive" position for the linker attachment that allows the release of active metabolites, similar to traditional prodrugs.

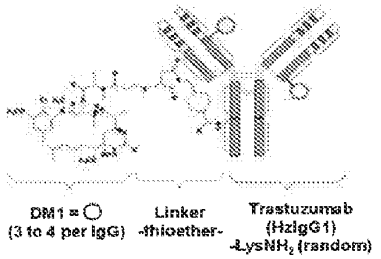


Figure 2A. Structure of trastuzumab emtansine. An ADC is a three-block "engine" — antibody-linker-drug — and each part of the composite molecule has to be carefully selected and assembled. Considered as an armed-antibody, an ADC is a bi-dentate construction where both parts (antibody and drug) of the molecule combine their effect to ensure selectivity and potency. The role of the linker arm is of paramount importance demanding a fine tuning to execute the controlled release and delivery of the two active components in the tumor environment.

Interestingly, one representative of each of the three cytotoxic-derived ADCs (trastuzumab emtansine, inotuzumab ozogamicin, and brentuximab vedotin) is currently in late clinical trials (Figure 2A-C), which indicates the maturity of these technologies and confirms their leadership in this field with these new generation ADCs (Reichert, 2010; Alley et al., 2010).

Trastuzumab emtansine (= T-DM1, anti-HER2 + DM1) (Figure 2A). Encouraging clinical phase I data have been recently reported for trastuzumab emtansine, an antibody-drug conjugate derived from trastuzumab and linked to a maytansinoid hemi-synthetic drug by a stable linker (Krop et al., 2010). From pharmacological standpoint, T-DM1 retains all the mechanisms of action of the naked parent antibody (Junttila et al., 2010). On July 7, 2010, Genentech/Roche has announced the submission of a Biologics License Application (BLA) to the FDA for trastuzumab emtansine for use in patients with advanced HER2-positive breast cancer who have previously received multiple HER2-targeted medicines and chemotherapies (Niculescu-Duvaz, 2010). The FDA submission was based on a Phase II pivotal study (TDM4374g, www.clinicaltrial.gov), a single-arm, multi-center trial designed to assess single-agent T-DM1 in 110 women with HER2-positive advanced breast cancer whose disease had worsened after receiving at least two prior HER2-targeted treatments (trastuzumab and lapatinib) in the metastatic setting and, often, an anthracycline, a taxane and capecitabine. Nevertheless, the FDA refused to accept the application for accelerated approval of the BLA by the end of August 2010. The FDA stated that the T-DM1 trials did not meet the standard for the accelerated approval process because all available treatment choices that were approved for metastatic breast cancer, regardless of HER2 status, had not been exhausted in the study population. Genentech will continue with its ongoing Phase III registrational T-DM1 trial to submit a new BLA in mid-2012. Genentech has licensed the technology for T-DM1 from ImmunoGen and Seattle Genetics. The fact that this leading biotech company has approximately 50 ADCs in early stages of research and development for multiple tumor types underlines the high level of hope and expectations for this ADC strategy.

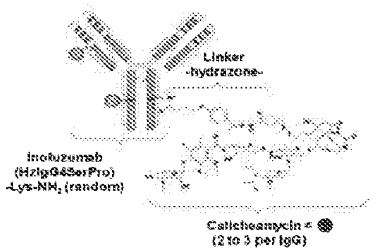


Figure 2B. Structure of inotuzumab ozogamicin.

Inotuzumab ozogamicin (= CMC-544, anti-CD22 + calicheamicin, Pfizer/Wyeth + UCB S.A.) (Figure 2B). Inotuzumab ozogamicin is investigated in B-cell non-Hodgkin's lymphoma (NHL) in combination with rituximab in a phase III trial (Advani et al., 2010; Alley et al., 2010). A humanized anti-CD22 mAb (G5/44, IgG4) was conjugated to calicheamycin with an acid labile linker (acetylphenoxy-butanoic) to provide the resulting conjugate, termed CMC-544. After binding to CD22, the molecule is internalized, and the calicheamicin portion then binds to the minor groove of DNA, leading to DNA-strand breaks and ultimately apoptosis. Preclinical studies indicated that the drug candidate significantly reduced levels of CD22 in cell lines, as well as in cells obtained from patients with B cell malignancies. The combination of inotuzumab ozogamicin and rituximab is being compared to a drug regimen selected by investigators in an ongoing phase III study of adult patients with follicular non-Hodgkin's lymphoma.

Brentuximab vedotin (= SGN-35, anti-CD30 + auristatin, Seattle Genetics + Millennium/Takeda) (Figure 2C). Brentuximab vedotin is investigated in relapsed and refractory Hodgkin's lymphoma (phase II/III) (Foyil and Bartlett, 2010). This ADC is a chimeric IgG1 conjugated, on an average of 3 to 5 cysteinyl residues and after mild reduction of interchain disulfide bonds, to monomethyl auristatin E (MMAE), via a maleimidocaproyl-valyl-citrullinyl-p-aminobenzylcarbamate linker. Upon internalization, cellular proteases cleave the bond and MMAE is released as a chemically unmodified active drug (Senter, 2009). Initial phase I studies of brentuximab vedotin showed a 52% overall response rate in relapsed Hodgkin's lymphoma, with minimal toxicity.

Rational Design and Optimization of Chemical Linkers

Linkers represent the key component of ADC structures (Rohrer, 2009; Erickson et al., 2010; Ducry and Stump, 2010). Among the reasons of failure of first generation ADCs the poor stability of the drugs in serum (and early release of the drugs in blood that triggered toxicity) or, conversely, non-release of the drugs in the tumor target cells stood out. Several classes of second generation linkers have been investigated. Acid-labile hydrazone linkers have been designed to be cleaved within the intracellular compartment of lysosomes due to lower pH compared to the systemic blood circulation (pH 5 vs. 7.4, respectively) and they have been applied to the production of gemtuzumab and inotuzumab ozogamicin, for example. Another class of linkers is disulfide-based in order to be selectively cleaved in the cytosol due to a more reductive intracellular environment (Lewis Phillips et al., 2008). Non-cleavable thioether linkers were developed more recently and intended to release the free active neoplastic drug by catabolic degradation of internalized ADC in the lysosomal compartment (e.g., trastuzumab emtansine). Peptide linkers like citruline-valine have the potential to be selectively cleaved by lysosomal proteases (e.g., cathepsin-B); they have demonstrated increased serum stability and improved anti-tumor effects compared to hydrazone linkers. A peptide linker is used for making brentuximab vedotin (Doronina et al., 2006).

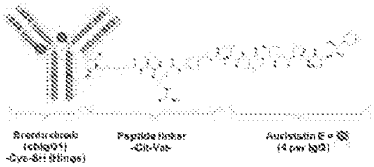


Figure 2C. Structure of brentuximab vedotin.

In addition, promising third generation linkers have been recently described that are processed as lipophilic metabolites of disulfide-linked conjugates or, conversely, hydrophilic linkers designed to bypass multidrug resistance (Kovtun et al., 2010). These later ones are processed in target cells to cytotoxic metabolites and retained by multi-drug-resistance 1 (molecule P-glycoprotein or ABCB1) expressing cells.

From a strategic perspective, it is interesting to note that a number of big pharmaceutical and biotech companies (e.g., Genentech/Roche, Medarex/BMS, Biogen Idec, Sanofi-Aventis) that have entered the complicated "ADC" field have first signed deals with ImmunoGen and/or Seattle Genetics to have access to their cytotoxic drugs (maytansinoids and auristatins, respectively), linker portfolio, and know-how to solve chemistry, manufacturing, and control (CMC) issues. In complement, they are developing their own ADC technologies (e.g., thiomabs by Genentech) or new synthetic DNA minor groove binding agents (Medarex/BMS).

Molecular Engineering of Optimized Antibodies for Site Directed Conjugation of Cytotoxic Drugs

In trastuzumab emtansine and other ADCs, the drug payloads may be randomly attached to exposed lysine residues distributed on Light and Heavy Chains of antibody (average of 80 to 95 per IgG) (Figure 1). Though fine-tuning of the labeling conditions could differentiate somewhat between the lysine residues, the theoretical risk exists as a result of coupling to lysine present in Complementary-Determining Regions (CDRs) or critical framework residues of the antibody variable region, thereby losing the antibody's capacity to bind to target antigens or Fc-receptors. Alternatively, site-specific-coupling to one or several of the eight cysteine residues involved in inter-chain disulfide bridges after mild reduction may be used as illustrated in the case for brentuximab (Figure 2C). For the same purpose, the glycan moiety can be subjected to mild oxidation and be used for site selective conjugation via a hydrazone linkage (Beck et al., 2008).

As further improvements for the third generation ADCs, design of optimized antibodies (e.g., engineered to contain free surface exposed cysteines for a site specific drug linkage) as well as drug loading level optimization are investigated, for example, to maintain the natural favorable pharmacokinetics of chimeric, humanized, and human IgGs. Site specific conjugation to antibodies results in homogeneous drug loading and avoids ADC subpopulations with altered antigen-binding (cross-link in the CDRs) or altered pharmacokinetics (Fc domain binding sites of FcRn receptors). Several such attempts have been recently described including the addition of two cysteines in the antibody variable domains (Junutula et al., 2008; Chen et al., 2009; Junutula et al., 2010) (Figure 3), in constant domains (Voynov et al., 2010), and the addition of C-terminal selenocysteines (Hofer et al., 2008); they represent very elegant ways to improve the overall homogeneity and to control the cytotoxic drug position and loading. Selenocysteine is co-translationally inserted into recombinant proteins and the nucleophilic selenol group allows region-specific covalent conjugation in the presence of the other natural amino acids (Hofer et al., 2009).

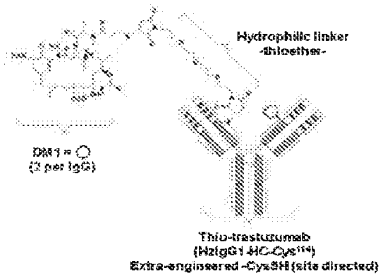


Figure 3. Structure of thio-trastuzumab emtansine. Homogeneous engineered entity based on a site directed covalent maytansinoid conjugate. Additional cysteine residues have been introduced at Ala114 position of both trastuzumab-heavy chains and a non-reducible bis-maleimido-trioxyethylene glycol linker (BMPEO) was used. This next generation immunoconjugate is much better chemically defined and shows an improved therapeutic index in in vivo oncology models that warrant interest for clinical testing (Junutula et al., 2010).

Further Challenges: Chemistry Manufacturing Control, Pharmacokinetics, and Biomarkers

From a pharmaceutical perspective, ADCs are much more complex molecules to develop than naked antibody or cytotoxic drugs (Wakankar, 2010). Chemistry Manufacturing Control issues are now clearly identified and addressed for the next generation of ADCs (Wakankar et al., 2010). Manufacturing of ADCs involves specific facilities to handle these highly cytotoxic drugs and to limit staff and environmental exposure (Rohrer, 2009). Sensitive mass-spectrometry methods are developed to assess the structure of these very large and complex molecules (150 kDa), to investigate the stability, and to insure batch to batch consistency. Tremendous progress has been made in these domains and there is no doubt that the methods that are currently developed for naked IgGs will also help to extensively characterize the structures of ADCs (Beck et al., 2005; Wagner-Rousset et al., 2008; Viasak et al., 2009; Atmanene et al., 2009). In addition, new formulation issues may be encountered and must be specifically addressed. Specific pharmacokinetics/pharmacodynamics studies including metabolism studies are designed to optimize the ADC loading and the administration schedules (Jumbe et al., 2010). Like for other targeted anti-cancer drugs, integrating molecular diagnostic and biomarkers to select the best patient sub-population is of prime importance for a successful ADC treatment (Hughes, 2009; Petak et al., 2010). Once again, trastuzumab-DM1 is a perfect paradigm since HER2 positive patient improvements have validated this oncoprotein as a biomarker (increased tumor cell proliferation and poor prognosis). Another good example was recently reported for glembatumumab vedotin that targets glycoprotein non-metastatic melanoma protein B (GPNMB) (Naumovski and Junutula, 2010). The expression of this antigen is associated with the basal/triple-negative subtype and is a prognostic marker of poor outcome in patients with breast cancer, a diseased population that currently lacks targeted-therapy options. Additionally, the better understanding of resistance mechanism to current treatments will help to design and provide the right ADC to the right patient population.

Conclusion

Combining the cytotoxicity of natural or synthetic highly potent anti-neoplastic agents with monoclonal antibodies conjugated by blood-stable optimized linkers is the key strategy of a new generation of antibody drug conjugates. The development of antibody drug conjugates in oncology takes a longer timeframe and is more complex than for naked antibodies, because much more parameters have to be finely tuned. As a sign of technological advancement, three of the ADCs (trastuzumab emtansine, inotuzumab ozogamicin, and brentuximab vedotin) have reached the late clinical development stages and shown encouraging therapeutic effects against both solid tumors and hematological malignancies. In addition, a dozen ADCs are investigated in earlier clinical trials including glembatumumab vedotin and lorvotuzumab mertansine in phase II trials. FDA and EMA have recently granted orphan drug designation for the latter one. Altogether these recent encouraging successes show that the next generation of antibody-drug conjugates has come of age. Renewed promises and hopes emerged, as it was the case 10 years ago. But it seems that at last we are close to the approval of novel ADC drugs.

Disclosure

The authors are employees of Pierre Fabre Research Institute (IRPF), which has collaboration agreements with Merck Research Laboratories for the development of anti-IGF-1R mAbs (h7C10, dalotuzumab) and with Abbott for the development of anti-cMet mAbs (h224G11).

(Corresponding author: Alain Beck, Ph.D., Centre d' Immunologie Pierre Fabre (CIPF), 5 Avenue Napoléon III, 74164 St Julien-en-Genevois, France.)

References

Advani A, Coiffier B, Czuczman MS, Dreyling M, Foran J, Gine E, Gisselbrecht C, Ketterer N, Nasta S, Rohatiner A, Schmidt-Wolf IG, Schuler M, Sierra J, Smith MR, Verhoef G, Winter JN, Boni J, Vandendries E, Shapiro M, Fayad L. Safety, pharmacokinetics, and preliminary clinical activity of inotuzumab ozogamicin, a novel immunoconjugate for the treatment of B-cell non-Hodgkin's lymphoma: results of a phase I study. J Clin Oncol 28(12):2085-2093, 2010.

Alley SC, Okeley NM, Senter PD. Antibody-drug conjugates: targeted drug delivery for cancer. Curr Opin Chem Biol 14(4):529-537, 2010.

Atmanene C, Wagner-Rousset E, Malissard M, Chol B, Robert A, Corvaia N, Van Dorsselaer A, Beck A, Sanglier-Cianferani S. Extending mass spectrometry contribution to therapeutic monoclonal antibody lead optimization: characterization of immune complexes using noncovalent ESI-MS. Anal Chem 81(15):6364-6373, 2009.

Bailly C. Ready for a comeback of natural products in oncology. Biochem Pharmacol 77(9):1447-1457, 2009.

Beck A, Bussat MC, Zorn N, Robillard V, Klinguer-Hamour C, Chenu S, Goetsch L, Corvaia N, Van Dorsselaer A, Haeuw JF. Characterization by liquid chromatography combined with mass spectrometry of monoclonal anti-IGF-1 receptor antibodies produced in CHO and NS0 cells. J Chromatogr B Analyt Technol Biomed Life Sci 819(2):203-218, 2005.

Beck A, Cochet O, Wurch T. GlycoFi's technology to control the glycosylation of recombinant therapeutic proteins. Expert Opin Drug Discov 5:95-111, 2010a.

Beck A, Reichert JM, Wurch T. 5th European Antibody Congress 2009: November 30 - December 2, 2009. MAbs 2(2):108-128, 2010b.

Beck A, Wagner-Rousset E, Bussat MC, Lokteff M, Klinguer-Hamour C, Haeuw JF, Goetsch L, Wurch T, Van Dorsselaer A, Corvaia N. Trends in glycosylation, glycoanalysis and glycoengineering of therapeutic antibodies and Fc-fusion proteins. Curr Pharm Biotechnol 9(6):482-501, 2008.

Beck A, Wagner-Rousset E, Wurch T, Corvaia N. Therapeutic antibodies and related products: choosing the right structure for success. Med Sci (Paris) 25(12):1024-1032, 2009.

Beck A, Wurch T, Bailly C, Corvaia N. Strategies and challenges for the next generation of therapeutic antibodies. Nat Rev Immunol 10(5):345-352, 2010c.

Bross PF, Beitz J, Chen G, Chen XH, Duffy E, Kieffer L, Roy S, Sridhara R, Rahman A, Williams G, Pazdur R. Approval summary: gemtuzumab ozogamicin in relapsed acute myeloid leukemia. Clin Cancer Res 7(6):1490-1496, 2001.

Chari RV. Targeted cancer therapy: conferring specificity to cytotoxic drugs. Acc Chem Res 41(1):98-107, 2008.

Chen XN, Nguyen M, Jacobson F, Ouyang J. Charge-based analysis of antibodies with engineered cysteines: from multiple peaks to a single main peak. MAbs 1(6):563-571, 2009.

Doronina SO, Mendelsohn BA, Bovee TD, Cerveny CG, Alley SC, Meyer DL, Oflazoglu E, Toki BE, Sanderson RJ, Zabinski RF, Wahl AF, Senter PD. Enhanced activity of monomethylauristatin F through monoclonal antibody delivery: Effects of linker technology on efficacy and toxicity. Bioconjug Chem 17(1):114-124, 2006.

Ducry L, Stump B. Antibody-drug conjugates: linking cytotoxic payloads to monoclonal antibodies. Bioconjug Chem 9(9):665-667, 2010.

Erickson HK, Widdison WC, Mayo MF, Whiteman K, Audette C, Wilhelm SD, Singh R. Tumor delivery and in vivo processing of disulfide-linked and thioether-linked antibody-maytansinoid conjugates. Bioconjug Chem 21(1):84-92, 2010.

Foyil KV, Bartlett NL. Anti-CD30 antibodies for Hodgkin lymphoma. Curr Hematol Malig Rep 5(3):140-147, 2010.

Gerber HP. Emerging immunotherapies targeting CD30 in Hodgkin's lymphoma. Biochem Pharmacol 79(11):1544-1552, 2010.

Gerber HP, Senter PD, Grewal IS. Antibody drug-conjugates targeting the tumor vasculature: Current and future developments. MAbs 1(3):247-253, 2009.

Haeuw JF, Caussanel V, Beck A. [Immunoconjugates, drug-armed antibodies to fight against cancer.] Med Sci (Paris) 25(12):1046-1052, 2009.

Hofer T, Skeffington LR, Chapman CM, Rader C. Molecularly defined antibody conjugation through a selenocysteine interface. Biochemistry 48(50):12047-12057, 2009.

Hofer T, Thomas JD, Burke TR Jr, Rader C. An engineered selenocysteine defines a unique class of antibody derivatives. Proc Natl Acad Sci U S A 105(34):12451-12456, 2008.

Hughes B. Gearing up for follow-on biologics. Nat Rev Drug Discov 8(3):181, 2009.

Hughes B. Antibody-drug conjugates for cancer: poised to deliver? Nat Rev Drug Discov 9(9):665-667, 2010.

Jumbe NL, Xin Y, Leipold DD, Crocker L, Dugger D, Mai E, Sliwkowski MX, Fielder PJ, Tibbitts J. Modeling the efficacy of trastuzumab-DM1, an antibody drug conjugate, in mice. J Pharmacokinet Pharmacodyn 37(3):221-242, 2010.

Junttila TT, Li G, Parsons K, Phillips GL, Sliwkowski M. Trastuzumab-DM1 (T-DM1) retains all the mechanisms of action of trastuzumab and efficiently inhibits growth of lapatinib insensitive breast cancer. Breast Cancer Res Treat,epub ahead of print, Aug. 21, 2010.

Junutula JR, Flagella KM, Graham RA, Parsons KL, Ha E, Bhakta S, Nguyen T, Dugger DL, Li G, Mai E, Lewis Phillips GD, Hiraragi H, Fuji RN, Tibbitts J, Vandlen R, Spencer SD, Scheller RH, Polakis P, Sliwkowski M. Engineered thio-trastuzumab-DM1 conjugate with an improved therapeutic index to target HER2-positive breast cancer. Clin Cancer Res,epub ahead of print, Aug. 30, 2010.

Junutula JR, Raab H, Clark S, Bhakta S, Leipold DD, Weir S, Chen Y, Simpson M, Tsai SP, Dennis MS, Lu Y, Meng YG, Ng C, Yang J, Lee CC, Duenas E, Gorrell J, Katta V, Kim A, McDorman K, et al. Site-specific conjugation of a cytotoxic drug to an antibody improves the therapeutic index. Nat Biotechnol 26(8):925-932, 2008.

Kovtun YV, Audette CA, Mayo MF, Jones GE, Doherty H, Maloney EK, Erickson HK, Sun X, Wilhelm S, Ab O, Lai KC, Widdison WC, Kellogg B, Johnson H, Pinkas J, Lutz RJ, Singh R, Goldmacher VS, Chari RV. Antibody-maytansinoid conjugates designed to bypass multidrug resistance. Cancer Res 70(6):2528-2537, 2010.

Krop IE, Beeram M, Modi S, Jones SF, Holden SN, Yu W, Tibbitts J, Yi JH, Sliwkowski MX, Jacobson F, Lutzker SG, Burris HA. Phase I study of trastuzumab-DM1, an HER2 antibody-drug conjugate, given every 3 weeks to patients with HER2-positive metastatic breast cancer. J Clin Oncol 28(16):2698-2704, 2010.

Kruser TJ, Wheeler DL. Mechanisms of resistance to HER family targeting antibodies. Exp Cell Res 316(7):1083-1100, 2010.

Labrijn AF, Buijsse AO, van den Bremer ET, Verwilligen AY, Bleeker WK, Thorpe SJ, Killestein J, Polman CH, Aalberse RC, Schuurman J, van de Winkel JG, Parren PW. Therapeutic IgG4 antibodies engage in Fab-arm exchange with endogenous human IgG4 in vivo. Nat Biotechnol 27(8):767-771, 2009.

Lewis Phillips GD, Li G, Dugger DL, Crocker LM, Parsons KL, Mai E, Blattler WA, Lambert JM, Chari RV, Lutz RJ, Wong WL, Jacobson FS, Koeppen H, Schwall RH, Kenkare-Mitra SR, Spencer SD, Sliwkowski MX. Targeting HER2-positive breast cancer with trastuzumab-DM1, an antibody-cytotoxic drug conjugate. Cancer Res 68(22):9280-9290, 2008.

Lutz RJ, Whiteman KR. Antibody-maytansinoid conjugates for the treatment of myeloma. MAbs 1(6):548-551, 2009.

Nahta R, Yu D, Hung MC, Hortobagyi GN, Esteva FJ. Mechanisms of disease: understanding resistance to HER2-targeted therapy in human breast cancer. Nat Clin Pract Oncol 3(5):269-280, 2006.

Naumovski L, Junutula JR. Glembatumumab vedotin, a conjugate of an anti-glycoprotein non-metastatic melanoma protein B mAb and monomethyl auristatin E for the treatment of melanoma and breast cancer. Curr Opin Mol Ther 12(2):248-257, 2010.

Niculescu-Duvaz I. Trastuzumab emtansine, an antibody-drug conjugate for the treatment of HER2+ metastatic breast cancer. Curr Opin Mol Ther 12(3):350-360, 2010.

Petak I, Schwab R, Orfi L, Kopper L, Keri G. Integrating molecular diagnostics into anticancer drug discovery. Nat Rev Drug Discov 9(7):523-535, 2010.

Polson AG, Calemine-Fenaux J, Chan P, Chang W, Christensen E, Clark S, de Sauvage FJ, Eaton D, Elkins K, Elliott JM, Frantz G, Fuji RN, Gray A, Harden K, Ingle GS, Kljavin NM, Koeppen H, Nelson C, Prabhu S, Raab H, et al. Antibody-drug conjugates for the treatment of non-Hodgkin's lymphoma: target and linker-drug selection. Cancer Res 69(6):2358-2364, 2009.

Polson AG, Williams M, Gray AM, Fuji RN, Poon KA, McBride J, Raab H, Januario T, Go M, Lau J, Yu SF, Du C, Fuh F, Tan C, Wu Y, Liang WC, Prabhu S, Stephan JP, Hongo JA, Dere RC, et al. Anti-CD22-MCC-DM1: an antibody-drug conjugate with a stable linker for the treatment of non-Hodgkin's lymphoma. Leukemia, in press, 2010.

Reichert JM. Antibodies to watch in 2010. MAbs 2(1):1-16, 2010.

Rohrer T. Potent weapons for the oncology arsenal. Chem Today 27(5):56-60, 2009.

Ryan MC, Kostner H, Gordon KA, Duniho S, Sutherland MK, Yu C, Kim KM, Nesterova A, Anderson M, McEarchern JA, Law CL, Smith LM. Targeting pancreatic and ovarian carcinomas using the auristatin-based anti-CD70 antibody-drug conjugate SGN-75. Br J Cancer 103(5):676-684, 2010.

Schmidt MM, Wittrup KD. A modeling analysis of the effects of molecular size and binding affinity on tumor targeting. Mol Cancer Ther 8(10):2861-2871, 2009.

Senter PD. Potent antibody drug conjugates for cancer therapy. Curr Opin Chem Biol 13(3):235-244, 2009.

Teicher BA. Antibody-drug conjugate targets. Curr Cancer Drug Targets 9(8):982-1004, 2009.

Vlasak J, Bussat MC, Wang S, Wagner-Rousset E, Schaefer M, Klinguer-Hamour C, Kirchmeier M, Corvaia N, Ionescu R, Beck A. Identification and characterization of asparagine deamidation in the light chain CDR1 of a humanized IgG1 antibody. Anal Biochem 392(2):145-154, 2009.

Voynov V, Chennamsetty N, Kayser V, Wallny HJ, Helk B, Trout BL. Design and application of antibody cysteine variants. Bioconjug Chem 21(2):385-392, 2010.

Wagner-Rousset E, Bednarczyk A, Bussat MC, Colas O, Corvaia N, Schaeffer C, Van Dorsselaer A, Beck A. The way forward, enhanced characterization of therapeutic antibody glycosylation: comparison of three level mass spectrometry-based strategies. J Chromatogr B Analyt Technol Biomed Life Sci 872(1-2):23-37, 2008.

Wakankar A. Antibody drug conjugates: The next wave of monoclonal antibody-mediated chemotherapeutics. AAPS News Mag 2010(May):15-21, 2010.

Wakankar AA, Feeney MB, Rivera J, Chen Y, Kim M, Sharma VK, Wang YJ. Physicochemical stability of the antibody-drug conjugate trastuzumab-DM1: changes due to modification and conjugation processes. Bioconjug Chem, in press,2010.

[Discovery Medicine; ISSN: 1539-6509; Discov Med 10(53):329-339, October 2010.]

Related Articles

* Mar 28, 2013 Cancer Immunotherapy: Present Status, Future Perspective, and a New Paradigm of Peptide Immunotherapeutics
* Nov 26, 2010 Histone Deacetylase Inhibitors in the Treatment of Lymphoma
* Mar 28, 2016 NK Cell-based Immunotherapy: Awakening the Innate Anti-cancer Response
* Feb 20, 2011 State of the Art and Future Perspectives for the Use of Insulin-like Growth Factor Receptor 1 (IGF-1R) Targeted Treatment Strategies in Solid Tumors
* Feb 22, 2013 Current Concepts in Diagnosing and Managing Primary Vitreoretinal (Intraocular) Lymphoma
* Dec 26, 2012 Infectious Pathogens and Hematologic Malignancy
* Mar 28, 2016 Integrative Understanding of Epidemiology and Genomics in B-cell Non-Hodgkin Lymphoma as a Pathway to Novel Management Strategies
* Dec 29, 2015 Statins as Anti-cancer Therapy: Can We Translate Preclinical and Epidemiologic Data into Clinical Benefit?
* Mar 30, 2010 Adoptive Immunotherapy for B-cell Malignancies with Autologous Chimeric Antigen Receptor Modified Tumor Targeted T Cells
* Mar 08, 2010 Treatment of Ovarian Cancer by Monoclonal Antibodies

More Related Articles

Access This PDF as a Subscriber | **Purchase/Download This**

Categories: Acute Myeloid Leukemia, Bevacizumab, Bispecific Antibody, Breast Cancer, Chemical Engineering, Chemotherapy, Follicular Lymphoma, Glycoengineering, Hodgkin's Lymphoma, Investigational New Drug, Leukemia, Lymphoma, Molecular Engineering, Multiple Myeloma, Non-Hodgkin's Lymphoma, Rituximab, Trastuzumab

Tags: antibody engineering, antibody-drug conjugate, brentuximab vedotin, calicheamycin, CD20, CD22, CD33, EGFR, endosialin, gemtuzumab ozogamicin, HER-2, immunoconjugate, inotuzumab ozogamicin, kinesin, monoclonal antibody, monoclonal antibody drug, Myeloma, PSMA, trastuzumab emtansine, tumor associated antigen, VEGF

Search

Search | Search Tips/Help

Journal Issues -- Current & Archive (Part)

Current Issue, Vol 21, No 116, Mar 2016 | No 114, Feb 2016 | No 113, Jan 2016 | No 112, Dec 2015 | No 111, Nov 2015 | No 110, Oct 2015 | No 109, Sep 2015 | No 108, Jul - Aug 2015 | No 107, Jun 2015 | No 106, May 2015 | No 105, Apr 2015 | No 104, Mar 2015 | No 103, Feb 2015 | No 102, Jan 2015 | No 101, Dec 2014 | No 100, Nov 2014 | No 099, Oct 2014 | No 098, Sep 2014 | No 097, Jul - Aug 2014 | No 096, Jun 2014 | No 095, May 2014 | No 094, Apr 2014 |

Global Categories

Medical Specialties
Addiction Medicine, Aging, Anesthesiology, Bacteriology, Cardiology, Cardiology and Circulation, Dermatology, Drug Discovery, Endocrinology, Epidemiology, Gastroenterology, Geriatric Medicine, Geriatrics, Gerontology, Gynecology, Hematology, Hepatology, Immunology, Infectious Diseases, Medical Genetics, Microbiology, Mycology, Neurology, Neurology, Neurosurgery, Nutrition, Oncology, Ophthalmology, Orthopedics, Otolaryngology, Pathology, Pediatrics, Personalized Medicine, Pharmacogenetics, Pharmacogenomics, Pharmacology, Plastic and Reconstructive Medicine, Preventive Medicine, Psychiatry, Psychology, Pulmonology, Radiology, Regenerative Medicine, Reproductive Medicine, Rheumatology, Surgery, Toxicology, Traditional Chinese Medicine, Translational Research, Transplantation, Urology, Virology
Life Sciences
Anatomy, Anthropology, Biochemistry, Bioinformatics, Biology, Biophysics, Cell Biology, Chemistry, Developmental Biology, Ecology, Embryology, Environmental Science, Epigenetics, Genetics, Genomics, Glycomics, Molecular Biology, Neuroscience, Physiology, Plant Biology, Proteomics
Species and Cell Types
Bacterium, Fungus, Human, Other Species, Parasite, Rodent, Streptococcus aerodoni, Virus
Research Technology
Antibody Production, Biotin-Avidin Technology, Bispecific Antibody, Carbohydrate, Cell Culture, Cell Fusion, Cell Tracking In Vivo, Cellular Electrophysiology, Chemiluminescence, Combinatorial Chemistry, Disease Gene Discovery, Drug Delivery, Flow Cytometry, Gene Knockout, Gene Targeting, Gene Transfer, Genetic Engineering, High Throughput Screening, Imaging, Immunotechnology, Microscopy, Molecular Engineering, Molecular Profiling, Nanotechnology, Nuclear Magnetic Resonance, Nuclear Transfer, Nucleic Acid, Organism Cloning, Protein, RNA Interference, Stem Cell Technology, Tissue Engineering, Transgenic Technology, X-Ray Crystallography
Therapeutic Technology and Methodology
Diagnosis, Experimental Therapy, Therapy
Pharmaceutical and Healthcare Industry
Biotechnology, Commercialization of Discoveries, FDA Drug Regulation, Pharmaceutical Industry

Global Tags

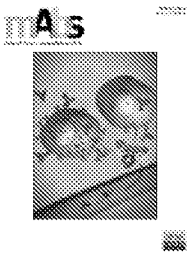
List of 100 Random Tags: (or View All Tags)

5-hydroxytryptamine receptor, Actor-Critic, adolescent, anticoagulation, antigenic shift, antithrombosis, APOE e4, AQP1, autoimmunity, B7-2, bacteriophage, Bayer, Behring, Pharma AG, BER, BOSER, BDNF, Bt-specific T cell engager, BMI, brain, calorie restriction, CCL21, CD30, CD40, CD52, CEA, CETP, chemerin, chemokine receptor, chromosome, cyclin D1, cystic fibrosis transmembrane conductance regulator, embryo, endothelial cell antigens, estriol, fibrinogen, gastroesophageal junction, genetic testing, genome, glycosphingolipid, growth and differentiation factor 9, heat shock protein, helper-dependent, adenovirus, hemagglutinin, HIV

latency HIV viral load Hsp90 humanized antibody hyperparathyroidism ICQVIR-5 IFN-beta IFN-gamma IL-4 immunoconjugate immunosuppression inotuzumab osteopenia interferon-gamma interleukin-21 interleukin-4 ion channel K-Ras karyotype lymphoma life expectancy lipogenesis LMNA major histocompatibility complex MC4R metabolic rate miRNA ML-N341 MRI mRNA splicing neurospheres NMDA receptor NOD-like receptor nucleoticamin p16INK4a paclitaxel oligonucleotide pattern recognition receptor peptide transduction domain PET platelet-derived microparticle Proteasome proteomic profiling PTCH radiation resistance receptor tyrosine kinase replicative senescence SARS single nucleotide variant stem cell plasticity STI571 super paramagnetic iron oxide nanoparticle teriparatide Thalidomide TNF inhibitors ursodeoxycholic acid UVB VapA VDR vesicle trafficking

Copyright 2016, Discovery Medicine. All Rights Reserved.

OnCusp
Ex. 1002



mAbs

ISSN: 1942-0862 (Print) 1942-0870 (Online) Journal homepage: http://www.tandfonline.com/loi/kmab20

Methods for site-specific drug conjugation to antibodies

Christopher R Behrens & Bin Liu

To cite this article: Christopher R Behrens & Bin Liu (2014) Methods for site-specific drug conjugation to antibodies, mAbs, 6:1, 46-53, DOI: 10.4161/mabs.26632

To link to this article: https://doi.org/10.4161/mabs.26632

Copyright © 2014 Landes Bioscience

Published online: 27 Sep 2013.

Submit your article to this journal

Article views: 2365

View Crossmark data

Citing articles: 76 View citing articles

Full Terms & Conditions of access and use can be found at
http://www.tandfonline.com/action/journalInformation?journalCode=kmab20

mAbs 6:1, 46–57; January/February 2014; © 2014 Landes Bioscience

Methods for site-specific drug conjugation to antibodies

Christopher R Behrens and Bin Liu*

Department of Anesthesia; UCSF Helen Diller Family Comprehensive Cancer Center; University of California at San Francisco; San Francisco, CA USA

Keywords: site-specific, antibody drug conjugate, ADC, targeted cancer therapy, therapeutic index, THIOMAB, transglutaminase, unnatural amino acids

Abbreviations: ADC, antibody drug conjugate; VC, valine citrulline; TDC, THIOMAB drug conjugate; MMAE, monomethylauristatin E; MMAD, monomethyl dolastatin 10; LC-MS, liquid chromatography-mass spectrometry; ESI-MS, electrospray ionization mass spectrometry; AUC, area under the curve

Antibody drug conjugates (ADCs) are an emerging class of targeted therapeutics with the potential to improve therapeutic index over traditional chemotherapy. Drugs and linkers have been the current focus of ADC development, in addition to antibody and target selection. Recently, however, the importance of conjugate homogeneity has been realized. The current methods for drug attachment lead to a heterogeneous mixture, and some populations of that mixture have poor in vivo performance. New methods for site-specific drug attachment lead to more homogeneous conjugates and allow control of the site of drug attachment. These subtle improvements can have profound effects on in vivo efficacy and therapeutic index. This review examines current methods for site-specific drug conjugation to antibodies, and compares in vivo results with their non-specifically conjugated counterparts. The apparent improvement in pharmacokinetics and the reduced off target toxicity warrant further development of this site-specific modification approach for future ADC development.

Introduction

Cancer has long been treated with a variety of cytotoxic drugs in an attempt to destroy the malignant cells without causing significant harm to the host cells.[1] Most existing chemotherapy drugs enter cells non-specifically through lipophilic interaction with the cell membrane.[2] Many of these drugs preferentially kill cell types with higher proliferation or metabolic rates, a class that includes most tumor cells but also many healthy cells such as those in the digestive system epithelium. In an attempt to increase the therapeutic index of these cytotoxic drugs, the drugs were attached to targeting groups that preferentially delivered the payload to tumor tissue. Monoclonal antibodies against cell surface antigens have been among the most popular targeting moieties. The attached antibody can significantly decrease non-specific uptake of the drug and increase specific uptake of the conjugate by tumor cells.[3] Assuming the antigen shows a significantly elevated expression on the target cells vs. healthy cells, the therapeutic index of the drug should increase. Early attempts to construct antibody drug conjugates (ADCs) utilized doxorubicin as the cytotoxic drug, but those conjugates showed insufficient potency (IC_{50} = 100 nM) and were ineffective anti-cancer agents.[4] In response to these results, new conjugates with more potent drugs such as calicheamicin[5] or maytansine[6] proved to have significantly higher potencies (IC_{50} = 0.01–0.04 nM, for maytansine conjugate), yet were still well-tolerated in mouse models. These conjugates showed promising results when used to treat mouse xenograft tumors, as complete regressions of the tumors were observed at non-toxic doses. This success prompted the development of a variety of drugs from the maytansine and dolastatin families[7,8] along with both cleavable and non-cleavable linkers.[9] The method for chemical attachment of drug to antibody, however, remained relatively unchanged. More recently, substantial efforts have gone toward investigation of new techniques that result in a more homogeneous mixture with greater control over the site of drug attachment, which could potentially result in an improved therapeutic index of the conjugates. This review will focus on these new techniques for site-specific drug attachment, as there are numerous other reviews that have already explained the important factors for selection of antibody, drug, and linker.[10-19]

*Correspondence author: Bin Liu; Email: liub@anesthesia.ucsf.edu
Submitted: 09/03/2013; Revised: 09/24/2013; Accepted: 09/26/2013
http://dx.doi.org/10.4161/mabs.26632

Current ADC Conjugation Methods

There are many techniques for chemical modification of proteins,[20-22] but two in particular are notable because they were used to construct the two ADCs with current FDA marketing approvals. Brentuximab vedotin, developed by Seattle Genetics, Inc., consists of an anti-CD30 monoclonal antibody conjugated to the highly cytotoxic drug monomethylauristatin E (MMAE) via modification of native cysteine side chain thiols.[23,24] This method involves reduction of the solvent-exposed disulfides with dithiothreitol (DTT) or tris(2-carboxyethyl)phosphine (TCEP) followed by modification of the resulting thiols with maleimide-containing drugs (**Fig. 1A**). For brentuximab vedotin, the thiols

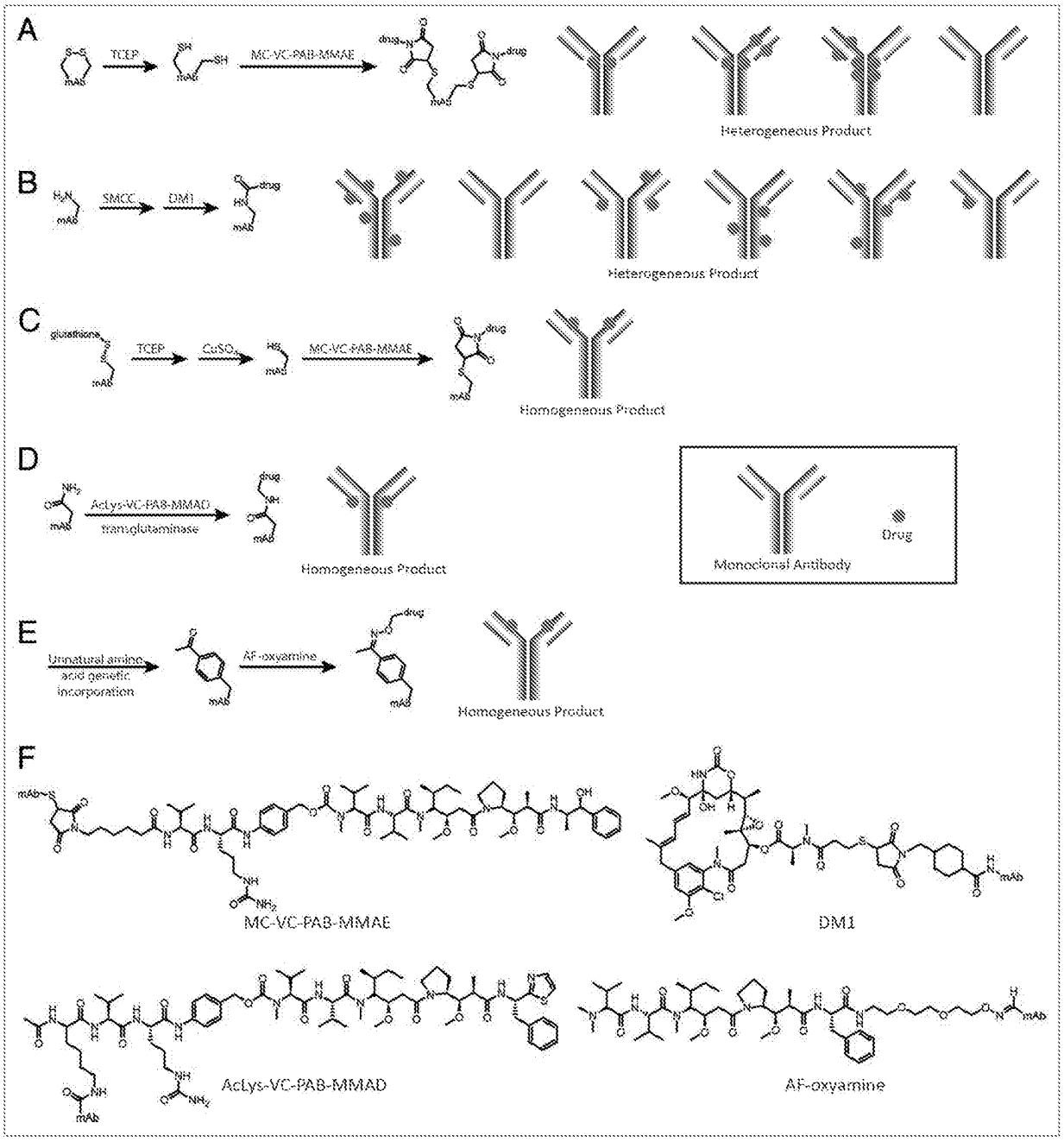


Figure 1. Please see page 3 for figure legend.

were modified with MC-VC-PAB-MMAE, which incorporates a cathepsin B protease cleavage site[25] (VC: valine, citrulline) and a self-immolative linker (PAB: *para*-aminobenzyloxycarbonyl) between the maleimide group (MC: maleimidocaproyl) and the cytotoxic drug (MMAE).[26] The cysteine attachment strategy resulted in two drugs per reduced disulfide; most human IgG molecules have four solvent-exposed disulfide bonds, and so a range of zero to eight drugs per antibody was possible. The exact number of drugs per antibody was determined by the extent of disulfide reduction. Full reduction of all four disulfide bonds gave a homogeneous construct with eight drugs per antibody while a partial reduction resulted in a heterogeneous mixture with zero, two, four, six, or eight drugs per antibody. Though the mixture is heterogeneous, there are still only eight potential sites for

OnCusp
Ex. 1002

Figure 1 (See previous page). Schemes for non-specific (**A, B**) and site-specific (**C, D, E**) drug conjugation to an antibody molecule. (**A**) After reduction of the interchain disulfide bonds with TCEP or DTT, MC-VC-PAB-MMAE (maleimidocaproyl-valinecitrulline-*p*-amino-benzyloxycarbonyl-monomethylauristatin E) was attached to the resulting cysteine side chain thiols using the maleimide functional group. The resulting conjugate was a heterogeneous mixture of antibodies with different numbers of drugs attached to the eight cysteine residues involved in interchain disulfide bonds. (**B**) DM1 (mertansine) was connected to the antibody with a maleimidocyclohexanecarboxylate bifunctional linker (SMCC) through the antibody lysine side chain amines. The resulting conjugate was a heterogeneous mixture with zero to eight drugs per antibody attached to as many as 40 different lysine residues.[34] (**C**) Site directed mutagenesis was utilized to install one additional cysteine residue in each heavy chain. Upon antibody expression this cysteine was found in a disulfide bond with glutathione. Reduction of all solvent exposed disulfide bonds followed by re-oxidation of the native disulfide bonds with $CuSO_4$ resulted in a single thiol on each heavy chain which could be modified with a maleimide-containing drug such as MC-VC-PAB-MMAE. This gave a homogeneous product with precisely two drugs attached at the sites of the mutant cysteines. (**D**) AcLys-VC-PAB-MMAD (acetyllysine-valinecitrulline-*p*-aminobenzyloxycarbonyl-monomethyldolastatin 10) was attached using the enzyme microbial transglutaminase to catalyze the site-specific reaction between the drug lysine and engineered glutamine side chains in the antibody. This method produced a homogeneous conjugate with two drugs per antibody, attached to the engineered glutamines. (**E**) The unnatural amino acid *p*-acetylphenylalanine was genetically incorporated into an antibody using an amber stop codon suppressor tRNA/aaRS pair. The resulting antibody contained one *p*-acetylphenylalanine in each heavy chain at the location of the genetically encoded amber stop codon. Site-specific modification of *p*-acetylphenylalanine with AF-oxyamine (auristatin F-oxyamine) resulted in a homogeneous conjugate with precisely two drugs per antibody. (**F**) Chemical structures and abbreviations of drugs drawn with relevant antibody amino acid side chain attached.

conjugation, which gives some measure of site control compared with the lysine modification strategy described below. Although these disulfide bonds aid in the stability of the antibody, there have been many examples of antibodies that bind their antigen with similar affinity after reduction.[26,27] Overall, this method has proven to be reliable and robust for many different antibody substrates. In addition to brentuximab vedotin, several other conjugates in clinical trials have also utilized this method.[28-31]

The other ADC with current FDA approval is ado-trastuzumab emtansine (Genentech, Inc.), which was constructed by coupling an anti-HER2 monoclonal antibody to the cytotoxic drug maytansine through modification of lysine side chain amines.[32] This version of maytansine (DM1) was modified to include a thiol that could be attached to a maleimide linker. A bifunctional linker (SMCC) with a maleimide at one end and an N-hydroxysuccinimidyl ester (NHS ester) at the other was reacted with lysine primary amine side chains to form a stable amide bond. The modified maytansine (DM1) was then attached to the antibody through conjugation to the maleimide end of the bifunctional linker (**Fig. 1B**). In contrast to the linker utilized in brentuximab vedotin, this linker had no protease cleavage site and thus required lysosomal degradation of the antibody to liberate the active DM1-linker-lysine metabolite. The attachment method resulted in a heterogeneous mixture of conjugates with an average of 3.0–3.6 drugs per antibody, but a range of zero to approximately six.[33] Compared with the cysteine method described above, this strategy gave a more heterogeneous mixture because 20[33] to 40[34] different lysine residues were found to be modified, while only 8 different cysteine residues are modified using the native cysteine modification method. Nonetheless, this method has proven effective as evidenced by the success of ado-trastuzumab emtansine and the numerous other conjugates in advanced trials that use this technology.[35-37]

Limitations of Current Conjugation Methods

Though the previously described methods have led to FDA-approved ADCs, and they are being used for most of the conjugates in clinical trials, there is still substantial room for improvement in the areas of therapeutic index, toxicity, and pharmacokinetics. While the exact mechanisms of ADC clearance and toxicity are still not fully understood, it has become clear from empirical evidence that the number of drugs per antibody can have a large effect on the important in vivo parameters of the conjugate. Hamblett et al. constructed ADCs using the cysteine modification strategy, and then used non-denaturing hydrophobic interaction chromatography to isolate conjugates with exactly four drugs per antibody from the heterogeneous mixture. While this method allowed comparison of different drug loading levels, it was not scalable. When equal concentrations of antibody were tested in cell toxicity assays, ADCs with eight drugs per antibody showed a lower IC_{50} than those with four drugs per antibody.[38] This trend did not translate to in vivo mouse xenograft experiments, however, as, at equivalent antibody doses, the conjugate with four drugs per antibody was equally potent as the conjugate with eight drugs per antibody. Further, on a per drug basis, the antibody with four drugs was twice as potent as the eight drugs per antibody conjugate. The differences observed between in vitro and in vivo potency was due to an increased rate of clearance for the more heavily modified conjugates (**Table 1**). These experiments led to the conclusion that the optimal loading was two to four drugs per antibody to maximize potency while avoiding rapid clearance from circulation. While the cysteine and lysine attachment methods can be adjusted to give an average drug loading of two to four per antibody, the resulting mixture will still be heterogeneous and contain species with both less and more drug loading than desired. It is sub-optimal to have a non-potent portion of antibody (no drug loading) and a portion that has the potential to be rapidly cleared and could contribute to toxicity (high loading).[34,38] Therefore, a conjugation strategy that results in a homogeneous mixture with two or four drugs per antibody would be ideal for maximizing the therapeutic index.

In addition to the issues with heterogeneous mixtures, there have been reports that the maleimide-thiol bond may have stability issues in circulation. Alley et al. were the first to show that drug transfer from antibody to cysteine-34 of albumin occurred slowly in serum.[39] They postulated that the maleimide was released via retro-Michael reaction and the high concentration of thiol-containing albumin scavenged the free maleimide drug. Transfer to the albumin was blocked by either adding an

Table 1. Relevant pharmacokinetic comparisons between antibody drug conjugates with different drug loading or site of drug attachment

Conjugation Method	ADC Description	Clearance (mL/day/kg)	AUC (μg hr/mL)	Model System	Ref.
Native Cysteine	anti-CD30 MMAE 4 drugs/Ab	6.0 ± 0.6	1,689 ± 187	Mouse	38
Native Cysteine	anti-CD30 MMAE 8 drugs/Ab	19.2 ± 0.8	520 ± 21	Mouse	
Native Cysteine	anti-Muc16 MMAE	16.1 ± 3.5	N/A	Rat	34
THIOMAB	anti-Muc16 MMAE	9.5 ± 2.9	N/A	Rat	
Transglutaminase	anti-M1S1 MMAD (Light chain)	N/A	30,610 ± 1,257	Rat	45
Transglutaminase	anti-M1S1 MMAD (Heavy chain)	N/A	9,422 ± 949	Rat	
Unnatural AA	anti-Her2 AF	7.4 ± 0.7	3,213 ± 304	Rat	54
Unnatural AA	anti-Her2 naked Ab	7 ± 2.6	3,632 ± 1,052	Rat	

From Hamblett et al., the four drugs/antibody conjugate showed a significantly slower rate of clearance than the eight drugs/antibody conjugate.[38] Junutula et al. demonstrated that the homogeneous THIOMAB drug conjugate with two drugs/antibody showed a slightly decreased rate of clearance compared with the corresponding ADC with an average of three drugs/antibody.[34] A new site selective method of drug attachment using transglutaminase described by Strop et al. was utilized to attach MMAD to the C-terminal region of either the heavy or light chain.[45] The two conjugates showed marked pharmacokinetic differences in rats, as the heavy chain mutant showed faster clearance and thus a lower area under the curve (AUC). These experiments demonstrated the impact of site of attachment on pharmacokinetic properties. Finally, an anti-Her2 auristatin F site-specific conjugate was synthesized using unnatural amino acid incorporation by Axup et al., and this conjugate showed similar pharmacokinetics to the naked antibody, thus demonstrating the feasibility of the unnatural amino acid method for constructing antibody drug conjugates.[54] Note that clearance and AUC data are only relevant when compared with the injected dose, so these values can only be compared within the same reference as the injected doses are identical. Comparisons between different methods are not valid given the available data.

excess of thiol to the serum or alkylating albumin cysteine-34. The conjugate was stable in buffered aqueous solution as long as there were no thiols present to scavenge the maleimide drug before it could re-attach to the antibody. The rate of this reaction in serum is slow, with a similar half-life to that of the IgG in circulation, and resulted in an approximately 25% drop in the exposure of drug to the tumor according to area under curve calculations. These experiments were performed using ADCs with the drug attached to the interchain disulfide cysteines, and do not necessarily represent the rate of maleimide exchange for thiols incorporated at different positions. Alley et al. showed that replacing the maleimidocaproyl group with bromoacetylcaproyl decreased the rate of drug release, but there is always a need for new conjugation chemistry that results in high stability linkages.

Site Specific Methods for Drug Attachment

To solve some of the issues described above, several research groups developed methods to site-specifically attach drugs at precise locations on the antibody. This strategy imparts advantages such as well-defined, homogeneous conjugates and, in some cases, new chemistry for attachment. With a tunable, homogeneous system, the pharmacokinetics of the conjugate can be optimized by changing the site of attachment of the drug, the linker chemistry, and the overall number of drugs. These factors are difficult to change with the standard attachment strategies and the resulting heterogeneous mixtures would require significant separation efforts to analyze each component.

THIOMAB drug conjugates

The first site-specific approach was developed by Junutula et al. at Genentech by introducing extra cysteine residues using site-directed mutagenesis.[34] This common practice in protein modification[40] was more complicated in an antibody because of the numerous native disulfide bonds already present. Introducing the extra cysteine residue in an unsuitable position could result in improper formation of the native disulfide bonds and therefore improper folding of the antibody. A further complication arose when the cysteine mutants were expressed, as the mutant residues were found as disulfides with cellular thiols such as glutathione or cysteine. In addition, a small portion of the antibodies were found to have three light chains due to a disulfide bond between engineered cysteine residues in the light chain, but this issue was resolved through purification and adjustment of cell culture methods.[41] Drug attachment to the mutant residues required reduction first, but there was no way to selectively reduce only the mutant cysteine disulfides without also reducing the native disulfide bonds. This problem was solved by reducing both the interchain and mutant disulfides, purifying the antibody away from the small molecule thiols, then reoxidizing the native cysteines using a gentle oxidant such as $CuSO_4$ or

OnCusp
Ex. 1002

dehydro-ascorbic acid. The resulting antibody had all of its native disulfide bonds intact, and a single reduced thiol in each heavy or light chain depending on the position of the mutation (**Fig. 1C**).

In addition to the mixed disulfide issue, some of the mutants were rendered unreactive by formation of a disulfide between the two mutant thiol side chains (light chain V110C). Other mutants (heavy chain A114C) showed excellent reactivity toward maleimide reagents, thus giving a mostly homogeneous conjugate with additions only at the mutated residues. MC-VC-PAB-MMAE was then attached to an anti-MUC16 antibody (heavy chain A114C—now referred to as a THIOMAB) to form a THIOMAB drug conjugate (TDC). This particular conjugate was studied with 1.6 drugs per antibody but later preparations achieved approximately 2.0 drugs per antibody. In comparison to the corresponding ADC constructed through the standard cysteine reduction strategy, the TDC showed slightly decreased efficacy in vitro and this difference was attributed to the 2-fold lower drug loading (1.6 for TDC, 3.1 for ADC). However, similar to the four vs. eight drugs per antibody case described by Hamblett et al.,[38] the TDC was equally or more potent than the ADC in vivo when equivalent antibody doses were injected. Additionally, the TDC showed much lower toxicity at equivalent doses compared with the ADC. In rats, the ADC at 16.6 mg/kg (1,500 μg/m^2 MMAE) showed depletion of circulating neutrophils five days after injection with a compensatory rebound by day 12, while the TDC at 36.4 mg/kg (1,500 μg/m^2 MMAE) showed no difference from the vehicle injection. Similar results were also observed in cynomolgus monkeys. In summary, the TDC was equally potent to the ADC in vivo when the injections were equivalent by antibody concentration, and the TDC showed fewer adverse effects when the injections were equivalent by total drug concentration. The serum clearance rate of the TDC was also slower than the ADC (**Table 1**), and a higher percentage of the TDC retained at least one drug. That the TDC both stayed in circulation longer and had fewer adverse effects strongly suggested that the source of much of the toxicity comes from the portion of drug conjugate that is degraded or removed from circulation. In addition to the MUC16 TDC, a TDC version of ado-trastuzumab emtansine showed similar efficacy to the corresponding ADC, but with fewer adverse effects, and thus it has a 2-fold higher therapeutic index.[42] The promising results of these studies demonstrate the importance of developing new methods to precisely control the drug loading of ADCs.

After showing the benefits of the controlled drug loading, the researchers examined how changing the site of drug attachment could alter the properties of the conjugates. To further investigate the role of the site of attachment on the properties of a TDC, Shen et al. made several TDC preparations with the mutant cysteine in different locations.[43] The three constructs compared were light chain V205C, heavy chain A114C, and Fc-S396C. Drug attachment to each resulted in conjugates with two drugs per antibody. All showed similar in vitro potency, but dramatic differences when tested in vivo. The light chain mutant showed slightly better anti-tumor efficacy than the heavy chain mutant, while the Fc mutant was significantly less potent than the other two.

In experiments meant to explain these results, the three TDC samples were incubated in serum at 37°C and the ratio of two-drug TDC to total antibody was determined by liquid chromatography-mass spectrometry (LC-MS). An increased rate of drug loss from the antibody correlated well with diminished efficacy of the conjugates. The less potent Fc mutant had little remaining two-drug TDC after only 24 h, while the other conjugates showed a much more gradual loss of drug. Other mutations in the Fc region did not have the same potency-reducing effect, so the effect was site-specific and not antibody region-specific. After cleavage from the antibody, the drug was found covalently attached to albumin, in agreement with observations by Alley et al.[39] Upon further examination of the LC-MS data, it was observed that the light chain V205C mutant showed mass shifts of +17 Da and +33 Da upon incubation in serum. These mass shifts corresponded to hydrolysis of one or both maleimide rings, which prevented the retro-Michael reaction that separates the drug from the antibody. It was then postulated that the high concentration of positive charges near the mutant cysteine catalyzed this hydrolysis, and this trend was observed on several different TDC mutants. It should be noted that these difficult LC-MS experiments were made significantly easier by the homogeneity of the sample, and might not be possible when analyzing a heterogeneous conjugate. Clearly the site of attachment plays a role in the pharmacokinetics of these conjugates, although these experiments do not allow determination of whether the solvent accessibility or the maleimide hydrolysis plays the larger role.

The engineered cysteine method proved rigorous enough to be used for the site-specific ADC SGN-CD33A from Seattle Genetics, Inc., which recently entered a Phase 1 study as a treatment of acute myeloid leukemia (AML). It was constructed using a proprietary engineered cysteine method to attach a dimer of the novel DNA crosslinking drug pyrrolobenzodiazepine.[44] The resulting conjugate mixture consisted of approximately 95% antibody with two linked drugs and an average loading of 1.9 drugs per antibody. No pharmacokinetic data has been released to date, but the conjugate showed full xenograft tumor regressions with single doses as low as 0.1 mg/kg.

Antibody drug conjugates via transglutaminase

In addition to the THIOMAB conjugation strategy, other methods for site-specific attachment of drugs have been developed. Strop et al. from Rinat-Pfizer demonstrated a new technique for conjugation using microbial transglutaminase to couple an amine-containing drug to an engineered glutamine on the antibody.[45] Transglutaminase is an enzyme that catalyzes bond formation between the acyl group of a glutamine side chain and the primary amine of a lysine side chain.[46] Previous experiments by other groups suggested that this method would result in site-specific conjugates. Jeger et al. showed that the enzyme does not modify any of the native glutamine residues in the antibody,[47] thus allowing selective modification of glutamine residues incorporated via site-directed mutagenesis. In addition, Ohtsuka et al. demonstrated that microbial transglutaminase could catalyze bond formation using a wide range of amino substrates, provided a four carbon linker separated the amine group from the rest of the molecule.[48] The group at Rinat-Pfizer

utilized these observations to develop a strategy that efficiently coupled cytotoxic drugs functionalized with a lysine or amino-PEG spacer to glutamine side chain residues (**Fig. 1D**). They incorporated the short sequence LLQG into 90 locations throughout the antibody, and 12 sites showed high levels of conjugation when exposed to microbial transglutaminase and a suitable amine substrate. Two conjugates were carried forward for analysis in animal models, both utilizing an anti-M1S1 antibody (C16). One contained the extra glutamine sequence at the C-terminus of the light chain (C16-LC) while the other incorporated the glutamine at the C-terminus of the heavy chain (C16-HC). Upon conjugation to AcLys-VC-MMAD (lysine with N-terminal amine acetylated, valine-citrulline protease cleavage site, and monomethyl dolastatin 10) the mutants had a loading of 1.9 (C16-HC) and 1.8 (C16-LC) drugs per antibody out of a maximum of 2.0, and peptide mapping demonstrated that the drugs were attached to the mutant glutamine residues. The resulting peptide bond between the glutamine side chain and lysine of the drug moiety did not have the stability issue found with the cysteine-maleimide conjugates described in the THIOMAB section above. This allowed the effect of the conjugation site on pharmacokinetics to be probed independent of chemical stability.

C16-LC and C16-HC were first compared with a traditional C16 ADC (3.6 drugs per antibody) in vitro. Both conjugates showed IC_{50} values in the 0.050–0.075 nM range for M1S1 overexpressing cell lines BxPC3 and A431, while the traditional C16 ADC showed values in the 0.030–0.040 nM range for the same cell lines. The difference in potency roughly corresponded to the ~2-fold difference in drug loading. Further, the site-specific conjugates showed similar in vivo efficacy to the traditional ADC in a mouse model with BxPC3 xenograft. Treatment with each of the three agents at a single dose of 3 mg/kg conjugate caused significant tumor regression that was stable over the 120 d of the study. Similar to the findings of Junutula et al.,[34] these site-specific conjugates showed similar efficacy at equivalent antibody doses, but double the potency when the drug loading was taken into consideration. While similar in mice, C16-LC and C16-HC showed significant pharmacokinetic differences in rats (**Table 1**). The C16-HC conjugate showed a much accelerated rate of clearance in rats as 83% of the antibody was lost from serum 24 h post-injection. In rats, the clearance of the C16-HC conjugate was similar to the anti-Muc1 ADC described by Junutula et al., whereas the C16-LC conjugate showed similar clearance to the anti-Muc1 site-specific THIOMAB drug conjugate. Because the C16-LC and C16-HC conjugates do not utilize maleimide chemistry and therefore do not suffer from the maleimide transfer issues, the marked differences between the two conjugates are likely due to the position of the attached drug. To verify that the C-terminal modification of the heavy chain did not interfere with FcRn interactions, the binding of both conjugates was tested and showed no difference from the respective naked antibodies. However, the C-terminal heavy chain mutation may affect other cellular interactions that impact conjugate clearance. Taken together, these experiments suggest that the placement of the drug on the antibody can have a significant effect on the pharmacokinetics, though the mechanism of this effect is unknown. Further experiments with the drug attached in a wider variety of positions could help elucidate some of these unknowns.

Unnatural amino acids in antibody drug conjugates

In addition to enzymatic conjugation, orthogonal chemistry conjugation has also been used to site-specifically modify a wide variety of proteins using unnatural amino acids.[49-51] One method for inserting unnatural amino acids into proteins uses an evolved tRNA/tRNA synthetase pair that specifically recognizes the unnatural amino acid and incorporates it as the 21st amino acid in place of the amber stop codon.[52,53] Recent experiments by Axup et al. demonstrated that this method was viable for producing IgG with unnatural amino acids.[54] They chose to introduce *p*-acetylphenylalanine as the unnatural amino acid because it contains a ketone functional group that is not found in any of the 20 natural amino acid side chains. This allows for specific modification of the ketone groups without interference from other amino acids, hence the term orthogonal conjugation. As a proof of concept, *p*-acetylphenylalanine was incorporated into an anti-Her2 IgG1. This was accomplished by first stably integrating the evolved tRNA and corresponding *p*-acetylphenylalanine-tRNA synthetase genes into Chinese hamster ovary cells. The light and heavy chain genes were then incorporated, with the heavy chain bearing a mutation that changed alanine-121 to the amber stop codon recognized by the evolved tRNA. The resulting cells produced over 300 mg/L of the mutant antibody from stable clones, which showed that the yield did not suffer from this technique. The mutant antibody showed similar affinity for its ligand as trastuzumab (Herceptin®), and electrospray ionization mass spectrometry (ESI-MS) of the deglycosylated heavy chain showed the expected mass given the mutation of one alanine to *p*-acetylphenylalanine.

With mutant antibody in hand, a drug containing the appropriate chemical moiety was required to make the desired ADC. Ketone groups can be modified with an alkoxyamine to form an oxime bond that is stable under physiological conditions (**Fig. 1E**).[55,56] Therefore, an auristatin F derivative attached to an oxyamine group using a short polyethylene glycol linker (AF-oxyamine) was synthesized. Similar to the DM1 molecule from ado-trastuzumab emtansine, this drug contained a non-cleavable linker so release of the drug was dependent on lysosomal degradation of the adjoining antibody.[32,57] After reaction of AF-oxyamine with the mutant antibody, the resulting conjugate (anti-Her2-IgG-nAF) contained two drugs per antibody, with less than 5% unreacted antibody as detected by ESI-MS. When tested in vitro the conjugate showed excellent potency against various $Her2^+$ cell lines with EC_{50} values in the 0.11–0.35 nM range, while showing significantly less potency (> 40 nM) against MCF-7 cells ($Her2^-$). Similarly impressive results were observed in vivo as the conjugate showed nearly full regressions of MDA-MB-435 $Her2^+$ xenograft tumors with a single injection at a dose of 5 mg/kg. To evaluate the pharmacokinetics, anti-Her2-IgG-nAF was injected into rats and the serum concentration of antibody was observed over time. The conjugate was indistinguishable from the naked mutant antibody (**Table 1**), thus suggesting that this conjugation

method and placement of drug were effective. In addition, the conjugate was incubated in mouse serum at 37 °C for 3 d before use in cell toxicity assays and showed nearly identical in vitro potency and selectivity as non-incubated conjugate. No toxicity was observed in Her2$^-$ cells for the incubated conjugate, which suggested there was no cleavage of drug from the antibody during incubation. This method provided an additional route for constructing ADCs with precisely two drugs per antibody. In addition, the oxime chemistry resulted in drug-antibody linkages with excellent biological stability.

This work only included pharmacokinetic data for one mutant, so it was not possible to draw any conclusions about the site of drug attachment. However, the unnatural amino acid method is particularly well suited for scanning potential positions of attachment on the antibody. Simple site-directed mutagenesis to incorporate an amber stop codon is all that is necessary to survey new mutants. The importance and potential of this method is illustrated by the number of companies pursuing various technologies for unnatural amino acid incorporation. Ambrx, Inc. (associated with Axup et al.), Allozyne, Inc., and Sutro Biopharma, Inc. are all developing ADC platforms using unnatural amino acids. Questions remain, however, about the potential immunogenicity of unnatural amino acids and their bio-orthogonal linkages. Though no evidence of immunogenicity was reported by Axup et al., further investigation is required to ensure the safety of these compounds.

Conclusion

The methods described in this review have provided three new routes to homogeneous ADCs with two drugs per antibody attached at precise locations. Compared with traditional methods, the site-specific methods showed an improvement in therapeutic index. Since ADC toxicity correlates roughly with the total amount of drug, the antibodies with high drug loading contribute more to toxicity, but are also more rapidly cleared from circulation than the low drug loading antibodies, so they not only contribute more to toxicity but also less to tumor killing efficacy. These site-specific methods eliminate the high drug loading antibodies while also limiting the amount of unconjugated antibody present. In addition, these site-specific methods will allow for further optimization of pharmacokinetic properties based on the site of attachment of the drug. Finally, these methods have proven to be relatively scalable, which makes them viable for clinical exploration.

Although the site-specific ADCs appear to improve upon the non-specific ADCs currently used in the clinic, these conclusions are based on fairly limited preclinical data and require more rigorous testing in clinical trials. Additionally, site-specific ADCs are still in the nascent stage of development. Further improvements are still possible, such as homogeneous conjugates with greater than two drugs per antibody, which could be more potent. While higher drug loading has been correlated with increased rate of clearance and toxicity, those conclusions were drawn from ADCs constructed using non-specific lysine or cysteine modification methods and may not be valid for site-specific ADCs. As the mechanisms for toxicity and ADC clearance are better understood, these site-specific methods can be engineered to produce ADCs with the desired properties. The area of ADCs is rapidly expanding and the contributions of site-specific chemistry will help fuel that expansion.

Disclosure of Potential Conflicts of Interest

No potential conflicts of interest were disclosed.

Acknowledgements

We thank the National Institutes of Health and National Cancer Institute for financial support (R01 CA118919, R01 CA129491, and R01 CA171315).

References

1. Chabner BA, Roberts TG Jr. Timeline: Chemotherapy and the war on cancer. Nat Rev Cancer 2005; 5:65-72; PMID:15630416; http://dx.doi.org/10.1038/nrc1529.
2. Minchinton AI, Tannock IF. Drug penetration in solid tumours. Nat Rev Cancer 2006; 6:583-92; PMID:16862189; http://dx.doi.org/10.1038/nrc1893.
3. Wu AM, Senter PD. Arming antibodies: prospects and challenges for immunoconjugates. Nat Biotechnol 2005; 23:1137-46; PMID:16151407; http://dx.doi.org/10.1038/nbt1141.
4. Yang HM, Reisfeld RA. Doxorubicin conjugated with a monoclonal antibody directed to a human melanoma-associated proteoglycan suppresses the growth of established tumor xenografts in nude mice. Proc Natl Acad Sci USA 1988; 85:1189-93; PMID:3422487; http://dx.doi.org/10.1073/pnas.85.4.1189.
5. Hinman LM, Hamann PR, Wallace R, Menendez AT, Durr FE, Upeslacis J. Preparation and characterization of monoclonal antibody conjugates of the calicheamicins: a novel and potent family of antitumor antibiotics. Cancer Res 1993; 53:3336-42; PMID:8324745.
6. Chari RV, Martell BA, Gross JL, Cook SB, Shah SA, Blättler WA, McKenzie SJ, Goldmacher VS. Immunoconjugates containing novel maytansinoids: promising anticancer drugs. Cancer Res 1992; 52:127-31; PMID:1727373.
7. Koehn FE. Natural Product Cytotoxins as Payloads for Antibody Drug Conjugates. Natural Products and Cancer Drug Discovery. 2013. 97–119.
8. Anderl J, Faulstich H, Hechler T, Kulke M. Antibody-drug conjugate payloads. Methods Mol Biol 2013; 1045:51-70; PMID:23913141; http://dx.doi.org/10.1007/978-1-62703-541-5_4.
9. Nolting B. Linker technologies for antibody-drug conjugates. Methods Mol Biol 2013; 1045:71-100; PMID:23913142; http://dx.doi.org/10.1007/978-1-62703-541-5_5.
10. Thudium K, Bilic S, Leipold D, Maller W, Kaur S, Meibohm B, Erickson H, Tibbitts J, Zhao H, Gupta M. American Association of Pharmaceutical Scientists National Biotechnology Conference Short Course: Translational Challenges in Developing Antibody-Drug Conjugates: May 24, 2012, San Diego, CA. MAbs 2013; 5:5-12; PMID:23255090; http://dx.doi.org/10.4161/mabs.22909.
11. Sievers EL, Senter PD. Antibody-drug conjugates in cancer therapy. Annu Rev Med 2013; 64:15-29; PMID:23043493; http://dx.doi.org/10.1146/annurev-med-050311-201823.
12. Teicher BA, Chari RV. Antibody conjugate therapeutics: challenges and potential. Clin Cancer Res 2011; 17:6389-97; PMID:22003066; http://dx.doi.org/10.1158/1078-0432.CCR-11-1417.
13. Chari RV. Targeted cancer therapy: conferring specificity to cytotoxic drugs. Acc Chem Res 2008; 41:98-107; PMID:17705444; http://dx.doi.org/10.1021/ar700108g.
14. Harper J, Mao S, Strout P, Kamal A. Selecting an optimal antibody for antibody-drug conjugate therapy: internalization and intracellular localization. Methods Mol Biol 2013; 1045:41-9; PMID:23913140; http://dx.doi.org/10.1007/978-1-62703-541-5_3.
15. Bander NH. Antibody-drug conjugate target selection: critical factors. Methods Mol Biol 2013; 1045:29-40; PMID:23913139; http://dx.doi.org/10.1007/978-1-62703-541-5_2.
16. Gerber H-P, Koehn FE, Abraham RT. The antibody-drug conjugate: an enabling modality for natural product-based cancer therapeutics. Nat Prod Rep 2013; 30:625-39; PMID:23525375; http://dx.doi.org/10.1039/c3np20113a.
17. Carter PJ, Senter PD. Antibody-drug conjugates for cancer therapy. Cancer J 2008; 14:154-69; PMID:18536555; http://dx.doi.org/10.1097/PPO.0b013e318172d704.

18. Ducry L, Stump B. Antibody-drug conjugates: linking cytotoxic payloads to monoclonal antibodies. Bioconjug Chem 2010; 21:5-13; PMID:19769391; http://dx.doi.org/10.1021/bc9002019.
19. Schrama D, Reisfeld RA, Becker JC. Antibody targeted drugs as cancer therapeutics. Nat Rev Drug Discov 2006; 5:147-59; PMID:16424916; http://dx.doi.org/10.1038/nrd1957.
20. Stephanopoulos N, Francis MB. Choosing an effective protein bioconjugation strategy. Nat Chem Biol 2011; 7:876-84; PMID:22086289; http://dx.doi.org/10.1038/nchembio.720.
21. Hermanson GT. Bioconjugate Techniques. Elsevier; 2008.
22. Baslé E, Joubert N, Pucheault M. Protein chemical modification on endogenous amino acids. Chem Biol 2010; 17:213-27; PMID:20338513; http://dx.doi.org/10.1016/j.chembiol.2010.02.008.
23. Senter PD, Sievers EL. The discovery and development of brentuximab vedotin for use in relapsed Hodgkin lymphoma and systemic anaplastic large cell lymphoma. Nat Biotechnol 2012; 30:631-7; PMID:22781692; http://dx.doi.org/10.1038/nbt.2289.
24. van de Donk NW, Dhimolea E. Brentuximab vedotin. MAbs 2012; 4:458-65; PMID:22684302; http://dx.doi.org/10.4161/mabs.20230.
25. Dubowchik GM, Firestone RA, Padilla L, Willner D, Hofstead SJ, Mosure K, Knipe JO, Lasch SJ, Trail PA. Cathepsin B-labile dipeptide linkers for lysosomal release of doxorubicin from internalizing immunoconjugates: model studies of enzymatic drug release and antigen-specific in vitro anticancer activity. Bioconjug Chem 2002; 13:855-69; PMID:12121142; http://dx.doi.org/10.1021/bc025536j.
26. Doronina SO, Toki BE, Torgov MY, Mendelsohn BA, Cerveny CG, Chace DF, DeBlanc RL, Gearing RP, Bovee TD, Siegall CB, et al. Development of potent monoclonal antibody auristatin conjugates for cancer therapy. Nat Biotechnol 2003; 21:778-84; PMID:12778055; http://dx.doi.org/10.1038/nbt832.
27. Sun MM, Beam KS, Cerveny CG, Hamblett KJ, Blackmore RS, Torgov MY, Handley FG, Ihle NC, Senter PD, Alley SC. Reduction-alkylation strategies for the modification of specific monoclonal antibody disulfides. Bioconjug Chem 2005; 16:1282-90; PMID:16173809; http://dx.doi.org/10.1021/bc050201y.
28. Pollack VA, Alvarez E, Tse KF, Torgov MY, Xie S, Shenoy SG, MacDougall JR, Arrol S, Zhong H, Gerwien RW, et al. Treatment parameters modulating regression of human melanoma xenografts by an antibody-drug conjugate (CR011-vcMMAE) targeting GPNMB. Cancer Chemother Pharmacol 2007; 60:423-35; PMID:17541593; http://dx.doi.org/10.1007/s00280-007-0490-z.
29. Ma D, Hopf CE, Malewicz AD, Donovan GP, Senter PD, Goeckeler WF, Maddon PJ, Olson WC. Potent antitumor activity of an auristatin-conjugated, fully human monoclonal antibody to prostate-specific membrane antigen. Clin Cancer Res 2006; 12:2591-6; PMID:16638870; http://dx.doi.org/10.1158/1078-0432.CCR-05-2107.
30. Li D, Poon KA, Yu S-F, Dere R, Go M, Lau J, Zheng B, Elkins K, Danilenko D, Kozak KR, et al. DCDT2980S, an anti-CD22-monomethyl auristatin E antibody-drug conjugate, is a potential treatment for non-Hodgkin lymphoma. Mol Cancer Ther 2013; 12:1255-65; PMID:23598530; http://dx.doi.org/10.1158/1535-7163.MCT-12-1173.
31. Govindan SV, Cardillo TM, Sharkey RM, Tat F, Gold DV, Goldenberg DM. Milatuzumab-SN-38 conjugates for the treatment of CD74+ cancers. Mol Cancer Ther 2013; 12:968-78; PMID:23427296; http://dx.doi.org/10.1158/1535-7163.MCT-12-1170.
32. Lewis Phillips GD, Li G, Dugger DL, Crocker LM, Parsons KL, Mai E, Blättler WA, Lambert JM, Chari RV, Lutz RJ, et al. Targeting HER2-positive breast cancer with trastuzumab-DM1, an antibody-cytotoxic drug conjugate. Cancer Res 2008; 68:9280-90; PMID:19010901; http://dx.doi.org/10.1158/0008-5472.CAN-08-1776.
33. Wang L, Amphlett G, Blättler WA, Lambert JM, Zhang W. Structural characterization of the maytansinoid-monoclonal antibody immunoconjugate, huN901-DM1, by mass spectrometry. Protein Sci 2005; 14:2436-46; PMID:16081651; http://dx.doi.org/10.1110/ps.051478705.
34. Junutula JR, Raab H, Clark S, Bhakta S, Leipold DD, Weir S, Chen Y, Simpson M, Tsai SP, Dennis MS, et al. Site-specific conjugation of a cytotoxic drug to an antibody improves the therapeutic index. Nat Biotechnol 2008; 26:925-32; PMID:18641636; http://dx.doi.org/10.1038/nbt.1480.
35. Tassone P, Gozzini A, Goldmacher V, Shammas MA, Whiteman KR, Carrasco DR, Li C, Allam CK, Venuta S, Anderson KC, et al. In vitro and in vivo activity of the maytansinoid immunoconjugate huN901-N2'-deacetyl-N2'-(3-mercapto-1-oxopropyl)-maytansine against CD56+ multiple myeloma cells. Cancer Res 2004; 64:4629-36; PMID:15231675; http://dx.doi.org/10.1158/0008-5472.CAN-04-0142.
36. Ikeda H, Hideshima T, Fulciniti M, Lutz RJ, Yasui H, Okawa Y, Kiziltepe T, Vallet S, Pozzi S, Santo L, et al. The monoclonal antibody nBT062 conjugated to cytotoxic Maytansinoids has selective cytotoxicity against CD138-positive multiple myeloma cells in vitro and in vivo. Clin Cancer Res 2009; 15:4028-37; PMID:19509164; http://dx.doi.org/10.1158/1078-0432.CCR-08-2867.
37. Blanc V, Bousseau A, Caron A, Carrez C, Lutz RJ, Lambert JM. SAR3419: an anti-CD19-Maytansinoid Immunoconjugate for the treatment of B-cell malignancies. Clin Cancer Res 2011; 17:6448-58; PMID:22003072; http://dx.doi.org/10.1158/1078-0432.CCR-11-0485.
38. Hamblett KJ, Senter PD, Chace DF, Sun MMC, Lenox J, Cerveny CG, Kissler KM, Bernhardt SX, Kopcha AK, Zabinski RF, et al. Effects of drug loading on the antitumor activity of a monoclonal antibody drug conjugate. Clin Cancer Res 2004; 10:7063-70; PMID:15501986; http://dx.doi.org/10.1158/1078-0432.CCR-04-0789.
39. Alley SC, Benjamin DR, Jeffrey SC, Okeley NM, Meyer DL, Sanderson RJ, Senter PD. Contribution of linker stability to the activities of anticancer immunoconjugates. Bioconjug Chem 2008; 19:759-65; PMID:18314937; http://dx.doi.org/10.1021/bc7004329.
40. Chalker JM, Bernardes GJL, Lin YA, Davis BG. Chemical modification of proteins at cysteine: opportunities in chemistry and biology. Chem Asian J 2009; 4:630-40; PMID:19235822; http://dx.doi.org/10.1002/asia.200800427.
41. Gomez N, Vinson AR, Ouyang J, Nguyen MD, Chen X-N, Sharma VK, Yuk IH. Triple light chain antibodies: factors that influence its formation in cell culture. Biotechnol Bioeng 2010; 105:748-60; PMID:19845001.
42. Junutula JR, Flagella KM, Graham RA, Parsons KL, Ha E, Raab H, Bhakta S, Nguyen T, Dugger DL, Li G, et al. Engineered thio-trastuzumab-DM1 conjugate with an improved therapeutic index to target human epidermal growth factor receptor 2-positive breast cancer. Clin Cancer Res 2010; 16:4769-78; PMID:20805300; http://dx.doi.org/10.1158/1078-0432.CCR-10-0987.
43. Shen B-Q, Xu K, Liu L, Raab H, Bhakta S, Kenrick M, Parsons-Reponte KL, Tien J, Yu S-F, Mai E, et al. Conjugation site modulates the in vivo stability and therapeutic activity of antibody-drug conjugates. Nat Biotechnol 2012; 30:184-9; PMID:22267010; http://dx.doi.org/10.1038/nbt.2108.
44. Kung Sutherland MS, Walter RB, Jeffrey SC, Burke PJ, Yu C, Kostner H, Stone I, Ryan MC, Sussman D, Lyon RP, et al. SGN-CD33A: a novel CD33-targeting antibody-drug conjugate using a pyrrolobenzodiazepine dimer is active in models of drug-resistant AML. Blood 2013; 122:1455-63; PMID:23770776; http://dx.doi.org/10.1182/blood-2013-03-491506.
45. Strop P, Liu S-H, Dorywalska M, Delaria K, Dushin RG, Tran T-T, Ho W-H, Farias S, Casas MG, Abdiche Y, et al. Location matters: site of conjugation modulates stability and pharmacokinetics of antibody drug conjugates. Chem Biol 2013; 20:161-7; PMID:23438745; http://dx.doi.org/10.1016/j.chembiol.2013.01.010.
46. Lorand L, Graham RM. Transglutaminases: crosslinking enzymes with pleiotropic functions. Nat Rev Mol Cell Biol 2003; 4:140-56; PMID:12563291; http://dx.doi.org/10.1038/nrm1014.
47. Jeger S, Zimmermann K, Blanc A, Grünberg J, Honer M, Hunziker P, Struthers H, Schibli R. Site-specific and stoichiometric modification of antibodies by bacterial transglutaminase. Angew Chem Int Ed Engl 2010; 49:9995-7; PMID:21110357; http://dx.doi.org/10.1002/anie.201004243.
48. Ohtsuka T, Sawa A, Kawabata R, Nio N, Motoki M. Substrate specificities of microbial transglutaminase for primary amines. J Agric Food Chem 2000; 48:6230-3; PMID:11141280; http://dx.doi.org/10.1021/jf000302k.
49. Kim CH, Axup JY, Schultz PG. Protein conjugation with genetically encoded unnatural amino acids. Curr Opin Chem Biol 2013; 17:412-9; PMID:23664497; http://dx.doi.org/10.1016/j.cbpa.2013.04.017.
50. Sletten EM, Bertozzi CR. Bioorthogonal chemistry: fishing for selectivity in a sea of functionality. Angew Chem Int Ed Engl 2009; 48:6974-98; PMID:19714693; http://dx.doi.org/10.1002/anie.200900942.
51. Best MD. Click chemistry and bioorthogonal reactions: unprecedented selectivity in the labeling of biological molecules. Biochemistry 2009; 48:6571-84; PMID:19485420; http://dx.doi.org/10.1021/bi9007726.
52. Wang L, Brock A, Herberich B, Schultz PG. Expanding the genetic code of Escherichia coli. Science 2001; 292:498-500; PMID:11313494; http://dx.doi.org/10.1126/science.1060077.
53. Wang L, Schultz PG. Expanding the genetic code. Angew Chem Int Ed Engl 2004; 44:34-66; PMID:15599909; http://dx.doi.org/10.1002/anie.200460627.
54. Axup JY, Bajjuri KM, Ritland M, Hutchins BM, Kim CH, Kazane SA, Halder R, Forsyth JS, Santidrian AF, Stafin K, et al. Synthesis of site-specific antibody-drug conjugates using unnatural amino acids. Proc Natl Acad Sci USA 2012; 109:16101-6; PMID:22988081; http://dx.doi.org/10.1073/pnas.1211023109.
55. Jencks WP. Mechanism and Catalysis of Simple Carbonyl Group Reactions. Prog Phys Org Chem 1964; 2:63-128; http://dx.doi.org/10.1002/9780470171813.ch2
56. Kalia J, Raines RT. Hydrolytic stability of hydrazones and oximes. Angew Chem Int Ed Engl 2008; 47:7523-6; PMID:18712739; http://dx.doi.org/10.1002/anie.200802651.
57. Doronina SO, Mendelsohn BA, Bovee TD, Cerveny CG, Alley SC, Meyer DL, Oflazoglu E, Toki BE, Sanderson RJ, Zabinski RF, et al. Enhanced activity of monomethylauristatin F through monoclonal antibody delivery: effects of linker technology on efficacy and toxicity. Bioconjug Chem 2006; 17:114-24; PMID:16417259; http://dx.doi.org/10.1021/bc0502917.

OnCusp
Ex. 1002

Clinical Medicine Insights: Oncology



OPEN ACCESS
Full open access to this and thousands of other papers at http://www.la-press.com.

REVIEW

Cytoplasmic Overexpression of HER2: a Key Factor in Colorectal Cancer

Erik J Blok[1], Peter JK Kuppen[1], Jeroen EM van Leeuwen[2] and Cornelis FM Sier[1]

[1]Department of Surgery, Leiden University Medical Center, Leiden, The Netherlands. [2]Department of Cell and Applied Biology, Faculty of Science, Radboud University, Nijmegen, The Netherlands.
Corresponding author email: c.f.m.sier@lumc.nl

Abstract: Trastuzumab, a humanized mouse monoclonal antibody directed against HER2 (Human Epidermal Growth Factor Receptor 2), is currently a keystone in the treatment of breast cancer. Meanwhile, trastuzumab has been validated for use in other types of cancer too. But the data on HER2 expression in colorectal cancer are ambiguous, with reported overexpression of HER2 varying between zero and 84%. In this review these studies are evaluated and compared. It shows that many factors influence the determination of HER2-expression, especially of the intracellular fraction of HER2. It is concluded that although membranous overexpression of HER2 is low in colorectal cancer with only 5% of all patients being positive, a significant proportion of the patients (30%) shows cytoplasmic HER2 overexpression. The clinical impact of enhanced intracellular HER2 is not known, because the nature and origin have not completely been revealed yet. Enlightening this process could be a stepping stone towards targeting of intracellular HER2 as a treatment option.

Keywords: HER2, ErbB2, Her2/neu, colorectal cancer, survival, membranous, cytoplasmic, immunohistochemistry, tissue microarray, biomarker, trastuzumab, herceptin

Clinical Medicine Insights: Oncology 2013:7 41–51

doi: 10.4137/CMO.S10811

This article is available from http://www.la-press.com.

© the author(s), publisher and licensee Libertas Academica Ltd.

This is an open access article. Unrestricted non-commercial use is permitted provided the original work is properly cited.

Background

Colorectal cancer is a major worldwide health problem with an annual incidence of 1.2 million and an annual mortality of over 600,000 people.[1,2] One of the reasons for the relatively high mortality is high tumor stage at the time of diagnosis, caused by the lack of symptoms or the presence of aspecific symptoms during the initial stages of disease. With an increase in tumor stage, the risk of recurrence after resection rises and the chances of survival deteriorate. Chemotherapy has shown to be an efficient strategy for adjuvant therapy, but is still not capable of preventing recurrence in all patients.[3] Therefore there is numerous ongoing research for alternative compounds to be used as adjuvant therapy. Monoclonal antibodies and other biologicals, targeting tumor-associated proteins and blocking essential processes of the tumor, are extensively studied. A crucial step in this process is the identification of tumor specific proteins that can be targeted by these compounds. One of these targets is HER2, which is primarily associated with breast cancer. This review provides an overview of all accessible studies that reported on HER2 overexpression in colorectal cancer, focusing especially on the differences between these studies.

HER2

Over the last two decades, the transmembrane tyrosine kinase receptor Human Epidermal Growth Factor Receptor 2 (HER2, also known as HER2/neu, ErbB2 or p185) has been shown to be an effective target for adjuvant therapy for especially breast cancer. HER2 is found to be upregulated in 20%–30% of all breast cancers. The 40–100 fold protein upregulation is due to a genetic amplification to 25–50 copies.[4] Slamon et al showed that tumors with overexpression of HER2 are more aggressive and, consequently, these patients have a worse prognosis compared to patients with HER2-negative tumors.[5,6] Trastuzumab (Herceptin®), a monoclonal antibody against the extracellular domain of HER2, showed a dramatic improvement in survival as well as recurrence rate when used as adjuvant therapy after breast cancer surgery. The recurrence risk dropped by 40% and the mortality rate by 30%.[7,8] This novel HER2-targeted therapy required a standardized scoring of immunohistochemical HER2 tumor staining to select the breast cancer patients that could benefit from trastuzumab. The scoring of HER2-status comprises four different outcomes: 0 (no staining or staining in <10% of the tumor cells), 1+ (a faint or incomplete membrane staining in >10% of the tumor cells), 2+ (a weak to moderate complete membrane staining in >10% of the tumor cells) and 3+ (an intense and complete membrane staining in >30% of the tumor cells).[9] There are multiple immunohistochemical kits available for HER2-staining, but the polyclonal antibody-based Herceptest (Dako, Glostrup, Denmark), which has been approved by the FDA (US Food and Drug Administration), is mostly used. Remarkably, it is reported that monoclonal antibody-based kits have a better agreement with HER2 gene amplification, as determined by FISH (fluorescence in situ hybridization).[10,11] Generally, the 3+ cases have an excellent concordance with FISH, while the 2+ results are more equivocal.[12] Current guidelines demand a FISH-analysis to determine the gene amplification in 2+ cases.[13]

Colorectal HER2 expression

After the breakthrough in breast cancer, HER2 has been evaluated as a target in other tumor types. After a 37% improvement in overall survival, this recently led to FDA-approval for the use of trastuzumab in HER2-positive metastatic gastric cancer.[14]

Several studies evaluating HER2 in colorectal cancer resulted in a large debate at the end of the last century because overexpression rates varied between zero and 84%.[15] Also the clinical significance of HER2 in these publications was not consistent, with some publications associating HER2 overexpression to survival,[16–18] while others failed to find such a correlation.[19–21] Most researchers agreed that the differences in expression were likely due to differences in technical approaches, antibodies, and scoring protocols, but conclusive data were never presented. Since then a large number of immunohistochemical studies have emerged about HER2 in colorectal cancer. The majority showed membranous overexpression rates between zero and 15%.[22–31] Remarkably, some studies reported both membranous and cytoplasmic overexpression with much higher rates up to 60%.[32–38] Up to now, there is no consistency about the proportion of HER2-overexpression in colorectal tumors.

Immunohistochemical detection of HER2

The major difficulty in comparing immunohistochemical studies is the variety in antibodies. Additionally, differences in technical procedures such as tissue fixation, slide storage procedures, antigen retrieval, and incubation time could influence the staining outcome. The type of HER2-antibody used varied widely in the 27 analyzed studies in this review. In total, 15 different types of antibodies were reported, eight monoclonals and seven polyclonals (Table 1). The claim of Arnaout et al in an early study that polyclonal antibodies mainly stain cytoplasmic HER2, in contrast to monoclonal antibodies staining primarily membranous HER2, was not confirmed in more recent publications.[41] For example, Half et al observed a cytoplasmic staining in 64% of the cases using monoclonal antibodies CB11 and 3B5.[23] Furthermore, there is evidence that some antibodies might not be completely specific for HER2, which could result in aberrant staining patterns. Schrohl et al showed that monoclonal antibody clones 4B5 and CB11 (respectively from PATHWAY®; Ventana Medical Systems Inc, Tucson, AZ, USA and Oracle®; Leica Microsystems GmbH, Wetzlar, Germany) cross-reacted with HER4. The antibodies used in the much used Herceptest, did not cross-react with any other HER-receptors.[47]

Although differences in antigen specificity are presumably the main cause for the differences between various reports, some studies using the same antibody still obtained varying results. For example, antibody NCL-CB11 (Novocastra Laboratories, Newcastle Upon Tyne, UK) is used in 5 different studies with a reported overexpression rate between 22% and 82%. Therefore, procedural variations might also substantially contribute to the variations found

Table 1. An overview of the antibodies used in the 27 studies analyzing HER2 overexpression in colorectal cancer. The antibodies are organized based on the scoring categories of their publications: studies that split into membranous overexpression and cytoplasmic overexpression (A), and studies without distinction between the overexpressing regions (B).

(A) Membrane and cytoplasm HER2 expression evaluated independently

Antibody	Company	Monoclonal/ polyclonal	Patients (n)	% membrane	% cytoplasmic
4D5[41]	Genentech	Monoclonal	70	0.00	0.00
HER14[41]	Genentech	Polyclonal	70	0.00	34.29
21N[41,42]		Polyclonal	93	1.08	5.38
NCL-CB11[16,22,26]	Novocastra	Monoclonal	310	2.58	30.97
No name[18,29]	Nichirei	Polyclonal	390	2.82	24.87
e2-4001[23]	Neomarkers	Monoclonal	96	5.21	63.54
3B5[23]	Oncogene science	Monoclonal	96	5.21	63.54
Herceptest[25,27,28,30,31]	Dako	Polyclonal	857	7.47	
4B5[24]	Ventana	Monoclonal	106	10.38	
CB11[43]	Biogenex	Monoclonal	86	13.95	
Z4881[36]	Zymed	Polyclonal	137	47.45	
A0485[34]	Dako	Polyclonal	74	51.35	

(B) Membrane and cytoplasm evaluated together

Antibody	Company	Monoclonal/ polyclonal	Patients (n)	% positive staining
e2-4001[38]	Neomarkers	Monoclonal	85	36.47
Unknown[20]	Triton	Polyclonal	32	37.50
A0485[33,35]	Dako	Polyclonal	310	47.42
NCL-CB11[21,44]	Novocastra	Monoclonal	541	49.91
300G-9[37]	Digiesi et al	Monoclonal	22	59.09
CB11[32,45]	Biogenex	Monoclonal	300	63.33
3B5[45]	Oncogene science	Monoclonal	176	82.39
NCL-CBE1[46]	Oncogene science	Monoclonal	35	82.86

in immunohistochemical HER2 studies. Incubation times of the antibodies in the various studies ranged from 60 minutes to overnight, and the antibody dilutions were between 1:20 and 1:250.[16,21,22,26,44] However, these variations do not entirely explain the differences in HER2 staining as no consistent correlation is observed between incubation time and overexpression. Both Kountourakis et al and Sun et al report an overexpression of approximately 22% (cytoplasmic and membranous); Kountourakis et al used 1:250 dilution and 60 minutes incubation, while Sun et al used 1:40 with an overnight incubation.[21,26] The two studies reported a highest overexpression of approximately 82%, incubation times of respectively 45 minutes and overnight respectively were used. In these studies, however, the comparability is hampered by the use of different antibodies.[45,46] We performed a comparison of incubation times in our own laboratory, incubating paraffin-embedded colorectal tumor tissue using A0485, an anti-HER2 polyclonal antibody (DAKO Glostrup, Denmark) after antigen retrieval. As shown in Figure 1, an incubation time longer than the 30 minutes indicated in the manufacturer's protocol for breast cancer tissues gives rise to a stronger cytoplasmic staining pattern, allowing better comparison between different colorectal tumors. Because the absolute amount of stainable HER2 in colorectal cancers seems low when compared to breast cancer, it seems advisable for immunohistochemical analysis of HER2-overexpression

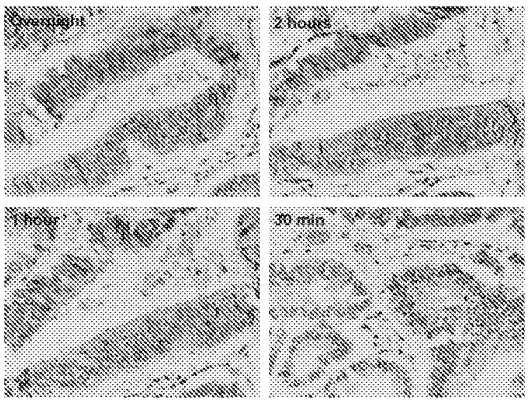


Figure 1. Paraffin-embedded colorectal cancer tissue was incubated with A0485 anti-HER2 antibody with increasing incubation times of 30 minutes, 1 hour, 2 hours and overnight.
Note: With longer incubation times, an increase in cytoplasmic staining (brown) can be observed.

to adapt the protocols for breast cancer for use in colorectal cancer.

Mirlacher et al showed a dramatic decrease in staining intensity for HER2 in tissue microarrays (TMAs) between freshly cut and stored slides.[39] We confirmed these results recently using our own TMA consisting of 500 colorectal cancer tissue samples obtained between 1991 and 2001. This TMA was produced using the same techniques as described earlier by our group for breast cancer.[40] Slides were incubated with A0485. The operation date, and therefore the length of storage time, had a great impact particularly on cytoplasmic HER2 expression. In the group of patients operated on before 1996, 8.4% showed overexpression of cytoplasmic HER2, while in the group of patients operated on in or after 1996, 42.7% expressed cytoplasmic overexpression. Tumors from patients operated on in 1998 or later showed the highest percentage of cytoplasmic staining (52%, manuscript in preparation). Therefore, it is likely that in studies having a long period of tissue collection the HER2 overexpression rate is underestimated especially in the older samples, which could partly explain the variation between studies.

These data emphasize the importance of standardized staining procedures, as relatively insignificant procedure variations might lead to completely different staining patterns and thereby different overexpression rates.

Scoring Procedure

A number of publications analyzed HER2-overexpression in colorectal tumors with genomic techniques like FISH, RT-PCR, Southern blotting, and Northern blotting. Kavanagh et al performed FISH on two 3+ cases and on nine 2+ cases. Both 3+ cases were confirmed to have gene amplification, but only one 2+ case was confirmed.[24] Nathanson et al found approximately the same results, confirming three out of three 3+ cases and one out of two 2+ cases with both FISH and PCR.[28] Ooi et al confirmed all 3+ and 2+ cases with FISH.[29] Together these results confirmed that for colorectal cancers, the observations are similar for those found in breast cancer, ie, that 3+ overexpression is conclusive for gene amplification, whereas 2+ staining is equivocal for gene amplification, and likely has other mechanisms of genetic overexpression.

When analyzing all accessible papers about HER2-overexpression on colon cancer tissue for their



scoring methods, it was observed that most publications follow the breast cancer protocol by examining only membranous overexpression,[24,25,27–31,34,36,42,43] or split their scoring in membranous and cytoplasmic overexpression.[16,18,22,23,26,41] In general, the membranous overexpression rates varied between 0% and 15%. Only Knösel et al and Park et al reported membranous overexpression of over 40%.[34,36] However, Park et al only confirmed two out of 27 3+ cases with FISH, which puts their results in a different perspective. Without these two outliers, the weighted average overexpression of membranous HER2 was 5%. For cytoplasmic overexpression however, the rates varied between 0% and 66%, with a weighted average of 30% (Table 2).

A number of publications did not split their scores into membranous and cytoplasmic overexpression, but took them together to determine positivity.[20,21,32,33,35,37,38,45,46] The observed overexpression rates varied between 22% and 83%, with a weighted average of 50% (Table 2). Unfortunately, no conclusions can be drawn about this percentage regarding the fraction of membranous or cytoplasmic overexpression. Based on the publications that used split results, it is

Table 2. An overview of all papers reporting about HER2 overexpression in colorectal cancer. The papers are organized based on the scoring categories: split into membranous overexpression and cytoplasmic overexpression (A), or papers without distinguishing between the overexpressing regions (B). The weighted average was calculated with and without outliers. When one paper used more than one antibody, all antibodies were examined separately for the weighted average.

(A) Membraneous and cytoplasmic HER2 overexpression evaluated separately

Authors	Year	Antibody	Patients (n)	% membrane	% cytoplasm
Kay et al[16]	1994	NCL-CB11	164	0	34
Arnaout et al[41]	1992	4D5, 21N, HER14	70	0	7–34
Kim et al[25]	2004	Herceptest	185	1	
Osako et al[18]	1998	Nichirei	146	2	66
Nathanson et al[28]	2003	Herceptest	169	3	
Ooi et al[29]	2004	Nichirei	244	3	
Schuell et al[30]	2006	Herceptest	77	4	
McCann et al[42]	1990	21N	23	4	
Half et al[23]	2004	e2-4001 and 3B5	96	5	64
Ochs et al[31]	2004	Herceptest	109	6	
Kountourakis et al[26]	2006	NCL-CB11	106	6	17
Gill et al[22]	2011	NCL-CB11	40	8	58
Kavanagh et al[24]	2009	4B5	106	10	
Dursun et al[43]	2001	CB11	86	14	
Li et al[27]	2011	Herceptest	317	15	
Park et al[36]	2007	Z4881	137	47*	
Knosel et al[34]	2002	A0485	74	51*	
Total % positive membrane				9.22	
Total % positive membrane without outliers (*)				5.38	
Total % positive cytoplasm					30.58

(B) Membrane and cytoplasm evaluated together

Authors	Year	Antibody	Patients (n)	% positive staining
Sun et al[21]	1995	NCL-CB11	293	23
Demirbas et al[32]	2005	CB11	124	36
Uner et al[38]	2005	e2-4001	85	36
Kluftinger et al[20]	1992	Triton	32	38
Kruszewski et al[35]	2010	A0485	202	47
Jesus et al[33]	2005	A0485	108	48
Porcelli et al[37]	2001	300G-9	22	59
McKay et al[44]	2002	NCL-CB11	248	82
Kapitanovic et al[45]	1997	3B5 and CB11	176	82
Maurer et al[46]	1998	NCL-CBE1	35	83
Total % positive staining				55.76

expected that the majority of overexpression in these publications is located in the cytoplasm, and only a minor fraction is overexpressed in the membrane.

Overall, it can be concluded that about 5% of colorectal tumors have membranous overexpression of HER2, while the cytoplasmic overexpression varies strongly with an average around 30%. However, it is likely that this value is an underestimation due to the loss of HER2 antigen in older tissue samples as described earlier.

Cytoplasmic HER2

The FDA-approved scoring system for breast cancer is based entirely on membranous HER-2 overexpression. Cytoplasmic overexpression in breast cancer occurs, but there are strict guidelines to ignore this.[48,49] These guidelines are very specific as trastuzumab is only capable of binding the extracellular domain of membranous HER2. In other words, cytoplasmic HER2 would not have any consequence for clinical decisions about therapy. For years cytoplasmic overexpression of HER2 has been regarded as not relevant for breast cancer. Intracellular HER2 cannot be targeted by trastuzumab, it does not correlate with HER2 mRNA levels,[51] it does not correlate to any clinical outcome,[52] and it may even be a different protein than membranous HER2.

In contrast to breast cancer, there is evidence that in colorectal cancer cytoplasmic HER2 could in fact be associated with survival prognosis. Of 15 publications that analyzed clinical prognostic parameters, six showed a worse patient survival with cytoplasmic tumor overexpression of HER2.[16,18,22,32,34,45] Seven studies showed no correlation with any clinical parameter.[20,21,26,33,35,44,46] Two other papers described a positive correlation between cytoplasmic overexpression and well-differentiated tumors.[23,38] Both publications hypothesize that enhanced cytoplasmic HER2 is an early marker in colorectal cancer, but decreases with progressing tumor stage and tumor dedifferentiation. This seems contradictory to the findings that patients with a HER2-cytoplasmic overexpressing tumor have a decreased survival rate as patients with progressed tumor (higher stage, dedifferentiation) would have less HER2 expression, but poorer prognosis. Moreover, one publication showed a worse differentiation and more lymph node metastases in cytoplasmic HER2-overexpressing tumors.[32]

When combining the distinction in scoring methods within those studies that report a clinical correlation, a remarkable pattern becomes clear. Of all seven studies that report a lack of clinical correlation, six of them do not split their scoring into membranous and cytoplasmic staining.[20,21,33,35,44,46] In contrast, out of the six studies that report a clinical correlation, four of them do split their results in membranous and cytoplasmic staining.[16,18,22,34] Although this has never been confirmed in a large multi-center trial, these studies strongly suggest a clinical relevance of cytoplasmic HER2 overexpression in colorectal cancer.

Assuming that cytoplasmic HER2 has a prognostic role in colorectal cancer, it might also be involved in tumor pathogenesis like membranous HER2 in breast cancer. A plausible explanation would be that cytoplasmic HER2 is forming homodimers, leading to an intracellular activation of the tyrosine kinase domain. Administration of trastuzumab will therefore not have any effect, as this antibody targets the extracellular domain only. Lapatinib, an intracellular tyrosine kinase inhibitor, has recently been approved for treatment of HER2-positive breast cancer patients.[50] If cytoplasmic HER2 is indeed actively involved in colorectal carcinogenesis the administration of lapatinib, or other intracellular HER2-targeting compounds, could be a breakthrough in the treatment of especially this type of cancer.

Biology of cytoplasmic HER2

In breast cancer, it was suggested that cytoplasmic HER2 is a truncated or different protein, based on the fact that a 155 kD peptide was found, in contrast to the 185 kD HER2 found on the membrane. However, for colorectal cancer there have been ambiguous observations. Osako et al performed a western blot analysis on one membranous overexpressing specimen, five membranous cytoplasmic specimens, and one negative sample. They observed 185 kD and 155 kD peptides in the membranous overexpressing specimen, but only 155 kD peptides in the cytoplasmic overexpressing specimens.[18] On the other hand, Kapitanovic et al performed a study in which they were able to split the cell lysate into a cytoplasmic and membranous fraction, and performed a western blot analysis with a different anti-HER2 antibody than Osako et al. They observed a 185 kD peptide in both fractions, and reported no 155 kD peptide. A western



blot using a P-Tyr antibody, detecting phosphorylated (activated) tyrosine kinase domains showed a 185 kD peptide in the intracellular fraction, indicating an intracellular activated HER2-receptor.[45] This would suggest that the activated HER2 was internalized upon activation, or that HER2 was activated intracellularly eg, via homodimerization. Half et al analyzed the localization of cytoplasmic HER2 in colorectal cancer by electron microscopy after labeling with an anti-HER2 antibody and a secondary colloidal gold-labeled antibody. HER2 was located in the rough endoplasmatic reticulum (rER), consistent with newly synthesized peptides. It was also detected in cytosolic vacuoles, at the plasma membrane, and at desmosomes in the intercellular junctions. Particularly because of the localization at the rER, it is likely that this HER2 is derived from original peptide synthesis, and thus would be of genomic origin. Most likely, however, HER2 internalization and synthesis are occurring at the same time. Until these experiments are repeated using an antibody which has been validated to be solely specific for HER2, the origin of cytoplasmic HER2 will not be clarified.

Based on the hypothesis that cytoplasmic HER2 in colorectal cancer is actually newly synthesized rather than internalized, three different studies analyzed genomic amplification to determine the genomic background of HER2-overexpression. Half et al discovered membranous overexpression in only five out of 96 colorectal tumors (5%), while they determined cytoplasmic overexpression in 61 tumors (63%). Four out of five membranous HER2-overexpressing tumors showed amplification with FISH, while no cytoplasmic HER2-overexpressing tumors were confirmed with this technique. Moreover, RT-PCR was performed and showed a 12-fold higher mRNA expression in membranous overexpressing tumors compared to cytoplasmic overexpressing tumors.[23] Pavlakis et al performed FISH-analysis on all cases described by Kountourakis et al. All 3+ cases of membranous overexpression were confirmed as being amplified, while only one of three 2+ cases was confirmed. No single cytoplasmic overexpressing tumor was confirmed.[26,54] These results clearly indicate that membranous overexpression is associated with gene amplification, while cytoplasmic overexpression is due to other mechanisms. Maurer et al performed a northern blot and a Southern blot on the 29 cases overexpressing HER2, without a distinction between membranous and cytoplasmic overexpression. Presumably this concerns cytoplasmic HER2 based on the high percentage of positive tumors (82%). They observed a 1.5 fold increase in mRNA via northern blot in tumors compared to healthy tissue, but the Southern blot did not show any gene amplification.[46] Again, this indicates that cytoplasmic HER2 overexpression is based on mechanisms other than gene amplification.

For other types of cancer, it has been shown that overexpression of HER2 can also occur via mechanisms other than gene amplification, eg, via increased levels of promoter-binding proteins as was observed by Kameda et al in gastric cancer. He observed elevated levels of binding proteins to the TATA-box located in the promoter-region of the HER2-gene, which led to overexpression of HER2.[55] Theoretically, mutations in downstream targets of HER2, for example KRAS, might also influence the expression of HER2 via affected feedback processes. These mechanisms could play a role in the observed cytoplasmic HER2 overexpression without any gene amplification. However, it is still unknown why HER2 does not migrate to the cell membrane, as it should being a transmembrane receptor. Whether it is a simple matter of quantities, and whether this transcriptional upregulation result in not enough HER2 to migrate to the cell membrane is unknown. It is controversial as the western blots from Kapitanovic et al and Osako et al exhibit a much denser signal when analyzing the cytoplasmic overexpressing cells, when compared to the membranous overexpressing cells.[18,45] However, the 12-fold higher mRNA expression in membranous HER2 overexpressing tumors compared to cytoplasmic overexpression as discovered by Half et al would support this theory. Perhaps there is an unknown HER2-transporter protein which is also regulated by the promoter-binding protein. Or perhaps the protein is in some way truncated when being overexpressed at a transcriptional level. Other possibilities include there being an actual 155 kD cleavage product incapable of migrating to the membrane or an immune-evasive strategy by the tumor. One theory is based on the influence of the unfolded protein response (UPR). Upon cellular stress, this response initially stimulates multiple chaperone proteins in the endoplasmic reticulum

in order to increase the glycosylation and folding capacity of the endoplasmic reticulum, and induces apoptosis when this initial response is insufficient. UPR activation in breast cancer cells has been demonstrated.[56] In normal, non-malignant cells there is a baseline expression of HER2, which leads to a HER2 on a cell membrane that cannot be detected by regular immunohistochemistry (Fig. 2A). A possible theory is that in the case of overexpression of the HER2-gene, there is a surplus of HER2 mRNA which, after being translated into protein, cannot be handled properly in the ER and thus leads to aberrant glycosylation or misfolding of the immature protein (Fig. 2C). In this case, either the Golgi apparatus is not capable of maturing the protein or the protein cannot be transported to the Golgi apparatus, both of which lead to accumulation of aberrant HER2 within the cytoplasm. This accumulation would trigger the UPR. The presence of an activated UPR will lead to an increase in properly glycosylated and folded protein, and the overexpression of HER2 by the cell at the membrane. However, for an unknown reason, gene amplification of HER2 in breast cancer leads to a more efficient UPR than HER2-overexpression in colorectal cancer (Fig. 2B). This difference in UPR could be influenced by other processes which affect cellular stress such as hypoxia, nutrient availability, treatment, or other genetic instabilities. This may lead to the situation that UPR in breast cancer is efficient enough to process the surplus of immature

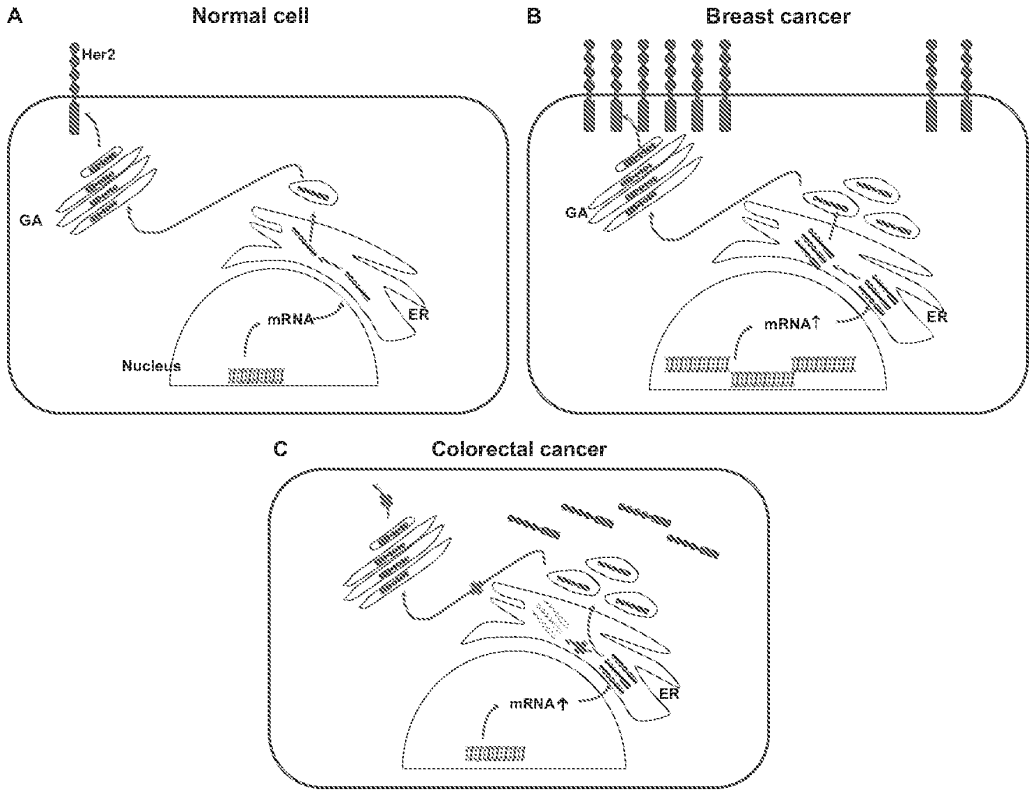


Figure 2. A schematic representation of the difference in HER2 expression between multiple cell types. In a normal cell (**A**), a single copy of the HER2-gene is transcribed to low levels of mRNA, which is then translated to HER2 which enters the endoplasmatic reticulum (ER). In the ER, HER2 is processed (eg, glycosylated), and transported to the Golgi apparatus (GA). There it undergoes final processing before being transported to the membrane. In breast cancer (**B**), this process is basically identical except that gene amplification leads to higher mRNA and HER2 levels. The processing capacity of the ER is improved, most likely due to the unfolded protein response (UPR). In colorectal cancer however (**C**), there is no gene amplification, but gene expression is upregulated during transcription.

Notes: The ER cannot keep up with the high amount of protein, therefore immature HER2 cannot to be completely processed in the ER, and cannot be transported to the GA and the cell membrane; instead incompletely folded HER2 might be extracted from the ER via the ER associated degradation pathway, deglycosylated into a 155–160 kDa protein prior to it accumulation and ultimately proteasomal degradation in the cytoplasm.[58]

HER2, while in colorectal cancer the UPR fails to do so which leads to accumulation of misfolded and aberrantly glycosylated HER2. This unglycosylated form of HER2 might be identical to the p155 variant mentioned before.

Conclusions

It is clear that most of the debate around HER2-overexpression in colorectal cancer is due to differences in staining/scoring techniques. When splitting the results in membranous and cytoplasmic overexpression, a clear pattern appears with approximately 5% of all patients having membranous overexpression, and about 30% of all patients having cytoplasmic overexpression. There is a strong correlation between genomic amplification and membranous overexpression, whereas no genomic amplification is observed in cases with cytoplasmic HER2 expression.[23,26,54]

With around 5% of all colorectal cancers overexpressing HER2 on their membrane, this would create a new treatment strategy with trastuzumab for approximately 60,000 patients worldwide per year. Unfortunately, a clinical trial was ended due to a lack of patient accrual.[57] A large, multicenter trial would be needed to include enough patients for sufficient analysis.

In contrast to membranous HER2 overexpression, a significant proportion of colorectal tumors (30%–50%) show cytoplasmic HER2 overexpression in most studies. The identity of cytoplasmic HER2 remains unclear, although there is some indirect evidence that it is derived from the upregulation of promoter-binding proteins leading to an increase in HER2 production. Additionally, the prognostic value of cytoplasmic HER2 is still unclear. An extensive study using standardized techniques on a large number of tumors is needed to elucidate this matter. If cytoplasmic HER2 has a pathophysiological role in colorectal cancer, intracellular HER2-targeting compounds, for example lapatinib, might be a new treatment option for the 30% of patients having cytoplasmic HER2 overexpression. This would impact about 360,000 patients per year; a clear breakthrough in the treatment of colorectal cancer.

Author Contributions

Conceived and designed the experiments: EB, CS. Analysed the data: EB. Wrote the first draft of the manuscript: EB. Contributed to the writing of the manuscript: EB, PK, CS. Agree with manuscript results and conclusions: EB, PK, JvL, CS. Jointly developed the structure and arguments for the paper: EB, PK, JvL, CS. Made critical revisions and approved final version: EB, PK, JvL, CS. All authors reviewed and approved of the final manuscript.

Funding

This research was performed within the framework of CTMM, the Center for Translational Molecular Medicine, project MUSIS (grant 03O-202).

Competing Interests

Author(s) disclose no potential conflicts of interest.

Disclosures and Ethics

As a requirement of publication author(s) have provided to the publisher signed confirmation of compliance with legal and ethical obligations including but not limited to the following: authorship and contributorship, conflicts of interest, privacy and confidentiality and (where applicable) protection of human and animal research subjects. The authors have read and confirmed their agreement with the ICMJE authorship and conflict of interest criteria. The authors have also confirmed that this article is unique and not under consideration or published in any other publication, and that they have permission from rights holders to reproduce any copyrighted material. Any disclosures are made in this section. The external blind peer reviewers report no conflicts of interest.

References

1. Ferlay J, Shin H, Bray F, Forman D, Mathers C, Parkin D. GLOBOCAN 2008 v1.2, Cancer incidence and mortality worldwide. Available at: http://globocan.iarc.fr. Accessed Jun 12, 2012.
2. Winawer SJ. The multidisciplinary management of gastrointestinal cancer. colorectal cancer screening. *Best Pract Res Clin Gastroenterol*. 2007; 2(6)1:1031–48.
3. André T, Boni C, Mounedji-Boudiaf L, et al. Oxaliplatin, fluorouracil, and leucovorin as adjuvant treatment for colon cancer. *N Engl J Med*. 2004; 350(23):2343–51.
4. Gutierrez C, Schiff R. HER2: Biology, detection, and clinical implications. *Arch Pathol Lab Med*. 2011;135(1):55–62.
5. Slamon DJ, Godolphin W, Jones LA, et al. Studies of the HER-2/neu proto-oncogene in human breast and ovarian cancer. *Science*. 1989;244(4905): 707–12.
6. Slamon DJ, Clark GM, Wong SG, Levin WJ, Ullrich A, McGuire WL. Human breast cancer: correlation of relapse and survival with amplification of the HER-2/neu oncogene. Science. 1987;235(4785):177–82.
7. Slamon DJ, Leyland-Jones B, Shak S, et al. Use of chemotherapy plus a monoclonal antibody against HER2 for metastatic breast cancer that overexpresses HER2. *N Engl J Med*. 2001;344(11):783–92.

8. Smith I, Procter M, Gelber RD, et al. 2-year follow-up of trastuzumab after adjuvant chemotherapy in HER2-positive breast cancer: a randomised controlled trial. *Lancet*. 2006;369(9555):29–36.
9. Liu YH, Xu FP, Rao JY, et al. Justification of the change from 10% to 30% for the immunohistochemical her2 scoring criterion in breast cancer. *Am J Clin Pathol*. 2009;132(1):74–9.
10. Rhodes A, Jasani B, Anderson E, Dodson AR, Balaton AJ. Evaluation of HER-2/neu immunohistochemical assay sensitivity and scoring on formalin-fixed and paraffin-processed cell lines and breast tumors: a comparative study involving results from laboratories in 21 countries. *Am J Clin Pathol*. 2002;118(3):408–17.
11. Seidman AD, Fornier MN, Esteva FJ, et al. Weekly trastuzumab and paclitaxel therapy for metastatic breast cancer with analysis of efficacy by HER2 immunophenotype and gene amplification. *J Clin Oncol*. 2001;19(20):2587–95.
12. Gouvea AP, Milanezi F, Olson SJ, Leitao D, Schmitt FC, Gobbi H. Selecting antibodies to detect HER2 overexpression by immunohistochemistry in invasive mammary carcinomas. *Appl Immunohistochem Mol Morphol*. 2006;14(1):103–8.
13. Press MF, Sauter G, Bernstein L, et al. Diagnostic evaluation of HER-2 as a molecular target: an assessment of accuracy and reproducibility of laboratory testing in large, prospective, randomized clinical trials. *Clin Cancer Res*. 2005;11(18):6598–607.
14. Bang YJ, Van Cutsem E, Feyereislova A, et al. Trastuzumab in combination with chemotherapy versus chemotherapy alone for treatment of HER2-positive advanced gastric or gastro-oesophageal junction cancer (ToGA): a phase 3, open-label, randomised controlled trial. *Lancet*. 1928;376(9742):687–97.
15. Ross JS. The HER-2/neu oncogene in tumors of the gastrointestinal tract. *Cancer Invest*. 2001;19(5):554–68.
16. Kay EW, Mulcahy H, Walsh CB, et al. Cytoplasmic c-erbB-2 protein expression correlates with survival in Dukes' B colorectal carcinoma. *Histopathology*. 1994;25(5):455–61.
17. Lazaris AC, Theodoropoulos GE, Anastassopoulos P, et al. Prognostic significance of p53 and c-erbB-2 immunohistochemical evaluation in colorectal adenocarcinoma. *Histol Histopathol*. 1995;10(3):661–8.
18. Osako T, Miyahara M, Uchino S, Inomata M, Kitano S, Kobayashi M. Immunohistochemical study of c-erbB-2 protein in colorectal cancer and the correlation with patient survival. *Oncology*. 1998;55(6):548–55.
19. Berney CR, Fisher RJ, Yang J, Russell PJ, Crowe PJ. Protein markers in colorectal cancer: predictors of liver metastasis. *Ann Surg*. 1999;230(2):179–84.
20. Kluftinger AM, Robinson BW, Quenville NF, Finley RJ, Davis NL. Correlation of epidermal growth factor receptor and c-erbB2 oncogene product to known prognostic indicators of colorectal cancer. *Surg Oncol*. 1992;1(1):97–105.
21. Sun XF, Carstensen JM, Stål O, Zhang H, Nordenskjöld B. c-erbB-2 oncoprotein in relation to DNA ploidy and prognosis in colorectal adenocarcinoma. *APMIS*. 1995;103(4):309–15.
22. Gill MK, Manjari M, Jain K, et al. Expression of Her-2/neu in colon carcinoma and its correlation with the histological grades and the lymph nodes status. *JCDR*. 2011;5:1564–8.
23. Half E, Broaddus R, Danenberg KD, Danenberg PV, Ayers GD, Sinicrope FA. HER-2 receptor expression, localization, and activation in colorectal cancer cell lines and human tumors. *Int J Cancer*. 2004;108:540–8.
24. Kavanagh D, Chambers G, O' Grady L, et al. Is overexpression of HER-2 a predictor of prognosis in colorectal cancer? *BMC Cancer*. 2009;9:1.
25. Kim JY, Lim SJ, Park K. Cyclooxygenase-2 and c-erbB-2 expression in colorectal carcinoma assessed using tissue microarrays. *Appl Immunohistochem Mol Morphol*. 2004;12(1):67–70.
26. Kountourakis P, Pavlakis K, Psyrri A, et al. Clinicopathologic significance of EGFR and Her-2/neu in colorectal adenocarcinomas. *Cancer J*. 2006;12(3):229–36.
27. Li Q, Wang D, Li J, Chen P. Clinicopathological and prognostic significance of HER-2/neu and VEGF expression in colon carcinomas. *BMC Cancer*. 2011;11:277.
28. Nathanson DR, Culliford AT, Shia J, et al. HER 2/neu expression and gene amplification in colon cancer. *Int J Cancer*. 2003;105(6):796–802.
29. Ooi A, Takehana T, Li X, et al. Protein overexpression and gene amplification of HER-2 and EGFR in colorectal cancers: an immunohistochemical and fluorescent in situ hybridization study. *Mod Pathol*. 2004;17(8):895–904.
30. Schuell B, Gruenberger T, Scheithauer W, Zielinski CH, Wrba F. HER 2/neu protein expression in colorectal cancer. *BMC Cancer*. 2006;6:123.
31. Ochs AM, Wong L, Kakani V, et al. Expression of vascular endothelial growth factor and HER2/neu in stage II colon cancer and correlation with survival. *Clin Colorectal Cancer*. 2004;4(4):262–7.
32. Demirbas S, Suculiu I, Yildirim S, Celenk T. Influence of the c-erb B-2, nm23, bcl-2 and p53 protein markers on colorectal cancer. *Turk J Gastroenterol*. 2006;17(1):13–9.
33. Jesus EC, Matos D, Artigiani R, Waitzberg AF, Goldenberg A, Saad SS. Assessment of staging, prognosis and mortality of colorectal cancer by tumor markers: receptor erbB-2 and cadherins. *Acta Cir Bras*. 2005;20(6):422–7.
34. Knösel T, Yu Y, Stein U, et al. Overexpression of c-erbB-2 protein correlates with chromosomal gain at the c-erbB-2 locus and patient survival in advanced colorectal carcinomas. *Clin Exp Metastasis*. 2002;19(5):401–7.
35. Kruszewski WJ, Rzepko R, Ciesielski M, et al. Expression of HER2 in colorectal cancer does not correlate with prognosis. *Dis Markers*. 2010;29(5):207–12.
36. Park DI, Kang MS, Oh SJ, et al. HER-2/neu overexpression is an independent prognostic factor in colorectal cancer. *Int J Colorectal Dis*. 2007;22(5):491–7.
37. Porcelli B, Frosi B, Terzuoli L, et al. Expression of P185 and P53 in benign and malignant colorectal lesions. *Histochem J*. 2001;33(1):51–7.
38. Uner A, Ebinc FA, Akyurek N, Unsal D, Mentes BB, Dursun A. Vascular endothelial growth factor, c-erbB-2 and c-erbB-3 expression in colorectal adenoma and adenocarcinoma. *Exp Oncol*. 2005;27(3):225–8.
39. Mirlacher M, Kasper M, Storz M, et al. Influence of slide aging on results of translational research studies using immunohistochemistry. *Mod Pathol*. 2004;17(11):1414–20.
40. van Nes J, de Kruijf E, Faratian D, et al. COX2 expression in prognosis and in prediction to endocrine therapy in early breast cancer patients. *Breast Cancer Res Treat*. 2011;125(3):671–85.
41. Arnaout AH, Dawson PM, Soomro S, et al. HER2 (c-erbB-2) oncoprotein expression in colorectal adenocarcinoma: an immunohistological study using three different antibodies. *J Clin Pathol*. 1992;45(8):726–7.
42. McCann A, Dervan PA, Johnston PA, Gullick WJ, Carney DN. c-erbB-2 oncoprotein expression in primary human tumors. *Cancer*. 1990;65(1):88–92.
43. Dursun A, Poyraz A, Suer O, Sezer C, Akyol G. Expression of Bcl-2 and c-ErbB-2 in colorectal neoplasia. *Pathol Oncol Res*. 2001;7(1):24–7.
44. McKay JA, Loane JF, Ross VG, et al. c-erbB-2 is not a major factor in the development of colorectal cancer. *Br J Cancer*. 2002;86(4):568–73.
45. Kapitanovic S, Radosevic S, Kapitanovic M, et al. The expression of p185(HER-2/neu) correlates with the stage of disease and survival in colorectal cancer. *Gastroenterology*. 1997;112(4):1103–13.
46. Maurer CA, Friess H, Kretschmann B, et al. Increased expression of erbB3 in colorectal cancer is associated with concomitant increase in the level of erbB2. *Hum Pathol*. 1998;29(8):771–7.
47. Schrohl AS, Pedersen HC, Jensen SS, Nielsen SL, Brünner N. Human epidermal growth factor receptor 2 (HER2) immunoreactivity: specificity of three pharmacodiagnostic antibodies. *Histopathology*. 2011;59(5):975–83.
48. Press MF, Hung G, Godolphin W, Slamon DJ. Sensitivity of HER-2/neu antibodies in archival tissue samples: potential source of error in immunohistochemical studies of oncogene expression. *Cancer Res*. 1994;54(10):2771–7.
49. Walker RA, Bartlett JMS, Dowsett M, et al. HER2 testing in the UK: further update to recommendations. *J Clin Pathol*. 2008;61(7):818–24.
50. Geyer CE, Forster J, Lindquist D, et al. Lapatinib plus capecitabine for HER2-positive advanced breast cancer. *N Engl J Med*. 2006;355(26):2733–43.
51. Taylor SL, Platt-Higgins A, Rudland PS, Winstanley JH, Barraclough R. Cytoplasmic staining of c-erbB-2 is not associated with the presence of detectable c-erbB-2 mRNA in breast cancer specimens. *Int J Cancer*. 1998;76(4):459–63.



52. Têtu B, Brisson J. Prognostic significance of HER-2/neu oncoprotein expression in node-positive breast cancer. The influence of the pattern of immunostaining and adjuvant therapy. *Cancer*. 1994;73(9):2359–65.
53. de Potter CR, van Daele S, van de Vijver MJ, et al. The expression of the neu oncogene product in breast lesions and in normal fetal and adult human tissues. *Histopathology*. 1989;15(4):351–62.
54. Pavlakis K, Kountourakis P, Stathopoulos E, et al. Her-2 protein expression, cellular localization, and gene amplification in colorectal carcinoma. *Appl Immunohistochem Mol Morphol*. 2007;15(4):441–5.
55. Kameda T, Yasui W, Yoshida K, et al. Expression of ERBB2 in human gastric carcinomas: relationship between p185erbb2 expression and the gene amplification. *Cancer Res*. 1990;50(24):8002–9.
56. Scriven P, Coulson S, Haines R, Balasubramanian S, Cross S, Wyld L. Activation and clinical significance of the unfolded protein response in breast cancer. *Br J Cancer*. 2009;101(10):1692–8.
57. Ramanathan RK, Hwang JJ, Zamboni WC, et al. Low overexpression of HER-2/Neu in advanced colorectal cancer limits the usefulness of trastuzumab (herceptin) and irinotecan as therapy. A Phase II Trial. *Cancer Invest*. 2004;22(6):858–65.
58. Meijer IMJ, van Leeuwen JEM. ERBB2 is a target for USP8-mediated deubiquitination. *Cell Signal*. 2011;23(2):458–67.

1242 *Bioconjugate Chem.* 2009, *20*, 1242–1250

Design, Synthesis, and Biological Evaluation of Antibody–Drug Conjugates Comprised of Potent Camptothecin Analogues

Patrick J. Burke,*,† Peter D. Senter,† David W. Meyer,† Jamie B. Miyamoto,† Martha Anderson,† Brian E. Toki,† Govindarajan Manikumar,‡ Mansukh C. Wani,‡ David J. Kroll,§ and Scott C. Jeffrey†

Seattle Genetics, Inc., 21823 30th Drive SE, Bothell, Washington 98021, Research Triangle Institute, Natural Products Laboratory, Research Triangle Park, North Carolina 27709, and North Carolina Central University, Pharmaceutical Sciences, BRITE, Durham, North Carolina 27707. Received March 12, 2009; Revised Manuscript Received April 10, 2009

Antibody–drug conjugates (ADCs) were prepared with potent camptothecin analogues attached to monoclonal antibodies (mAbs) via dipeptide or glucuronide-based linkers. Aniline-containing camptothecin analogues were employed to provide a site of linker attachment via carbamate bonds that would be stable in circulation. The camptothecin analogues, 7-butyl-10-amino-camptothecin and 7-butyl-9-amino-10,11-methylenedioxy-camptothecin, are generally 10–1000 times more potent than camptothecin. Dipeptide and glucuronide drug linkers were employed containing self-immolative spacers that release drug following lysosomal degradation upon ADC internalization into antigen-positive cell lines. The camptothecin drug linkers were conjugated to three antibodies: chimeric BR96, chimeric AC10, and humanized 1F6, which bind to the Lewis-Y antigen on carcinomas, CD30 on hematologic malignancies, and CD70 present on hematologic malignancies and renal cell carcinoma, respectively. ADCs bearing the potent camptothecin analogue, 7-butyl-9-amino-10,11-methylenedioxy-camptothecin, were highly potent and immunologically specific on a panel of cancer cell lines in vitro, and efficacious at well-tolerated doses in a renal cell carcinoma xenograft model.

INTRODUCTION

In an attempt to enhance activity and mitigate toxicity of cancer chemotherapy, there has been a great deal of interest in the use of monoclonal antibodies (mAbs) for the targeted delivery of cytotoxic agents to cancer cells (*1*–*3*). The principle behind this approach is that, by covalent attachment of a cytotoxic drug to a mAb that binds selectively to a tumor-specific antigen, the activity of the drug could be enhanced through high intratumoral concentrations while sparing normal, nontarget tissue from indiscriminant damage. Early-generation ADCs[1] have demonstrated that several parameters are important for efficient targeted cell kill, such as drug potency, drug linker stability, efficient on-target drug release, mAb immunogenicity, and normal tissue expression of the tumor antigen (*1*–*3*). More recently, significant progress in ADC design has led to the clinical advancement of two new immunoconjugates: SGN-35 for CD30-positive hematologic malignancies (*3*–*5*) and trastuzumab-DM1 for HER2-positive metastatic breast cancer (*6, 7*). In phase I clinical trials both ADCs induced tumor regressions at well-tolerated doses (*6, 8*–*10*), providing further validation of the use of ADCs as an emerging treatment modality.

We are interested in all classes of drugs that may be suitable for empowering mAbs. Early immunoconjugates used clinically approved cytotoxic agents due to their availability and known toxicological properties. This approach is exemplified by BR96-doxorubicin ADC targeted to the Lewis-Y antigen present on human carcinomas. Doxorubicin was attached to the mAb via an acid-sensitive hydrazone linker, and free drug was released upon ADC internalization into acidic lysosomes (*11*). In vivo efficacy was observed in tumor-bearing mice, albeit at elevated (>100 mg ADC/kg) dose levels. Clinical trials revealed low levels of activity in patients with Lewis-Y positive carcinomas (*11*–*13*). The limitations associated with this ADC included drug linker instability, antigen expression on normal tissues, and low drug potency. It has been proposed that optimized ADCs must address these issues to achieve maximal therapeutic efficacy (*1, 2*).

As part of our search for new chemotypes suitable for use in ADCs, we sought to evaluate conjugates consisting of potent camptothecin (CPT) analogues. Camptothecin (**1**) is a natural product that exerts cytotoxic activity through the inhibition of topoisomerase I, leading to cell death (*14*). As a consequence of its broad-spectrum antitumor activity and cytotoxic mechanism, there has been a substantial effort toward the development of clinical camptothecin analogues. To date, two water-soluble analogues have received FDA approval: topotecan and irinotecan. Topotecan is used primarily in the treatment of advanced ovarian cancer and non-small cell lung cancer and was recently approved for cervical cancer (*15*). Irinotecan is a prodrug that is converted into SN-38, a more potent CPT analogue, under the action of carboxylesterases (*16*) and is used primarily in the treatment of colorectal cancer (*15*). Clinical studies with irinotecan, topotecan, and other camptothecin analogues in development indicate that optimal efficacy is achieved with dosing regimens that provide for prolonged exposure to low levels of camptothecin (*17*). This suggests that camptothecin, or potent CPT analogues, may be ideally suited for mAb targeting, as antibodies often have extended circulation half-lives, ranging from many days to weeks (*1, 3*).

* To whom correspondence should be addressed. Phone: 425-527-4766; Fax: 425-527-4109; email: pburke@seagen.com.
† Seattle Genetics, Inc.
‡ Research Triangle Institute.
§ North Carolina Central University.

[1]Abbreviations: ADC, antibody-drug conjugate; AUC, area under the curve; CPT, camptothecin; DIPEA, *N,N*-diisopropylethylamine; DMF, dimethylformamide; DMSO, dimethyl sulfoxide; DOX, doxorubicin; ES, electrospray; IC_{50}, concentration that inhibits 50% cell growth; mAb, monoclonal antibody; mc-val-cit, maleimidocaproyl-valine-citrulline; NHS, *N*-hydroxysuccinimide; PABA, *para*-aminobenzyl alcohol; PBS, phosphate-buffered saline; SCID, severe combined immunodeficient; THF, tetrahydrofuran.

10.1021/bc9001097 CCC: $40.75 © 2009 American Chemical Society
Published on Web 05/26/2009

OnCusp
Ex. 1002

An ADC of CPT has already been described (*18*). It was found that BR96-CPT had a similar level of potency as BR96-DOX (*18, 19*). In addition, the CPT-containing ADC was relatively unstable, due to the use of a labile carbonate linker (*18*). Other camptothecin ADCs bearing SN-38 were more potent, but were also composed of labile linkers (*20*). On the basis of our previous work with optimized auristatin-containing ADCs (*4*), we felt that it was necessary to use camptothecin analogues with much higher potency than CPT, and to incorporate linkers that provide high serum stability.

Camptothecins have been subjected to extensive structure−activity relationship studies (*21*), which indicate that 7-position alkyl substituents and a methylenedioxy group spanning the 10 and 11 positions confer enhanced biochemical and cellular potency (*22, 23*). The selected camptothecin analogues, 7-butyl-10-amino-CPT (**2**) and the des-amino precursor (**12**) to 7-butyl-9-amino-10,11-methylenedioxy-CPT (**3**), are substantially more potent (1−3 logs) than camptothecin (*22, 24, 25*). These molecules are ideally suited for ADC application, not only because of their potencies, but also because they (**2** and **3**) contain functional groups that allow for stable mAb attachment. We now report the design, synthesis, and biological evaluation of ADCs comprising highly potent camptothecin analogues. This investigation resulted in CPT ADCs that were well-defined, potent, and immunologically specific in vitro and displayed good in vivo efficacy at well-tolerated doses.

EXPERIMENTAL PROCEDURES

General Methods and Materials. All commercially available anhydrous solvents were used without further purification and were stored under a nitrogen atmosphere. NMR spectral data were collected on a Varian Mercury 400 MHz spectrometer. Chemical shifts (δ) were reported in ppm and referenced off the deuterium solvent signal. Coupling constants (J) are reported in hertz. Mass spectral data were obtained on a ZMD Micromass mass spectrometer interfaced to an HP Agilent 1100 HPLC instrument configured for LC-MS analysis. 7-Butyl-10-amino-camptothecin (**2**) and 7-butyl-10,11-methylenedioxy-camptothecin (**12**) were prepared via Friedlander condensation as previously described (*23*).

Analytical HPLC was performed on two different HPLC systems. Data collected by "gradient A" were obtained on an HP Agilent 1100 HPLC equipped with a C12 Phenomenex Synergi 2.0 × 150 mm, 4 μm, 80 Å reverse-phase column. The acidic eluent consisted of a linear gradient of acetonitrile from 5% to 95% in 0.1% aqueous formic acid over 10 min, followed by isocratic 95% acetonitrile for 5 min (flow rate = 0.4 mL/min). Data collected by "gradient B" were obtained on a Waters 2690 HPLC interfaced with a Waters 996 PDA and Millenium^{32} software. Samples were eluted over a C12 Phenomenex Synergi 2.0 × 150 mm, 4 μm, 80 Å reverse-phase column. The neutral eluent consisted of a linear gradient of acetonitrile from 10% to 90% in 5 mM ammonium phosphate pH 7 over 10 min, followed by isocratic 90% acetonitrile for 5 min (flow rate = 1.0 mL/min).

Preparative HPLC was carried out on a Varian ProStar 210 solvent delivery system configured with a Varian ProStar 330 PDA detector. Products were purified over a C12 Phenomenex Synergi 10.0 × 250 mm, 4 μm, 80 Å reverse-phase column eluting with 0.05% TFA in water (solvent A) and 0.05% TFA in acetonitrile (solvent B). Purification Method A consisted of the following gradient of solvent A to solvent B: 90:10 from 0 to 5 min; 90:10 to 40:60 from 5 to 45 min; 40:60 to 10:90 from 45 to 50 min; followed by isocratic 10:90 for 5 min. The flow rate was 4.6 mL/min with monitoring at 254 nm. Purification Method B consisted of the following gradient of solvent A to

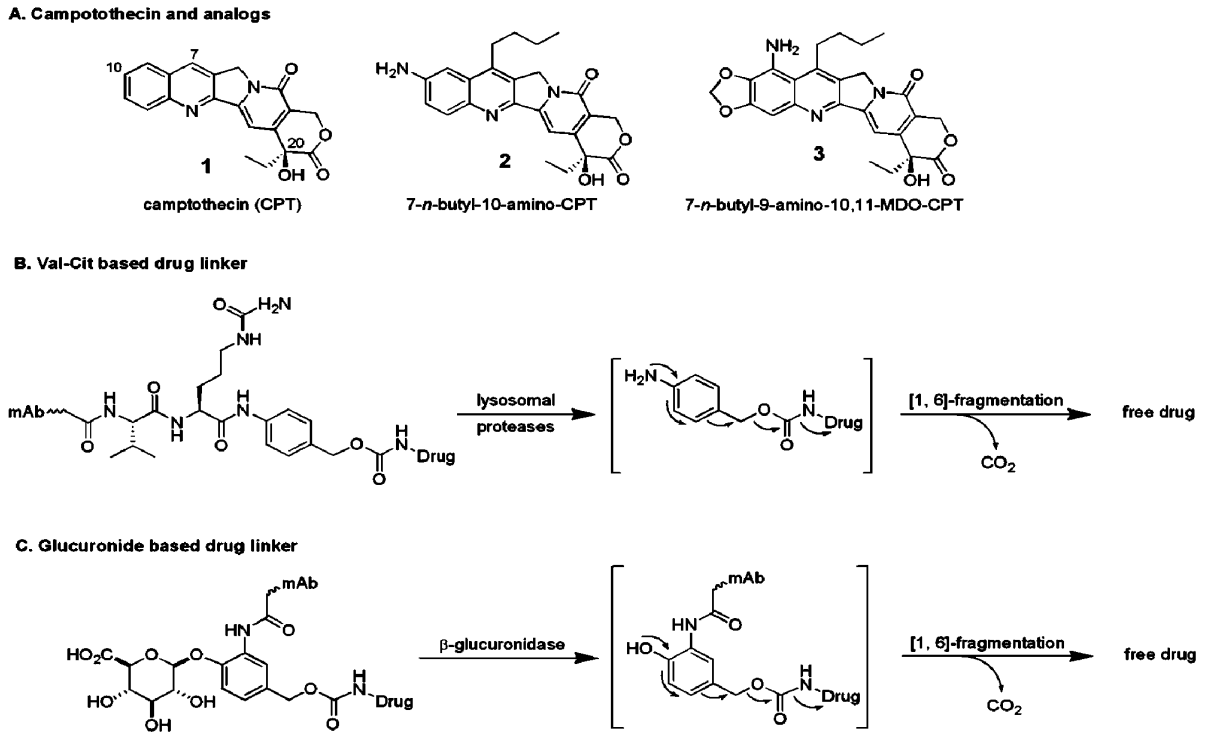


Figure 1. Structures and mechanism of release of active CPT drugs; (A) camptothecin and potent analogues prepared via Friedlander condensation; (B) val-cit dipeptide based drug linker; (C) glucuronide based drug linker.

solvent B: isocratic 90:10 from 0 to 5 min; 90:10 to 60:40 from 5 to 45 min; 60:40 to 10:90 from 45 to 50 min; followed by isocratic 10:90 for 5 min. The flow rate was 4.6 mL/min with monitoring at 254 nm.

Analytical thin layer chromatography was performed on silica gel 60 F_{254} aluminum sheets (EMD Chemicals, Gibbstown, NJ). Whatman 60 Å 230−400 mesh silica gel was used for flash chromatographic purification. Radial chromatography was performed on a Chromatotron instrument (Harris Research, Palo Alto, CA).

7-Butyl-9-amino-10,11-methylenedioxy-camptothecin (3). To a stirred solution of 7-butyl-10,11-methylenedioxy-camptothecin (**12**, 50 mg, 112 μmol) was added 2 mL of concentrated sulfuric acid. The reaction was cooled to 0 °C and sodium nitrate (14 mg, 166 μmol) was added. The reaction was warmed to room temperature and stirred for 30 min, at which time LC/MS revealed complete conversion to product. The reaction was then poured into ice-water and extracted with methylene chloride. The combined extracts were washed with water and concentrated under reduced pressure to provide the nitrated material (54 mg, 98%). UV λ_{max}: 225, 305, and 385 nm. LC-MS: *m/z* (ES^+) found 494.14 $(M+H)^+$, *m/z* (ES^-) found 492.10 $(M-H)^-$. The material was carried forward without further characterization. A stirred solution of the nitrated material (54 mg, 110 μmol) in ethanol was warmed to facilitate dissolution, and then the reaction vessel was purged with nitrogen. At room temperature, 10% palladium on carbon (100 mg) was added, and the reaction mixture was exposed to a hydrogen atmosphere. After 30 min, LC-MS indicated conversion to product. The reaction was filtered through a plug of Celite that was subsequently washed with 300 mL methanol. The filtrate was concentrated under reduced pressure and purified by radial chromatography on a 1 mm plate eluted with a CH_2Cl_2/MeOH mixture (97:3 to 95:5 CH_2Cl_2/MeOH) to provide **3** (29 mg, 57%). ^1H NMR ($CDCl_3$) δ (ppm): 1.02 (m, 6H), 1.57 (m, 3H, under HOD), 1.82 (m, 2H), 1.87 (m, 3H), 3.35 (m, 3H), 3.73 (m, 1H), 5.21 (s, 1H), 5.22 (s, 1H), 5.51 (AB, J = 16.4 Hz, 2H), 6.17 (d, J = 2.0 Hz, 2H). UV λ_{max} 229, 280, 335, and 381 nm. Analytical HPLC: gradient A, t_R = 12.56 min, AUC_{255} = 97.9%; gradient B, t_R = 8.35 min, AUC_{255} = 97.5%. LC-MS: *m/z* (ES^+) found 464.00 $(M+H)^+$, *m/z* (ES^-) found 461.97 $(M-H)^-$.

4-((*S*)-2-((*S*)-2-(6-(2,5-Dioxo-2*H*-pyrrol-1(5*H*)-yl)hexanamido)-3-methylbutanamido)-5-ureidopentanamido)benzyl-(7-butyl-10-aminocamptothecin)carbamate (4). An oven-dried flask was charged with a solution of **2** (10 mg, 23.8 μmol) in 0.5 mL anhydrous CH_2Cl_2. The solution was stirred at room temperature under nitrogen, and 0.4 mL of a 20% phosgene solution in toluene was added. The resultant brown suspension was stirred for 18 h at room temperature. The solution was then evaporated to dryness with a stream of nitrogen gas and further concentrated by rotary evaporation. To the residue obtained was added maleimidocaproyl-valine-citrulline-*para*-aminobenzyl alcohol (**13**, 20.5 mg, 35.7 μmol) (henceforth called mcVal-Cit-PABA (*26*)) dissolved in 0.5 mL anhydrous DMF. The solution was then heated to 45 °C under nitrogen. LC/MS revealed the formation of a product corresponding to the desired molecular weight. The reaction was diluted with 1.5 mL of DMSO and desired product isolated by preparative HPLC (Method A) to give **4** (3.6 mg, 15%). ^1H NMR (DMSO-d_6) δ (ppm): 0.87 (m, 9H), 0.97 (t, J = 7.6 Hz, 3H), 1.19 (m, 2H), 1.48 (m, 8H), 1.70 (m, 4H), 1.85 (m, 4H), 2.15 (m, 4H), 3.10 (m, 5H), 4.19 (m, 1H), 4.38 (m, 1H), 5.17 (s, 2H), 5.29 (s, 2H), 5.43 (s, 2H), 5.98 (m, 1H), 7.00 (s, 2H), 7.28 (s, 1H), 7.41 (d, J = 8.6 Hz, 2H), 7.65 (d, J = 8.0 Hz, 2H), 7.81 (d, J = 9.2 Hz, 1H), 7.90 (m, 1H), 8.10 (d, J = 9.0 Hz, 2H), 8.43 (s, 2H), 10.03 (s, 1H), 10.27 (s, 1H). UV λ_{max}: 225, 267, and 385 nm. Analytical HPLC: gradient A, t_R = 12.38 min, AUC_{255} = 98.5%; gradient B, t_R = 7.81 min, AUC_{255} = 93.9%. LC-MS: *m/z* (ES^+) found 1018.33 $(M+H)^+$, *m/z* (ES^-) found 1017.06 $(M-H)^-$.

4-((*S*)-2-((*S*)-2-(6-(2,5-Dioxo-2*H*-pyrrol-1(5*H*)-yl)hexanamido)-3-methylbutanamido)-5-ureidopentanamido)benzyl-(7-butyl-9-amino-10,11-methylendioxycamptothecin)carbamate (5). Drug linker **5** was prepared from CPT **3** (24 mg, 51.8 μmol) in an analogous reaction to that described for **4**. The crude reaction material was purified by flash chromatography on silica gel eluted with MeOH in CH_2Cl_2 (98:2 to 95:5 to 90:10 CH_2Cl_2/MeOH) to yield **5** (11.2 mg, 20%). ^1H NMR (DMF-d_7) δ (ppm): 0.96 (m, 9H), 1.28 (m, 3H), 1.56 (m, 8H), 2.00 (m, 3H), 2.16 (m, 1H), 2.29 (m, 2H), 3.08 (q, J = 6.2 Hz, 1H), 3.26 (m, 3 H), 3.46 (t, J = 6.8 Hz, 2H), 4.36 (t, J = 7.6 Hz, 1H), 4.63 (bt, 1H), 5.20 (s, 2H), 5.31 (s, 2H), 5.51 (s, 2H), 5.66 (m, 1H), 6.27 (bt, 1H), 6.37 (s, 1H), 6.49 (s, 1H), 7.02 (s, 2H), 7.37 (s, 1H), 7.45 (d, J = 8.0 Hz, 1H), 7.55 (s, 1H), 7.84 (d, J = 8.0 Hz, 1H), 7.90 (d, J = 8.4 Hz, 1H), 8.16 (d, J = 7.6 Hz, 1H), 9.37 (s, 1H), 10.11 (s, 1H). UV λ_{max}: 227, 253, and 383 nm. Analytical HPLC: gradient A, t_R = 12.11 min, AUC_{255} = 96.2%; gradient B, t_R = 7.41 min, AUC_{255} = 94.9%. LC-MS: *m/z* (ES^+) found 1062.45 $(M+H)^+$, *m/z* (ES^-) found 1060.29 $(M-H)^-$.

(2*S*,3*S*,4*S*,5*R*,6*S*)-Methyl 6-(2-(3-(((9*H*-fluoren-9-yl)methoxy)-carbonylamino)propanamido)-4-(((7-butyl-10-aminocamptothecin)carbamoyloxy)methyl)phenoxy)-3,4,5-triacetoxy-tetrahydro-2*H*-pyran-2-carboxylate (6). A flame-dried flask was charged with the known (*27*) protected glucuronide linker fragment (**14**, 28.5 mg, 38.1 μmol) dissolved in 1.5 mL anhydrous CH_2Cl_2. Anhydrous pyridine (37 μL, 457 μmol) was added, and the solution was cooled to −78 °C under a nitrogen atmosphere. Diphosgene (5.5 μL, 46 μmol) was added; the light yellow, limpid solution was stirred for 3 h at −78 °C. A solution of **2** (16.0 mg, 38.1 μmol) in 1.5 mL anhydrous THF was then added, and the reaction was warmed to 0 °C over 1 h. Analytical HPLC at 1 h revealed the formation of product. The reaction was poured into 50 mL EtOAc, and the organic phase was washed with 20 mL water, then 20 mL brine. The organic layer was dried over Na_2SO_4, filtered, and concentrated. The residue so obtained was purified by flash chromatography on silica gel eluted with a CH_2Cl_2/MeOH mixture (98:2 to 97:3 CH_2Cl_2/MeOH) to provide **6** (28.8 mg, 64%). ^1H NMR ($CDCl_3$) δ (ppm) 0.95 (t, J = 7.6 Hz, 3H), 0.99 (t, J = 7.2 Hz, 3H), 1.46 (m, 3H), 1.66 (m, 3H), 1.86 (m, 3H), 2.03 (s, 3H), 2.05 (s, 6H), 2.73 (m, 2H), 3.05 (q, J = 8.0 Hz, 1H), 3.57 (m, 2H), 3.72 (s, 3H), 4.12 (t, J = 7.2 Hz, 1H), 4.31 (m, 4H), 5.15 (m, 7H), 5.42 (m, 1H), 5.59 (m, 1H), 5.76 (bt, 1H), 6.95 (d, J = 8.4 Hz, 1H), 7.04 (d, J = 8.0 Hz, 1H), 7.21 (m, 1H), 7.22 (s, 1H), 7.32 (t, J = 7.2 Hz, 2H), 7.52 (d, J = 7.2 Hz, 2H), 7.59 (d, J = 8.4 Hz, 1H), 7.68 (m, 3H), 8.06 (m, 2H), 8.29 (s, 1H), 8.41 (s, 1H). UV λ_{max}: 267 and 385 nm. LC-MS: *m/z* (ES^+) found 1194.84 $(M+H)^+$, *m/z* (ES^-) found 1192.57 $(M-H)^-$.

(2*S*,3*S*,4*S*,5*R*,6*S*)-Methyl 6-(2-(3-(((9*H*-fluoren-9-yl)methoxy)-carbonylamino)propanamido)-4-(((7-butyl-9-amino-10,11-methylendioxycamptothecin)carbamoyloxy)methyl)phenoxy)-3,4,5-triacetoxy-tetrahydro-2*H*-pyran-2-carboxylate (7). A flame-dried flask was charged with **3** (10 mg, 21 μmol) dissolved in 0.5 mL anhydrous CH_2Cl_2. The solution was stirred at room temperature under nitrogen, and 0.4 mL of a 20% phosgene solution in toluene was added. The reaction was stirred for 18 h at room temperature; a small aliquot of the reaction was quenched with methanol, and the methyl carbamate (indicating formation of the isocyanate) was detected by LC-MS. The solution was then evaporated to dryness with a stream of nitrogen gas and further concentrated by rotary evaporation. To the residue obtained was added the known (*27*) protected glucuronide linker fragment (**14**, 30 mg, 40 μmol) dissolved in 0.2 mL anhydrous DMF. The reaction was stirred at room

OnCusp
Ex. 1002

temperature for 2 h, after which time LC-MS revealed conversion to product. The reaction was then concentrated, redissolved in minimal CH_2Cl_2, and purified by radial chromatography eluting CH_2Cl_2/MeOH (97:3 to 95:5 CH_2Cl_2/MeOH) to give **7** (10 mg, 38%). ^{1}H NMR ($CDCl_3$) δ (ppm): 0.88 (m, 3H), 1.00 (t, J = 7.6 Hz, 3H), 1.26 (s, 2H), 1.42 (m, 3H), 1.87 (m, 2H), 2.06 (s, 9H), 2.74 (m, 2H), 2.99 (bs, 1H), 3.18 (bs, 1H), 3.61 (m, 2H), 3.74 (s, 3H), 4.19 (q, J = 6.8 Hz, 2H), 4.39 (q, J = 10 Hz, 2H), 5.16 (m, 9H), 5.43 (q, J = 8.8 Hz, 1H), 5.65 (d, J = 16.4 Hz, 1H), 5.85 (s, 1H), 6.17 (s, 3H), 6.96 (m, 3H), 7.22 (s, 1H), 7.32 (t, J = 6.8 Hz, 2H), 7.45 (s, 1H), 7.59 (m, 3H), 7.67 (d, J = 7.2 Hz, 2H), 8.14 (s, 1H), 8.47 (s, 1H). UV λ_{max}: 229, 263, and 383 nm. LC-MS: m/z (ES^+) found 1237.95 $(M+H)^+$, m/z (ES^-) found 1236.85 $(M-H)^-$.

(2*S*,3*S*,4*S*,5*R*,6*S*)-6-(2-(3-Aminopropanamido)-4-(((7-butyl-10-aminocamptothecin)carbamoyloxy)methyl)phenoxy)-3,4,5-trihydroxy-tetrahydro-2*H*-pyran-2-carboxylic Acid (8). A flask charged with **6** (24.0 mg, 20.1 μmol) dissolved in a solvent mixture of 2.5 mL MeOH, 3.0 mL THF, and 2.5 mL water, was cooled to 0 °C. To the stirred solution was added LiOH monohydrate (8.6 mg, 212 μmol) and the reaction was warmed to room temperature. After 3 h, LC-MS revealed complete conversion to product. Glacial acetic acid (12.7 μL, 222 μmol) was added, and the reaction was evaporated to dryness. Purification of residue by preparative HPLC using Method B gave **8** (12.7 mg, 67%). ^{1}H NMR (CD_3OD) δ (ppm) 0.96 (t, J = 7.6 Hz, 3H), 0.99 (t, J = 7.2 Hz, 3H), 1.49 (q, J = 7.2 Hz, 2H), 1.65 (m, 2H), 1.89 (m, 2H), 2.62 (s, 1H), 2.86 (t, J = 6.0 Hz, 2H), 2.95 (bt, 2H), 3.53 (m, 3H), 3.93 (m, 1H), 4.84 (d, J = 7.6 Hz, 1H), 4.91 (s, 2H), 5.11 (s, 2H), 5.34 (AB, J = 16.0 Hz, 2H), 7.20 (m, 2H), 7.40 (s, 1H), 7.60 (m, 1H), 7.82 (d, J = 8.8 Hz, 1H), 8.12 (s, 1H), 8.22 (s, 1H), 9.63 (s, 1H). UV λ_{max}: 227, 267, 385 nm. LC-MS: m/z (ES^+) found 832.20 $(M+H)^+$, m/z (ES^-) found 830.27 $(M-H)^-$.

(2*S*,3*S*,4*S*,5*R*,6*S*)-6-(2-(3-Aminopropanamido)-4-(((7-butyl-9-amino-10,11-methylendioxycamptothecin)carbamoyloxy)-methyl)phenoxy)-3,4,5-trihydroxy-tetrahydro-2*H*-pyran-2-carboxylic Acid (9). Drug linker **9** was prepared from **7** (25.0 mg, 25.2 μmol) in the same manner as that described for **8**. The reaction gave **9** (17.6 mg, 92%). UV λ_{max}: 223 and 383 nm. LC-MS: m/z (ES^+) found 875.94 $(M+H)^+$, m/z (ES^-) found 873.95 $(M-H)^-$. The material was carried forward without further characterization.

(2*S*,3*S*,4*S*,5*R*,6*S*)-6-(2-(3-(6-(2,5-Dioxo-2*H*-pyrrol-1-(5*H*)-yl)hexanamido)propanamido)-4-(((7-butyl-10-aminocamptothecin)carbamoyloxy)methyl)phenoxy)-3,4,5-trihydroxy-tetrahydro-2*H*-pyran-2-carboxylic Acid (10). To a solution of **8** (23.0 mg, 27.6 μmol) dissolved in 1.5 mL anhydrous DMF was added maleimidocaproyl NHS ester (12.8 mg, 41.4 μmol), followed by DIPEA (14.4 μL, 82.8 μmol). The reaction was stirred at room temperature under nitrogen for 4 h, at which time LC-MS revealed conversion to product. The crude reaction was diluted in DMSO and purified by preparative HPLC (Method A) to give **10** (20.5 mg, 72%). ^{1}H NMR (DMF-d_7) δ (ppm): 0.99 (m, 6H), 1.26 (p, J = 8.4 Hz, 2H), 1.57 (m, 6H), 1.81 (p, J = 7.2 Hz, 2H), 2.01 (m, 2H), 2.16 (t, J = 7.2 Hz, 2H), 2.68 (t, J = 6.8 Hz, 2H), 3.21 (t, J = 8.0 Hz, 2H), 3.57 (m, 10H), 4.10 (d, J = 9.6 Hz, 2H), 5.03 (m, 1H), 5.23 (s, 2H), 5.36 (s, 2H), 5.52 (d, J = 2.4 Hz, 2H), 6.52 (bs, 1H), 7.01 (s, 2H), 7.19 (dd, J = 8.4, 2.0 Hz, 1H), 7.27 (d, J = 8.4 Hz, 1H), 7.43 (s, 1H), 7.94 (t, J = 5.6 Hz, 1H), 8.09 (dd, J = 9.2, 2.0 Hz, 1H), 8.18 (d, J = 9.2 Hz, 1H), 8.48 (s, 1H), 8.57 (s, 1H), 9.36 (s, 1H), 10.37 (s, 1H). UV λ_{max}: 267 and 385 nm. Analytical HPLC: gradient A, t_R = 11.93 min, AUC_{255} = 94.7%; gradient B, t_R = 5.76 min, AUC_{255} = 97.1%. LC-MS: m/z (ES^+) found 1025.40 $(M+H)^+$, m/z (ES^-) found 1023.29 $(M-H)^-$.

(2*S*,3*S*,4*S*,5*R*,6*S*)-6-(2-(3-(6-(2,5-Dioxo-2*H*-pyrrol-1-(5*H*)-yl)hexanamido)propanamido)-4-(((7-butyl-9-amino-10,11-methylendioxycamptothecin)carbamoyloxy)methyl)phenoxy)-3,4,5-trihydroxy-tetrahydro-2*H*-pyran-2-carboxylic Acid (11). Drug linker **11** was prepared from **9** (16.3 mg, 18.6 μmol) in the same manner as that described for **10**. The reaction gave **11** (12.9 mg, 65%). ^{1}H NMR (DMF-d_7) δ (ppm): 0.93 (t, J = 7.2 Hz, 3H), 0.99 (t, J = 8.0 Hz, 3H), 1.27 (m, 2H), 1.56 (m, 8H), 1.70 (m, 2H), 1.98 (m, 2H), 2.17 (t, J = 7.6 Hz, 2H), 2.69 (m, 2H), 3.52 (m, 10H), 4.10 (d, J = 9.2 Hz, 2H), 5.03 (d, J = 6.4 Hz, 2H), 5.19 (s, 2H), 5.30 (s, 2H), 5.51 (d, J = 2.8 Hz, 2H), 6.37 (m, 3H), 7.02 (d, J = 3.6 Hz, 2H), 7.18 (d, J = 8.4 Hz, 1H), 7.28 (d, J = 8.4 Hz, 1H), 7.37 (s, 1H), 7.55 (s, 1H), 8.50 (s, 1H), 9.36 (s, 1H), 9.43 (s, 1H). UV λ_{max}: 223 and 383 nm. Analytical HPLC: gradient A, t_R = 11.70 min, AUC_{255} = 97.2%; gradient B, t_R = 5.47 min, AUC_{255} = 97.7%. LC-MS: m/z (ES^+) found 1069.44 $(M+H)^+$, m/z (ES^-) found 1067.37 $(M-H)^-$.

Antibody−Drug Conjugate Preparation. The immunoconjugates were prepared as previously described (*4*, *28*). Briefly, the mAbs (4−5 mg/mL) in PBS containing 50 mM sodium borate at pH 7.4 were reduced with tris(carboxyethyl)phosphine hydrochloride at 37 °C. The progress of the reaction, which reduces interchain disulfides, was monitored by reaction with 5,5′-dithiobis(2-nitrobenzoic acid) and allowed to proceed until the desired level of thiols/mAb was achieved. The reduced antibody was then cooled to 0 °C and alkylated with 1.5 equiv of maleimide drug linker per antibody thiol. After 1 h, the reaction was quenched by the addition of 5 equiv of *N*-acetyl cysteine (NAC). Quenched drug linker was removed by gel filtration over a PD-10 column. The ADC was then sterile-filtered through a 0.22 μm syringe filter. Protein concentration and drug loading were determined by spectral analysis at 280 and 375 nm, respectively, with correction for the contribution of drug absorbance at 280 nm. Size-exclusion chromatography was used to determine the extent of antibody aggregation, and RP-HPLC confirmed the absence of remaining NAC-quenched drug linker.

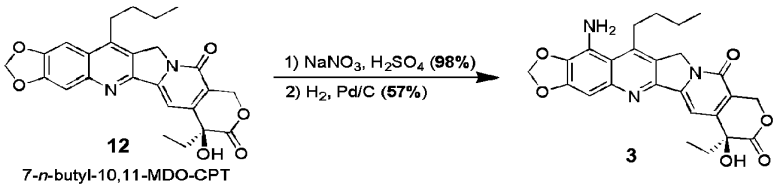
ADC Binding Assay. Karpas 299 cells were treated with serial dilutions of cAC10 or cAC10-**10** in PBS. cBR96-**10** was also included as a nonbinding control. After 30 min on ice, the cells were washed and resuspended in 4 °C PBS. Secondary goat antibody-FITC was added to detect bound mAb or ADC. The cells were then washed, fixed with paraformaldehyde, and analyzed by flow cytometry.

Stability Assay. The stability of cBR96-**10** was assessed by incubation in citrated CD-1 mouse plasma. cBR96-**10** was incubated at 37 °C in plasma over the course of two weeks. Aliquots were withdrawn as a function of time and protein precipitated through the addition of 5 volumes ice-cold methanol containing 0.1% formic acid and spiked with a camptothecin reference standard. The protein was then removed by centrifugation for 5 min at 16 100 *g*; the supernatant was collected and analyzed by LC-MS (ES^+ mode) using gradient A for the detection of counts at m/z 420.2 $(M+H)^+$ at a retention time of 11.78 min, corresponding to free drug **2**. A standard calibration curve spanning the range 1−100% drug release was employed to convert the m/z 420.2 AUC at 11.78 min to a concentration value.

In Vitro Growth Inhibition. The cytotoxic activity of the immunoconjugates was assessed using a resazurin (Sigma, St. Louis, MO, USA) reduction assay (*4*). Karpas 299 (2000 cells/well), H3396 (2000 cells/well), L540cy (7000 cells/well), and Caki-1 (1000 cells/well) cells cultured in log-phase growth were seeded for 24 h in 96-well plates containing 150 μL RPMI 1640 supplemented with 20% FBS. Serial dilutions of ADC in cell culture media were prepared at 4× working concentration; 50 μL of each dilution was added to the 96-well plates. Following

OnCusp
Ex. 1002

Scheme 1



addition of ADC, the cells were incubated with test articles for 4 or 8 d at 37 °C. Resazurin was then added to each well to achieve a 50 μM final concentration, and the plates were incubated for an additional 4 h at 37 °C. The plates were then read for the extent of dye reduction on a Fusion HT plate reader (Packard Instruments, Meridien, CT, USA) with excitation and emission wavelengths of 530 and 590 nm, respectively. The IC_{50} value, determined in triplicate, is defined here as the concentration that results in a 50% reduction in cell growth relative to untreated controls.

In Vivo Therapy Experiments. All experiments were conducted in concordance with the Animal Care and Use Committee in a facility fully accredited by the Association for Assessment and Accreditation of Laboratory Animal Care. In vivo tolerability was first assessed to ensure that the conjugates were tolerated at clinically relevant doses. BALB/c mice were treated with escalating doses of ADC formulated in PBS with 0.01% Tween 20. Mice were monitored for weight loss following drug treatment; those that experienced 20% weight loss or other signs of morbidity were euthanized.

The efficacy experiment was conducted in a renal cell carcinoma xenograft model. Caki-1 tumor fragments were implanted into the right flank of Nude mice. Mice were randomized to study groups ($n = 5$) on day nine with each group averaging around 100 mm^3 tumor volume. The ADC or controls were dosed ip according to a q4dx4 schedule. Tumor volume as a function of time was determined using the formula $(L \times W^2)/2$. Animals were euthanized when tumor volumes reached 1000 mm^3. Mice showing durable regressions were terminated on day 96 post-implant.

RESULTS

Drug Linker Design. There are two significant challenges associated with designing an immunoconjugate with camptothecin: lack of a suitable functional group for conjugation, and hydrophobicity, which can cause antibody aggregation. The first obstacle requires designing a drug linker that combines a high level of stability in circulation with rapid drug release upon internalization into targeted cells. The only readily accessible functional group in camptothecin is the C20 tertiary hydroxyl. The use of ester or carbonate linkages to assemble conjugates with aliphatic alcohols is common (*18, 20, 29−31*). However, as cited earlier, this can be a liability, as mouse plasma contains high levels of esterase activity and readily cleaves ester and carbonate functional groups (*32*).

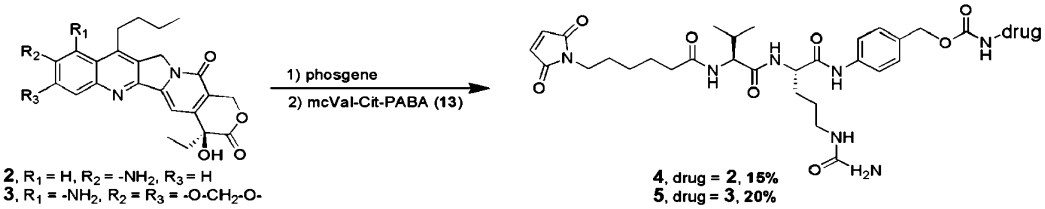
To address drug linker stability, we envisioned employing a carbamate bond to an amine-containing camptothecin such as 7-butyl-10-amino-CPT (**2**) shown in Figure 1. Carbamate bonds typically provide superior stability relative to ester and carbonate bonds with respect to hydrolysis (*33*). Alternatively, we installed an amine into the known (*23, 24*) analogue 7-butyl-10,11-methylenedioxy-CPT (**12**, Scheme 1). In both cases, the presence of the amine provided for the use of a cathepsin B-cleavable valine-citrulline-PABA dipeptide linker (val-cit) system (Figure 1B). The val-cit dipeptide linker system is designed to achieve circulation stability and rapid lysosomal drug release upon internalization into the targeted cancer cells (*4, 34*).

A second obstacle associated with this class is manifest in the hydrophobic nature of these compounds. Camptothecins possess a rigid, extended aromatic ring system that confers limited aqueous solubility and can induce significant antibody aggregation. To address this issue, hydrophilic glucuronide-based CPT drug linkers (Figure 1C) were pursued in addition to dipeptide drug linkers. The glucuronide linker system is characterized by its ability to provide monomeric ADCs with a high degree of circulation stability and rapid drug release in the presence of endogenous β-glucuronidase at the target site (*27*).

Drug Linker Synthesis. The syntheses of CPT analogues **2** and **12** were achieved by the well-precedented Friedlander condensation route (*23, 25*). Regioselective nitration and subsequent hydrogenation of **12** provided the 9-amino analogue **3** in 56% overall yield, as shown in Scheme 1. The protease-cleavable dipeptide drug linkers were prepared in two synthetic steps (Scheme 2). Camptothecins **2** and **3** were treated with phosgene to convert their respective amines to isocyanates in situ. The isocyanates were subsequently trapped by benzyl alcohol linker **13** (*26*) (mcVal-Cit-PABA), forming the carbamate linkages in drug linkers **4** and **5**, respectively.

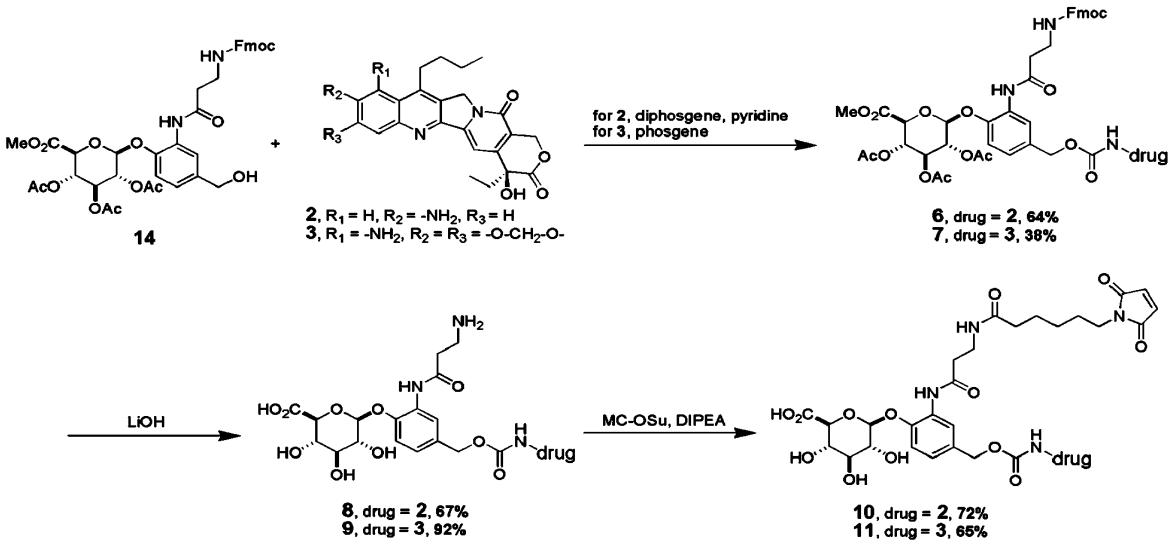
The glucuronide drug linkers were prepared according to the synthetic sequence in Scheme 3. The synthesis commenced by converting the protected glucuronide benzyl alcohol **14** (*27*) to the chloroformate with diphosgene, which was then trapped in situ with camptothecin **2** to provide intermediate **6**. The more sterically hindered amine in **3** was converted to the isocyanate with phosgene and trapped with glucuronide benzyl alcohol **14**. Exhaustive saponification and simultaneous Fmoc-deprotection of **6** and **7** yielded free amines **8** and **9**, respectively. The synthetic sequence was then completed via the coupling of amines **8** and **9** with the NHS ester of maleimidocaproic acid

Scheme 2



OnCusp
Ex. 1002

Scheme 3



(MC-OSu), providing drug linkers **10** and **11**, respectively, in moderate overall yield.

Preparation of Antibody−Drug Conjugates. Conjugates comprising antibodies cBR96, cAC10, and h1F6 and drug linkers **4**, **5**, **10**, and **11** were prepared following standard protocols (*4*, *28*). Reduced interchain disulfides were alkylated with drug linker, forming Michael adducts between the mAb cysteines and drug linker maleimide. Upon completion of the conjugation reaction, excess drug linker was quenched with *N*-acetylcysteine and removed by gel filtration, which was confirmed by HPLC. Drug loading was assessed by chromatographic analysis and UV absorption of the ADCs with correction for the contribution of the camptothecin chromophore at 280 nm.

The extent of ADC aggregation was determined by size-exclusion chromatography. Glucuronide drug linkers **10** and **11** provided ADCs with 4 drugs or 8 drugs per antibody with minimal (<5%) aggregation (Tables 1 and 2). The dipeptide drug linkers **4** and **5** led to antibody aggregation to a greater extent than the more hydrophilic glucuronide drug linkers. ADCs loaded with 4 drugs per antibody contained 4−16% aggregate. ADCs comprising **4** or **5** loaded with 8 drugs/mAb gave much higher levels of aggregation. For example, cAC10 loaded with drug linker **4** was >80% aggregated (Table 1). Highly aggregated (>20%) ADCs were excluded from the biological evaluation.

ADC Binding. As previously shown (*4*), alkylation of interchain disulfides typically has negligible effect on ADC antigen binding activity. To ensure that this was the case with the camptothecins, cAC10-**10** (7 drug/mAb) was assayed for binding affinity relative to unconjugated mAb with CD30+ Karpas 299 cells. The results, shown in Figure 2, indicate that conjugation did not significantly impact the antigen binding. Antigen-negative cBR96 displayed no appreciable binding.

Drug Linker Stability. Val-Cit-PAB and glucuronide carbamate drug linkers have been previously shown to be highly stable toward hydrolysis in various matrices, including plasma (*4*,*28*). To corroborate these observations with the camptothecin series, cBR96-**10** (7 drug/mAb) was incubated in mouse plasma, and the appearance of free drug was assessed by a calibrated LC/MS assay. After 14 d at 37 °C, the free drug (**2**) signal was below the limit of detection of the assay, which is <1% of the theoretical maximum drug release. This suggests that the carbamate linkage is stable to hydrolysis in mouse plasma. Control experiments established efficient recovery of free drug from the matrix.

In Vitro Biological Evaluation. The activities of ADCs containing 7-butyl-10-amino-CPT (**2**) incorporated via dipeptide (**4**) or glucuronide (**10**) drug linker were assessed on Karpas 299 (CD30+) ALCL and H3396 (LeY+) breast carcinoma cell lines following 4 or 8 d treatment (Table 1). ADCs comprising dipeptide drug linker **4** displayed negligible activity following a 4 d treatment (data not shown). When the treatment time was extended to 8 d, modest immunologically specific activity was observed. ADCs bearing glucuronide drug linker **10** were weakly

Table 1. Cytotoxic Activities of ADCs Containing 2

					IC_{50} values (nM)	
cytotoxic agent	treatment time (d)	antigen	drug/mAb ratio	percent aggregate	Karpas 299[a] (CD30+, LeY−)	H3396[a] (CD30−, LeY+)
cAC10−**4**		CD30	8	>80	nt	nt
cBR96−**4**		LeY	8	>80	nt	nt
cAC10−**4**	8	CD30	3.7	9	26	no effect
cBR96−**4**	8	LeY	4.2	16	110	13
cAC10−**10**	4	CD30	7	<5	160	>500[b]
cBR96−**10**	4	LeY	7	<5	>500[b]	22
cAC10−**10**	8	CD30	7	<5	1.8	460
cBR96−**10**	8	LeY	7	<5	170	21
1	4	--	--	--	9.7	7.4
2	4	–	–	–	1.0	0.9

[a] Cells were treated with test articles for 4 or 8 d, and cell viability was determined by resazurin conversion. The IC_{50} values represent the concentrations (nM) of the drug component of the ADC. [b] IC_{50} values are greater than the highest concentration tested.

OnCusp
Ex. 1002

Table 2. Cytotoxic Activities of ADCs Containing 3 Following 4 d Treatment

				IC_{50} (nM)		
cytotoxic agent	antigen	drug/mAb ratio	percent aggregate	Karpas 299[a] (CD30+, CD70−)	L540cy[a] (CD30+, CD70−)	Caki-1[a] (CD 30−, CD70+)
cAC10−**5**	CD30	3.8	8	4.4	0.32	>150[b]
h1F6−**5**	CD70	4.2	4	>190[b]	no effect	6.2
cAC10−**11**	CD30	4.4	3	0.91	0.23	>210[b]
h1F6−**11**	CD70	4.5	1	>220[b]	190	1.5
cAC10−**11**	CD30	8	2	0.89	0.41	510
h1F6−**11**	CD70	8	1	650	280	3.3
1	–	–	–	9.7	7.4	7.0
3	–	–	–	0.06	0.03	0.05

[a] Cells were treated with test articles for 4 d, and cell viability was determined by resazurin conversion. The IC_{50} values represent the concentrations (nM) of the drug component of the ADC. [b] IC_{50} values are greater than the highest concentration tested.

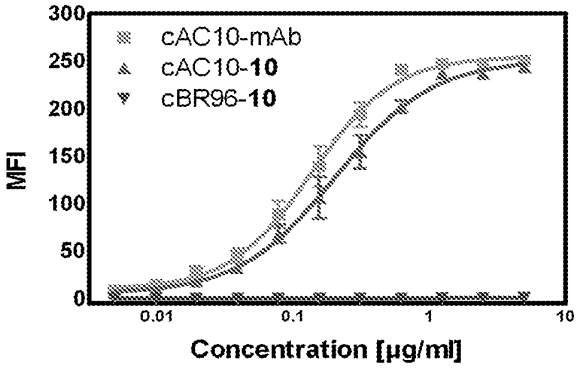


Figure 2. FACS analysis of antigen binding of glucuronide drug linker cAC10-**10** relative to cAC10 mAb and nonbinding cBR96-**10** on CD30+ Karpas 299 cells.

active, albeit more potent than mAb−**4** conjugates, over the course of a 4 d drug treatment with IC_{50} values of 160 nM and 22 nM on Karpas 299 and H3396, respectively. When drug treatment was extended to 8 d, cAC10−**10** displayed a substantial increase in potency on Karpas 299. An analogous increase in potency on H3396 cells was not observed. The activities of conjugates comprising h1F6 or cAC10 and **5** and **11** were tested on Karpas 299, L540cy (Hodgkin lymphoma), and Caki-1 (renal cell carcinoma) following a 4 d treatment (Table 2). The conjugates were immunologically specific and highly potent on the three cell lines, with IC_{50} values ranging from 0.23 to 4.4 nM across the panel.

In Vivo Biological Evaluation. In light of the superior in vitro potency of ADCs armed with camptothecin analogue **3** relative to **2**, in vivo evaluation focused on ADCs bearing drug linkers **5** and **11**. ADCs were initially evaluated for mouse tolerability prior to efficacy experiments. BALB/c mice were injected once ip with cAC10−**5** (4 drug/mAb) or cAC10−**11** (4 drug/mAb) and evaluated for weight loss and morbidity. Both the glucuronide (cAC10−**11**) and the val-cit dipeptide (cAC10−**5**) conjugates were well-tolerated at 50 mg/kg. At 100 mg/kg, cAC10−**5** resulted in moderate weight loss (5−10%) and cAC10−**11** was toxic. From these results, the maximum tolerated doses (MTD) for cAC10−**5** and cAC10−**11** are approximately 100 mg/kg and 50 mg/kg, respectively.

An efficacy experiment with immunoconjugates h1F6−**5** and h1F6−**11** was carried out in the Caki-1 renal cell carcinoma model. Nude mice bearing Caki-1 tumors were treated four times every 4 d (q4d × 4) with ADCs once the average tumor size was approximately 100 mm^3 (Figure 3). At 3 mg/kg, the val-cit immunoconjugate (h1F6−**5**) had no effect on tumor growth. In contrast, the glucuronide conjugate (h1F6−**11**) induced substantial tumor growth delay. At 10 mg/kg, the glucuronide conjugate again

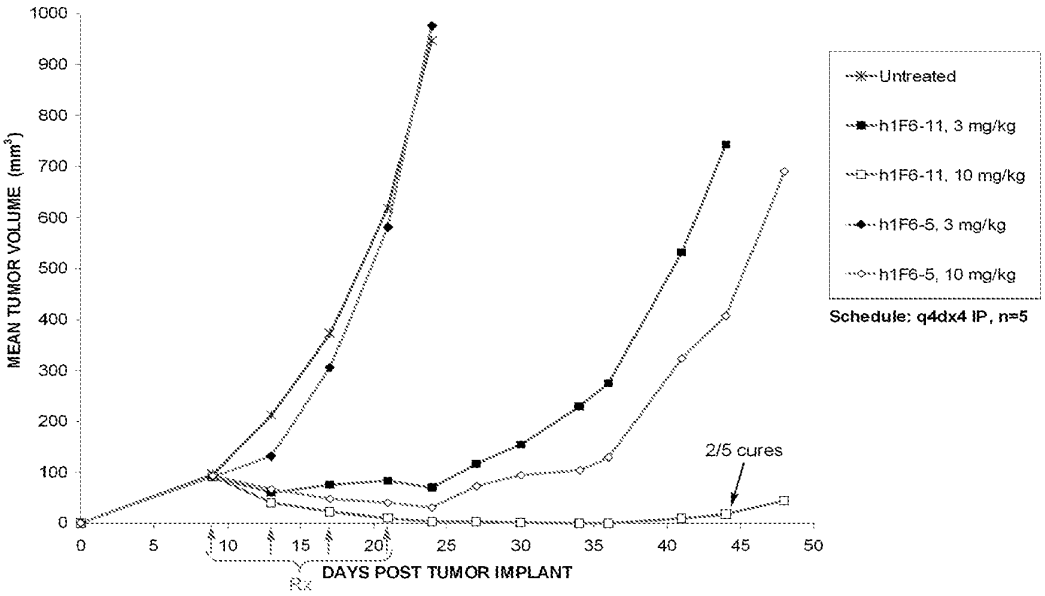


Figure 3. In vivo efficacy of camptothecin ADCs in a Caki-1 renal cell carcinoma xenograft model; all ADCs contain 4 dr/mAb.

outperformed the val-cit conjugate. Mice treated with h1F6—**5** achieved 5/5 partial regressions, while mice treated with h1F6—**11** had 5/5 complete regressions with 2/5 mice cured.

DISCUSSION

Early work on ADCs established drug potency as an important parameter contributing to the conjugate activity. The camptothecin analogues employed here are substantially more potent than CPT or related clinical analogues, irinotecan and topotecan. Among the two CPT analogues evaluated, the more potent analogue (**3**) provided significantly more potent ADCs (Tables 1 and 2). ADCs bearing **3** provided in vitro potencies 20- to 400-fold greater than CPT ADCs (*18*). More recently, ADCs bearing SN-38 were reported to be active at the single-digit nM level (*20*). Specificity controls were not included, however, and it is possible that nonspecific drug release from the carbonate or ester drug linker significantly contributed to the observed conjugate potency. The ADCs bearing **3** led to high levels of immunologically specific cell kill at subsaturating doses (Table 2). Immunological specificity implies that the linker is stable since the cells were continuously exposed to the ADCs for 96 h. The binding ADCs were less potent than the respective free drugs (Tables 1 and 2). It is possible that free drug accumulation via passive cellular uptake over the course of the 96 h treatment exceeds the intracellular drug concentration achieved through antigen-mediated delivery. This has been previously observed with other ADCs (*5*, *35*, *36*).

Camptothecins are an especially compelling drug class for ADCs because they can be produced synthetically, modified to give analogues with high potency, and have been shown to possess pronounced clinical activity. However, aqueous insolubility presents a significant challenge in utilizing the CPT drug class. Clinical camptothecins, irinotecan and topotecan, were designed to overcome this by inclusion of solubilizing amine groups (*15*). From the standpoint of ADC development, upon conjugation, CPT hydrophobicity can lead to significant mAb aggregation. The glucuronide linker system is ideal in addressing this issue. The glucuronide drug linkers consistently provided monomeric ADCs when loaded at 4 and 8 drug/mAb, whereas the dipeptide drug linkers tended to provide ADCs with a greater degree of aggregation (Tables 1 and 2). This is consistent with our previous work with hydrophobic minor groove binders (*37*).

We have described the preparation and biological evaluation of ADCs empowered with camptothecin analogues that were selected on the basis of the presence of an amine functional group and enhanced cellular potency. The amine functional group was deemed important because it facilitated the use of carbamate-based linkers such as the val-cit dipeptide and the glucuronide linker systems. On the basis of these results, immunoconjugates comprising the more potent analogue (**3**) linked via val-cit dipeptide or glucuronide drug linker systems are well-suited for further development.

LITERATURE CITED

(1) Carter, P. J., and Senter, P. D. (2008) Antibody-drug conjugates for cancer therapy. *Cancer J. 14*, 154–169.

(2) Chari, R. V. J. (2008) Targeted cancer therapy: conferring specificity to cytotoxic drugs. *Acc. Chem. Res. 41*, 98–107.

(3) Wu, A. M., and Senter, P. D. (2005) Arming antibodies: prospects and challenges for immunoconjugates. *Nat. Biotechnol. 23*, 1137–1146.

(4) Doronina, S. D., Toki, B. E., Torgov, M. Y., Mendelsohn, B. A., Cerveny, C. G., Chace, D. F., DeBlanc, R. L., Gearing, R. P., Bovee, T. D., Siegall, C. B., Francisco, J. A., Wahl, A. F., Meyer, D. L., and Senter, P. D. (2003) Development of potent monoclonal antibody auristatin conjugates for cancer therapy. *Nat. Biotechnol. 21*, 778–784.

(5) Francisco, J. A., Cerveny, C. G., Meyer, D. L., Mixan, B. J., Klussman, K., Chace, D. F., Rejniak, S. X., Gordon, K. A., DeBlanc, R. L., Toki, B. E., Law, C.-L., Doronina, S. D., Siegall, C. B., Senter, P. D., and Wahl, A. F. (2003) cAC10-vcMMAE, an anti-CD30-monomethyl auristatin E conjugate with potent and selective antitumor activity. *Blood 102*, 1458–1465.

(6) Beeram, M., Krop, I. E., Modi, S., Tolcher, A. W., Rabbee, N., Girish, S., Tibbitts, J., Holden, S. N., Lutzker, S. G., and Burris, H. A. (2007) A phase I study of trastuzumab-MCC-DM1 (T-DM1), a first-in-class HER2 antibody-drug conjugate (ADC), in patients (pts) with HER2+ metastatic breast cancer (BC). *J. Clin. Oncol.* 25 Abstract 1042.

(7) Phillips, G. D. L., Li, G., Dugger, D. L., Crocker, L. M., Parsons, K. L., Mai, E., Blattler, W. A., Lambert, J. M., Chari, R. V. J., Lutz, R. J., Wong, W. L. T., Jacobson, F. S., Koeppen, H., Schwall, R. H., Kenkare-Mitra, S. R., Spencer, S. D., and Sliwkowski, M. X. (2008) Targeting HER2-positive breast cancer with trastuzumab-DM1, an antibody-drug conjugate. *Cancer Res. 68*, 9280–9290.

(8) Krop, I. E., Beeram, M., Modi, S., Rabbee, N., Girish, S., Tibbitts, J., Holden, S. N., Lutzker, S. G., and Burris, H. A. 30th Annual San Antonio Breast Cancer Symposium, 2007, Abstract 310.

(9) Younes, A., Forero-Torres, A., Bartlett, N. L., Leonard, J. P., Lynch, C., Kennedy, D. A., and Sievers, E. L. American Society of Hematology National Meeting, 2008a, Abstract 1006.

(10) Younes, A., Forero-Torres, A., Bartlett, N. L., Leonard, J. P., Rege, B., Kennedy, D. A., Lorenz, J. M., and Sievers, E. L. American Society of Clinical Oncology, 2008b, Abstract 8526.

(11) Trail, P. A., Willner, D., Lasch, S. J., Henderson, A. J., Hofstead, S., Casazza, A. M., Firestone, R. A., Hellstrom, I., and Hellstrom, K. E. (1993) Cure of xenografted human carcinomas by BR96-doxorubicin immunoconjugates. *Science 261*, 212–215.

(12) Saleh, M. N., Sugarman, S., Murray, J., Ostroff, J. B., Healey, D., Jones, D., Daniel, C. R., LeBherz, D., Brewer, H., Onetto, N., and LaBuglio, A. F. (2000) Phase I trial of the anti-Lewis Y drug immunoconjugate BR96-doxorubicin in patients with Lewis Y-expressing epithelial tumors. *J. Clin. Oncol. 18*, 2282–2292.

(13) Tolcher, A. W., Sugarman, S., Gelman, K. A., Cohen, R., Saleh, M., Isaacs, C., Young, L., Healey, D., Onetto, N., and Slichenmyer, W. (1999) Randomized phase II study of BR96-doxorubicin conjugate in patients with metastatic breast cancer. *J. Clin. Oncol. 17*, 478–484.

(14) Pommier, Y. (2006) Topoisomerase I inhibitors: camptothecins and beyond. *Nat. Rev. Cancer 6*, 789–802.

(15) Garcia-Carbonero, R., and Supko, J. G. (2002) Current perspectives on the clinical experience, pharmacology, and continued development of the camptothecins. *Clin. Cancer Res. 8*, 641–661.

(16) Satoh, T., Hosokawa, M., Atsumi, R., Suzuki, W., Hakusui, H., and Nagai, E. (1994) Metabolic activation of CPT-11, 7-ethyl-10-[4-(1-piperidino)-1-piperidino]carbonyloxycamptothecin, a novel antitumor agent, by carboxylesterase. *Biol. Pharm. Bull. 17*, 662–664.

(17) Gerrits, C. J. H., de Jonge, M. J. A., Schellens, J. H. M., Stoter, G., and Verweij, J. (1997) Topoisomerase I inhibitors: the relevance of prolonged exposure for present clinical development. *Br. J. Cancer 76*, 952–962.

(18) Walker, M. A., Dubowchik, G. M., Hofstead, S. J., Trail, P. A., and Firestone, R. A. (2002) Synthesis of an immunoconjugate of camptothecin. *Bioorg. Med. Chem. Lett. 12*, 217–219.

(19) Willner, D., Trail, P. A., Hofstead, S. J., King, H. D., Lasch, S. J., Braslawsky, G. R., Greenfield, R. S., Kaneko, T., and Firestone, R. A. (1993) (6-Maleimidocaproyl)hydrazone of doxorubicin - A new derivative for the preparation of immunoconjugates of doxorubicin. *Bioconjugate Chem. 4*, 521–527.

OnCusp
Ex. 1002

(20) Moon, S. J., Govindan, S. V., Cardillo, T. M., D'Souza, C. A., Hansen, H. J., and Goldenberg, D. M. (2008) Antibody conjugates of 7-ethyl-10-hydroxycamptothecin (SN-38) for targeted cancer chemotherapy. *J. Med. Chem. 51*, 6916–6926.

(21) Thomas, C. J., Rahier, N. J., and Hecht, S. M. (2004) Camptothecin: current perspectives. *Bioorg. Med. Chem. 12*, 1585–1604.

(22) Adams, D. J., Webba da Silva, M., Flowers, J. L., Kohlhagen, G., Pommier, Y., Colvin, O. M., Manikumar, G., and Wani, M. C. (2006) Camptothecin analogs with enhanced activity against human breast cancer cells. I. Correlation of potency with lipophilicity and persistence in the cleavage complex. *Cancer Chemother. Pharmacol. 57*, 135–144.

(23) Wani, M. C., Manikumar, G., Wall, M. E., and Wall, M. A. (2004) (US PTO, Ed.), US 2004/0266803 A1, Research Triangle Institute, USA.

(24) Vladu, B., Woynarowski, J. M., Manikumar, G., Wani, M. C., Wall, M. A., Von Hoff, D. D., and Wadkins, R. M. (2000) 7- and 10-substituted camptothecins: dependence of topoisomerase I-DNA cleavable complex formation and stability on the 7- and 10-substituents. *Mol. Pharmacol. 57*, 243–251.

(25) Wall, M. A., Wani, M. C., Nicholas, A. W., Manikumar, G., Tele, C., Moore, L., Truesdale, A., Leitner, P., and Besterman, J. M. (1993) Plant antitumor agents. 30. Synthesis and structure activity of novel camptothecin analogs. *J. Med. Chem. 36*, 2689–2700.

(26) Dubowchik, G. M., Firestone, R. A., Padilla, L., Willner, D., Hofstead, S. J., Mosure, K., Knipe, J. O., Lasch, S. J., and Trail, P. A. (2002) Cathepsin B-labile dipeptide linkers for lysosomal release of doxorubicin from internalizing immunoconjugates: model studies of enzymatic drug release and antigen-specific in vitro anticancer activity. *Bioconjugate Chem. 13*, 855–869.

(27) Jeffrey, S. C., Andreyka, J. B., Bernhardt, S. X., Kissler, K. M., Kline, T., Lenox, J. S., Moser, R. F., Nguyen, M. T., Okeley, N. M., Stone, I. J., Zhang, X., and Senter, P. D. (2006) Development and properties of beta-glucuronide linkers for monoclonal antibody-drug conjugates. *Bioconjugate Chem. 17*, 831–840.

(28) Jeffrey, S. C., Torgov, M. Y., Andreyka, J. B., Boddington, L., Cerveny, C. G., Denny, W. A., Gordon, K. A., Gustin, D., Haugen, J., Kline, T., Nguyen, M. T., and Senter, P. D. (2005) Design, synthesis, and in vitro evaluation of dipeptide-based antibody minor groove binder conjugates. *J. Med. Chem. 48*, 1344–1358.

(29) de Groot, F. H. M., Busscher, G. F., Aben, R. W. M., and Scheeren, H. W. (2002) Novel 20-carbonate linked prodrugs of camptothecin and 9-aminocamptothecin designed for activation by tumour-associated plasmin. *Bioorg. Med. Chem. Lett. 12*, 2371–2376.

(30) de Groot, F. H. M., Loos, W. J., Koekkoek, R., van Berkom, L. W. A., Busscher, G. F., Seelen, A. E., Albrecht, C., de Bruijn, P., and Scheeren, H. W. (2001) Elongated multiple electronic cascade and cyclization spacer systems in activatible anticancer prodrugs for enhanced drug release. *J. Org. Chem. 66*, 8815–8830.

(31) Lerchen, H. G., Baumgarten, J., von dem Bruch, K., Lehmann, T. E., Sperzel, M., Kempka, G., and Fiebig, H. H. (2001) Design and optimization of 20-O-linked camptothecin glycoconjugates as anticancer agents. *J. Med. Chem. 44*, 4186–4195.

(32) Liederer, B. M., and Borchardt, R. T. (2006) Enzymes involved in the bioconversion of ester-based prodrugs. *J. Pharm. Sci. 95*, 1177–1195.

(33) Huang, T. L., Szekacs, A., Uematsu, T., Kuwano, E., Parkinson, A., and Hammock, B. D. (1993) Hydrolysis of carbonates, thiocarbonates, carbamates, and carboxylic esters of alpha-naphthol, beta-naphthol, and para-nitrophenol by human, rat, and mouse liver carboxylesterases. *Pharm. Res. 10*, 639–648.

(34) Dubowchik, G. M., and Firestone, R. A. (1998) Cathepsin B-sensitive dipeptide prodrugs. 1. A model study of structural requirements for efficient release of doxorubicin. *Bioorg. Med. Chem. Lett. 8*, 3341–3346.

(35) Jeffrey, S. C., Nguyen, M. T., Andreyka, J. B., Meyer, D. L., Doronina, S. D., and Senter, P. D. (2006) Dipeptide-based highly potent doxorubicin antibody conjugates. *Bioorg. Med. Chem. Lett. 16*, 358–362.

(36) Tassone, P., Gozzini, A., Goldmacher, V., Shammas, M. A., Whiteman, K. R., Carrasco, D. R., Li, C., Allam, C. K., Venuta, S., Anderson, K. C., and Munshi, N. C. (2004) In vitro and in vivo activity of the maytansinoid immunoconjugate huN901-N2′-deacetyl-N2′-(3-mercapto-1-oxopropyl)-maytansine against CD56+ multiple myeloma cells. *Cancer Res. 64*, 4629–4636.

(37) Jeffrey, S. C., Nguyen, M. T., Moser, R. F., Meyer, D. L., Miyamoto, J. B., and Senter, P. D. (2007) Minor groove binder antibody conjugates employing a water soluble beta-glucuronide linker. *Bioorg. Med. Chem. Lett. 17*, 2278–2280.

BC9001097

Gene Mapping Report

Cytogenet Cell Genet 92:164–165 (2001)

Cytogenetics and Cell Genetics

Assignment[1] of TACSTD1 (alias TROP1, M4S1) to human chromosome 2p21 and refinement of mapping of TACSTD2 (alias TROP2, M1S1) to human chromosome 1p32 by in situ hybridization

G. Calabrese,[a] C. Crescenzi,[b] E. Morizio,[a] G. Palka,[a] E. Guerra[b] and S. Alberti[b]

[a]Section of Medical Genetics, Department of Biomedical Sciences, University of Chieti;
[b]Laboratory of Experimental Oncology, Department of Cell Biology and Oncology, Istituto di Ricerche Farmacologiche Mario Negri – Consorzio Mario Negri Sud, Santa Maria Imbaro, Chieti (Italy)

[1] This is discordant with the previous assignment of TACSTD1 to chromosome 4 and a more precise localization of TACSTD2 previously mapped to 1p32→p31 or 1p13→q12 by Linnenbach et al. (1993).

Rationale and significance

TACSTD1 (alias TROP1, M4S1; OMIM 600718) and TACSTD2 (alias TROP2, M1S1; OMIM 137290) encode cell-surface glycoproteins expressed in epithelial cells. Trops are calcium signal transducers (Ripani et al., 1998), are over-expressed by human carcinomas and play a role in the control of tumor cell growth (manuscript in preparation). TACSTD2 (originally called M1S1; Fornaro et al., 1995) is responsible for the gelatinous drop-like corneal dystrophy (OMIM 204870) (Tsujikawa et al., 1999). Although placed within a YAC/BAC/cosmid contig on 1p (Tsujikawa et al., 1999), its chromosome location still is undecided at 1p32→p31 or 1p13→q12 (Linnenbach et al., 1993; UniGene Hs.23582). By fluorescence in situ hybridization (FISH) we assign TACSTD2 to 1p32. The growth-suppressing properties of TACSTD2 and the frequent deletion of 1p32 in human tumors (White et al., 1999) suggest that this gene is a candidate to be a novel oncosuppressor. TACSTD1 (formerly called M4S1) shares a 49%-similar cDNA sequence with TACSTD2. TACSTD1 was localized to 4q by human/rodent somatic cell hybrid analyses (Linnenbach et al., 1993) (UniGene Hs.692). We reassign TACSTD1 to human chromosome 2p21, a region which contains the MSH2 and MSH6 DNA mismatch repair genes (Papadopoulos et al., 1995). In agreement with the HUGO Gene Nomenclature Committee, the M4S1 and M1S1 genes have been renamed TACSTD (tumor-associated calcium signal transducer) 1 and 2, respectively.

Materials and methods

FISH was performed according to Calabrese et al. (1994). Hybridization of biotin-14-dATP-labeled probes was detected by indirect staining with avidin-FITC. Chromosomes were counterstained with DAPI. Images were captured using a CCD camera (Photometrics) driven by a Vidas-Zeiss image analyzer.

Probe names: hTROP1 (TACSTD1); hTROP2 (TACSTD2).
Probe type: human genomic
Insert size: multiple inserts of 6–8 kb for hTROP1 (TACSTD1), 15 kb for hTROP2 (TACSTD2).
Vector: pBluescript for hTROP1 (TACSTD1); EMBL-4 for hTROP2 (TACSTD2).
Proof of authenticity: DNA sequencing.
Gene reference: (TACSTD1) Linnenbach et al. (1993); (TACSTD2) Fornaro et al. (1995), Tsujikawa et al. (1999).

Supported by the Italian Association for Cancer Research (AIRC, Milan, Italy), the Italian National Research Council (Convenzione CNR – Consorzio Mario Negri Sud).We are grateful to Dr. Linnenbach for the gift of the GA733-2/TROP1/TACSTD1 probes.

Received 5 September 2000; manuscript accepted 29 September 2000.

Request reprints from Dr. Saverio Alberti, Head,
Lab. of Experimental Oncology, Consorzio Mario Negri Sud,
66030 Santa Maria Imbaro Chieti (Italy); telephone: (39) 0872-570.293;
fax: (39) 0872-570.412; e-mail: alberti@emms.mnegri.it

KARGER
Fax + 41 61 306 12 34
E-mail karger@karger.ch
www.karger.com

© 2001 S. Karger AG, Basel

0301–0171/01/0922–0164$17.50/0

Accessible online at:
www.karger.com/journals/cog

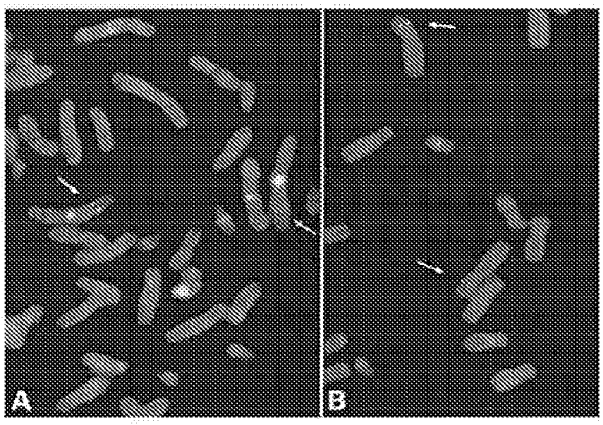


Fig. 1. Chromosome location of the human TACSTD2 gene at 1p32 (**A**) and of the TACSTD1 gene at 2p21 (**B**), as shown by FISH analysis (arrows).

Results

Mapping data

TACSTD1

Location: 2p21

Number of cells examined: 25

Number of cells with specific signal: 1 (0), 2 (1), 3 (6), and 4 (18) chromatids per cell

Most precise assignment: 2p21

Location of background signals (sites with >2 signals): none observed

TACSTD2

Location: 1p32

Number of cells examined: 30

Number of cells with specific signal: 1 (1), 2 (2), 3 (4), and 4 (23) chromatids per cell

Most precise assignment: 1p32

Location of background signals (sites with >2 signals): none observed

References

Calabrese G, Sallese M, Stornaiuolo A, Stuppia L, Palka G, De Blasi A: Chromosome mapping of the human arrestin (SHG), beta-arrestin 2 (ARB2), beta-adrenergic receptor kinase 2 (ADRBK2) genes. Genomics 23:286–288 (1994).

Fornaro M, Dell' Arciprete R, Stella M, Bucci C, Nutini M, Capri MG, Alberti S: Cloning of the gene encoding Trop-2, a cell surface glycoprotein expressed by human carcinomas. Int J Cancer 62:610–618 (1995).

Limnenbach AJ, Seng BA, Wu S, Robbins S, Scollon M, Pyrc JJ, Druck T, Huebner K: Retroposition in a family of carcinoma-associated antigene genes. Molec Cell Biol 13:1507–1515 (1993).

OMIM: Online Mendelian Inheritance in Man. URL: http://www.ncbi.nlm.nih.gov/omim/

Papadopoulos N, Nicolaides NC, Liu B, Parsons R, Lengauer C, Palombo F, D'Arrigo A, Markowitz S, Willson JKV, Kinzler KW, Jiricny J, Vogelstein B: Mutations of GTBP in genetically unstable cells. Science 268:1915–1917 (1995).

Ripani E, Sacchetti A, Corda D, Alberti S: The human Trop-2 is a tumor-associated calcium signal transducer. Int J Cancer 76:671–676 (1998).

Tsujikawa M, Kurahashi H, Tanaka T, Nishida K, Shimomura Y, Tano Y, Nakamura Y: Identification of the gene responsible for gelatinous drop-like corneal dystrophy. Nature Genet 21:420–423 (1999).

White PS, Forus A, Matise TC, Schutte BC, Spieker N, Stanier P, Vance JM, Gregory SG: Report of the fifth international workshop on human chromosome 1 mapping 1999. Cytogenet Cell Genet 87:143–171 (1999).

Office de la propriété intellectuelle du Canada
Un organisme d'Industrie Canada

Canadian Intellectual Property Office
An Agency of Industry Canada

SMART & BIGGAR
CIPOmail@smart-biggar.ca

28 March 2017 (28-03-2017)

Application No.	:	**2,885,800**
PCT No.	:	**JP2013006069**
Owner	:	DAIICHI SANKYO COMPANY, LIMITED
Title	:	**ANTIBODY-DRUG CONJUGATE**
Classification	:	C07K 5/103 (2006.01)
Your File No.	:	**51481-31**
Examiner	:	Colleen MacFarlane

THIS LETTER IS NOT A REQUISITION. NO RESPONSE IS REQUIRED.

This letter acknowledges the phone conversation of 24 March 2017 (24-03-2017). We confirm that the report dated 17 March 2017 (17-03-2017) requires clarification.

As discussed with the Examiner's Section Head on 24 March 2017 (24-03-2017), the Applicant's Agent would like clarification of the defect related to claim 15 as being cited for anticipation using common general knowledge without pointing to a source. The compound of claim 15 is the compound exatecan which is commonly known in the art as Applicant acknowledges throughout the description (p. 2, for example). The only difference between the known exatecan compound and the compound of claim 15 is the addition of the –COCOH- functional group to the nitrogen in position 1 (to allow conjugation with the linker), a strategy which would be well known to a skilled person. Applicant also cites references to known derivatives of exatecan (DE-310, for example), which comprise peptide linkers attached to the amino group (p.3-4, for example). The synthesis of exatecan as described in U.S. Patent 5,834,476 (Terasawa et al.,1998) (and reproduced in Wikipedia) discloses the structure of exatecan comprising **–NHCOC**F_3- in position 1, the F_3 in the place of the -OH group in the instant application. For these reasons, it is contended that the structure of exatecan is considered as common general knowledge, as is the functional group, COCOH, and thus the compound of claim 15 is anticipated by the common general knowledge in the art.

2,885,800 2

As agreed during the conversation, to accelerate the prosecution of the application, we will not withdraw the report. Therefore, the deadline to respond to the examiner's requisition on this application remains the one indicated in said report.

Colleen MacFarlane
Patent Examiner (B1)
819-639-1402

As per CIPO Client Service Standards, a response to a telephone enquiry or voice mail should be provided by the end of the next business day. In the event that attempts to reach the examiner are unsuccessful, the examiner's Section Head, Nicholas Ohan, can be reached at 819-639-5250.

Innovation, Sciences et Développement économique Canada
Office de la propriété intellectuelle du Canada

Innovation, Science and Economic Development Canada
Canadian Intellectual Property Office

SMART & BIGGAR
CIPOmail@smart-biggar.ca

13 April 2018 (13-04-2018)

Application No.	:	**2,939,802**
PCT No.	:	**JP2015002020**
Owner	:	DAIICHI SANKYO COMPANY, LIMITED; DAIICHI SANKYO EUROPE GMBH
Title	:	**ANTI-HER3 ANTIBODY-DRUG CONJUGATE**
Classification	:	C07K 16/28 (2006.01)
Your File No.	:	**51481-38**
Examiner	:	Jacinth Abraham

YOU ARE HEREBY NOTIFIED OF A REQUISITION BY THE EXAMINER IN ACCORDANCE WITH SUBSECTION 30(2) OF THE *PATENT RULES*. IN ORDER TO AVOID ABANDONMENT UNDER PARAGRAPH 73(1)(*a*) OF THE *PATENT ACT*, A WRITTEN REPLY MUST BE RECEIVED WITHIN THE **SIX (6)** MONTH PERIOD AFTER THE ABOVE DATE.

This application has been examined taking into account the:

Description,	pages 1 - 226, as originally filed;
Claims,	1 - 38, as received on 15 August 2016 (15-08-2016) during the national phase; and
Drawings,	pages 1 - 26, as originally filed.

The number of claims in this application is 38.

As the application is apparently directed to a plurality of inventions, as detailed below, the examiner has proceeded on the presumption that the applicant will elect the claims of **Group A**. This presumption does not affect the applicant's right to elect, one time, a different invention for prosecution. The scope of the search and examination of the claims was therefore restricted to the subject-matter of the claims of **Group A** (directed to an Her3-binding antibody known by its arbitrary designation as U1-59, has full-length heavy and light chains represented by SEQ ID NOs 583 and 584, has VH and VL represented by SEQ ID NOs 70 and 72, and CDRs in the VH represented by SEQ ID NOs 562 to 564, and CDRs in the VL represented by SEQ ID NOs 565 to 567).

Documents Applied

D1	CA2815154	Hettmann, T. et al.	9 February 2012 (09-02-2012)

D2	CA2859255	Lerchen, H-G., et al.	20 June 2013 (20-06-2013)
D3	CA2927832	Eliasof, S.D.	14 November 2011 (24-11-2011)
D4	Ochi, Y. et al., Cancer Chemother & Pharmacol., Vol. 55, Pages 323-332, April 2005 (04-2005)		

D1 discloses the use of U1-59, an Her3 antibody, in treating disease (paragraph 4). The antibody may be attached to a drug by means of a linker/spacer: "Various methods of attaching effector groups to polypeptides or glycopeptides (such as antibodies) are known in the art, and may be used in making and carrying out the compositions and methods described herein. In some embodiments, it may be useful to have effector groups attached to a binding protein by spacer arms of various lengths to, for example, reduce potential steric hindrance" (paragraph 65). Maytansine, T-DM1, is provided as an example of an antibody-drug conjugate (paragraph 104). Examples of other drugs are in paragraph 121. Please see also paragraphs 123 and 124.

D2 discloses an antibody-drug conjugate wherein the antibody binds FGFR2, the drug is exactecan (page 151, line 30), and wherein the antibody is linked to exatecan via a linker (page 9).

D3 discloses the conjugate of exatecan to a cyclodextrin-containing polymer (CDP), wherein the former is attached to the latter via a linker.

D4 discloses a GGFG tetrapeptide linker to link exatecan to a biomolecule carrier. A protease *in vivo* cleaves and releases exatecan from the carrier.

The examiner has identified the following defects in the application.

Claims 1 - 38 do not comply with section 28.3 of the *Patent Act*. These claims are directed to subject-matter that would have been obvious at the claim date to a person skilled in the art or science to which it pertains having regard to D1 in view of D2 – D4. The subject matter of these claims is the combination of the following three entities to form an antibody-drug conjugate (ADC; please see the present description, paragraphs 12 and 13):
1. an Her3 antibody,
2. exatecan (a cytotoxic drug), and
3. a linker that links the Her3 antibody to exatecan.

With regard to the above, Her2 antibodies are old and known. In fact, a simple search finds numerous disclosures in the Canadian Patent Database of treatment of disease with the U1-59 antibody. Please see D1.

Likewise, exatecan is and old and known drug, which is conjugated to an antibody via linker to treat disease. Please see D2. Exatecan is also conjugated to other molecules to treat disease. Please see D3 and D4.

Linkers that link an antibody to a drug are old and known. For example, please see the Written Opinion of the PCT for WO2015098099, and prosecution before the EPO for corresponding EP3088419, and before the USPTO for 15/187179, for examples of disclosures of linkers prior to

the claim date of the present application. For example, disclosures in the above, for e.g., D4 – D6 before the EPO, wherein EPO's D6 is D4 cited herein, disclose a GGFG tetrapeptide linker to link exatecan to a biomolecule carrier. A protease *in vivo* cleaves and releases exatecan from the carrier. Moreover, a linker is a simple molecule that is devised to hold a drug onto an antibody (please see description for D1 under "Documents Applied". Linkers are well known, and the chemistry for generating and testing these are also common general knowledge; hence, in the realm of linking a known antibody to a known drug, a linker is a trivial feature. Hence, Applicant cannot lay claim to every Her3 antibody (known, and yet to be developed) and the known exatecan as an antibody-drug conjugate by specifying a trivial feature – a linker. Moreover, GGFG tetrapeptide on its own suffices to link exatecan to a carrier; hence, there is no further invention in adding other molecules in addition to GGFG to arrive at a different linker; i.e., there is no inventive advantage to such a linker with added-on molecules. 1

Therefore, it would be obvious to one skilled in the art to link an Her3 antibody (disclosed in D1) to exactecan (disclosed in D2 – D4) via any linker that will hold the antibody to exatecan as disclosed in D1 including a linker comprising GGFG disclosed in D4 (see also the previous paragraph for further disclosures of linkers) to arrive at the subject matter of these claims. Therefore, the subject matter of each of claims 1 – 38 is obvious, and fails to comply with section 28.3 of the *Patent Act*.

The application does not comply with subsection 36(1) of the *Patent Act* as the claims are directed to more than one invention. The phrase "one invention only" in section 36 of the *Patent Act*, when understood in its full context and in view of section 36 of the *Patent Rules*, has a meaning equivalent to "one invention only or to a group of inventions so linked as to form a single general inventive concept" in Rule 13.1 of the *Regulations Under the PCT*.

Identifying a defect arising from non-compliance with the requirements of section 36 of the *Patent Act* does not contravene PCT article 27(1).

Following an evaluation of the claims, the examiner has identified that the claims are directed to the following groups of inventions:

> **Group A** - Claims 1 - 34 and 36 - 38 (all partial), and claim 35 (whole), directed to an Her3-binding antibody known by its arbitrary designation as U1-59, has full-length heavy and light chains represented by SEQ ID NOs 583 and 584, has VH and VL represented by SEQ ID NOs 70 and 72, and CDRs in the VH represented by SEQ ID NOs 562 to 564, and CDRs in the VL represented by SEQ ID NOs 565 to 567; and 2
>
> **Groups Undetermined** - Claims 1 - 34 and 36 - 38 (all partial), directed to an undetermined number of Her3-binding antibodies.

The following are all old and known: (1) anti-Her3 antibody U1-59 (see, for example, D1); (2) conjugates of exatecan and its derivatives linked to an antibody or biomolecule to form a conjugate, which conjugate treats disease (D2 – D4); and (3) organic molecule and peptide linkers that link an antibody to a drug (D1, D2 and D4). Applicant is referred to the indication above for lack of an inventive step. Hence, there is no inventive special technical feature that will link the subject matter in the claims into a single invention. Please note that linkers are well

known, and the chemistry for generating and testing these are also common general knowledge; hence, in the realm of linking a known antibody to a known drug, a linker is a trivial feature that cannot serve as an inventive special technical feature.

2

According to subsection 36(2) of the *Patent Act*, after limiting the claims of the present application to one invention only, the applicant may make any other invention disclosed the subject of a divisional application. The applicant is advised that once an election has been made, further prosecution of the present application will be limited to the invention so elected.

Claims 1, 10, 11, 14 and 16 are indefinite and do not comply with subsection 27(4) of the *Patent Act*. The language used to indicate the positions on the molecules on which they are found, and the attachment sites on the linker, antibody and exatecan, are so unclear that it is not possible to clearly discern where exactly the linker is attached to the antibody, and where exactly the linker is attached to exatecan (claims 1, 14 and 16). Please see page 227, lines 6, 7, 11 and 12; page 228, last two lines; page 232, lines 8 – 11; page 234, lines 5, 6, 10 and 11; and page 235, lines 11 and 12.

3

Also, in claims 10 and 11, the following phrases cause a lack of clarity, respectively: "partial structure having a chain length of 4 to 7 atoms" (claim 10) and "partial structure having a chain length of 5 or 6 atoms" (claim 11).

4

Claims 1 – 4, 14 and 16 are indefinite and do not comply with subsection 27(4) of the *Patent Act*. The term "residue" does not serve to correctly and clearly define a peptide, and causes a lack of clarity to each of claims 1 – 4, 14 and 16. In the art, this term is used to refer to a single amino acid. On the contrary, a peptide is made of a plurality of amino acids.

5

Claims 1, 3, 12 – 16 and 20 are indefinite and do not comply with subsection 27(4) of the *Patent Act*. Absence of an appropriate conjunction at the following locations causes a lack of clarity to each of claims 1, 3, 12 – 16 and 20: page 228, between lines 8 and 9; page 229, between lines 16 and 17; page 230, between lines 17 and 18, and between lines 22 and 23; page 232, between lines 3 and 4; page 233, before line 3, and between lines 11 and 12; page 235, between lines 7 and 8; and page 236, between lines 9 and 10.

6

In view of the above, the groups in claims 3, 14 and 15 are not defined correctly (see section 11.11 of the *Manual of Patent Office Practice*).

Claims 1, 14, 16, and 21 – 23 are indefinite and do not comply with subsection 27(4) of the *Patent Act*. The following lack clear antecedence, and cause a lack of clarity to the corresponding claims:

7

"the linker structure" (claims 1, 14 and 16);
"the drug-linker structure moiety" (claim 14); and
"the selected one drug-linker structure" (claims 21 – 23).

Claims 11 and 13 are indefinite and do not comply with subsection 27(4) of the *Patent Act*. The term "followings" causes a lack of clarity to each of claims 11 and 13.

8

Claims 14 and 16 are indefinite and do not comply with subsection 27(4) of the *Patent Act*. Stating a different number for the same formula causes a lack of clarity to claims 14 and 16, as it gives the impression that Formulae 3, 5 and 6 are different from the corresponding ones in claim 1. 9

Claims 14, 15 and 21 – 23 are indefinite and do not comply with subsection 27(4) of the *Patent Act*. The expression "one drug-linker structure" is not correctly and fully defined, and causes a lack of clarity to each of claims 14, 15 and 21 – 23; it is unclear what exactly it signifies in the antibody-drug conjugate. In this regard, the relationship of "the drug-linker structure moiety" and "one drug-linker structure" within the antibody-drug conjugate should be defined at first instance in every set of claims that depend from an independent claim. 10

Claims 24 – 26, 30, 31, 37 and 38 are indefinite and do not comply with subsection 27(4) of the *Patent Act*. The term "medicine" is vague and imprecise, and does not serve to correctly and clearly define the intended subject matter. Please note that the term "drug" is already present in the expression "antibody-drug conjugate", and will cause a lack of clarity if used to replace the term "medicine". 11

Claims 26, 28, 30 and 38 are indefinite and do not comply with subsection 27(4) of the *Patent Act*. The expression "is applied" is an active step in a method of medical treatment, and causes a lack of clarity to each of claims 26, 28 and 38. For a similar reason, the phrase "is used" in claim 30 (line 3), can be taken to cause a similar lack of clarity. 12

It follows that claims 26, 28, 29, 30 and 38 encompass subject-matter that lies outside the definition of "invention" and do not comply with section 2 of the *Patent Act*. The defined method is a method of medical treatment and is consequently not a statutory "art" or "process" (see section 17.02.03a of the *Manual of Patent Office Practice*). 13

Claims 27, 31 and 36 are indefinite and do not comply with subsection 27(4) of the *Patent Act*. The article "an" in "an active ingredient" implies, but does not clearly specify, the presence of other active ingredients. 14

Claim 31 is indefinite and does not comply with subsection 27(4) of the *Patent Act*. The phrase "even an additional medicine as an active ingredient" lacks clarity (claim 31). 15

Claim 33 is indefinite and does not comply with subsection 27(4) of the *Patent Act*. The preposition "on" in the phrase "on the heavy and light chains" causes a lack of clarity. Please see claim 32. 16

Claim 34 is not fully supported by the description and does not comply with section 84 of the *Patent Rules*. There is no SEQ ID NO: 33 in the sequence listings of amino acid sequences. 17

Claim 35 unnecessarily refers to the drawings and does not comply with subsection 86(1) of the *Patent Rules*. Features of the invention should not, unless required, rely on references to the description or drawings. The technical features being defined can be defined in terms of the stated SEQ ID NOs; hence, reference to the drawings is not required. In particular, references such as "(Figure 1)" and "(Figure 2)" should be removed. 18

The description contains statements that incorporate by reference other documents and does not comply with subsection 81(1) of the *Patent Rules*. Several such statements are found in the description, and should be removed. 19

The description does not comply with section 76 of the *Patent Rules*, which requires that trade-marks mentioned in the application be identified as such. If "Sephadex" in paragraph 123, "Triton" in paragraph 268, "Celite" in paragraph 241 and "Tween-20" in paragraph 268 are trade-marks, they must be so identified. 20

In view of the foregoing defects, the applicant is requisitioned, under subsection 30(2) of the *Patent Rules*, to amend the application in order to comply with the *Patent Act* and the *Patent Rules* or to provide arguments as to why the application does comply.

Under section 34 of the *Patent Rules*, any amendment made in response to this requisition must be accompanied by a statement explaining the nature thereof, and how it corrects each of the above identified defects.

Jacinth Abraham
Patent Examiner (Section B2)
819-639-7687

As per CIPO Client Service Standards, a response to a telephone enquiry or voice mail should be provided by the end of the next business day. In the event that attempts to reach the examiner are unsuccessful, the examiner's Section Head, Dr. Robert Rymerson, can be reached at 819-743-2713.

For general inquiries: 1-866-997-1936 or for more options see http://www.ic.gc.ca/eic/site/cipointernet-internetopic.nsf/eng/wr00006.html.

CIPO values your feedback and invites you to complete a short and anonymous ongoing survey on patent examination products and services. You can access the survey at the following link: http://ic.sondages-surveys.ca/s/SCB-OPS/langeng.

2939802A_jab.docm

The Examination Search Report is provided for reference only and is not part of any requisition made by the examiner in accordance with the *Patent Act* or *Rules*. The applicant is not required to respond to the information contained in the Examination Search Report.

Examination Search Report

Box I: General Information			
Application No.	2,939,802	Search Report Date	2017-08-24
Title	ANTI-HER3 ANTIBODY-DRUG CONJUGATE		
Examiner	Jacinth Abraham	Search Conducted?	Yes

Box II: Family Prosecution		
Family Member	File Wrapper Reviewed	Status of Prosecution
US2017021031A1	2017-08-24	In Progress
EP3129063A1	2017-08-24	In Progress

Box III: Search History			
Claims Searched	1 - 38	Date of Search	2017-08-24

Type of Search Conducted (select all that apply):

Canadian first to file search	■	Supplemental/top up search	■
Inventor/applicant search	■	Non laid open search	□
Comprehensive search	□	In-house searcher	□

Search History from Databases Consulted:

```
##### CANADIAN PATENT DATABASE/INTELLECT ##########

"U1-59" <AND> publication-date <= 2014-04-10

("U1-59" <AND> exatecan) <AND> publication-date <= 2014-04-10

(antibody <AND> exatecan <AND> conjugate) <AND> publication-date <= 2014-04-10

(antibody <AND> exatecan <AND> GGFG <AND> linker <AND> conjugate) <AND> publication-date
<= 2014-04-10

(GGFG <AND> linker <AND> antibody <AND> conjugate) <AND> publication-date <= 2014-04-10

(GGFG <AND> linker <AND> conjugate) <AND> publication-date <= 2014-04-10

((Daiichi <OR> U3) <IN> interested-party) <AND> linker <AND> conjugate <AND> GGFG
```

```
##### STN CAplus, Medline, DWPI, EMBASE, Biosis, CANPATFULL, USFULL, EPFULL and
PCTFULL##########

pd<20140410 AND (antibody AND exatecan AND GGFG AND linker AND conjugate)

pd<20140410 AND (exatecan AND GGFG AND linker AND conjugate)

pd<20140410 AND (antibody AND exatecan AND linker AND conjugate)

pd<20140410 AND (antibody AND exatecan AND linker AND conjugate AND Her3)

pd<20140410 AND (antibody AND exatecan AND linker AND conjugate AND succinimid*)

pd<20140410 AND (antibody AND exatecan AND linker AND conjugate AND succinimid* AND GGFG)


##### GOOGLE ##########

(succinimid-3-yl-N)-Ch2Ch2Ch2-C(=O)-GGFG-NH-CH2CH2-C(=O)-(NH-DX)


##### GENOMEQUEST ##########


Audit trail

    Report generated on the 24 Aug 2017 : 18:24 (EDT)
    Queries: download queries

Title  CA2939802 U1-59 Ab CDRs, VH, VL, HC and LC
Description
Owner and Launch Date    This run is launched by Jacinth Abraham at 2017-08-24 14:30:54,
and its status is FINISHED, at 2017-08-24 14:36:27.
Location     It is located at [My Data].
Workflow     IP. Total Nb. of Results: 5000. Storage size: 215.54 MB. (Id: 3414007, See
Log)
Query Database
Protein Databases (10 sequences):

Database     Version  Release Date      Database Status
.query database     20170824     2017-08-24 14:30:54       Most Recent
Subject Database
No nucleotide database selected.

Protein Databases (117,707,210 sequences):

Sequences with length less than 6 or more than 100,000 are not searched.

Database     Version  Release Date      Database Status
GQ-Pat GoldPlus Protein - Patent sequences     20170821     2017-08-21 10:22:53       M
GQ-Pat Platinum protein - Patent sequences     20170821     2017-08-21 10:20:36       M
```

Thomson-Reuters Geneseq - Protein sequences 201716 2017-08-12 02:54:16 M
Protein Data Bank - protein seqs 20170822 2017-08-22 14:00:14 Most Recent
Genpept - Translated Genbank 220 2017-08-15 12:16:59 Most Recent
Search Strategy

The search strategy was GenePAST.
This strategy fits the shorter sequence (query or subject) into the longer one, keeping the number of mismatches and gaps to a minimum.
Alignments with less than 80% identity over query are discarded.

Keep Best Alignments Best 500 alignments are kept.

Version 9

OnCusp
Ex. 1002

The State Intellectual Property Office of People's Republic of China

100020

北京市朝阳区东三环中路 1 号环球金融中心办公楼东楼 20 层 北京市金杜律师事务所
杨宏军 牛蔚然

Issuing Date:

Application No. or Pubilcation No.:201380053256.2 **Issue No.:**

Applicant or Patentee: DAIICHI SANKYO COMPANY, LTD.

Title of Invention: Antibody-drug conjugate

The First Office Action

(PCT Application Entering the National Phase)

1. ☒Upon the request of substantive examination of the applicant, in accordance with Article 35.1 of the Patent Law, the State Intellectual Property Office performs the substantive examination for the aforesaid application for a patent for invention.

☐In accordance with Article 35.2 of the Patent Law, the State Intellectual Property Office proceeds to examine the aforesaid application for a patent for invention as to its substance on its own initiative.

2. ☒The applicant requests on the basis of:

JP 专利局的申请日 2012 年 10 月 11 日为优先权日。

3. ☐Upon examination, the amendment submitted by the applicant on_____, shall not be accepted for not in conformity with Rule 51.1 of the Implementing Regulations of the Patent Law.

4. ☐Examination is proceeded on the basis of Chinese document or the Chinese translation of the original filing international application.

☒Examination is proceeded on the basis of the following applicant documents:

依据专利合作条约第 28 条或者第 41 条提交的修改的权利要求第 1-49 项;

2015 年 4 月 10 日提交的说明书附图第 1-22 幅、说明书摘要、说明书第 1-7, 22-2581 段、说明书核苷酸和氨基酸序列表;

2015 年 9 月 6 日提交的说明书第 8-21 段。

5. ☒The following reference documents are cited in this Office Action(the serial number(s) of which will be used in follow-on examination)

No.	Document number or Document title	publication date (or application date of the conflicting application)
1	CN 101490087A	20090722

6. Conclusive opinions of the examination:

About the description:

☐The application falls into the scope of subject matter which is nonpatentable according to Article 5 of the Patent Law.

☐The description fails to comply with the provisions of Article 26.3 of the Patent Law.

☐The description fails to comply with the provisions of Article 33 of the Patent Law.

☐The drafting of the description fails to comply with Rule 17 of the Implementing Regulations of the Patent Law.

☐_____

About the claims:

☐The claim(s)_____fail(s) to comply with the provisions of Article 2.2 of the Patent Law.

☐The claim(s)_____fail(s) to comply with the provisions of Article 9.1 of the Patent Law.

☐The claim(s)_____fail(s) to comply with the novelty requested by Article 22.2 of the Patent Law.

☒The claim(s) 1-33fail(s) to comply with the inventive steps requested by Article 22.3 of the Patent Law.

☐The claim(s)_____fail(s) to comply with the applicability requested by Article 22.4 of the Patent Law.

☒The claim(s) 34 fall(s) into the scope of subject matter which is nonpatentable according to Article 25 of the Patent Law.

☐The claim(s)_____fail(s) to comply with the provisions of Article 26.4 of the Patent Law.

☒The claim(s) 1-49（具体参见通知书正文）fail(s) to comply with the provisions of Article 31.1 of the Patent Law.

☐The claim(s)_____fail(s) to comply with the provisions of Article 33 of the Patent Law.

☐The claim(s)_____fail(s) to comply with the provisions of Rule 19 of the Implementing Regulations of the Patent Law.

☐The claim(s)_____fail(s) to comply with the provisions of Rule 20 of the Implementing Regulations of the Patent Law.

☐The claim(s)_____fail(s) to comply with the provisions of Rule 21 of the Implementing Regulations of the Patent Law.

☐The claim(s)_____fail(s) to comply with the provisions of Rule 22 of the Implementing Regulations of the Patent Law.

☐_____

☐The application fails to comply with the provisions of Article 26.5 of the Patent Law or Rule 26 of its Implementing Regulations.

☐The application fails to comply with the provisions of Article 20.1 of the Patent Law.

☐The divisional application fails to comply with the provisions of Rule 43.1 of the Implementing Regulations of the Patent Law.

The detailed analyses of the above conclusive opinions refer to the text of this Office Action.

7. On the basis of the conclusive opinions, the examiner suggests:

☐The applicant should amend the application documents according to the text of this Office Action.

☒The applicant should state the reasons why the patent application should be granted in the observation, and amend the part which fails to comply with the provisions according to this Office Action; otherwise the patent application should not be granted.

☐The substantive content that might be granted can not be found in the application, if the applicant does not state the reasons or the stated reasons are not sufficient, the application shall be rejected.

☐_____

8. The applicant should pay attention to the followings statements:

(1) In accordance with Article 37 of the Patent Law, the applicant should submit the written opinion within four months from the date of receipt of this Office Action. If, without any justified reason, the time limit for reply is not met, the application shall be deemed to have been withdrawn.

(2) The amendment of the application document by the applicant should be in conformity with

The State Intellectual Property Office of People's Republic of China

Article 33 of the Patent Law, and it should not exceed the scope specified in the initial description and claims. Meanwhile, the amendment of the application document by applicant should be in conformity with Rule 51.3 of the Implementing Regulations of the Patent Law, and in accordance with this Office Action.

(3) The written opinion and/or amendment document of the applicant should be sent by mail or submitted directly to the Receiving Division of the Patent Office of the State Intellectual Property Office, otherwise it will be considered to have no legal effect.

(4) Without appointment, the applicant and/or the agent should not come to the Patent Office of the State Intellectual Property Office to have an interview with the examiner.

9. The text of this Office Action has 7 pages, and the attachments are as follows:

☐The total number of copies of the reference documents cited is _____ copies and _____ pages.

☐7

Name of the Examiner:李翠莹 Tel:020-28950489 Examination Department:专利审查协作广东中心 医药生物发明审查部

The State Intellectual Property Office of People's Republic of China

First Office Action

(PCT Appication of Entering the National Phase)

Application Number:2013800532562

This application relates to antibody - medicine conjugate. Through the examination. Draw following examination reports at present.,

一. The unicity.

This application relates to following 3 and compiles and publishes the Ming Dynasty.

(1) claim 1-34. Relate to antibody - medicine conjugate., Relevant medicine., Anticancer drugs., Pharmaceutical composition and treatment method., Medicine wherein is antitumor nature compound., Shown antitumor nature compound and antibody via following formula., The articulate of the shown structure of - L1-L2-LP-NH- (CH2) n1-La-Lb-Lc- forms., Wherein., Antibody is connected in L1char(39)s end., The amino nitrogen-atoms that antitumor nature compound used 1 is for connecting the position., Connect in Lcchar(39)s end wherein L1 express - (succinimide - 3- base - N) (CH2) n2-C (O)., -CH2-C(=O)-NH-(CH2)n3-C(=O)- -C(=O)-cyc.Hex(1 4)-CH2-(N-ly-3-diminiccuS)- Or - C (O) (CH2) n4-C (O)., Wherein., N2 expresses 2-8char(39)s integer., N3 expresses 1-8char(39)s integer., N4 expresses 1-8char(39)s integer.

(2) claim 35-48. Relate to medicine - joint midbody compound Q- (CH2) nQ-C (O) L2a-LP-NH- (CH2) n1-La-.Lb-Lc-(NH-DX) Q wherein expresses (maleimide - N- base)., HS- X-CH2-C(=O)-NH- Or (pyrrolidine - 2., 5-diketone - N- base), O-C (O)., X expresses bromine atom or iodine atom., NQ expresses 2-8char(39)s integer.

(3) claim 49 relates to - shown the connecing of L1-L2-LP-NH- (CH2) n1-La-Lb-Lc-.The head. It is used for obtaining via connecting antibody - the medicine conjugate that is formed by connecting medicine and antibody., Wherein L1 expresses - (succinimide - 3- base - N) (CH2) n2-C (O)., -CH2-C(=O)-NH-(CH2)n3-C(=O)- -C(=O)-cyc.Hex(1 4)-CH2-(N-ly-3-diminiccuS)- Or - C (O) (CH2) n4-C (O)., Wherein., N2 expresses 2-8char(39)s integer., N3 expresses 1-8char(39)s integer., N4 expresses 1-8char(39)s integer.

Above-mentioned 3 compile and publish only have the same or corresponding technical characterictic between the bright technical scheme char(39) be used for be connected medicine and antibody joint design char(39). Yet. 1 (CN101490087 A of contrast file., 2009.07.22) disclose a joint design., char(39) connect char(39) (L) antibody - medicine conjugate for can be used to connect one or more medicine modules (D) and antibody unit (Ab) formation general formula I.(ADC), difunctional or multi-functional module (seeing the 1st section the 148th page of reciprocal in contrast 1 description of file). ., It is thus clear that above-mentioned the same or corresponding technical characterictic char(39) be used for be connected medicine and antibody joint design char(39) not the

technical characterictic of making contributions to the prior art., Not specific technical characterictic promptly. Consequently, Relate to char(39) be used for be connected medicine and antibody joint design char(39) the technical scheme between do not have a the same or corresponding specific technical characterictic., Do not belong to a total inventive concept., It is unrelated in the technique., Consequently, does not possess the unicity., Be not conform to the regulation of the 31st the 1st section of patent law.

二. Compile and publish bright examination reports as follows to first.

1, claim 34 belongs to the diagnosis and the treatment method of the said disease of the 25th the 1st section (3) item of patent law. Can not be granted patent.

The ask for protection treatment method of tumour and / or cancer of claim 34. This method is for making the human body or the animal body that have life recover or obtain healthily or reduce painfully., Block., The process of the cause of disease or focus is alleviated or eliminated., The diagnosis and the treatment method that belong to the said disease of the 25th the 1st section (3) item of sharp method., Therefore can not be granted patent.

2、 Claim 1 is not conform to the regulation of the 22nd the 3rd section of patent law.

Claim 1 antibody - the medicine conjugate of asking for protection. Be 1 as n1. L1 is - (succinimide - 3- base - N) (CH2) n2-C (O)., N2 is 5., L2 and La and Lb are the single bond., Lc is - during C (O)., Contrast file 1 discloses following structure., Wherein R17 is - (CH2) 5-., Ab is the antibody unit., D is the medicine module., Ww is the amino acid unit., Yy is that the space group unit (sees the 1st section the 148th page of reciprocal in contrast 1 description of file., The 149th page of reciprocal 3-11 is capable., The 151st page of reciprocal is the 3rd section to the 152nd page the 1st section). The technical scheme that claim 1 was asked for protection is compared with 1 disclosed technological content of contrast file. The difference lies in that (1) claim 1 has prescribed a limit to the concrete type of medicine. The mode of medicine with the articulate has been prescribed a limit to to (2) claim 1. Lp and Lcchar(39)s concrete structure has still been prescribed a limit to to (2) claim 1. The actual technical matters of solving of claim 1 provides another kind of antibody - medicine conjugate.

To distinguishing characteristics (1). Contrast file 1 discloses the invention provides immune conjugate or antibody - the medicine conjugate that contains the coupling and have the antibody of cell toxic agent., Said cell toxic agent includes the chemotherapeutic agent. And multiple chemotherapeutic agent has been enumerated. Analog including the camptothecin asks the pool for the well-being., Yi Li (sees the 2nd section the 22nd page of reciprocal in contrast 1 description of file for the well-being., The 72nd page the 3rd section). Though the said antitumor nature

compound of contrast 1 unexposed claim 1 of file. Nevertheless the antitumor nature compound of claim 1 also is the common camptothecin derivant in this field., Those skilled in the art expect the type according to the cancer easily., Concrete therapeutic schedule., Be used for preparing said antibody - medicine conjugate through the suitable antitumor nature compound of limited experimental selection., The technological effect of its reinforcing medicine curative effect can be expected.

To distinguishing characteristics (2) - (3). It is dipeptide - seven peptide unit that contrast file 1 discloses Ww., And the sept unit can select - Gly-Gly- or - Gly- (sees the 8th line contrast the 153rd page of reciprocal in 1 description of file., The 155th page the 3rd section). It is thus clear that. Yy in contrast file 1 formula II is - Gly-Gly- or - during Gly-., Be equivalent to that the Lc in the claim 1 is - C (O)., And make the antitumor nature compound to connect in Lc terminally with 1 amino nitrogen-atoms. It is thus clear that. Those skilled in the art select Lp and Lcchar(39)s concrete structure easily in 1 disclosed technological content of contrast file., Its technological effect of connecting antibody and medicine can be expected.

In sum. The known general knowledge that combines this field on the basis of contrast file 1 technical scheme in order to obtain claim 1 and ask for protection., Conspicuous as far as those skilled in the art., Claim 1 does not possess outstanding substantive characteristics and remarkable progress., Be not conform to the regulation of the 22nd the 3rd section of patent law.

3、Claim 2-14 is not conform to the regulation of the 22nd the 3rd section of patent law.

Claim 1 is quoted to claim 2. Further prescribe a limit to Lpchar(39)s peptide residue. Yet. Contrast file 1 still discloses the amino acid unit and has included the dipeptide, kyrine, tetrapeptide, or pentapeptide. The dipeptide of illustration nature includes. Valine - citrulline (vc or val-cit). Alanine - phenylalanine (af or ala-phe). The kyrine of illustration nature includes. Glycine - valine - citrulline (gly-val-cit) and glycine - glycine - glycine (gly-gly-gly). The amino acid residue that constitutes amino acid joint member can be including the amino acid residue of natural existence. And there are the amino acid analog in less important amino acid and non-natural., Such as citrulline (seeing the 3rd section the 154th page of reciprocal in contrast 1 description of file). . It is thus clear that. The peptide that contrast file 1 disclosed the amino acid unit can be selected from the phenylalanine., The glycine., The valine., The citrulline., And the amino acid of other types also is the conventional selection of amino acid joint design.

Claim 1 is quoted to claim 3. The further structure that connects of prescribing a limit to. Yet. Contrast file 1 discloses La and Lb is the single bond., Lc is - C (O)., And Lp can be for tetrapeptide (seeing the examination reports of claim 2). .

Claim 1 is quoted to claim 4. The further structure that connects of prescribing a limit to. Yet. Contrast file 1 discloses La and Lb is the single bond., Lc is - C (O)., And Lp can be for tetrapeptide (seeing the examination reports of claim 2). ., Though 1 unexposed GGFGchar(39)s of contrast file tetrapeptide residue., Nevertheless it discloses said amino acid unit and can be selected from G and F., Those skilled in the art are easily through the limited experimental shown amino acid unit of GGFG that obtains., It is connected the effect and can expect.

Claim 1 is quoted to claim 5. Further prescribe a limit to L1char(39)s structure. Yet. Be at 5 ochar(39)clock as n2., Contrast file 1 discloses structure - (succinimide - 3- base - N) (CH2) n2-C (O)., Contrast file 1 still discloses the structure., Wherein R17 (sees the 2nd line the 152nd page of reciprocal in contrast 1 description of file for - (CH2) 5- ., The 153rd page of reciprocal is the 8th line)., Structure - CH2-C (O) NH- (CH2) n3-C (O) is disclosed promptly.

Claim 1 is quoted to claim 6. Further prescribe a limit to L1char(39)s structure. Please see the examination reports of claim 5.

Claim 1 is quoted to claim 7. Further prescribe a limit to L1char(39)s structure. Yet. 1 selection of having instructed multiple extension unit of contrast file., Including - (CH2CH2O) r- (seeing the 150th page the 1st section in 1 description of contrast file). ., As r > 1 ochar(39)clock., Contained promptly - C (O) (CH2) n4-Cchar(39)s (O) structure.

Claim 1-6 is quoted to claim 8. Further prescribe a limit to the integer that n2 is 2-5., L2 is the single bond. Yet. Contrast file 1 discloses n2 and has been 5., L2 is single bond (seeing preceding examination reports). .

Claim 1-6 is quoted to claim 9. Further prescribe a limit to n2 and L2. Yet. Contrast file 1 discloses as 5 (seeing preceding examination reports). . 1 selection of still having instructed multiple extension unit of contrast file. Including - (CH2) rC (O) NRb (CH2CH2O) r- (seeing the 150th page the 1st section in 1 description of contrast file). ., When r=3., Contained promptly - NH- (CH2CH2O) n5-CH2-CH2-Cchar(39)s (O) structure.

Claim 10-11 quotes claim 1-7 respectively. Further prescribing a limit to - NH- (CH2) n1-La-Lb-Lc-char(39)s atom number. Yet. The Lc excellent choice (seeing the 155th page of 2-3 section in contrast 1 description of file). that contrast file 1 disclosed., Those skilled in the art obtain the partial structure of the said number of the atoms purpose chain length of claim 10-11 easily through limited experiment., Its technological effect can be expected.

Claim 1-7 is quoted to claim 12. Further prescribing a limit to - NH- (CH2) n1-La-Lb-Lc-char(39)s structure. Yet. 1 selection of still having instructed multiple extension unit of contrast file., Including - (CH2) rC (O) NRb (CH2CH2O) r- (seeing the 150th page the 1st section in 1 description of contrast file). ., It is thus clear that wherein contained - NH-., -(CH2)rC(O)- - CH2CH2O-char(39)s structure., Those skilled in the art carry out conventional the transformation in order to obtain this claim several kinds of said structures to above-mentioned structure easily., Its

technological effect can be expected.

Claim 13-14 all further prescribes a limit to specific joint design. Yet. The extension unit has been instructed to contrast file 1., The selection of amino acid unit., And DXchar(39)s enlightenment has been given to select., Those skilled in the art obtain the said antibody of claim 13-14 - medicine conjugate through limited experiment easily., Antibody - medicine conjugate that contrast file 1 provided has the technological effect of dwindling internal tumour volume equally., The said conjugate of claim 13-14 does not possess unexpected technological effect (seeing 1 embodiment part of contrast file). .

In sum. When its claim of quoting does not possess creativeness., It does not possess outstanding substantive characteristics and remarkable progress to subordinate to claim 2-14 yet., Be not conform to the regulation of the 22nd the 3rd section of patent law.

4、Claim 15 is not conform to the regulation of the 22nd the 3rd section of patent law.

Claim 15 antibody - the medicine conjugate of asking for protection. Be 1 as n1. N2 is 5., When L2 and La and Lb are the single bond., Contrast file 1 discloses following structure., Wherein R17 is - (CH2) 5-., Ab is the antibody unit., D is the medicine module., Ww is the amino acid unit., Yy is that the space group unit (sees the 1st section the 148th page of reciprocal in contrast 1 description of file., The 149th page of reciprocal 3-11 is capable., The 151st page of reciprocal is the 3rd section to the 152nd page the 1st section)., It is thus clear that contrast file 1 open - (succinimide - 3- base - N) (CH2) 5-C (O) is connected to antibody via the thioether bond., And - (succinimide - 3- base - N) 3 are connected with antibody., On 1 nitrogen-atoms with the joint design that contains this structure in the methene be connected. The technical scheme that claim 15 was asked for protection is compared with 1 disclosed technological content of contrast file. The difference lies in that (1) claim 15 has prescribed a limit to the concrete type of medicine. (2) claim 15 still prescribes a limit to - and (succinimide - 3- base - N) (CH2) n2-C (O) is via being present in.The thioether bond that forms in the disulfide bond of the hinge portion of the antibody part and be connected to antibody. And Lp and Lcchar(39)s concrete structure. The actual technical matters of solving of claim 15 provides another kind of antibody - medicine conjugate.

To distinguishing characteristics (1). Contrast file 1 discloses the invention provides immune conjugate or antibody - the medicine conjugate that contains the coupling and have the antibody of cell toxic agent., Said cell toxic agent includes the chemotherapeutic agent. And multiple chemotherapeutic agent has been enumerated. Analog including the washing room asks the pool for the well-being., Yi Li (sees the 2nd section the 22nd page of reciprocal in contrast 1 description of file for the well-being., The 72nd page the 3rd section). Though the said antitumor nature

compound of contrast 1 unexposed claim 15 of file. Nevertheless the antitumor nature compound of claim 15 also is the common camptothecin derivant in this field., Those skilled in the art expect the type according to the cancer easily., Concrete therapeutic schedule., Be used for preparing said antibody - medicine conjugate through the suitable antitumor nature compound of limited experimental selection., The technological effect of its reinforcing medicine curative effect can be expected.

To distinguishing characteristics (2). Structure that contrast file 1 disclosed L1 with and antibody is connected to through the thioether bond., Those skilled in the art influence Fab and regional its function of performance of Fc of antibody in order to avoid sterically hindered., Expect easily being connected the disulfide bond part that connects with the hinge area., Its technological effect can be expected. It is dipeptide - seven peptide unit that contrast file 1 still discloses Ww. And the sept unit can select - Gly-Gly- or - Gly- (sees the 8th line contrast the 153rd page of reciprocal in 1 description of file., The 155th page the 3rd section). It is thus clear that. Yy in contrast file 1 formula II is - Gly-Gly- or - during Gly-., Be equivalent to that the Lc in the claim 1 is - C (O)., And make the antitumor nature compound to connect in Lc terminally with 1 amino nitrogen-atoms. It is thus clear that. Those skilled in the art select Lp and Lcchar(39)s concrete structure easily in 1 disclosed technological content of contrast file., Its technological effect of connecting antibody and medicine can be expected.

In sum. The known general knowledge that combines this field on the basis of contrast file 1 technical scheme in order to obtain claim 15 and ask for protection., Conspicuous as far as those skilled in the art., Claim 15 does not possess outstanding substantive characteristics and remarkable progress., Be not conform to the regulation of the 22nd the 3rd section of patent law.

5、Claim 16-21 is not conform to the regulation of the 22nd the 3rd section of patent law.

Claim 15 is quoted to claim 16. Further prescribe a limit to n2, L2, La, Lbchar(39)s structure. Yet. Contrast file 1 discloses n2 and has been 5., L2 is single bond (seeing preceding examination reports). . 1 selection that still discloses multiple extension unit of contrast file. Including - (CH2) rC (O) NRb (CH2CH2O) r-CH2- (seeing the 150th page the 1st section in 1 description of contrast file). ., Be at 1 ochar(39)clock as r., It has included the second kind structure that this claim was prescribed a limit to.

Claim 15 is quoted to claim 17. Further prescribe a limit to n2, L2char(39)s structure. Yet. Contrast file 1 discloses n2 and has been 5., L2 is single bond (seeing preceding examination reports). .

Claim 15 is quoted to claim 18. Further prescribe a limit to n2, L2char(39)s structure. Contrast file 1 discloses n2 and has been 5. (seeing preceding examination reports). Yet. 1 selection of still having instructed multiple